



AUG 29 2003

QA: NA

RECEIVED BY BSC CCU

DATE: 09/03/2003

Joseph D. Ziegler, Director
 Office of License Application and Strategy
 U.S. Department of Energy
 Office of Civilian Radioactive Waste Management
 Office of Repository Development
 P.O. Box 364629
 North Las Vegas, NV 89036-8629

CONTRACT NO. DE-AC28-01RW12101 – TRANSMITTAL OF REPORT *TECHNICAL BASIS DOCUMENT NO. 11: SATURATED ZONE FLOW AND TRANSPORT* ADDRESSING TWENTY-FIVE KEY TECHNICAL ISSUE (KTI) AGREEMENTS RELATED TO SATURATED ZONE FLOW AND TRANSPORT

This letter transmits *Technical Basis Document No. 11: SATURATED ZONE FLOW AND TRANSPORT*. This technical basis document contains a summary of the current conceptual understanding of flow and transport in the saturated zone (SZ) and provides the context within which individual KTI agreements related to flow and transport in the saturated zone are addressed. Appendices A through M provide direct responses to the following Unsaturated and Saturated Zone Flow Under Isothermal Conditions (USFIC), Radionuclide Transport (RT), Total System Performance Assessment and Integration (TSPAI) Key Technical Issue (KTI), and related General (GEN) 1.01 agreements:

- Appendix A – The Hydrologic Framework Model/Geologic Framework Model Interface (Response to USFIC 5.10*)
- Appendix B – Hydrostratigraphic Cross Sections (Response to RT 2.09 AIN-1 and USFIC 5.05 AIN-1)
- Appendix C – Potentiometric Surface and Vertical Gradients (Response to USFIC 5.08 AIN-1*)
- Appendix D – Regional Model and Confidence Building (Response to USFIC 5.02*, USFIC 5.12*, and USFIC 5.11 AIN -1)
- Appendix E – Horizontal Anisotropy (Response to USFIC 5.01*)
- Appendix F – Flow-C¹⁴ Residence Time (Response to USFIC 5.06*)
- Appendix G – Uncertainty in Flow Path Lengths in Tuff and Alluvium (Response to RT 2.08*, RT 3.03*, and USFIC 5.04*)
- Appendix H - Transport Properties (Response to RT 1.05*, RT 2.01*, RT 2.10*, GEN 1.01 #28 and #34, and RT 2.03 AIN-1)
- Appendix I – Transport-Spatial Variability of Parameters (Response to RT 2.02*, TSPAI 3.32*, and TSPAI 4.02*)
- Appendix J – Determination of Whether Kinetic Effects Should Be Included in the Transport Model (Response to RT 1.04)

AUG 29 2003

Appendix K – Transport- K_d s in Alluvium (Response to RT 2.06*, RT 2.07*, and GEN 1.01 #41 and #102)

Appendix L – Transport-Temporal Changes in Hydrochemistry (Response to TSPA I 3.31*)

Appendix M – Microspheres as Analogs (Response to RT 3.08 AIN-1 and GEN 1.01 #43 and 45)

These Appendices provide the responses to eighteen of the KTI agreements listed in Table II of Performance Based Incentive 1-2.11, Develop Integrated Response Package for KTI agreements. The relevant KTI agreements are highlighted with an asterisk.

The subject report is one in a series of technical basis documents that are being prepared to describe the Yucca Mountain repository system components and processes that are important for predicting the likely postclosure performance of the repository. The information presented in these documents, along with the associated references, forms an outline of the postclosure safety analysis that is being developed for the license application. This information also responds to open KTI Agreements made between the U.S. Nuclear Regulatory Commission (NRC) and the U.S. Department of Energy (DOE). Placing the DOE responses to individual KTI agreements in the context of the applicable repository system components and processes allows for a more direct discussion of the relevance of the agreements to the postclosure safety analyses that will be presented in the License Application. The mapping of KTI agreements to key processes described in the technical basis documents is also consistent with the Yucca Mountain Review Plan abstraction groups (see Enclosure 1). The goal of this approach is to provide a more direct and transparent discussion of the relevant KTI agreements.

The enclosed technical basis document discusses the methods used to model the conceptual understanding of flow and transport in the SZ. It includes a description of processes and features that are important to understanding the regional groundwater flow system, the site-scale groundwater flow system, and the site-scale radionuclide transport model for the SZ. This document places the responses to individual KTI agreements related to SZ flow and transport within the context of the overall conceptual understanding of flow and transport in the SZ, explains their relationship to the postclosure safety analyses, and provides a discussion of the relevance of KTI agreements in the context of the SZ flow and transport models.

Bechtel SAIC Company, LLC (BSC) considers the KTI agreements covered in *Technical Basis Report 11: Saturated Zone Flow and Transport* to be fully addressed, and pending review and acceptance by the NRC, they should be closed.

Also enclosed is a draft letter for submittal to the NRC.

AUG 29 2003

0828038612

Page 3

We are ready to assist you in any way that will be beneficial to the Project. Please contact Martha Pendleton at (702) 295-3267 or Thom Booth at (702) 295-2486 for any additional information you may require.



Nancy H. Williams
Manager of Projects

8-29-03
Date Signed

TB:cg - 0828038612

Enclosures:

1. Table 1 – Correlation of Abstraction Groups in the Yucca Mountain Review Plan and Technical Basis Documents
2. *Technical Basis Document No. 11: Saturated Zone Flow and Transport*
3. NRC Draft Letter

cc:

R. W. Andrews, BSC, Las Vegas, NV
D. L. Barr, DOE, Las Vegas, NV
D. A. Beckman, BSC, Las Vegas, NV
T. C. Booth, BSC, Las Vegas, NV
S. J. Cereghino, BSC, Las Vegas, NV
D. H. Coleman, DOE, Las Vegas, NV
A. A. Eddebarh, BSC, Las Vegas, NV
T. C. Gunter, DOE, Las Vegas, NV
C. L. Hanlon, DOE, Las Vegas, NV
R. J. Henning, BSC, Las Vegas, NV
C. M. Newbury, DOE, Las Vegas, NV
M. W. Pendleton, BSC, Las Vegas, NV
M. C. Tynan, DOE, Las Vegas, NV
M. D. Voegele, BSC, Las Vegas, NV
M. R. Wisenburg, BSC, Las Vegas, NV

Enclosure 1

Table 1. Correlation of Abstraction Groups in the Yucca Mountain Review Plan and Technical Basis Documents

Yucca Mountain Review Plan Abstraction Group	Technical Basis Documents(s)
1. Degradation of Engineered Barriers	6. Waste Package and Drip Shield \ Corrosion
2. Mechanical Disruption of Engineered Barriers	4. Mechanical Degradation and Seismic Effects 14. Low-Probability Seismic Effects
2. Quantity and Chemistry of Water Contacting Waste Packages and Waste Forms	3. Water Seeping into Drifts 5. In-drift Chemical Environment 7. In-package Environment
4. Radionuclide Release Rates and Solubility Limits	7. Waste Form Degradation and Solubility 8. Colloids 9. Engineered Barrier System Transport
5. Climate and Infiltration	1. Climate and Infiltration
6. Flow Paths in the Unsaturated Zone	2. Unsaturated Zone Flow
7. Radionuclide Transport in the Unsaturated Zone	10. Unsaturated Zone Transport
8. Flow Paths in the Saturated Zone	11. Saturated Zone Flow and Transport
9. Radionuclide Transport in the Saturated Zone	11. Saturated Zone Flow and Transport
10. Volcanic Disruption of Waste Packages	13. Volcanic Disruptive Events
11. Airborne Transport of Radionuclides	13. Volcanic Disruptive Events
12. Concentration of Radionuclides in Ground Water	11. Saturated Zone Flow and Transport
13. Redistribution of Radionuclides in Soil	12. Biosphere Transport
14. Biosphere Characteristics	12. Biosphere Transport

OVERNIGHT MAIL

ATTN: Document Control
Chief, High-Level Waste Branch, DWM/NMSS
U.S. Nuclear Regulatory Commission
11555 Rockville Pike
Rockville, MD 20852-2738

TRANSMITTAL OF REPORT "*TECHNICAL BASIS DOCUMENT NO. 11: SATURATED ZONE FLOW AND TRANSPORT*" ADDRESSING KEY TECHNICAL ISSUE (KTI) AGREEMENTS RELATED TO SATURATED ZONE FLOW AND TRANSPORT

This letter transmits *Technical Basis Document No. 11: SATURATED ZONE FLOW AND TRANSPORT*. This technical basis document contains a summary of the current conceptual understanding of flow and transport in the saturated zone (SZ) and provides the context within which individual KTI agreements related to flow and transport in the saturated zone are addressed. Appendices A through M provide direct responses to the following Unsaturated and Saturated Zone Flow Under Isothermal Conditions (USFIC), Radionuclide Transport (RT), Total System Performance Assessment and Integration (TSPAI) Key Technical Issue (KTI), and related General (GEN) 1.01 agreements:

- Appendix A – The Hydrologic Framework Model/Geologic Framework Model Interface (Response to USFIC 5.10)
- Appendix B – Hydrostratigraphic Cross Sections (Response to RT 2.09 AIN-1 and USFIC 5.05 AIN-1)
- Appendix C – Potentiometric Surface and Vertical Gradients (Response to USFIC 5.08 AIN-1)
- Appendix D – Regional Model and Confidence Building (Response to USFIC 5.02, USFIC 5.12, and USFIC 5.11 AIN -1)
- Appendix E – Horizontal Anisotropy (Response to USFIC 5.01)
- Appendix F – Flow- C^{14} Residence Time (Response to USFIC 5.06)
- Appendix G – Uncertainty in Flow Path Lengths in Tuff and Alluvium (Response to RT 2.08, RT 3.03, and USFIC 5.04)
- Appendix H - Transport Properties (Response to RT 1.05, RT 2.01, RT 2.10, GEN 1.01 #28 and #34, and RT 2.03 AIN-1)
- Appendix I – Transport-Spatial Variability of Parameters (Response to RT 2.02, TSPAI 3.32, and TSPAI 4.02)
- Appendix J – Determination of Whether Kinetic Effects Should Be Included in the Transport Model (Response to RT 1.04)
- Appendix K – Transport- K_d s in Alluvium (Response to RT 2.06, RT 2.07, and GEN 1.01 #41 and #102)

Appendix L – Transport-Temporal Changes in Hydrochemistry (Response to TSPA I 3.31)

Appendix M – Microspheres as Analogs (Response to RT 3.08 AIN-1 and GEN 1.01 #43 and 45)

The subject report is one in a series of technical basis documents that are being prepared to describe the Yucca Mountain repository system components and processes that are important for predicting the likely postclosure performance of the repository. The information presented in these documents, along with the associated references, forms an outline of the postclosure safety analysis that is being developed for the license application. This information also responds to open KTI Agreements made between the U.S. Nuclear Regulatory Commission (NRC) and the U.S. Department of Energy (DOE). Placing the DOE responses to individual KTI agreements in the context of the applicable repository system components and processes allows for a more direct discussion of the relevance of the agreements to the postclosure safety analyses that will be presented in the License Application. The mapping of KTI agreements to key processes described in the technical basis documents is also consistent with the Yucca Mountain Review Plan abstraction groups (see Enclosure 1). The goal of this approach is to provide a more direct and transparent discussion of the relevant KTI agreements.

The enclosed technical basis document discusses the methods used to model the conceptual understanding of flow and transport in the SZ. It includes a description of processes and features that are important to understanding the regional groundwater flow system, the site-scale groundwater flow system, and the site-scale radionuclide transport model for the SZ. This document places the responses to individual KTI agreements related to SZ flow and transport within the context of the overall conceptual understanding of flow and transport in the SZ, explains their relationship to the postclosure safety analyses, and provides a discussion of the relevance of KTI agreements in the context of the SZ flow and transport models.

DOE considers the KTI agreements covered in *Technical Basis Report 11: Saturated Zone Flow and Transport* to be fully addressed, and pending review and acceptance by NRC, they should be closed.

There are no new regulatory commitments in the body or the enclosure to this letter.

Please direct any questions concerning this letter and its enclosure to Timothy C. Gunter at (702) 794-1343.

Joseph D. Ziegler, Director
Office of License Application and Strategy



QA: NA

August 2003

Technical Basis Document No. 11: Saturated Zone Flow and Transport

By:
Robert W. Andrews, Al A. Eddebbbarh

With Contributions By:
Roger J. Henning, Scott C. James, August C. Matthusen, Arend Meijer,
Hari Viswanathan, Timothy J. Vogt, Jim L. Boone, Thomas C. Booth, Mei Ding,
Paul R. Dixon, Ernest L. Hardin, Charles Haukwa, Edward M. Kwicklis,
Terry A. Miller, Paul W. Reimus, Richard W. Spengler, and Patrick Tucci

Prepared for:
U.S. Department of Energy
Office of Civilian Radioactive Waste Management
Office of Repository Development
P.O. Box 364629
North Las Vegas, Nevada 89036-8629

Prepared by:
Bechtel SAIC Company, LLC
1180 Town Center Drive
Las Vegas, Nevada 89144

Under Contract Number
DE-AC28-01RW12101

CONTENTS

	Page
1. INTRODUCTION	1-1
1.1 OBJECTIVE AND SCOPE	1-3
1.2 DESCRIPTION OF PROCESSES AFFECTING THE PERFORMANCE OF THE SATURATED ZONE	1-5
1.3 SUMMARY OF CURRENT UNDERSTANDING	1-6
1.4 ORGANIZATION OF THIS REPORT	1-8
1.5 NOTE REGARDING THE STATUS OF SUPPORTING TECHNICAL INFORMATION	1-8
2. SATURATED ZONE GROUNDWATER FLOW	2-1
2.1 INTRODUCTION	2-1
2.2 REGIONAL GROUNDWATER FLOW SYSTEM.....	2-1
2.2.1 Regional Groundwater Recharge and Discharge.....	2-2
2.2.2 Regional Potentiometric Surface	2-9
2.2.3 Death Valley Regional Hydrogeology.....	2-12
2.2.4 Regional Geochemistry.....	2-17
2.2.5 Groundwater Flow Model and Results	2-25
2.3 SITE-SCALE GROUNDWATER FLOW SYSTEM.....	2-28
2.3.1 Site Characterization and Data Collection.....	2-29
2.3.2 Site-Scale Recharge and Discharge	2-29
2.3.3 Site-Scale Potentiometric Surface.....	2-33
2.3.4 Site-Scale Hydrogeologic Framework.....	2-39
2.3.5 Site-Scale Hydrogeology	2-47
2.3.6 Site-Scale Geochemistry: Analyses of Water Types and Mixing.....	2-55
2.3.7 Site Scale Groundwater Flow Model and Results	2-57
2.4 Summary.....	2-68
3. SATURATED ZONE RADIONUCLIDE TRANSPORT.....	3-1
3.1 Introduction.....	3-1
3.2 Advection, Matrix Diffusion, AND Dispersion PROCESSES.....	3-3
3.2.1 Advection, Diffusion, and Dispersion Processes and Parameters for Fractured Volcanic Tuffs	3-3
3.2.2 Advection, Diffusion, and Dispersion Processes and Parameters for Alluvium	3-13
3.2.3 Corroboration of Tuff and Alluvial Advective Transport Representations Using Carbon Isotope Information	3-17
3.3 RADIONUCLIDE Sorption PROCESSES	3-25
3.3.1 Radionuclide Sorption on Fractured Tuff.....	3-26
3.3.2 Radionuclide Sorption in the Alluvium	3-32
3.3.3 Colloid-Facilitated Transport.....	3-39
3.4 Site-Scale Radionuclide Transport Model.....	3-40
4. SUMMARY AND CONCLUSIONS	4-1

CONTENTS (Continued)

	Page
4.1 SUMMARY OF SATURATED ZONE FLOW PROCESSES AND RELEVANCE TO REPOSITORY PERFORMANCE	4-2
4.2 SUMMARY OF SATURATED ZONE TRANSPORT PROCESSES AND RELEVANCE TO REPOSITORY PERFORMANCE	4-3
4.3 CONCLUDING REMARKS.....	4-5
5. REFERENCES	5-1
5.1 Documents Cited	5-1
5.2 SOURCE DATA, LISTED BY DATA TRACKING NUMBER	5-6
APPENDIX A – THE HYDROGEOLOGIC FRAMEWORK MODEL/GEOLOGIC FRAMEWORK MODEL INTERFACE (RESPONSE TO USFIC 5.10).....	A-1
APPENDIX B – HYDROSTRATIGRAPHIC CROSS SECTIONS (RESPONSE TO RT 2.09 AIN-1 AND USFIC 5.05 AIN-1)	B-1
APPENDIX C – POTENTIOMETRIC SURFACE AND VERTICAL GRADIENTS (RESPONSE TO USFIC 5.08 AIN-1).....	C-1
APPENDIX D – REGIONAL MODEL AND CONFIDENCE BUILDING (RESPONSE TO USFIC 5.02, USFIC 5.12, AND USFIC 5.11 AIN-1)	D-1
APPENDIX E – HORIZONTAL ANISOTROPY (RESPONSE TO USFIC 5.01).....	E-1
APPENDIX F – FLOW-C14 RESIDENCE TIME (RESPONSE TO USFIC 5.06)	F-1
APPENDIX G – UNCERTAINTY IN FLOW PATH LENGTHS IN TUFF AND ALLUVIUM (RESPONSE TO RT 2.08, RT 3.08, AND USFIC 5.04).....	G-1
APPENDIX H – TRANSPORT PROPERTIES (RESPONSE TO RT 1.05, RT 2.01, RT 2.10, GEN 1.01 (#28 AND #34), AND RT 2.03 AIN-1)	H-1
APPENDIX I – TRANSPORT—SPATIAL VARIABILITY OF PARAMETERS (RESPONSE TO RT 2.02, TSPA I 3.32, AND TSPA I 4.02).....	I-1
APPENDIX J – DETERMINATION OF WHETHER KINETIC EFFECTS SHOULD BE INCLUDED IN THE TRANSPORT MODEL (RESPONSE TO RT 1.04)	J-1
APPENDIX K – TRANSPORT- K_{Ds} IN ALLUVIUM (RESPONSE TO RT 2.06, RT 2.07, AND GEN 1.01 (#41 AND #102)).....	K-1
APPENDIX L – TRANSPORT-TEMPORAL CHANGES IN HYDROCHEMISTRY (RESPONSE TO TSPA I 3.31)	L-1
APPENDIX M – MICROSPHERES AS ANALOGS (RESPONSE TO RT 3.08 AIN-1 AND GEN 1.01 (#43 AND #45)).....	M-1

FIGURES

	Page
1-1. Components of the Postclosure Technical Basis for the License Application	1-1
1-2. Conceptual Representation of Radionuclide Transport Pathways from the Repository to the Biosphere.....	1-4
2-1. Major Physiographic Features in the Death Valley Regional Flow System.....	2-3
2-2. Location of Principal Recharge Areas and Amounts in the Death Valley Regional Flow System.....	2-5
2-3. Location of Principal Naturally Occurring Discharge Areas in the Death Valley Regional Flow System	2-7
2-4. Location of Principal Anthropogenic Groundwater Discharge Areas in the Death Valley Regional Flow System	2-10
2-5. Regional-Scale Potentiometric Surface Map	2-11
2-6. Inferred Groundwater Flow Paths in the Central Death Valley Subregion	2-13
2-7. Outcrops of Major Hydrogeologic Units in the Death Valley Region	2-14
2-8. Representative Hydrogeologic Cross Sections through the Death Valley Region	2-15
2-9. Depth Dependency of Regional Hydraulic Conductivity Estimates.....	2-16
2-10. Location of Geochemical Groundwater Types and Regional Flow Paths Inferred from Hydrochemical and Isotopic Data.....	2-19
2-11. Regional Groundwater Chloride Concentrations and Inferred Regional Flow Paths.....	2-20
2-12. Areal Distribution of Sulfate in Groundwater	2-21
2-13. Regional Groundwater delta-Deuterium.....	2-22
2-14. Comparison of Predicted and Observed Hydraulic Heads in the Death Valley Regional Groundwater Flow Model	2-27
2-15. Simulated and Observed Groundwater Discharge for Major Discharge Areas.....	2-28
2-16. Location of Boreholes used to Characterize the Site-Scale Groundwater Flow System in the Vicinity of Yucca Mountain.....	2-30
2-17a. Flux Zones used for Comparing Regional and Site-Scale Flux.....	2-32
2-17b. Map of Recharge to the Saturated Zone Site-Scale Flow Model.....	2-33
2-18. Nominal Site-Scale Potentiometric Surface.....	2-35
2-19. Alternative Site-Scale Potentiometric Surface.....	2-36
2-20. Outcrop Geology of the Site-Scale Hydrogeologic Framework Model	2-41
2-21. Representative Cross-Sections through the Site-Scale Hydrogeologic Framework Model.....	2-42
2-22. Locations of Nye County Alluvium Cross Sections.....	2-44
2-23. Nye County Alluvium Cross Sections	2-45
2-24. Alluvial Zone Total Thickness in the Site-Scale Hydrogeologic Model.....	2-46
2-25. Alluvial Zone Saturated Thickness in the Site Scale Hydrogeologic Model.....	2-47
2-26. Location of the C-Wells Complex	2-48
2-27. Stratigraphy, Lithology, Matrix Porosity, Fracture Density, and Inflow from Open-Hole Surveys at the C-Wells.....	2-49
2-28. Distribution of Drawdown in Observation Wells at Two Times After Pumping Started in UE-25 C#3.....	2-50

FIGURES (Continued)

	Page
2-29. Drawdowns Observed in Wells Adjacent to the C-Wells Complex during the Long Term Pumping Test	2-51
2-30. Summary of Lithology and Flow Characteristics at Wells NC-EWDP-19D of the Alluvial Testing Complex.....	2-53
2-31. Fitting the Injection-Pumpback Tracer Tests in Screen #1 of NC-EWDP-19D1 Using the Linked-Analytical Solutions Method	2-55
2-32. Groundwater U and $^{234}\text{U}/^{238}\text{U}$ Ratios in the Vicinity of Yucca Mountain	2-56
2-33. Three-Dimensional Representation of the Computation Grid.....	2-58
2-34. Comparison of Observed and Predicted Hydraulic Heads in the Site-Scale Groundwater Flow Model.....	2-60
2-35. Comparison of Calibrated and Observed Permeabilities from Yucca Mountain Pump Test Data in the Site-Scale Groundwater Flow Model.....	2-63
2-36. Comparison of Calibrated and Observed Permeabilities from Nevada Test Site Pump Test Data in the Site-Scale Groundwater Flow Model.....	2-63
2-37. Predicted Groundwater Flowpath Trajectories Compared to Flowpaths Inferred from Geochemistry	2-65
2-38. Predicted Saturated Zone Particle Trajectories from Yucca Mountain	2-67
3-1. Conceptual Model of Radionuclide Transport Processes in the Saturated Zone.....	3-2
3-2. Conceptual Representation of Flowing Interval Spacing	3-5
3-3. Cumulative Probability Density Function of Flowing Interval Spacing	3-6
3-4. Uncertainty in Effective Flow Porosity in Fractured Tuffs at Yucca Mountain.....	3-8
3-5. Normalized Tracer Responses in the Bullfrog Tuff Multiple Tracer Test Illustrating the Effect of Matrix Diffusion.....	3-9
3-6. Distribution of Matrix Diffusion Coefficients Applicable to Fractured Tuffs at Yucca Mountain.....	3-10
3-7. Dispersivity as a Function of Length Scale	3-11
3-8. Comparison of Effective Modeled Dispersivity versus Specified Dispersivities using the Site-Scale Radionuclide Transport Model	3-12
3-9. Schematic Illustration of Alternative Conceptual Transport Models for the Valley-Fill Deposits South of Yucca Mountain.....	3-15
3-11. Effective Porosity Distribution used in Yucca Mountain Transport Model.....	3-16
3-12. Areal Distribution of Delta Carbon-13 in Groundwater in the Vicinity of Yucca Mountain.....	3-19
3-13. Carbon-14 Activities in Groundwater in the Vicinity of Yucca Mountain	3-20
3-14. Comparison of Observed Dissolved Organic and Inorganic Carbon-14 Ages in Groundwaters in the Vicinity of Yucca Mountain.....	3-21
3-15. Correlation of Carbon-14 and Delta-Carbon-13 in Perched Waters and Groundwaters in the Vicinity of Yucca Mountain.....	3-22
3-16. Bromide and Lithium Breakthrough Curves and Comparison to Model Fits.....	3-26
3-17. Comparison of Lithium Tracer Test Results and Model Predicted Results at the C-Wells Complex.....	3-27
3-18. Neptunium Sorption Coefficients on Devitrified Tuff Versus Experiment Duration for Sorption (Forward) and Desorption (Backward) Experiments	3-29

FIGURES (Continued)

	Page
3-19. Neptunium Sorption Coefficients on Zeolitic Tuff Versus Experiment Duration for Sorption (Forward) and Desorption (Backward) Experiments	3-29
3-20. Plutonium Sorption Coefficients on Devitrified Tuff Versus Experiment Duration for Sorption (Forward) and Desorption (Backward) Experiments	3-30
3-21. Plutonium Sorption Coefficients on Zeolitic Tuff Versus Experiment Duration for Sorption (Forward) and Desorption (Backward) Experiments	3-30
3-22. Uranium Sorption Coefficients on Devitrified Tuff Versus Experiment Duration for Sorption (Forward) and Desorption (Backward) Experiments	3-31
3-23. Uranium Sorption Coefficients on Zeolitic Tuff as a Function of Experiment Duration	3-31
3-24. Distribution Coefficients of ¹²⁹ I and ⁹⁹ Tc in Alluvium.....	3-33
3-25. Sorption of ²³³ U onto Alluvium as a Function of Time.....	3-33
3-26. Distribution Coefficients of ²³⁷ Np and ²³³ U in Alluvium	3-34
3-27. Sorption of ²³³ U in 19D Zone 1 and Zone 4 Waters.....	3-35
3-28. Distribution Coefficients of ²³⁷ Np(V) as a Function of Test Interval and Size Fraction Determined from Batch Experiments.....	3-36
3-29. Sorption of Np(V) in NC-EWDP-3S and NC-EWDP-19D Well Waters.....	3-37
3-30. Relationship Between Surface Area, the Amount of Smectite (S) and Clinoptilolite (C), and Measured K_d of ²³⁷ Np(V) of Alluvium.....	3-38
3-31. Tritium and ²³³ U Breakthrough Curve for a Column Test.....	3-38
3-32. Predicted Breakthrough Curves for Radionuclides of Potential Interest to a Repository	3-42
3-33a. Mass Breakthrough Curves (upper) and Median Transport Times (lower) for Carbon, Technetium, and Iodine at 18-km Distance	3-43
3-33b. Mass Breakthrough Curves (upper) and Median Transport Times (lower) for Neptunium at 18-km Distance	3-44
3-33c. Mass Breakthrough Curves (upper) and Median Transport Times (lower) for Plutonium at 18-km Distance.....	3-45
3-34. Comparison of Breakthrough Curves for the Base Case and Radionuclides Irreversibly Attached to Colloids: 18-km Boundary	3-46

INTENTIONALLY LEFT BLANK

TABLES

	Page
1-1. List of Appendices and the KTI Agreements that are Addressed.....	1-9
2-1. Summary of Precipitation, Modeled Net Infiltration, and Estimated Recharge using Maxey-Eakin Methods for the Area of the Death Valley Regional Groundwater Flow Model.....	2-6
2-2. Inferred Naturally Occurring Discharge Amounts in the Death Valley Regional Flow System.....	2-8
2-3. Summary of Bases for Regional Flow Paths and Mixing Zones Derived from Geochemistry Observations.....	2-23
2-4. Comparison of Regional and Site-Scale Fluxes.....	2-31
2-5. Summary of Vertical Head Observations at Boreholes in the Vicinity of Yucca Mountain.....	2-38
2-6. Correspondence between Units of the Revised- and Base-Case Hydrogeologic Framework Models.....	2-43
2-7. Specific Discharges and Seepage Velocities Estimated from the Different Drift Analysis Methods as a Function of Assumed Flow Porosity.....	2-54
2-8. Comparison of Water Levels Observed and Predicted at Nye County Early Warning Drilling Program Wells.....	2-61
3-1. Summary of Effective Flow Porosity from Conservative Tracer Tests.....	3-6
3-2. Summary of Flow Porosity Values from Multiple Tracer Tests.....	3-7
3-3. Chemistry and Ages of Groundwater from Seven Boreholes at Yucca Mountain.....	3-23
3-4. Sorption-Coefficient Distributions for Saturated Zone Units from Laboratory Batch Tests.....	3-28

INTENTIONALLY LEFT BLANK

ACRONYMS AND ABBREVIATIONS

AIN	Additional Information Needed
AMR	analysis and model report
ATC	Alluvial Testing Complex
DOE	U.S. Department of Energy
DVRFS	Death Valley Region Flow System
EWDP	Early Warning Drilling Program
GFM	Geologic Framework Model
HFM	Hydrogeologic Framework Model
KTI	Key Technical Issue
NRC	U.S. Nuclear Regulatory Commission
PA	performance assessment
PMR	process model report
TSPA-LA	total system performance assessment for the licence application
USGS	U.S. Geological Survey

INTENTIONALLY LEFT BLANK

1. INTRODUCTION

This Technical Basis Document provides a summary of the conceptual understanding of the flow of groundwater and the transport of radionuclides that may be potentially released to the saturated zone beneath and downgradient from Yucca Mountain. This document is one in a series of Technical Basis Documents prepared for each component of the Yucca Mountain repository system relevant to predicting the likely postclosure performance of the repository. The relationship of saturated zone flow and transport to the other components is illustrated in Figure 1-1.

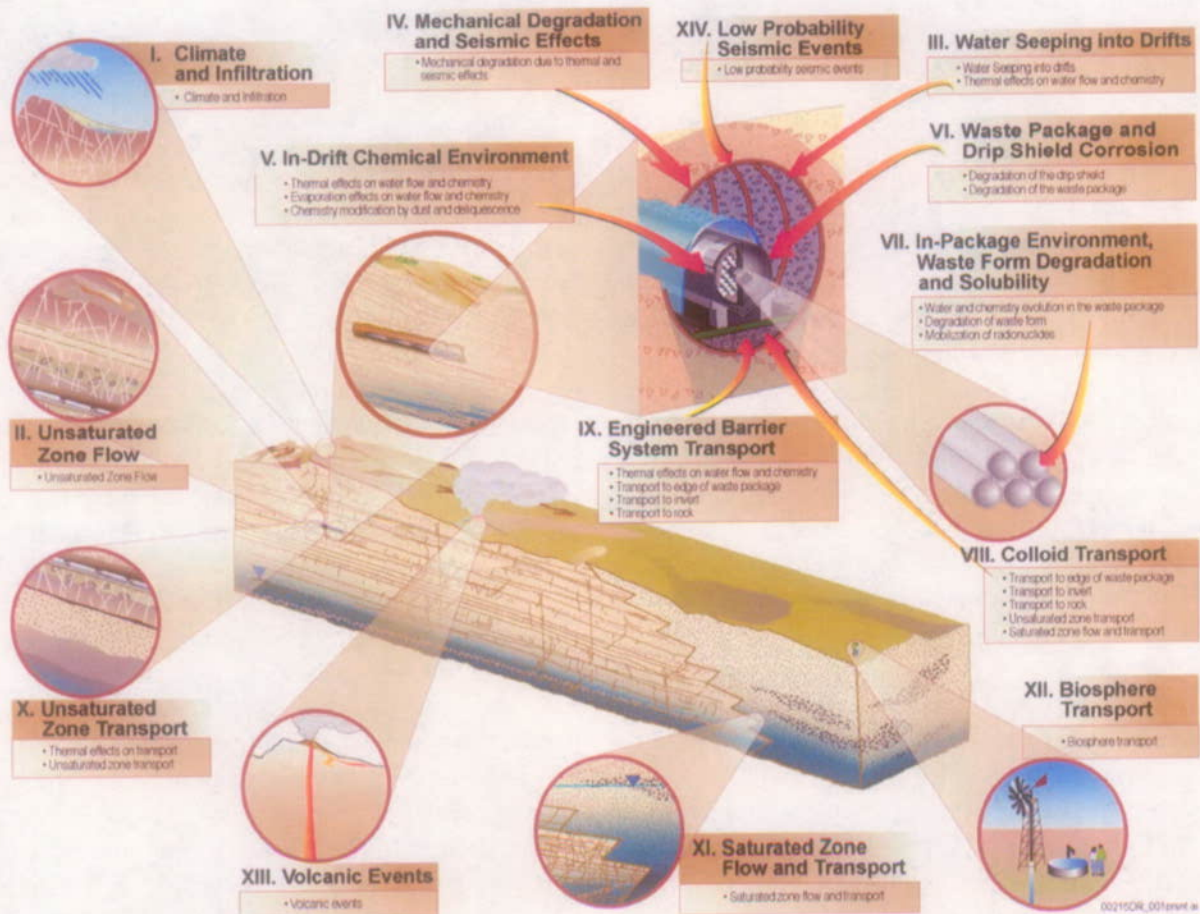


Figure 1-1. Components of the Postclosure Technical Basis for the License Application

The information presented in this document, and the associated references, forms an outline of the ongoing development of the postclosure safety analysis that will comprise the license application. This information is also used to respond to open Key Technical Issue (KTI) agreements made between the U.S. Nuclear Regulatory Commission (NRC) and the U.S. Department of Energy (DOE). Placing the DOE responses to individual KTI agreements and NRC Additional Information Needed (AIN) requests within the context of the overall saturated zone flow and transport process, as they relate to postclosure safety analyses, allows for a more direct discussion of the relevance of the agreement.

Appendices to this document are designed to allow for a transparent and direct response to each KTI agreement and AIN requests. Each appendix addresses one or more of the agreements. If agreements apply to similar aspects of the saturated zone subsystem, they were grouped in a single appendix. In some cases, appendices provide detailed discussions of data, analyses, or information related to the further conceptual understanding presented in this Technical Basis Document. In these cases, the appendices are referenced from the appropriate section of the Technical Basis Document. In other cases, the appendices provide information that is related to the Technical Basis Document information but at a level of detail that relates more to the uncertainty in a particular data set or feature, event, or process that is less relevant to the overall technical basis. In these cases, the appendices reference the relevant section of the Technical Basis Document to put the particular KTI agreement into context, but the Technical Basis Document does not reference the appendices.

This Technical Basis Document and appendices are responsive to agreements made between the DOE and the NRC during Technical Exchange and Management Meetings on Radionuclide Transport (Reamer and Williams 2000a), Total System Performance Assessment and Integration (Reamer 2001), and Unsaturated and Saturated Flow Under Isothermal Conditions (Reamer and Williams 2000b), and to AIN requests from the NRC to the DOE dated August 16, 2002 (Schlueter 2002a), August 30, 2002 (Schlueter 2002b), December 19, 2002 (Schlueter 2002c), and February 5, 2003 (Schlueter 2003).

Most of the agreements were based on questions that NRC staff developed from their review of the Site Recommendation support documents and presentations by the DOE at the technical exchanges. The agreements, in general, required the DOE to present additional information, conduct further testing, perform sensitivity or validation exercises for models, or provide justification for assumptions used in the *Yucca Mountain Site Suitability Evaluation* (DOE 2002). Since those technical exchanges, the DOE has conducted the additional analysis and testing necessary to meet the commitments. The appendices present the additional information that forms the technical basis for addressing the intent of the KTI agreements.

This Technical Basis Document provides a summary-level synthesis of many relevant aspects of the saturated zone flow and transport modeling that is being completed to support development of the Yucca Mountain license application. This information is consistent with the *Yucca Mountain Review Plan* (NRC 2003) and the DOE risk-informed prioritization planning process (BSC 2002), but it does not attempt to address all the detailed acceptance criteria identified in the *Yucca Mountain Review Plan*. For example, this Technical Basis Document describes the geological, hydrological, and geochemical aspects of the saturated zone that affect the determination of the flow paths and radionuclide transport and includes a summary of the technical basis that supports how this information is integrated into the total system performance assessment abstraction. In addition, it presents the most important data and parameters used to justify the model abstraction and the methods used to characterize and propagate data and parameter uncertainty through the abstraction. Therefore, it addresses elements of the identified areas of review for the abstraction groups entitled *Flow Paths in the Saturated Zone* (Section 2.2.1.3.8) and *Radionuclide Transport in the Saturated Zone* (Section 2.2.1.3.9) of the *Yucca Mountain Review Plan*.

This document presents a summary and synthesis of the detailed technical information presented in the analyses and model reports and other technical products that are used as the basis for the description of the saturated zone barrier and the incorporation of this barrier into the postclosure performance assessment. Several analyses, model reports, and other technical products support this summary:

- *A Three-Dimensional Numerical Model of Predevelopment Conditions in the Death Valley Regional Ground-Water Flow System, Nevada and California* (D'Agnesse et al. 2002)
- *Water-Level Data Analysis for the Saturated Zone Site-Scale Flow and Transport Model* (USGS 2001a)
- *Site-Scale Saturated Zone Transport* (BSC 2003a)
- *Saturated Zone Colloid Transport* (BSC 2003b)
- *Site-Scale Saturated Zone Flow Model* (BSC 2003c)
- *SZ Flow and Transport Abstraction* (BSC 2003d)
- *Saturated Zone In-Situ Testing* (BSC 2003e).
- *Geochemical and Isotopic Constraints on Groundwater Flow Directions and Magnitudes, Mixing, and Recharge at Yucca Mountain* (BSC 2003f)

The basic approach of this document is to provide a comprehensive summary of the saturated zone flow and transport understanding, the details of which are presented in the supporting analyses, model reports, and related products.

1.1 OBJECTIVE AND SCOPE

The objectives of this Technical Basis Document are to:

- Describe the processes relevant to the performance of the saturated zone flow and transport component of the post-closure performance assessment
- Present the relevant data, analyses, and models used to project the behavior of the saturated zone flow and transport processes
- Summarize the development of the site-scale saturated zone flow and transport models and key subprocess models that are used to analyze data from the saturated zone
- Summarize the results of the flow and transport models used in the assessment of postclosure performance at Yucca Mountain.

The purpose of the site-scale saturated zone flow and transport model is to describe the spatial and temporal distribution of groundwater as it moves from the water table below the repository,

through the saturated zone, and to the point of uptake by a potential downgradient receptor. The saturated zone processes that control the movement of groundwater and the movement of dissolved radionuclides and colloidal particles that might be present, and the processes that reduce radionuclide concentrations in the saturated zone, are described in this document.

The evaluation of the saturated zone in the Yucca Mountain area considers the possibility of radionuclide transport from their introduction at the water table beneath the repository to a hypothetical well located along the compliance boundary downgradient from the site. The likely pathway for radionuclides potentially released from the repository to reach the accessible environment is through groundwater aquifers below the repository. These aquifers, collectively referred to as the saturated zone, delay the transport of any radionuclides released to the saturated zone and reduce the concentration of radionuclides before they reach the accessible environment.

A simplified conceptualization of the saturated zone flow and transport for Yucca Mountain and its relationship to transport in the unsaturated zone and biosphere is provided in Figure 1-2. Radionuclides released into seepage water contacting breached waste packages in the repository would migrate downward through the unsaturated zone for approximately 210 to 390 m to the water table. At that point, radionuclides would enter the saturated zone and migrate downgradient within the tuff and alluvial aquifers to the accessible environment. At a distance of 15 to 22 km along the flow path from the repository, groundwater flow enters the alluvial aquifer and remains in the alluvium for an additional 1 to 10 km until it is subject to uptake into the accessible environment.

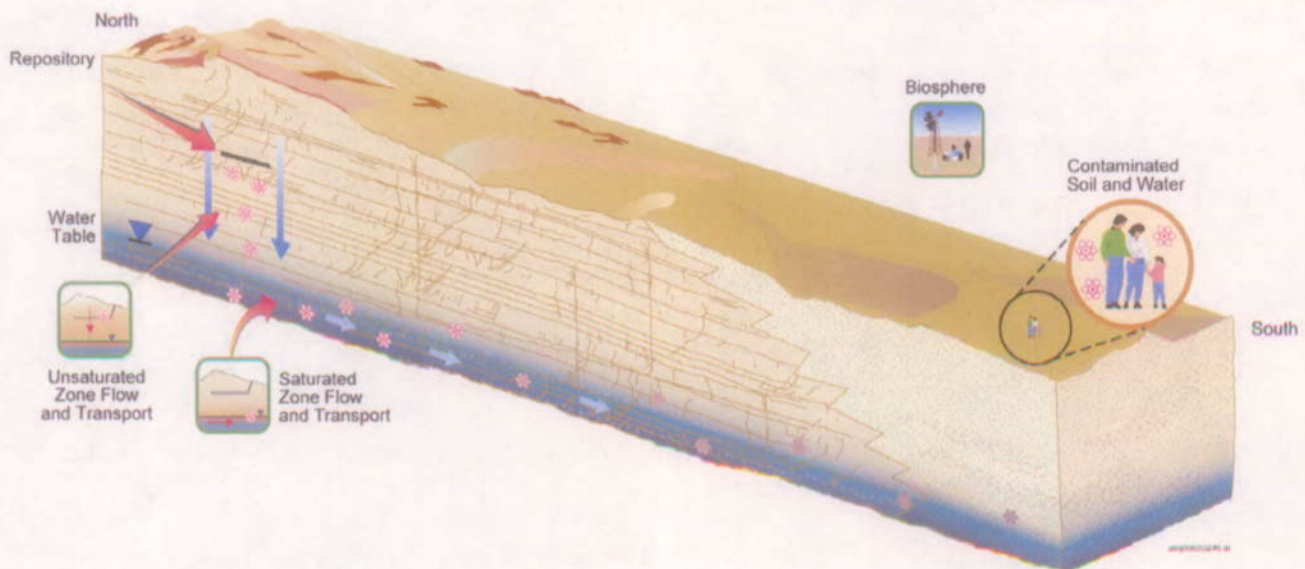


Figure 1-2. Conceptual Representation of Radionuclide Transport Pathways from the Repository to the Biosphere

1.2 DESCRIPTION OF PROCESSES AFFECTING THE PERFORMANCE OF THE SATURATED ZONE

The saturated zone at Yucca Mountain is a barrier to the migration of dissolved and colloidal radionuclides that may be released from the unsaturated zone. This barrier delays the transport of radionuclides that potentially enter the saturated zone to the time they are withdrawn from the well used by the hypothetical person who comprises the reasonably maximally exposed individual.

Any radionuclides which enter the saturated zone are expected to do so over a spatial and temporal scale that is dependent on the degradation modes and rates of the engineered barriers as well as transport processes from the degraded engineered barriers to the saturated zone. For example, it is possible that the engineered barriers fail either over a broad temporal scale that ranges from thousands to hundreds of thousands of years due to natural degradation processes or they fail over a relatively short time interval associated with a low probability disruptive event such as a large seismic event or a volcanic event. The spatial scale over which radionuclides enter the saturated zone may be either (a) relatively confined to an area on the order of 100 square meters for each degraded waste package (for cases where the flow is predominantly vertical through the unsaturated zone), (b) concentrated at locations where the bulk of the unsaturated ground water flow intersects the water table or (c) dispersed over a significant fraction of the total repository footprint of several square kilometers. The timing and extent of the radionuclides that enter the saturated zone is considered in the performance assessment using a range of spatial locations and combining the transport times within the saturated zone to those times when radionuclides are predicted to reach the saturated zone. This abstraction process is described in *SZ Flow and Transport Abstraction* (BSC 2003d).

The processes that affect the performance of the saturated zone barrier include both groundwater flow and radionuclide transport processes. The groundwater flow processes determine the rate of water movement within the saturated zone and the flow paths through which the water is likely to travel. These flow paths extend from where the radionuclides may possibly enter the saturated zone to where they exit at the point of compliance. These flow paths define the different geologic materials through which potentially released radionuclides are likely to be transported.

The radionuclide transport processes include those that determine the advective velocity of dissolved radionuclides within the saturated fractures or pores of the geologic media as well as the processes that relate to the interaction of the dissolved or colloidal radionuclides with the rock or alluvium materials with which they come into contact. The advective transport processes are determined by the rate of groundwater flow and the effective porosity of the media through which that flow occurs. Lower effective porosities yield higher groundwater velocities and shorter transport times. The dispersive processes are affected by small scale velocity heterogeneity that allows some dissolved constituents to travel faster than the average advective transport time and others to travel slower than the average advective transport time. Dispersive processes also cause a net spreading of the radionuclide mass concentration, although this spreading is not significant to post closure performance due to the mixing which occurs when the radionuclide mass flux is mixed with the annual water demand of 3.7 million cubic meters (3,000 acre-feet).

Dissolved radionuclides diffuse from the fractures in which they are advectively transported into the matrix, which does not have significant advective flux. This matrix diffusion process tends to slow the net transport time of these dissolved species. The effectiveness of this process is dependent on the diffusive properties of the matrix and the degree of spacing between the flowing fracture zones. Larger diffusion coefficients or a smaller spacing between flowing fracture zones result in a slower net transport time within the fractured rock mass.

Many radionuclides of potential significance to repository performance are sorbed within the matrix of the rock mass. Although these radionuclides may also be sorbed on the fracture surfaces, this retardation mechanism has not been considered in the performance assessment. The degree of sorption is dependent on the individual radionuclide. Some radionuclides such as technetium, iodine and carbon are not sorbed. These radionuclides are transported considering only advection, dispersion and matrix diffusion processes. Other radionuclides such as neptunium, uranium, plutonium, among others, are sorbed in the matrix or pores of the fractured tuffs or alluvium. The stronger the sorption, the longer the delay in the transport time of the radionuclides is compared to the advective-dispersive transport times.

The above saturated zone flow and transport processes are represented by different conceptual and numerical models that are used to predict the expected behavior of the saturated zone barrier as it relates to the performance of the Yucca Mountain repository system. These models include models of groundwater flow at the regional and site scale and models of radionuclide transport. The bases of these models is derived from site-specific *in-situ* observations as well as field and laboratory tests to determine the relevant parameter values used in these models. This Technical Basis Document presents a summary of the bases for these models and parameters and a discussion of the uncertainty associated with these models, the included parameters and the predicted results, i.e., radionuclide transport times, relevant to post-closure performance.

1.3 SUMMARY OF CURRENT UNDERSTANDING

An understanding of saturated zone flow and transport in the vicinity of Yucca Mountain has been gained through the collection of regional and site data and through the incorporation of these data into models that describe processes affecting the behavior of the saturated zone barrier. Hydrogeologic data have been collected from boreholes that penetrate the saturated zone and from nonintrusive field investigations (i.e., geophysical surveys). These data were used to develop a scientific understanding of the subsurface hydrogeology and to assemble the database necessary to evaluate the expected performance characteristics of the saturated zone. In general, the rate and direction of groundwater flow within the saturated zone is controlled by the spatial configuration of the potentiometric surface and the hydrologic properties and characteristics of the materials that constitute the saturated zone below the water table. Based on the potentiometric surface in the Yucca Mountain area and vicinity, groundwater within the saturated zone beneath the repository is inferred to move from upland areas of recharge (located north of Yucca Mountain) towards areas of natural discharge (springs and playas south of Yucca Mountain). This flow direction is supported by hydrochemistry and isotope distributions.

Groundwater flow in the saturated zone below and directly downgradient from the repository occurs in fractured, porous volcanic tuffs at a relatively shallow depth below the water table, and in fractured carbonate rocks of Paleozoic age (limestones and dolomites) at much greater depths.

At distances of about 15 to 18 km downgradient from the repository, where the volcanic rocks thin out beneath valley fill materials, the water table transitions from the volcanic rocks to the valley-fill (alluvial) material.

The most likely pathway for radionuclides to reach the accessible environment is through the uppermost groundwater aquifers below the repository. These aquifers, collectively referred to as the saturated zone, delay the transport of any potentially released radionuclides to the accessible environment and reduce the concentration of these radionuclides before they reach the accessible environment. Delay in the release of radionuclides to the accessible environment allows radioactive decay to diminish the mass of radionuclides that are ultimately released. Dilution of radionuclide concentrations in the groundwater used by the potential receptor occurs during transport and in the process of extracting groundwater from wells. The key processes that affect the performance of this barrier are summarized in the following text.

To determine the characteristics of the saturated zone, flow and transport processes need to be considered. Pertinent data for characterizing groundwater flow in the saturated zone includes measurements of water levels in boreholes and wells (which defines the configuration of the water table and associated potentiometric surface) and hydraulic testing to determine hydraulic properties (hydraulic conductivity, permeability, and storage coefficient) of the rock unit and alluvium materials.

Data on hydraulic properties have been obtained from more than 150 hydraulic tests conducted in boreholes and wells in the Yucca Mountain area. These hydraulic tests include constant-discharge pumping tests, slug injection (falling head) tests, pressure injection tests, and fluid logging techniques (e.g., temperature measurement and tracer injection surveys). Multiple-well pumping and tracer tests have been conducted in the three C-wells; a complex of boreholes located about 3 km east of the repository site. Multiple-well hydraulic tests, and single-well hydraulic and tracer tests have been conducted in cooperation with Nye County at the Alluvial Testing Complex, a complex of wells located close to U.S. Highway 95.

Hydrochemical data (e.g., chloride and sulfate concentrations) and isotopic data (e.g., uranium-234/uranium-238 ratios, and strontium and carbon isotope ratios) also have been collected from a number of boreholes and wells. These data were used to independently define likely groundwater flow paths from the repository area.

Processes important to the transport of radionuclides in the saturated zone include advection, sorption, diffusion (in particular matrix diffusion), hydrodynamic dispersion, decay and ingrowth, and filtration of colloids carrying radionuclides. These characteristics have been evaluated through a range of in situ tests (such as at the C-Wells and Alluvial Testing complexes) and laboratory tests. In situ tests generally are used to evaluate properties such as effective porosity and longitudinal dispersivity, while laboratory tests are used to evaluate sorption characteristics. Sorption coefficients (K_{ds}) have been measured in the laboratory for a number of important radionuclides based on crushed-rock batch and column tests that used borehole core samples for selected saturated zone rock units at Yucca Mountain. Estimates of K_{ds} have been developed for various radionuclides such as americium, thorium, uranium, protactinium, neptunium, and plutonium.

Estimates of colloid attachment and detachment rates in saturated fractured volcanic rocks have been obtained from tracer tests conducted at the C-Wells complex using polystyrene microspheres as surrogate colloids. Physical data applicable to the attachment, detachment, and transport of radionuclides on natural colloidal substrates (e.g., silica and clay minerals) have been obtained for selected radionuclides (e.g., plutonium-239 and americium-243) through laboratory experiments and testing.

Analyses conducted using the saturated zone transport model indicate that the saturated zone is expected to be a barrier to the transport of any radionuclides potentially released from the unsaturated zone to the accessible environment within the 10,000-year period of regulatory concern for the repository at Yucca Mountain. The expected behavior of the saturated zone system is to delay the transport of sorbing radionuclides and radionuclides associated with colloids for many thousands of years, even under wetter climatic conditions in the future. Nonsorbing radionuclides are expected to be delayed for hundreds of years during transport in the saturated zone.

1.4 ORGANIZATION OF THIS REPORT

The report is organized as follows:

Section 1. Introduction—The objectives and scope of this Technical Basis Document, and a discussion of the saturated zone as a barrier, are presented in this section.

Section 2. Saturated Zone Flow—A description of field and laboratory testing, data collection activities, and modeling of groundwater flow processes in the saturated zone are described at the regional and site scales.

Section 3. Saturated Zone Radionuclide Transport—Field and laboratory testing, data collection activities and the modeling of radionuclide transport processes at the site scale are described in this section.

Section 4. Summary—A summary of the results of the saturated zone flow and transport processes, as they relate to postclosure performance projections of the repository, are described in this section.

Section 5. References—Sources of information used in this document are listed in this section.

Appendices—Thirteen appendices, as listed in Table 1-1, address specific KTI agreement items and AIN requests.

1.5 NOTE REGARDING THE STATUS OF SUPPORTING TECHNICAL INFORMATION

This document was prepared using the most current information available at the time of its development. This Technical Basis Document and its appendices providing KTI agreement responses that were prepared using preliminary or draft information reflect the status of the Yucca Mountain Project's scientific and design bases at the time of submittal. In some cases, this involved the use of draft Analysis and Model Reports (AMRs) and other draft references

whose contents may change with time. Information that evolves through subsequent revisions of the AMRs and other references will be reflected in the License Application (LA) as the approved analyses of record at the time of LA submittal. Consequently, the Project will not routinely update either this Technical Basis Document or its KTI agreement appendices to reflect changes in the supporting references prior to submittal of the LA.

Table 1-1. List of Appendices and the KTI Agreements that are Addressed

Appendix	Appendix Title	Key Technical Issues Addressed
A	The Hydrogeologic Framework Model/Geologic Framework Model Interface	USFIC 5.10
B	Hydrostratigraphic Cross Sections	RT 2.09 AIN-1 AND USFIC 5.05 AIN-1
C	Potentiometric Surface and Vertical Gradients	USFIC 5.08 AIN-1
D	Regional Model and Confidence Building	USFIC 5.02, USFIC 5.12, AND USFIC 5.11 AIN-1
E	Horizontal Anisotropy	USFIC 5.01
F	Carbon-14 Residence Time	USFIC 5.06
G	Uncertainty in Flow paths Lengths in Tuff and Alluvium	RT 2.08, RT 3.08, and USFIC 5.04
H	Transport Properties	RT 1.05, RT 2.01, RT 2.10, AND RT 2.03 AIN-1
I	Transport—Spatial Variability of Parameters	RT 2.02, TSPA 3.32 and TSPA 4.02.
J	Determination of Whether Kinetic Effects Should be Included in the Transport Model	RT 1.04.
K	Transport— K_d s in Alluvium	RT 2.06, RT 2.07, and GEN 1.01#102
L	Transport—Temporal Changes in Hydrochemistry	TSPA 3.31
M	Microspheres as Analogs	RT 3.08 AIN-1 and GEN 1.01#45

INTENTIONALLY LEFT BLANK

2. SATURATED ZONE GROUNDWATER FLOW

2.1 INTRODUCTION

The following sections summarize the understanding of saturated zone flow processes, models, and parameters. This understanding is important to describing the likely groundwater flow paths and flow rates, as well as the geologic units through which groundwater is likely to flow in the vicinity of Yucca Mountain. This summary includes discussion of the regional and site-scale geologic setting, hydrogeologic setting, hydrogeochemistry, and groundwater flow modeling.

The hydrogeologic setting in the Death Valley region in general, and in the vicinity of Yucca Mountain in particular, has been the focus of data collection, interpretation, and analysis over the last several decades. This focus has, in part, been due to Federal government interest in understanding the groundwater flow system within the Nevada Test Site and in the region around Death Valley National Park, as well as State of Nevada and Nye County interest in understanding the available groundwater resources in the area. Early work by Maxey and Eakin (1950) provided a quantitative basis for estimating groundwater recharge as a function of precipitation in the arid southwest, and Winograd and Thordarson (1975) established the likely groundwater flow paths controlling the discharge of groundwater to springs in and around Death Valley. Since these early investigations, studies of groundwater flow in the Death Valley region have benefited from additional geologic and hydrologic characterization conducted via drilling and testing numerous boreholes and wells in the area.

A general understanding of the regional-scale groundwater flow system is important for understanding the Yucca Mountain groundwater flow system because the regional-scale system sets the context for the site-scale geologic and hydrologic systems. An important aspect of the regional hydrogeologic system is that the system occurs in an enclosed basin without any surface or subsurface points of discharge to the ocean (i.e., all water that naturally leaves the region does so exclusively through the processes of evaporation or evapotranspiration). This regional basin, which includes the natural discharge at springs in the Death Valley area, is referred to as the Death Valley Regional Groundwater Flow System.

The site-scale conceptual model is a synthesis of what is known about flow and transport processes at the scale required for postclosure performance assessment analyses, that is, at a scale relevant to assess potential radionuclide transport from beneath Yucca Mountain to the point about 18 km south of Yucca Mountain where the reasonably maximally exposed individual may hypothetically extract groundwater from the aquifer. This knowledge builds on, and is consistent with, knowledge that has accumulated at the regional scale, but it is more detailed because a higher density of data is available at the site-scale level.

2.2 REGIONAL GROUNDWATER FLOW SYSTEM

The Death Valley regional groundwater flow system (Death Valley Regional Flow System) encompasses an area of about 70,000 km² in southern California and southern Nevada, between latitudes 35° and 38° 15' north and longitudes 115° and 118° 45' west. The region varies topographically and geologically, and these features tend to control the regional groundwater flow system. The topographic highs are generally above 3,600-m elevation in the Spring

Mountains and above 2,900 m in the Sheep Mountains. The topographic lows occur in Death Valley and major intermittent tributaries of the Amargosa River. The major physiographic features within the regional flow system are illustrated in Figure 2-1.

Groundwater in the Death Valley region flows through a variety of rock types, ranging from Paleozoic carbonate to Tertiary volcanic rocks (such as those in the Yucca Mountain area) to alluvial aquifers (such as those from which water is extracted for irrigation and other domestic purposes in the Amargosa Farms area). Within the Death Valley region, the presence of hydrostratigraphic discontinuities due to tectonic features, such as faults, has caused many of the aquifers to be heterogeneous. Faults, which disrupt the hydrostratigraphic continuity, divert water in regional circulation to subregional and local discharge.

The following discussion summarizes regional recharge and discharge areas and amounts, hydraulic potentials, hydrogeologic characteristics, and hydrochemistry observations and inferences that are used to constrain the groundwater flow system in the vicinity of Yucca Mountain.

2.2.1 Regional Groundwater Recharge and Discharge

One of the first steps in developing a consistent representation of the groundwater flow regime in a groundwater basin is to identify the major recharge and discharge locations, types, and amounts. By comparing these distributions, an overall understanding of the water budget within the basin can be developed. Differences between the annual average recharge and discharge amounts are indicative of conditions when water is either added to or taken from the total water in storage within the aquifers of the basin.

Groundwater recharge in the Death Valley region is principally the result of water that directly infiltrates the soil horizon due to precipitation (rainfall and snowmelt) and that is not lost from the soil horizon due to evaporation or transpiration before being available to recharge the groundwater. Although some recharge can occur along intermittent rivers and streams in the area, most notably the Amargosa River and tributaries, the areal and temporal extent of this recharge is negligible from an overall water budget perspective (although local geochemistry and isotopic variations have, in part, been attributed to such local intermittent recharge; Hevesi et al. 2002, p. 12). Although this intermittent recharge has not been explicitly incorporated in the regional flow model, its effect on the site-scale flow model has been included (see Section 2.3.2). Net infiltration in the region is controlled by variability in precipitation and other factors, including the timing of precipitation, elevation, slope, soil or rock type, and vegetation. Net infiltration usually is episodic and generally occurs after periods of winter precipitation when evapotranspiration is low (Hevesi et al. 2002, p. 10).



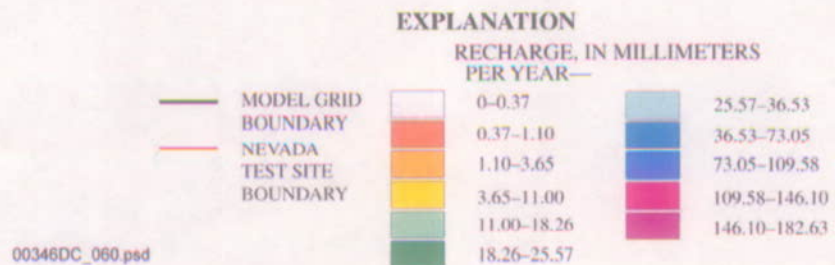
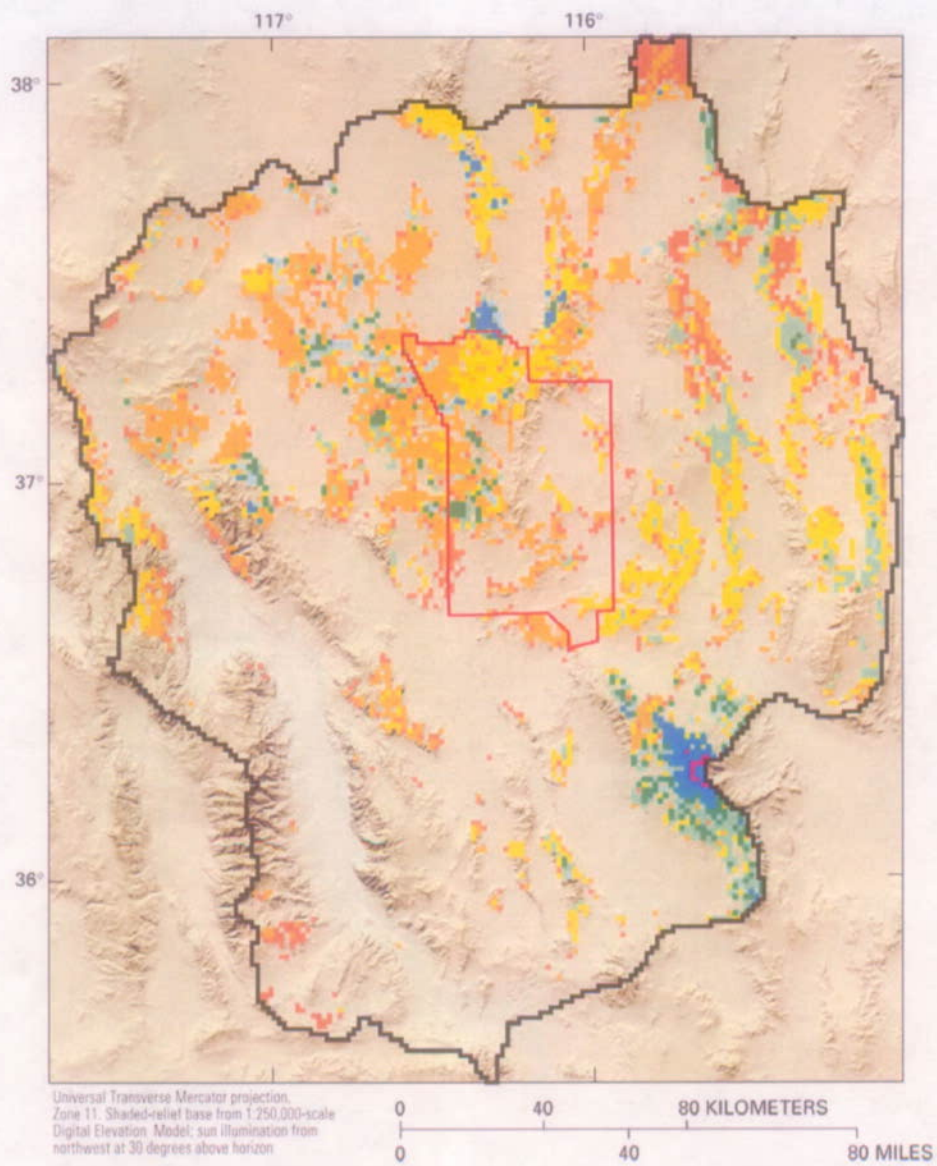
Source: Belcher et al. 2002, Figure 1.

NOTE: The different model boundaries reflect different regional model studies that are discussed and referenced in the source.

Figure 2-1. Major Physiographic Features in the Death Valley Regional Flow System

Estimates of net infiltration have been developed based on a number of approaches. A traditional approach has been to empirically correlate net infiltration to average annual precipitation. This approach was originally postulated by Maxey and Eakin (1950). A more process-based approach has been recently developed by scientists at the U.S. Geological Survey, in which the estimated recharge is a function of precipitation, soil depth, evapotranspiration, and soil and rock permeability, among other factors. The application of this approach has resulted in an estimate of net infiltration in the Yucca Mountain region (Figure 2-2 and Table 2-1). Although there is uncertainty (about a factor of three) in the range of estimates of average annual net infiltration over the Death Valley region, the results of the infiltration distribution generally confirm that most of the recharge occurs at higher elevations in the Spring and Sheep Mountains, and at other locations above about 1,500 m elevation.

Naturally occurring discharge from aquifers in the Death Valley region generally occurs due to evapotranspiration from the shallow water table beneath playas or at surface springs. Locations of surface features where regional discharge is expected are described by D'Agnese et al. (2002). The current understanding of discharge locations and rates are summarized in Figure 2-3 and Table 2-2. These estimates have been compiled from estimates of evapotranspiration rates and observations of spring discharge in the area.



Source: D'Agnese et al. 2002, Figure 21.

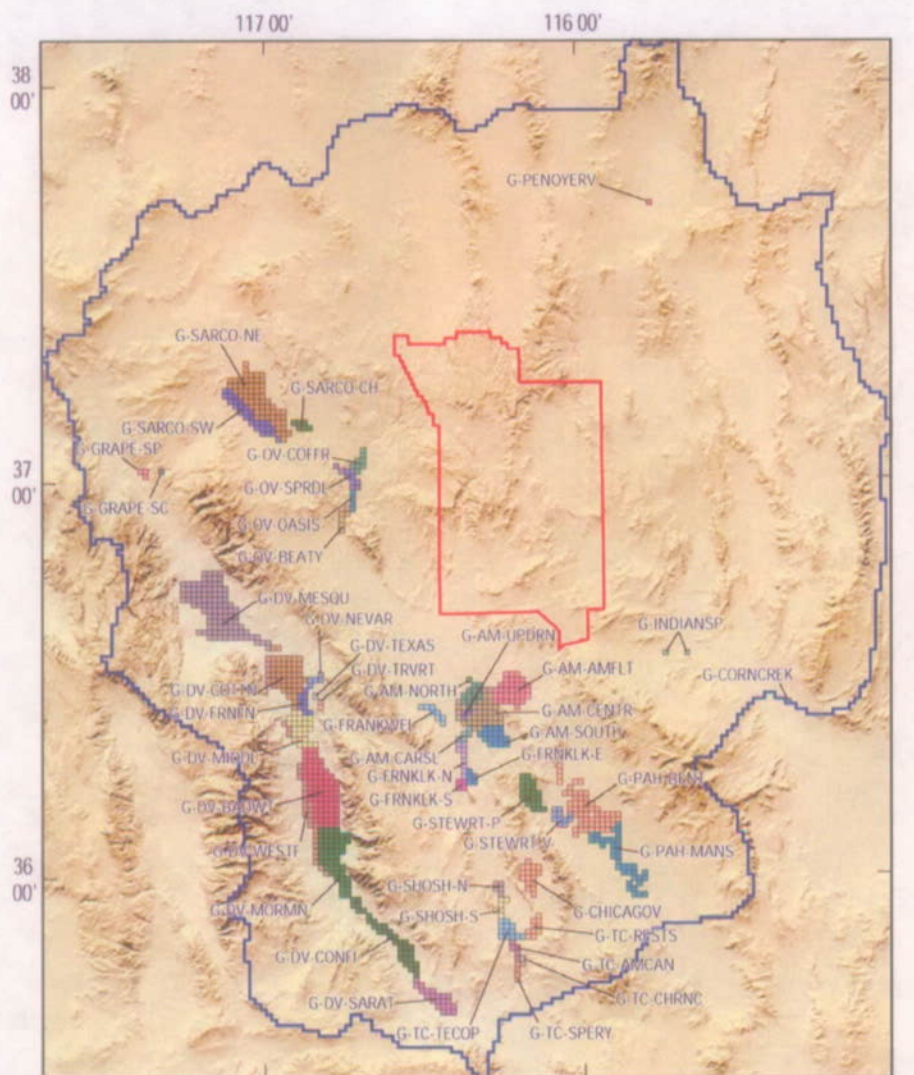
Figure 2-2. Location of Principal Recharge Areas and Amounts in the Death Valley Regional Flow System

Table 2-1. Summary of Precipitation, Modeled Net Infiltration, and Estimated Recharge using Maxey-Eakin Methods for the Area of the Death Valley Regional Groundwater Flow Model.

Precipitation Model	Model Type	Average Value for Area of Death Valley Groundwater Flow Model (mm/yr.)	Total Area Volume (million m ³ /yr)	Net Infiltration or Recharge as a Percentage of Precipitation
1980 to 1995 Modeled Precipitation		202	7,980	—
	Model net infiltration	7.8	310	3.9
	Model net infiltration of areas with >200 mm/yr. precipitation	4.8	190	6.2
	Modified Maxey-Eakin estimated recharge	6.3	250	3.1
	Modified Maxey-Eakin of areas with >200 mm/yr. precipitation	2.6	110	5.1
	Original Maxey-Eakin estimated recharge	4.8	190	2.4
1920 to 1993 Cokriged Precipitation		188	7,430	—
	Modified Maxey-Eakin estimated recharge	5.1	200	2.7
	Original Maxey-Eakin estimated recharge	3.7	150	2.0




Source: Based on Hevesi et al. 2002, Table 2.

NOTE: Volumetric flows rounded to the nearest 10 million m³/yr.



Universal Transverse Mercator projection, Zone 11. Shaded-relief base from 1:250,000-scale Digital Elevation Model; sun illumination from northwest at 30 degrees above horizon

EXPLANATION

-  Model grid boundary
-  Nevada Test Site boundary
-  Model cells representing drains with observation name (observation descriptions provided in table 3)

Source: Based on D'Agness et al. 2002, Figure 18.

Figure 2-3. Location of Principal Naturally Occurring Discharge Areas in the Death Valley Regional Flow System

Table 2-2. Inferred Naturally Occurring Discharge Amounts in the Death Valley Regional Flow System

Observation description	Observation name	Observed discharge (m ³ /day)
Ash Meadows, Amargosa Flat	G-AM-AMFLT	6,019
Ash Meadows, Carson Slough	G-AM-CARSL	498
Ash Meadows, central area	G-AM-CENTR	21,444
Ash Meadows, upper drainage	G-AM-UPDRN	3,219
Ash Meadows, northern area	G-AM-NORTH	19,499
Ash Meadows, southern area	G-AM-SOUTH	10,085
Chicago Valley	G-CHICAGOV	1,452
Corn Creek Springs	G-CORNCREK	676
Death Valley, Badwater basin area	G-DV-BADWT	5,019
Death Valley, Confidence Hills area	G-DV-CONFI	6,651
Death Valley, Cottonball basin area	G-DV-COTTN	3,547
Death Valley, Furnace Creek alluvial fan	G-DV-FRNFN	10,185
Death Valley, Mesquite Flat area	G-DV-MESQU	29,075
Death Valley, Middle basin	G-DV-MIDDL	2,587
Death Valley, Mormon Point area	G-DV-MORMN	7,225
Death Valley, Nevares Springs	G-DV-NEVAR	1,884
Death Valley, Saratoga Springs area	G-DV-SARAT	6,535
Death Valley, Texas Spring	G-DV-TEXAS	1,220
Death Valley, Travertine Springs	G-DV-TRVRT	4,633
Death Valley, western alluvial fans	G-DV-WESTF	13,637
Franklin Well area	G-FRANKWEL	1,182
Franklin Lake, eastern area	G-FRNKLLK-E	411
Franklin Lake, northern area	G-FRNKLLK-N	2,254
Franklin Lake, southern area	G-FRNKLLK-S	711
Grapevine Springs, Scotty's Castle area	G-GRAPE-SC	1,035
Grapevine Springs, spring area	G-GRAPE-SP	2,450
Indian Springs and Cactus Springs	G-INDIANSP	2,240
Oasis Valley, Beatty area	G-OV-BEATY	2,774
Oasis Valley, Coffers Ranch area	G-OV-COFFR	5,343
Oasis Valley, middle Oasis Valley area	G-OV-OASIS	3,157
Oasis Valley, Springdale area	G-OV-SPRDL	8,113
Pahrump Valley, Bennett Spring area	G-PAH-BENT	16,753
Pahrump Valley, Manse Spring area	G-PAH-MANS	5,375
Penoyer Valley area	G-PENOYERV	12,833
Sarcobatus Flat, Coyote Hills area	G-SARCO-CH	1,503
Sarcobatus Flat, northeastern area	G-SARCO-NE	30,421
Sarcobatus Flat, southwestern area	G-SARCO-SW	11,960
Shoshone basin, northern area	G-SHOSH-N	2,259
Shoshone basin, southern area	G-SHOSH-S	4,831
Stewart Valley, predominantly playa area	G-STEWRT-P	995
Stewart Valley, predominantly vegetation area	G-STEWRT-V	2,381
Tecopa basin, Amargosa Canyon area	G-TC-AMCAN	3,394
Tecopa basin, China Ranch area	G-TC-CHRNC	1,784
Tecopa basin, Resting Spring area	G-TC-RESTS	2,537
Tecopa basin, Sperry Hills area	G-TC-SPERY	1,341
Tecopa basin, central area	G-TC-TECOP	12,221
TOTAL:		105,776,270 m³ per year

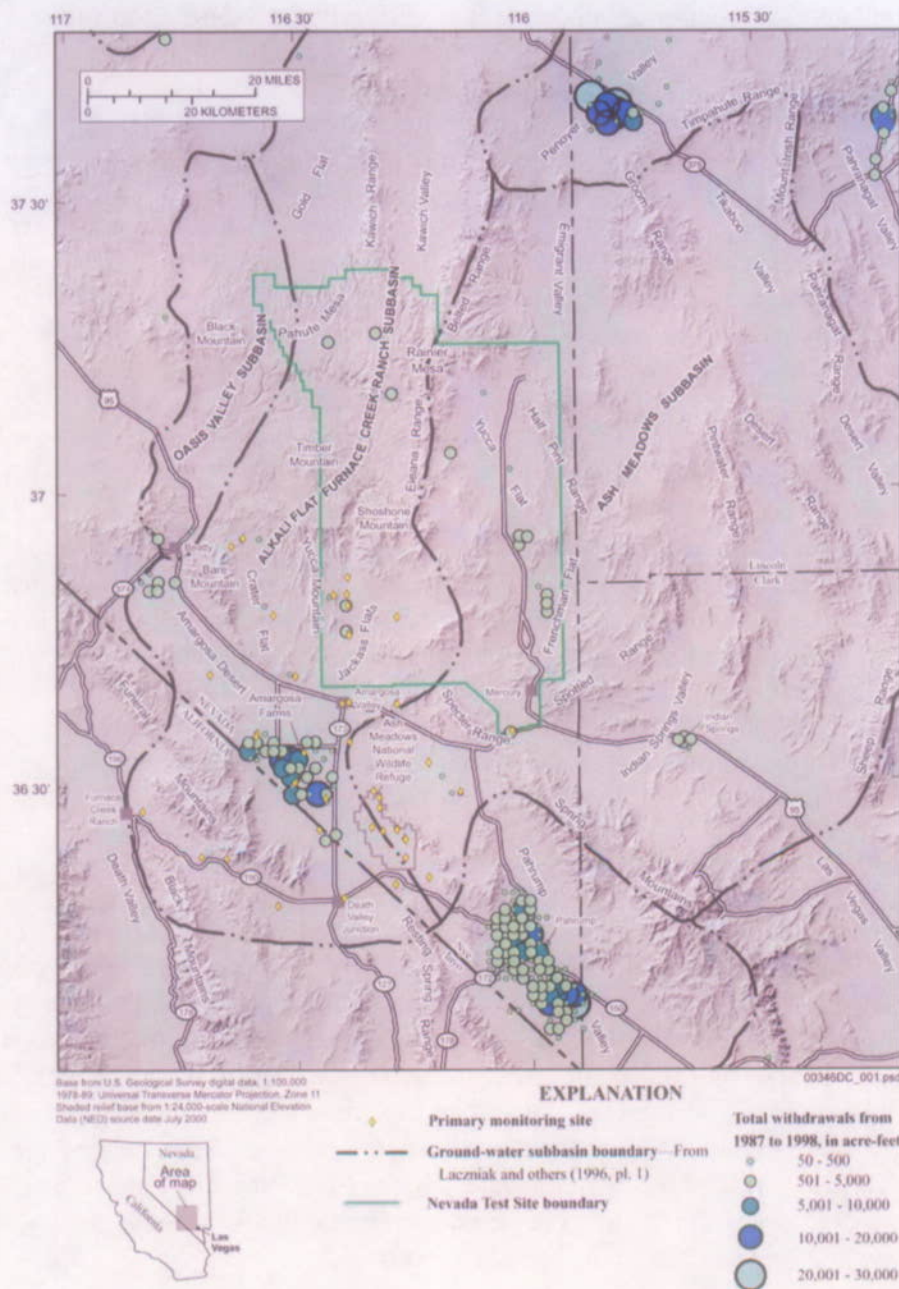
Source: Based on D'Agnesi et al. 2002.

In addition to natural discharge, groundwater has been withdrawn from the aquifers in the Death Valley regional groundwater basin for various domestic, agricultural, industrial, and government purposes over the last several decades. Locations and estimates of groundwater extraction are summarized in Figure 2-4. Although these discharges from the regional aquifers are small in comparison to natural discharge, they potentially affect the flow paths and flow rates in the vicinity of the pumping centers.

In comparing areas of recharge and discharge, it is apparent that most of the recharge occurs at higher elevations, while most discharge occurs at lower elevations. The total volumetric annual recharge and discharge rates in the basin should be similar assuming there is no net water gain or loss from the aquifers within the basin. The differences between Tables 2-1, 2-2, and Figure 2-4 might be the result of several factors. For example, they may reflect the degree of temporal averaging in the different techniques used to estimate net infiltration or in the estimation method used to determine the net infiltration (Hevesi et al. 2002). Alternatively, the differences may reflect that there is a nonsteady component of the regional flow system and that recharge and discharge are not in equilibrium. However, it is more likely that the estimates of recharge and discharge are essentially equivalent, and the differences simply represent the precision of the estimation method. Therefore, given the vastness of the groundwater basin, it is not surprising that the regional estimates of recharge and discharge only agree to within a factor of about three, as the regional recharge estimate varies from about 110 to 310 million m³/yr, and the regional discharge estimate is about 106 million m³/yr. This uncertainty in the estimate of the overall water budget has been considered in the estimate of the aquifer characteristics that affect the local flow system around Yucca Mountain.

2.2.2 Regional Potentiometric Surface

A regional-scale potentiometric map has been constructed by D'Agnese et al. (1997) for the Death Valley Regional Flow System (Figure 2-5). This regional-scale map was constructed using data sets describing water levels from monitoring wells in the region, boundaries of perennial marshes and ponds, regional spring locations, general inferences based on the distribution of recharge and discharge areas in the region, and a general understanding of the regional hydrogeology. The regional potentiometric surface corresponds to the major recharge and discharge areas identified above, with the major recharge being represented by potential highs in the Spring and Sheep Mountains and other areas with elevations greater than 1,500 m above sea level and discharge being represented by areas with a very low potential gradient or in areas with elevations less than 500 m above sea level.



Source: Fenelon and Moreo 2002, Figure 11.

NOTE: To convert total withdrawals over the reported period to annual water withdrawals, divide by 12 to convert to acre-feet/yr. or multiply by about 100 to convert to m^3/yr (there are 1,233 m^3 in 1 acre-foot). Therefore, the largest pumping center in the Amargosa Valley during this period was discharging 1 to 2 million m^3/yr on average.

Figure 2-4. Location of Principal Anthropogenic Groundwater Discharge Areas in the Death Valley Regional Flow System



Regional-Scale Potentiometric Surface Map

Source: After D'Agness et al. 1997, Figure 27.

NOTE: The regional flow system model boundary indicated on this figure reflects the boundaries used in D'Agness et al. (1997) which have been revised in the more recent interpretations described in D'Agness et al. (2002) and presented in Figures 2-1 to 2-3.

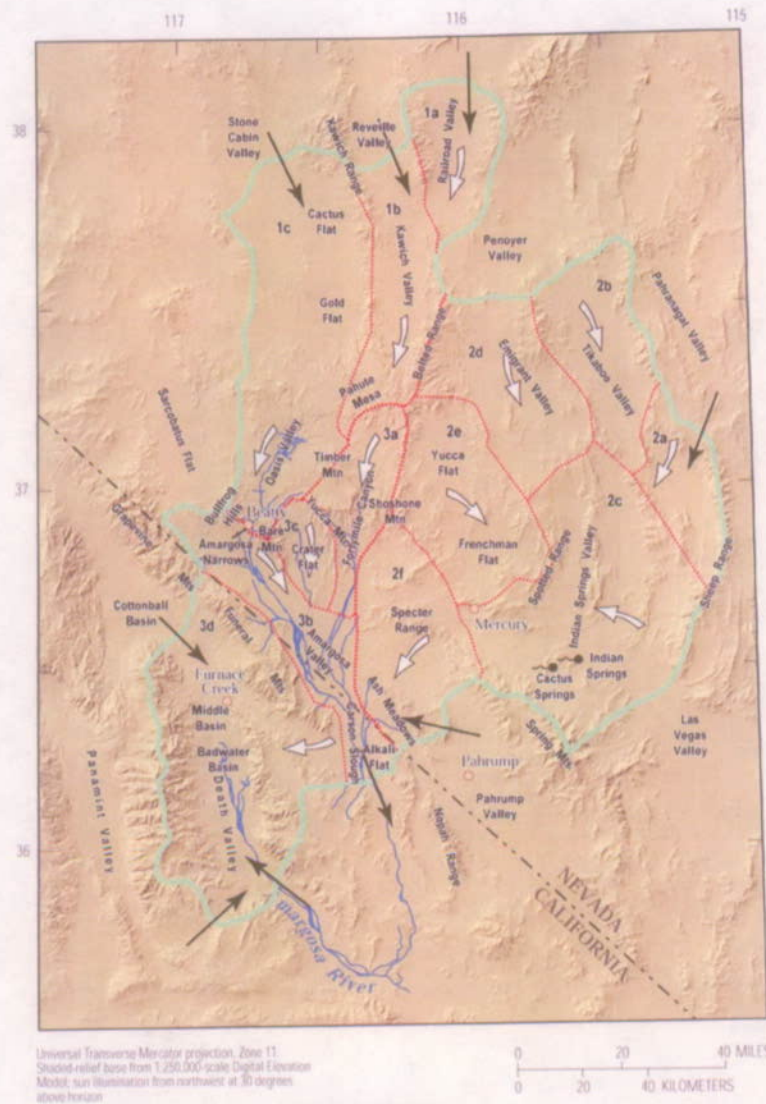
Figure 2-5. Regional-Scale Potentiometric Surface Map

Using only the potentiometric information and knowledge of major recharge and discharge areas, D'Agnese et al. (2002) have inferred the general regional groundwater flow directions in the central Death Valley subregion of the Death Valley regional flow system (Figure 2-6), which generally is southerly in the vicinity of Yucca Mountain. Although these interpreted flow directions are useful indicators of general trends, they do not directly quantify the uncertainty in the flow paths, and they primarily are used to confirm the flow directions developed at the scale of the site model.

2.2.3 Death Valley Regional Hydrogeology

The Death Valley regional hydrogeology is characterized by rocks of differing lithology and hydraulic characteristics depending in part on the location and proximity to major tectonic features. The faults also have effects on the flow system, ranging from acting as barriers to groundwater flow when flow is perpendicular to the fault strike, to providing preferential flow paths (horizontally and vertically) when flow is parallel to the fault strike.

The major hydrogeologic units from oldest to youngest are: the Lower Clastic Confining Unit, the Lower Carbonate Aquifer, the Upper Clastic (Eleana) Confining Unit, the Upper Carbonate Aquifer, the Volcanic Aquifers, the Volcanic Confining Units, and the Alluvial Aquifer. The Lower Clastic Confining Unit forms the basement and is generally present beneath the other units except in caldera complexes. The Lower Carbonate Aquifer is the most extensive and transmissive unit in the region, and it is the source of regional discharge in the springs of Death Valley National Park. The Upper Clastic Confining Unit is present in the north-central part of the Nevada Test Site. It typically impedes flow between the overlying Upper Carbonate Aquifer and the underlying Lower Carbonate Aquifer, and is associated with many of the large hydraulic gradients in and around the Nevada Test Site. The Volcanic Aquifers and Volcanic Confining Units form a stacked series of alternating aquifers and confining units in and around the Nevada Test Site. The Volcanic Aquifers are moderately transmissive and are saturated in the western sections of the Nevada Test Site. The Alluvial Aquifer forms a discontinuous aquifer in the region. Regional outcrops of these hydrogeologic units are depicted in Figure 2-7, and representative cross sections through the region, depicting the correlation of these different units, are presented in Figure 2-8.



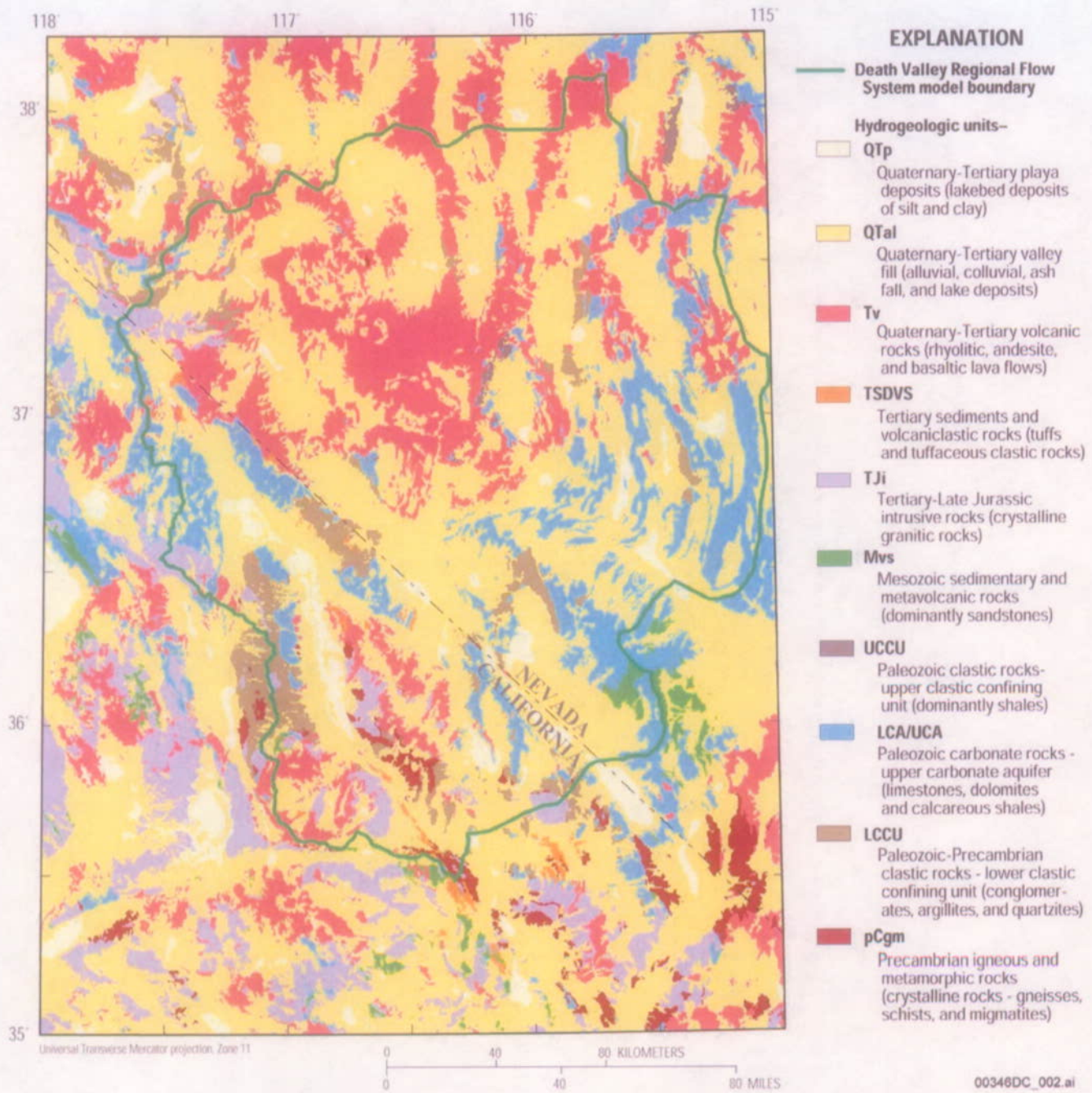
EXPLANATION

Subregion boundary	Ground-water basins and sections -
Ground-water section boundary	(1) Pahute Mesa-Oasis Valley Ground-Water Basin
Arrows designate dominant regional flowpath associated with ground-water section discussed in text	a Southern Railroad Valley
Potential flow into or between subregions	b Kawich Valley Section
Location of spring	c Oasis Valley Section
Location of populated-place	(2) Ash Meadows Ground-Water Basin
	a Pahranaqat Section
	b Tikaboo Valley Section
	c Indian Springs Section
	d Emigrant Valley Section
	e Yucca-Frenchman Flat Section
	f Specter Range Section
	(3) Alkali Flat-Furnace Creek Ground-Water Basin
	a Fortymile Canyon Section
	b Amargosa River Section
	c Crater Flat Section
	d Funeral Mountains Section

Source: Based on D'Agness et al. 2002, Figure 11.

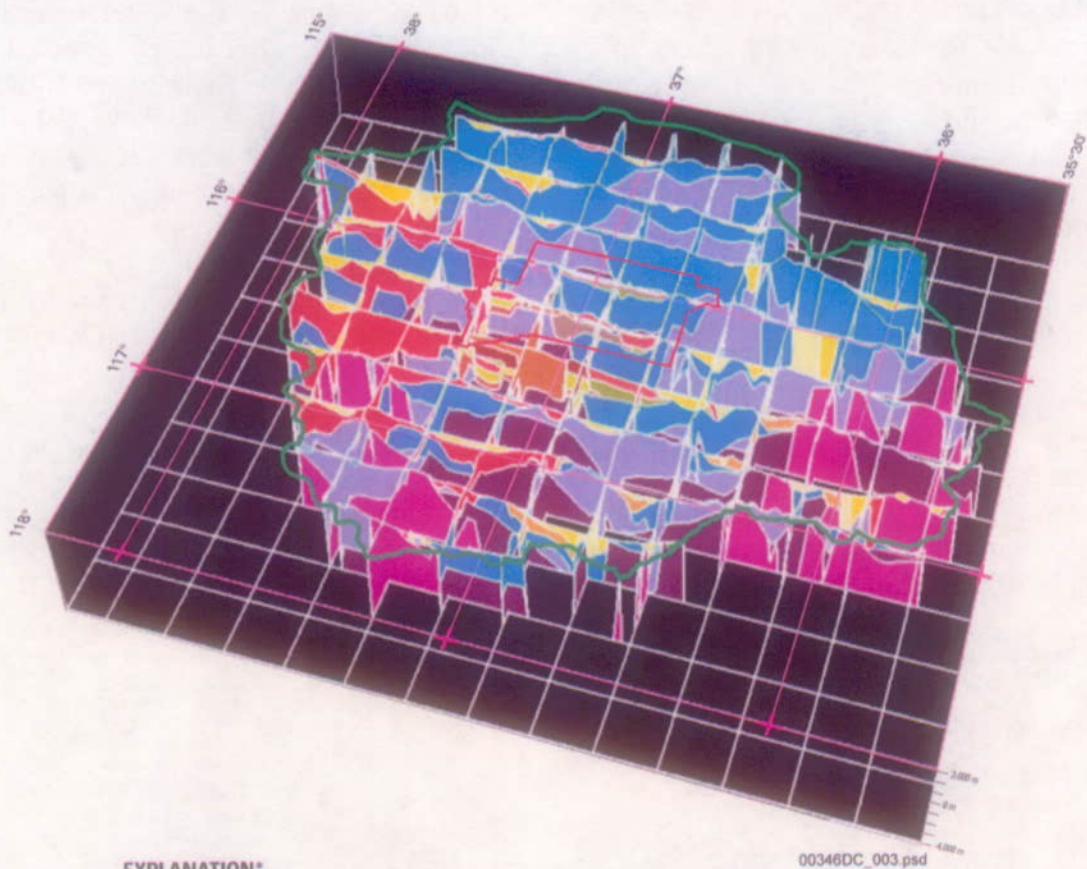
NOTE: The Central Death Valley Subregion is one of three subregions identified in the Death Valley Regional Flow Model (D'Agness et al. 2002).

Figure 2-6. Inferred Groundwater Flow Paths in the Central Death Valley Subregion
























Source: Belcher et al. 2002, Figure 4.

Figure 2-7. Outcrops of Major Hydrogeologic Units in the Death Valley Region



EXPLANATION*

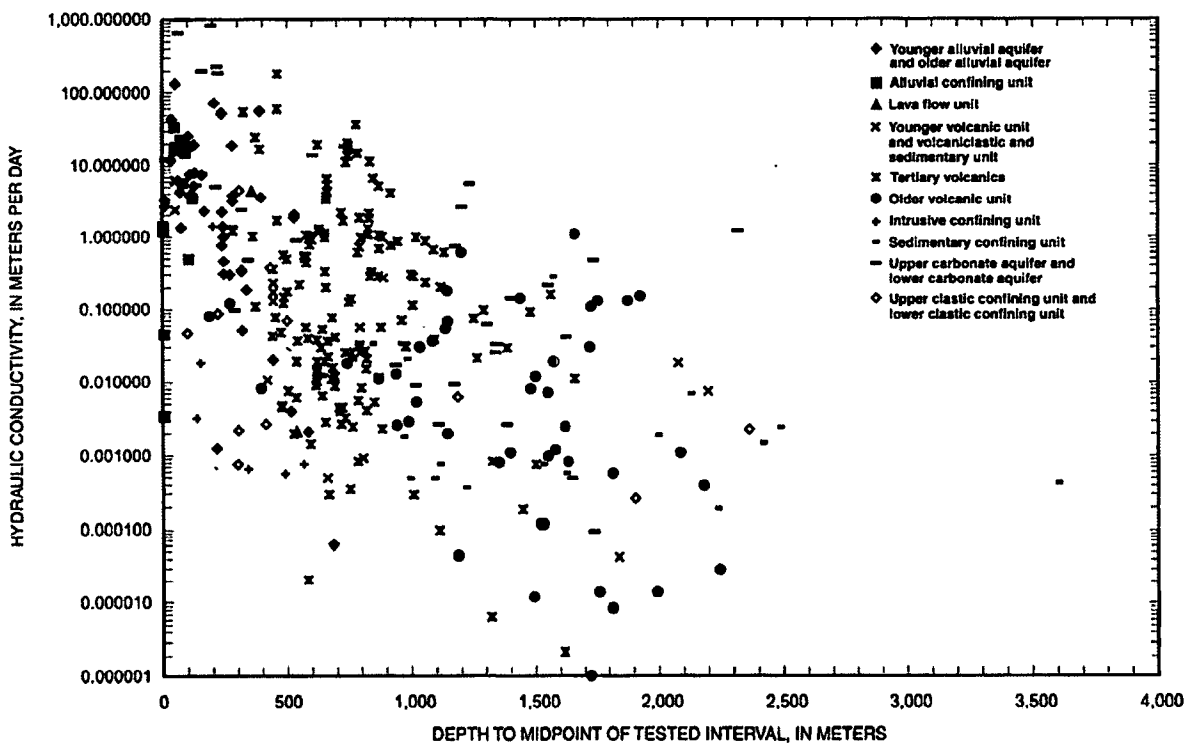
- | | | | |
|---|---|---|---|
|  | QTal – Valley-fill alluvium |  | Mvs – Mesozoic volcanoclastic and sedimentary rocks |
|  | QTp – Valley-fill playa deposits |  | UCA – Upper carbonate aquifer |
|  | VU – Undifferentiated volcanic rocks |  | UCCU – Upper clastic confining unit |
|  | VA – Volcanic aquifer |  | LCA – Lower carbonate aquifer |
|  | VCU – Volcanic confining unit |  | LCCU – Lower clastic confining unit |
|  | TMA – Timber Mountain aquifer |  | pCgm – Precambrian granites and metamorphic rocks |
|  | TC – Paintbrush/Calico Hills tuff cone |  | TJi – Tertiary-Jurassic intrusives |
|  | TCB – Bullfrog confining unit |  | Death Valley Regional Flow System model boundary |
|  | TBA – Belted Range aquifer |  | Nevada Test Site boundary |
|  | TBCU – Basal confining unit | | |
|  | TBQ – Basal aquifer | | |
|  | TSDVS – Tertiary sediments/Death Valley section | | |

*All units indicated are present in the model, but some do not appear in the diagram due to the scale selected.

Source: Belcher et al. 2002, Figure 35.

Figure 2-8. Representative Hydrogeologic Cross Sections through the Death Valley Region

Understanding of the regional groundwater flow requires evaluating the water transmitting capability of the major lithologic units in the Death Valley region. Belcher et al. (2001) have compiled estimates of transmissivity, hydraulic conductivity, storage coefficients, and anisotropy ratios for major hydrogeologic units within the Death Valley region. Belcher et al. (2002) used a compilation of 930 hydraulic conductivity measurements to derive estimates of the hydraulic characteristics for several hydrogeologic units within the Death Valley regional groundwater system. Regional variability in aquifer characteristics are summarized in Figure 2-9. Although this figure illustrates an apparent depth dependency of hydraulic conductivity, the objective in presenting the information in this format primarily to depict the variability in hydraulic conductivity as a function of rock type. The depth dependency, which is presumably related to confining stress, has not been directly incorporated in the hydrogeologic models of the region. Although presenting the information as a function of rock type, it is also probable that the range of variation within a particular rock type is largely affected by the degree of fracturing of the rock in the vicinity of the borehole that was tested (i.e., they reflect the local heterogeneity of the rock mass). Uncertainty and variability in hydraulic conductivity are evaluated in the construction of the regional and site-scale hydrogeologic models. Uncertainty in hydraulic conductivities does not greatly constrain the flow models.



Source: Belcher and Elliot 2001, Figure 4.

Figure 2-9. Depth Dependency of Regional Hydraulic Conductivity Estimates

2.2.4 Regional Geochemistry

In addition to hydraulic observations, an understanding of regional flow systems can be ascertained from interpretations of the regional hydrogeochemistry. The application of hydrogeochemical and isotopic methods make it possible to reduce some uncertainties concerning regional groundwater flow patterns and flow rates. They also provide some bounds on the magnitude and timing of recharge of saturated zone groundwater.

The main processes that control groundwater chemistry are:

- Precipitation (atmospheric) quantities and compositions
- Soil-zone processes in recharge areas
- Rock-water interactions in the unsaturated zone between the zone of infiltration and the water table
- Rock-water interactions in the saturated zone along the flow path from the recharge location to the point where the water is sampled
- Mixing of groundwater from different flow systems.

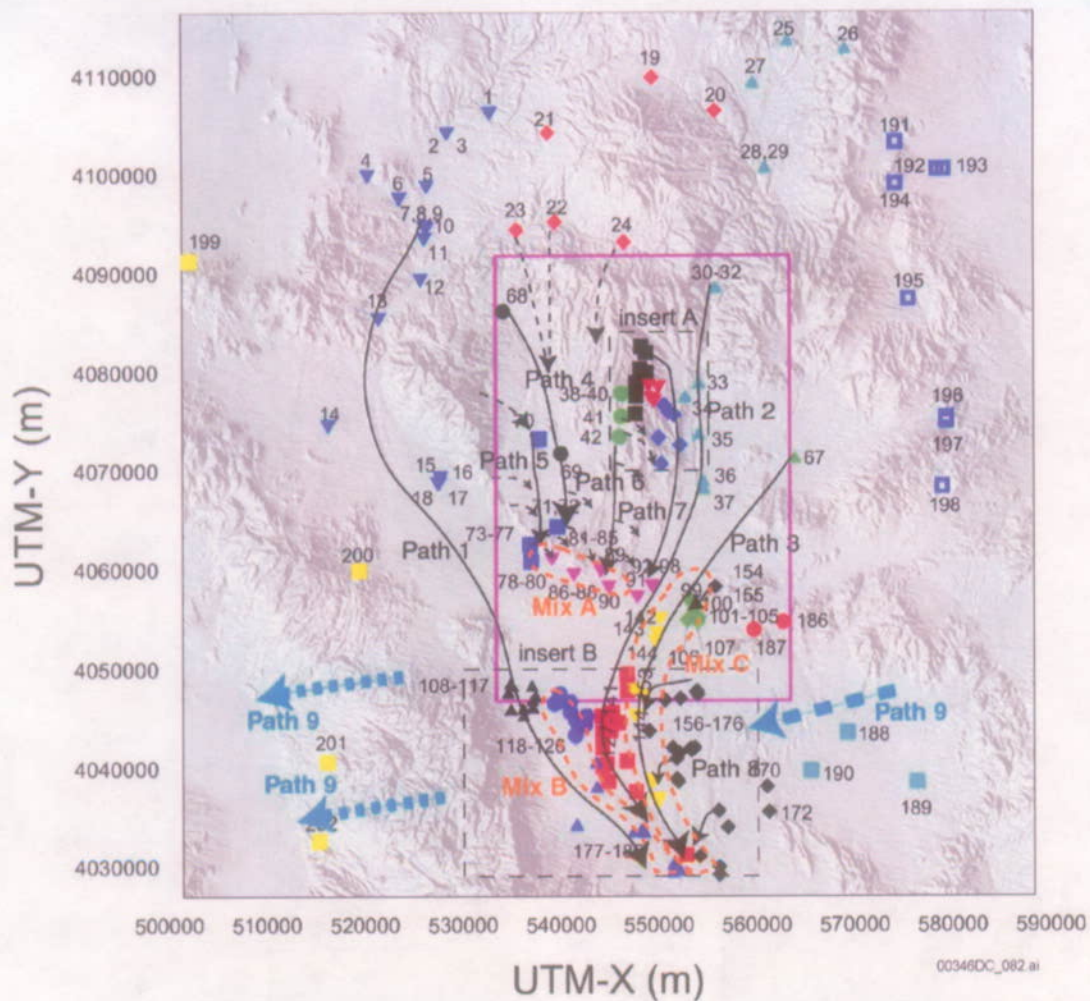
Groundwater is influenced to differing degrees by these processes, and as a result, groundwater extracted from different places (and therefore traveling by different pathways) can attain different chemical signatures that reflect individual pathway histories. The first three of the main processes do not affect the composition of groundwater after it enters the aquifer. However, input compositions differ in the recharge area because of evapotranspiration (which affects ion concentrations), recharge temperatures (which affect delta-deuterium and delta-oxygen-18), precipitation compositions, soil-zone mineral dissolution, and precipitation reactions.

After entering an aquifer, chemical characteristics can be affected by interactions between the groundwater and the rocks. Conservative geochemical constituents (i.e., those that show the least impact from interactions with water and rocks) are particularly important for delineating flow paths because their concentrations primarily reflect inputs and processes that operate in recharge areas. Generally, conservative constituents, for which analytical data are available, include chloride, sulfate, delta-deuterium, and delta-oxygen-18. Where a lack of downgradient continuity in chemical and isotopic compositions was observed, the possibility of groundwater mixing was further evaluated and quantified with inverse geochemical mixing and reaction models.

Areal distribution maps of groundwater solutes and isotopes were used by BSC (2003f) to obtain initial estimates of groundwater flow paths. Water type locations and the corresponding observation points used to evaluate geochemical signatures are depicted in Figure 2-10. Figure 2-11 illustrates the same information while showing chloride concentrations in the identified wells. Both figures depict the site-scale model domain boundaries. Table 2-3 summarizes the basis for the flow paths illustrated on Figure 2-11. Similar plots for sulfate and delta-deuterium were also used in interpreting these flow paths (Figures 2-12 and 2-13, respectively).

Flow paths were interpreted based on a number of approaches, including (1) examination of areal distribution plots (e.g., Figures 2-11, 2-12, and 2-13) for spatial trends, (2) examination of scatterplots between chemical or isotopic variables that indicate relationships (including mixing) between groundwater from the different geographic areas identified in Figure 2-10, and (3) inverse geochemical models that were used to estimate the mixing fractions of various upgradient groundwater's present in a downgradient groundwater, recognizing that groundwater composition can be a result of mixing and water-rock interactions (BSC 2003f). The first two approaches focus on patterns and relationships displayed among relatively nonreactive species (e.g., chloride, sulfate and delta-deuterium). The potential groundwater sources and mixing relationships suggested by the first two approaches were examined more quantitatively by inverse mixing and reaction models that also considered the evolution of more reactive species through water-rock interaction. The first approach is essentially two dimensional, but the second and third approaches incorporate the effects of three-dimensional mixing with local recharge or with groundwater upwelled from the deep carbonate aquifer.

The regional flow paths and mixing zones identified based on the groundwater geochemical signatures are consistent with the general flow directions and recharge-discharge relationships discussed above. For example, the southwesterly flow in the deep carbonate aquifer across the Amargosa Desert is consistent with recharge in the Spring Mountains and Sheep Range areas and discharge in the springs around Death Valley. Similarly, the relatively shallow southerly flow through tuff and alluvium from recharge in the Rainer Mesa area along the Fortymile Canyon and under Fortymile Wash discharges in the wells in Amargosa Valley or at natural discharge areas such as Franklin Lake Playa. All of the above plots illustrate a general southerly flow of regional groundwater in the vicinity of Yucca Mountain and a mixing of different groundwater types in the alluvial aquifer underlying the Amargosa Valley.

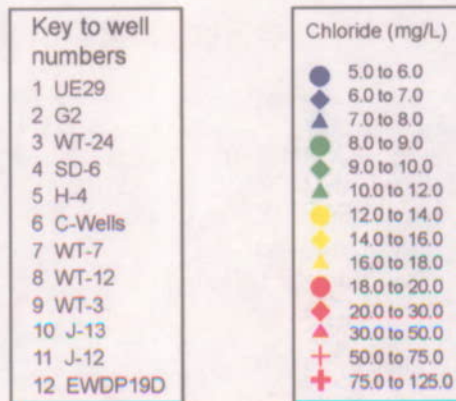
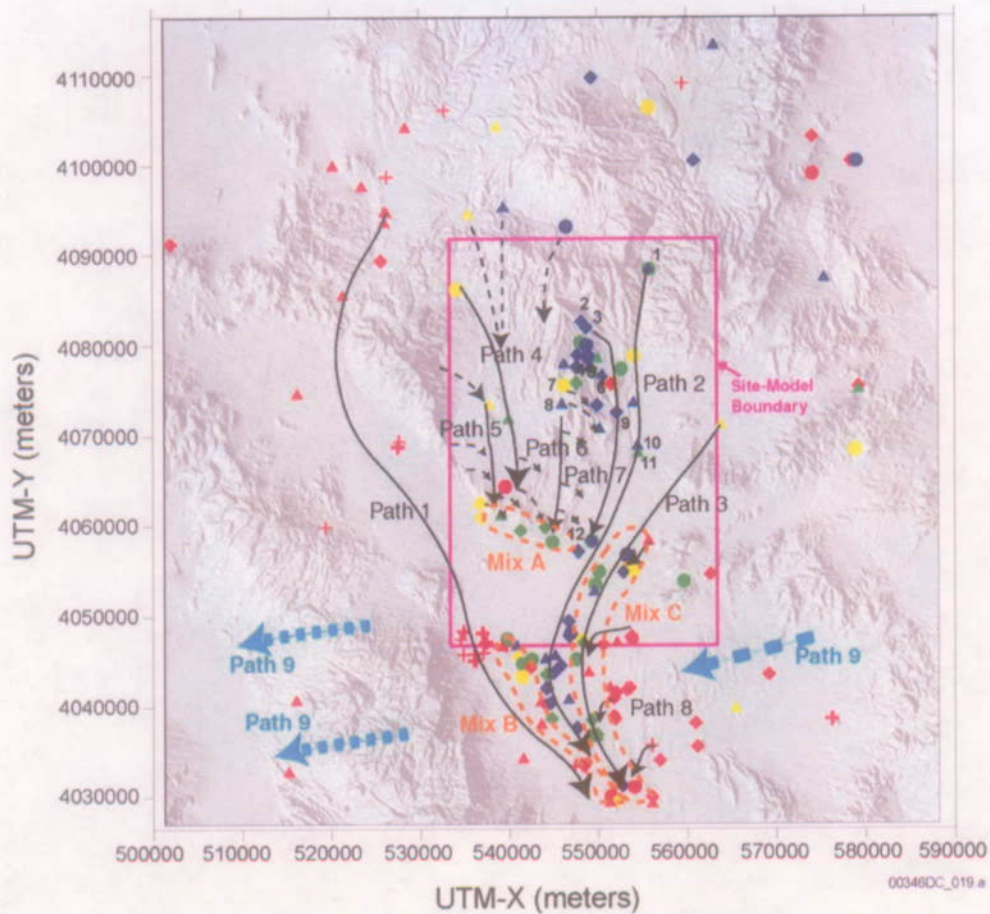


- | | |
|--------------------------------------|------------------------------------|
| ▼ Oasis Valley/NW Amargosa (OV/NWA) | ◆ Lathrop Wells (LW) |
| ◆ Timber Mountain (TM) | ▲ Amargosa River (AR) |
| ▲ Fortymile Wash North (FMW-N) | ● Fortymile Wash - West (FMW-W) |
| ● Solitario Canyon Wash (SCW) | ■ Fortymile Wash - South (FMW-S) |
| ■ Yucca Mountain - Crest (YM-CR) | ▼ Fortymile Wash - East (FMW - E) |
| ▼ Yucca Mountain - Central (YM-C) | ◆ Gravity Fault (GF) |
| ◆ Yucca Mountain - Southeast (YM-SE) | ▲ Amarg. Riv./Fortymile W (AR/FMW) |
| ▲ Jackass Flats | ● Skeleton Hills (SH) |
| ● Crater Flat (CF) | ■ Amargosa Flat (AF) |
| ■ Crater Flat - Southwest (CF-SW) | ■ Mine Mountain (MM) |
| ▼ Yucca Mountain - South (YM-S) | ■ Funeral Mountains (FMT) |

Source: BSC 2003f, Figure 62.

NOTE: The termination of flow paths implies that the flow paths could not be traced from geochemical information downgradient from these areas because of mixing or dilution by more actively flowing groundwater; flow path terminations do not imply that groundwater flow has stopped.

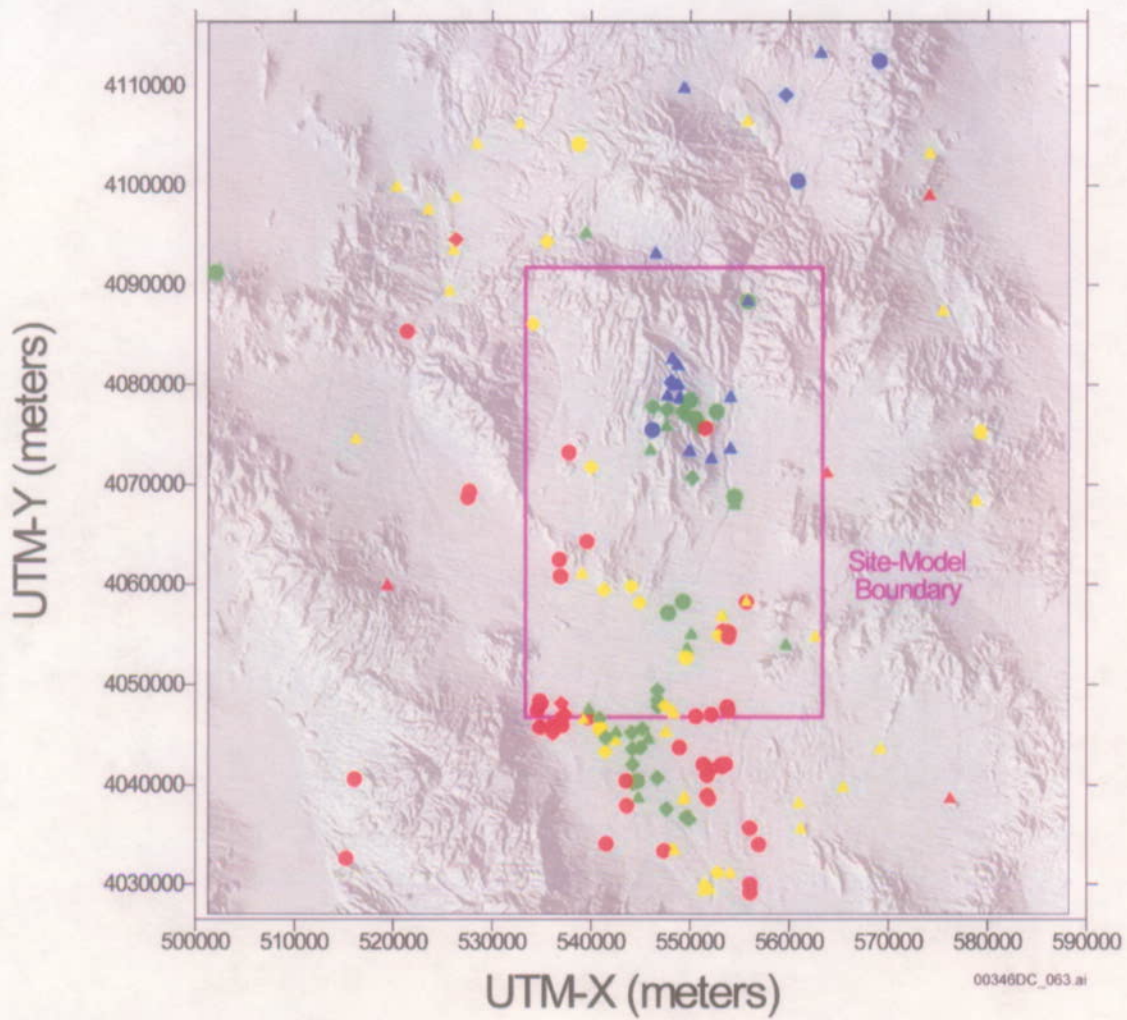
Figure 2-10. Location of Geochemical Groundwater Types and Regional Flow Paths Inferred from Hydrochemical and Isotopic Data



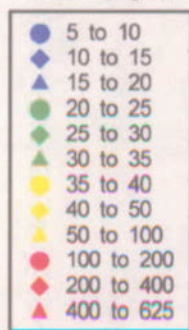
Source: Based on BSC 2003f; chloride from Figure 15; flow paths from Figure 62.

NOTE: The termination of flow paths implies that the flow paths could not be traced from geochemical information downgradient from these areas because of mixing or dilution by more actively flowing groundwater; flow path terminations do not imply that groundwater flow has stopped.

Figure 2-11. Regional Groundwater Chloride Concentrations and Inferred Regional Flow Paths



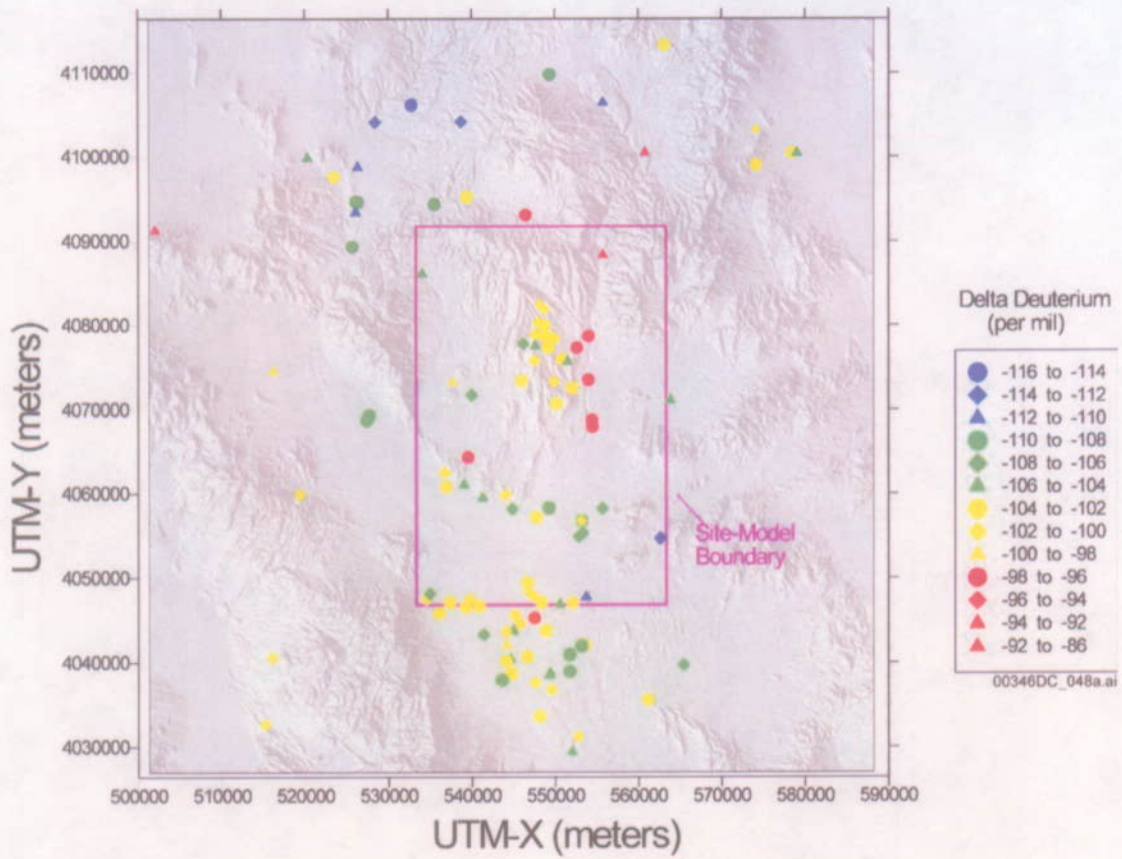
Sulfate (mg/L)



data as of 2/18/03

Source: BSC 2003f, Figure 16.

Figure 2-12. Areal Distribution of Sulfate in Groundwater



Source: Based on BSC 2003f, Figure 24.

Figure 2-13. Regional Groundwater delta-Deuterium

Table 2-3. Summary of Bases for Regional Flow Paths and Mixing Zones Derived from Geochemistry Observations

Flow path or Mixing Zone (Figure 2-10)	Geochemical Flowpath or Mixing Zone Description	Geochemical Evidence of Flowpath or Mixing Zone
1	Oasis Valley through the Amargosa Desert along the axis of the Amargosa River to its confluence with Fortymile Wash	Areal plots of chloride and scatterplots of SO ₄ versus Cl. Groundwater along this flow path becomes more dilute to the south as it becomes increasingly mixed with groundwater near Fortymile Wash. Upstream of this mixing zone, high groundwater ¹⁴ C activities and variable δD and δ ¹⁸ O compositions indicate the presence of relatively young recharge in the groundwater due to runoff or irrigation in the area
2	Fortymile Canyon area southward along the axis of Fortymile Wash into the Amargosa Desert	Similar anion and cation concentrations along the flow line and dissimilarities compared to regions to the east and west. Groundwater along the northern part of this flow path is distinguished from groundwater at Yucca Mountain by δD and δ ¹⁸ O compositions that are heavier or more offset from the Yucca Mountain meteoric water line than the groundwater found under Yucca Mountain. Some part of the groundwater along Fortymile Wash may also be derived by recharge due to runoff or irrigation in the area based on the observation that ¹⁴ C activities do not decrease systematically southward in either the northern or southern segments of the wash.
3	Jackass Flats in the vicinity of well J-11 southward along the western edge of the Lathrop Wells area and southward through the FMW-E area wells	High SO ₄ and low δ ³⁴ S characteristics of groundwater from well J-11 distinguish it from the high SO ₄ and high δ ³⁴ S groundwater characteristic of the Gravity fault and the low SO ₄ and low δ ³⁴ S groundwater of the Fortymile Wash. A scatterplot of δ ³⁴ S versus 1/SO ₄ indicates a mixing trend involving well J-11 as an end member, with wells in the Lathrop Wells and FMW-E groups having up to 20 percent of a J-11-like groundwater. These mixing relations were confirmed with PHREEQC inverse models involving selected wells in these groups.
4	Lower Beatty Wash area into northwestern Crater Flat. This groundwater flows predominantly southward in Crater Flat past borehole VH-1 and NC-EWDP-3D.	Scatterplots and PHREEQC inverse models show that a mixture of groundwater is required to account for the Cl, δD, and δ ¹⁸ O compositions characteristic of this flow path. East of Flow Path 4, the extremely light δ ¹³ C and high δ ⁸⁷ Strontium of groundwater in northern Yucca Mountain compared to Timber Mountain groundwater, indicates that groundwater from the Timber Mountain and Beatty Wash areas is not the dominant component of groundwater at Yucca Mountain north of Drillhole Wash.
5	SW Crater Flat Group	Chemically and isotopically distinct from groundwater that characterizes Flow Path 4, with higher concentrations of most major ions (but lower concentrations of F and SiO ₂), and relatively high δ ¹⁸ O and δD. Groundwater in Oasis valley has some of the lightest oxygen and hydrogen isotopic composition of groundwater in the Yucca Mountain area, eliminating flow from Oasis Valley under Bare Mountain as a possible source of groundwater in southwest Crater Flat. A more likely source for groundwater along this flow path is local recharge at Bare Mountain, a source suggested by the similarly heavy δD and δ ¹⁸ O compositions of perched water emanating from a spring at Bare Mountain (Specie Spring) and groundwater in southwest Crater Flat. This similarity indicates that local recharge and runoff from Bare Mountain may be the source of groundwater along this flow path, as schematically indicated by the dashed nature of the beginning of this flow path in Figure 2-10.

Table 2-3. Summary of Bases for Regional Flow Paths and Mixing Zones Derived from Geochemistry Observations (Continued)

Flow path or Mixing Zone (Figure 2-10)	Geochemical Flowpath or Mixing Zone Description	Geochemical Evidence of Flowpath or Mixing Zone
6	From well WT-10 southward toward well NC-EWDP-15P	This flow path is identified from PHREEQC models that indicate that groundwater from well NC-EWDP-15P is formed from subequal amounts of groundwater from wells WT-10 and VH-1, and a small percentage (<5 percent) of groundwater from the carbonate aquifer. Although the predominant direction of flow from the Solitario Canyon area is southward along the Solitario Canyon fault, evidence for the leakage of small amounts of groundwater eastward across the fault is provided by similarities in the concentrations of many ions and isotopes between the Solitario Canyon Wash and Yucca Mountain - Crest area wells. This chemical and isotopic similarity indicates that groundwater as far east as borehole H-4 may have some component of groundwater from the Solitario Canyon Wash area and possibly NC-EWDP-19D. The short southeast-oriented dashed lines from Solitario Canyon Group wells schematically illustrate this leakage.
7	From northern Yucca Mountain southeastward toward YM-SE wells in the Dune Wash area and then southwestward along the western edge of Fortymile Wash.	The upper segment of this flow path is motivated by the high groundwater $^{234}\text{U}/^{238}\text{U}$ activity ratios found in the northern Yucca Mountain and Dune Wash areas. High $^{234}\text{U}/^{238}\text{U}$ activity ratios (greater than 7) typify both perched water and groundwater along and north of Drill Hole Wash but not groundwater along Yucca Crest at borehole SD-6 or perched water at borehole SD-7. Based on the conceptual model for the evolution of $^{234}\text{U}/^{238}\text{U}$ activity ratios, congruent dissolution of thick vitric tuffs that underlie the Topopah Spring welded tuff along Yucca Crest south of Drill Hole Wash would be expected to decrease the $^{234}\text{U}/^{238}\text{U}$ activity ratios of deep unsaturated-zone percolation south of the Wash. High $^{234}\text{U}/^{238}\text{U}$ activity ratios are expected only where these vitric tuffs are absent, as in northern Yucca Mountain.
8	Leakage of groundwater from the carbonate aquifer across the Gravity fault.	Hydrogeologists and geochemists have recognized this leakage across the fault (Winograd and Thordarson 1975; Claassen 1985). The carbonate aquifer component in this groundwater is recognized by many of the same chemical and isotopic characteristics that typify groundwater discharging from the carbonate aquifer at Ash Meadows. These characteristics include high concentrations Ca and Mg, low SiO_2 , heavy $\delta^{13}\text{C}$ values, low ^{14}C activity, and comparable $\delta^{18}\text{O}$ and δD values as the Ash Meadows groundwater.
9	Deep underflow of groundwater from the carbonate beneath the Amargosa Desert and Funeral Mountains to the discharge points in Death Valley.	The similarity in the chemical and isotopic characteristics of groundwater found in the Gravity fault area and groundwater that discharges from springs at Nevares Spring and Travertine Spring support this interpretation. The dissimilarity in Cl, Mg, and SiO_2 concentrations in these springs compared to the groundwater from the alluvial aquifer along the Amargosa River suggests that this alluvial groundwater is not the predominant source of the spring discharge in Death Valley.
Mix A	NC-EWDP and SW Crater Flat samples along Interstate 95.	The zone is demonstrated by groundwater compositions of samples that are intermediate between the compositionally distinct groundwater of the carbonate aquifer and dilute groundwater of the volcanic aquifer that is interpreted to have originated in the Yucca Mountain area (see flow paths 6 and 7 discussion).

Table 2-3. Summary of Bases for Regional Flow Paths and Mixing Zones Derived from Geochemistry Observations (Continued)

Flow path or Mixing Zone (Figure 2-10)	Geochemical Flowpath or Mixing Zone Description	Geochemical Evidence of Flowpath or Mixing Zone
Mix B	Samples from the FMW-W, AR/FMW and a few samples from the FMW-S groups.	The zone highlights groundwater with compositions that are intermediate between the distinct and consistent groundwater compositions of the Amargosa River Group and the dilute groundwater of the FMW-S group.
Mix C	Consists of all samples from the Lathrop Wells and FMW-E groups, a few of the more westerly samples from the Gravity fault group and at least one sample (#141) from the FMW-S group.	Characterized by small percentages of the distinctively high SO ₄ groundwater from Well J-11. Groundwater with this distinctive signature is mixed to variable degrees with dilute water from the FMW-S group to the west, or groundwater from the carbonate aquifer (Gravity fault group) to the east.

Source: BSC 2003f.

2.2.5 Groundwater Flow Model and Results

Several models have been constructed over the past decade to describe the hydrogeology in the Death Valley region. The current three-dimensional digital hydrogeologic framework model developed for the Death Valley Regional Flow System contains elements from both of the hydrogeologic framework models used in previous investigations: the 1997 Death Valley Regional Flow System model (D'Agnese et al. 1997) and the Under Ground Test Area regional model (DOE 1997).

The Death Valley Regional Flow System has been analyzed by the U.S. Geological Survey using a three-dimensional steady-state model. The required model parameter values were supplied by discretization of the three-dimensional hydrogeologic framework model and digital representations of the remaining conceptual model components. The three-dimensional simulation and corresponding sensitivity analysis supported the hypothesis of interactions between a relatively shallow local and subregional flow system and a deeper dominant regional system controlled by the carbonate aquifer.

Model calibration was completed to estimate hydraulic parameters to best fit observed hydraulic data and evaluate alternative conceptual models of the flow system. The results of the model are illustrated in Figure 2-14 where the residual difference between the simulated and observed heads is plotted. Acceptable matches to observed hydraulic heads generally occur in areas of low hydraulic gradients. Poorer fits to observed heads generally occur in areas with steep hydraulic gradient. Although some of the observed and simulated heads differ by more than 100 m, the general flow directions and recharge and discharge relationships are preserved.

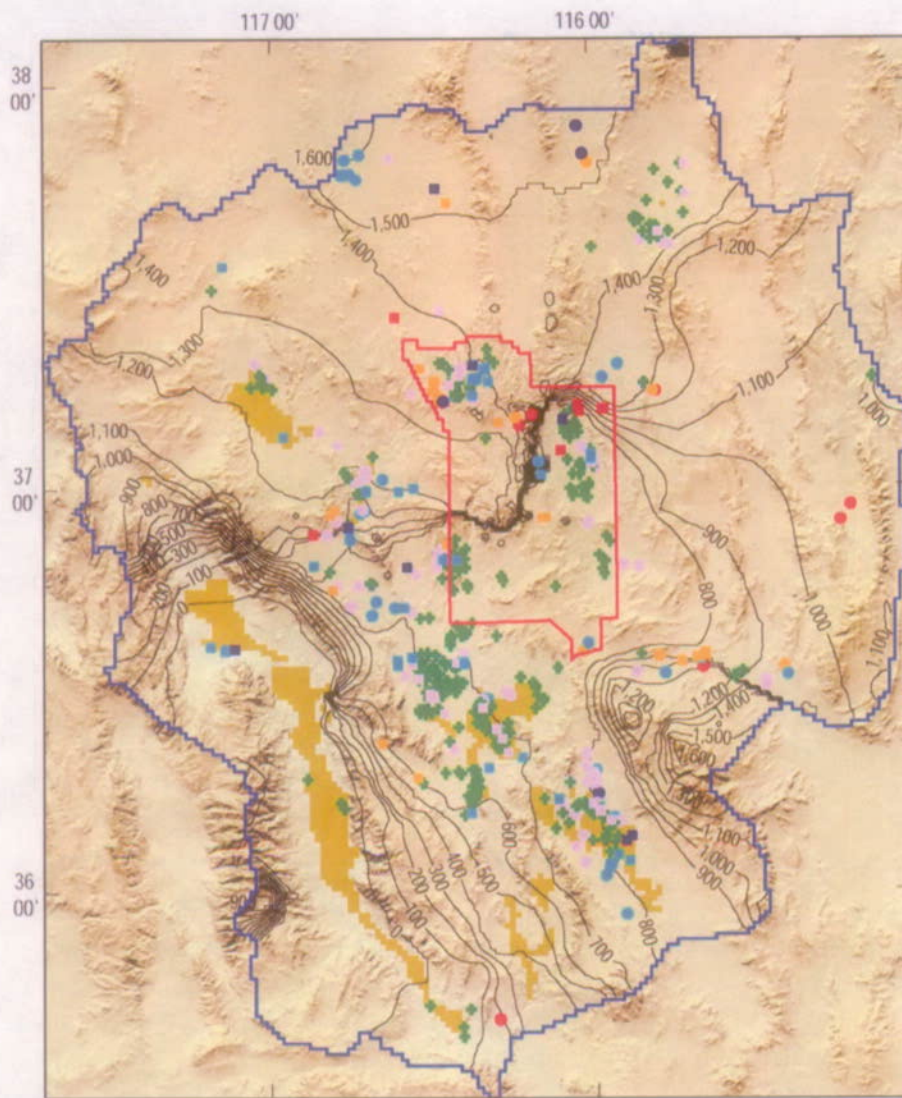
Figure 2-14 indicates that in some parts of the regional flow model, the data are too sparse to sufficiently constrain the model. That is, the model attempts to reduce the hydraulic head residual with equal weight applied to all observations. In areas where more wells exist to constrain the predicted hydraulic heads, the residuals are generally lower. This is the case in the Amargosa Farms area, Yucca Flat, Oasis Valley and in the vicinity of Yucca Mountain. In areas

with less hydraulic constraint, such as north of Indian Springs and along the Eleana Range, the residuals are generally greater.

Although significant uncertainty exists in the observed and predicted hydraulic heads in the regional flow model, the general trends which are indicative of major recharge and discharge areas are consistent with the observed areas presented in Figures 2-1 and 2-2.

Comparison of modeled discharge and inferred discharge is presented in Figure 2-15. Given the large uncertainty in the hydraulic characteristics and the sparseness of the observations, the match is believed to be acceptable for the purposes of understanding the overall flow system and estimating the flow rates in the vicinity of Yucca Mountain.

Uncertainties in the regional flow model can be attributed to: (1) uncertainties in the hydrogeology represented in the framework model, (2) water levels being represented as static as opposed to perched conditions, and (3) resolution of detailed hydrostratigraphy in the coarse grid of the regional model. Considering these constraints, the regional representation of groundwater flow is sufficiently characterized to define a general southerly flow direction in the vicinity of Yucca Mountain.



Universal Transverse Mercator projection,
 Zone 11. Shaded-relief base from
 1:250,000-scale Digital Elevation
 Model; sun illumination from northwest
 at 30 degrees above horizon

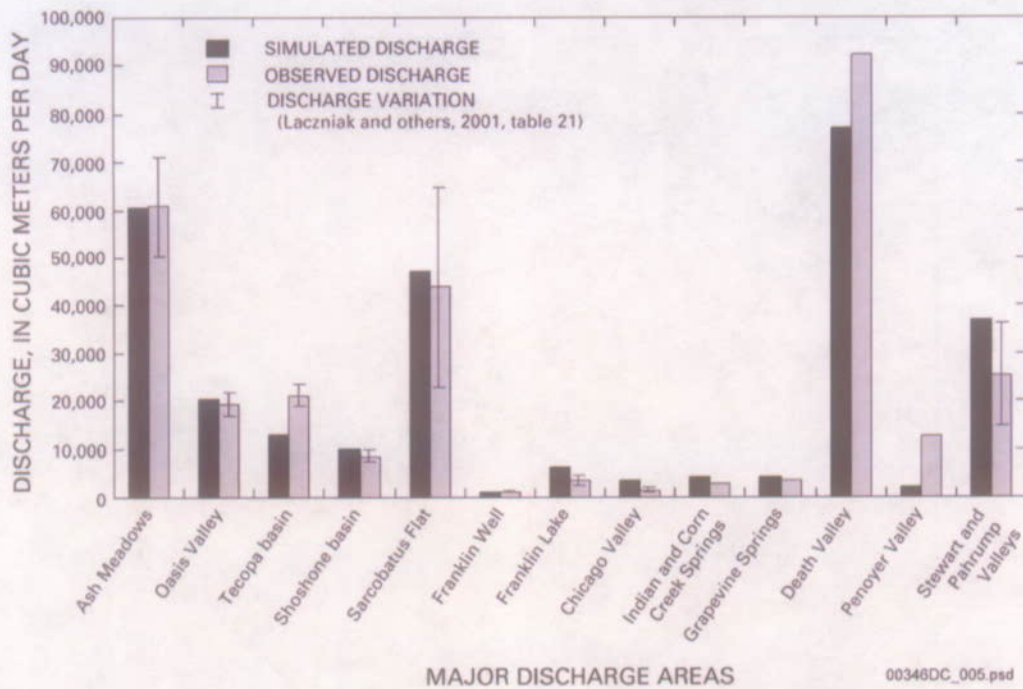
00348DC_022.a

EXPLANATION

- Drain cells
 - Model grid boundary
 - Nevada Test Site boundary
 - Simulated hydraulic-head contour
- Contour interval is 100 meters
- Hydraulic-head residuals -**
 - >100
 - 50 to 100
 - 35 to 50
 - 20 to 35
 - 10 to 20
 - 10 to -10
 - 10 to -20
 - 20 to -35
 - 35 to -50
 - 50 to -100
 - <-100

Source: Based on D'Agness et al. 2002, Figure 40.

Figure 2-14. Comparison of Predicted and Observed Hydraulic Heads in the Death Valley Regional Groundwater Flow Model



Source: D'Agness et al. 2002, Figure 43.

Figure 2-15. Simulated and Observed Groundwater Discharge for Major Discharge Areas

2.3 SITE-SCALE GROUNDWATER FLOW SYSTEM

To better represent the groundwater flow system at the scale of interest for the repository, it is necessary to develop a more refined estimate of the groundwater regime than is possible using only the regional characterization. The regional groundwater flow characterization provides the context of the site-scale representation by constraining the likely groundwater flow paths (through regional understanding of recharge, discharge, hydraulic potentials, and geochemistry) and the average volumetric flow rates (through regional understanding of the hydraulic characteristics and the regional water budget). The regional representation is not suitable for evaluating the details of the groundwater flow rates (e.g., specific discharge) or the distribution of those flow rates along the paths of likely radionuclide migration from Yucca Mountain to the compliance point specified in the regulations.

Figure 2-1 depicts the location and scale of the site-scale groundwater flow representation. This model encompasses an area of 30×45 km and extends from the top of the water table to the lower clastic confining unit. Although the site-scale model resides within the regional-scale representation and must be consistent with the regional characterization, the details of the flow paths and hydrogeology at the scale of hundreds of meters to kilometers necessitates a finer resolution of understanding than the scale of kilometers to tens of kilometers used in the regional model.

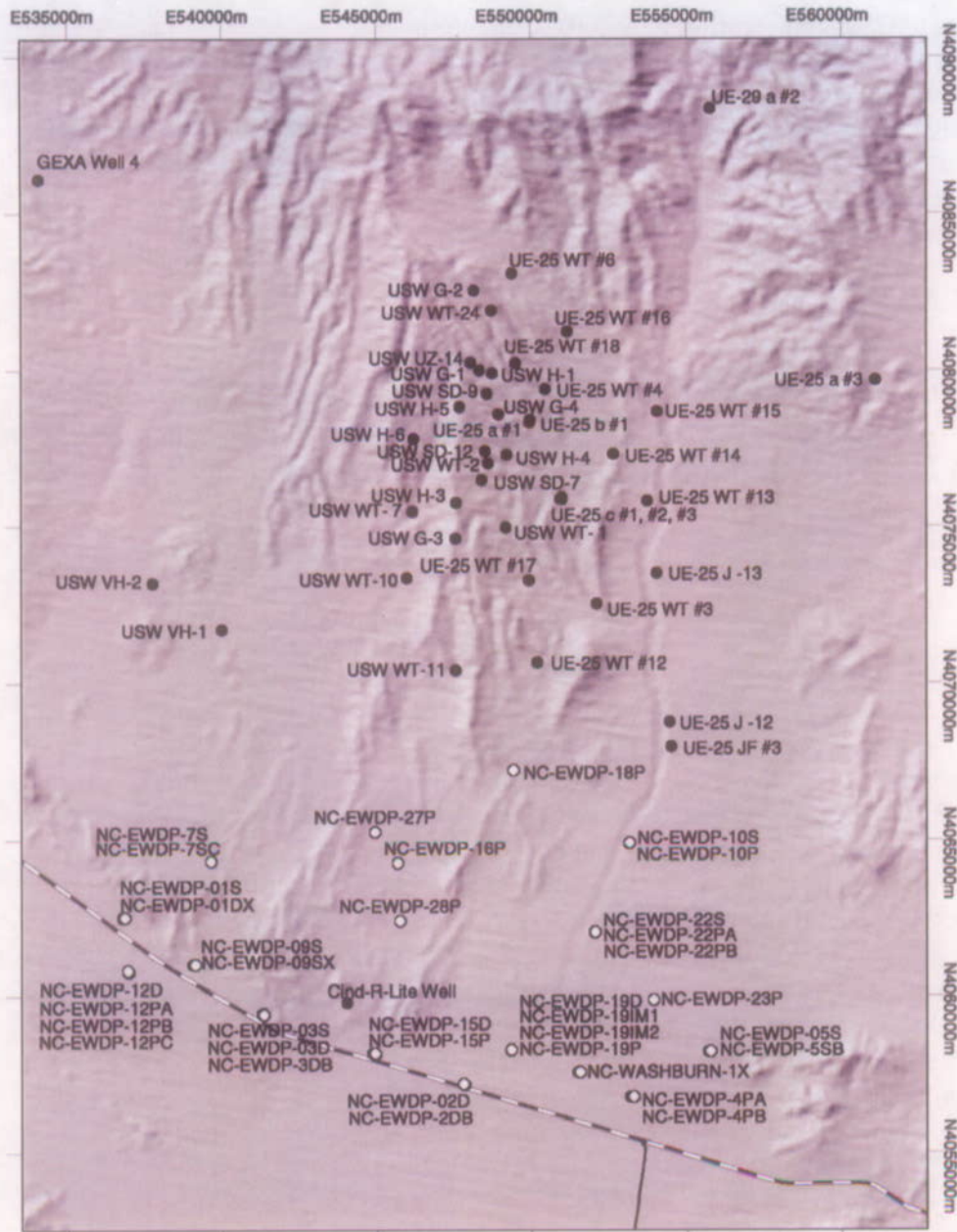
2.3.1 Site Characterization and Data Collection

Drilling for evaluation of the Yucca Mountain site began in 1978, and the first hydrologic test well completed in 1981. Detailed site characterization commenced in 1986. Water levels were measured as each well was completed, and long-term water-level monitoring commenced in 1983. Periodic measuring of water levels continues through the present. The network of monitoring boreholes has evolved over the years and continues to increase as additional wells are installed as part of the ongoing Nye County Early Warning Drilling Program. The monitoring wells provide measurements at various depths, and a number of wells monitor more than one depth interval.

The location of monitoring wells used to characterize the groundwater flow system in the vicinity of Yucca Mountain are illustrated in Figure 2-16. This figure includes those wells drilled and tested by the DOE in support of the Yucca Mountain Site Characterization Project and those drilled and tested by Nye County as part of the Nye County Early Warning Drilling Program.

2.3.2 Site-Scale Recharge and Discharge

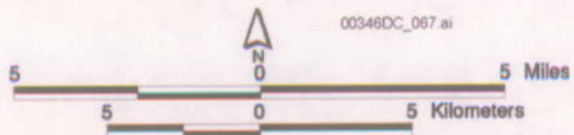
Within the scale of the site model of saturated zone groundwater flow, the bulk of the recharge and discharge occurs along the lateral boundaries with the regional model (Figure 2-17a). Inflow generally occurs along the northern and eastern boundaries, and discharge is generally along the southern boundary (Table 2-4). Figure 2-17a shows the segments of the north, east, and west boundaries listed in Table 2-4. Inflow from the north is generally the result of regional recharge that occurs at Timber Mountain, Pahute Mesa, and Rainer Mesa. Inflow from the east is generally the result of regional underflow in the carbonate aquifers that were recharged in the Specter Range. Outflow to the south is the result of both carbonate underflow and flow in the alluvial aquifers which ultimately discharge either in wells in Amargosa Valley or naturally discharge at Ash Meadows. Table 2-4 shows the site-scale base-case flow model and the 1997 Death Valley Regional Flow System model. Appendix D also compares the 2001 Death Valley Regional Flow System model. Local recharge due to infiltration along Yucca Mountain and, to a lesser extent, along Fortymile Wash is also considered. The distributions of vertical recharge in the site-scale model are depicted in Figure 2-17b.



Legend

- Saturated Zone Borehole
- Nye County Early Warning Drilling Program Borehole

Map Projection: Universal Transverse Mercator, Zone 11



YMP-03-042_0

Source: CRWMS M&O 2000a, Figure 3-7.

Figure 2-16. Location of Boreholes used to Characterize the Site-Scale Groundwater Flow System in the Vicinity of Yucca Mountain

Of the total volumetric recharge and discharge in the regional flow basin (on the order of 100 to 300 million m³/yr), about 10 to 30 percent (depending on the assumed regional flow balance) flows through the site-scale model boundaries. The bulk of the flow is within the carbonate aquifers that are recharged to the east and north of the site model area. Groundwater flows into and across the site model boundaries, and it ultimately discharges to the south of the site model.

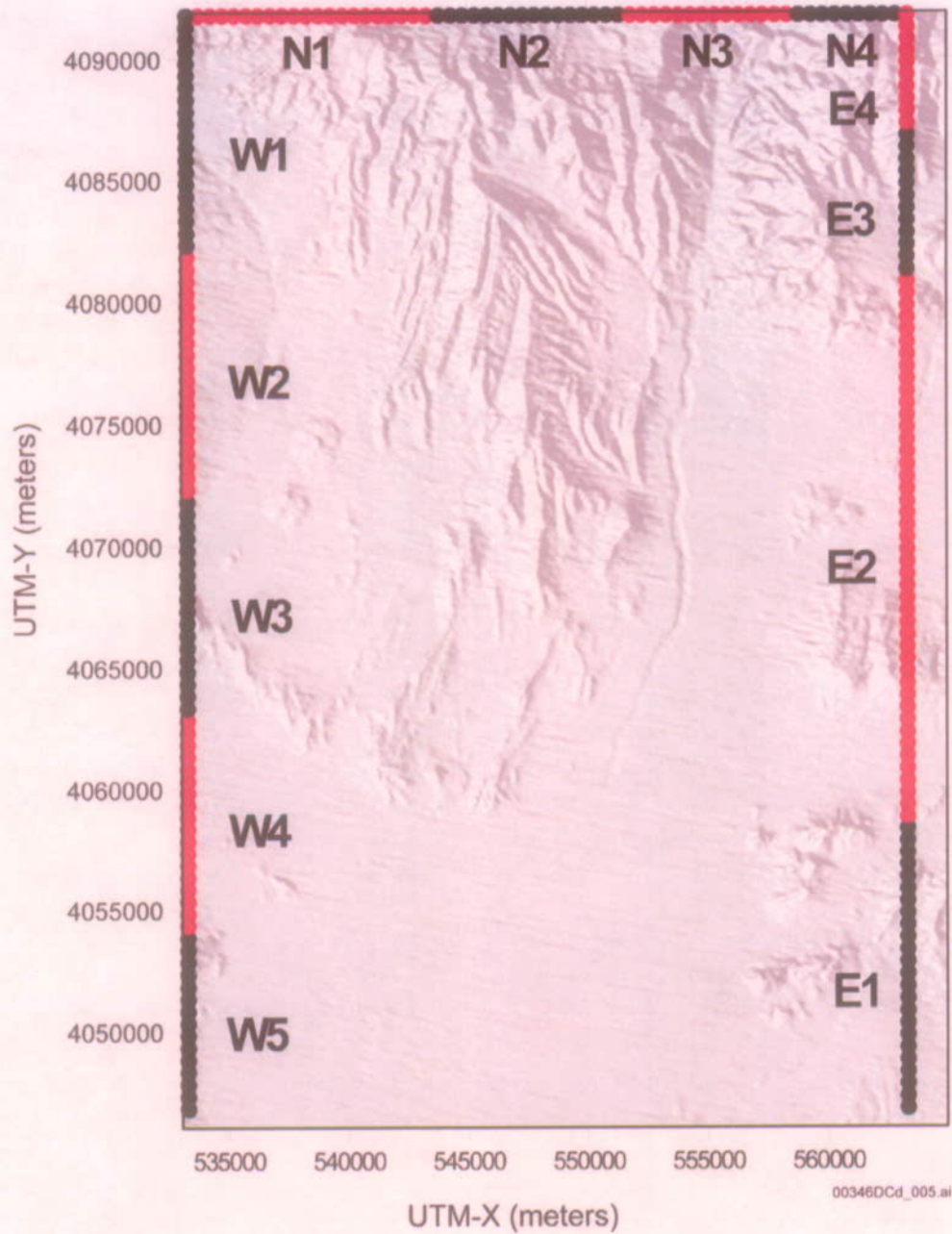
Table 2-4 compares the regional- and site-scale model fluxes for an evaluation of consistency. Based on the discussion of the uncertainty in the regional potentiometric surface, the uncertainty and variability in regional aquifer characteristics and the uncertainty in the regional recharge and discharge amounts and distribution, the uncertainty in these boundary fluxes (which is not quantified on this table) is considerable. All three types of information (hydraulic heads, hydraulic conductivity, and recharge-discharge amounts) are integrated into the site-scale model to develop an integrated and self-consistent representation of the overall flow system. Although uncertainty exists in each type of information, the integrated representation appropriately reflects all three observations.

Table 2-4. Comparison of Regional and Site-Scale Fluxes

Boundary Zone	Regional Flux (million m ³ /yr)	Site-Scale Flux (million m ³ /yr)
N1	-3.2	-1.9
N2	-0.5	-1.1
N3	-1.7	-1.0
N4	-0.6	-1.4
Subtotal of North Boundary Fluxes	-6.1	-5.4
W1	0.1	0.1
W2	-2.2	<<0.1
W3	-0.2	<<0.1
W4	0.1	<<0.1
W5	-1.5	-0.2
Subtotal of West Boundary Fluxes	-3.7	-0.1
E1	-17.5	-17.5
E2	-0.2	0.1
E3	0.1	0.5
E4	-0.1	0.5
Subtotal of East Boundary Fluxes	-17.7	-16.4
S	28.9	22.8

Source: Based on BSC 2001, Table 14.

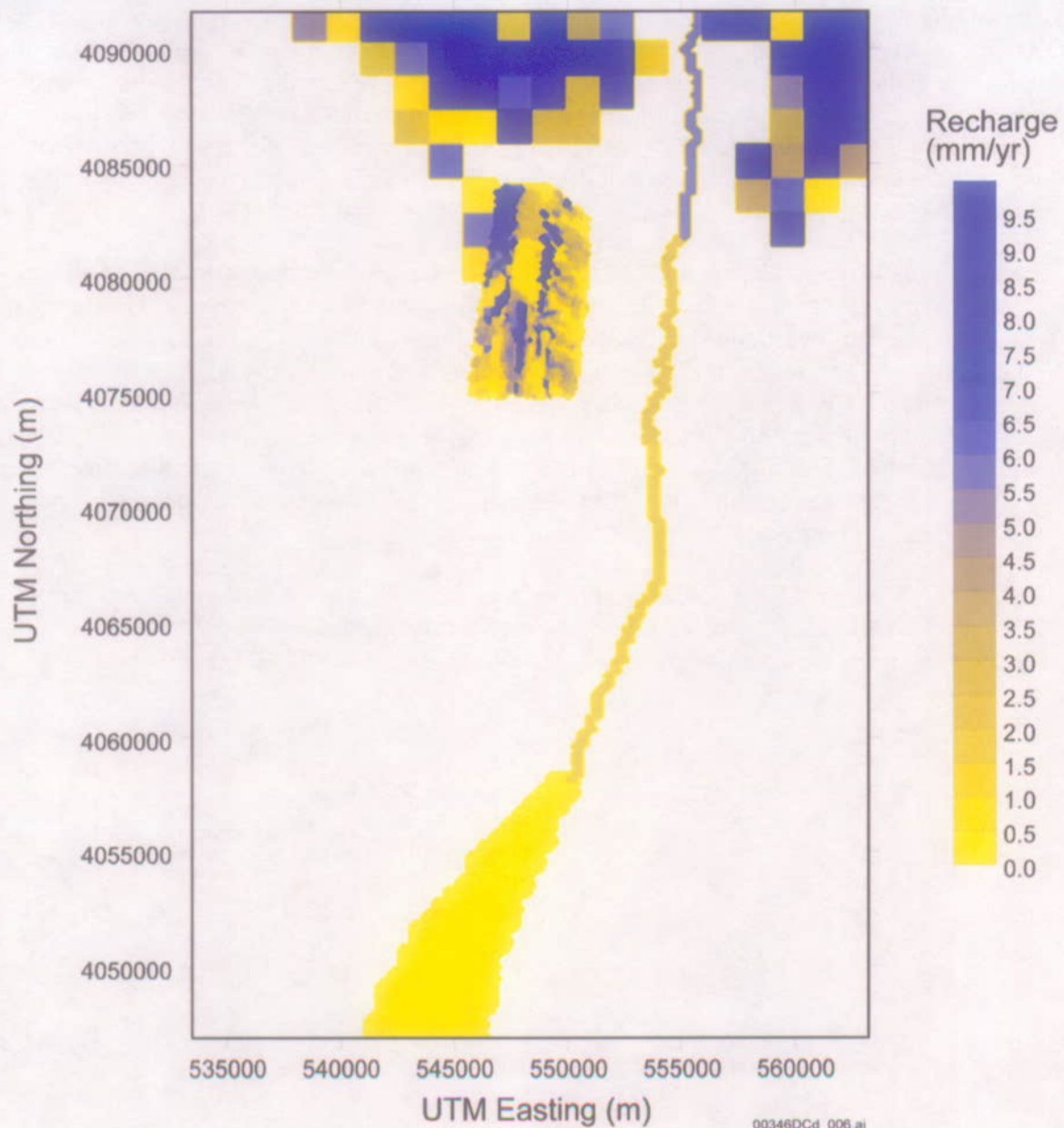
NOTES: A negative value indicates flow into the model. Values were converted from mass flux to volumetric flux and rounded to the nearest 0.1 million m³/yr.



Source: BSC 2001, Figure 16.

NOTE: Locations indicate discrete places where boundary fluxes from the regional model are applied to the site-scale flow model. The Southern boundary is not coded S because it is one segment.

Figure 2-17a. Flux Zones used for Comparing Regional and Site-Scale Flux



Source: BSC 2002, Figure 6.1.3-2.

Figure 2-17b. Map of Recharge to the Saturated Zone Site-Scale Flow Model

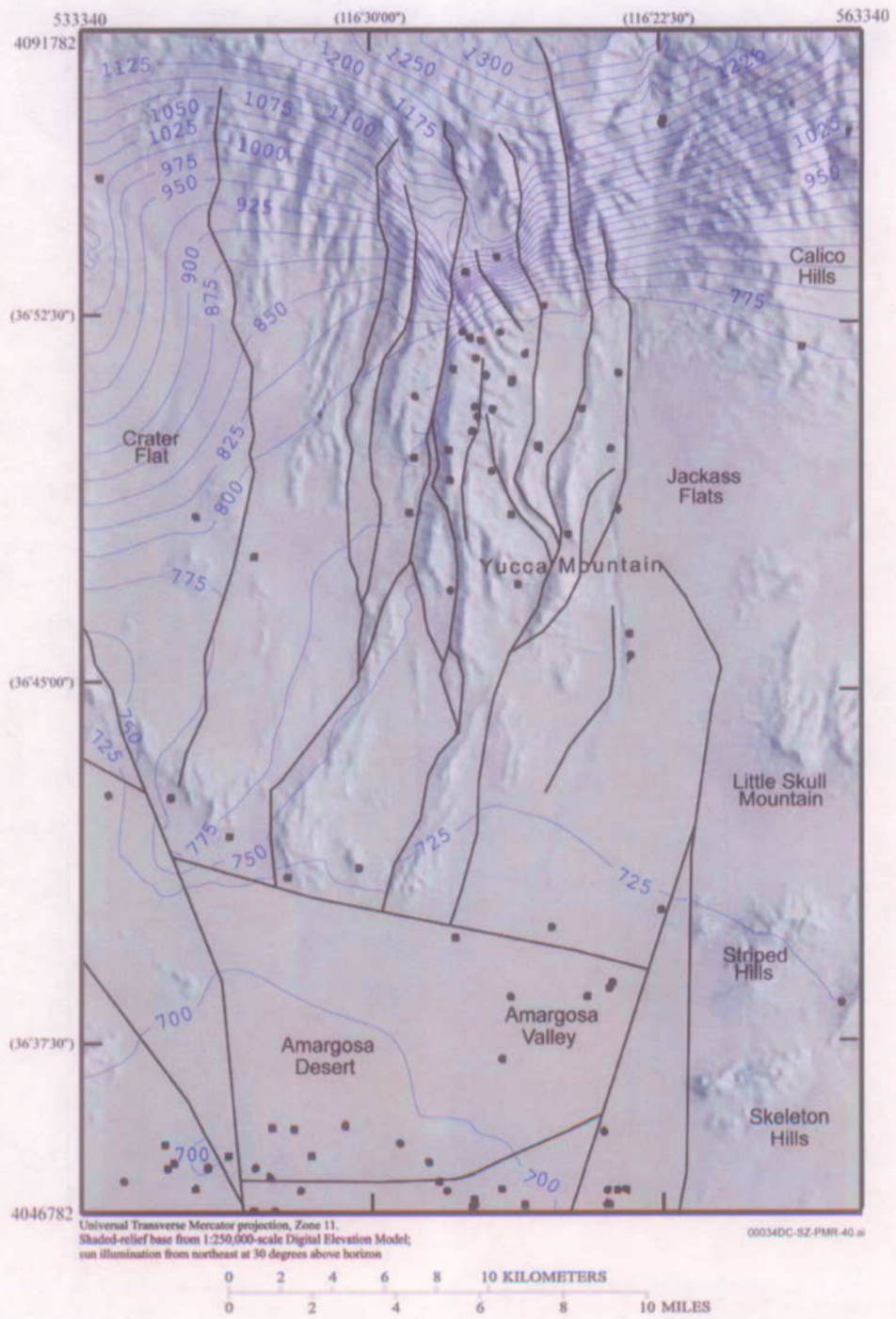
2.3.3 Site-Scale Potentiometric Surface

Figure 2-18 depicts the results of an analysis of water-level data prepared by the U.S. Geological Survey to provide the potentiometric surface within the site-scale model domain and target water-level data for model calibration (USGS 2001b). During this analysis, the water-level data were used to generate a single representative potentiometric surface for the saturated zone site-scale model domain. When developing the potentiometric surface, water-level altitudes

representing the uppermost aquifer system, typically the volcanic or alluvial system, were used. The water-level altitudes in some boreholes represent composite heads from multiple hydrogeologic units and fracture zones. Generally, water levels in the uppermost saturated zone appear to represent a laterally continuous, well-connected aquifer system. However, locally, it is possible that either the observed uppermost potential represents a perched or semiconfined interval, or that a more transmissive unit deeper in the borehole controls the local potential. The faults depicted in Figure 2-18 are described by BSC (2003c) and USGS (2001b).

The USGS (2001a) provided an updated analysis of water-level data (Figure 2-19). This analysis included water-level data collected through December 2000, including water-level data obtained from the expanded Nye County Early Warning Drilling Program and data from borehole USW WT-24. In addition to the inclusion of new water-level data, the primary difference in the approach taken to generate the revised potentiometric surface was the assumption that water levels in the northern portion of the model domain from boreholes USW G-2 and UE-25 WT #6 represent perched conditions and are not representative of the regional potentiometric surface. As a result, the revised potentiometric surface map represents an alternate concept for the large hydraulic gradient area north of Yucca Mountain.

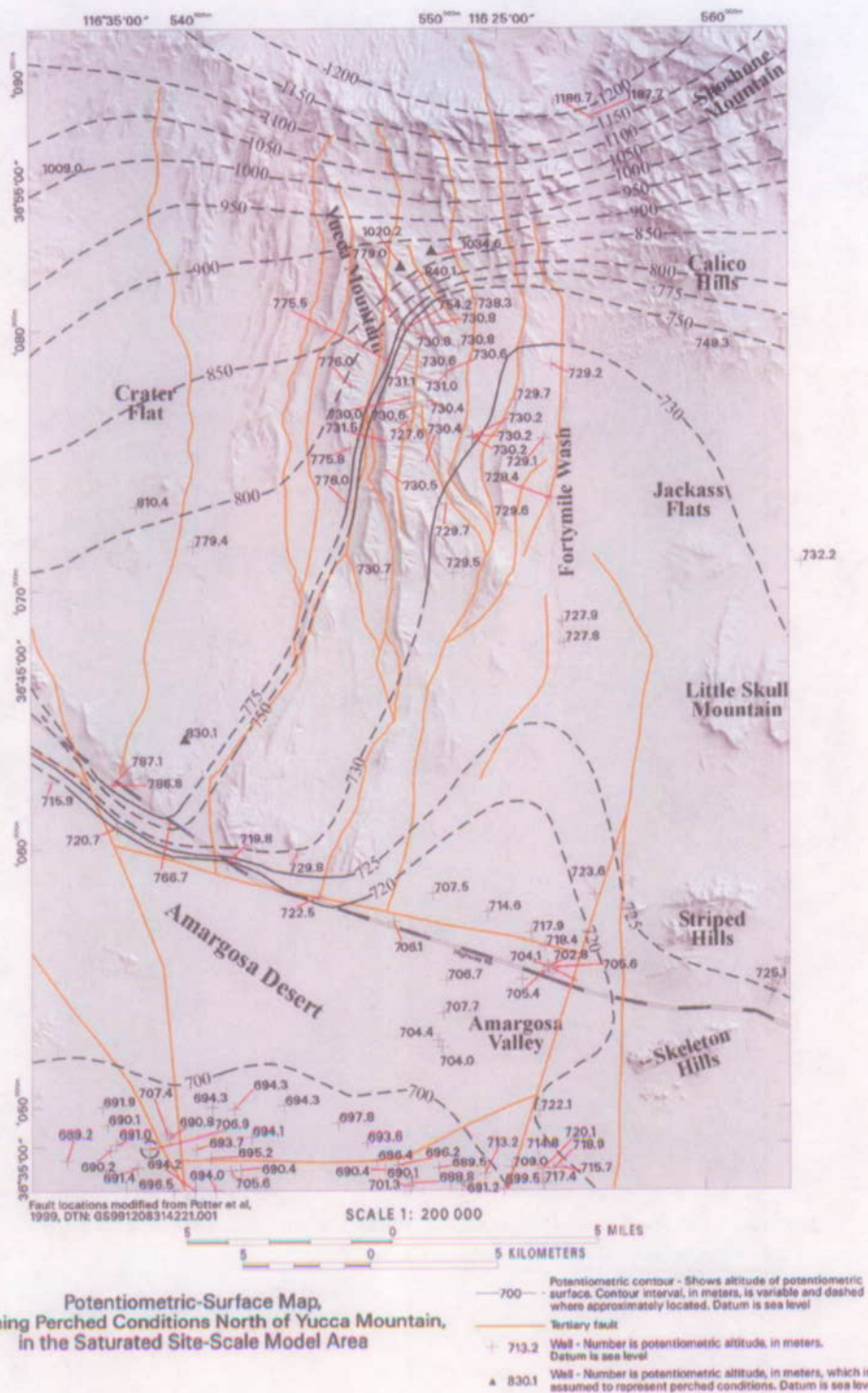
Comparison of Figures 2-18 and 2-19 indicate that the potentiometric surface maps are similar. Although differences can be noted in these two conceptualizations, both potentiometric surfaces indicate a predominately southerly component of groundwater flow in this area.



Source: USGS 2001b, Figure 1-2.

NOTE: Black lines indicate major faults, which are identified in the source document.

Figure 2-18. Nominal Site-Scale Potentiometric Surface



Source: USGS 2001a, Figure 6-1.

Figure 2-19. Alternative Site-Scale Potentiometric Surface

Based on the above potentiometric surface maps, three distinct hydraulic gradient areas in the vicinity of Yucca Mountain have been identified: (1) a large hydraulic gradient between water-level altitudes of 1,030 m and 750 m at the northern end of Yucca Mountain, (2) a moderate hydraulic gradient west of the crest of Yucca Mountain, and (3) a small hydraulic gradient extending from Solitario Canyon to Fortymile Wash.

A number of explanations have been proposed to explain the presence of the large hydraulic gradient at the north end of Yucca Mountain (Czarnecki and Waddell 1984; Ervin et al. 1994). Explanations proposed for the large hydraulic gradient include:

1. Faults that contain nontransmissive fault gouge
2. Faults that juxtapose transmissive tuff against nontransmissive tuff
3. The presence of a less fractured lithologic unit
4. A change in the direction of the regional stress field and a resultant change in the intensity, interconnectedness, and orientation of open fractures on either side of the area with the large hydraulic gradient
5. A disconnected, perched or semi-perched water body (i.e., the high water-level altitudes are caused by local hydraulic conditions and are not part of the regional saturated zone flow system).

The cause of the moderate hydraulic gradient is generally believed to be the result of the Solitario Canyon fault and its splays functioning as a barrier to flow from west to east due to the presence of low-permeability fault gouge or to the juxtaposition of more permeable units against less permeable units (Luckey et al. 1996, p. 25).

The small hydraulic gradient occupies most of the repository area and the downgradient area eastward to Fortymile Wash. Over a distance of 6 km, the hydraulic gradient declines only about 2.5 m between the crest of Yucca Mountain and Fortymile Wash. The small gradient could indicate highly transmissive rocks, little groundwater flow in this area, or a combination of both (Luckey et al. 1996, p. 27).

In addition to an understanding of the areal hydraulic potential gradient distribution, local vertical potential gradients have been observed in individual boreholes that have isolated test intervals. The results of these individual head observations are tabulated in Table 2-5. Depending on the location of the borehole, small vertical potential differences are probably not indicative of vertical flow, but, instead, represent the degree of horizontal heterogeneity within the aquifer that is tested. However, large vertical potential differences, such as those between the carbonate aquifer and the overlying tuff or alluvial aquifers, are generally representative of more extensive flow field differences.

The vertical hydraulic gradients in the vicinity of Yucca Mountain are generally oriented upward (i.e., they are positive values in Table 2-5). These upward gradients effectively limit the downward potential for migration of water within the tuff aquifers or between the tuff aquifers

Table 2-5. Summary of Vertical Head Observations at Boreholes in the Vicinity of Yucca Mountain

Borehole	Open Interval (m below land surface)	Potentiometric Level (m above sea level)	Head Difference deepest to shallowest intervals (m)
USW H-1 tube 4	573-673	730.94	54.7
USW H-1 tube 3	716-765	730.75	
USW H-1 tube 2	1097-1123	736.06	
USW H-1 tube 1	1783-1814	785.58	
USW H-3 upper	762-1114	731.19	28.9
USW H-3 lower	1114-1219	760.07	
USW H-4 upper	525-1188	730.49	0.1
USW H-4 lower	1188-1219	730.56	
USW H-5 upper	708-1091	775.43	0.2
USW H-5 lower	1091-1219	775.65	
USW H-6 upper	533-752	775.99	2.2
USW H-6 lower	752-1220	775.91	
USW H-6	1193-1220	778.18	
UE-25 b #1 upper	488-1199	730.71	-1.0
UE-25 b #1 lower	1199-1220	729.69	
UE-25 p #1 (volcanic)	384-500	729.90	21.4
UE-25 p #1 (carbonate)	1297-1805	751.26	
UE-25 c #3	692-753	730.22	0.4
UE-25 c #3	753-914	730.64	
USW G-4	615-747	730.3	-0.5
USW G-4	747-915	729.8	
UE-25 J -13 upper	282-451	728.8	-0.8
UE-25 J -13	471-502	728.9	
UE-25 J -13	585-646	728.9	
UE-25 J -13	820-1063	728.0	
NC-EWDP-1DX (shallow)	WT-419	786.8	-38.0
NC-EWDP-1DX (deep)	658-683	748.8	
NC-EWDP-2D (volcanic)	WT-493	706.1	7.6
NC-EWDP-2DB (carbonate)	820-937	713.7	
NC-EWDP-3S probe 2	103-129	719.8	-1.5
NC-EWDP-3S probe 3	145-168	719.4	
NC-EWDP-3D	WT-762	718.3	
NC-EWDP-4PA	124-148	717.9	5.7
NC-EWDP-4PB	225-256	723.6	
NC-EWDP-7SC probe 1	24-27	818.1	-77.9
NC-EWDP-7SC probe 2	55-64	786.4	
NC-EWDP-7SC probe 3	82-113	756.6	
NC-EWDP-7SC probe 4	131-137	740.2	
NC-EWDP-9SX probe 1	27-37	766.7	0.1
NC-EWDP-9SX probe 2	43-49	767.3	
NC-EWDP-9SX probe 4	101-104	766.8	
NC-EWDP-12PA	99-117	722.9	2.2
NC-EWDP-12PB	99-117	723.0	
NC-EWDP-12PC	52-70	720.7	
NC-EWDP-19P	109-140	707.5	5.3
NC-EWDP-19D	106-433	712.8	

Source: Based on USGS 2001a, Table 6-1.

NOTE: Negative values indicate downward gradient.

and the underlying carbonate aquifer. Although locally downward hydraulic gradients are possible, these have been attributed to the presence of local recharge conditions and low permeability confining units. Additional details on observed vertical gradients in the vicinity of Yucca Mountain are presented in Appendix B.

Only two sites, UE-25 p #1 and NC-EWDP-2D/2DB, provide information on vertical gradients between volcanic rocks and the underlying Paleozoic carbonate rocks. At UE-25 p #1, water levels currently are monitored only in the carbonate aquifer; however, water-level data were obtained from within the volcanic rocks as the borehole was drilled and tested. At this site, water levels in the Paleozoic carbonate rocks are about 20 m higher than those in the overlying volcanic rocks. Borehole NC-EWDP-2DB penetrated Paleozoic carbonate rocks toward the bottom of the borehole (Spengler 2001a). Water levels measured within that deep part of the borehole are about 8 m higher than levels measured in volcanic rocks penetrated by borehole NC-EWDP-2D.

Water levels monitored in the lower part of the volcanic-rock sequence at Yucca Mountain also are generally higher than levels monitored in the upper part of the volcanics. For examples, boreholes USW H-1 (tube 1) and USW H-3 (lower interval) both monitor water levels in the lower part of the volcanic rock sequence, and upward gradients are observed at these boreholes with head differences of 55 and 29 m, respectively. The gradient at USW H-3 is not completely characterized because the water levels in the lower interval had been continuously rising before the packer that separates the upper and lower intervals failed in 1996.

An upward gradient is also observed between the alluvial deposits monitored in borehole NC-EWDP-19P and underlying volcanic rocks monitored in borehole NC-EWDP-19D. The vertical head difference at this site is 5.3 m; however, levels reported for NC-EWDP-19D represent a composite water level for the alluvium and volcanics, so that the true head difference between those units is not completely known.

Several downward gradients have also been observed within the saturated zone site-scale flow and transport model area (Table 2-5). The largest downward gradient is observed between the deep and shallow monitored intervals at borehole NC-EWDP-1DX (head difference of 38 m) and NC-EWDP-7S (head difference of about 78 m). The depth to water at both of these locations is anomalously shallow and probably represents either locally perched conditions or the presence of a low permeability confining unit close to the surface that effectively impedes the downward migration of water to the more contiguous tuff and alluvium aquifers at greater depths.

2.3.4 Site-Scale Hydrogeologic Framework

The site-scale hydrogeologic framework represents the site hydrostratigraphy at a scale commensurate with the scale of the flow system and sufficient to define the different hydrogeologic units through which water may migrate from the repository block to a compliance point about 18 km south of Yucca Mountain. Understanding the various lithologic units through which water migrates is important due to the unique transport characteristics of the different lithologies in the vicinity of Yucca Mountain. In particular, the transport characteristics of fractured and porous welded tuffs are different from fractured nonwelded tuffs, which are both different from the porous alluvium. Of particular interest to the behavior of the saturated zone

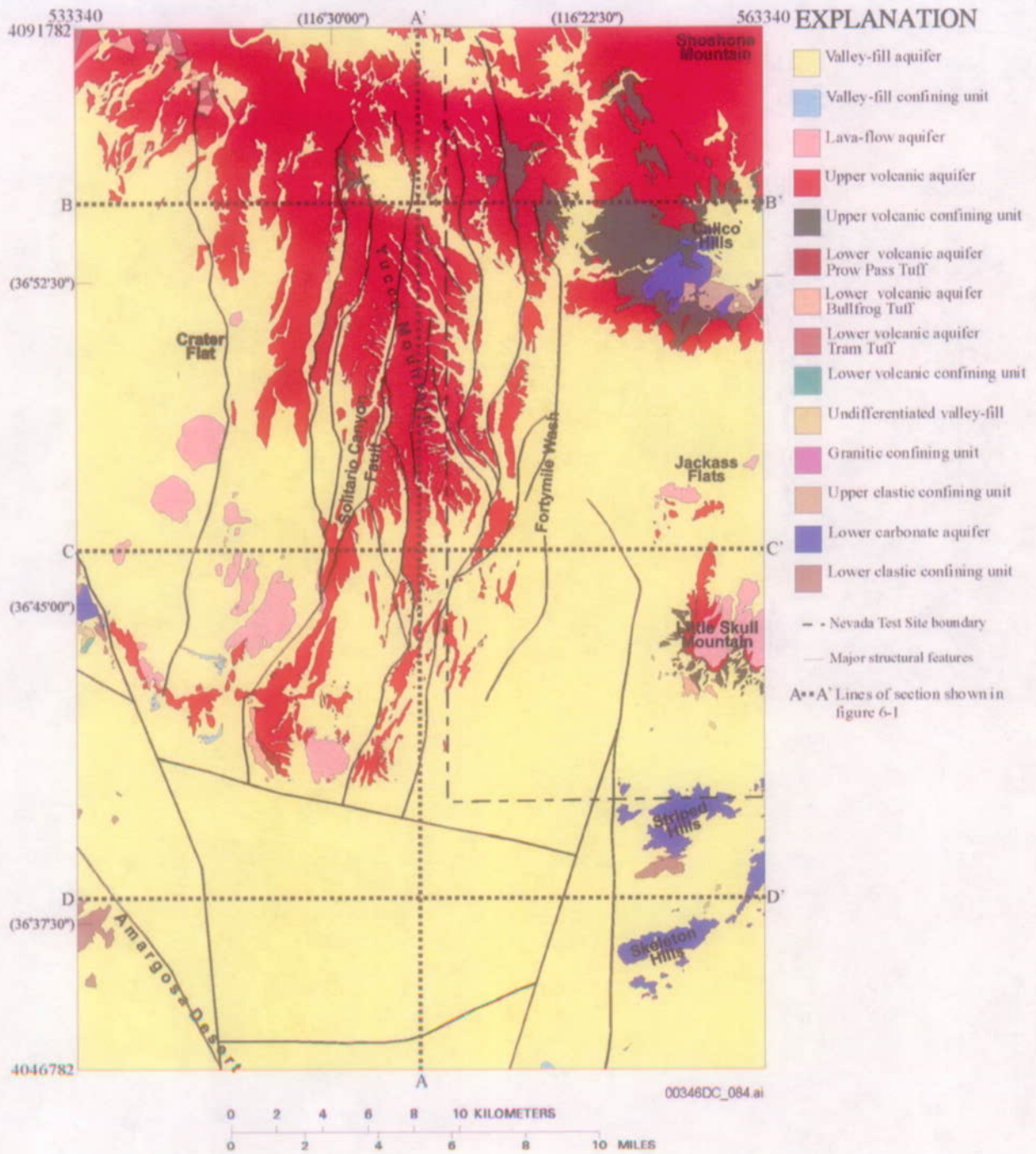
barrier at Yucca Mountain are the effective porosity and retardation characteristics of the different lithologies, as well as the relative travel length in the alluvial aquifer.

The hydrogeologic framework sets the lithologic constraints through which water is likely to flow. This framework is based on direct outcrop observations (Figure 2-20), geologic observations from boreholes in the area, interpolation from the regional hydrogeology, geophysical logs (in particular resistivity and seismic surveys), and geologic inferences of lithologic unit thicknesses from regional facies variations. Representative portions of the site-scale hydrogeologic framework model are presented in Figure 2-21.

Aspects of the site-scale geology that pertain to groundwater flow are represented in the site-scale hydrogeologic framework model. A detailed description of the hydrogeologic framework model, assumptions, and methods used to develop the model are given by USGS (2001c). A comparison of the hydrogeologic framework model revision with the geologic framework model used to evaluate the detailed site geology is presented in Appendix A.

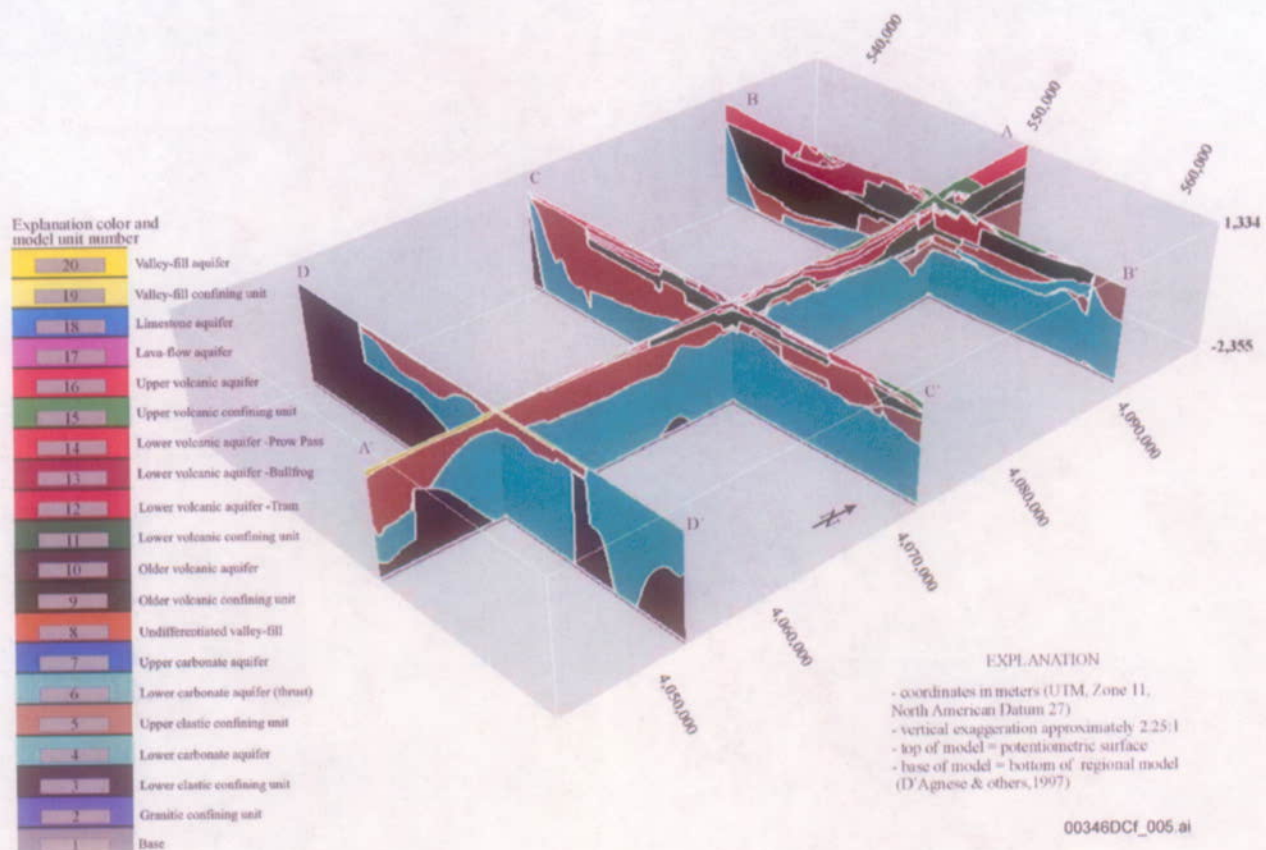
Since the development of the hydrogeologic framework model used in the license application base-case model, the Yucca Mountain hydrogeologic framework model has been reinterpreted incorporating data recently obtained from the Nye County Early Warning Drilling Program and through the reinterpretation of existing data from other areas (including geophysical data in the northern area of the site). The major changes in the revised hydrogeologic framework model are in the southern part of the model and include new information on the depths and extent of the alluvial layers.

As a result of the reinterpretation of the hydrogeologic framework model, the number and distribution of hydrogeologic units has been modified in the 2002 hydrogeologic framework model and now correspond to the units in the regional hydrogeologic framework model. A comparison of the hydrogeologic units identified in the hydrogeologic framework models used in the base-case and 2002 models is provided in Table 2-6. The table indicates that while there were 19 hydrogeologic units in the base-case hydrogeologic framework model, there are 27 hydrogeologic units in the 2002 hydrogeologic framework model. Four of the 27 units present in the regional model are not found within the boundary of the site-scale hydrogeologic framework model because they are pinched out by adjacent units. The hydrogeologic framework model revision has the same units and is consistent with the regional Death Valley Regional Flow System model (D'Agnese et al. 2002).



Source: USGS 2001c, Figure 4-2.

Figure 2-20. Outcrop Geology of the Site-Scale Hydrogeologic Framework Model



Source: USGS 2001c, Figure 6-1.

Note: On the figure, "D'Agnese & others, 1997" refers to D'Agnese et al. (1997).

Figure 2-21. Representative Cross-Sections through the Site-Scale Hydrogeologic Framework Model

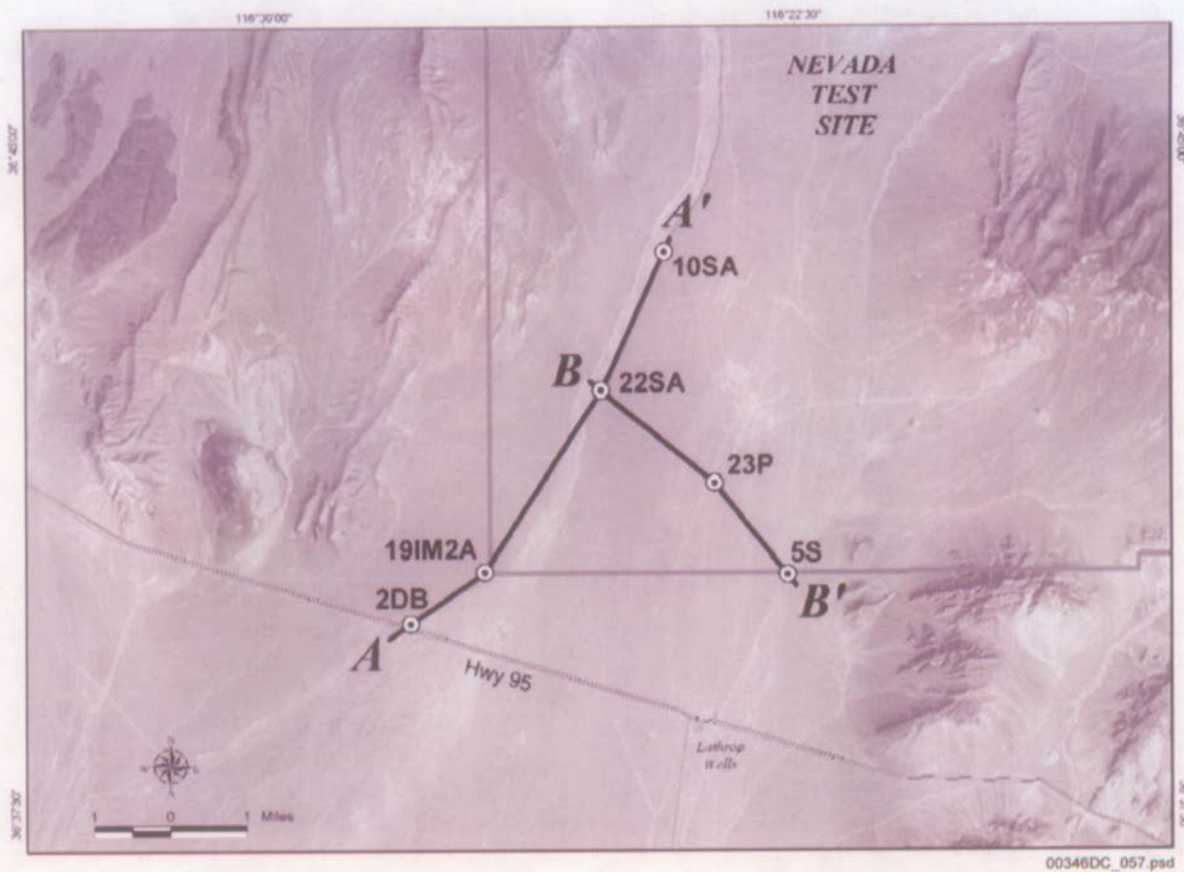
Table 2-6. Correspondence between Units of the Revised- and Base-Case Hydrogeologic Framework Models

Abbreviation	Revised (Site and Regional Transient Model in Preparation)		Base-Case Hydrogeologic Framework Model	
	Hydrogeologic Name	Unit	Unit	Hydrogeologic Name
Base	Base (-4000 m)	1	1	Base (bottom of regional flow model)
ICU	Intrusive Confining Unit	2	2	Granitic confining unit (granites)
XCU	Crystalline Confining Unit	3	3	Lower Clastic Confining Unit (lccu)
LCCU	Lower Clastic Confining Unit	4	3	Lower Clastic Confining Unit (lccu)
LCA	Lower Carbonate Aquifer	5	4	Lower Carbonate Aquifer (lca)
UCCU	Upper Clastic Confining Unit	6	5	Upper Clastic Confining Unit, Upper Clastic Confining Unit-thrust 2 (uccu, uccut2)
UCA	Upper Carbonate Aquifer	7	NA	NA
LCCU_T1	Lower Clastic Confining Unit – thrust	8	NA	Lower Clastic Confining Unit-thrust 1 (lccut1)
LCA_T1	Lower Carbonate Aquifer – thrust	9	6	Lower Carbonate Aquifer thrusts 1 and 2 (lcat1, lcat2)
VSU Lower	Lower Volcanic and Sedimentary Units	11	8	Undifferentiated valley-fill (leaky)
OVU	Older Volcanic Units	12	9,10,11	Older Volcanic Confining Unit, Older Volcanic Aquifer, Lower Volcanic Confining Unit (lvcu, lva, mvcu)
BRU	Belted Range Unit (none in site area)	NA	NA	NA
CFTA	Crater Flat - Tram Aquifer	14	12	Lower Volcanic Aquifer-Tram Tuff (tct)
CFBCU	Crater Flat - Bullfrog Confining Unit	15	13	Lower Volcanic Aquifer-Bullfrog Tuff (tcb)
CFPPA	Crater Flat - Prow Pass Aquifer	16	14	Lower Volcanic Aquifer-Prow Pass Tuff (tcp)
WVU	Wahmonie Volcanic Unit	17	15	Upper Volcanic Confining Unit (uvcu)
CHVU	Calico Hills Volcanic Unit	18	15	Upper Volcanic Confining Unit (uvcu)
PVA	Paintbrush Volcanic Aquifer	19	16	Upper Volcanic Aquifer (uva)
TMVA	Timber Mountain Volcanic Aquifer	20	16	Upper Volcanic Aquifer (uva)
VSU	Volcanic and Sedimentary Units	21	8	Undifferentiated valley-fill (leaky)
YVU	Young Volcanic Units (none in site area)	NA	NA	NA
LFU	Lavaflow Unit	23	17	Lava-flow Aquifer (basalts)
LA	Limestone Aquifer	24	18	Limestone Aquifer (amarls)
OACU	Older Alluvial Confining Unit (none in site area)	NA	NA	NA
OAA	Older Alluvial Aquifer	26	20	Valley-fill Aquifer (alluvium), Undifferentiated valley-fill (leaky)
YACU	Young Alluvial Confining Unit	27	19	Valley-fill Confining Unit (playas)
YAA	Young Alluvial Aquifer	28	20	Valley-fill Aquifer (alluvium)

Source: BSC 2003c, Table 7.5-2.

NOTE: These units do not have a one-to-one correlation. This table approximately relates the new hydrogeologic units to the base-case version. Four units that do not occur in the site-scale hydrogeologic framework model (OACU, YVU, BRU, and SCU) are included here to maintain the relationship to the regional model.

The development of the 2002 site-scale hydrogeologic framework model revision was influenced primarily by geologic observations made from Nye County wells drilled since the earlier version of the model. Although these wells serve multiple geologic and hydrogeologic purposes, an important use has been to better characterize the thickness and lateral extent of the alluvial aquifer north of U.S. Highway 95. The location of these Nye County wells and cross-section lines are illustrated in Figure 2-22.

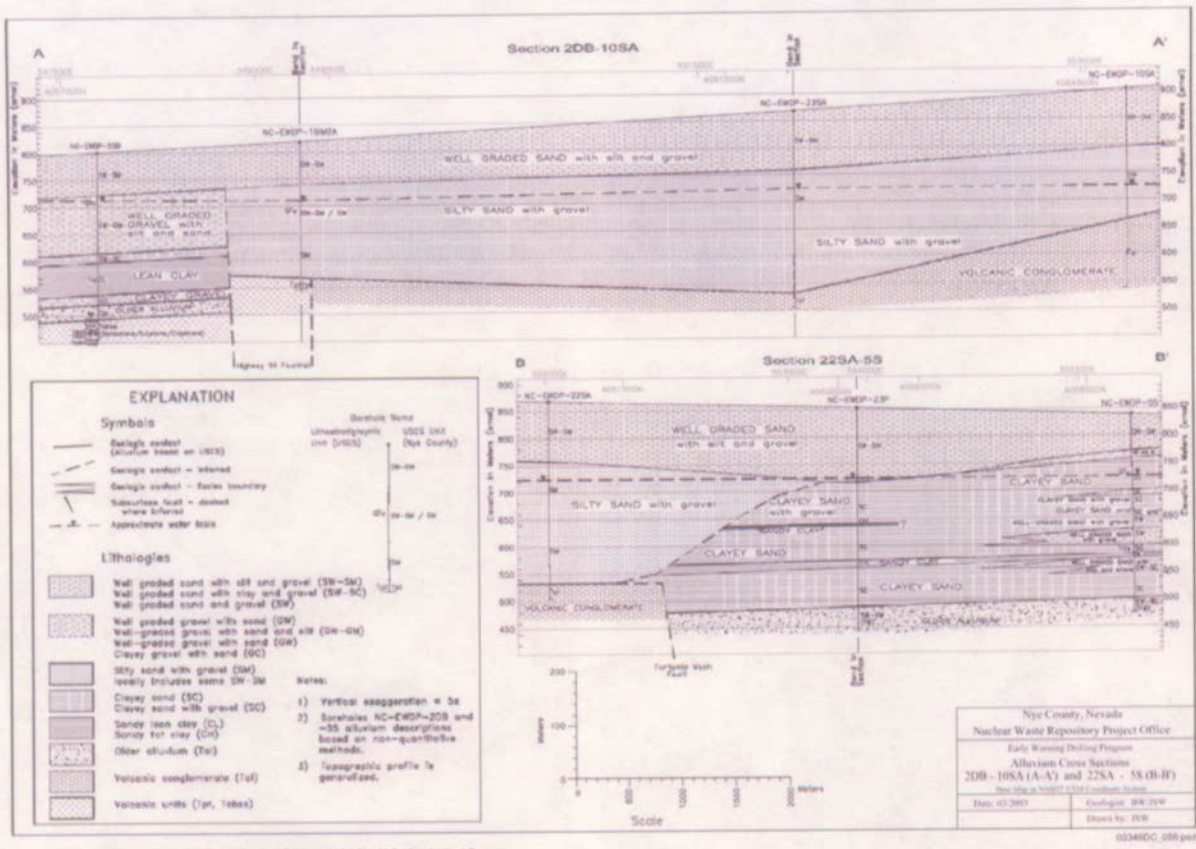


Source: Nye County Department of Natural Resources and Federal Facilities 2003, Figure 4.5-3.

NOTE: The cross sections A-A' and B-B' are shown in Figure 2-23.

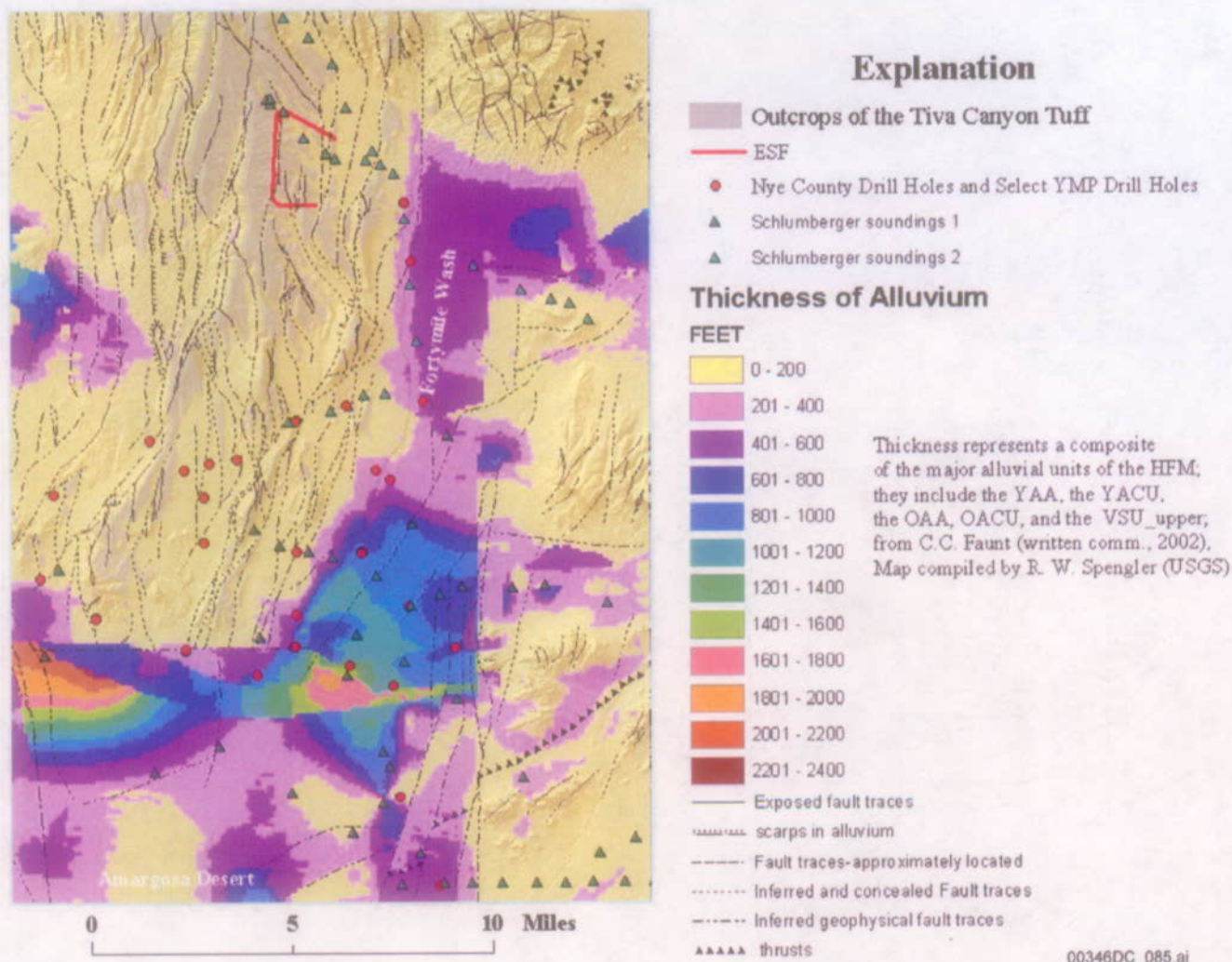
Figure 2-22. Locations of Nye County Alluvium Cross Sections

Figure 2-23 shows the cross-sections for these Nye County wells. Figures 2-24 and 2-25 depict the total alluvial thickness and saturated alluvial thickness derived from borehole observations and geophysical logging completed in the area between Yucca Mountain and U.S. Highway 95.



Source: Nye County Department of Natural Resources and Federal Facilities 2003, Figure 4.5-4.

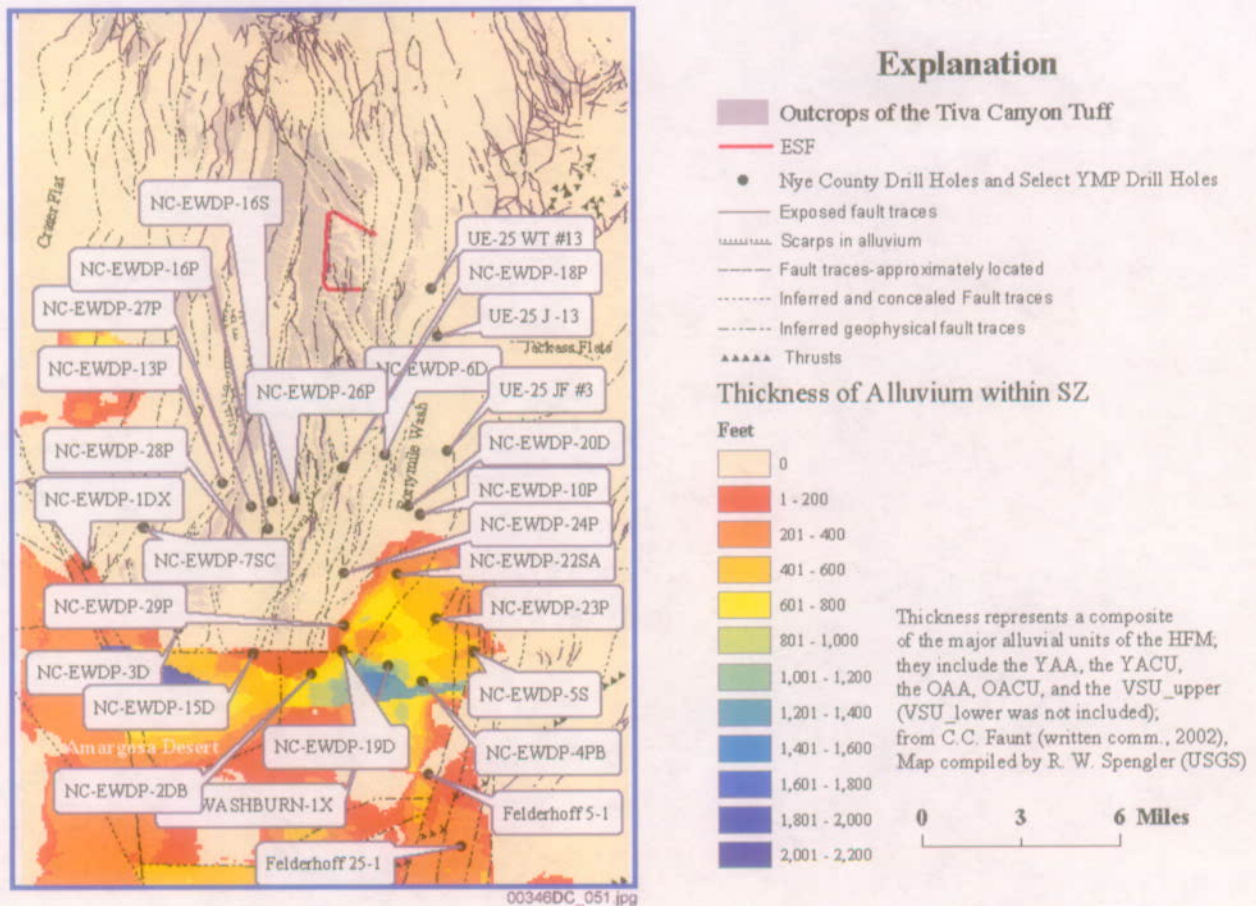
Figure 2-23. Nye County Alluvium Cross Sections



Thickness of Alluvial Deposits in the Vicinity of Yucca Mountain

Source: DTN: GS021008312332.002.

Figure 2-24. Alluvial Zone Total Thickness in the Site-Scale Hydrogeologic Model



Source: DTN: GS021008312332.002.

Figure 2-25. Alluvial Zone Saturated Thickness in the Site Scale Hydrogeologic Model

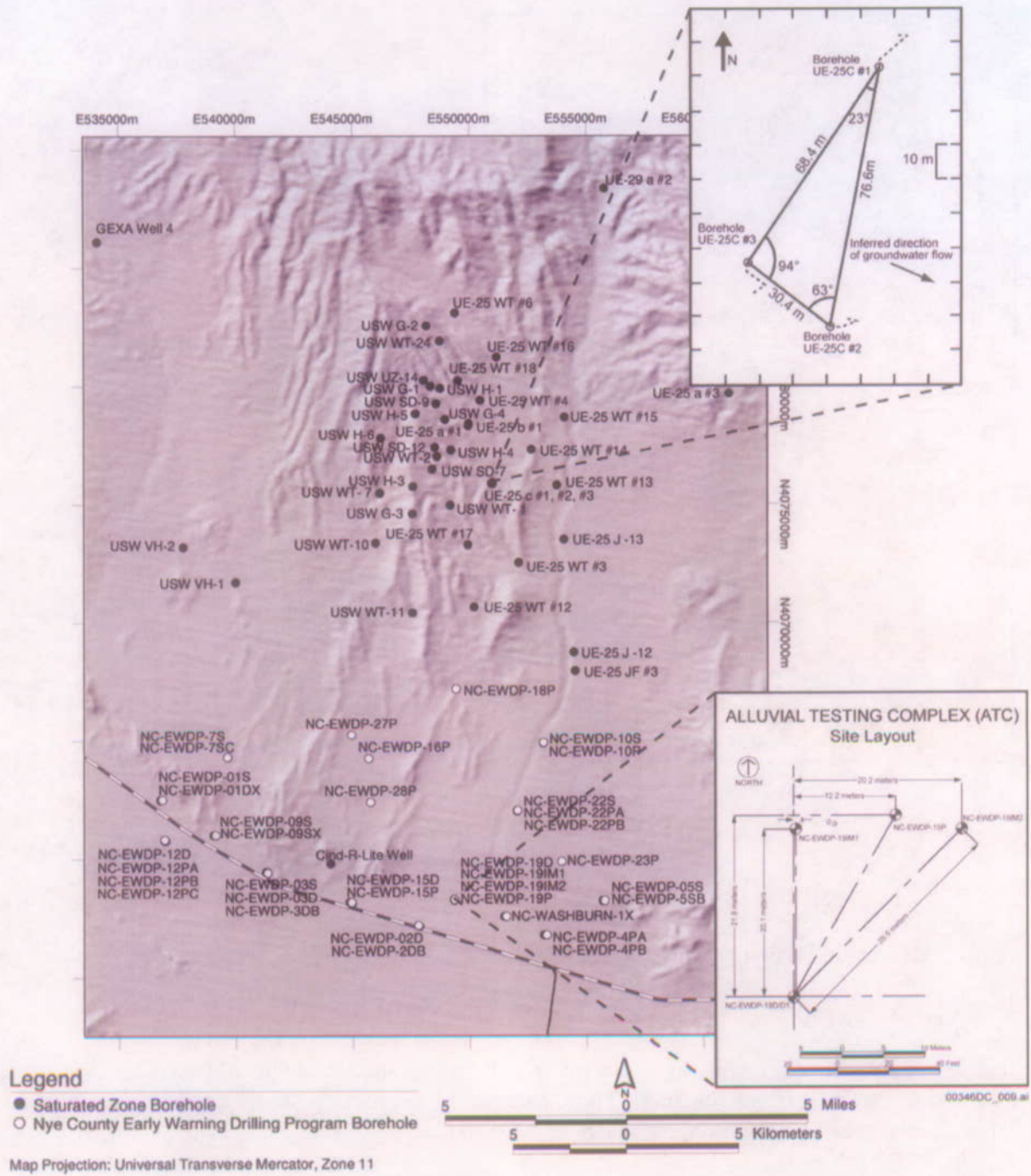
2.3.5 Site-Scale Hydrogeology

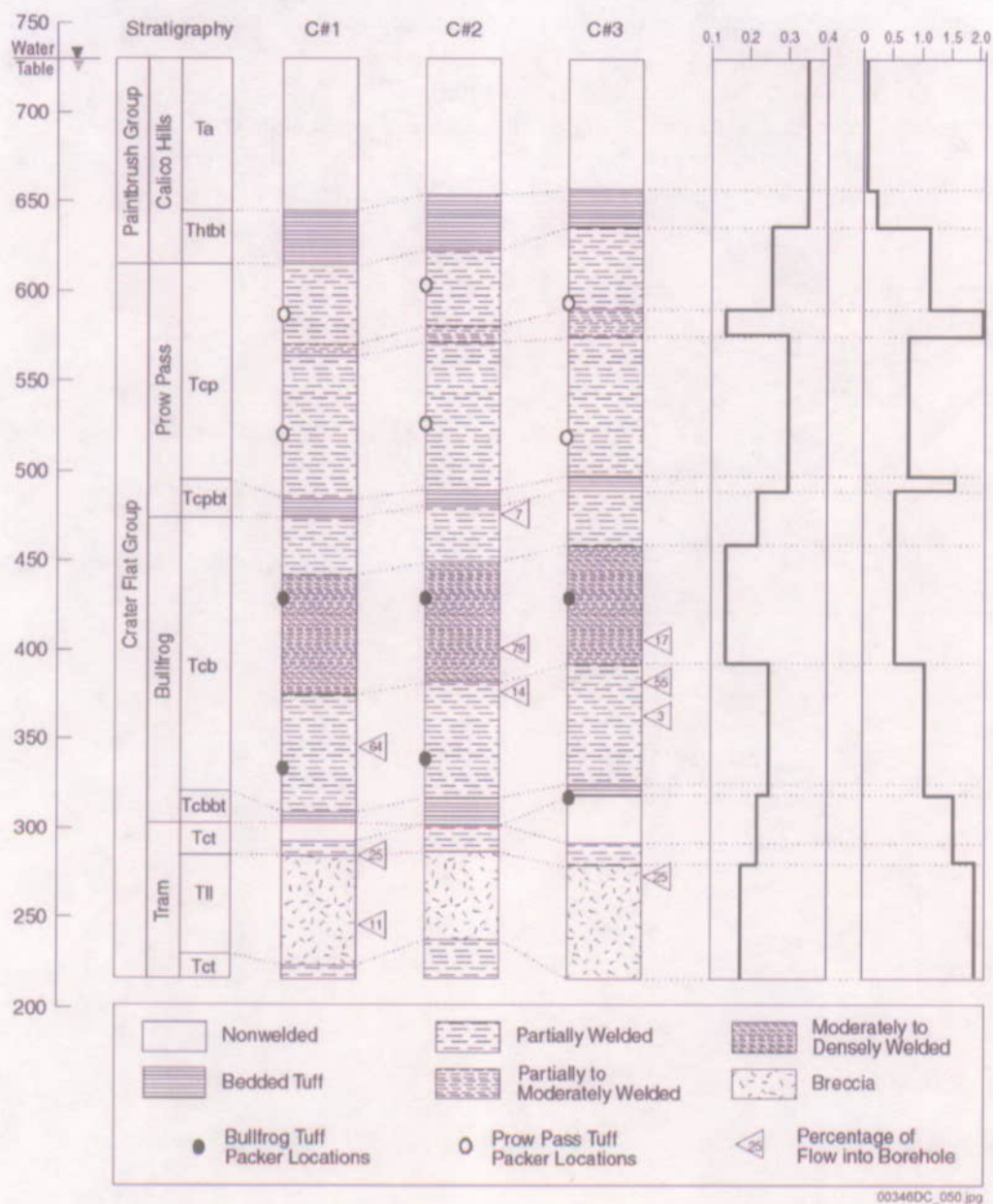
2.3.5.1 Site-Scale Hydrogeologic Characteristics

The permeability of rock units in the vicinity of Yucca Mountain has been determined by single well and crosshole hydraulic testing. These data have been used as starting points to support the calibration of the site-scale flow model (Section 2.3.7).

2.3.5.2 Tuff Hydrogeologic Characteristics Derived from Testing at the C-Wells

The C-Wells complex comprises a three-well configuration drilled and packed off in the Crater Flat Group. This complex is located about 700 m southeast of the South Portal of the Exploratory Study Facility (Figure 2-26), and has been used to test the hydraulic and transport characteristics of the tuff aquifers along the likely travel path of groundwater from Yucca Mountain. Figure 2-27 summarizes the well construction and identifies the major flowing intervals observed in these three wells.



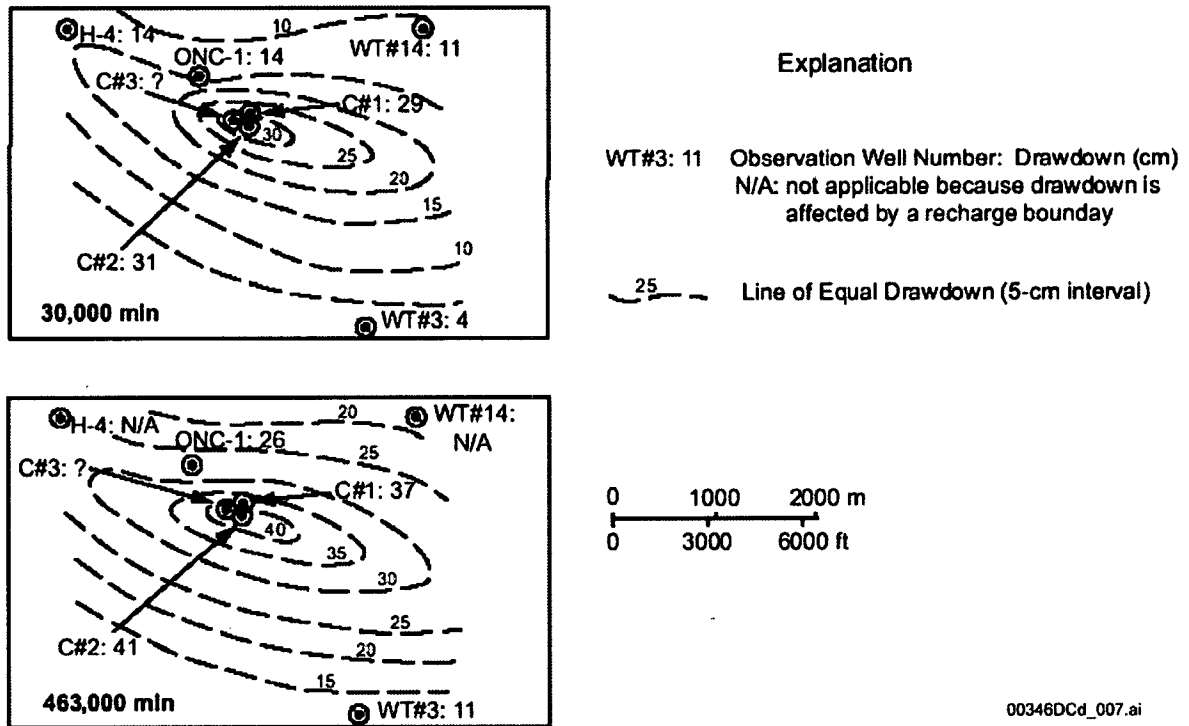


Source. BSC 2003e, Figure 6.1-2.

NOTE: Packer locations indicate intervals in which trace tests described in this report were conducted. (Note that the tracer tests were conducted between UE-25 C#2 and UE-25 C#3.) The two well logs represent the matrix porosity (dimensionless) and fracture density (number of fractures per meter), from left to right respectively

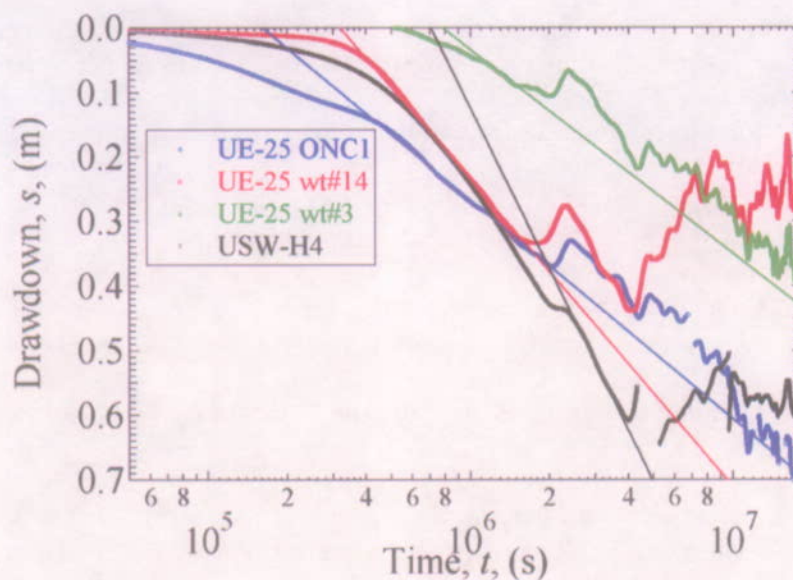
Figure 2-27. Stratigraphy, Lithology, Matrix Porosity, Fracture Density, and Inflow from Open-Hole Surveys at the C-Wells

In addition to the single- and cross-hole testing performed at the C-Wells, a large-scale pump test was performed in this complex. This test was conducted for more than a year and resulted in discernible drawdowns in wells located several kilometers away (Figures 2-28 and 2-29). These drawdowns indicate the lateral continuity of the saturated zone aquifer in these tuff rock units as well as the similarity in the transmissivities derived from this long-term test and the average hydraulic characteristics of these rocks in the vicinity of Yucca Mountain.



Source: BSC 2003e, Figure 6.2-36.

Figure 2-28. Distribution of Drawdown in Observation Wells at Two Times After Pumping Started in UE-25 C#3



Source: BSC 2003e, Figure 6.2-39.

Figure 2-29. Drawdowns Observed in Wells Adjacent to the C-Wells Complex during the Long Term Pumping Test

2.3.5.3 Site-Scale Permeability Anisotropy

Anisotropic conditions exist if the permeability of media varies as a function of direction. Because groundwater primarily flows in fractures within the volcanic units downgradient of Yucca Mountain, and because fractures and faults occur in preferred orientations, it is possible that anisotropic conditions of horizontal permeability exist along the pathway of potential radionuclide migration in the saturated zone (BSC 2003e, Section 6.2.6). Performance of the repository could be affected by horizontal anisotropy if the permeability tensor is oriented in a north-south direction because the groundwater flow could be diverted to the south, causing any transported solutes to remain in the fractured volcanic tuff for longer distances before moving into the valley-fill alluvial aquifer (Figures 2-24 and 2-25). More southerly oriented flow directions would, therefore, reduce the travel path length through the alluvium to the compliance point. A reduction in the length of the flow path in the alluvium would decrease the amount of radionuclide retardation that could occur for radionuclides with greater sorption capacity in the alluvium than in fractured volcanic rock matrix. In addition, potentially limited matrix diffusion in the fractured volcanic units could lead to shorter transport times in the volcanic units relative to the alluvium.

A conceptual model incorporating horizontal anisotropy in the tuff aquifer is acceptable, given that flow in the tuff aquifer generally occurs in a fracture network that exhibits a preferential north-south strike azimuth. Major faults near Yucca Mountain that have been mapped at the surface and that have been included in the site-scale hydrogeologic framework model also have a similar preferential orientation (Figure 2-20). In addition, north to north-northeast striking structural features are optimally oriented perpendicular to the direction of least principal

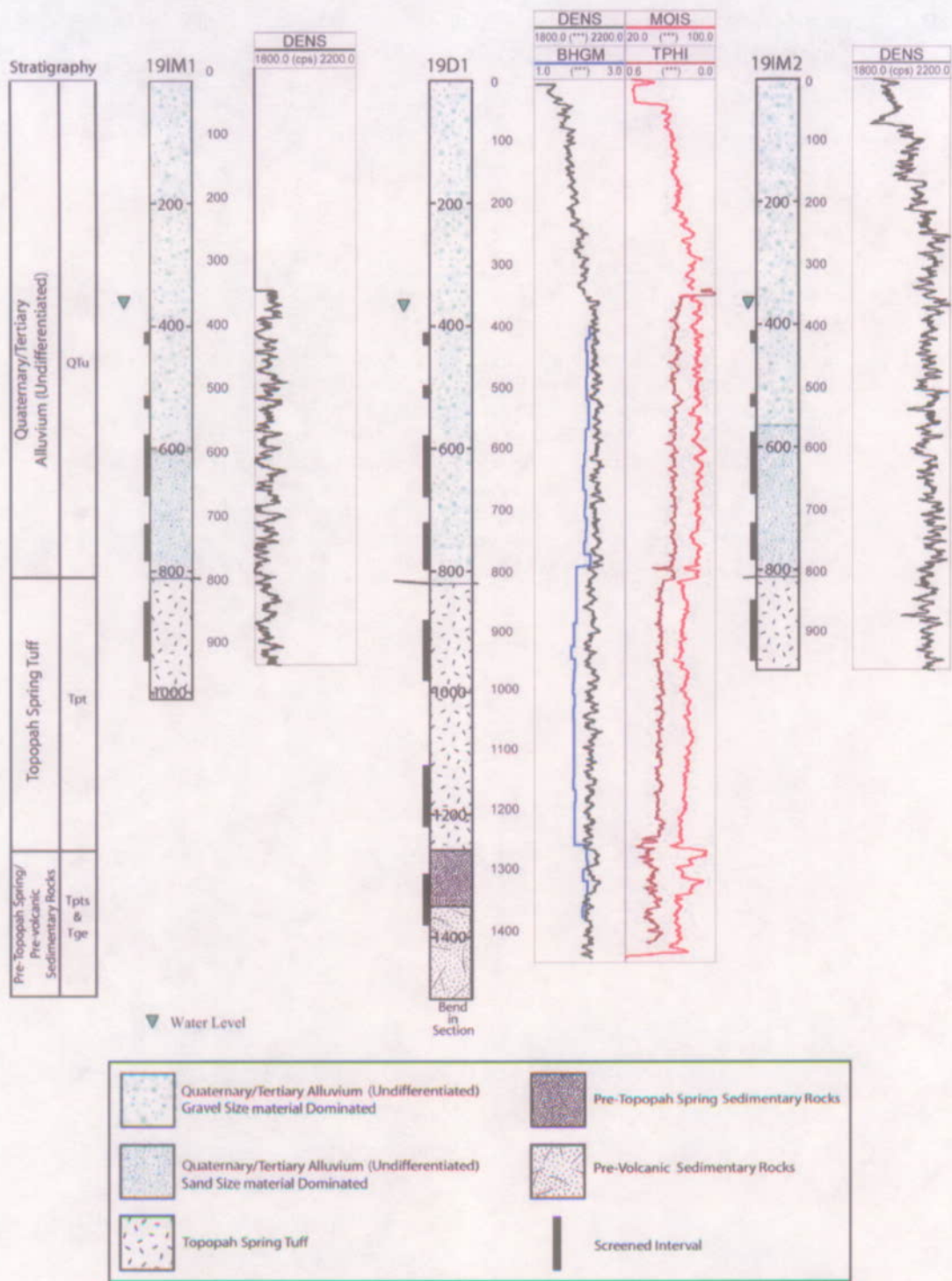
horizontal compressive stress, thus promoting flow in that direction, suggesting a tendency toward dilation and potentially higher permeability (Ferrill et al. 1999, pp. 5 to 6).

Evaluation of the long-term pumping tests at the C-Wells complex supports the conclusion that large-scale horizontal anisotropy of aquifer permeability may occur in the saturated zone. Results of this hydrologic evaluation presented in Appendix E generally are consistent with the structural analysis of potential anisotropy and indicate anisotropy that is oriented in a north-northeast to south-southwest direction, assuming the response in borehole H-4 is not considered. The response in borehole H-4 is consistent with the effect of the Antler Wash fault being superimposed on this uniform anisotropy, resulting in a north-west to south-east anisotropy.

2.3.5.4 Hydrogeologic Characteristics of the Alluvium Derived from Nye County Testing

Hydraulic testing of the alluvium has been performed at a number of Nye County wells. Of particular note is testing in the Alluvial Testing Complex (Figure 2-26). Figure 2-30 presents a summary of the lithology in the boreholes at the Alluvial Testing Complex.

One of the most important results of the testing at the Alluvial Testing Complex has been the interpretation of the "huff-puff" injection-withdrawal tracer test. In this test, a tracer is added to the wellbore and briefly injected into the aquifer. After a period of time (ranging from 0.5 days to 30 days), the tracer is pumped back. The migration of the tracer during the intervening time is controlled by the natural groundwater flux. The results of this test are illustrated in Figure 2-31. Although uncertainty exists in the interpretation of such tests, using reasonable ranges of effective porosity (varying between 5 and 30 percent), a range of specific discharges in the vicinity of the borehole can be determined. Table 2-7 presents the results of this analysis and indicates a specific discharge in the range of 1.2 to 9.4 m/yr.



Source: Questa Engineering Corporation 2002; lithostratigraphic logs Spengler 2001b; Spengler 2003a; Spengler 2003b.

Figure 2-30. Summary of Lithology and Flow Characteristics at Wells NC-EWDP-19D of the Alluvial Testing Complex

Table 2-7. Specific Discharges and Seepage Velocities Estimated from the Different Drift Analysis Methods as a Function of Assumed Flow Porosity

Assumed Flow Porosity ^a	Specific Discharge (m/yr.) / Seepage Velocity (m/yr.)		
	0.05	0.18	0.3
Peak Arrival Analysis	1.2 / 24.5	2.4 / 13.1	3.0 / 9.9
Late Arrival Analysis ^b	3.9 / 77.1	7.3 / 40.4	9.4 / 31.3
Mean Arrival Analysis ^c	2.0 / 40.3	3.8 / 20.9	4.9 / 16.4
Mean Arrival Analysis ^d	2.5 / 49.1	4.6 / 25.8	6.0 / 20.2
Linked Analytical Solutions	1.5 / 15 with a flow porosity of 0.10 and a longitudinal dispersivity of 5 m.		

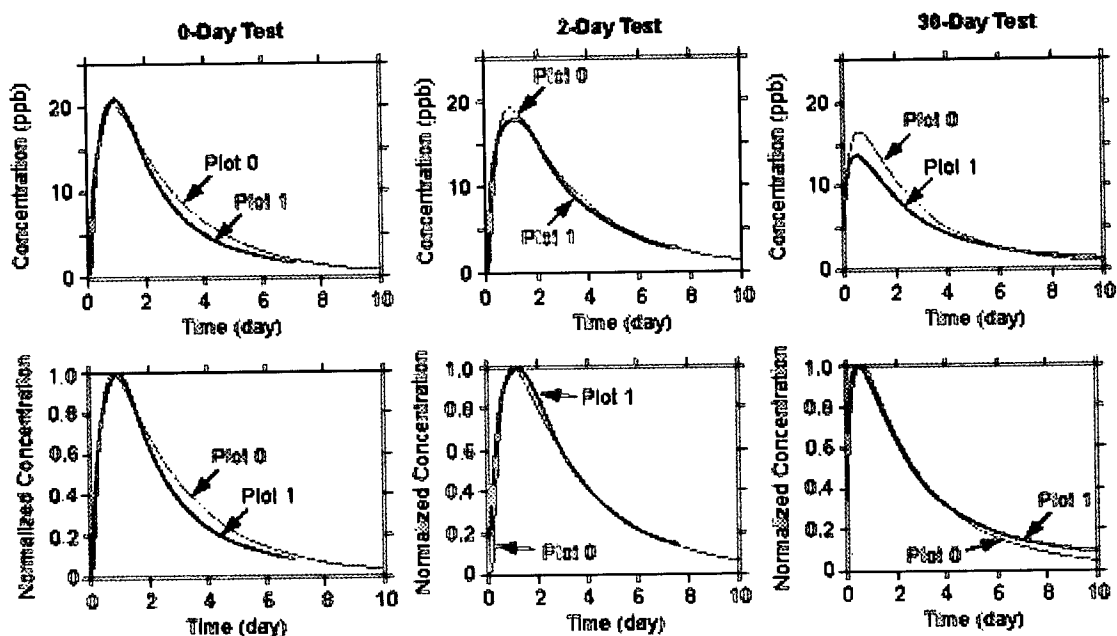
Source: BSC 2003e, Table 6.5-7.

NOTE: ^aThe three values are approximately the lowest, expected, and highest values of the alluvium flow porosity used in Yucca Mountain performance assessments (BSC 2001a).

^bTime/Volume associated with ~86.4 percent recovery in each test (the final recovery in the 0.5-hr rest period test, which had the lowest final recovery of any test).

^cMean arrival time calculated by truncating all tracer response curves at ~86.4 percent recovery in each test.

^dAlternative mean arrival time calculated by extrapolating the tracer response curves in the 0.5-hr rest period test to 91.3 percent and truncating the response curves in the two-day rest period test to 91.3 percent recovery (the final recovery in the 30-day rest period test).



Source: BSC 2003e, Figure 6.5-26.

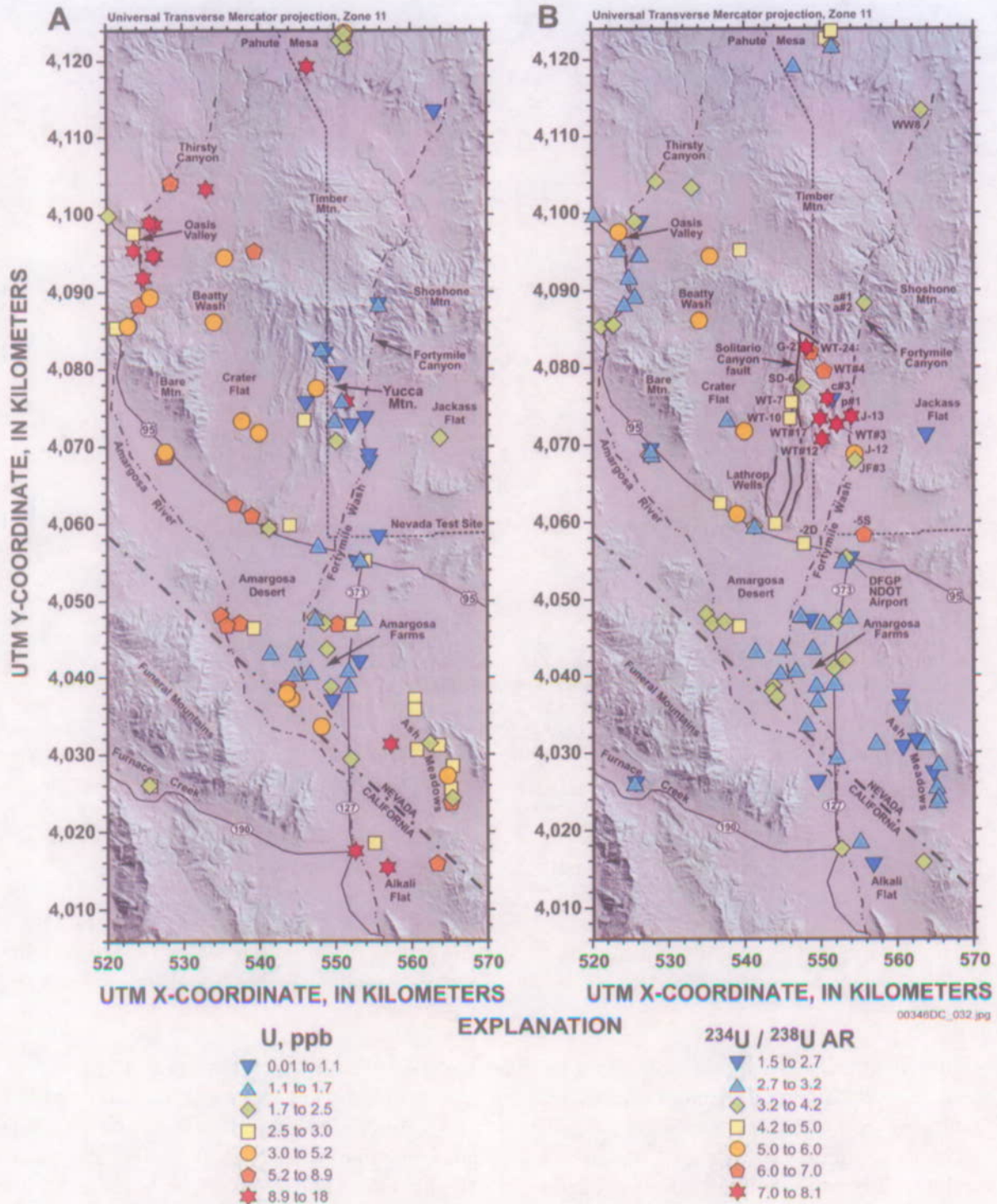
NOTE: The plots are fits of three injection-pumpback tracer tests with theoretical curves that result from three solutions to the advection-dispersion equation for the three phases of injection, drift, and pumpback. "Plot 0" is the model fit and "Plot 1" is the data curve. The parameters used in the calculations are: flow porosity = 0.1, matrix porosity = 0.0, longitudinal dispersivity = 5.05 m, transverse dispersivity = 1.00 m, test interval thickness = 32.0 ft, tracer volume injected = 2800 gal, chase volume injected = 22,000 gal, injection rate = 15.0 gpm, mass injected = 5.0 kg, natural gradient = 0.002 m/m, T for gradient = 20.0 m²/d, specific discharge = 1.5 m/yr., the Q values for the 0-, 2-, and 30-day tests are 13.41, 11.00, and 13.50, respectively.

Figure 2-31. Fitting the Injection-Pumpback Tracer Tests in Screen #1 of NC-EWDP-19D1 Using the Linked-Analytical Solutions Method

2.3.6 Site-Scale Geochemistry: Analyses of Water Types and Mixing

Hydrochemical data provide information on several important site-scale issues, including the existence and magnitude of local recharge, flow directions from the repository to downgradient locations, and the potential for mixing and dilution of groundwater that could be released from the repository.

Hydrochemical and isotopic data from perched water at Yucca Mountain compared to similar data from the regional groundwater system suggests that local recharge is a component of the saturated zone waters in volcanic aquifers beneath Yucca Mountain. The data examined included uranium isotopes (uranium-234/uranium-238; Figure 2-32) and major anions and cations. It is possible that shallow groundwater beneath Yucca Mountain is composed entirely of local recharge. For example, by comparing the isotopic signature of water obtained from the perched waters in wells USW UZ-14 and WT-24 with those of the saturated zone groundwater obtained from wells to the southeast, it is apparent that these waters have a similar origin, which is predominately from vertical recharge through the unsaturated tuff units in the vicinity of Yucca Mountain (BSC 2003f Section 6.7.6.6).



Source: Paces et al 2002, Figure 5.

Figure 2-32. Groundwater U and $^{234}\text{U}/^{238}\text{U}$ Ratios in the Vicinity of Yucca Mountain

The chloride concentrations of the groundwater identified from uranium isotopes as having originated from Yucca Mountain have been used to estimate the recharge flux through Yucca Mountain (BSC 2003f, Section 6.7.6.6). Based on the chloride data at these wells, and assuming that the chloride flux from precipitation was between one and two times its estimated present-day value, past infiltration rates ranged between about 6.5 and 16.5 mm/yr. These groundwater probably infiltrated during the late Pleistocene when the climate was cooler and wetter, so the relatively high infiltration rates should be interpreted as reflecting past, rather than present-day, conditions.

Despite the sometimes large distances between wells, the differences in regional groundwater chemical and isotopic compositions are often large enough that groundwater flow paths at a regional scale can be identified with some confidence (Figure 2-10). In contrast, despite the closer well spacing, the compositions of groundwaters in the immediate vicinity of Yucca Mountain are often too similar to allow detailed flow paths from the repository to be identified with certainty. However, because flow paths do not cross in plan view, possible flow directions from the repository area are constrained by regional Flow Paths 6 and 2 to be dominantly south or southeastward from the repository area. Geochemical inverse models (BSC 2003f, Section 6.7.8) for well NC-EWDP-19D indicated that groundwater at this well could have originated from the area of well WT-3 at the mouth of Dune Wash (as depicted by Flow Path 7), or as a result of the mixing of groundwater flowing from the vicinity of well USW WT-10 and local Yucca Mountain recharge (indicated schematically by small eastward-pointing arrows on Flow Path 6; Figure 2-10). An origin for NC-EWDP-19D groundwater from the Solitario Canyon area would imply groundwater from the repository area should be forced to flow southeastward toward Fortymile Wash; conversely, an origin for well NC-EWDP-19D groundwater from the Dune Wash area near well WT-3 implies that groundwater from the repository area flows along a more southerly trajectory.

2.3.7 Site Scale Groundwater Flow Model and Results

2.3.7.1 Site-Scale Groundwater Flow Model Development

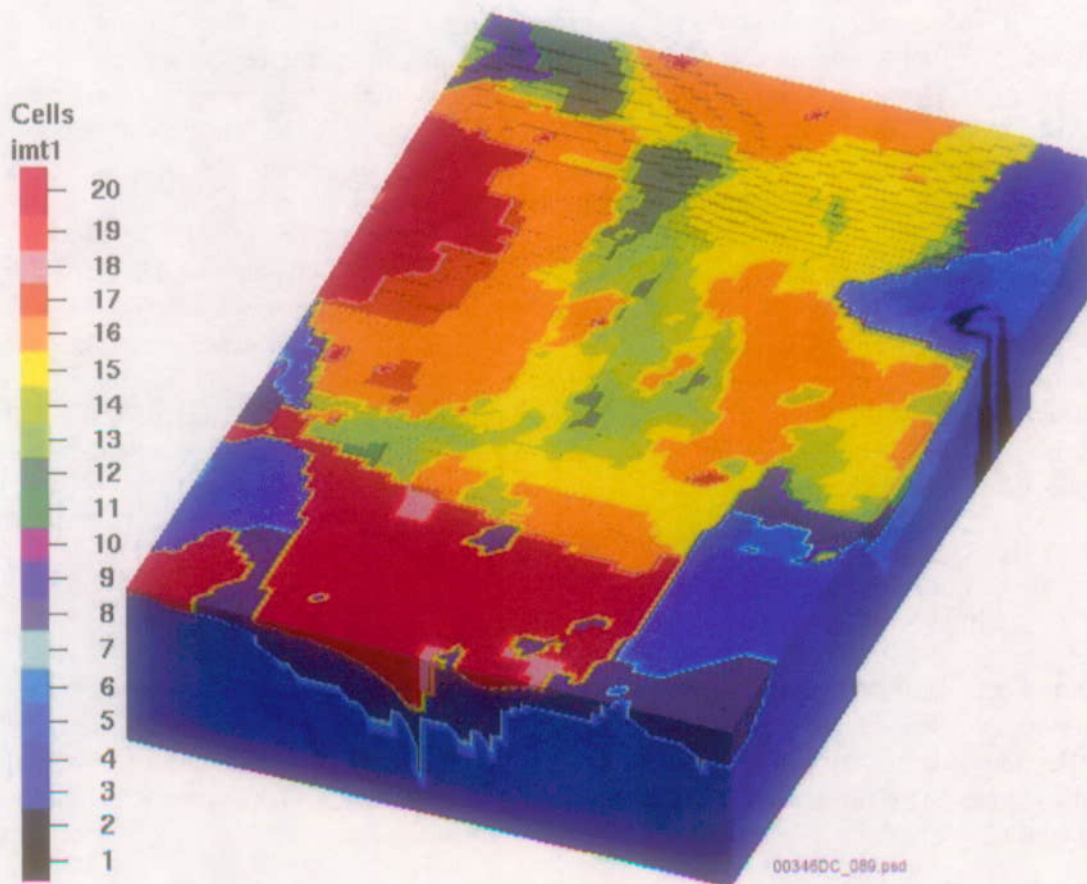
Development of the site-scale groundwater flow model requires the generation of a computational grid, the identification of the hydrogeologic unit at each node on the grid, the specification of boundary conditions, the specification of recharge values, and the assignment of nodal hydrogeologic properties. Each of these elements of model development is discussed in this section.

The computational grid developed for the site-scale saturated zone flow and transport model was formulated so that the horizontal grid is coincident with the grid cells in the regional-scale flow model. The depth of the computational grid is approximately the same as depth of the regional-scale saturated zone flow model. The computational grid begins at the water table surface and extends to a depth of 2,750 m below sea level.

The vertical grid spacing was established to provide the resolution necessary to represent flow and transport along critical flow and transport pathways in the saturated zone. A finer grid spacing was adopted for shallower portions of the model, while a progressively coarser grid was adopted for deeper portions of the aquifer. The vertical grid spacing ranged from 10 m near the

water table to 550 m at the bottom of the model domain. The vertical dimension of the model domain was divided into 11 zones, and constant vertical grid spacing was adopted in each of these 11 zones. In total, 38 model layers were included in the vertical dimension.

A three-dimensional representation of the base-case computational grid is provided in Figure 2-33. The grid is truncated at the water table surface, which is at 1,200 m in the north and 700 m in the south. The grid extends from Universal Transverse Mercator coordinates (Zone 11, North American Datum 1927) 533340E to 563340E in the east-west direction, and from 4046780N to 4091780N north-south direction. This representation of the computation grid illustrates the complex three-dimensional spatial relation among units within the site-scale model area.



Source: BSC 2003c, Figure 6.5-2.

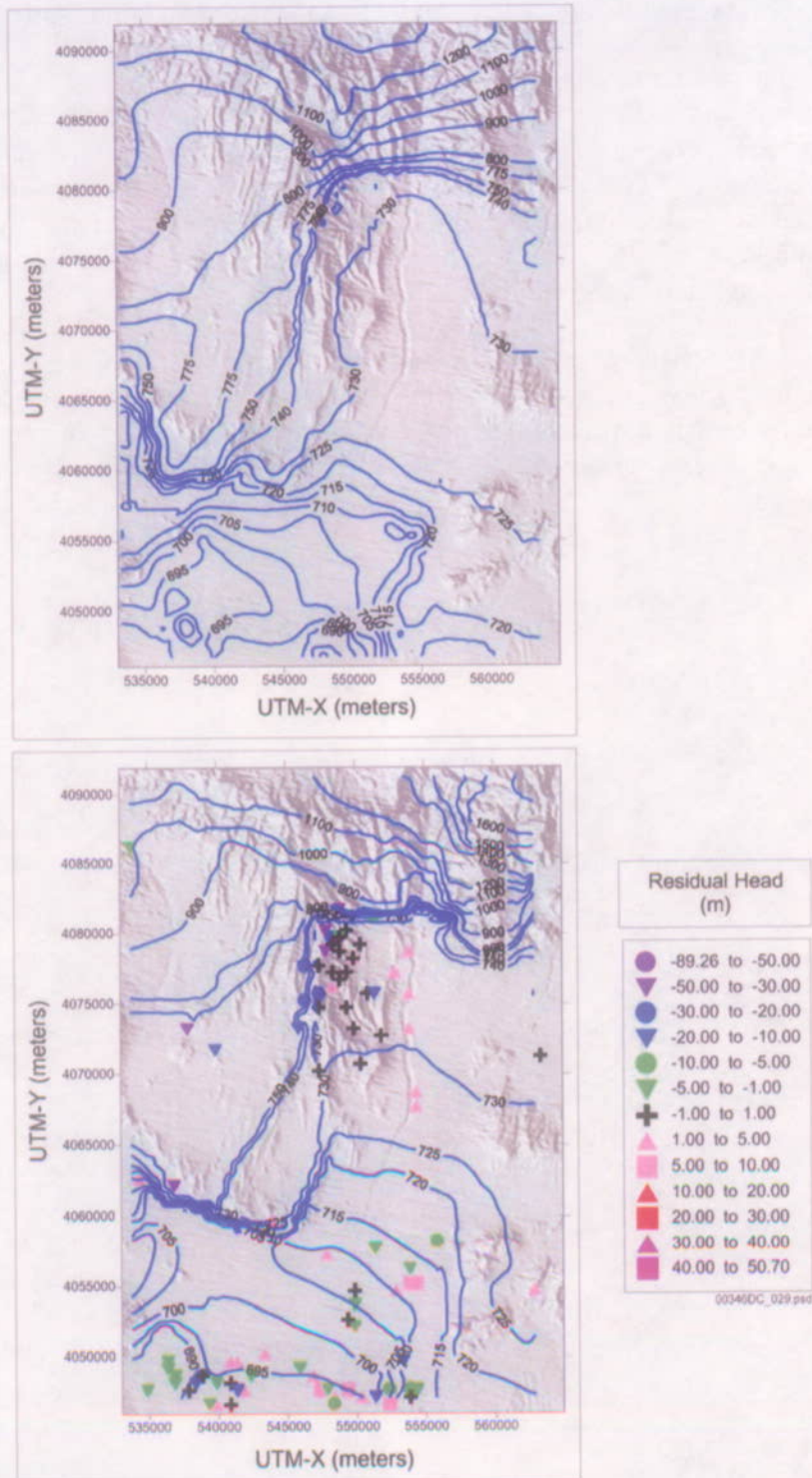
NOTE: Shading represents different hydrogeologic features included in the model. View (500 m, 3x elevation) showing node points colored by hydrogeologic unit values from the hydrogeologic framework model.

Figure 2-33. Three-Dimensional Representation of the Computation Grid

2.3.7.2 Site-Scale Groundwater Flow Model Comparisons to Observations

The results of the calibrated site-scale saturated zone flow and transport model have been compared to direct and indirect indicators of groundwater flow processes. These analyses include a comparison between: (1) the observed and predicted water-level data, (2) calibrated and observed permeability data, (3) boundary fluxes predicted by the regional-scale flow model and the calibrated site-scale saturated zone flow model, (4) the observed and predicted gradients between the carbonate aquifer and overlying volcanic aquifers, (5) hydrochemical data and particle pathways predicted by the model, and (6) thermal data.

Predicted and Observed Water-Level Elevations—Predicted and observed heads from the site-scale groundwater flow model are illustrated in Figure 2-34. As in the case of the regional model, the comparison is favorable in areas of low hydraulic gradient, but becomes more uncertain in areas of steep gradients. In the areas downgradient from Yucca Mountain, the match is acceptable.



Source: Based on BSC 2003c, Figures 6.4-5 and 6.4-6.

NOTE: Upper figure represents observed hydraulic heads and lower figure represents predicted hydraulic heads and head residuals (predicted minus observed heads)

Figure 2-34. Comparison of Observed and Predicted Hydraulic Heads in the Site-Scale Groundwater Flow Model

Since the calibration of the site-scale flow model, a number of additional wells have been installed as part of the Nye County Early Warning Drilling Program. These additions include both wells installed at new locations and wells completed at depths different from those previously available at existing locations. Comparison of the water levels observed in the new Nye County Early Warning Drilling Program wells with water levels predicted by the calibrated site-scale flow model at these new locations and depths offered an opportunity to validate the site-scale flow model using new data not used for development and calibration of the flow model.

The predicted and observed water levels are provided in Table 2-8.

Table 2-8. Comparison of Water Levels Observed and Predicted at Nye County Early Warning Drilling Program Wells

Site Name	x (m)	y (m)	Observed Head (m)	Modeled Head (m)	Residual Error (m)
NC-EWDP-1DX, deep	536768	4062502	748.8	762.7	13.9
NC-EWDP-1DX, shallow	536768	4062502	786.8	756.7	-30.1
NC-EWDP-1S, P1	536771	4062498	787.1	767.3	-19.8
NC-EWDP-1S, P2	536771	4062498	786.8	767.3	-19.5
NC-EWDP-2DB	547800	4057195	713.7	717.0	4.3
NC-EWDP-2D	547744	4057164	706.1	709.2	3.3
NC-EWDP-3D	541273	4059444	718.3	703.7	-14.6
NC-EWDP-3S, P2	541269	4059445	719.8	702.5	-17.3
NC-EWDP-3S, P3	541269	4059445	719.4	702.6	-16.8
NC-EWDP-5SB	555676	4058229	723.6	718.0	-6.6
NC-EWDP-9SX, P1	539039	4061004	766.7	731.7	-35.0
NC-EWDP-9SX, P2	539039	4061004	767.3	731.7	-35.6
NC-EWDP-9SX, P4	539039	4061004	766.8	731.7	-35.1
NC-Washburn-1X	551465	4057563	714.6	714.5	-0.1
NC-EWDP-4PA	553167	4056766	717.9	715.5	-2.4
NC-EWDP-4PB	553167	4056766	723.6	715.5	-8.1
NC-EWDP-7S – Zone 1	539638	4064323	818.1	769.6	-48.5
NC-EWDP-7S – Zone 2	539638	4064323	786.4	769.6	-16.8
NC-EWDP-7S – Zone 3	539638	4064323	756.6	769.6	13.0
NC-EWDP-7S – Zone 4	539638	4064323	740.2	769.6	29.4
NC-EWDP-12PA	536951	4060814	722.9	705.3	-17.6
NC-EWDP-12PB	536951	4060814	723.0	705.3	-17.7
NC-EWDP-12PC	536951	4060814	720.7	704.3	-16.4
NC-EWDP-15P	544848	4058158	722.5	711.0	-11.5
NC-EWDP-19P	549329	4058292	707.5	713.2	5.7
NC-EWDP-19D	549317	4058270	712.8	713.2	0.4
NC-EWDP-16P	545648	4064247	730.9	711.0	-19.9
NC-EWDP-27P	544936	4065266	730.3	713.2	-17.1
NC-EWDP-28P	545723	4062372	729.7	713.2	-16.5

Source: BSC 2003c, Table 7.1-2.

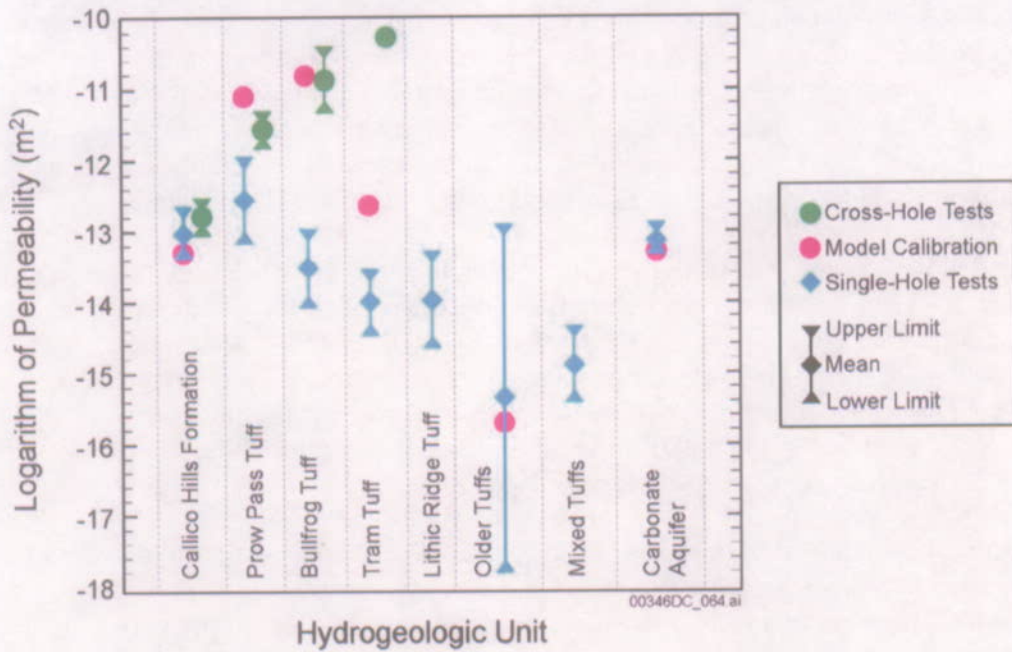
Examination of the residuals reported in Table 2-8 indicates that the uncertainty associated with predicted water levels is dependent on their location within the site-scale model domain. The residuals are generally higher in the western portion of the Nye County Early Warning Drilling Program area. The gradients are steeper in this area, and the calibrated model is generally less capable of predicting the steeper gradients in this area.

The observed residuals tend to improve as the wells are located further to the east. For example, residuals in the general area of NC-Washburn-1X, NC-EWDP-4, and NC-EWDP-5 are low. These wells are in the predicted flow path from the repository and that inferred by hydrochemical data. Thus, these additional water-level data confirm the capability of the site-scale flow model to predict water levels in this portion of the flow path from the repository.

Permeability—For model validation, the permeabilities estimated during calibration of the site-scale saturated zone flow and transport model were compared to permeabilities determined from aquifer test data from the Yucca Mountain area and elsewhere at the Nevada Test Site (BSC 2003c, Section 7). The logarithms of permeability estimated during calibration of the model were compared to the mean logarithms of permeability determined from aquifer test data from Yucca Mountain (Figure 2-35) and to data from elsewhere at the Nevada Test Site (Figure 2-36). For most of the geologic units, the calibrated permeabilities were within the 95 percent confidence limits of the mean permeabilities estimated from the data. Given these available data, the agreement between the model-calibrated value and the estimated site permeability value for the carbonate aquifer is considered to provide an adequate basis for confidence in the validity and representativeness of the site-scale flow model.

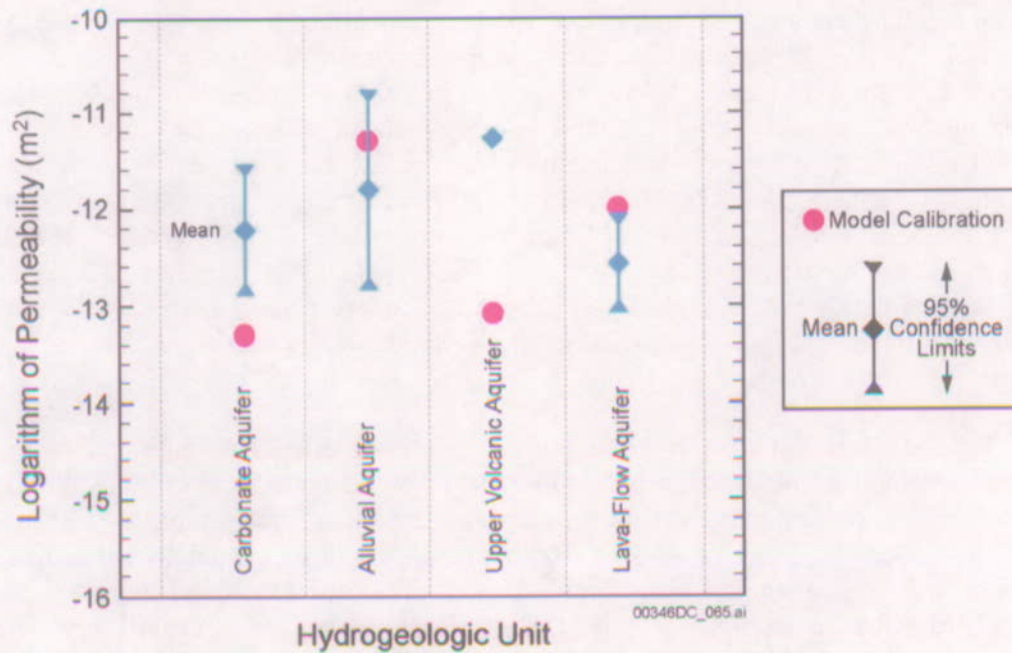
With the exception of the calibrated values for the upper volcanic aquifer, the calibrated permeabilities generally are consistent with most of the permeability data from Yucca Mountain and elsewhere at the Nevada Test Site. A discrepancy exists between the calibrated permeability for the Tram Tuff and the mean permeability derived from the cross-hole tests. However, the permeabilities measured for the Tram Tuff of the Crater Flat Group may have been enhanced by the presence of a breccia zone in the unit at boreholes UE-25 C#2 and UE-25 C#3 (Geldon et al. 1997, Figure 3; BSC 2003e).

The permeability data obtained from single-hole and cross-hole testing in the alluvial testing complex also compare acceptably well to the permeabilities predicted in the site-scale flow model. Single-well hydraulic testing of the saturated alluvium in well NC-EWDP-19D1 of the Alluvial Testing Complex was conducted between July 2000 and November 2000. During this testing, a single-well test of the alluvial aquifer to a depth of 247.5 m (812 ft) below land surface at the NC-EWDP-19D1 resulted in a permeability measurement of $2.7 \times 10^{-13} \text{ m}^2$ for the alluvial aquifer (BSC 2003c; Table 7.2-1). A cross-hole hydraulic test was also conducted at the Alluvial Testing Complex in January 2002. During this test, borehole NC-EWDP-19D1 was pumped in the open-alluvium section, while water-level measurements were made in two adjacent wells. The intrinsic permeability measured in this test for the tested interval of alluvium is $2.7 \times 10^{-12} \text{ m}^2$. The calibrated permeability for the Alluvial Uncertainty Zone was $3.2 \times 10^{-12} \text{ m}^2$. Because the cross hole tests intercepted a larger volume of rock they are considered to be more representative of the water transmitting capability of the alluvium at this location, and therefore are more appropriate for comparison to the calibrated permeability values.



Source: Based on BSC 2001, Figure 14.

Figure 2-35. Comparison of Calibrated and Observed Permeabilities from Yucca Mountain Pump Test Data in the Site-Scale Groundwater Flow Model



Source: BSC 2001, Figure 15.

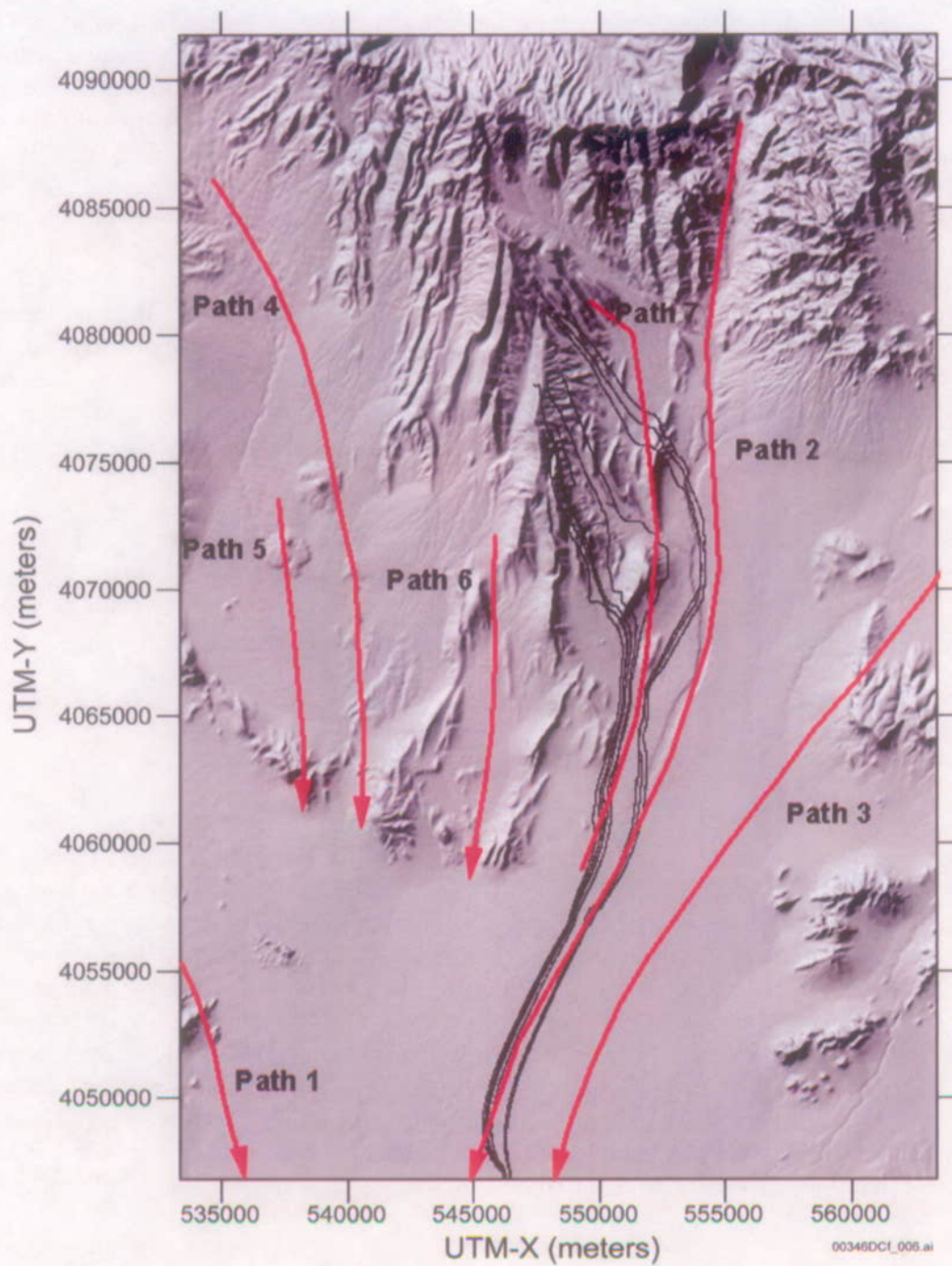
Figure 2-36. Comparison of Calibrated and Observed Permeabilities from Nevada Test Site Pump Test Data in the Site-Scale Groundwater Flow Model

Boundary Fluxes—A comparison of the fluxes predicted at the boundary of the site-scale model domain by the calibrated site-scale saturated zone flow and transport model and by the regional-scale model was used to further validate the model (CRWMS M&O 2000a, Section 3.4.2). The volumetric fluxes computed along the boundaries by the two models match acceptably well (Table 2-4). The total fluxes across the northern boundary computed by the regional-scale model and the site-scale saturated zone flow and transport model were 6.0×10^6 m³/yr and 5.3×10^6 m³/yr, respectively. The comparison of the boundary fluxes computed along the east side of the site-scale saturated zone flow model domain also indicates a good match. The total fluxes across the eastern boundary computed by the regional-scale model and the site-scale model were 1.8×10^7 and 1.6×10^7 m³/yr, respectively. The match is particularly good along the lower thrust area, where both models predict large fluxes across the model boundary. Both models also predicted small fluxes across the remainder of the eastern boundary. The effect of the small differences between the two model flux predictions on the specific discharge is within the uncertainty range used.

The southern boundary flux is simply a sum of the other boundary fluxes plus the recharge. A comparison of the fluxes across the southern boundary computed by the regional-scale model and the site-scale saturated zone flow and transport model indicates a relatively good match. The difference in the fluxes computed by the two models across the southern boundary is approximately 2.3×10^7 (site scale) and 2.9×10^7 (regional scale) m³/yr.

Upward Hydraulic Gradient—An upward hydraulic gradient between the lower carbonate aquifer and the overlying volcanic rocks has been observed in the vicinity of Yucca Mountain. Principal evidence for this upward gradient is provided by data from the only borehole at Yucca Mountain that has been drilled into the upper part of the carbonate aquifer (UE-25 p#1) and Nye County well NC-EWDP-2DB. Hydraulic head measurements in UE-25 p#1 borehole indicate that the head in the carbonate aquifer is about 752 m (2,470 ft), about 21 m (69 ft) higher than the head measured in this borehole in the overlying volcanic rocks. The head in the carbonate aquifer at this borehole location was estimated as part of the model calibration process. An increasing head with depth at this location was preserved during model calibration, although the head difference was only 12.73 m instead of the observed 21 m (BSC 2003c, Table 16). The difference in predicted and observed values of the upward hydraulic gradient at this location results, in part, because the constant vertical head boundary conditions imposed on the lateral boundaries of the model domain constrained the vertical groundwater flow and gradients within the model interior (CRWMS M&O 2000a, Sections 6.7.11 and 6.1.2).

Hydrochemical Data Trends—To provide further validation of the site-scale saturated zone flow and transport model, the flow paths (Figure 2-37) predicted by the calibrated model were compared with those estimated using groundwater chemical and isotopic data (Figure 2-11). Flow paths predicted by the calibrated site-scale saturated zone flow model were generated using the particle-tracking capability of the Finite Element Heat and Mass Transfer Code (Zyvoloski et al. 1997) by placing particles at different locations beneath the repository and running the model to trace the paths of these particles across a range of horizontal anisotropies.



Source: BSC 2003c, Figure 7.3-1b.

Figure 2-37. Predicted Groundwater Flowpath Trajectories Compared to Flowpaths Inferred from Geochemistry

Comparison of the flow paths predicted by the calibrated model with those estimated using groundwater chemical and isotopic data indicate that most of the particles travel within the envelop formed by flow paths 6 and 2, and roughly follow the trajectory of path 7 through the alluvium along the west side of Fortymile Wash. These particle trajectories from the repository are permitted by the constraints provided by the groundwater geochemical and isotopic data.

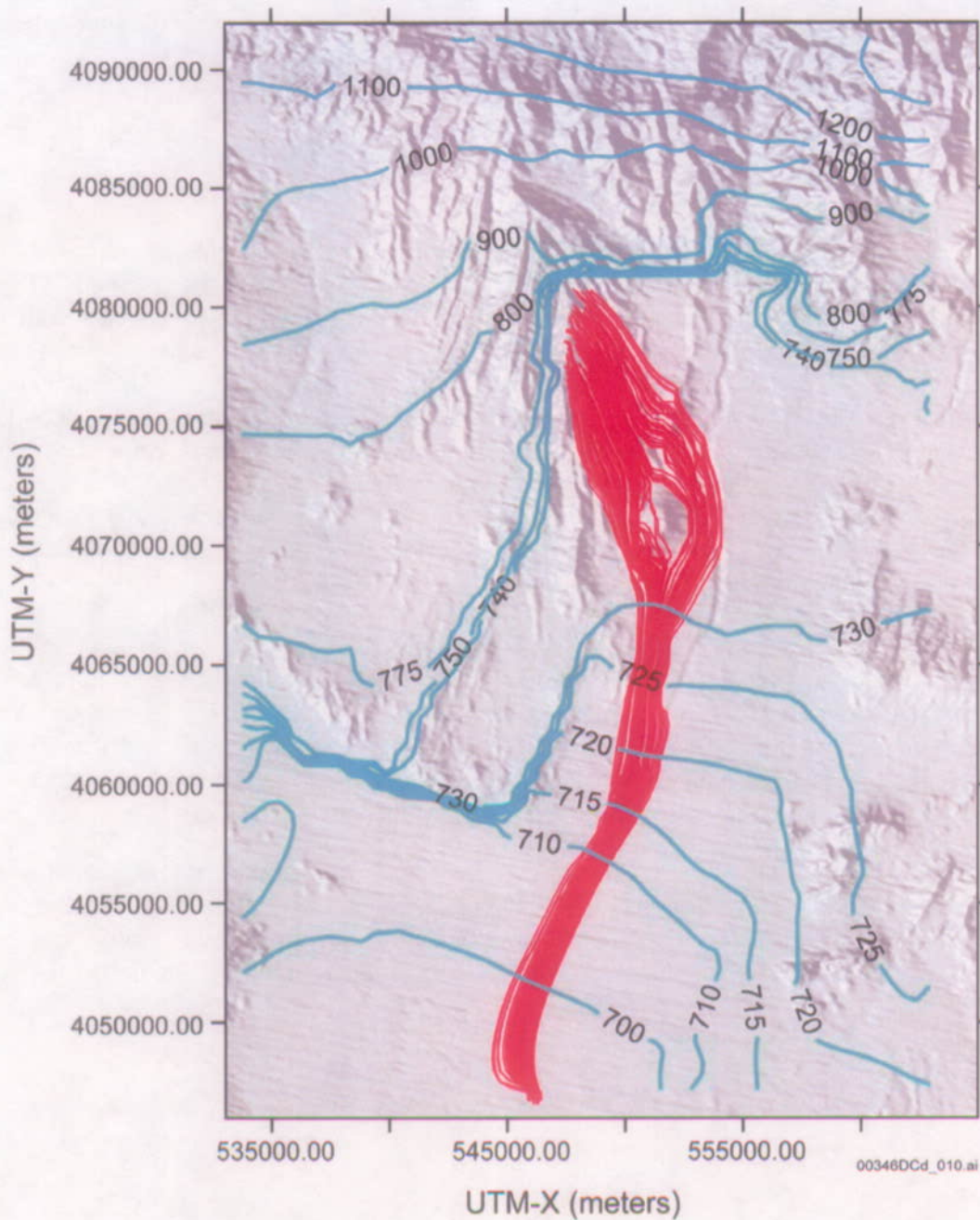
Thermal Modeling—Temperature measurements can be used as an indirect indicator of groundwater flow. Although uncertainty exists in the interpretation of the thermal anomalies in that they could result from thermal properties (notably thermal conductivity), heat flux, or overburden variability, and not the result of areal or vertical groundwater flux, an acceptable comparison of observed and simulated temperatures for the site-scale flow model has been obtained. The temperature data used in the thermal modeling are taken from temperature profiles measured within the model domain. The temperature data were extracted at 200-m intervals from these temperature profiles, and a total of 94 observations from 35 wells were obtained.

Coupled thermal modeling and conduction-only model have been completed to evaluate the consistency of the saturated zone flow model with the available thermal observations. The details related to this thermal modeling are presented in Appendix D. The results presented in Appendix D provide a reasonable comparison even given the uncertainties associated with the interpretation of the thermal anomalies.

2.3.7.3 Model Results

Using the calibrated flow model, specific discharge was estimated for a nominal fluid path leaving the repository area and traveling 0 to 5 km, 5 to 20 km, and 20 to 30 km. The specific discharge simulated by the flow model for each segment of the flow path from the repository was determined using the median travel time for a group of particles released beneath the repository. Values for specific discharge of 0.67, 2.3, and 2.5 m/yr. were obtained, respectively, for the three segments of the flow path. The first segment reflects flow within the tuff aquifers, and the last segment (from 20 to 30 km) reflects flow within the alluvial aquifer. It warrants noting that an expert elicitation panel convened prior to the Site Recommendation (CRWMS M&O 1998, Figure 3-2e) estimated a specific discharge of 0.71 m/yr. for the 5-km distance. Thus, agreement is found between the specific discharge predicted by the calibrated model and that estimated by the expert elicitation panel for the 5-km (3-mi) distance. In addition, the lower end of the range of inferred specific discharges from the single well tracer-injection test of between 1.2 and 9.4 m/yr., acceptably reproduces the median-modeled specific discharge at this location (about 2.3 m/yr.).

The particle-tracking capability of the Finite Element Heat and Mass Transfer Code (Zyvoloski et al. 1997) was used to demonstrate flow paths predicted by the calibrated site-scale saturated zone flow and transport model. One hundred particles were distributed uniformly over the area of the repository and allowed to migrate until they reached the model boundary (Figure 2-38). The pathways leave the repository and generally travel in a south-southeasterly direction to the 18-km compliance boundary.



Source: Based on BSC 2003c, Figure 6.6-3.

Figure 2-38. Predicted Saturated Zone Particle Trajectories from Yucca Mountain

The flow paths from the water table beneath the repository to the accessible environment directly affect breakthrough curves and associated radionuclide travel times. Because the flow paths and water table transition from the volcanic tuffs to the alluvium, flow path uncertainty directly affects the length of flow in the volcanic tuffs and in the alluvium. Uncertainty in flow paths is affected by permeability anisotropy of the volcanic tuffs. Large-scale anisotropy and

heterogeneity were implemented in the saturated zone site-scale flow model through direct incorporation of known hydraulic features, faults, and fractures. Detailed discussion of the uncertainty in flow path lengths in the tuff aquifers prior to intersecting the alluvial aquifers is discussed in Appendix G.

2.4 SUMMARY

The regional and site-scale groundwater flow representations indicate that groundwater in the shallow tuff aquifers flows south-southeasterly from Yucca Mountain and parallels Fortymile Wash to the point where it discharges from the shallow tuff aquifers and mixes with other groundwater in the alluvium under Amargosa Desert. The flow paths are acceptably constrained by the available hydrogeologic and geochemical information, and the location of the alluvium-tuff contact is also acceptably constrained by recent drilling and geophysics conducted by Nye County. The exact location where the groundwater at the water-table enters the alluvium is uncertain. This uncertainty is due, in part, to uncertainty in the flow paths, which is due to uncertainty in anisotropy and in the alluvium-tuff contact. The uncertainty in the alluvium-tuff contact has been included in the uncertainty of radionuclide transport times along the paths of likely radionuclide migration in the saturated zone.

In addition to the flow paths being acceptably constrained, the average flow rates, as defined by the specific discharge distribution in the alluvium, has been independently evaluated to be about 2.5/yr in the alluvium with a range of between about 1.2 to 9.4 m/yr. To account for the uncertainty in the hydraulic properties and specific discharge a range of specific discharge values have been used in the assessment of repository performance. The range considered varies from a factor of three to a factor of one-third of the median specific discharge.

The regional and site-scale groundwater flow models have been calibrated with potentiometric, recharge, discharge, and hydraulic characteristic observations. In addition, these flow models have been independently corroborated with geochemical observations (conservative tracers and stable isotopes), thermal observations, and tracer test determination of specific discharge.

3. SATURATED ZONE RADIONUCLIDE TRANSPORT

If radionuclides are released in the aqueous phase from the repository and migrate through the unsaturated zone either as dissolved species or sorbed onto colloids, they will enter the groundwater flow regime in the saturated zone. Released radionuclides would be expected to travel along the groundwater flow paths described in Section 2 (Figure 2-38). The rate at which these radionuclides are transported is a function of key radionuclide transport processes and parameters such as effective porosity, matrix diffusion, hydrodynamic dispersion, and radionuclide sorption or retardation. The transport of radionuclides as solute is affected by advection, diffusion, and dispersion, and for reactive constituents, sorption. Transport of radionuclides sorbed onto colloids is affected by filtering, where colloids with diameters greater than the pore openings are filtered by the medium, and by attachment-detachment processes. Mixing and dilution of radionuclides in the groundwater affects the concentration of radionuclides released to the environment. This section presents observations and test data that provide the conceptual basis and understanding of radionuclide transport through the saturated zone.

3.1 INTRODUCTION

The processes relevant to the performance of the saturated zone barrier at Yucca Mountain are described conceptually in Figure 3-1. Advection, matrix diffusion, dispersion, and sorption processes occur over different scales of interest within the saturated zone. The effect and significance of these processes is also different in the fractured tuff units than in the porous alluvium.

In the fractured tuffs, advective transport occurs within the fractures, thus the effective fracture spacing and porosity are important for describing the advective velocity of any dissolved constituents. Major flowing fracture zones (termed flowing intervals) are generally spaced on the order of meters to tens of meters apart, while fractures themselves may be more closely spaced and have sub millimeter apertures. Radionuclides that are transported through the fractures may diffuse into the surrounding matrix or sorb onto the fracture surface. If the radionuclides diffuse into the matrix, they may also be sorbed within the matrix of the rock.

In the porous tuff units, advective transport occurs through the porous matrix. Because the effective porosity of the alluvium is considerably greater than that of the fractured tuff, the transport velocity in the alluvium is greatly reduced in comparison to that of the tuff (even though as discussed in Section 2.3.7 the specific discharge in the alluvium is about a factor three greater than that of the tuff). Radionuclides transported through the porous alluvium can also sorb onto minerals within the alluvium.

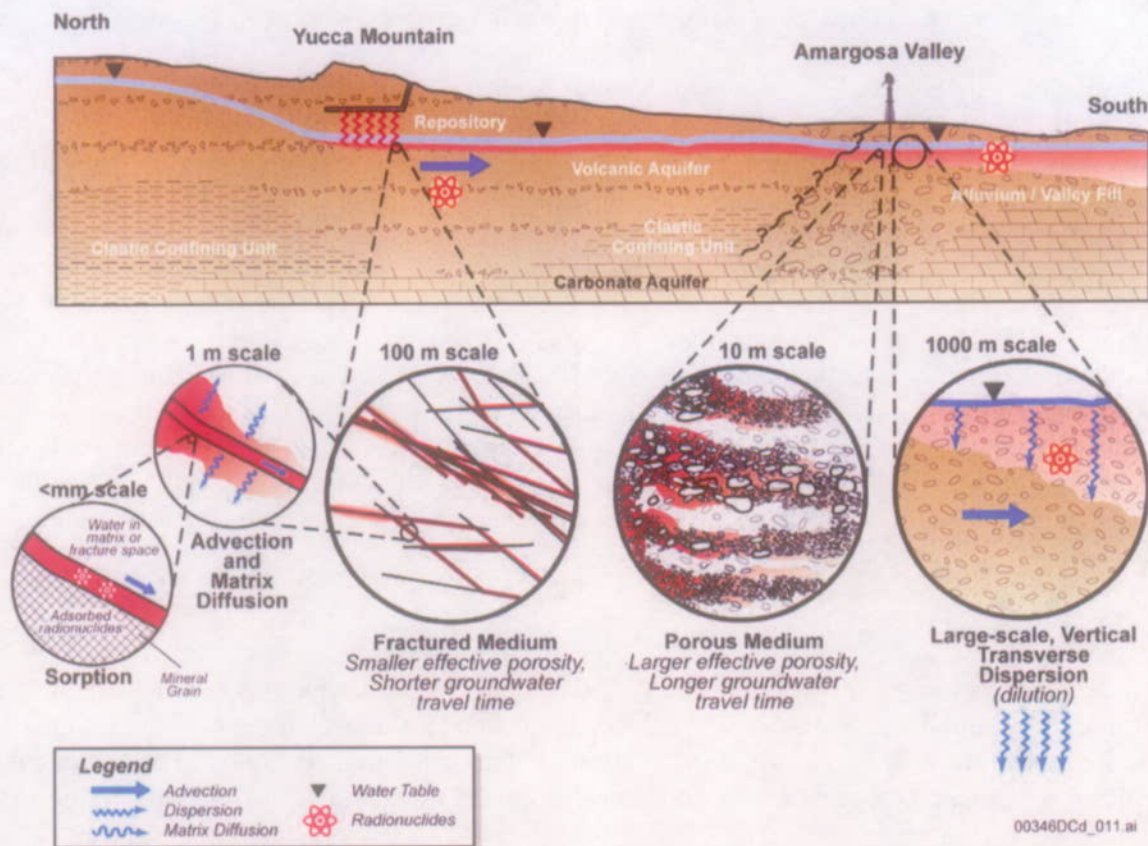


Figure 3-1. Conceptual Model of Radionuclide Transport Processes in the Saturated Zone

In addition to the advective, diffusive, and retardation mechanisms, small-scale heterogeneities in aquifer characteristics, which result in a small-scale variability in advective velocities, can effectively disperse the radionuclides as they migrate through the saturated zone. This dispersive phenomenon tends to allow some radionuclides released at a particular point to migrate either faster than or slower than the average velocity along the groundwater flow trajectory.

Finally, although it is possible for groundwater beneath Yucca Mountain to mix with other groundwater as they flow southward towards Amargosa Valley, it is apparent that the likely flow paths remain acceptably constrained over an aquifer width of a few kilometers. At the compliance point, located about 18 km south of Yucca Mountain, the reasonably maximally exposed individual uses well water that has been extracted from the aquifer at a rate of $3.7 \times 10^6 \text{ m}^3/\text{yr}$ (3,000 acre-ft/yr.). This well is located in the center of the groundwater flow trajectories to maximize the concentration of any dissolved radionuclides that may be contained within the groundwater. This pumping discharge is likely to extract all radionuclides that are in the groundwater at that point as well as mix with other groundwater that does not contain any radionuclides. The effective concentration within the water that is used by the reasonably maximally exposed individual reflects this mixing process for the purposes of determining the potential dose attributed to these radionuclides.

It is possible to present the conceptual basis for radionuclide transport using different logical foundations. For example, one could present each process that could potentially affect transport and describe the basis for the understanding of each without regard to whether the process occurred in the fractured tuff or the alluvium. Alternatively, one could describe the transport processes in the fractured tuff and then those processes in the alluvium. The following presentation combines these two approaches. In Section 3.2, the processes affecting advective transport of radionuclides for which little retardation is expected by sorption processes are presented (i.e., advection, matrix diffusion, and dispersion). Section 3.2.1 presents these processes for the fractured tuff and Section 3.2.2 presents these processes for the alluvium. In Section 3.3 the processes affecting radionuclide sorption are presented. Again, Section 3.3.1 presents these processes for the fractured tuff and Section 3.3.2 presents these processes for the alluvium. Section 3.4 then presents the combined affect of flow and transport processes for both the fractured tuff and alluvium and for the relevant nonsorbing and sorbing radionuclides in terms of the expected radionuclide arrival time profiles (e.g., breakthrough curves) illustrating the effect of only the saturated zone barrier on radionuclide transport.

3.2 ADVECTION, MATRIX DIFFUSION, AND DISPERSION PROCESSES

Advection drives the movement of dissolved constituents in flowing groundwater. The rate of advection is determined by the groundwater velocity, which is controlled by specific discharge and effective porosity. The effective porosity (i.e., the void volume through which the dissolved constituents are likely to flow) is a function of the material properties of the hydrostratigraphic units along the flow paths.

Diffusion of dissolved or colloidal radionuclides into regions of slowly moving groundwater is an important retardation process. Dissolved radionuclides will diffuse from water flowing in the fractures into the matrix, or nonfractured, portion of the rocks, as well as from water in pores between rock grains in the alluvium into porosity within the rock grains. They will eventually diffuse back into the moving groundwater; however, diffusion into and out of the rock matrix and grains will slow the rate of transport.

Hydrodynamic dispersion, the spreading of solutes along the flow path, decreases the concentration of radionuclides in groundwater. Dispersion occurs because of heterogeneity in flow velocities resulting from heterogeneity of permeability. This heterogeneity can occur at scales ranging from microscopic to the scale of the rock units.

3.2.1 Advection, Diffusion, and Dispersion Processes and Parameters for Fractured Volcanic Tuffs

The advective-diffusive transport properties of relevance to potential radionuclide transport through the fracture tuffs beneath and downgradient from Yucca Mountain include the fracture or flowing interval spacing, the effective fracture porosity, matrix diffusion, and hydrodynamic dispersion. The first two of these greatly affect the mean advective velocity and the second two affect the spread of the distribution of advective transport times through the fractured rock mass.

The transport characteristics of the fractured tuff aquifers in the vicinity of Yucca Mountain have generally been inferred from hydraulic testing in the wells that penetrate the saturated zone. This

general information has been enhanced by detailed hydraulic and single- and multiple-well tracer testing conducted at the C-Wells complex. Both of these sources of discrete test information have been supplemented by analyses of Carbon-14 to confirm the understanding of advective transport over a more integrated scale relevant to performance of the Yucca Mountain repository.

Results from the hydraulic and tracer testing completed at the C-Wells complex (Figure 2-26) were used to identify and confirm the conceptualization of flow and transport in the fractured tuff and to derive flow and transport parameters for modeling. These tests have confirmed the dual-porosity conceptualization of transport, in which transport takes place in the fracture and matrix porosity of the fractured rock mass. The testing sequence is briefly summarized below and the details relevant to the determination of transport characteristics are presented in their appropriate section.

A series of cross-hole radial converging tracer tests were performed in the Bullfrog-Tram and Prow Pass units at the C-Wells complex (Figure 2-27) using suites of reactive and nonreactive tracers to determine parameters necessary to model advection, dispersion, diffusion, and sorption processes. Conservative tracer tests conducted at the C-Wells complex included:

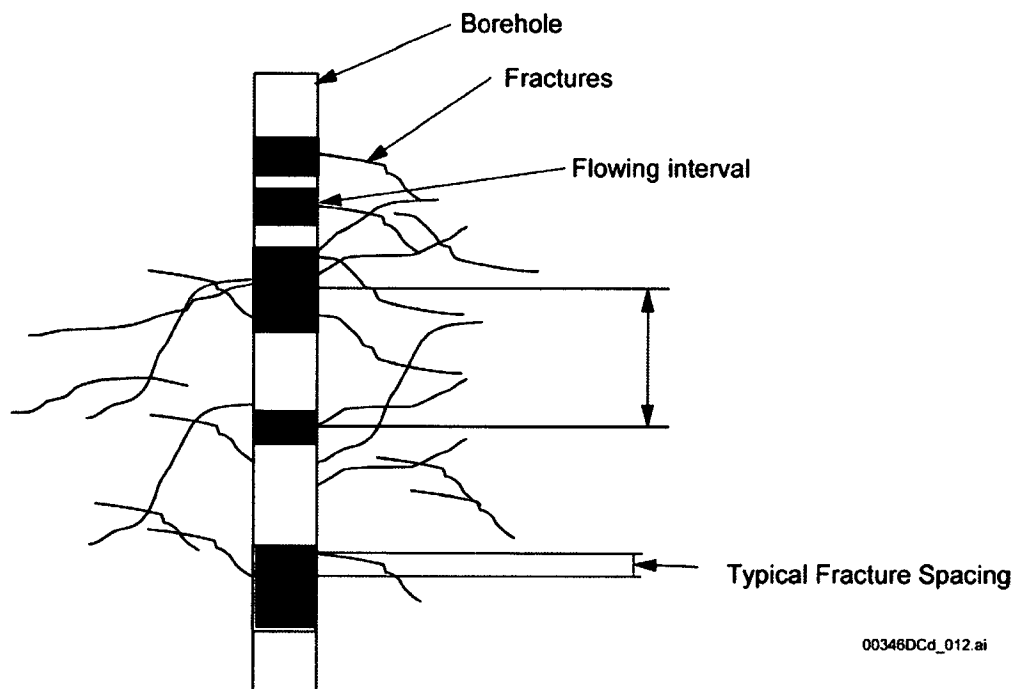
- Iodide injection into the combined Bullfrog-Tram interval
- Injection of iodide into the Lower Bullfrog interval
- Injection of 2,6 difluorobenzoic acid into the lower Bullfrog interval
- Injection of 3-carbamoyl-2-pyridone into the Lower Bullfrog interval
- Injection of iodide and 2,4,5 trifluorobenzoic acid into the Prow Pass formation
- Injection of 2,3,4,5 tetrafluorobenzoic acid into the Prow Pass formation
- Injection of pentafluorobenzoic acid into the Lower Bullfrog interval
- Injection of multiple solute and colloid tracers (carboxylate-modified latex microspheres) between wells UE-25 C#2 and UE-25 C#3. One test was conducted in the Lower Bullfrog Tuff and the other was conducted in the Prow Pass Tuff.

3.2.1.1 Fracture Flowing Interval Spacing

Hydrologic evidence at Yucca Mountain supports the model of fluid flow within fractures in the moderately to densely welded tuffs of the saturated zone (CRWMS M&O 2000a, Section 3.2.2). For example, the bulk hydraulic conductivities measured in the field (which are dominated by fracture flow) tend to be several orders of magnitude higher than hydraulic conductivities of intact (primarily unfractured) tuff core samples measured in the laboratory. Also, there is a positive correlation between fractures identified using acoustic televiewer or borehole television tools and the zones of high transmissivity and flow (Erickson and Waddell 1985, Figure 3). The implication is that flow is primarily through the fracture system, not through the matrix between fractures. Fractures generally are found within the moderately to densely welded tuffs.

Flowing interval spacing, illustrated in Figure 3-2 is a parameter in the dual porosity transport model. A flowing interval is defined as a fractured zone that transmits fluid in the saturated zone, as identified through borehole flow meter surveys. Flowing interval spacing is distinct from the fracture spacing, which is typically used in the literature. Fracture spacing was not used because the available field data (e.g., see the fluid logging and fracture mapping conducted in the C-Wells complex presented in Figure 2-27) identified zones (i.e., flowing intervals) that contain fluid-conducting fractures but do not distinguish how many or which fractures comprise the flowing interval. These data also indicate that numerous fractures between flowing intervals do not transmit groundwater. The flowing interval spacing is measured between the midpoints of each flowing interval.

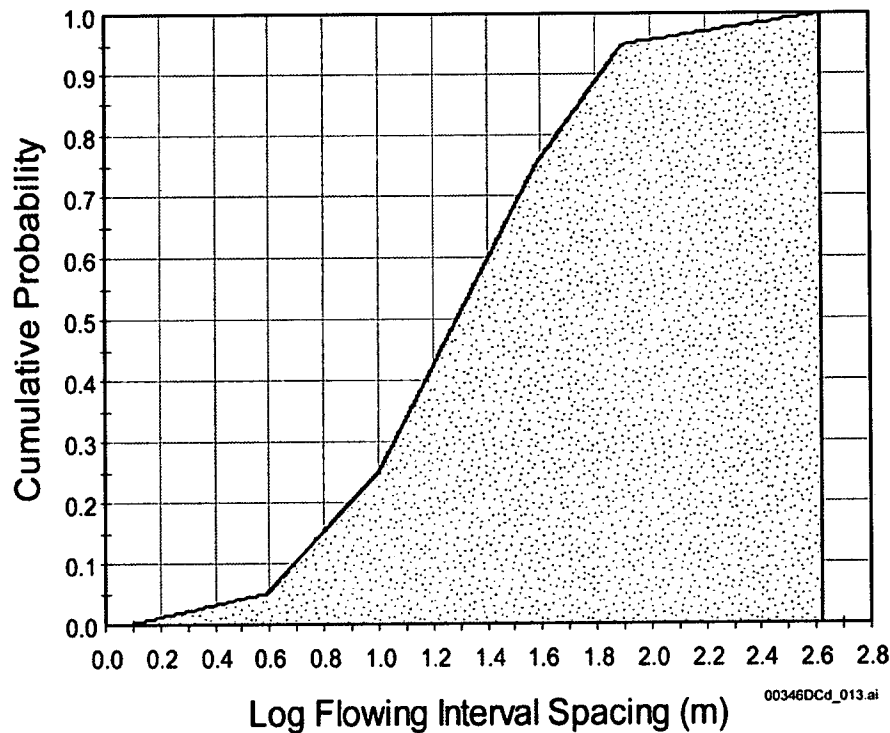
Uncertainty in the flowing interval spacing was directly included in the transport model. This uncertainty is manifested principally in an effect on matrix diffusion. The larger the spacing between flowing intervals, the less effect matrix diffusion has on delaying radionuclide transport times.



Source: BSC 2001b, Figure 1.

Figure 3-2. Conceptual Representation of Flowing Interval Spacing

There is uncertainty associated with the flowing interval spacing parameter due to limited data. The data set used for the analysis consisted of borehole flow meter survey data. This analysis is described in detail in *Probability Distributions for Flowing Interval Spacing* (BSC 2001b), and resulted in the distribution for flowing interval spacings indicated in Figure 3-3.



Source: BSC 2003d, Figure 6-12.

Figure 3-3. Cumulative Probability Density Function of Flowing Interval Spacing

3.2.1.2 Fracture Effective Porosity

The flowing interval porosity is defined as the volume of the pore space through which large amounts of groundwater flow occurs, relative to the total volume. The fracture porosity characterizes the effective porosity within flowing intervals rather than within each fracture. The advantage to this definition of fracture porosity is that in situ well data may be used to characterize the parameter. The flowing interval porosity may also include the matrix porosity of small matrix blocks within fracture zones.

The estimated effective flow porosity values from conservative tracer tests are summarized in Table 3-1.

Table 3-1. Summary of Effective Flow Porosity from Conservative Tracer Tests

Tracer Test	Flow Porosity
Iodide test from UE-25 C#2 to C#3 in Bullfrog-Tram	8.6%
DFBA test from UE-25 C#2 to C#3 in Lower Bullfrog	7.2% - 9.9%
Pyridone test from UE-25 C#1 to C#3 in Lower Bullfrog	NA
Single-Porosity, Partial-Recirculating Solution: 2,4,5 DFBA: UE-25 C#3 to C#2 in Prow Pass	0.045%
Dual-Porosity, Partial-Recirculating Solution: 2,4,5 DFBA: UE-25 C#3 to C#2 in Prow Pass	0.045%

Source: Based on BSC 2003e, Tables 6.3-2 and 6.3-3.

NOTE: DFBA = 2,6 difluorobenzoic acid.

Advective transport in the Prow Pass is interpreted to be through an interconnected network of fractures whereas in the Bullfrog-Tram intervals, the relatively large flow porosity suggests a less well-connected fracture network where transport occurs through sections of matrix between fractures. If on the other hand, transport occurs through the tortuous path along the poorly connected network of fractures which is much longer than the straight line distance between wells, the resulting flow porosities would be much less than the 7.2 to 9.9 percent range indicated in Table 3-1. In all cases, the data corroborate the concept of flow primarily through fractures.

Table 3-2 summarizes the effective flow porosity values derived from the two multiple tracer tests, one in the Prow Pass, the other in the Lower Bullfrog. The upper and lower bounds in the table were calculated using mean tracer residence times assuming linear and radial flow, respectively.

Table 3-2. Summary of Flow Porosity Values from Multiple Tracer Tests

Tracer Test	Lower Bound Flow Porosity	Upper Bound Flow Porosity
Prow Pass	0.3%	0.6%
Lower Bullfrog	0.3%	3.1%

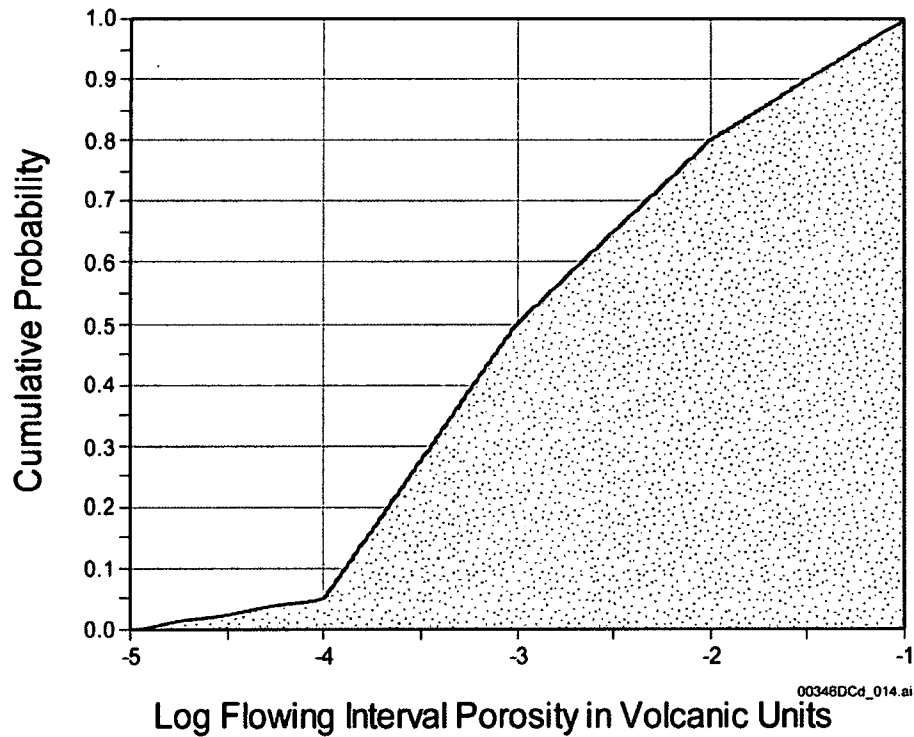
Source: BSC 2003e, Table 6.3-10.

Figure 3-4 illustrates the range of likely effective flow porosities derived from the C-Wells tests and other site-specific observations. This information has been used to define the uncertainty in the effective porosity relevant for post closure performance assessment at Yucca Mountain. The lower end of the uncertainty range reflects some non-site-specific information on effective flow porosities of fractured rock masses (BSC 2003d).

3.2.1.3 Matrix Diffusion

When a dissolved species travels with the groundwater within a fracture, it may migrate by molecular diffusion into the relatively stagnant fluid in the rock matrix. When a molecule enters the matrix, its velocity effectively goes to zero until Brownian motion carries it back into a fracture. The result of moving into the stagnant matrix is a delay in the arrival of the solute at a downgradient location from that predicted if the solute had remained in the fracture.

Matrix diffusion has been demonstrated to occur in the volcanic rocks within the vicinity of Yucca Mountain (Reimus, Haga et al. 2002; Reimus, Ware et al. 2002). Reimus, Ware et al. (2002) developed an empirical relationship between the effective diffusion coefficient and porosity and permeability measurements based on diffusion cell experiments on rock samples from the Yucca Mountain area. Diffusing species are ⁹⁹Tc (as TcO₄), ¹⁴C (as HCO₃) and tritiated water (³HHO). Rock samples were taken from within the vicinity of Yucca Mountain, underneath Pahute Mesa, and Area 25 of the Nevada Test Site. Reimus, Haga et al. (2002) found that differences in rock type account for the largest variability in the effective diffusion coefficients, rather than variability between diffusing species, size, and charge.

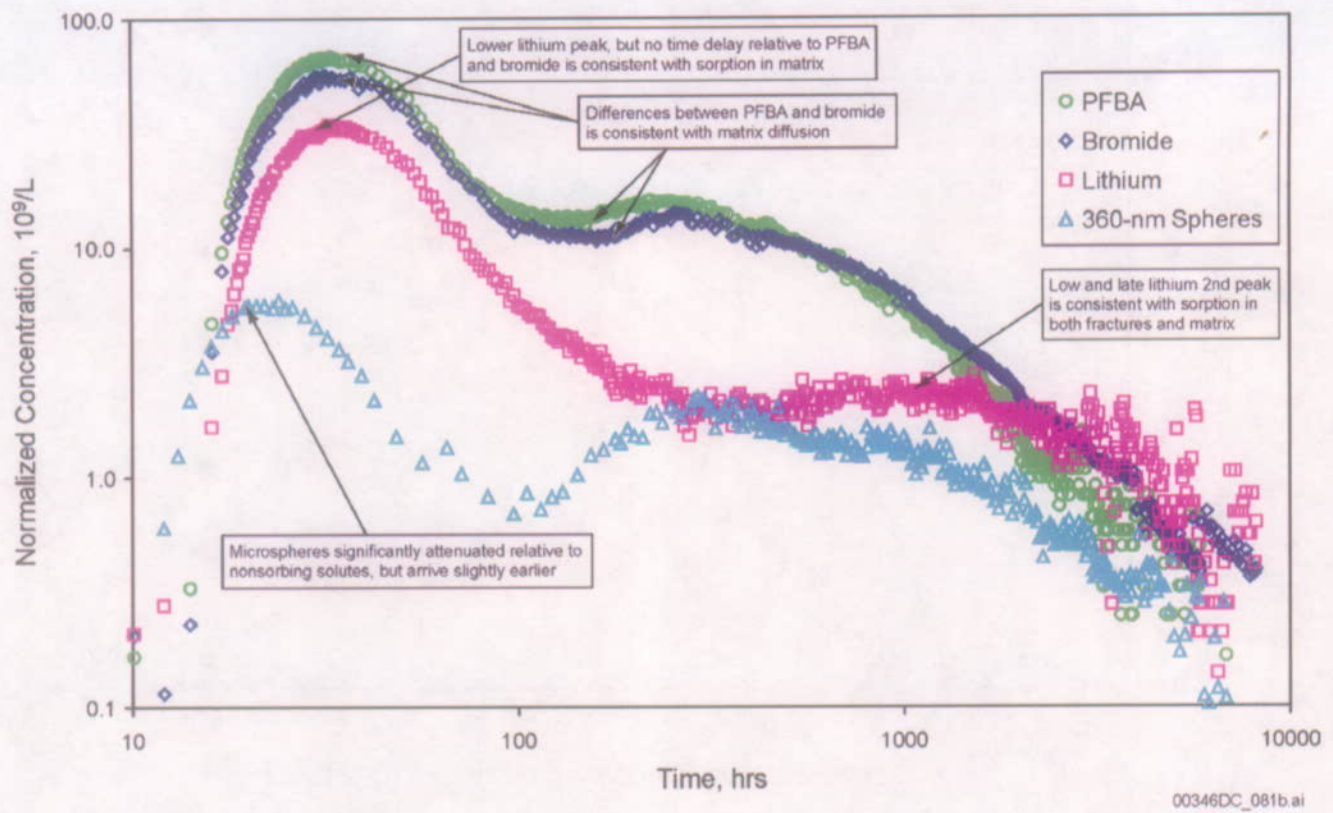


Source: BSC 2003d, Figure 6-13.

Figure 3-4. Uncertainty in Effective Flow Porosity in Fractured Tuffs at Yucca Mountain

In the field, cross-hole tracer tests that demonstrate the effect of matrix diffusion have been conducted (BSC 2001c, Section 6). The C-Wells reactive tracer test (BSC 2003e; CRWMS M&O 2000a, Section 3.1.3.2), demonstrated that observed tracer breakthrough is explained by models incorporating matrix diffusion (Figure 3-5).

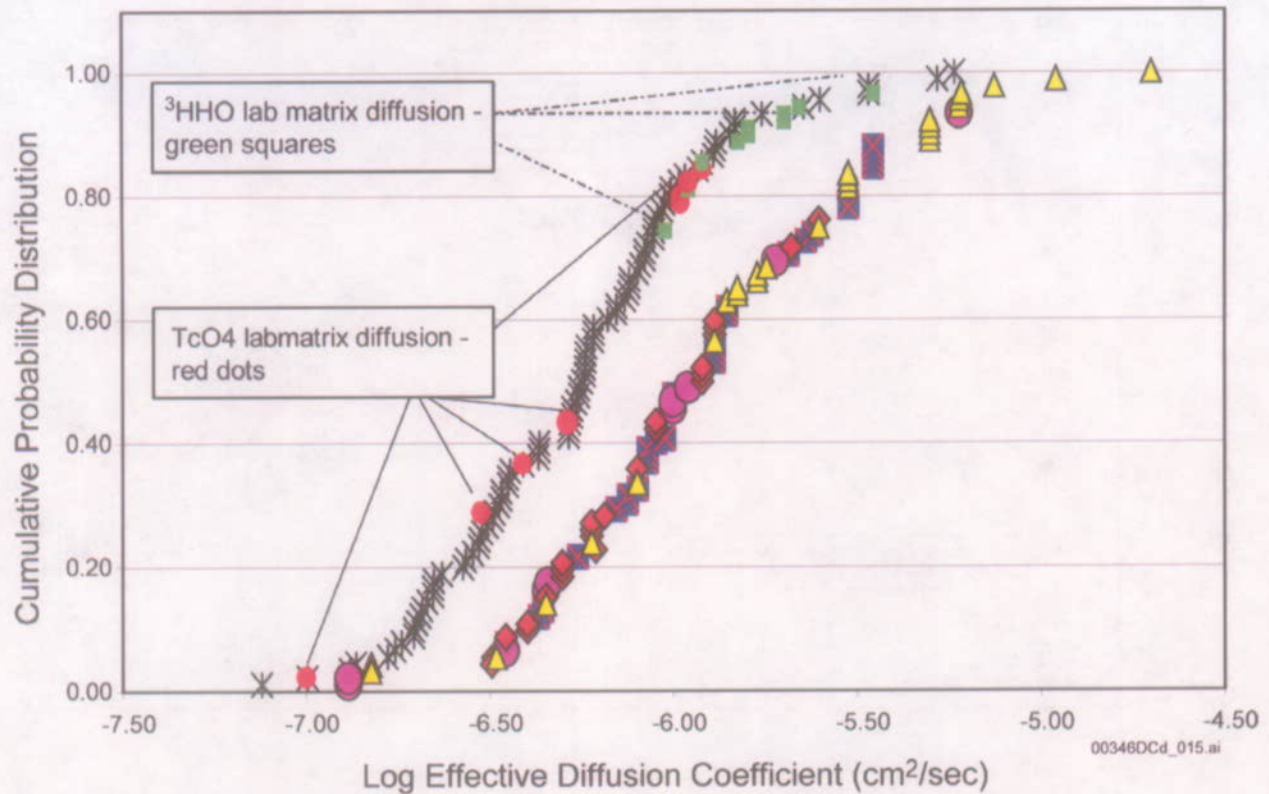
Laboratory experiments and field tests demonstrated the validity of matrix diffusion and provided a basis for quantifying the effect of matrix diffusion on radionuclide migration through the moderately and densely welded tuffs of the saturated zone at Yucca Mountain. The cumulative distribution of the matrix diffusion coefficient applicable to Yucca Mountain tuffs is illustrated in Figure 3-6.



Source: BSC 2001, Figure 96.

NOTE: Tracer recoveries were about 69 percent for pentafluorobenzoic acid, 69 percent for bromide, 39 percent for lithium, and 15 percent for microspheres. Concentrations are normalized to mass injected; both axes are log scale.

Figure 3-5. Normalized Tracer Responses in the Bullfrog Tuff Multiple Tracer Test Illustrating the Effect of Matrix Diffusion



Source: BSC 2003d, Figure 6-14.

NOTE: The curve to the left represents values of effective diffusion coefficient derived using a linear regression relationship based on porosity and permeability values and diffusion cell results (Reimus et al. 2002, p. 2.25). Included in the plot are laboratory measurements of effective diffusion coefficient from Triay 1993 and Rundberg et al. 1987 to demonstrate the reasonableness of the derived values of effective diffusion coefficient. The curve to the right represents laboratory and field-derived estimates; Triangles - ^{14}C laboratory values; Squares - ^3HHO laboratory values; Diamonds - TcO_4 laboratory values; Circles - Br^- and PFBA field values presented in Reimus et al., 2002 and Reimus et al., 2003.

Figure 3-6. Distribution of Matrix Diffusion Coefficients Applicable to Fractured Tuffs at Yucca Mountain

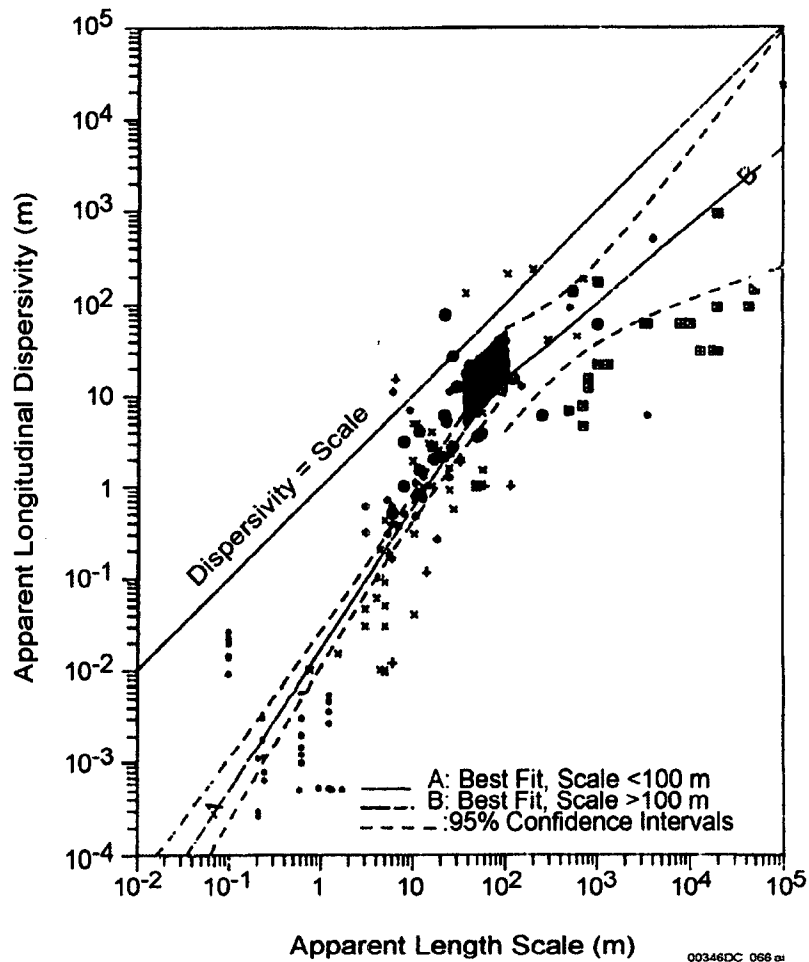
3.2.1.4 Hydrodynamic Dispersion

Dispersive processes can occur at a range of scales and at directions longitudinal and transverse to the average groundwater flow direction. Longitudinal dispersion is a function of several factors including the relative concentrations of the solute, the flow field, and the rock properties. An important component of this dispersion is the dispersivity, a coarse measure of the solute (mechanical) spreading properties of the rock. Longitudinal dispersivity will be important only at the leading edge of the advancing plume, while transverse dispersivity (horizontal transverse and vertical transverse) affects the plume width.

Dispersion is caused by heterogeneities from the scale of individual pore spaces to the thickness of individual strata and the length of structural features such as faults. The spreading and dilution of radionuclides that results from these heterogeneities could be important to

performance of the repository. Although heterogeneities at the scale of kilometers are represented explicitly in the site-scale saturated zone flow and transport model, dispersion at smaller scales is characterized using an anisotropic dispersion coefficient tensor consisting of a three-dimensional set of values: longitudinal, horizontal-transverse, and vertical-transverse dispersivities.

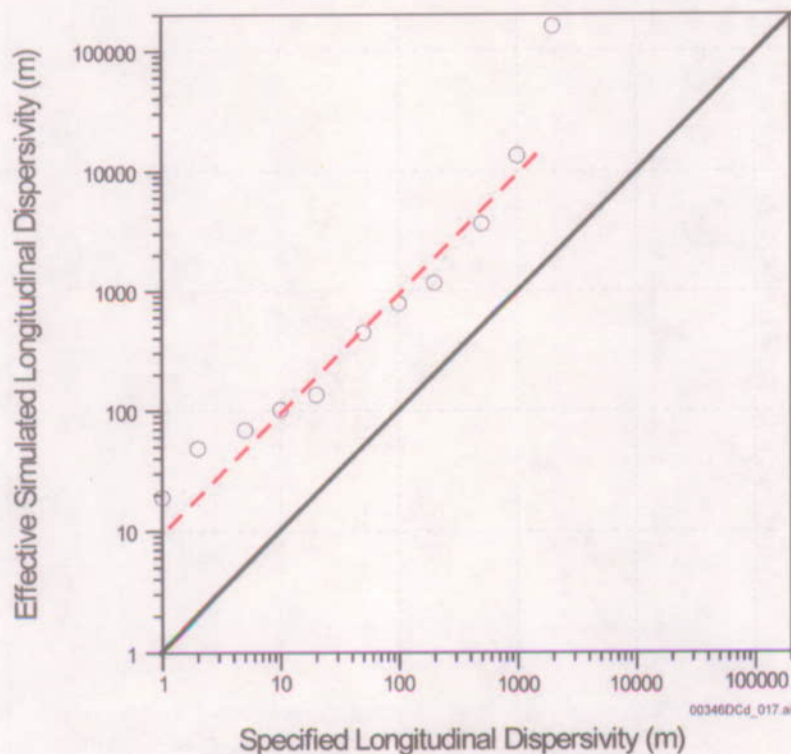
Transport field studies have been conducted at a variety of length scales from meters to kilometers to address the issue of dispersion. Figure 3-7 shows estimated dispersivity as a function of length scale. Dispersivity has been shown to increase as a function of observation scale, attributed mainly to mixing as more heterogeneities are sampled at larger scales (Gelhar et al. 1992). The dispersivity values determined for the C-Wells reactive tracer experiment (CRWMS M&O 2000a, Section 3.1.3.2), shown as a black diamond on Figure 3-7, illustrate a trend toward larger dispersion coefficients for transport over longer distances.



Source: BSC 2001c, Figure 100.

Figure 3-7. Dispersivity as a Function of Length Scale

Dispersion in saturated zone transport at Yucca Mountain has been simulated using a random-walk displacement algorithm to model dispersion phenomenon on the local scale (10s to 100s of meters). In addition, the spatial distribution of hydrogeologic units of contrasting permeability within the model imparts an additional dispersion at the scale of kilometers to the simulated transport of particles as flow paths diverge during transport. The effective longitudinal dispersivity due to both processes may be considerably larger than the specified value due to the additive effects of these two processes. The effective longitudinal dispersivity has been analyzed for a range of values of specified longitudinal dispersivity to evaluate the magnitude of this effect. The results of this analysis (BSC 2003d) indicate that the effective simulated longitudinal dispersivity is about one order of magnitude higher than the specified longitudinal dispersivity (Figure 3-8). To account for this numerical effect, the dispersivity used in the model is reduced by an order of magnitude to allow the effective modeled diffusion to be equivalent to the observed dispersivity distribution (Figure 3-8). Because all the radionuclide mass is captured in the representative volume, transverse vertical and horizontal dispersivity are not pertinent to TSPA-LA modeling.



Source: BSC 2003d, Figure 6-19.

Figure 3-8. Comparison of Effective Modeled Dispersivity versus Specified Dispersivities using the Site-Scale Radionuclide Transport Model

3.2.2 Advection, Diffusion, and Dispersion Processes and Parameters for Alluvium

Due to the porous nature of the alluvial material, fluid flow in the alluvium is well represented using a porous continuum conceptual model. As a result, the principal transport characteristic of the alluvium relevant to nonsorbing radionuclide migration is the effective porosity.

3.2.2.1 Effective Porosity of the Alluvium

A range of effective porosities for alluvial materials has been presented in the literature (BSC 2003d). To supplement this distribution, site-specific testing has been performed in some single-well tracer tests at the Alluvial Testing Complex. A site-specific value of 0.10 (10 percent) was determined for effective porosity from well NC-EWDP-19D1 at the Alluvial Testing Complex based on a single-well pumping test (BSC 2003e). There are also total porosity values from the same well based on borehole gravimeter surveys, which are used in developing the upper bound of the effective porosity in the alluvium uncertainty distribution.

Single-well hydraulic testing of the saturated alluvium was conducted in well NC-EWDP-19D1 between July 2000 and November 2000. In January 2002, two cross-hole hydraulic tests were performed where well NC-EWDP-19D1 was pumped and wells NC-EWDP-19IM1 and NC-EWDP-19IM2 were used for monitoring.

The total porosity of the alluvium was determined to be about 33 percent from analysis of grain size distributions. An estimate of total porosity using the storage coefficient from the cross-hole hydraulic test, the thickness of the tested interval, and the barometric efficiency of the formation was determined to be 40 percent. These values represent upper bounds of possible porosities, which need to be adjusted to account for the effective porosity through which water and any radionuclides are likely to be transported.

In addition, three single-well injection-withdrawal tracer tests were conducted in well NC-EWDP-19D1 between December 2000 and April 2001. In each tracer test, two nonsorbing solute tracers with different diffusion coefficients were simultaneously injected (a halide and a fluorobenzoic acid dissolved in the same solution). The three conceptual transport models that were considered for the saturated valley-fill deposits located south of Yucca Mountain prior to single-well tracer testing at NC-EWDP-19D/D1 are depicted in Figure 3-9 and described below:

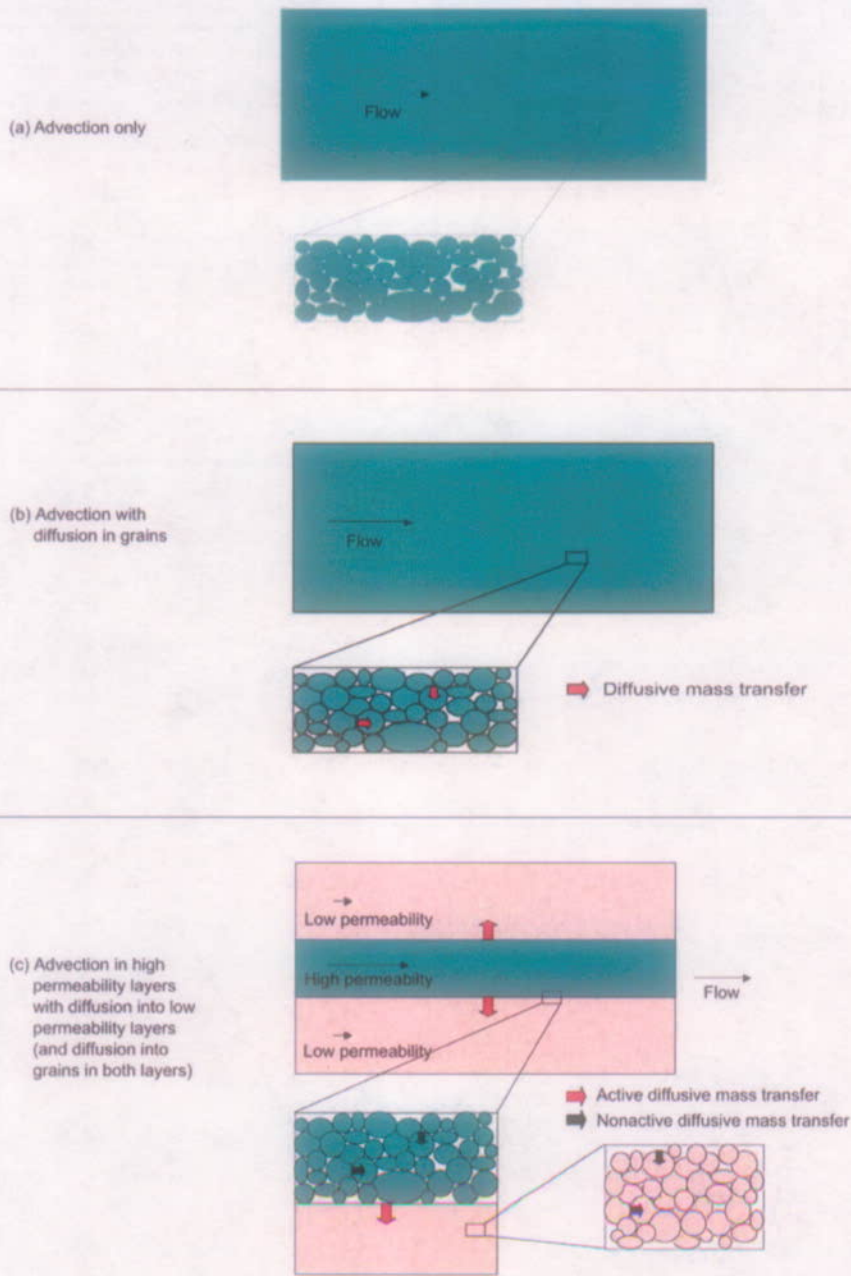
- The first model assumes purely advective transport through a porous medium with no diffusive mass transfer into either the grains of the medium or between advective and nonadvective regions of the aquifer. This model does not necessarily imply a homogeneous flow field, but it does preclude a system with alternating layers of relatively narrow thickness, considerable differences in permeability, or both. Such a conceptual model might be valid in a sandy aquifer with grains of relatively low porosity.
- The second model is similar to the first except that it assumes diffusive mass transfer into the grains of the porous medium. These grains are internally porous, but the porosity is not well connected over the scale of the grains; therefore, the grains transmit negligible flow.

- The third model assumes diffusive mass transfer between advective and nonadvective layers in the aquifer. In this model, the flow system is assumed to alternate between high and low conductivity layers, a simplified representation that is consistent with some depositional scenarios. Diffusive mass transfer in this case is only between the two layers, not into grains within the layers. However, one variation of this model is to assume that diffusion also occurs into grains in both the advective and nonadvective layers. This variation is essentially a combination of the second and third conceptual models, with an additional level of complexity allowing for diffusion in the nonadvective layer into both the inter- and intragranular pore spaces.

Figure 2-31 is an example of the tracer response, showing nearly identical responses of the paired tracers. Because the response of the paired tracers with different diffusion coefficients are the same it implies that the conceptual model of a single porosity medium (i.e., model 1) is valid.

Four methods were used to estimate the ambient groundwater velocity from the differences in tracer breakthrough for the various drift periods during the single-well tracer tests. These four methods include the peak arrival, late arrival, and two mean arrival methods. Table 2-7 summarizes the specific discharge and seepage velocity estimates for three different assumed flow porosities. Estimates of specific discharge range from 1.2 to 9.4 m/yr., which falls within the range of specific discharges derived from the site-scale flow model. Flow porosity and longitudinal dispersivity estimates of 0.10 and 5 m, respectively, were obtained using a linked-analytical-solution method.

Based on the above observations and literature surveys, a range of effective porosities is possible for the alluvium. Figure 3-10 illustrates the possible distributions and Figure 3-11 is the actual distribution used in the model.



For illustration purposes only

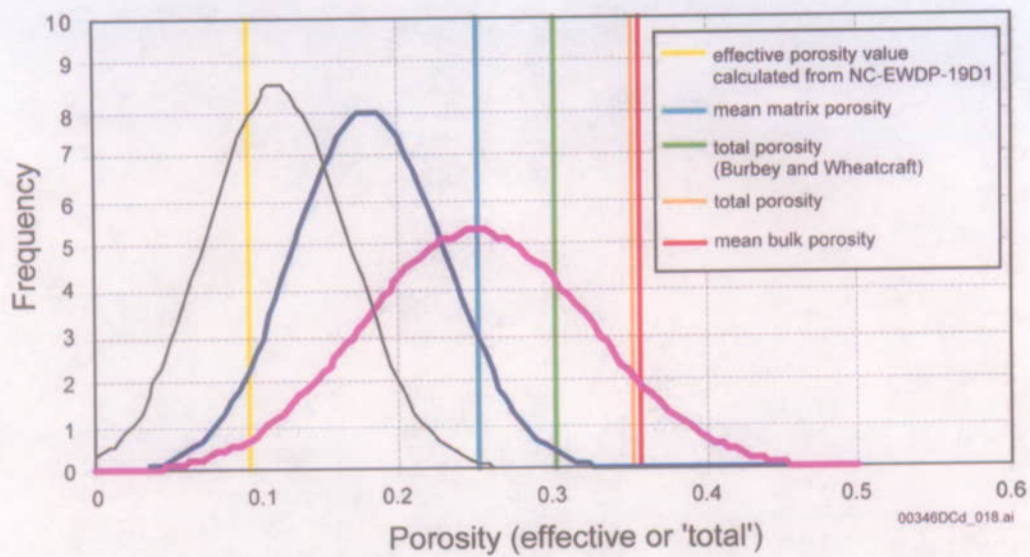
NOTES: Red arrows in (c) indicate diffusive mass transfer options that were exercised in this scientific analysis, and black arrows indicate options that were not exercised.

00346DC_059.psd

Source: BSC 2003e, Figure 6.5-1.

NOTES: Red arrows in (c) indicate diffusive mass transfer options that were exercised in this scientific analysis, and black arrows indicate options that were not exercised.

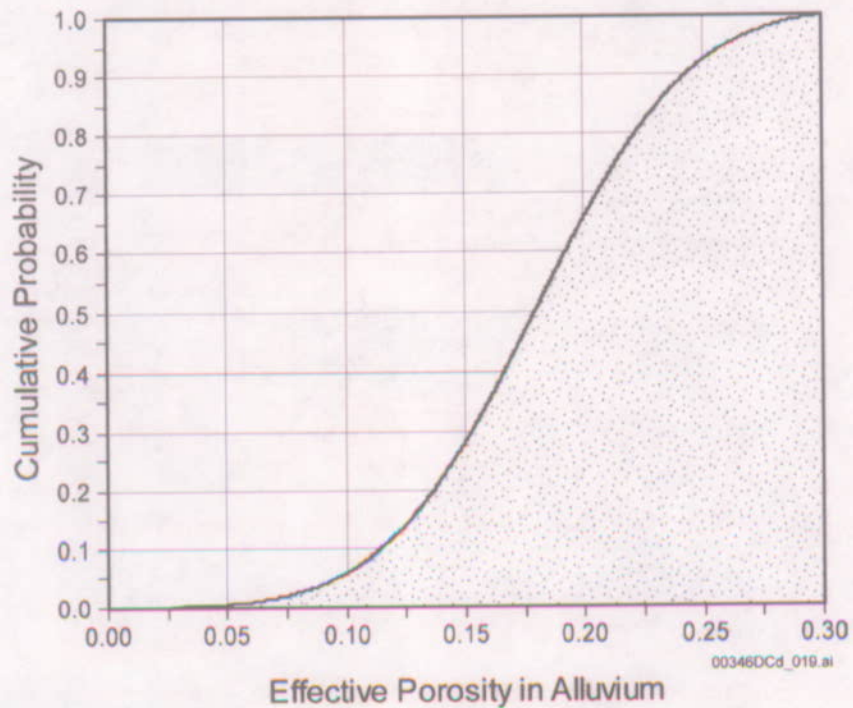
Figure 3-9. Schematic Illustration of Alternative Conceptual Transport Models for the Valley-Fill Deposits South of Yucca Mountain



Source: BSC 2003d, Figure 6-8.

NOTE: Solid black distribution is MO0003SZFWTEEP.000; the solid blue distribution is MO010SHCONEPOR.000; the solid pink distribution is MO0003SZWTEEP.000. All data are from DOE 1997 except for total porosity (Burbey and Wheatcraft), which is from Burbey and Wheatcraft 1986.

Figure 3-10. Range of Observed and Literature Effective Porosities in Alluvial Materials



Source: BSC 2003d, Figure 6-9.

Figure 3-11. Effective Porosity Distribution used in Yucca Mountain Transport Model

3.2.2.2 Alluvium Diffusion

The fact that there was virtually no difference in the normalized responses of the halide and fluorobenzoic acid tracers in the three single-well tracer tests conducted in NC-EWDP-19D1 strongly suggests that a single-porosity conceptual model is appropriate for modeling radionuclide transport in the saturated alluvium south of Yucca Mountain (BSC 2003e). Further evidence for a single-porosity flow and transport system was provided by the lack of an increase in tracer concentrations after flow interruptions during the tailing portions of the tracer responses in two of the tests. This lack of increase in tracer concentrations indicates a lack of diffusive mass transfer between flowing and stagnant water in the flow system. As a result of these observations, diffusion was not considered in transport in the alluvium.

3.2.2.3 Alluvium Dispersivity

Field scale values of dispersivity in the alluvium have not been measured. However, several column tracer experiments were conducted using groundwater and alluvium from the site of well NC-EWDP-19D1 and the sorbing tracer, lithium bromide. The dispersivity values obtained from these experiments range from 1.8 to 5.4 cm (BSC 2003e). The small dispersivity values are consistent with the scale of the column experiments. However, as discussed above, these values are not appropriate for larger scale simulations due to the scale dependency of this parameter. A common scale-dependent dispersivity for fractured tuff and alluvium has been used in numerical models of transport at Yucca Mountain (Figure 3-7; see also BSC 2001c).

3.2.3 Corroboration of Tuff and Alluvial Advective Transport Representations Using Carbon Isotope Information

Although the advective transport properties are acceptably constrained by in-situ observations from boreholes, these observations are limited by the time and space scale over which the testing was conducted. For example, the scale of the C-Wells and Alluvial Testing Complex are representative of spatial scales of 10s of meters and temporal scales of days to months. The transport processes of relevance to repository performance occur over spatial scales of kilometers and temporal scales of 1000s of years.

One of the few methods to investigate relevant transport processes over the spatial and temporal scale of interest to repository performance is the use of naturally occurring radioisotopes such as ^{14}C . The following discussion summarizes the observations of carbon isotopes used to substantiate the properties developed at the smaller scales.

3.2.3.1 Carbon-14 Background

The radioactive decay of ^{14}C , with a half-life of 5,730 years, forms the basis for radiocarbon dating. The ^{14}C age of a sample is calculated as

$$t = (-1/\lambda) \ln (^{14}\text{A}/^{14}\text{A}_0) \quad (\text{Eq. 3-1})$$

where t is the mean groundwater age (yr.), λ is the radioactive decay constant ($1.21 \times 10^{-4} \text{ yr}^{-1}$), ^{14}A is the measured ^{14}C activity, and $^{14}\text{A}_0$ is the assumed initial activity. Carbon-14 ages typically are expressed in percent modern carbon (pmc). A ^{14}C activity of 100 pmc is taken as

the ^{14}C activity of the atmosphere in the year 1890, before the natural ^{14}A of the atmosphere was diluted by large amounts of carbon-14-free carbon dioxide gas from the burning of fossil fuel.

Theoretically, the activity of ^{14}C in a groundwater sample reflects the time when the water was recharged. Unfortunately, precipitation generally has low carbon concentrations and has a high affinity for dissolution of solid phases in the soil zone, unsaturated zone, and saturated zone. In particular, in the transition from precipitation compositions to groundwater compositions, the concentration of combined bicarbonate and carbonate in the water commonly increases by orders of magnitude (Langmuir 1997, Table 8.7; Meijer 2002). Because bicarbonate is the principal ^{14}C -containing species in most groundwater, the source of this additional bicarbonate can have a major impact on the "age" calculated from the ^{14}C activity of a given water sample. If the source is primarily decaying plant material in an active soil zone, the calculated age for the water sample should be close to the true age. In contrast, if the source of the bicarbonate is dissolution of old (i.e., older than 10^4 yr.) calcite with low ^{14}C activity, or oxidation of old organic material, then the calculated age for the sample will be over estimated.

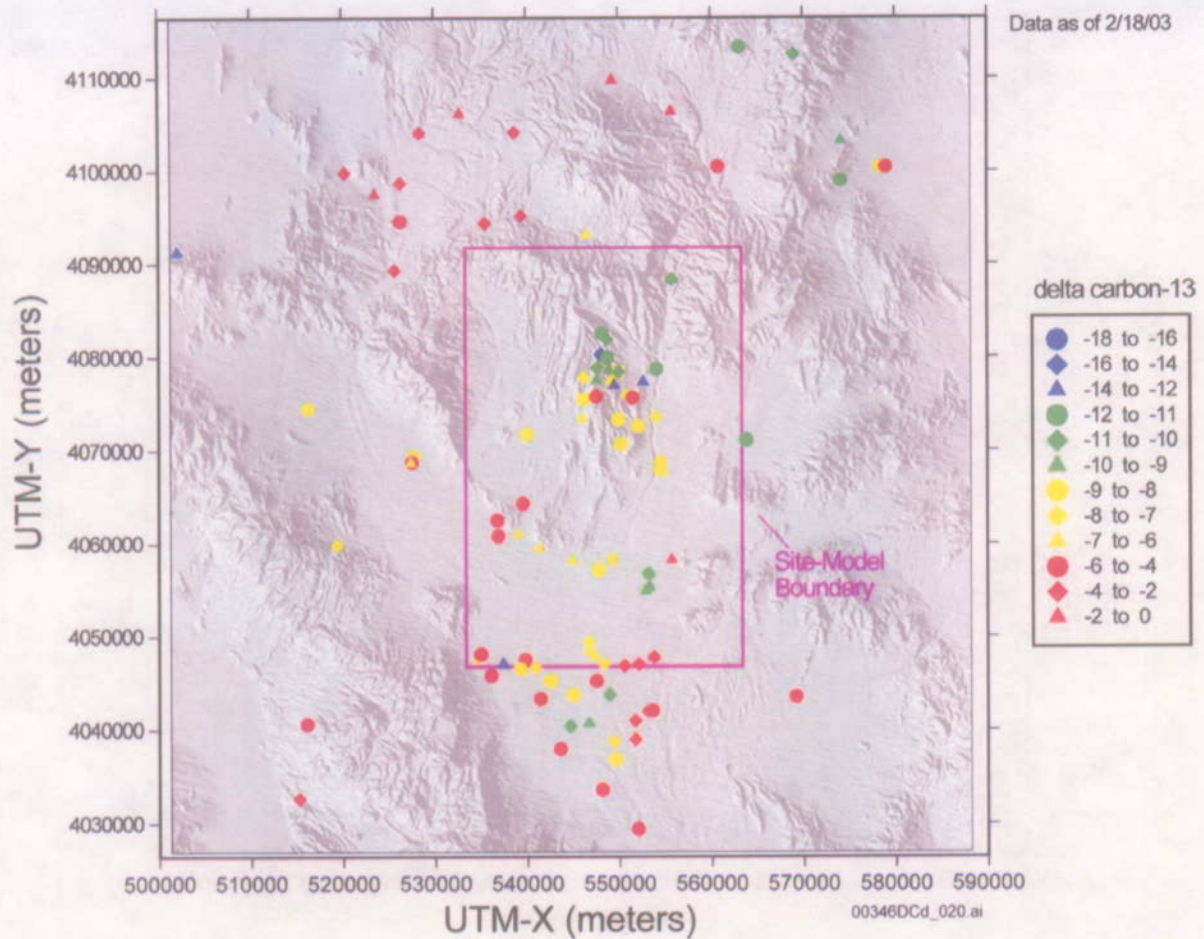
A useful measure of the source of the carbon in a water sample is the delta carbon-13 ($\delta^{13}\text{C}$) value of the sample because this value is different for organic materials compared to calcites. The $\delta^{13}\text{C}$ value, in units of per mil, is defined as

$$\delta^{13}\text{C} = \left[\frac{(^{13}\text{C}/^{12}\text{C})_{\text{sample}}}{(^{13}\text{C}/^{12}\text{C})_{\text{standard}}} - 1 \right] \times 1000 \quad (\text{Eq. 3-2})$$

The $\delta^{13}\text{C}$ values of carbon species typical of the soil waters in arid environments range from -25 to -13 per mil (Forester et al. 1999, p. 36). At Yucca Mountain, pedogenic carbonate minerals have $\delta^{13}\text{C}$ values that generally are between -8 and -4 per mil, although early formed calcites are also present that have $\delta^{13}\text{C}$ values greater than 0 per mil (Forester et al. 1999, Figure 16; Whelan et al. 1998, Figure 5). Paleozoic carbonate rocks typically have $\delta^{13}\text{C}$ values close to 0 per mil (Forester et al. 1999, Figure 16; Whelan et al. 1998, Figure 5).

3.2.3.2 Delta Carbon-13 Observations in Groundwater in the Vicinity of Yucca Mountain

The areal distribution of $\delta^{13}\text{C}$ values is shown in Figure 3-12. Groundwater in the northernmost part of Yucca Mountain is generally lighter in $\delta^{13}\text{C}$ than groundwater found toward the central and southern parts of the mountain. North of Yucca Mountain, groundwater $\delta^{13}\text{C}$ values are generally considerably heavier than the groundwater $\delta^{13}\text{C}$ values found at Yucca Mountain. Overall, the $\delta^{13}\text{C}$ values of groundwater in Nye County Early Warning Drilling Program boreholes at the southern edge of Crater Flat increase toward the west, reflecting the increasing component of groundwater from carbonate rocks with $\delta^{13}\text{C}$ values around zero. The groundwater $\delta^{13}\text{C}$ values near Fortymile Wash are generally lower than the $\delta^{13}\text{C}$ values toward the western and eastern parts of the Amargosa Desert, where groundwater $\delta^{13}\text{C}$ values reflect the proximity to carbonate rocks of the southern Funeral Mountains and discharge from the carbonate aquifer across the Gravity Fault, respectively.

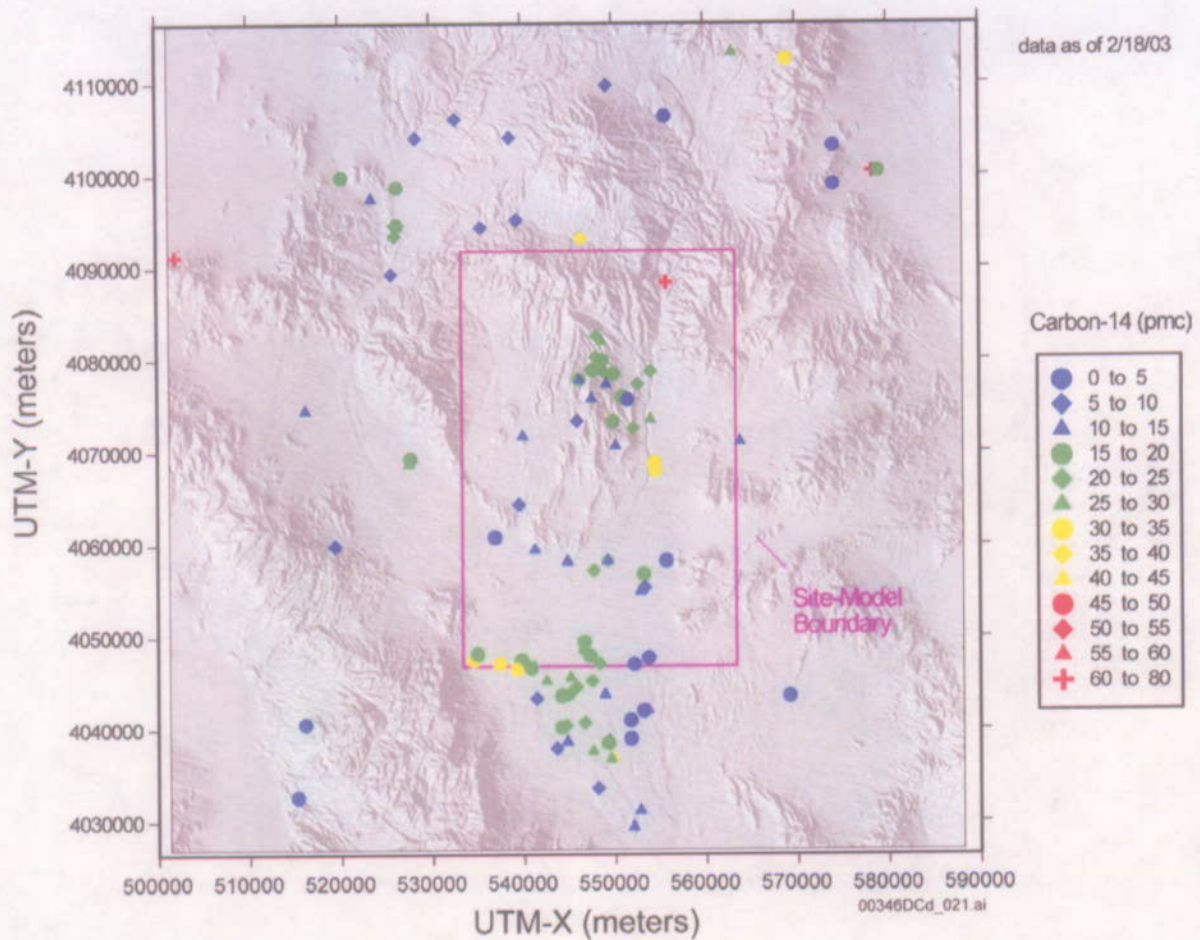


Source: BSC 2003f, Figure 27.

Figure 3-12. Areal Distribution of Delta Carbon-13 in Groundwater in the Vicinity of Yucca Mountain

3.2.3.3 Carbon-14 Observations in Groundwater in the Vicinity of Yucca Mountain

The areal distribution of ^{14}C activity is shown in Figure 3-13. Groundwater at the eastern edge of Crater Flat near Solitario Canyon has some of the lowest ^{14}C activities of groundwater in the map area. Groundwater at several Nye County boreholes in the Yucca Mountain-South grouping to the south of borehole USW VH-1 has similar ^{14}C activities. The groundwater at boreholes NC-EWDP-2D, NC-EWDP-19P, and some zones in NC-EWDP-19D have a ^{14}C activities of 20 pmc or more, similar to the ^{14}C activities of groundwater in Dune Wash and Fortymile Wash. Groundwater near Fortymile Wash has ^{14}C activities that range from about 76 pmc near the northern boundary of the model area to values under 20 pmc near the southern boundary of the model area. South of the site-model boundary, groundwater ^{14}C activities near Fortymile Wash range from 10 to 40 pmc.



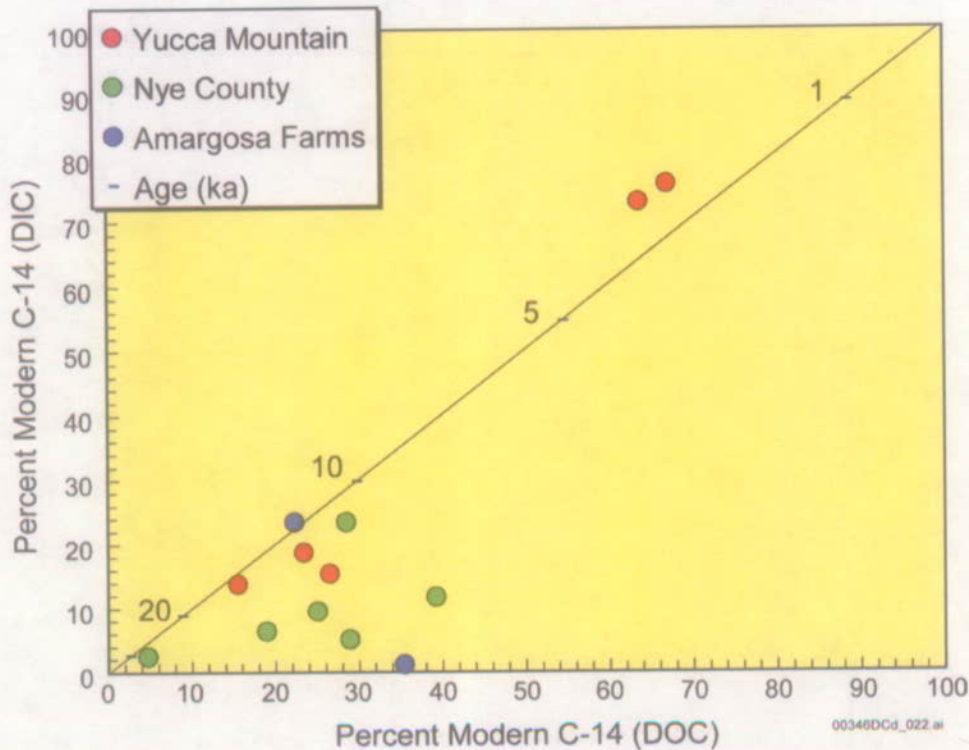
Source: BSC 2003f, Figure 28.

Figure 3-13. Carbon-14 Activities in Groundwater in the Vicinity of Yucca Mountain

The above observations have been based on measurements of dissolved inorganic carbon isotopes. As interpretation of such measurements has considerable uncertainty due to the varied water-rock interactions that can greatly affect the measured isotope ratios, measurements of dissolved organic carbon content have also been made. Carbon isotopes of dissolved organic carbon provide a means independent of dissolved inorganic carbon model age corrections to determine travel times of groundwater in aquifers. Groundwater ages can be calculated directly from dissolved organic carbon ^{14}C values if the ^{14}C of the recharge area groundwater is known. Ages calculated from dissolved organic carbon ^{14}C are maximum ages because any organic aquifer material would contain no ^{14}C . The exception is newly drilled boreholes that can contain modern dissolved organic carbon.

Thirteen dissolved organic carbon measurements have been made on samples of groundwater the Yucca Mountain area. A correlation of the ages determined from dissolved inorganic and dissolved organic carbon is presented in Figure 3-14. Most of the dissolved inorganic carbon ages for these waters are greater than 12,000 yrs. The dissolved organic carbon ages for these groundwater are younger ranging from 8,000 to 16,000 yrs. The youngest dissolved organic

carbon and dissolved inorganic carbon radiocarbon ages are for water from upper Fortymile Canyon, and these ages show a slight reverse discordance, that is the dissolved inorganic carbon ages are slightly younger than the dissolved organic carbon ages.



Source: Peters 2003, Slide 36 of 68.

Note: The numbers on the one-to-one line are groundwater ages in thousands of years, calculated assuming $^{14}A_0$ is 100 pmc.

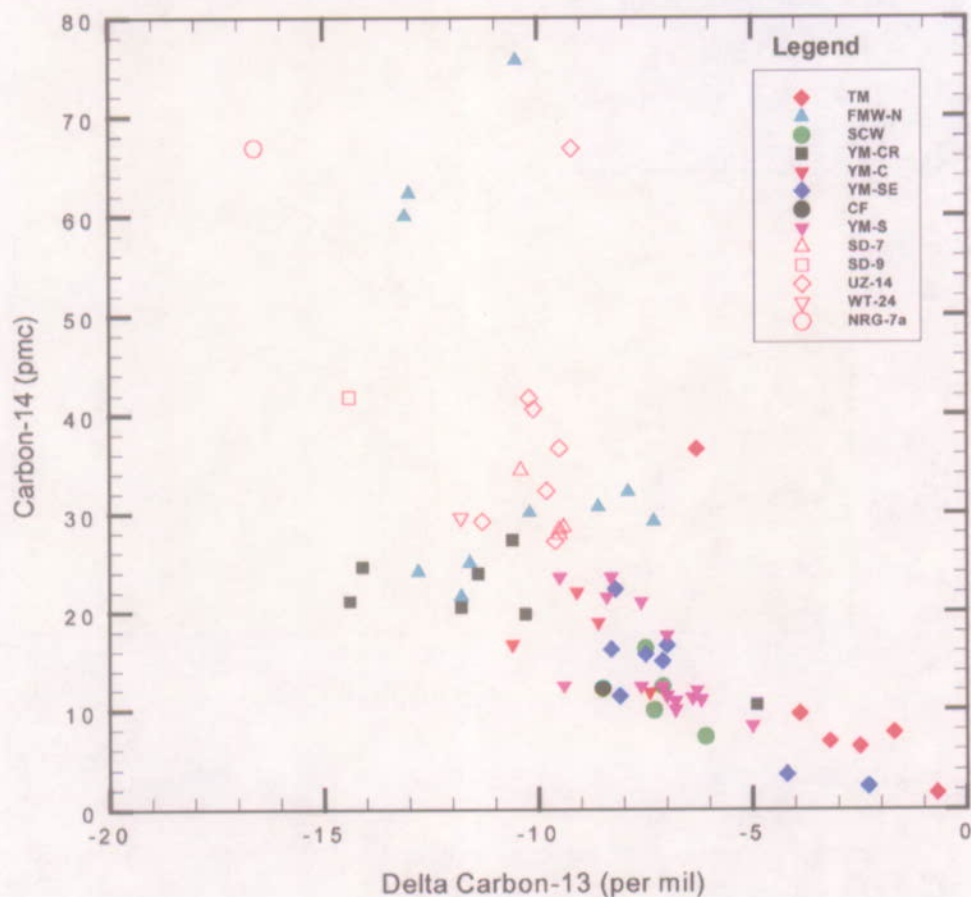
Figure 3-14. Comparison of Observed Dissolved Organic and Inorganic Carbon-14 Ages in Groundwater in the Vicinity of Yucca Mountain

3.2.3.4 Interpretation of Carbon Isotope Data

The measured activity of ^{14}C indicates that most groundwater contain less than 30 pmc, with a few notable exceptions in northern Fortymile Wash. Trends of decreasing ^{14}C along potential flow paths from the repository are not evident from most of the data. The carbon reservoir (principally as bicarbonate) in groundwater is readily modified through reaction with aquifer rock along the flow path. It is therefore necessary to evaluate potential sources of carbon in the groundwater before using ^{14}C data to evaluate flow paths or residence times.

Although carbon isotopes are not used to evaluate flow paths, ^{14}C data from groundwater along the potential flow paths can be used to infer relative advective transport times. The measured ^{14}C activities are corrected to account for decrease in ^{14}C activity that results from water-rock interactions and the mixing of groundwater as identified by mixing and chemical reaction models (see Appendix F). This process estimates decreases in ^{14}C activity due to radioactive decay

during transit between boreholes, which is converted into a transit time using the radioactive decay equation. After determining the transit time between boreholes from the radioactive decay equation, linear groundwater velocities are determined by dividing the distance between the boreholes by the transit time.



00346DCd_023

Source: BSC 2003f, Figure 45.

Figure 3-15. Correlation of Carbon-14 and Delta-Carbon-13 in Perched Waters and Groundwater in the Vicinity of Yucca Mountain

The variability in $\delta^{13}\text{C}$ values (Figure 3-12) suggests that groundwater in the Yucca Mountain area have interacted to varying degrees with carbonate rock, minerals, or with groundwater from the carbonate aquifer, and therefore require different amounts of correction to account for these effects. This conclusion is also indicated by the variable degrees of agreement between the organic and inorganic ^{14}C activities of groundwater in the Yucca Mountain area (Figure 3-14) and by a scatterplot of ^{14}C activity versus $\delta^{13}\text{C}$ for Yucca Mountain and upgradient areas (Figure 3-15). The scatterplot indicates that perched water at Yucca Mountain, groundwater in northern Yucca Mountain (YM-CR wells), and groundwater beneath Fortymile Wash have the highest ^{14}C activities and lightest $\delta^{13}\text{C}$ values, whereas groundwater from the Timber Mountain area and from the carbonate aquifer in the Yucca Mountain Southeast (YM-SE) group have the

lowest ^{14}C activities and heaviest $\delta^{13}\text{C}$ values. Collectively, the data display a trend that can be interpreted in a number of ways. Calcite dissolution or mixing of local recharge with isotopic characteristics of perched water with groundwater from the carbonate aquifer or from Timber Mountain are possible explanations for the observed trend between $\delta^{13}\text{C}$ and ^{14}C . Both of these processes tend to introduce dissolved inorganic carbon with heavy $\delta^{13}\text{C}$ and little ^{14}C . This explanation assumes that points on the trend are of the same age, but that the water dissolved different amounts of calcite. However, the scatter of points about the trend could be due to inclusion of samples of different ages. The scatterplot (Figure 3-15) also substantiates the argument that groundwater in northernmost Yucca Mountain at some Yucca Mountain Crest (YM-CR) group wells originates primarily from local recharge rather than by the southerly flow of groundwater from Timber Mountain.

To provide an estimate of groundwater ages, corrected ^{14}C ages were calculated for locations within 18 km of the repository where groundwater had been identified from anomalously high $^{234}\text{U}/^{238}\text{U}$ ratios as having originated mostly from local recharge (Paces et al. 1998). Corrections were also made to the ^{14}C ages of groundwater from several locations for which $^{234}\text{U}/^{238}\text{U}$ activity ratios were not measured but which may contain substantial fractions of local Yucca Mountain recharge based on proximity to groundwater with high $^{234}\text{U}/^{238}\text{U}$ activity ratios.

Table 3-3. Chemistry and Ages of Groundwater from Seven Boreholes at Yucca Mountain

Borehole	$^{234}\text{U}/^{238}\text{U}$ Activity Ratio	^{14}C Activity (pmc)	DIC, as HCO_3 , (mg/L)	Corrected ^{14}C age (years)	Uncorrected ^{14}C age (years)
USW G-2	7 to 8	20.5	127.6	13,100	13,100
UE-25 WT #17	7 to 8	16.2	150.0	13,750 to 14,710	15,040
UE-25 WT #3	7 to 8	22.3	144.3	11,430 to 12,380	12,400
UE-25 WT #12	7 to 8	11.4	173.9	15,430 to 16,390	17,950
UE-25 C #3	7 to 9	15.7	140.2	14,570 to 15,300	15,300
UE-25 B #1 (Tcb) ^b	---	18.9	152.3	12,350 to 13,300	13,770
USW G-4	---	22.0	142.8	11,630 to 12,510	12,500

Source: BSC 2003f, Table 16.

NOTE: DIC = dissolved inorganic carbon,
pmc = percent modern carbon

3.2.3.5 Evaluation of Groundwater Velocities in the Yucca Mountain Region

Under ideal circumstances, the decrease in groundwater ^{14}C activities along a flow path can be used to calculate groundwater velocities. The calculation is straightforward when groundwater recharge occurs in a single location and groundwater downgradient from this location does not receive addition recharge or mix with other groundwater. In the Yucca Mountain area, the calculation of groundwater velocity based on ^{14}C activity is complicated by the possible presence of multiple, distributed recharge areas. If relatively young recharge were added along a flow

path, the ^{14}C activity of the mixed groundwater would be higher and the calculated transport times shorter than for the premixed groundwater without the downgradient recharge. Unfortunately, the chemical and isotopic characteristics of the recharge from various areas at Yucca Mountain may not be sufficiently distinct to identify separate sources of local recharge in the groundwater. Conversely, if groundwater from the carbonate aquifer were to mix downgradient with Yucca Mountain recharge, the mixture would have a lower ^{14}C activity than the Yucca Mountain recharge component because of the high carbon alkalinity and low ^{14}C activity of the carbonate aquifer groundwater. However, the presence of groundwater from the carbonate aquifer in the mixture would be recognized because of the distinct chemical and isotopic composition of that groundwater compared with the recharge water, and the effect on the ^{14}C activity of the groundwater mixture could be calculated.

In this section, groundwater velocities are estimated along various flow path segments using the ^{14}C activities of the groundwater along the flow path. The measured ^{14}C activities at the upgradient borehole defining the segment are adjusted to account for decreases in the ^{14}C activity that result from water-rock interactions the groundwater undergoes between boreholes, as identified by PHREEQC mixing and chemical reaction models described by BSC (2003f). This adjustment to the initial ^{14}C activity is necessary to distinguish between the decrease in ^{14}C activity caused by water-rock interaction and the decrease in ^{14}C activity due to transit time between the boreholes. After determining the transit time between boreholes, linear groundwater velocities are determined by dividing the distance between the boreholes by the transit time. Groundwater velocities were calculated for several possible flow paths south of the repository, as described below.

Flow path Segment USW WT-3 to NC-EWDP-19D—PHREEQC inverse models (BSC 2003f, Section 6.5.8) indicate that groundwater sampled from various zones in borehole NC-EWDP-19D could have evolved from groundwater at borehole USW WT-3. Transit times were calculated using the dissolved inorganic carbon of groundwater at borehole USW WT-3 and PHREEQC estimates of the carbon dissolved by this groundwater as it moves toward various zones at borehole NC-EWDP-19D. Groundwater in the composite borehole and alluvial groundwater require approximately 1,000 to 2,000 years to travel the approximately 15-km distance between boreholes USW WT-3 and NC-EWDP-19D. This equates to linear groundwater velocities of approximately 7.5 to 15 m/yr. The groundwater in the deeper alluvial zones (Zones 3 [145.6 to 206.0 m] and 4 [220.2 to 242.4 m]) requires approximately 1,500 to 3,000 years, and thus travels at a linear groundwater velocity of 5 to 10 m/yr. In contrast, the transit times calculated for groundwater from shallow Zones 1 (125.9 to 131.4 m) and 2 (151.8 to 157.3 m) have transit times that range from 0 to about 350 years. Using the upper age of 350 years, groundwater flow from borehole USW WT-3 to Zones 1 and 2 in borehole NC-EWDP-19D is about 40 m/yr. This higher velocity may indicate that some of the shallow groundwater at borehole USW WT-3 moves along major faults like the Paintbrush Canyon fault or that groundwater is more representative of local recharge conditions.

For comparison, similar analyses in the tuff aquifers in the vicinity of Yucca Mountain have been conducted by White and Chuma (1987) and Chapman et al. (1995). White and Chuma (1987) estimated flow velocities between 3 and 30 m/yr. (9.8 and 98 ft/yr.), while Chapman et al. (1995) estimated flow velocities of between 1.9 and 2.4 m/yr. (6.2 and 7.9 ft/yr.).

Flow path Segment USW WT-24 to WT 3—Transit times were calculated using the dissolved inorganic carbon of groundwater at borehole USW WT-24 and PHREEQC estimates of the carbon dissolved by this groundwater as it moves toward borehole UE-25 WT #3. The transit time estimate based on the differences in dissolved inorganic carbon of groundwater at boreholes USW WT-24 and UE-25 WT #3 is 216 years. Using this estimate of transit time and a linear distance between boreholes USW WT-24 and UE-25 WT #3 of 10 km, results in a linear groundwater velocity of 46 m/yr.

3.2.3.6 Summary of Interpretations of Carbon Isotope Observations

Although uncertainty and variability exists in the ^{14}C and $\delta^{13}\text{C}$ observations, they generally indicate advective transport times of unretarded species that range from a few hundred to a few thousand years along likely flow paths within the tuff and alluvium aquifers to a downgradient point (NC-EWDP-19D) close to the compliance boundary. These advective travel times are similar to those that result from the saturated zone flow and transport model that is presented in Section 3.4.

3.3 RADIONUCLIDE SORPTION PROCESSES

Sorption reactions are chemical reactions that involve the attachment of dissolved chemical constituents to solid surfaces. Although these reactions can be complex, they are typically represented in transport calculations by a constant called the sorption coefficient. In the literature, the sorption coefficient (K_d) is often referred to as the distribution coefficient, both terms are used interchangeably in this document. The sorptive properties of the tuff and alluvial aquifers have been studied in a range of laboratory and in situ tests.

In addition to radionuclide transport being affected by interactions between the dissolved species and the solid aquifer materials through sorption processes, radionuclide migration can also be affected by precipitation reactions caused by variable geochemical conditions along the groundwater travel path. The most significant control on precipitation reactions in the saturated zone at Yucca Mountain is the possible affect that reducing conditions could have on the behavior of several redox-sensitive radionuclides such as technetium.

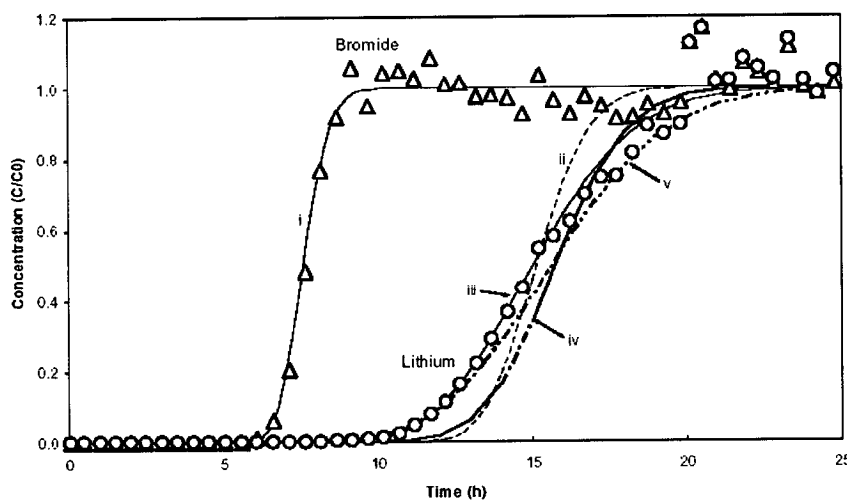
Reducing conditions have been observed in the groundwater of several boreholes in the vicinity of Yucca Mountain. A summary of this information is presented in Appendix K. In addition, there is a range of redox conditions in alluvial groundwater, as measured in groundwater pumped from Nye County boreholes. For example, groundwater in the central portion of the expected flow path (e.g., at NC-EWDP-19D and -22S) has generally oxidizing conditions (with the exception of zone 4) while groundwater to the east (i.e., at NC-EWDP-5S) and west (i.e., at NC-EWDP-1DX and -3D) show reducing characteristics.

Although the presence of reducing conditions has been observed in the saturated zone at Yucca Mountain; as described in Appendix K, the groundwater chemistry along the likely flow paths is generally oxidizing. Because oxidizing conditions yield a more conservative transport behavior, the possible precipitation reactions have not been considered in the post closure performance assessment analyses.

3.3.1 Radionuclide Sorption on Fractured Tuff

Sorption reaction interactions can potentially occur on the surfaces of fractures and within the rock matrix of the fractured tuff in the vicinity of Yucca Mountain. However, because of a lack of data and to be conservative, sorption on fracture surfaces is neglected, and only sorption within the matrix is included in the saturated zone transport model. Testing of sorptive characteristics has been performed in situ at the C-Wells complex using analog tracers and in the laboratory using actual radionuclides of interest to repository performance at Yucca Mountain.

The C-Wells reactive tracer field experiments build on the detailed understanding of flow and advective transport characteristics obtained through the range of hydraulic and nonreactive tracer tests summarized in Section 3.2.1. By having a reasonable understanding of the flow and advective transport properties at the C-Wells complex, interpretation of the reactive tracer test data can be accomplished using extrapolation to determine the sorption characteristics. The reactive tracer chosen as the analog was lithium. An example lithium test conducted in the laboratory is represented in Figure 3-16. The range of laboratory-derived lithium sorption coefficients (K_{ds}) is between 0.084 to 0.32 ml/g (BSC 2003e, Table 6.3-11).



Source: BSC 2003e, Figure 6.3-60.

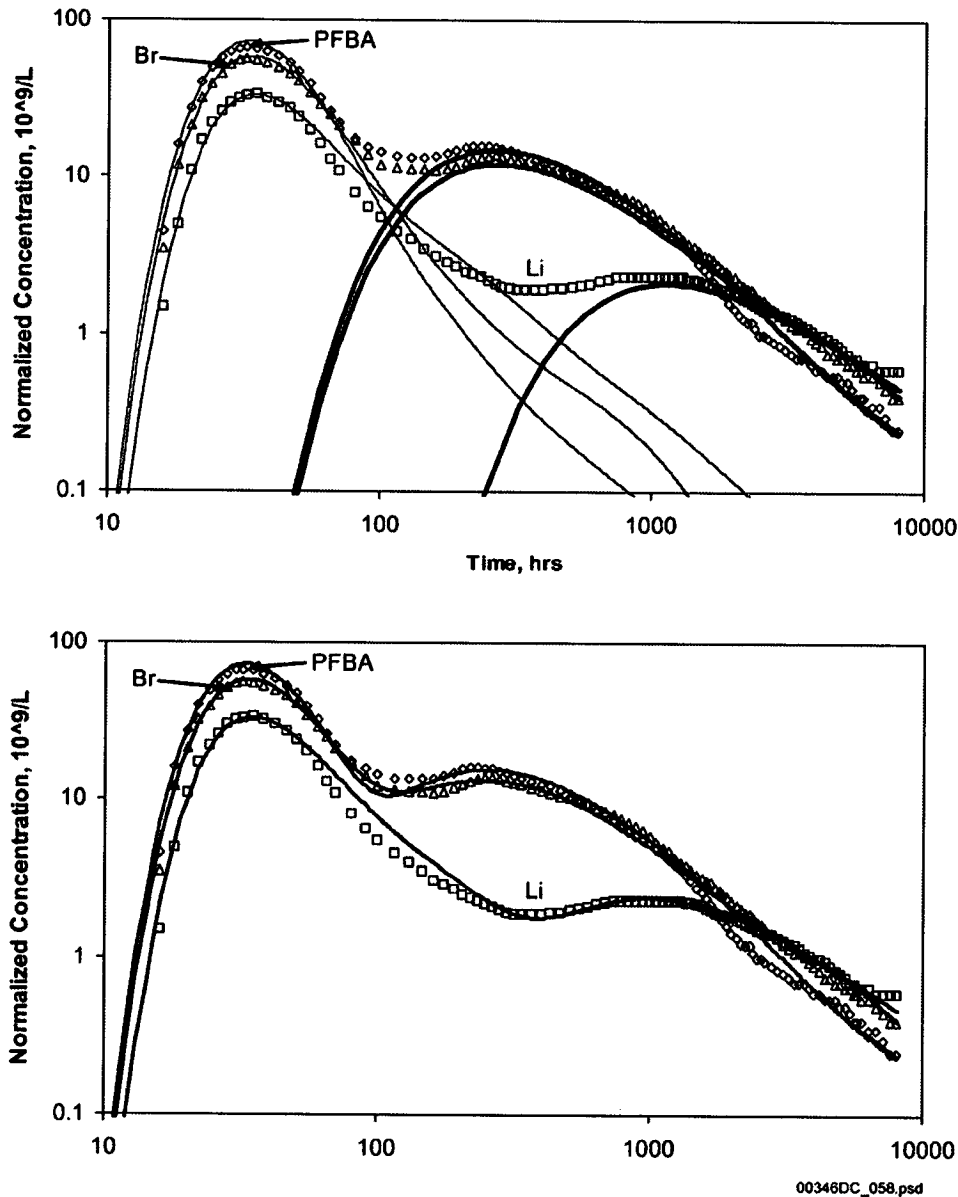
NOTES: The curves above are numbered as follows:

- (i) fit to bromide data with a Peclet number of 250
 - (ii) fit to lithium data assuming linear isotherm ($R_F = 2.0$) with equilibrium sorption
 - (iii) fit to lithium data assuming linear isotherm with a forward rate constant of 3.1 1/hr (and $R_F = 2.0$)
 - (iv) fit to lithium data assuming a Langmuir isotherm with equilibrium sorption
 - (v) fit to lithium data assuming a Langmuir isotherm with a forward rate constant of 3.2 1/hr.
- Langmuir isotherm parameters: $K_L = 0.0058$ mL/ μ g and $S_{max} = 105.8$ μ g/g (batch isotherm values obtained for lithium on central Bullfrog Tuff from UE-25 C#2).

Figure 3-16. Bromide and Lithium Breakthrough Curves and Comparison to Model Fits

The results of one of the multiple-well injection-withdrawal tests are illustrated in Figure 3-17. The interpretation of these test results was modeled using a matrix-diffusion model with the

sorption coefficient of the matrix as an adjustable parameter (CRWMS M&O 2000a, Section 3.1.3.2). The model results are compared to the field observations in Figure 3-17, and the model fit to the data agreed well with the laboratory sorption test data. Thus in addition to confirming the sorption characteristics of the tuff aquifer materials, this match provides an additional degree of confidence in the matrix-diffusion model. The fact that the early breakthrough of lithium had the same timing as that of the nonsorbing tracers, but with a lower normalized peak concentration, is consistent with matrix diffusion followed by sorption in the matrix.



Source: BSC 2003e, Figure 6.3-28; DTN: LA0007PR831231.001 (data); output DTN: LA0303PR831231.003 (model).

Figure 3-17. Comparison of Lithium Tracer Test Results and Model Predicted Results at the C-Wells Complex

Lithium sorption parameters were deduced from the field tracer tests. In these tests, lithium sorption always was approximately equal to or greater than the sorption measured in the laboratory (CRWMS M&O 2000a, Table 3-4). Details of the methods used to obtain the field lithium sorption parameters and discussions of possible alternative interpretations of the lithium responses are provided by Reimus et al. (1999; BSC 2003e).

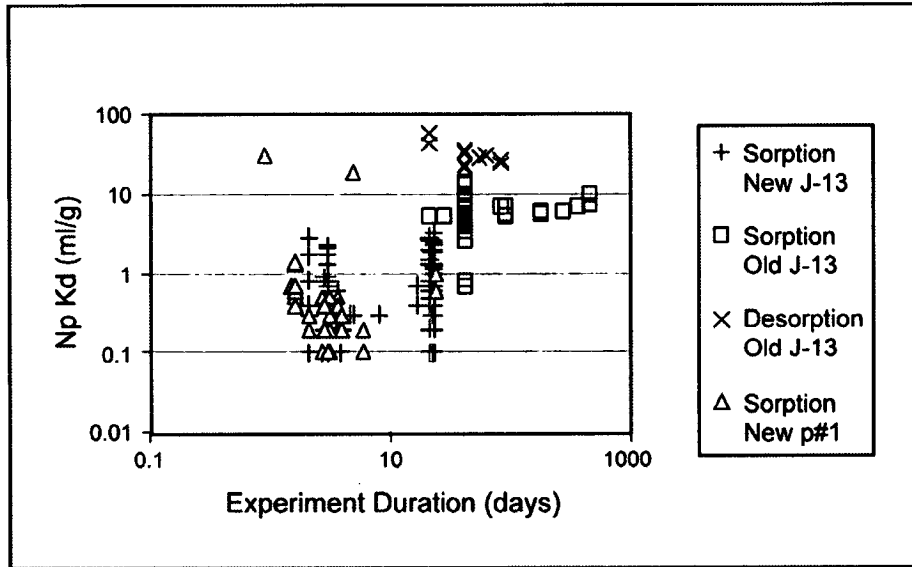
Experimental sorption coefficients (K_d values) were obtained using rock samples collected from the Topopah Spring welded and Calico Hills nonwelded hydrogeologic units at Busted Butte. The fine particles produced during sample crushing were not removed during the Busted Butte sorption study (BSC 2001c, Section 6.8.5.1.2.2) to duplicate in situ conditions, whereas fine materials were removed in the standard batch-sorption tests documented by Ding et al. (2003). Values for K_d could be influenced by small crushed-rock sizes used for sorption measurement, with the fine materials generating large K_d values. Sorption data determined during batch experiments are presented in Table 3-4.

Table 3-4. Sorption-Coefficient Distributions for Saturated Zone Units from Laboratory Batch Tests

Parameter Name	Parameter Value Range (ml/g)	Distribution Type
Am K_d (volcanics)	1,000 - 10,000	Truncated normal
Am K_d (alluvium)	1,000 - 10,000	Truncated normal
Cs K_d (volcanics)	100 - 7500	Cumulative
Cs K_d (alluvium)	100 - 1000	Truncated normal
Np K_d (volcanics)	0.0 - 6.0	Cumulative
Np K_d (alluvium)	1.8 - 13	Cumulative
Pa K_d (volcanics)	1,000 - 10,000	Truncated normal
Pa K_d (alluvium)	1,000 - 10,000	Truncated normal
Pu K_d (volcanics)	10 - 300	Cumulative
Pu K_d (alluvium)	50 - 300	Beta
Ra K_d (volcanics)	100 - 1000	Uniform
Ra K_d (alluvium)	100 - 1000	Uniform
Sr K_d (volcanics)	20 - 400	Uniform
Sr K_d (alluvium)	20 - 400	Uniform
Th K_d (volcanics)	1,000 - 10,000	Truncated normal
Th K_d (alluvium)	1,000 - 10,000	Truncated normal
U K_d (volcanics)	0 - 20	Cumulative
U K_d (alluvium)	1.7 - 8.9	Cumulative
C/Tc/I K_d (volcanics, alluvium)	0.0	None

Source: Based on BSC 2003d, Table 4-3.

The sorption data that were used as the basis of the distributions for neptunium, uranium, and plutonium (Table 3-4) are also presented in Figures 3-18 through 3-23. These data represent different types of experiments (sorption versus desorption), different water chemistries (derived from well J-13 and well UE-25 p#1), different times when the experiment was performed ("old" are tests performed prior to 1990 and "new" are tests performed after 1990) and different durations of the experiment.

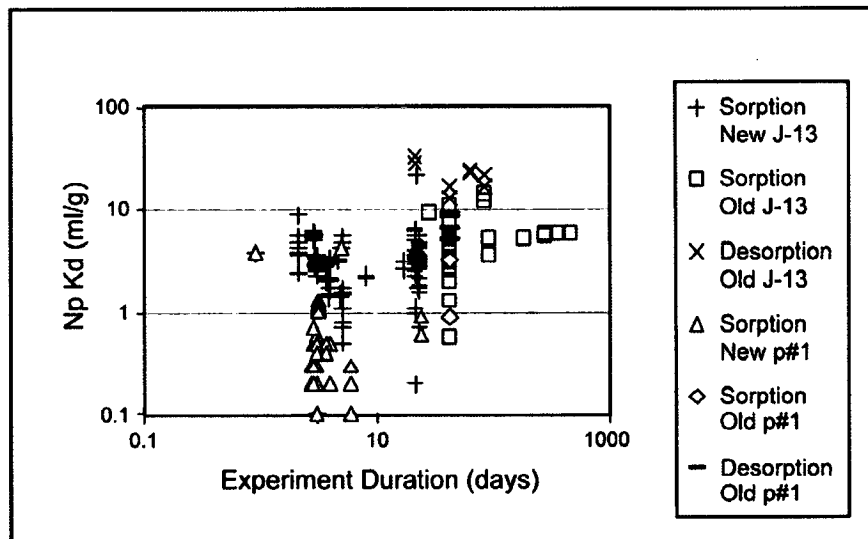


00346DCd_024.ai

Source: BSC 2003a, Figure I-16.

NOTE: Experiments oversaturated with Np_2O_5 have been omitted.

Figure 3-18. Neptunium Sorption Coefficients on Devitrified Tuff Versus Experiment Duration for Sorption (Forward) and Desorption (Backward) Experiments

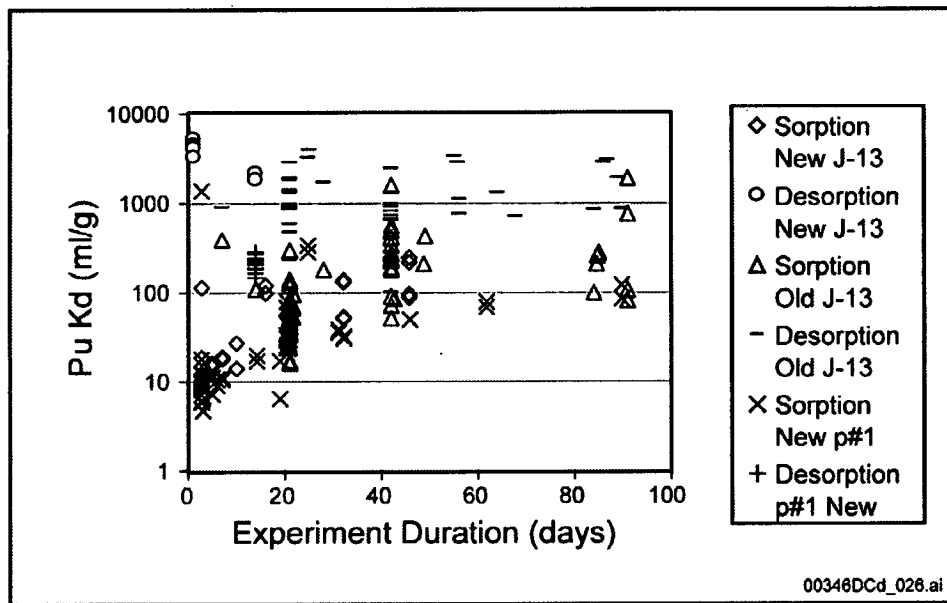


00346DCd_025.ai

Source: BSC 2003a, Figure I-20.

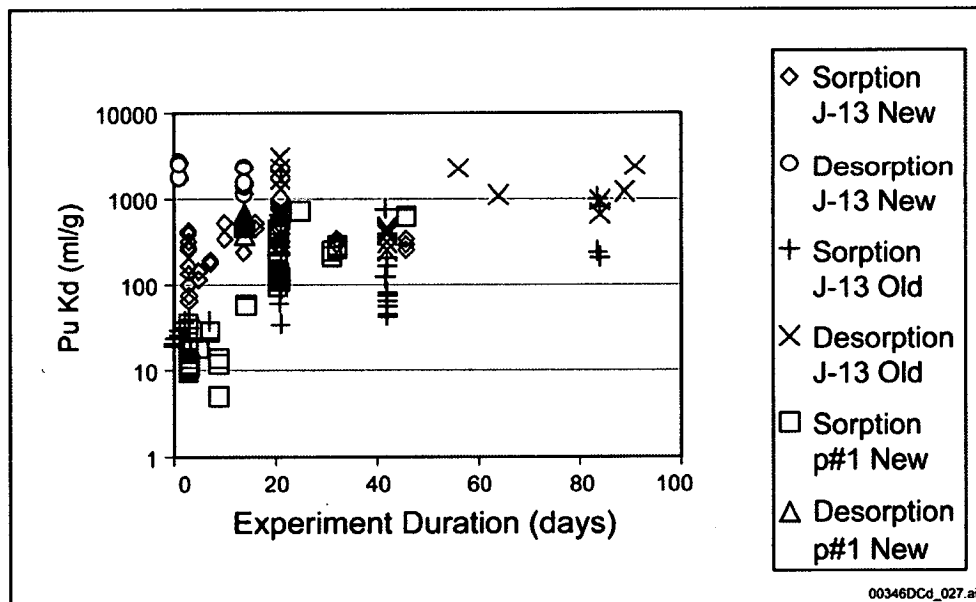
NOTE: Over saturated experiments have been omitted.

Figure 3-19. Neptunium Sorption Coefficients on Zeolitic Tuff Versus Experiment Duration for Sorption (Forward) and Desorption (Backward) Experiments



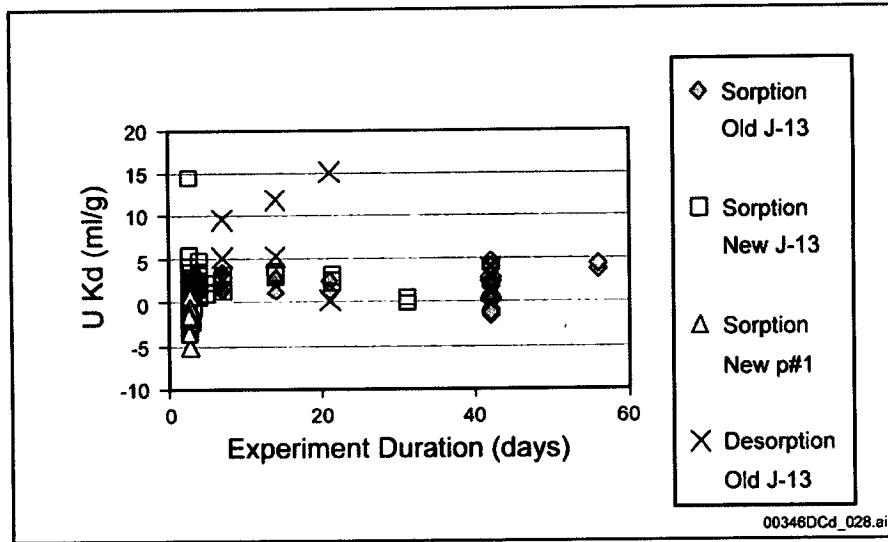
Source: BSC 2003a, Figure I-24.

Figure 3-20. Plutonium Sorption Coefficients on Devitrified Tuff Versus Experiment Duration for Sorption (Forward) and Desorption (Backward) Experiments



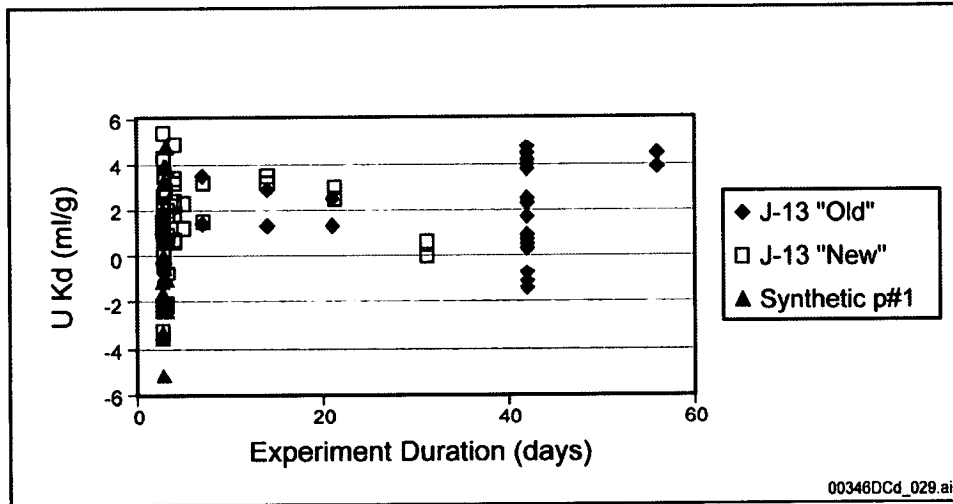
Source: BSC 2003a, Figure I-29.

Figure 3-21. Plutonium Sorption Coefficients on Zeolitic Tuff Versus Experiment Duration for Sorption (Forward) and Desorption (Backward) Experiments



Source: BSC 2003a, Figure I-48.

Figure 3-22. Uranium Sorption Coefficients on Devitrified Tuff Versus Experiment Duration for Sorption (Forward) and Desorption (Backward) Experiments



Source: BSC 2003a, Figure I-52.

Figure 3-23. Uranium Sorption Coefficients on Zeolitic Tuff as a Function of Experiment Duration

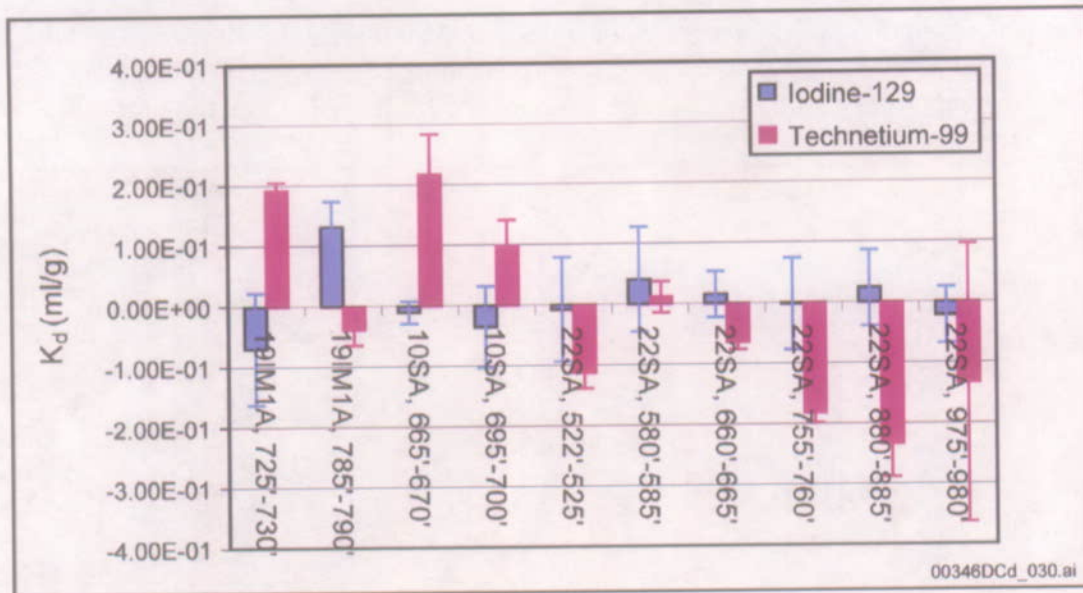
3.3.2 Radionuclide Sorption in the Alluvium

The migration behavior of sorbing radionuclides in the saturated alluvium south of Yucca Mountain has been studied through a series of laboratory scale tests. The alluvium consists primarily of materials with a volcanic origin similar to those found at Yucca Mountain (with some enrichment of clays and zeolites relative to common volcanic tuffs, plus the existence of secondary mineral coatings on the detritus), and it is expected that the sorption characteristics of the alluvium and tuffs are similar.

The experiments conducted using the alluvial material focused on the transport characteristics of the radionuclides ^{129}I , ^{99}Tc , ^{237}Np , and ^{233}U . The first two were determined to be nonsorbing on tuff rocks, while the second two were moderately sorbed on tuff rocks. The goal of these experiments was to determine the sorption coefficient of the alluvial materials under conditions relevant to the field. To achieve these objectives, many batch sorption, batch desorption, and flow-through column experiments have been carried out under ambient conditions to determine the distribution coefficients of these radionuclides between groundwater and alluvium from different boreholes.

The alluvium samples used in the experiments were obtained at various depths from three Nye County boreholes located south of Yucca Mountain (NC-EWDP-19IM1A, -10SA, and -22SA). The alluvium samples used for batch experiments were dry sieved and size fractions of less than 75 μm , 75 to 500 μm , and 75 to 2,000 μm were used in different experiments. For column experiments, alluvium samples within a particle size range of 75 to 2000 μm were wet sieved to remove fine particles that would clog the columns. The groundwater used in the experiments was obtained from borehole NC-EWDP-19D (Zones 1 and 4) and NC-EWDP-10SA. Mineral characterization of alluvium used in the experiments was determined by quantitative X-ray diffraction. Although the dominant minerals in the alluvium are quartz, feldspar, and plagioclase, considerable amounts of the sorbing minerals smectite (ranging from 3 to 8 percent) and clinoptilolite (ranging from 4 to 14 percent) were identified in the alluvial samples (see Appendix K).

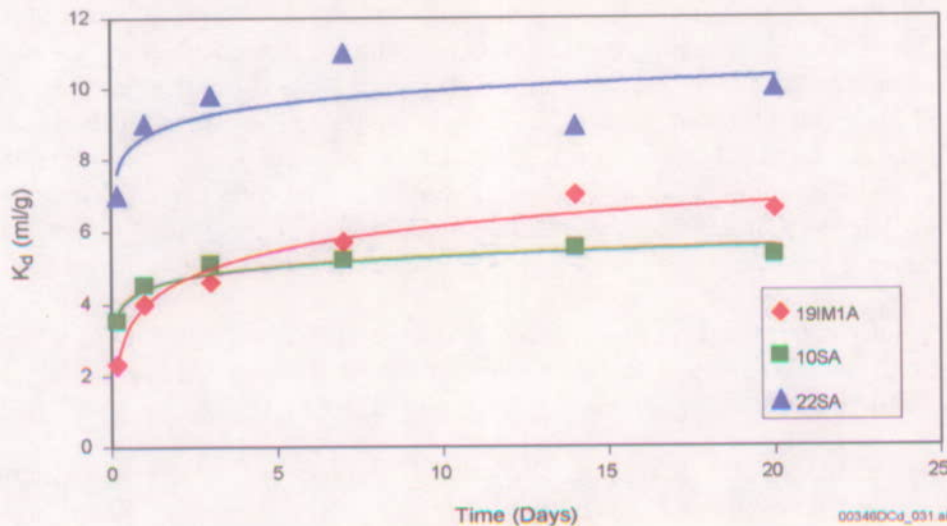
The results of the batch sorption tests (Figure 3-24) indicate there is little sorption of ^{129}I and ^{99}Tc on the alluvium. The scatter of the results around a K_d of zero is representative of the degree of precision of the testing method. Negative K_d s are not physically possible.



Source: Based on Ding et al. 2003, Figure 1.

Figure 3-24. Distribution Coefficients of ¹²⁹I and ⁹⁹Tc in Alluvium

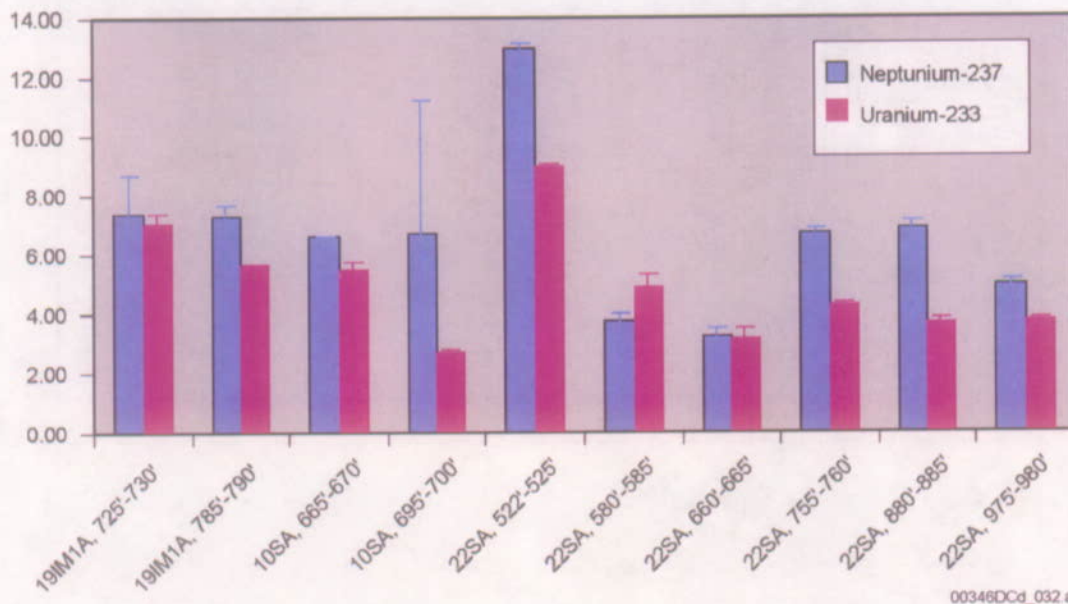
Figure 3-25 presents kinetic sorption of ²³³U in three alluvium samples. The results show that sorption of ²³³U onto alluvium is rather fast and that after one day of exposure, the amount of ²³³U adsorbed onto the alluvium changed little with time in all three tests. The higher K_d value from sample 22SA may be due to its higher smectite and clinoptilolite content (see Appendix K).



Source: See Appendix K, Figure K-2.

Figure 3-25. Sorption of ²³³U onto Alluvium as a Function of Time

The experimentally determined K_d values of ^{237}Np and ^{233}U in alluvium are presented in Figure 3-26. The results suggest that the distribution coefficients of ^{237}Np and ^{233}U in the alluvium range from about 3 to 13 ml/g for ^{237}Np , and from about 3 to 9 ml/g for ^{233}U .



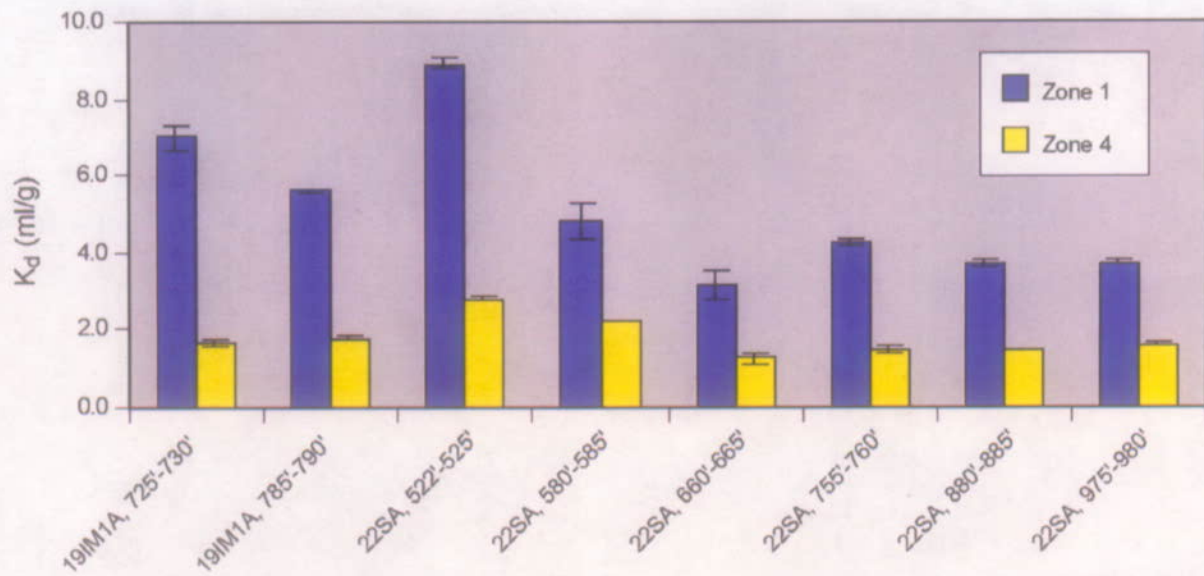
Source: See Appendix K, Figure K-3.

Figure 3-26. Distribution Coefficients of ^{237}Np and ^{233}U in Alluvium

To test if ^{233}U sorption behavior differs when using groundwater from different zones of the alluvial aquifer, adsorption experiments of ^{233}U on the same alluvium with two zone waters (19D Zone 1 and Zone 4) were conducted. As shown in Figure 3-27, K_d values of ^{233}U measured in Zone 4 water is much less than that of in Zone 1 water. The major differences in these two waters are: (1) the concentration of divalent cations in Zone 4 water is lower than that of Zone 1 water, and (2) the pH of Zone 4 water is slightly higher than that of Zone 1 water (see Appendix K). These differences may cause the solubility of ^{233}U in Zone 4 water to be higher resulting in less sorption.

The experimentally determined K_d values for ^{237}Np are presented in Figure 3-28. The K_d values range from about 4 to 500 ml/g. The particle size of the sample appears to affect the measured K_d value, as the smaller the particle sizes generally have larger K_d values.

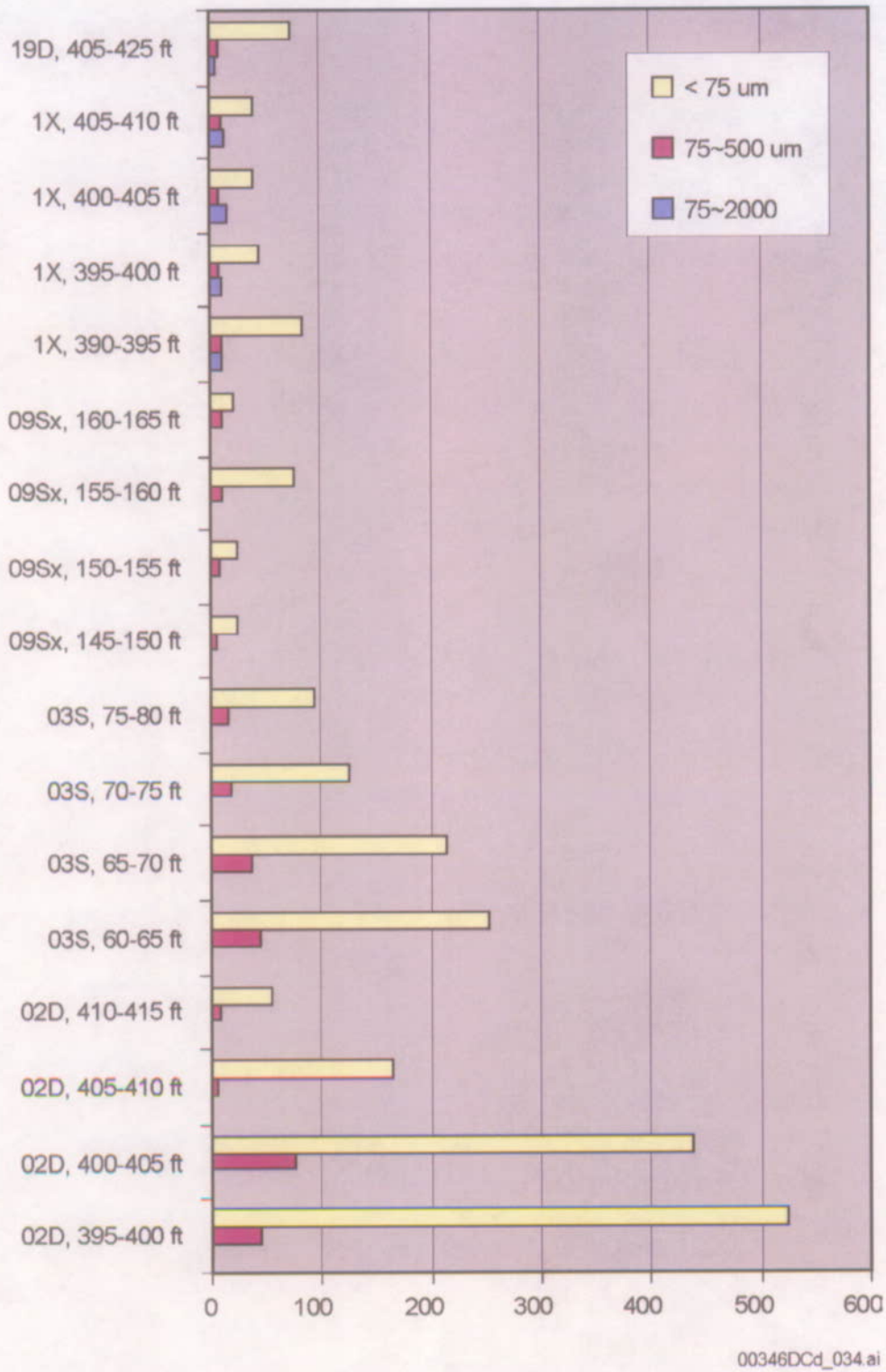
Adsorption experiments of ^{237}Np were performed on the same alluvial materials with groundwater from two wells, NC-EWDP-03S and -19D (see Appendix K). As shown in Figure 3-29, the influence of groundwater from different wells on distribution coefficients of ^{237}Np is negligible.



00346DCd_033.ai

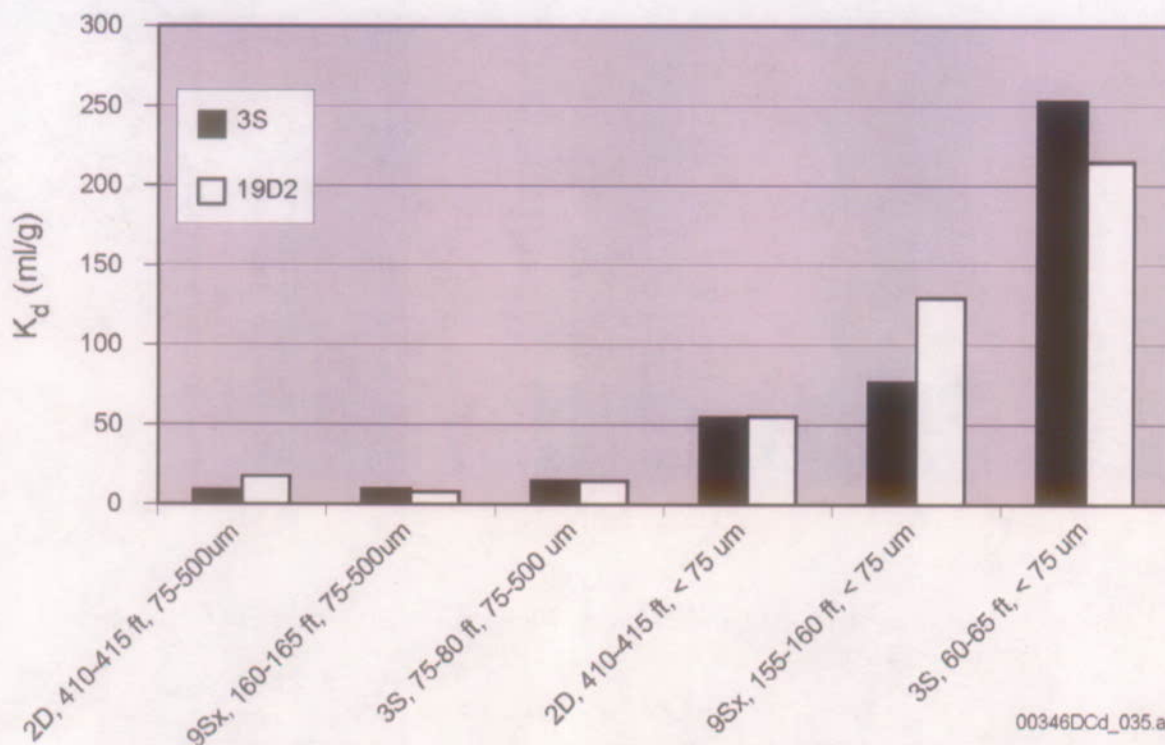
Source: See Appendix K, Figure K-4.

Figure 3-27. Sorption of ²³³U in 19D Zone 1 and Zone 4 Waters.



Source: Ding et al. 2003, Figure 2.

Figure 3-28. Distribution Coefficients of $^{237}\text{Np(V)}$ as a Function of Test Interval and Size Fraction Determined from Batch Experiments

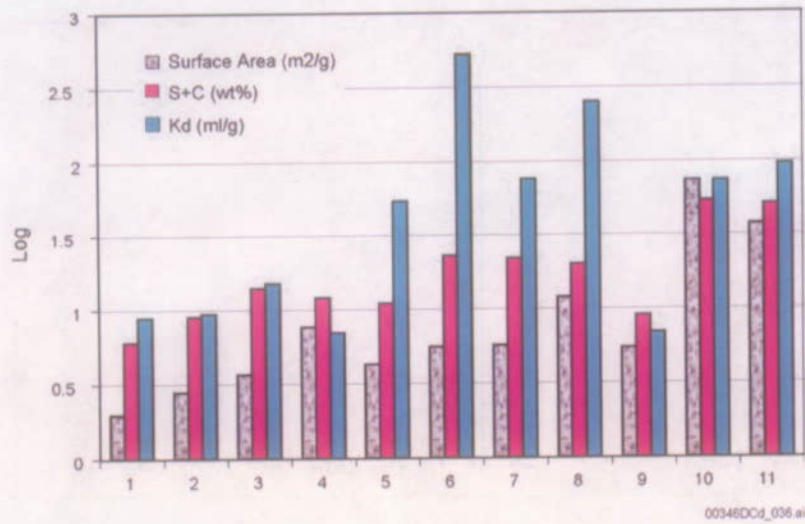


Source: See Appendix K, Figure K-10.

Figure 3-29. Sorption of Np(V) in NC-EWDP-3S and NC-EWDP-19D Well Waters

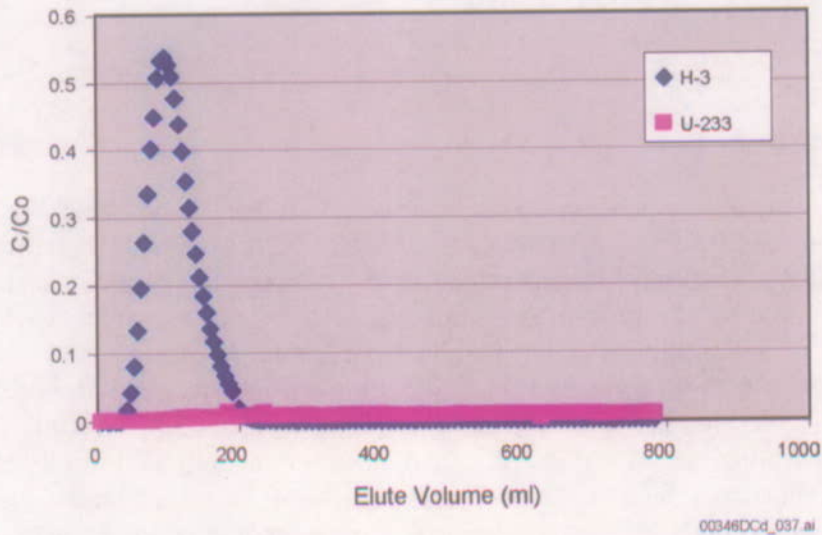
Adsorption is generally dependent on the surface properties of the materials. In general, the larger the surface area of the sample, the larger K_d value under the same experimental conditions. Clay and zeolite minerals have larger surface areas than the primary minerals such as quartz and Fledspar that compose the bulk of the alluvium. Therefore, alluvium, which contains large amounts of clay and zeolites, will generally have larger K_d values than the volcanic tuffs. Figure 3-30 presents ^{237}Np K_d values with respect to surface area and secondary minerals (the amount of smectite and clinoptilolite) content in alluviums. These results indicate that the correlation between sorption, surface area, and smectite plus clinoptilolite is as expected, with the exception that two high K_d samples do not have correspondingly high smectite and clinoptilolite content. These results suggest that trace amount of minerals such as amorphous iron and manganese oxides may affect the sorption of ^{237}Np in alluvium (see Appendix K). Additional studies of ^{237}Np sorption to vitric tuffs of Busted Butte indicated that sorption of radionuclides increases with increasing levels of smectite and Fe and Mn oxides in the rock (BSC 2003a).

In addition to the batch experiments described above, column experiments were conducted. Figure 3-31 presents the results of a representative column test using ^{233}U compared to the nonsorbing tracer tritium. Although the degree of ^{233}U sorption varies from column to column, the interpreted sorption coefficients are consistent with those observed in the batch experiments.



Source: See Appendix K, Figure K-12.

Figure 3-30. Relationship Between Surface Area, the Amount of Smectite (S) and Clinoptilolite (C), and Measured K_d of $^{237}\text{Np(V)}$ of Alluvium



Source: See Appendix K, Figure K-7a.

NOTE: The total recovery of tritium is about 94 percent, and that of ^{233}U is about 10 percent. The flow rate is 10 ml/h.

Figure 3-31. Tritium and ^{233}U Breakthrough Curve for a Column Test

In summary, ^{237}Np is considerably sorptive on the porous materials of the alluvial aquifer, with sorption strongly dependent on the presence of clay minerals and iron and magnesium oxides that have large surface areas available for sorption.

3.3.3 Colloid-Facilitated Transport

Radionuclide transport may be enhanced if the radionuclides sorb onto colloids. Colloid transport in the saturated zone is governed by several factors, including (1) the percentage of the colloids that irreversibly filter or attach to surfaces of subsurface materials, (2) the rate radionuclides desorb from the colloids, and (3) the colloid concentrations that may compete with immobile surfaces for radionuclides. Analyses of colloid concentrations and size distributions in Yucca Mountain groundwater have not found high concentrations of colloids (BSC 2003b).

The filtering or attachment of colloids onto subsurface materials has been studied using polystyrene microsphere data from the C-Wells field tests to obtain conservative estimates of colloid attachment and detachment rates in fractured tuffs. Published data have been used to obtain bounding estimates of attachment and detachment rates in alluvium.

Laboratory experiments have been conducted to determine the magnitude and rates of sorption and desorption for strongly sorbing, long-lived radionuclides onto several different types of colloids that may be present in the near-field (iron oxides such as goethite and hematite that might result from degradation of waste package materials) or in the far-field (silica, montmorillonite clay) environment at Yucca Mountain (CRWMS M&O 2000b, Section 3.8). These studies used the radionuclides ^{239}Pu and ^{243}Am , with the plutonium being prepared in two different forms: colloidal plutonium (IV) and soluble plutonium (V). Also, water from Well J-13 and a synthetic sodium-bicarbonate solution have been used in the experiments. Colloid concentrations were varied in some of the experiments to determine the effect of colloid concentration. Details of the experiment and summaries of the ^{239}Pu sorption and desorption rates onto the different colloids are provided in *Colloid-Associated Radionuclide Concentration Limits* (CRWMS M&O 2001). The results can be summarized as follows:

- The sorption of ^{239}Pu onto hematite, goethite, and montmorillonite colloids was strong and rapid, but the sorption of ^{239}Pu onto silica colloids was slower and not as strong.
- The desorption rates of ^{239}Pu from hematite colloids were so slow that they are essentially impossible to measure after 150 days. Desorption from goethite and montmorillonite colloids was also slow, but not as slow as hematite. The desorption rates of ^{239}Pu from silica colloids was rapid relative to the other colloids.
- For a given form of ^{239}Pu , sorption was generally stronger, faster, and less reversible in the synthetic sodium-bicarbonate water than in the natural Well J-13 water. Apparently, the presence of other ions, probably most notably calcium, in the natural water tended to suppress the sorption of ^{239}Pu .
- There was no clear trend of colloidal plutonium (IV) or soluble plutonium (V) being more strongly sorbed onto colloids. In general, it appeared that plutonium (V) was sorbed slightly more to hematite and silica, while plutonium (IV) was sorbed slightly more to goethite and montmorillonite.

- The sorption of ^{239}Pu was greatest per unit mass of colloid at the lowest colloid concentrations, which implies that the most conservative K_d values for performance assessment will come from sorption data generated at low colloid concentrations.

The sorption of ^{243}Am onto hematite, montmorillonite, and silica colloids showed the same trends as ^{239}Pu sorption (i.e., for both ^{243}Am and ^{239}Pu , sorption onto hematite was stronger than sorption onto montmorillonite, and sorption onto montmorillonite was stronger than it was onto silica), and the magnitudes of sorption for the two radionuclides were similar for the different colloids.

This ongoing work indicates (BSC 2003b):

- Waste form colloids such as hematite pose the greatest risk for colloid-facilitated transport within the engineered barriers but their significance to saturated zone transport is mitigated by the fact that these colloids would have to migrate through the waste package, invert and unsaturated zone before reaching the saturated zone.
- Natural clay colloids are likely to facilitate plutonium or americium transport more than silica colloids in the saturated zone.

Additional details of colloid-facilitated transport through the saturated zone are provided in *Saturated Zone Colloid Transport* (BSC 2003b).

3.4 SITE-SCALE RADIONUCLIDE TRANSPORT MODEL

The saturated zone site-scale radionuclide transport model is designed to provide an analysis tool that facilitates understanding of solute transport in the aquifer beneath and downgradient from the repository. The transport model builds on the flow model and the regional and site hydrogeologic and geochemical understanding obtained through field and laboratory studies. The data used in the development of the relevant transport parameters (e.g., sorption coefficient), submodel processes (e.g., advection and sorption), and site-scale model processes (e.g., flow paths and transit times) are based on laboratory testing, field tests, and analog literature information.

The principal output of the site-scale radionuclide transport model is the arrival time of important radionuclides at the point of compliance, which is located about 18 km south of Yucca Mountain. The arrival times are expressed as a breakthrough curve of mass versus time. A representative plot of normalized mass arrival is illustrated in Figure 3-32. This figure illustrates mass breakthrough for an unretarded radionuclide species (e.g., technetium) and a moderately sorbing radionuclide (e.g., neptunium). For the retarded species, this figure illustrates the relative contribution of sorption in the alluvium versus sorption in the fractured tuff aquifers. For this representation, the total sorption is dominated by sorption that occurs on the alluvial materials. This is the result of the combined effects of lower advective velocities in the alluvium (due to the effective porosity being greater than that in the fractured tuffs) and the higher sorption coefficient in the alluvium (Table 3-4).

Variability and uncertainty exist in the hydrogeologic properties and parameters that affect the prediction of radionuclide transport through the saturated zone. Variability of properties can occur over different spatial scales. For example, the effective porosity for developing advective transport velocity should be different at the scale of a core sample or in-situ field test, as well as differing among hydrogeologic units. This difference was noted in the C-Wells test interpretation presented in Section 3.2.1.2. Knowing that the properties are variable allows for reducing the total variance of the property if the degree of spatial correlation of the property also is known.

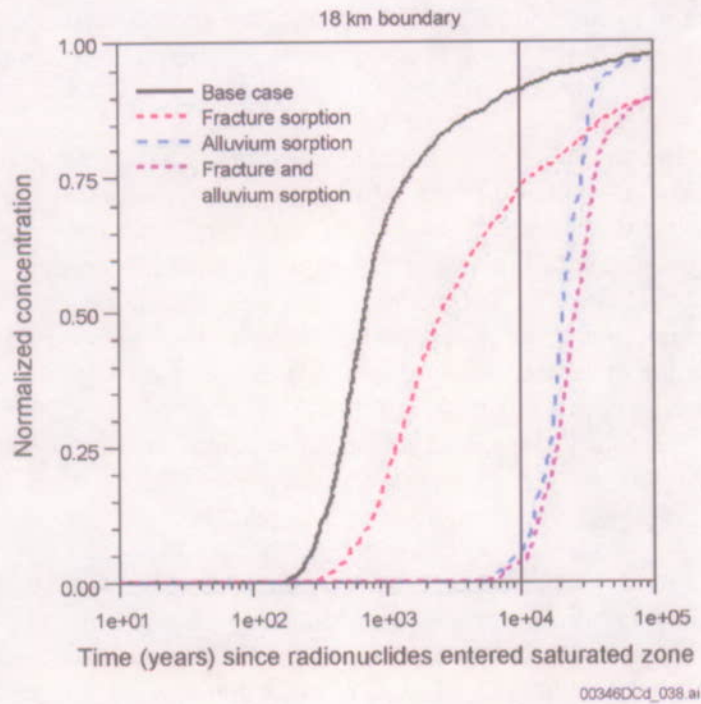
Rather than quantifying the degree of spatial correlation in flow and transport properties, the approach taken in the evaluation of saturated zone barrier performance was to first develop an integrated, self-consistent representation of the flow and transport processes that can be independently corroborated with other information (e.g., geochemistry and isotope information). After this model is developed, the approach consists of propagating uncertainty in all relevant flow and transport properties through the transport model to develop a distribution of possible breakthrough curves for different radionuclides. These breakthrough curves, all of which are equally likely based on current information, reflect the expected range of possible performance. In so doing, spatial variability has effectively been captured in the uncertainty reflected in the breakthrough curves. Appendix I presents additional discussion of the spatial variability of transport properties important to saturated zone performance.

Uncertainty exists in many of the parameters that affect radionuclide transport through the tuff rocks and alluvium downgradient from Yucca Mountain. This uncertainty includes flow-related parameter uncertainty such as (1) the boundary condition fluxes from the regional model, (2) the hydraulic properties of the saturated tuff and alluvial aquifers, (3) the hydraulic potential and gradients, and (4) the anisotropy of the tuff aquifers. This uncertainty manifests itself in uncertainty in the flow path orientation, uncertainty in the flow path distance in the tuff and alluvium to the compliance boundary, and uncertainty in the specific discharge within the saturated rocks and alluvium.

Uncertainty also exists in the transport-related parameters such as (1) the flowing interval spacing within the fractured tuff aquifers, (2) the effective fracture porosity within the flowing intervals, (3) the matrix diffusion between the fractures in the flowing intervals and the matrix between the flowing intervals, (4) the effective dispersivity within the fractured tuff, (5) the effective porosity of the porous alluvial materials, (6) the sorption characteristics of the tuff matrix, (7) the sorption characteristics of the alluvial materials, and (8) the filtration and attachment-detachment characteristics of colloiddally transported materials.

The above uncertainties result in a range of projected advective-dispersive transport times for different radionuclides of interest to a repository. Application of the transport model, considering this range of uncertainty, results in a range of possible breakthrough curves for different radionuclides. The results for three representative radionuclides are illustrated in Figure 3-33). Figure 3-33a illustrates that for nonsorbing radionuclides (e.g., carbon, technetium, and iodine), and the distribution of travel times is between several hundred and several thousand years. This is analogous to the distribution inferred from carbon isotope information presented in Section 3.2.3.4. For moderately sorbing radionuclides such as ^{237}Np (with K_d s in the range of 1 to 10 ml/g; Figure 3-33b), the travel time ranges from several

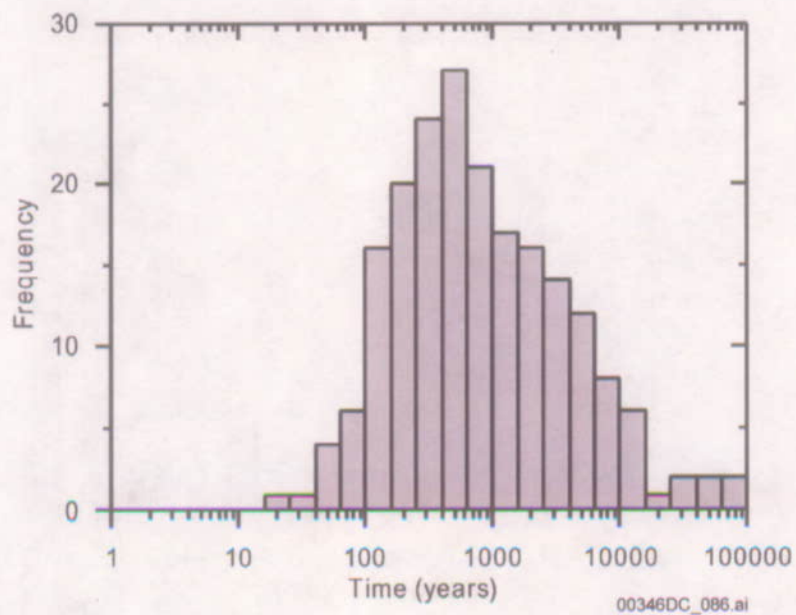
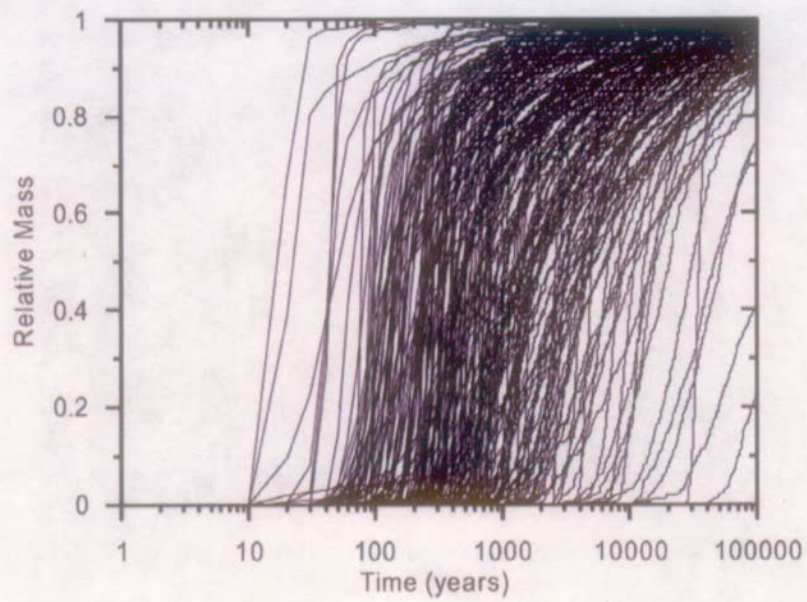
thousand to over ten thousand years. For highly sorbing radionuclides (e.g., plutonium), travel times generally are greater than 10,000 years (Figure 3-33b). For particles irreversibly attached to colloids, transport times are longer than 10,000 years (Figure 3-34). These ranges in effective mass breakthrough reflect the combined effects of the above uncertainties.



Source: BSC 2003a, Figure 6.7-1a.

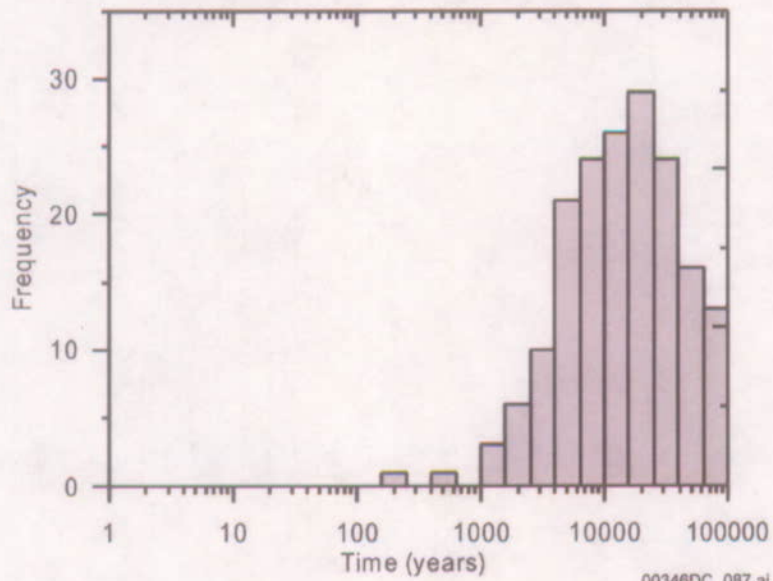
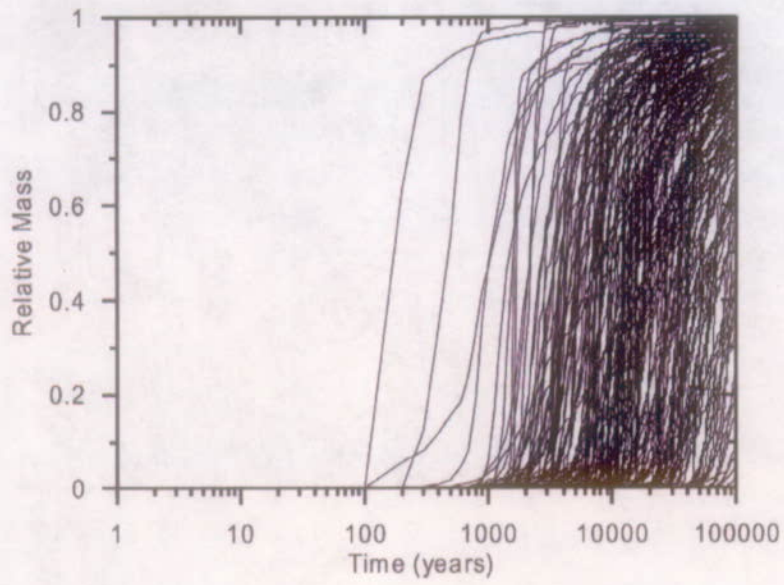
NOTE: Transport trajectories start in the saturated zone beneath the repository and migrate to the compliance point about 18-km south of the repository.

Figure 3-32. Predicted Breakthrough Curves for Radionuclides of Potential Interest to a Repository



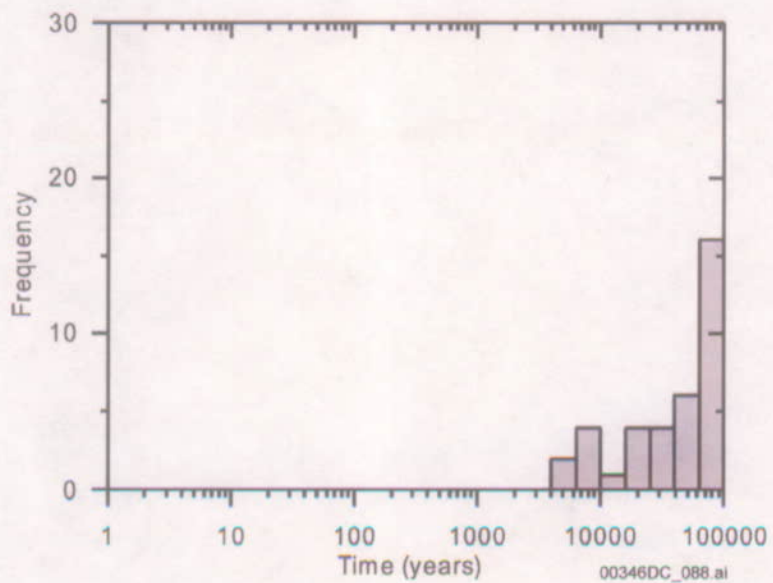
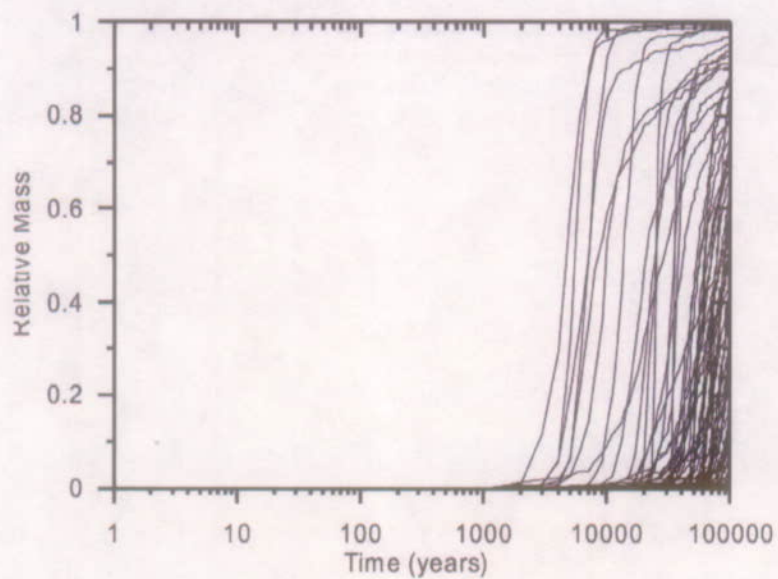
Source: BSC 2003d, Figure 6-28.

Figure 3-33a. Mass Breakthrough Curves (upper) and Median Transport Times (lower) for Carbon, Technetium, and Iodine at 18-km Distance



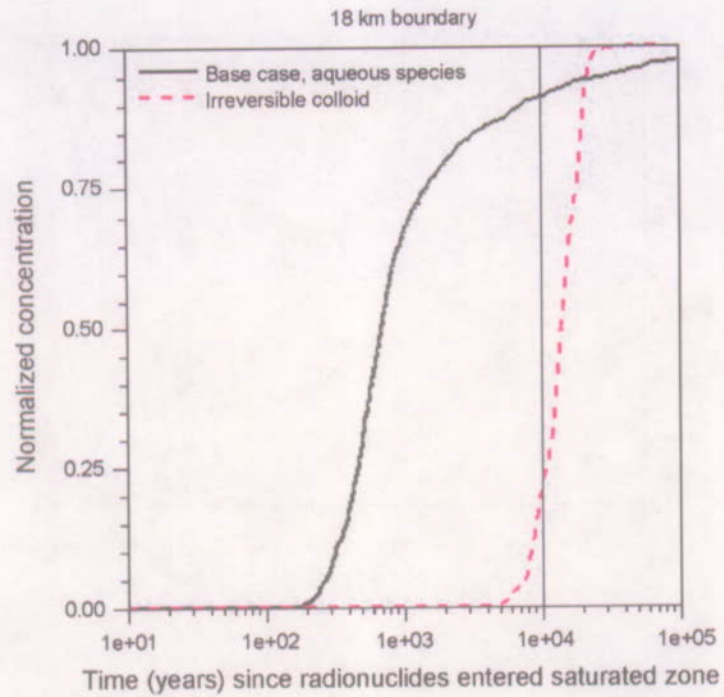
Source: BSC 2003d, Figure 6-32.

Figure 3-33b. Mass Breakthrough Curves (upper) and Median Transport Times (lower) for Neptunium at 18-km Distance



Source: BSC 2003d, Figure 6-31.

Figure 3-33c. Mass Breakthrough Curves (upper) and Median Transport Times (lower) for Plutonium at 18-km Distance



Source: BSC 2003a, Figure 6.7-5a.

Figure 3-34. Comparison of Breakthrough Curves for the Base Case and Radionuclides Irreversibly Attached to Colloids: 18-km Boundary

4. SUMMARY AND CONCLUSIONS

This Technical Basis Document has presented the technical data and related analyses and models that form the conceptual basis for the understanding of the saturated zone flow and transport processes that are relevant to the postclosure performance of the Yucca Mountain repository. The various data sets, including geologic, hydrogeologic, and geochemical data sets, assist in constraining the groundwater flow directions and rates between Yucca Mountain and the accessible environment. Field and laboratory data related to radionuclide transport characteristics have been used to constrain the advective transport times between the repository and the accessible environment for nonsorbing and sorbing radionuclides. The nonsorbing advective transport times and velocities have been further corroborated using naturally occurring ^{14}C tracers. In-situ field transport tests using surrogates to radionuclides and colloids of importance to repository performance have been used to build confidence in the radionuclide transport conceptual models and to develop transport properties for use in evaluating the performance of the saturated zone barrier. Finally, laboratory tests of the sorption behavior of radionuclides of importance to performance have been conducted to develop the sorption characteristics of these radionuclides in the saturated zone.

The saturated zone flow and transport processes described in this Technical Basis Document are represented by different conceptual and numerical models that are used to predict the expected behavior of the saturated zone barrier as it relates to the performance of the Yucca Mountain repository system. These models include models of groundwater flow at the regional and site scale and models of radionuclide transport. These models are constructed using parameter values generated using *in-situ* field observations as well as field and laboratory tests. The relevant parameters that most significantly affect the predicted performance of the saturated zone barrier are enumerated below:

- Hydraulic gradient
- Hydraulic conductivity
- Recharge and discharge
- Specific discharge
- Flowing interval spacing
- Flow path length in fractured tuff and alluvium
- Effective porosity of fractured tuff and porous alluvium
- Dispersivity
- Matrix diffusion
- Sorption coefficient

Uncertainty in these parameters has been considered in the development of the uncertainty in the radionuclide transport travel times from the base of the unsaturated zone to the point of compliance.

All of the above information has been used to develop the conceptual basis of the behavior of the saturated zone barrier. In each aspect important to postclosure repository performance, the uncertainty in the flow and transport properties has been considered. This uncertainty is reflected in the projection of the performance of the saturated zone flow and transport barrier at

Yucca Mountain. It reflects data and parameter uncertainty as well as the uncertainty in the conceptual representation. This uncertainty results in a wide range of possible advective transport times for each of the important radionuclides potentially affecting repository performance.

The following sections summarize the understanding of the saturated zone and the relevance of this understanding to repository performance.

4.1 SUMMARY OF SATURATED ZONE FLOW PROCESSES AND RELEVANCE TO REPOSITORY PERFORMANCE

The saturated zone flow processes control the direction and rate of groundwater flow. The groundwater flow direction affects the location where radionuclides released from the Yucca Mountain repository may be intercepted by a hypothetical well located along the compliance boundary. In addition, the groundwater flow path between the point where radionuclides enter the saturated zone (generally beneath the repository) and the point where water in the saturated zone is extracted by the hypothetical well, the hydrogeologic units and geochemical environments along the flow path, which in turn affects the flow and transport characteristics. The rate of groundwater flow (the advective flux through the saturated zone), affects the transport velocity when the effects of flow porosity are considered.

The groundwater flow direction from Yucca Mountain downgradient to the point of compliance has been determined based on observations of hydraulic head and hydraulic conductivity near Yucca Mountain. Although the observed hydraulic head gradient directly beneath Yucca Mountain is extremely small, heads upgradient and downgradient of the repository have been used to infer a generally south-easterly groundwater flow direction at Yucca Mountain and a generally southerly flow direction in the vicinity of Fortymile Wash. Although a range of flow directions has been developed to accommodate uncertainty in the horizontal anisotropy of the tuff aquifers, these flow directions all tend to parallel the orientation of Fortymile Wash.

Groundwater flow directions near Yucca Mountain are consistent with the general flow directions developed from the understanding of the regional groundwater flow system. This understanding is summarized in Section 2.2. This regional understanding includes the most important hydrogeologic units that affect flow directions, as well as bounding the overall flow rates (by comparing groundwater recharge and discharge to the water budget in the Death Valley region). This regional understanding has been used to determine the natural recharge and discharge areas, and the amounts for all groundwater in the basin.

Groundwater flow directions in the vicinity of Yucca Mountain are also consistent with the general flow directions inferred from geochemical and isotopic signatures (Section 2.2.4). The use of geochemical and isotopic signatures can be a valuable method to evaluate alternative hypotheses of flow directions because generally such geochemical samples integrate over a larger spatial and temporal scale than would discrete head or hydraulic conductivity measurements. While the general geochemical (as represented by chloride and sulfate observations) and isotopic (as represented by δD , ^{14}C , and $^{234}U/^{238}U$ activity ratios) trends support the southerly groundwater flow direction near Yucca Mountain, local geologic and

hydrogeologic heterogeneity affects the detailed interpretation of different mixing zones at any particular borehole.

An important consideration in understanding the saturated zone flow system is the relationship between flow in the fractured tuff aquifers immediately beneath and downgradient from Yucca Mountain, and the alluvial aquifer from which groundwater discharges in the Amargosa Valley. The location of the tuff-alluvium contact has been a focus of investigations being performed as part of the Nye County Early Warning Drilling Program. Although uncertainty exists in the exact location of this contact, results of these investigations better constrain the location, and the remaining uncertainty has been incorporated in the saturated zone transport model.

Information on geology, hydrogeology, recharge-discharge relationships, and hydrochemistry have been used to develop integrated models of the saturated zone flow system near Yucca Mountain. These models exist at the regional and site scales. Uncertainty in hydrogeologic properties and boundary conditions have been addressed in these models. The site-scale flow model has been used to project a range of possible flow paths and flow rates from the repository to the accessible environment for use in assessing the performance of the saturated zone barrier in postclosure performance assessment. The results of this model (e.g., flow rates and the fraction of the flow path length in the alluvium) have been used as input to the assessment of radionuclide transport in the saturated zone. This model is described in Section 2.3.7.

4.2 SUMMARY OF SATURATED ZONE TRANSPORT PROCESSES AND RELEVANCE TO REPOSITORY PERFORMANCE

After the groundwater flow fields have been defined, assessment of the radionuclide transport processes within the flow fields can be quantified. Laboratory and in-situ field tests have been performed to develop transport-related parameters that support the development of the transport model.

Saturated zone transport processes affect how fast dissolved or colloidal species are transported with the flowing groundwater. Transport is affected by the velocity of the flowing groundwater within the fractured or porous geologic media and the interactions of any dissolved or colloidal species with this media, either by matrix diffusion or various retardation mechanisms.

The velocity of the flowing groundwater is a function of the specific discharge derived from the understanding of the groundwater flow system and the effective porosity of the zones through which the water flows. Water flow through the fractured tuff aquifers is generally confined to isolated fracture intervals, while flow in the alluvial aquifer is dispersed through the porous material. Cross-hole tracer tests conducted in fractured tuff aquifers at the C-Wells complex have investigated the effective porosity of the fractured tuffs at the scale of 10s of meters. Single-hole tracer tests conducted in the alluvium at the Alluvial Tracer Complex have investigated effective porosity at the scale of a few meters. Given the paucity of direct in-situ observations of effective porosity at the scale of interest to repository performance, a wide range of uncertainty has been applied to this property. This uncertainty is summarized in Section 3.2.1 and 3.2.2.

Although there is no direct observation of groundwater velocity, radioisotopes can be used to infer a range of possible advective velocities. Carbon-14 ages and age differences have been used to support the groundwater velocities developed from specific discharge and effective porosity information. Both lines of evidence (Section 3.2.3) indicate that the possible range of advective velocities of unretarded species is between about 2 and 40 m/yr.

Dissolved radionuclides may diffuse into the matrix of fractured media (or into stagnant pore spaces of porous alluvium), causing a delay in transport times from that determined solely from advective transport. Matrix diffusion processes have been observed in tracer testing at the C-Wells complex and appropriate parameters for combined advective-diffusive transport have been developed based on these tests. The effect of matrix diffusion in delaying radionuclide transport is a function of the spacing between the fractures that contain the flowing groundwater. The flowing interval spacing, which has been developed based on observations in the C-Wells complex and in other tuff aquifers, is at the conservative end of the distribution of possible matrix diffusion effects.

Dissolved radionuclides that are transported with the groundwater have differing affinities to be retarded or adsorbed onto the mineral surfaces with which they come into contact. These differences are a function of rock type, differing mineral assemblages within the different rocks and alluvium, differences in groundwater chemistry, and differences in radionuclides. A number of laboratory tests have been conducted to evaluate the range of possible sorption coefficients. The results of these tests are summarized in Section 3.3. Some radionuclides important to repository performance are not sorbed (e.g., technetium and iodine), some are moderately sorbed (e.g., neptunium and uranium), and others are largely sorbed (e.g., americium, plutonium and cesium) on the geologic media of the saturated zone.

A saturated-zone transport model has been developed to integrate the effects of flow and transport processes relevant to repository performance. This model incorporates uncertainty in the processes and parameters describing these processes into an assessment of the overall behavior of the saturated zone barrier. The uncertainties included in this representation include specific discharge, flow path length in the alluvium, effective porosity of the tuff and alluvial aquifers, flowing interval spacing of the alluvial aquifer, matrix diffusion, and sorption coefficients for different radionuclides.

Incorporating this uncertainty in the performance assessment yields a range of breakthrough curves for different radionuclides being transported from the point they enter the saturated zone under Yucca Mountain to the point they are extracted in the hypothetical well located at the compliance point about 18 km south of Yucca Mountain. The range of breakthrough times for nonsorbing radionuclides (e.g., carbon, technetium and iodine) are between 10s of years and 10s of thousands of years, with a median time of about 700 years. For moderately sorbing radionuclides, exemplified by neptunium, the range of breakthrough times is between several hundred years to over 100,000 years, with a median time of about 20,000 years. For highly sorbing radionuclides, (e.g., plutonium), the range of breakthrough times is between several thousand years and over 100,000 years, with a median time in excess of 100,000 years.

Saturated-zone performance is portrayed in light of its role as a barrier to radionuclide transport in that it delays the arrival of radionuclides at the point of compliance where the reasonably

maximally exposed individual extracts water from a hypothetical well. In reality, the barrier delays the arrival of radionuclides and reduces the concentration of radionuclides that may be discharged from the well. However, for postclosure performance, the concentration is the average concentration based on an annual water demand of 3.7 million m³ (3,000 acre-feet). The details associated with determining the concentration of radionuclides in the aquifer is not required, as the annual water demand exceeds the average volumetric flow rate in the portion of the aquifer containing radionuclides. Therefore, the barrier performance may be represented as a mass breakthrough or activity breakthrough rather than a concentration.

4.3 CONCLUDING REMARKS

Hydrogeologic investigations have been undertaken near Yucca Mountain over the last several decades. These investigations have resulted in a broad understanding of the geology, hydrogeology, and geochemistry of the saturated zone in and around Yucca Mountain. The data and interpretations have been published in documents prepared by scientific staff at Los Alamos and Sandia National Laboratories, Open File and related monographs by the staff of the U.S. Geological Survey, and other peer reviewed publications. The data, analyses, and models developed by DOE contractors to support this Technical Basis Document have been collected and reviewed in accordance with the Quality Assurance requirements applicable at the time they were generated. The most important references describing elements of the saturated zone performance have been cited in this document. Other documents have developed an understanding of specific aspects of the saturated zone, and these documents largely are cited in the documents that support this document.

This document is a summary and synthesis of the data, analyses, and models that are used to evaluate the performance of the saturated zone barrier at Yucca Mountain. This barrier is important in that it affects the arrival time of any potentially released radionuclides at the potential receptor location (about 18 km south of Yucca Mountain). Uncertainty in the performance of this barrier is included in the results, which will be used as input to the total system performance assessment. The importance of this uncertainty, from the perspective of total risk (i.e., dose) to the reasonably maximally exposed individual, will be evaluated as part of the sensitivity analyses performed after the postclosure total system performance model is complete and validated.

INTENTIONALLY LEFT BLANK

5. REFERENCES

5.1 DOCUMENTS CITED

- Belcher, W.R. and Elliot, P.E. 2001. *Hydraulic-Property Estimates for use with a Transient Ground-Water Flow Model of the Death Valley Regional Ground-Water Flow System, Nevada and California*. Water-Resources Investigations Report 01-4210. Carson City, Nevada: U.S. Geological Survey. TIC: 252585.
- Belcher, W.R.; Faunt, C.C.; and D'Agnese, F.A. 2002. *Three-Dimensional Hydrogeologic Framework Model for Use with a Steady-State Numerical Ground-Water Flow Model of the Death Valley Regional Flow System, Nevada and California*. Water-Resources Investigations Report 01-4254. Denver, Colorado: U.S. Geological Survey. TIC: 252875.
- BSC (Bechtel SAIC Company) 2001a. *Input and Results of the Base Case Saturated Zone Flow and Transport Model for TSPA*. ANL-NBS-HS-000030 REV 00 ICN 01. Las Vegas, Nevada: Bechtel SAIC Company. ACC: MOL.20011112.0068.
- BSC 2001b. *Probability Distribution for Flowing Interval Spacing*. ANL-NBS-MD-000003 REV 00 ICN 02. Las Vegas, Nevada: Bechtel SAIC Company. ACC: MOL.20010625.0304.
- BSC 2001c. *Unsaturated Zone and Saturated Zone Transport Properties (U0100)*. ANL-NBS-HS-000019 REV 00 ICN 02. Las Vegas, Nevada: Bechtel SAIC Company. ACC: MOL.20020311.0017.
- BSC 2002. *Risk Information to Support Prioritization of Performance Assessment Models*. TDR-WIS-PA-000009 REV 01 ICN 01. Las Vegas, Nevada: Bechtel SAIC Company. ACC: MOL.20021017.0045.
- BSC 2003a. *Site-Scale Saturated Zone Transport*. MDL-NBS-HS-000010 REV 01A. Las Vegas, Nevada: Bechtel SAIC Company. ACC: MOL.20030626.0180.
- BSC 2003b. *Saturated Zone Colloid Transport*. ANL-NBS-HS-000031 REV 01A. Las Vegas, Nevada: Bechtel SAIC Company. ACC: MOL.20030602.0288.
- BSC 2003c. *Site-Scale Saturated Zone Flow Model*. MDL-NBS-HS-000011 REV 01A. Las Vegas, Nevada: Bechtel SAIC Company. ACC: MOL.20030626.0296.
- BSC 2003d. *SZ Flow and Transport Model Abstraction*. MDL-NBS-HS-000021 REV 00A. Las Vegas, Nevada: Bechtel SAIC Company. ACC: MOL.20030612.0138.
- BSC 2003e. *Saturated Zone In-Situ Testing*. ANL-NBS-HS-000039 REV 00A. Las Vegas, Nevada: Bechtel SAIC Company. ACC: MOL.20030602.0291.
- BSC 2003f. *Geochemical and Isotopic Constraints on Groundwater Flow Directions and Magnitudes, Mixing, and Recharge at Yucca Mountain*. ANL-NBS-HS-000021 REV 01A. Las Vegas, Nevada: Bechtel SAIC Company. ACC: MOL.20030604.0164.

Burbey, T.J. and Wheatcraft, S.W. 1986. *Tritium and Chlorine-36 Migration from a Nuclear Explosion Cavity*. DOE/NV/10384-09. Reno, Nevada: University of Nevada, Desert Research Institute, Water Resources Center. TIC: 201927.

Chapman, N.A.; Andersson, J.; Robinson, P.; Skagius, K.; Wene, C-O.; Wiborgh, M.; and Wingefors, S. 1995. *Systems Analysis, Scenario Construction and Consequence Analysis Definition for SITE-94*. SKI Report 95:26. Stockholm, Sweden: Swedish Nuclear Power Inspectorate. TIC: 238888.

Claassen, H.C. 1985. *Sources and Mechanisms of Recharge for Ground Water in the West-Central Amargosa Desert, Nevada—A Geochemical Interpretation*. U.S. Geological Survey Professional Paper 712-F. Washington, [D.C.]: United States Government Printing Office. TIC: 204574.

CRWMS M&O (Civilian Radioactive Waste Management System Management & Operating Contractor) 1998. *Saturated Zone Flow and Transport Expert Elicitation Project*. Deliverable SL5X4AM3. Las Vegas, Nevada: CRWMS M&O. ACC: MOL.19980825.0008.

CRWMS M&O 2000a. *Saturated Zone Flow and Transport Process Model Report*. TDR-NBS-HS-000001 REV 00 ICN 02. Las Vegas, Nevada: CRWMS M&O. ACC: MOL.20001102.0067.

CRWMS M&O 2000b. *Waste Form Degradation Process Model Report*. TDR-WIS-MD-000001 REV 00 ICN 01. Las Vegas, Nevada: CRWMS M&O. ACC: MOL.20000713.0362.

CRWMS M&O 2001. *Colloid-Associated Radionuclide Concentration Limits: ANL*. ANL-EBS-MD-000020 REV 00 ICN 01. Las Vegas, Nevada: CRWMS M&O. ACC: MOL.20010216.0003.

Czarnecki, J.B. and Waddell, R.K. 1984. *Finite-Element Simulation of Ground-Water Flow in the Vicinity of Yucca Mountain, Nevada-California*. Water-Resources Investigations Report 84-4349. Denver, Colorado: U.S. Geological Survey. ACC: NNA.19870407.0173.

D'Agnese, F.A.; Faunt, C.C.; Turner, A.K.; and Hill, M.C. 1997. *Hydrogeologic Evaluation and Numerical Simulation of the Death Valley Regional Ground-Water Flow System, Nevada and California*. Water-Resources Investigations Report 96-4300. Denver, Colorado: U.S. Geological Survey. ACC: MOL.19980306.0253.

D'Agnese, F.A.; O'Brien, G.M.; Faunt, C.C.; Belcher, W.R.; and San Juan, C. 2002. *A Three-Dimensional Numerical Model of Predevelopment Conditions in the Death Valley Regional Ground-Water Flow System, Nevada and California*. Water-Resources Investigations Report 02-4102. Denver, Colorado: U.S. Geological Survey. TIC: 253754.

Ding, M.; Reimus, P.W.; Ware, S.D.; and Meijer, A. 2003. "Experimental Studies of Radionuclide Migration in Yucca Mountain Alluvium." *Proceedings of the 10th International High-Level Radioactive Waste Management Conference (IHLRWM), March 30-April 2, 2003, Las Vegas, Nevada*. Pages 126-135. La Grange Park, Illinois: American Nuclear Society. TIC: 254559.

- DOE (U.S. Department of Energy) 1997. *Regional Groundwater Flow and Tritium Transport Modeling and Risk Assessment of the Underground Test Area, Nevada Test Site, Nevada*. DOE/NV-477. Las Vegas, Nevada: U.S. Department of Energy. ACC: MOL.20010731.0303.
- DOE 2002. *Yucca Mountain Site Suitability Evaluation*. DOE/RW-0549. Washington, D.C.: U.S. Department of Energy, Office of Civilian Radioactive Waste Management. ACC: MOL.20020404.0043.
- Erickson, J.R. and Waddell, R.K. 1985. *Identification and Characterization of Hydrologic Properties of Fractured Tuff Using Hydraulic and Tracer Tests—Test Well USW H-4, Yucca Mountain, Nye County, Nevada*. Water-Resources Investigations Report 85-4066. Denver, Colorado: U.S. Geological Survey. ACC: NNA.19890713.0211.
- Ervin, E.M.; Luckey, R.R.; and Burkhardt, D.J. 1994. *Revised Potentiometric-Surface Map, Yucca Mountain and Vicinity, Nevada*. Water-Resources Investigations Report 93-4000. Denver, Colorado: U.S. Geological Survey. ACC: NNA.19930212.0018.
- Fenelon, J.M. and Moreo, M.T. 2002. *Trend Analysis of Ground-Water Levels and Spring Discharge in the Yucca Mountain Region, Nevada and California, 1960–2000*. Water-Resources Investigations Report 02-4178. Carson City, Nevada: U.S. Geological Survey. ACC: MOL.20030812.0306.
- Ferrill, D.A.; Winterle, J.; Wittmeyer, G.; Sims, D.; Colton, S.; Armstrong, A.; and Morris, A.P. 1999. "Stressed Rock Strains Groundwater at Yucca Mountain, Nevada." *GSA Today*, 9, (5), 1-8. Boulder, Colorado: Geological Society of America. TIC: 246229.
- Forester, R.M.; Bradbury, J.P.; Carter, C.; Elvidge-Tuma, A.B.; Hemphill, M.L.; Lundstrom, S.C.; Mahan, S.A.; Marshall, B.D.; Neymark, L.A.; Paces, J.B.; Sharpe, S.E.; Whelan, J.F.; and Wigand, P.E. 1999. *The Climatic and Hydrologic History of Southern Nevada During the Late Quaternary*. Open-File Report 98-635. Denver, Colorado: U.S. Geological Survey. TIC: 245717.
- Geldon, A.L.; Umari, A.M.A.; Fahy, M.F.; Earle, J.D.; Gemmell, J.M.; and Darnell, J. 1997. *Results of Hydraulic and Conservative Tracer Tests in Miocene Tuffaceous Rocks at the C-Hole Complex, 1995 to 1997, Yucca Mountain, Nye County, Nevada*. Milestone SP23PM3. [Las Vegas, Nevada]: U.S. Geological Survey. ACC: MOL.19980122.0412.
- Gelhar, L.W.; Welty, C.; and Rehfeldt, K.R. 1992. "A Critical Review of Data on Field-Scale Dispersion in Aquifers." *Water Resources Research*, 28, (7), 1955-1974. Washington, D.C.: American Geophysical Union. TIC: 235780.
- Hevesi, J.A.; Flint, A.L.; and Flint, L.E. 2002. *Preliminary Estimates of Spatially Distributed Net Infiltration and Recharge for the Death Valley Region, Nevada-California*. Water-Resources Investigations Report 02-4010. Sacramento, California: U.S. Geological Survey. TIC: 253392.
- Langmuir, D. 1997. *Aqueous Environmental Geochemistry*. Upper Saddle River, New Jersey: Prentice Hall. TIC: 237107.

Luckey, R.R.; Tucci, P.; Faunt, C.C.; Ervin, E.M.; Steinkampf, W.C.; D'Agnesse, F.A.; and Patterson, G.L. 1996. *Status of Understanding of the Saturated-Zone Ground-Water Flow System at Yucca Mountain, Nevada, as of 1995*. Water-Resources Investigations Report 96-4077. Denver, Colorado: U.S. Geological Survey. ACC: MOL.19970513.0209.

Maxey, G.B. and Eakin, T.E. 1950. *Ground Water in White River Valley, White Pine, Nye, and Lincoln Counties, Nevada*. Water Resources Bulletin No. 8. Carson City, Nevada: State of Nevada, Office of the State Engineer. TIC: 216819.

Meijer, A. 2002. "Conceptual Model of the Controls on Natural Water Chemistry at Yucca Mountain, Nevada." *Applied Geochemistry*, 17, (6), 793-805. New York, New York: Elsevier. TIC: 252808.

NRC (U.S. Nuclear Regulatory Commission) 2003. *Yucca Mountain Review Plan, Final Report*. NUREG-1804, Rev. 2. Washington, D.C.: U.S. Nuclear Regulatory Commission, Office of Nuclear Material Safety and Safeguards. TIC: 254568.

Nye County Department of Natural Resources and Federal Facilities. 2003. *Nye County Drilling, Geologic Sampling and Testing, Logging, and Well Completion Report for the Early Earning Drilling Program Phase III Boreholes*. NWRPO-2002-04. [Pahrump], Nevada: U.S. Department of Energy, Nuclear Waste Repository Project Office. ACC: MOL.20030812.0307.

Paces, J.B.; Ludwig, K.R.; Peterman, Z.E.; and Neymark, L.A. 2002. "²³⁴U/²³⁸U Evidence for Local Recharge and Patterns of Ground-Water Flow in the Vicinity of Yucca Mountain, Nevada, USA." *Applied Geochemistry*, 17, (6), 751-779. New York, New York: Elsevier. TIC: 252809.

Paces, J.B.; Ludwig, K.R.; Peterman, Z.E.; Neymark, L.A.; and Kenneally, J.M. 1998. "Anomalous Ground-Water ²³⁴U/²³⁸U Beneath Yucca Mountain: Evidence of Local Recharge?" *High-Level Radioactive Waste Management, Proceedings of the Eighth International Conference, Las Vegas, Nevada, May 11-14, 1998*. Pages 185-188. La Grange Park, Illinois: American Nuclear Society. TIC: 237082.

Peters, M.T. 2003. *Status of Ongoing Testing*. Presented to: Nuclear Waste Technical Review Board, June 14, 2003. 68 pages. Washington, D.C.: Bechtel SAIC Company. ACC: MOL.20030820.0045.

Questa Engineering Corporation 2002. *Preliminary Analysis of Pump-Spinner Tests and 48-Hour Pump Tests in Wells NC-EWDP-19IM1 and -19IM2, Near Yucca Mountain, Nevada*. NWRPO-2002-05. [Pahrump], Nevada: Nye County Nuclear Waste Repository Project Office. ACC: MOL.20030821.0001.

Reamer, C.W. 2001. "U.S. Nuclear Regulatory Commission/U.S. Department of Energy Technical Exchange and Management Meeting on Total System Performance Assessment and Integration (August 6 through 10, 2001)." Letter from C.W. Reamer (NRC) to S. Brocoum (DOE/YMSCO), August 23, 2001, with enclosure. ACC: MOL.20011029.0281.

Reamer, C.W. and Williams, D.R. 2000a. Summary Highlights of NRC/DOE Technical Exchange and Management Meeting on Radionuclide Transport. Meeting held December 5-7, 2000, Berkeley, California. Washington, D.C.: U.S. Nuclear Regulatory Commission. ACC: MOL.20010117.0063.

Reamer, C.W. and Williams, D.R. 2000b. Summary Highlights of NRC/DOE Technical Exchange and Management Meeting on Unsaturated and Saturated Flow Under Isothermal Conditions. Meeting held August 16-17, 2000, Berkeley, California. Washington, D.C.: U.S. Nuclear Regulatory Commission. ACC: MOL.20001201.0072.

Reimus, P.W.; Adams, A.; Haga, M.J.; Humphrey, A.; Callahan, T.; Anghel, I.; and Counce, D. 1999. *Results and Interpretation of Hydraulic and Tracer Testing in the Prow Pass Tuff at the C-Holes*. Milestone SP32E7M4. Los Alamos, New Mexico: Los Alamos National Laboratory. TIC: 246377.

Reimus, P.W.; Haga, M.J.; Humphrey, A.R.; Counce, D.A.; Callahan, T.J.; and Ware, S.D. 2002. *Diffusion Cell and Fracture Transport Experiments to Support Interpretations of the BULLION Forced-Gradient Experiment*. LA-UR-02-6884. Los Alamos, New Mexico: Los Alamos National Laboratory. TIC: 253859.

Reimus, P.W.; Ware, S.D.; Benedict, F.C.; Warren, R.G.; Humphrey, A.; Adams, A.; Wilson, B.; and Gonzales, D. 2002. *Diffusive and Advective Transport of ^3H , ^{14}C , and ^{99}Tc in Saturated, Fractured Volcanic Rocks from Pahute Mesa, Nevada*. LA-13891-MS. Los Alamos, New Mexico: Los Alamos National Laboratory. TIC: 253905.

Schlueter, J.R. 2002a. "Radionuclide Transport Agreement 3.08." Letter from J. Schlueter (NRC) to J.D. Ziegler (DOE/YMSCO), August 16, 2002, 0822023934, with enclosure. ACC: MOL.20021014.0097.

Schlueter, J.R. 2002b. "Radionuclide Transport Agreement 2.03 and 2.04." Letter from J. Schlueter (NRC) to J.D. Ziegler (DOE/YMSCO), August 30, 2002, 0909024110. ACC: MOL.20020916.0098.

Schlueter, J.R. 2002c. "Additional and Corrected Information Needs Pertaining to Unsaturated and Saturated Flow Under Isothermal Conditions (USFIC) Agreement 5.05 and Radionuclide Transport (RT) Agreement 2.09." Letter from J.R. Schlueter (NRC) to J.D. Ziegler (DOE/ORD), December 19, 2002, 1223025549, with attachment. ACC: MOL.20030214.0140.

Schlueter, J.R. 2003. "The U.S. Nuclear Regulatory Commission Review of the U.S. Department of Energy Documents Pertaining to Agreement Unsaturated and Saturated Flow under Isothermal Conditions (USFIC). 3.02 (Status: Additional Information Needs) and Agreement Total System Performance Assessment and Integration (TSPAI).3.22 (Status: Additional Information Needs)." Letter from J.R. Schlueter (NRC) to J.D. Ziegler, (DOE), February 26, 2003, 0304036305, with attachment. ACC: MOL.20030424.0627.

Spengler, R.W. 2001a. "Pz in NC-EWDP-2DB." E-mail from R. Spengler to P. McKinley, August 30, 2001. ACC: MOL.20010907.0001.

Spengler, R.W. 2001b. Interpretation Of The Lithostratigraphy In Drill Hole NC-EWDP-19D1 ACC: MOL.20020402.0393.

Spengler, R.W. 2003a. Technical Data Record For Interpretation of the Lithostratigraphy in Drill Hole NC-EWDP-19IM1A (NC-EWDP-19IM1) ACC: MOL.20030218.0304.

Spengler, R.W. 2003b. Technical Data Record For Interpretation of the Lithostratigraphy in Drill Hole NC-EWDP-19IM2A (NC-EWDP-19IM2) ACC: MOL.20030218.0305.

USGS (U.S. Geological Survey) 2001a. *Water-Level Data Analysis for the Saturated Zone Site-Scale Flow and Transport Model*. ANL-NBS-HS-000034 REV 01. Denver, Colorado: U.S. Geological Survey. ACC: MOL.20020209.0058.

USGS 2001b. *Water-Level Data Analysis for the Saturated Zone Site-Scale Flow and Transport Model*. ANL-NBS-HS-000034 REV 00 ICN 01. Denver, Colorado: U.S. Geological Survey. ACC: MOL.20010405.0211.

USGS 2001c. *Hydrogeologic Framework Model for the Saturated-Zone Site-Scale Flow and Transport Model*. ANL-NBS-HS-000033 REV 00 ICN 02. Denver, Colorado: U.S. Geological Survey. ACC: MOL.20011112.0070.

Whelan, J.F.; Moscati, R.J.; Roedder, E.; and Marshall, B.D. 1998. "Secondary Mineral Evidence of Past Water Table Changes at Yucca Mountain, Nevada." *High-Level Radioactive Waste Management, Proceedings of the Eighth International Conference, Las Vegas, Nevada, May 11-14, 1998*. Pages 178-181. La Grange Park, Illinois: American Nuclear Society. TIC: 237082.

White, A.F. and Chuma, N.J. 1987. "Carbon and Isotopic Mass Balance Models of Oasis Valley - Fortymile Canyon Groundwater Basin, Southern Nevada." *Water Resources Research*, 23, (4), 571-582. Washington, D.C.: American Geophysical Union. TIC: 237579.

Winograd, I.J. and Thordarson, W. 1975. *Hydrogeologic and Hydrochemical Framework, South-Central Great Basin, Nevada-California, with Special Reference to the Nevada Test Site*. Geological Survey Professional Paper 712-C. Washington, D.C.: United States Government Printing Office. ACC: NNA.19870406.0201.

Zyvoloski, G.A.; Robinson, B.A.; Dash, Z.V.; and Trease, L.L. 1997. *User's Manual for the FEHM Application—A Finite-Element Heat- and Mass-Transfer Code*. LA-13306-M. Los Alamos, New Mexico: Los Alamos National Laboratory. TIC: 235999.

5.2 SOURCE DATA, LISTED BY DATA TRACKING NUMBER

GS021008312332.002. Hydrogeologic Framework Model for the Saturated-Zone Site-Scale Flow and Transport Model, Version YMP_9_02. Submittal date: 12/09/2002.

GS991208314221.001. Geologic Map of the Yucca Mountain Region. Submittal date: 12/01/1999.

LA0007PR831231.001. Bullfrog Reactive Tracer Test Data. Submittal date: 07/21/2000.

LA0303PR831231.003. Model Interpretations of C-Wells Field Tracer Transport Experiments. Submittal date: 03/31/2003.

MO0003SZFWTEEP.000. Data Resulting from the Saturated Zone Flow and Transport Expert Elicitation Project. Submittal date: 03/06/2000.

MO0105HCONEPOR.000. Hydraulic Conductivity and Effective Porosity for the Basin and Range Province, Southwestern United States. Submittal date: 05/02/2001.

UN0102SPA008KS.003. Concentration Dataset for Tracers (2, 6-Difluorobenzoic Acid and Iodide) Used for 48 Hour Shut in Tracer Test at the Alluvial Tracer Complex in Nye County. Submittal date: 06/11/2001.

UN0109SPA008IF.006. Concentration Dataset for Tracers (2,4-Difluorobenzoic Acid and Chloride) Used for the 30-Day Shut in Tracer Test at the Alluvial Tracer Complex in Nye County Nevada. Submittal date: 09/28/2001.

UN0109SPA008KS.007. Concentration Dataset for Tracer (Pentafluorobenzoic Acid) Used for the 30Day-Shut in Tracer Test at the Alluvial Tracer Complex in Nye County Nevada. Submittal date: 09/21/2001.

INTENTIONALLY LEFT BLANK

APPENDIX A

**THE HYDROGEOLOGIC FRAMEWORK MODEL/
GEOLOGIC FRAMEWORK MODEL INTERFACE
(RESPONSE TO USFIC 5.10)**

Note Regarding the Status of Supporting Technical Information

This document was prepared using the most current information available at the time of its development. This Technical Basis Document and its appendices providing Key Technical Issue Agreement responses that were prepared using preliminary or draft information reflect the status of the Yucca Mountain Project's scientific and design bases at the time of submittal. In some cases this involved the use of draft Analysis and Model Reports (AMRs) and other draft references whose contents may change with time. Information that evolves through subsequent revisions of the AMRs and other references will be reflected in the License Application (LA) as the approved analyses of record at the time of LA submittal. Consequently, the Project will not routinely update either this Technical Basis Document or its Key Technical Issue Agreement appendices to reflect changes in the supporting references prior to submittal of the LA.

APPENDIX A

THE HYDROGEOLOGIC FRAMEWORK MODEL/ GEOLOGIC FRAMEWORK MODEL INTERFACE (RESPONSE TO USFIC 5.10)

This appendix provides a response for Key Technical Issue (KTI) Unsaturated and Saturated Flow under Isothermal Conditions (USFIC) agreement USFIC 5.10. This KTI agreement relates to providing more information about the apparent discontinuity between the geologic framework model (GFM) and the site-scale hydrogeologic framework model (HFM).

A.1 KEY TECHNICAL ISSUE AGREEMENT

A.1.1 USFIC 5.10

KTI agreement USFIC 5.10 was reached during the NRC/DOE technical exchange and management meeting on unsaturated and saturated flow under isothermal conditions held during October 31 through November 2, 2000 in Albuquerque, New Mexico (Reamer and Williams 2000). The saturated zone portion of KTI subissues 5 and 6 was discussed at the meeting. During the meeting, the DOE presentation included a discussion of the site-scale HFM, which provides the fundamental geometric framework for developing a site-scale three-dimensional groundwater flow and transport model. The DOE stated the framework provides a basis for the mathematical model, which incorporates site-specific subsurface information and will continue to be updated. The regional HFM is also being revised by the USGS.

The NRC expressed concerns about the site-scale HFM report (USGS 2000) regarding the boundary between the GFM and areas to the south that present problems in correlating geologic units in faults and maintaining unit thickness. The DOE stated that the HFM is being updated to include new data.

Wording of the agreement is as follows

USFIC 5.10

Provide, in updated documentation of the HFM that the noted discontinuity at the interface between the GFM and the HFM does not impact the evaluation of repository performance. DOE will evaluate the impact of the discontinuity between the Geologic Framework Model and the Hydrogeologic Framework Model on the assessment of repository performance and will provide the results in an update to the Hydrogeologic Framework Model for the Saturated-Zone Site-Scale Flow and Transport Model AMR during FY 2002.

A.1.2 Related Key Technical Issue Agreements

USFIC 5.05 and RT 2.09 (both delivered in FY02) presented the revised geologic cross-sections, including new Nye County borehole data, and presented a discussion of the correlation between the geostratigraphy and hydrostratigraphy. The response to the additional information needed for USFIC 5.05 and RT 2.09 is presented in Appendix B.

A.2 RELEVANCE TO REPOSITORY PERFORMANCE

Conceptual representations of the hydrogeology at the regional and site scale may differ due to the scale-dependency of significant hydrogeologic features. Although different conceptual representations can characterize subsurface systems at different scales, the boundaries between these conceptual representations should be shown to not affect the results at the scale of interest. In the case of the boundary between the GFM used to develop a detailed geologic profile at the scale of the repository (i.e., several kilometers in the areal plane and several hundred meters in the vertical plane) and the HFM used to develop a hydrostratigraphic profile in the scale of the site (i.e., several tens of kilometers in the areal plane and several kilometers in the vertical plane), the boundary conditions should not affect the predicted flux of groundwater across this boundary. It is conceivable that model discontinuities at the boundary could affect the water flow and hence radionuclide transport across the boundary.

Documentation available at the time of the Site Recommendation indicated the presence of a framework model discontinuity between the detailed GFM model used for unsaturated zone flow and transport and the coarser site-scale HFM used to evaluate saturated zone flow and transport.

The Technical Basis Document Saturated Zone and Transport summary main text that describes the hydrogeologic understanding used in assessing the flow of groundwater and transport of radionuclides in the saturated zone beneath and downgradient from Yucca Mountain is found in Section 2.3.4.

A.3 RESPONSE

Since this KTI Agreement item was made, the site-scale HFM and GFM used in the site recommendation have been revised to newer versions for license application, mostly in response to needs of the models they support. The apparent discontinuities were investigated and some adjustments were made (Section A.4.2.4).

Because no new data are expected within the GFM domain, there are no plans to update or revise the GFM beyond its current version (GFM 2000) (BSC 2002). The regional-scale HFM will continue to be updated as new data become available. New data have been obtained from the Nye County Early Warning Drilling Program and other information has been obtained from Inyo County, the National Park Service in Death Valley, and affected Indian Tribes in Inyo County. The new data has been incorporated into the new version of the USGS Death Valley regional model. Of the new information that has become available since the last update to the site-scale HFM (USGS 2001), only the Nye County data are within the domain of the Yucca Mountain site-scale model, and those data are not in the area where the apparent discontinuities were observed. The last update to the site-scale HFM (USGS 2001) addressed issues discovered by Wilson (2001) and documented in a data qualification report. The new Nye County data are also the subject of an NRC Additional Information Needed request for RT 2.09 and USFIC 5.05 which is addressed in Appendix B. Because the models that support the license application are completed and have been accepted by the downstream user (i.e., the Total Systems Performance Assessment organization) as adequate for the intended use, the DOE does not intend to update the Yucca Mountain Project site-scale HFM report until the Nye County drilling program is complete, which is not planned to occur until after the license application is submitted.

The following excerpt from *Hydrogeologic Framework Model for the Saturated-Zone Site-Scale Flow and Transport Model* (USGS 2001) documents the apparent discontinuities in unit thicknesses of the four units within the site-scale HFM that have the GFM as the principal source of data:

Within the immediate site area, the site GFM was used as the principal source of subsurface data for the Upper Volcanic Confining Unit and the Prow Pass, Bullfrog, and Tram Tuffs within the Lower Volcanic Aquifer in the HFM. For these units, the GFM is essentially embedded within the HFM. However, because of differences between how data external to the GFM were used to construct the HFM and were used to establish the thicknesses of units along the lateral boundaries of the GFM, the process of embedding the GFM within the HFM introduced some apparently anomalous discontinuities in some unit thicknesses across the GFM model boundaries. These apparent discontinuities are artifacts of differences between the HFM and GFM model grids and the data interpolation and extrapolation methods used in constructing the GFM, and they do not affect the applicability of the HFM in providing a hydrogeologic framework for the site-scale saturated zone flow model.

These apparent discontinuities at the interface between the GFM and HFM do not affect the evaluation of repository performance because:

- Only one of the four units in the HFM (USGS 2001) identified as having the GFM as the principal source of subsurface data, demonstrate a discontinuity, and that discontinuity has been resolved in the most recent revision of the site-scale HFM (DTN: GS021008312332.002).
- The two models, GFM and HFM, are used by different subsystems within performance assessment and both models have been validated for their intended uses.

A.4 BASIS FOR THE RESPONSE

A.4.1 Summary of the Issue

The following sections contain descriptions of the GFM, site-scale HFM, the process of incorporating GFM data into the site-scale HFM, and the apparent discrepancies that resulted from this process. A description of the site-scale HFM and its use in the context of the saturated zone conceptual understanding of the flow of groundwater and transport of radionuclides in the saturated zone beneath and downgradient from Yucca Mountain is found in Section 2.3.4.

A.4.1.1 Geologic Framework Model

The GFM represents a three-dimensional interpretation of the stratigraphy and structural features developed to represent the rock layers, rock properties, and mineralogy of the Yucca Mountain site. The GFM provides a baseline representation of the locations and distributions of 50 rock layers and 44 faults in the subsurface of the Yucca Mountain area for use in geologic modeling and repository design. Input data from geologic mapping and boreholes provide controls at the ground surface and to the depths of the boreholes; however, most of the modeled volume is

unsampled and therefore poorly constrained. The GFM is an interpretative and predictive tool that provides a representation of the subsurface system on a smaller scale. The GFM portrays the distribution of rock layers that are most important to TSPA-related models and analyses that are in close proximity to the repository horizon, the largest of which are in the unsaturated zone model. The site-scale HFM directly uses some units from the GFM model as input.

The GFM represents a three-dimensional interpretation of the geology surrounding the geologic repository and encompasses an area of 168 km² (65 mi²) and a volume of 771 km³ (185 mi³). The boundaries of the GFM were chosen to encompass the exploratory boreholes and to provide a geologic framework over the area of interest for hydrologic flow and radionuclide transport modeling through the unsaturated zone. The depth of the model is constrained by the inferred depth of the Tertiary-Paleozoic unconformity. The GFM was constructed from geologic maps and borehole data. Additional information from measured stratigraphic sections, gravity profiles, and seismic profiles was considered. The GFM generally uses a horizontal grid spacing of 61 m; however, the topography is spaced at 30 m. This spacing was determined to be the largest that would adequately represent the input data over the area of interest without unreasonable computation expense.

The GFM was validated by predicting the subsurface geology for two boreholes (USW WT#24 and USW SD-6) and one tunnel (ECRB Cross-Drift) using GFM3.0 (DTN: MO9804MWDGFM03.001), and comparing the predictions to the actual results in GFM3.1 (DTN: MO9901MWDGFM31.000). Because the same data and methods were used in GFM2000 (BSC 2002), the previous validation applies to the latest model revision. No new data are available to apply the same kind of validation directly to GFM2000; however, "jack-knife" uncertainty estimates provide a useful comparison to the model validation results and show similar results. GFM2000 also was evaluated for a match to available input data. Boreholes USW WT#24 and USW SD-6, and the ECRB Cross-Drift are in close proximity to the repository footprint.

A.4.1.2 Site-Scale Hydrogeologic Framework Model

The site-scale HFM is a simplified three-dimensional interpretation of the hydrostratigraphy and structure within the site-scale saturated zone model domain. The HFM was built from geologic maps and sections, borehole data, geophysical data and existing geologic framework models, and was constructed specifically for groundwater flow through the saturated zone. The HFM provides a simplified and generalized geometric foundation for the groundwater flow model and provides a representation of the location and distribution of hydrogeologic units in the saturated zone for use in groundwater flow modeling.

The lower boundary of the model is coincident with that of the regional flow model (DTN: GS960808312144.003). This boundary is generally consistent with no vertical flow in or out of the base of the site-scale model domain. A geologic map and cross sections developed for the model domain was the main input to the HFM (DTN: GS991208314221.001). Data from all available boreholes were incorporated in the construction of the HFM; however, borehole lithologic data from Nye County boreholes and boreholes USW SD-6 and USW WT#24 were not available at the time of model construction. The top of the HFM was set to an updated potentiometric surface map (DTN: GS000508312332.001). The HFM uses horizontal grid

spacing of 125 m, which was chosen based on flow modeling requirements. Because of the large grid spacing, the HFM simplifies the available data near the repository by combining and averaging detailed GFM data. The HFM also extrapolates from the widely spaced data in the poorly constrained areas of the model domain. However, the HFM resolution is at a greater detail than used for the saturated zone model computational grid, which uses a 500-m vertical resolution.

The current HFM (USGS 2001) represents the hydrogeologic setting for the Yucca Mountain area that covers about 1,350 km² and includes a saturated thickness of about 2.75 km. The HFM extends from Universal Transverse Mercator (UTM) Zone 11 easting coordinates 533340 to 563340 and northing coordinates 4046782 to 4091782. In depth, the model domain extends from the interpreted top of the water table to the base of the regional groundwater flow model (DTN: GS960808312144.003). The domain was selected to be: (1) coincident with grid cells in the regional groundwater flow model (DTN: GS960808312144.003) such that the base of the site model was equivalent to the base of the regional model (2,750 meters below a smoothed version of the potentiometric surface); (2) sufficiently large to minimize the effects of boundary conditions on estimating permeability values at Yucca Mountain; (3) sufficiently large to assess groundwater flow at distances beyond the 18 km compliance boundary from the repository area; (4) small enough to minimize the number of computational nodes in the model; (5) thick enough to include part of the regional Paleozoic carbonate aquifer; and (6) large enough to include borehole control in the Amargosa Desert at the southern end of the modeled area.

The HFM is intended for, and restricted to, the development of the site-scale saturated zone groundwater flow and transport model, including use of hydrogeologic unit definitions in performance assessment parameter development. Preliminary validations of techniques used to construct the model indicate that the HFM agrees with the input data within expected tolerances and is suitable for the intended use. The HFM was examined and corrected for geologic inconsistencies; however, the model is not intended for precise geologic unit locations or identification. The HFM provides a simplified and generalized geometric foundation for the groundwater flow model.

A.4.1.3 Incorporation of Geologic Framework Model Data into the Hydrogeologic Framework Model

Within the immediate site-scale area, the GFM was used as the principal source of subsurface data for the Upper Volcanic confining unit and the Prow Pass, Bullfrog, and Tram Tuffs within the Lower Volcanic Aquifer in the HFM. For these units, the GFM essentially is embedded within the HFM.

The HFM, because of its larger size, requires simplification of geostatigraphically identified units into units of hydrologic importance to the saturated zone models (site-scale and regional). The wider spacing of control points results in different model interpretations for some units common to the HFM and GFM.

The models show differences in stratigraphic units because they have different purposes and focus on different stratigraphic units of interest. In addition, because they cover different areas, some assumptions and details that apply to the GFM can not be incorporated with uniformity

into the HFM where large areas with minimal field data exist. The portrayal of faults and the distinction between units that are mineralogically and stratigraphically distinguishable in Yucca Mountain boreholes, but act as similar hydrogeologic units regionally are two examples. The HFM is a representation of the hydrogeologic units and major structural features within the saturated zone flow system encompassed by the domain of the site-scale saturated zone flow and transport model. These units are subjected to different stresses and facies changes, and therefore have different hydraulic properties.

In the HFM and GFM borehole databases, differences in the depths of contacts between hydrogeologic units were identified during data qualification (Wilson 2001, Section 3.4.2.1). Differences exceeding 30 feet, which approximates the minimum vertical nodal spacing in the site-scale saturated zone flow model, were found for 17 of the hundreds of data points used in constructing the hydrogeologic unit surfaces, and many of these were attributed to changes in stratigraphic unit definitions that occurred after the HFM database was compiled (Wilson 2001, Section 3.4.2.1). The software used to generate the HFM unit surfaces (USGS 2001, Section 6.3) integrates information from many data points and provides a smoothing that minimizes the effects of discrepancies at individual locations. Wilson (2001) summarized the differences: "Most of the observed differences were minor and would not affect generalized uses of the data. Most of the larger differences were related to either variation in the application of the HFM unit top definitions or were the result of changes in stratigraphic contact definitions."

A.4.1.4 Resulting Documented Apparent Discontinuities

The following excerpt from *Hydrogeologic Framework Model for the Saturated-Zone Site-Scale Flow and Transport Model* (USGS 2001) documents the apparent discontinuities in unit thicknesses of the four units within the HFM that have the GFM as the principal source of data:

Within the immediate site area, the site GFM was used as the principal source of subsurface data for the Upper Volcanic Confining Unit and the Prow Pass, Bullfrog, and Tram Tuffs within the Lower Volcanic Aquifer in the HFM. For these units, the GFM is essentially embedded within the HFM. However, because of differences between how data external to the GFM were used to construct the HFM and were used to establish the thicknesses of units along the lateral boundaries of the GFM, the process of embedding the GFM within the HFM introduced some apparently anomalous discontinuities in some unit thicknesses across the GFM model boundaries. These apparent discontinuities are artifacts of differences between the HFM and GFM model grids and the data interpolation and extrapolation methods used in constructing the GFM, and they do not affect the applicability of the HFM in providing a hydrogeologic framework for the site-scale saturated zone flow model

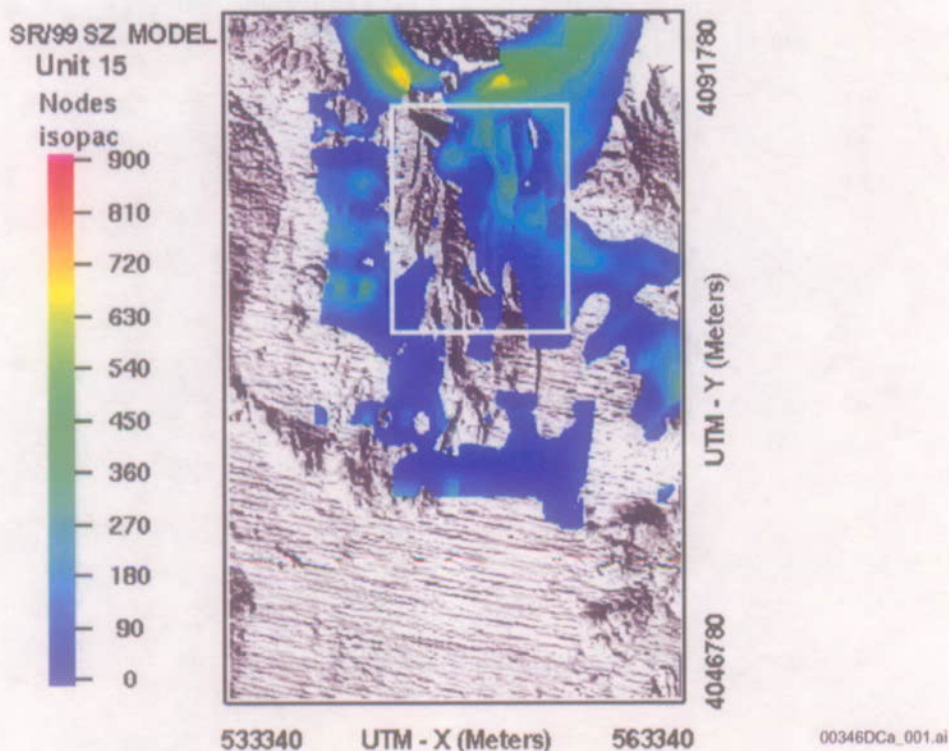
A.4.2 Discussion of Documented Apparent Discontinuities

In the following sections, isochore maps (maps showing vertical thicknesses) are used to identify apparent discontinuities in unit thickness that may occur as a result of differences between the GFM and HFM. Discontinuities that result from thickness differences occur near the boundary of the GFM and are nearly parallel to the boundary of the GFM. The following figures (A-1 through A-5) show that only the Tram Tuff contains a large discontinuity as a result of a

thickness difference. No discontinuities are apparent in the Upper Volcanic confining unit, Prow Pass Unit, or the Bullfrog Unit.

A.4.2.1 Upper Volcanic Confining Unit

Within and adjacent to the GFM area, no discontinuities are apparent in this isopach map of the Upper Volcanic confining unit (Figure A-1).



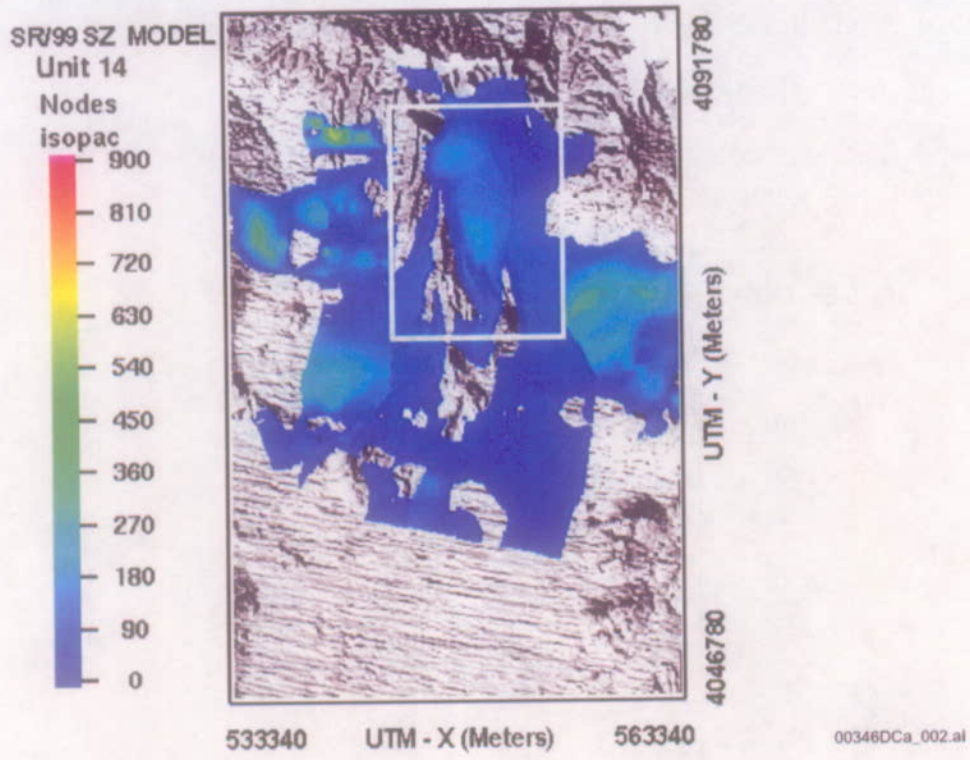
Source: DTN: LA0304TM831231.001

NOTE: The rectangular box shows the borders indicating the approximate GFM area with lower left corner at 544067, 4070099 UTM meters and the upper right corner at 555341, 4085070 UTM meters. A shaded relief map is used for the background and shows where the unit is pinched out to zero thickness by other units or truncated by the water table surface.

Figure A-1. Site Recommendation HFM Upper Volcanic Confining Unit Thickness

A.4.2.2 Prow Pass

Within and adjacent to the GFM area, no discontinuities are apparent in this isopach map of the Prow Pass unit (Figure A-2).



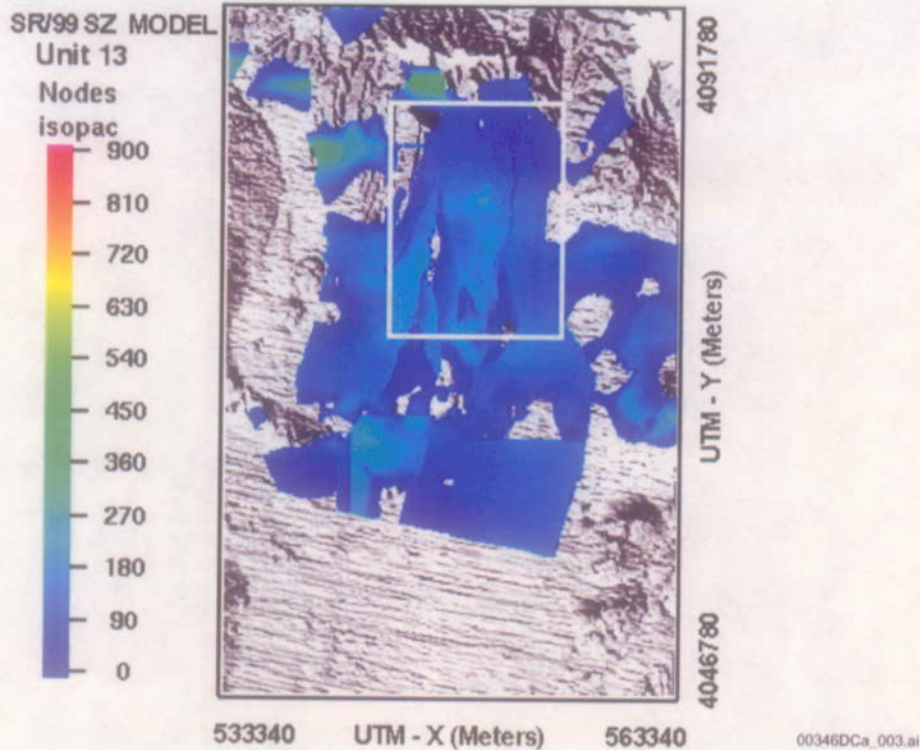
Source: DTN: LA0304TM831231.001

NOTE: See note for Figure A-1.

Figure A-2. Site Recommendation HFM Prow Pass Unit Thickness

A.4.2.3 Bullfrog

Within and adjacent to the GFM area, no discontinuities are apparent in this isopach map of the Bullfrog unit (Figure A-3).



Source: DTN: LA0304TM831231.001

NOTE: See note for Figure A-1.

Figure A-3. Site Recommendation HFM Bullfrog Unit Thickness

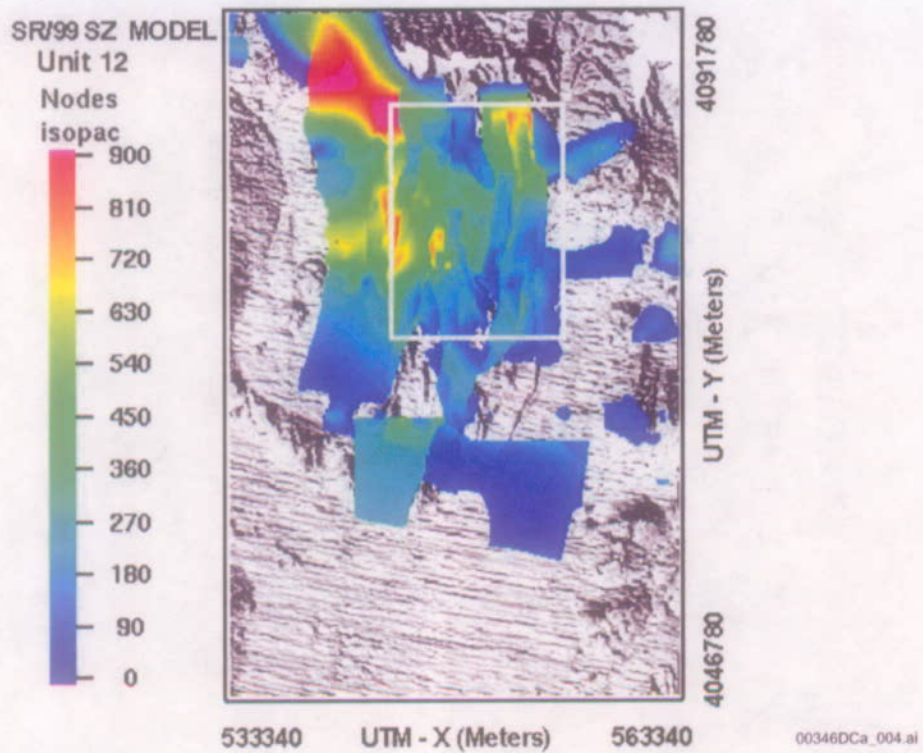
A.4.2.4 Tram Tuff

A discontinuity was identified in the northwest corner of the GFM model area where the Tram Tuff pinches out in the GFM, but it thickens in the HFM. This can be seen as an abrupt change (Figure A-4, see a straight, north-south line in northwest corner of GFM area) where the HFM shows the unit thickness as 1,000 m next to a 350 m thickness within the GFM boundary.

This apparent discontinuity was identified, and Yucca Mountain Project personnel worked to insure that the units common to both models were handled in a uniform manner. The discontinuity was resolved within the HFM by adding contours with increasing elevation to the GFM and by continuing this incline in the HFM definition, resulting in a smooth transition from the lower Tram tuff thickness in the northeast corner to the greater thicknesses seen towards Claim Canyon Caldera and beyond the GFM boundaries. The current version of the HFM (DTN: GS021008312332.002) is consistent with data from drill holes and is consistent with the GFM. The smooth transition enhances the applicability of the HFM in providing a hydrogeologic framework for the site-scale flow and transport model.

Figures A-4 and A-5 show the thickness of the Tram Tuff unit in the area of the GFM. The new HFM (Figure A-5) shows a smooth transition from the GFM defined thickness to the area

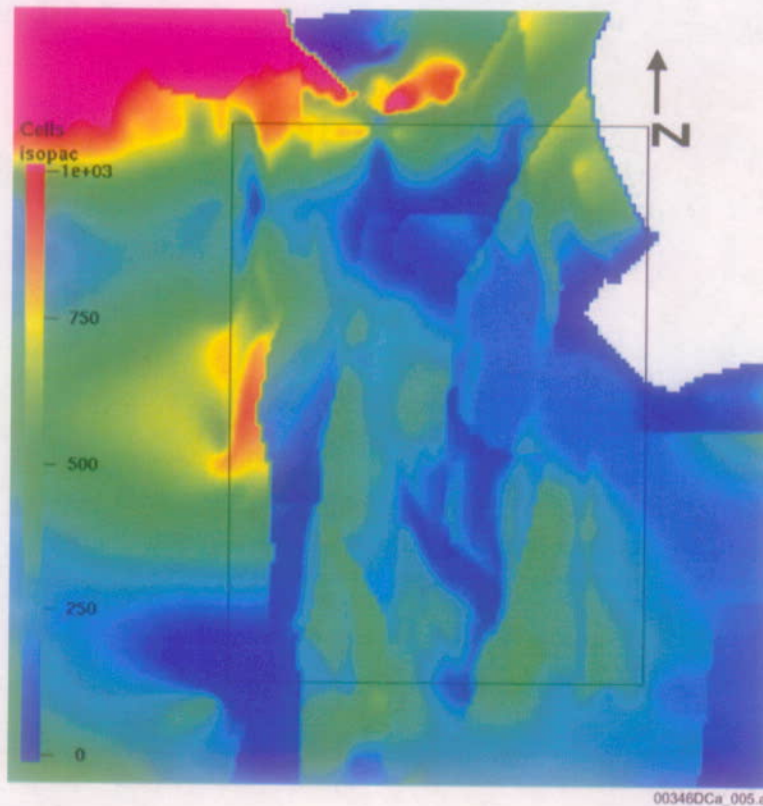
outside of the GFM. In general, the newer HFM shows fewer anomalies (e.g., trenches and peaks). Normally these features do not show up in coarser 500-m computational grids, but they are addressed and resolved in the new HFM and create a smoother surface.



Source: DTN: LA0304TM831231.001

NOTE: See note for Figure A-1.

Figure A-4. SR 1999 Tram Unit Thickness



Source: DTN: GS021008312332.002

NOTES: The rectangular box shows the borders indicating the approximate GFM area with lower right corner at 544067, 4070099 UTM meters and the upper right corner at 555341, 4085070 UTM meters. This figure was scaled such that the rectangular box approximately matches the size of the rectangular box in the previous four figures. White gaps appear where this unit is zero thickness or truncated by the water table surface.

Figure A-5. 2002 V10 Tram Unit Thickness

A.4.3 Summary

The two models, GFM and HFM, are used by different subsystems within the Performance Assessment organization. Both models have been validated for the intended uses, the GFM being close to the repository horizon and focusing on geologic units, and the HFM covering a large geographical area and focusing on hydrogeologic units. The HFM and GFM are different model interpretations of the area and have different intended purposes.

The apparent discontinuity is not relevant to the assessment of repository performance because the two models are used by different subsystems within performance assessment. The unsaturated zone (BSC 2001a) is one of the principal users of information from the GFM, whereas the saturated zone is the only user of the HFM (BSC 2001b).

A.5 REFERENCES

A.5.1 Documents Cited

BSC (Bechtel SAIC Company) 2001a. *UZ Flow Models and Submodels*. MDL-NBS-HS-000006 REV 00 ICN 01. Las Vegas, Nevada: Bechtel SAIC Company. ACC: MOL.20020417.0382.

BSC 2001b. *Calibration of the Site-Scale Saturated Zone Flow Model*. MDL-NBS-HS-000011 REV 00 ICN 01. Las Vegas, Nevada: Bechtel SAIC Company. ACC: MOL.20010713.0049.

BSC 2002. *Geologic Framework Model (GFM2000)*. MDL-NBS-GS-000002 REV 01. Las Vegas, Nevada: Bechtel SAIC Company. ACC: MOL.20020530.0078.

Reamer, C.W. and Williams, D.R. 2000. Summary Highlights of NRC/DOE Technical Exchange and Management Meeting on Unsaturated and Saturated Flow Under Isothermal Conditions. Washington, D.C.: U.S. Nuclear Regulatory Commission. ACC: MOL.20001128.0206.

USGS (U.S. Geological Survey) 2000. *Hydrogeologic Framework Model for the Saturated-Zone Site-Scale Flow and Transport Model*. ANL-NBS-HS-000033 REV 00. Denver, Colorado: U.S. Geological Survey. ACC: MOL.20000802.0010.

USGS 2001. *Hydrogeologic Framework Model for the Saturated-Zone Site-Scale Flow and Transport Model*. ANL-NBS-HS-000033 REV 00 ICN 02. Denver, Colorado: U.S. Geological Survey. ACC: MOL.20011112.0070.

Wilson, C. 2001. Data Qualification Report: Stratigraphic Data Supporting the Hydrogeologic Framework Model for Use on the Yucca Mountain Project. TDR-NBS-HS-000013 REV 00. Las Vegas, Nevada: Bechtel SAIC Company. ACC: MOL.20010725.0225.

A.5.2 Source Data, Listed by Data Tracking Number

GS000508312332.001. Water-Level Data Analysis for the Saturated Zone Site-Scale Flow and Transport Model. Submittal date: 06/01/2000.

GS021008312332.002. Hydrogeologic Framework Model for the Saturated-Zone Site-Scale Flow and Transport Model, Version YMP_9_02. Submittal date: 12/09/2002.

GS960808312144.003. Hydrogeologic Evaluation and Numerical Simulation of the Death Valley Regional Ground-Water Flow System, Nevada and California, Using Geoscientific Information Systems. Submittal date: 08/29/1996.

GS991208314221.001. Geologic Map of the Yucca Mountain Region. Submittal date: 12/01/1999.

LA0304TM831231.001. SZ Flow and Transport Model, Hydrogeologic Surface Files. Submittal date: 04/07/2003.

MO9804MWDGFM03.001. An Update to GFM 3.0; Corrected Horizon Grids for Four Fault Blocks. Submittal date: 04/14/1998.

MO9901MWDGFM31.000. Geologic Framework Model. Submittal date: 01/06/1999.

INTENTIONALLY LEFT BLANK

APPENDIX B
HYDROSTRATIGRAPHIC CROSS SECTIONS
(RESPONSE TO RT 2.09 AIN-1 and USFIC 5.05 AIN-1)

Note Regarding the Status of Supporting Technical Information

This document was prepared using the most current information available at the time of its development. This Technical Basis Document and its appendices providing Key Technical Issue Agreement responses that were prepared using preliminary or draft information reflect the status of the Yucca Mountain Project's scientific and design bases at the time of submittal. In some cases this involved the use of draft Analysis and Model Reports (AMRs) and other draft references whose contents may change with time. Information that evolves through subsequent revisions of the AMRs and other references will be reflected in the License Application (LA) as the approved analyses of record at the time of LA submittal. Consequently, the Project will not routinely update either this Technical Basis Document or its Key Technical Issue Agreement appendices to reflect changes in the supporting references prior to submittal of the LA.

APPENDIX B

HYDROSTRATIGRAPHIC CROSS SECTIONS (RESPONSE TO RT 2.09 AIN-1 and USFIC 5.05 AIN-1)

This appendix provides a response to an additional information needed (AIN) request from the U.S. Nuclear Regulatory Commission (NRC) for Key Technical Issue (KTI) agreements Radionuclide Transport (RT) 2.09 and Unsaturated and Saturated Flow under Isothermal Conditions (USFIC) 5.05. These KTI agreements relate to providing updated hydrostratigraphic cross sections that include additional borehole data.

B.1 KEY TECHNICAL ISSUE AGREEMENT

B.1.1 RT 2.09 and USFIC 5.05

KTI agreement USFIC 5.05 was reached during the NRC/DOE technical exchange and management meeting on unsaturated and saturated flow under isothermal conditions held during October 31 through November 2, 2000 in Albuquerque, New Mexico (Reamer and Williams 2000a). The saturated zone portion of KTI subissues 5 and 6 was discussed at the meeting.

KTI agreement RT 2.09 was reached during the NRC/DOE technical exchange and management meeting on radionuclide transport held December 5 through 7, 2000, in Berkeley, California. Radionuclide transport KTI subissues 1, 2 and 3 were discussed at that meeting (Reamer and Williams 2000b).

A letter report responding to this agreement (Ziegler 2002) was prepared. The report included hydrostratigraphic and geologic cross sections with Nye County data. Specific additional information was requested by the U. S. Nuclear Regulatory Commission after the staff's review of this letter report was completed, resulting in RT 2.09 AIN-1 and USFIC 5.05 AIN-1 (Schlueter 2002). The comments for these two AINs are identical.

Wording of these agreements is as follows:

USFIC 5.05

Provide the hydrostratigraphic cross sections that include the Nye County data. DOE will provide the hydrostratigraphic cross sections in an update to the Hydrogeologic Framework Model for the Saturated Zone Site-Scale Flow and Transport Model AMR expected to be available during FY 2002, subject to availability of the Nye County data.

RT 2.09

Provide the hydrostratigraphic cross sections that include the Nye County data. DOE will provide the hydrostratigraphic cross sections in an update to the Hydrogeologic Framework Model for the Saturated Zone Site-Scale Flow and Transport Model AMR expected to be available during FY 2002, subject to availability of the Nye County data.

USFIC 5.05 AIN-1 and RT 2.09 AIN-1

DOE should provide hydrostratigraphic cross sections containing Nye County data in the forthcoming revised Hydrogeologic Framework Model AMR or separate report. NRC staff suggests the revised report also address the two comments for corrected information and the seven comments for additional information needs previously discussed in the staff comments section of this review.

The seven comments relating to additional information needed to fulfill the intent of USFIC 5.05 and RT 2.09 agreements (Schlueter 2002) are as follows:

1. One of the critical underlying technical goals of the agreements was to develop information about geologic cross sections that are important to reducing uncertainties in groundwater flow and transport. For example, information derived from properly constructed and technically defensible geologic cross sections could greatly reduce uncertainties with regard to the location of the tuff-alluvium contact and the thickness and identification of tuff and alluvium within the upper several hundred meters of the basin sections. The cross sections presented in the June 28, 2002 letter report are insufficient to support these technical goals. The cross sections instead depict approximately 6,000 m [20,000 ft] of section in which the details of the near surface stratigraphy are obscured by the gross scale of cross-section construction.
2. Figures 4 through 12 present hydrogeologic cross sections extracted from a "2002 Hydrogeologic Framework Model." No reference is provided for this hydrogeologic framework model, which is apparently an updated model based on the stratigraphic interpretations in Plate 1 of the report. The hydrogeologic framework model used in DOE performance assessments to date—the one reviewed by NRC—was published in 2000 (CRWMS M&O 2000). It is not clear whether this revised hydrogeologic framework model will be used to update the site-scale saturated zone flow model and the performance assessment abstraction for saturated zone flow and transport. If the revised model is not to be used as input to performance assessment analyses, then a comparison of the revised model, which is presumed to be the best DOE interpretation, to the older model used in performance assessments should be provided.
3. Critical information and discussion of the identification of the various tuff units encountered in the Nye County Wells are absent from the report. In parallel with the technical goals stated in [AIN-1] #1 above, identification of the tuff units in these wells could provide the DOE with the necessary information to either validate or improve the flow and transport model depiction of groundwater in the shallow alluvial aquifer of Fortymile Wash. Staff anticipated that the report would include such information as it was informally presented at a previous technical exchange (Spengler 2000).

4. The technical basis for identification of the geologic or hydrologic units encountered in the Nye County wells is not provided in the report. The geologic units are simply named in summary tables with references to other data sources. The report lacks sufficient technical discussion of the criteria used to identify the geologic units or the resulting data and interpretations used to generate the stratigraphic units from the Nye County well cuttings. Without such information, there is insufficient technical basis to support interpretations in the cross sections.
5. There is no technical basis or discussion provided in the report about how the geophysical data were used to develop the stratigraphic information in the cross sections. The report simply identifies the data sources and associated reports and papers. Without such information, there is insufficient technical basis to support interpretations in the cross sections.
6. There is no technical basis or technical discussion provided in the report about how the regional geologic data from geologic maps or cross sections were used to develop the stratigraphic information in the cross sections. The report simply identifies the data sources and associated reports and papers. Without such information, there is insufficient technical basis to support interpretations in the cross sections.
7. Many of the lithologic identifications used in the report are unique to these cross sections (e.g., lithologic units Tgeg1-Tgeg6 in Table 2 of the letter report), without apparent consideration of existing geologic information. Many of these similar aged units have been identified, described, and mapped in the surrounding outcrop exposures of bedrock⁵. It is not clear whether the previously identified lithologic units have been renamed, or whether new lithologic units are being proposed.

[Footnote 5 from NRC document: Murray, D.A., Stamatakos, J.A., and Ridgway, K.D., "Regional Stratigraphy of Oligocene and Lower Miocene Strata in the Yucca Mountain Region." Center for Nuclear Waste Regulatory Analyses San Antonio Texas, July 2002, IM01402.220.]

B.1.2 Related Key Technical Issue Agreements

None.

B.2 RELEVANCE TO REPOSITORY PERFORMANCE

The purpose of this appendix is to provide a technical response to the NRC AIN request to the agreements described in Section B.1. The subject of the original agreements was the update of stratigraphic and hydrostratigraphic cross sections based on additional borehole data. The AIN responses are offered in the context of the technical adequacy of the original KTI agreement transmittal to satisfy that agreement.

B.3 RESPONSE

B-3.1 Response to AIN-1 #1—Additional characterization obtained from Nye County Early Warning Drilling Program (EWDP) borehole lithologies and aeromagnetic studies helped reduce uncertainties in the tuff-alluvium contact (Appendix G), and groundwater flow and transport in the areas covered by the Nye County cross sections. Additional information on the tuff-alluvium contact is provided in the Saturated Zone (SZ) Technical Basis Document (TBD) section 2.3.4. Flow and transport parameter uncertainty is captured in the stochastic parameter distributions that are sampled for the saturated zone flow and transport model simulations. Specifically, the alternative conceptual model of “channeling in the alluvium” with the key assumption that high permeability channels exist in the alluvium that can provide preferential pathways for flow and transport is implicitly included in the saturated zone transport model through the range of uncertainty in the effective porosity values (BSC 2003, Table 6.4-1)

B3.2 Response to AIN-1 #2—The hydrogeologic framework model has been updated to include new geologic data, primarily from the Nye County EWDP boreholes. Together with the 2002 revision to the Death Valley Regional Flow System and water level elevation from the new Nye County EWDP wells an alternate site-scale flow model was developed to update the base-case site-scale model. The alternate model has been calibrated and used to validate the existing base-case model. More detail on the alternate model and the use of the updated regional DVRFS is provided in section D-4.2 of appendix D.

The use of the site-scale hydrogeologic framework model is discussed in relationship to overall saturated zone flow and transport in Section 2.3.4.

The models to support the License Application are completed and have been accepted by the DOE as adequate for their intended use in the Total Systems Performance Assessment.

Cross sections were constructed to augment the hydrogeologic framework model (HFM; USGS 2001) (as stated in the KTI agreement items), which extends to depths on the order of 3 km. The printed version of the cross sections included in the June 28, 2002, letter report to NRC were formatted to display at a scale of approximately 1:25,000. However, because the cross sections were prepared in AutoCAD, they can be plotted at a larger scale if additional resolution is desired. New information continues to be gathered and evaluated and will continue to be provided as the project schedule requires it. For example, updated information on geologic cross sections has recently been completed and is available in PDF format (DTN: GS030408314211.002). Work continues on the HFM as new information becomes available, and if updates become available before the license application, an impact analysis will be conducted under AP-2.14Q, *Review of Technical Products and Data*, to evaluate if current products that depend on the revised product require modification to meet Yucca Mountain Project goals. The current HFM (USGS 2001) is valid for the TSPA-LA.

Response to AIN-1 #3—The technical basis for the identification of tuff units are available in many of the references included with the cross sections (DTN: GS030408314211.002) which refer to lithostratigraphic descriptions in all Nye County EWDP drill holes. The lithostratigraphic data packages for Nye County EWDP boreholes contain the technical bases for the identification of tuff units along with additional information such as the “level of confidence” associated with

each stratigraphic interpretation and a description of any corroborative geophysical log responses. Additional information concerning the technical basis for the identification of lithostratigraphic units encountered in Nye County EWDP boreholes can be found in Sections 4.1 and 4.3 of the June 28, 2002 letter report to the NRC (DIRS 164589).

Response to AIN-1 #4—The technical basis for identification of the lithostratigraphic units encountered in the Nye County EWDP wells is provided in the supporting documentation, as cited in the June 28, 2002, letter report to NRC. Selected references in Section 4.1 and Section 4.3 provide information on the criteria used to identify lithostratigraphic units. This supporting documentation is available to NRC onsite staff.

Response to AIN-1 #5—Descriptions of the use of borehole geophysical data are presented in references on the lithostratigraphic interpretations of Nye County EWDP Phases I, II, and, III. Additional illustrative information regarding the use and spatial relation of surface based geophysical information used in construction of the cross sections can now be found in the data package titled "Subsurface Interpretations along Cross Sections Nye-1, Nye-2, and Nye-3, southern Nye County, Nevada"—2002, by R.W. Spengler and R. P. Dickerson, DTN: GS030408314211.002. This data package, in part, developed to aid in satisfying some of the concerns identified in this Appendix B, is composed of 2 poster-size presentations (sheets). Sheet 1 contains four maps that illustrate the spatial position of all the information used in the construction of the cross sections. These data include: 1) locations of Nye County EWDP drill holes used in the construction of Nye-1, Nye-2, and Nye-3, 2) interpretive locations of faults, 3) locations of isostatic gravity anomalies, 4) locations of aeromagnetic anomalies, 5) depth-to-basement contours, 6) locations of seismic refraction profiles (near the Nye-2 section only), 7) locations of outcrops, and 8) location of potentiometric contours. Sheet 2 now contains updated versions of the 3 cross sections provided in the June 28, 2002 letter report to the NRC. These cross sections are all presented on one poster-size sheet and are presented in color, which greatly enhances the readability of the cross sections even at the printed scale of 1:25,000. Much of the earlier problems regarding the difficulty in seeing detailed lithostratigraphic relations near the upper part of the sections (close to the water table) have been resolved through the use of color in the cross sections. A "water table" profile has been included on all cross sections to facilitate inspection of this part of the cross sections.

The June 28, 2002 letter report to NRC, Table 1 and Section 3.3, provides a discussion of how the referenced geophysical data were used as corroborative data to develop the more detailed cross sections, and specifically to help locate the top of the Paleozoic strata and identify possible buried structures.

Response to AIN-1 #6—Revised cross sections in the 2-poster sheet format (Subsurface Interpretations Along Cross Sections Nye-1, Nye-2, and Nye-3, Southern Nye County, Nevada—2002, by R.W. Spengler and R. P. Dickerson, DTN: GS030408314211.002) now include a display of outcrops and structures relevant to the locations of Nye-1, Nye-2, and Nye-3. These geologic features were drawn or revised based on geologic information contained on regional geologic maps and cross sections.

Response to AIN-1 #7—The lithologic identifications are not unique to these cross sections and existing geologic information was considered. Existing geologic information described by Wahl

et al. (1997), Buesch et al. (1996), and the data report for NC-EWDP-2DB (DTN: GS011008314211.001) were considered. Lithologic units Tgeg1-Tgeg6 represent subunits within unit Tge (unit Tge [Prevolcanic sedimentary rocks] as described by Wahl et al. 1997). The data report for NC-EWDP-2DB (DTN: GS011008314211.001) indicates that the nomenclature of lower volcanic units and Tertiary sedimentary strata in NC-EWDP-2DB, for the most part, follows that of Wahl et al. (1997) and Buesch et al. (1996). The thin Tgeg1-Tgeg6 gravel layers, as described in the data report for NC-EWDP-2DB (DTN: GS011008314211.001), contain unique lithologic components that are currently found in the vicinity of borehole NC-EWDP-2DB, and potentially represent important marker beds, traceable from one borehole to another. Therefore, they were informally assigned a subunit status (i.e., g1, g2, g3, g4, g5, and g6, for these gravels). Wahl et al. (1997) note that these rocks were formerly designated as the Horse Spring Formation, but are older than the Miocene type Horse Spring Formation of the Lake Mead area.

The internal CNWRA report dated July, 2002, cited in Footnote 5 of the AIN-1 #7, postdates all of these references as well as the subject letter report (Ziegler 2002). In particular reference to the internal CNWRA report dated July, 2002, the general correlations shown and described in this report, which begin in the Frenchman Flat area, extend west to Fortymile Wash, and terminate in the Funeral Mountains, lack fundamental correlations of regional pyroclastic deposits. Without concerted attempt to correlate these key marker horizons with well constrained time lines, erroneous interpretations and correlations of the regional Tertiary sedimentary stratigraphy are likely to occur.

B.4 BASIS FOR THE RESPONSE

The seven parts of this AIN comprise a request for information that was provided in Section B3.

B.5 REFERENCES

B.5.1 Documents Cited

BSC (Bechtel SAIC Company) 2003. *Site-Scale Saturated Zone Transport*. MDL-NBS-HS-000010 REV 01A. Las Vegas, Nevada: Bechtel SAIC Company. ACC: MOL.20030626.0180.

Buesch, D.C.; Spengler, R.W.; Moyer, T.C.; and Geslin, J.K. 1996. *Proposed Stratigraphic Nomenclature and Macroscopic Identification of Lithostratigraphic Units of the Paintbrush Group Exposed at Yucca Mountain, Nevada*. Open-File Report 94-469. Denver, Colorado: U.S. Geological Survey. ACC: MOL.19970205.0061.

Reamer, C.W. and Williams, D.R. 2000a. Summary Highlights of NRC/DOE Technical Exchange and Management Meeting on Unsaturated and Saturated Flow Under Isothermal Conditions. Washington, D.C.: U.S. Nuclear Regulatory Commission. ACC: MOL.20001128.0206.

Reamer, C.W. and Williams, D.R. 2000b. Summary Highlights of NRC/DOE Technical Exchange and Management Meeting on Radionuclide Transport. Meeting held December 5-7, 2000, Berkeley, California. Washington, D.C.: U.S. Nuclear Regulatory Commission. ACC: MOL.20010117.0063.

Schlueter, J.R. 2002. "Additional and Corrected Information Needs Pertaining to Unsaturated and Saturated Flow Under Isothermal Conditions (USFIC) Agreement 5.05 and Radionuclide Transport (RT) Agreement 2.09." Letter from J.R. Schlueter (NRC) to J.D. Ziegler (DOE/ORD), December 19, 2002, 1223025549, with attachment. ACC: MOL.20030214.0140.

USGS (U.S. Geological Survey) 2000. *Hydrogeologic Framework Model for the Saturated-Zone Site-Scale Flow and Transport Model*. ANL-NBS-HS-000033 REV 00. Denver, Colorado: U.S. Geological Survey. ACC: MOL.20000802.0010.

USGS 2001. *Hydrogeologic Framework Model for the Saturated-Zone Site-Scale Flow and Transport Model*. ANL-NBS-HS-000033 REV 00 ICN 02. Denver, Colorado: U.S. Geological Survey. ACC: MOL.20011112.0070.

Wahl, R.R.; Sawyer, D.A.; Minor, S.A.; Carr, M.D.; Cole, J.C.; Swadley, W C; Laczniak, R.J.; Warren, R.G.; Green, K.S.; and Engle, C.M. 1997. *Digital Geologic Map Database of the Nevada Test Site Area, Nevada*. Open-File Report 97-140. Denver, Colorado: U.S. Geological Survey. TIC: 245880.

Williams, N. and Fray, R. 2002. "Contract No. DE-AC08-01RW12101 - Key Technical Issue (KTI) Agreements: Unsaturated and Saturated Flow Under Isothermal Conditions (USFIC) 5.05 and Radionuclide Transport (RT) 2.09." Letter from N. Williams (BSC) and R. Fray (BSC) to J.D. Ziegler (DOE/YMSCO), June 28, 2002, TB:cg - 0628023173, with enclosure. ACC: MOL.20020820.0068.

Ziegler, J.D. 2002. "Transmittal of a Report Addressing Key Technical Issue (KTI) Agreement Items Unsaturated and Saturated Zone Flow Under Isothermal Conditions (USFIC) 5.05 and Radionuclide Transport (RT) 2.09." Letter from J.D. Ziegler (DOE/YMSCO) to J.R. Schlueter (NRC), July 2, 2002, OL&RC:TCG-1351, 0703023215. ACC: MOL.20020911.0119, MOL.20020820.0068.

B.5.2 Codes, Standards, Regulations, and Procedures

AP-2.14Q, Rev. 2, ICN 2. *Review of Technical Products and Data*. Washington, D.C.: U.S. Department of Energy, Office of Civilian Radioactive Waste Management. ACC: DOC.20030206.0001.

B.5.3 Source Data, Listed by Data Tracking Number

GS011008314211.001. Interpretation of the Lithostratigraphy in Deep Boreholes NC-EWDP-19D1 and NC-EWDP-2DB Nye County Early Warning Drilling Program. Submittal date: 01/16/2001.

GS030408314211.002. Subsurface Geologic Interpretations Along Cross Sections Nye-1, Nye-2, and Nye-3, Southern Nye County, Nevada - 2002. Submittal date: 05/09/2003.

INTENTIONALLY LEFT BLANK

APPENDIX C
POTENTIOMETRIC SURFACE AND VERTICAL GRADIENTS
(RESPONSE TO USFIC 5.08 AIN-1)

Note Regarding the Status of Supporting Technical Information

This document was prepared using the most current information available at the time of its development. This Technical Basis Document and its appendices providing Key Technical Issue Agreement responses that were prepared using preliminary or draft information reflect the status of the Yucca Mountain Project's scientific and design bases at the time of submittal. In some cases this involved the use of draft Analysis and Model Reports (AMRs) and other draft references whose contents may change with time. Information that evolves through subsequent revisions of the AMRs and other references will be reflected in the License Application (LA) as the approved analyses of record at the time of LA submittal. Consequently, the Project will not routinely update either this Technical Basis Document or its Key Technical Issue Agreement appendices to reflect changes in the supporting references prior to submittal of the LA.

APPENDIX C

POTENTIOMETRIC SURFACE AND VERTICAL GRADIENTS (RESPONSE TO USFIC 5.08 AIN-1)

This appendix provides a response to the additional information needed (AIN) request from the U.S. Nuclear Regulatory Commission (NRC) for Key Technical Issue (KTI) agreement Unsaturated and Saturated Flow under Isothermal Conditions (USFIC) 5.08. This KTI agreement relates to providing more information about the potentiometric surface and vertical gradients.

C.1 KEY TECHNICAL ISSUE AGREEMENT

C.1.1 USFIC 5.08 AIN-1

KTI agreement USFIC 5.08 was reached during the NRC/DOE technical exchange and management meeting on unsaturated and saturated flow under isothermal conditions held October 31 through November 2, 2000 in Albuquerque, New Mexico. The saturated zone portion of KTI subissues 5 and 6 were discussed at that meeting (Reamer and Williams 2000).

A letter report responding to this agreement and containing an updated potentiometric surface map and explanatory text (Ziegler 2002) was prepared. Specific additional information was requested by the U. S. Nuclear Regulatory Commission after the staff's review of this letter report was completed, resulting in USFIC 5.08 AIN-1 (Reamer and Williams 2000).

The wording of these agreements is as follows:

USFIC 5.08

Taking into account the Nye County information, provide the updated potentiometric data and map for the regional aquifer, and an analysis of vertical hydraulic gradients within the site scale model. DOE will provide an updated potentiometric map and supporting data for the uppermost aquifer in an update to the Water-Level Data Analysis for the Saturated Zone Site-Scale Flow and Transport Model AMR expected to be available in October 2001, subject to receipt of data from the Nye County program. Analysis of vertical hydraulic gradients will be addressed in the site-scale model and will be provided in the Calibration of the Site-Scale Saturated Zone Flow Model AMR expected to be available during FY 2002.

USFIC 5.08 AIN-1

1. Incorporate data for well SD-6, which was drilled several years ago (DOE 1999) and provide key information about hydraulic heads close to the Solitario Canyon Fault, into the analysis of water levels near Yucca Mountain and provide the analysis for NRC review. The same data given in tables in the water-level AMR for other wells should be provided for SD-6.

2. Provide a hydrogeologic interpretation for the high heads observed in wells UZ-14 and H-5.
3. Provide an updated hydrogeologic interpretation for groundwater elevations in wells G-2 and WT-#6 (i.e., wells that define the large hydraulic gradient) based on newly available data from well WT-24.
4. Provide the basis for assuming that the water level in Well NC-EWDP-7S represents perched water.

C.1.2 Related Key Technical Issue Agreements

None.

C.2 RELEVANCE TO REPOSITORY PERFORMANCE

The purpose of this appendix is to provide a technical response to the NRC AIN request to the agreement described in Section C.1. The subject of the original agreements was the update of the potentiometric surface map based on additional well data. The AIN responses are offered in the context of the technical adequacy of the original KTI agreement transmittal to satisfy that agreement.

Additional related discussion can be found in Section 2.3.4.

Potentiometric surface interpretations are important to the saturated zone flow model because the information generated is one of the primary datasets used for calibration. It is also important that some information be used for model validation. At the time the original potentiometric interpretations were made, some of the more recent data points were not yet qualified or had not stabilized from the stress of drilling. Therefore these data were not used in the potentiometric interpretations. Rather, the datapoints were used in the validation process to see if the interpretation without them would be able to predict where the head measurements should have been if the model interpretation was adequate for its intended purpose.

C.3 RESPONSE

In addition to the response to the four AIN questions, a discussion of an updated potentiometric surface and vertical hydraulic gradient analyses are provided in the basis for response. The two analyses provide the relationship of water level elevations in the subject wells to the potentiometric surface and use in the flow modeling.

Response to AIN-1 #1—The water-level information requested for borehole USW SD-6 was used for model validation in *Calibration of the Site-Scale Saturated Zone Flow Model* (BSC 2001). The predicted head at borehole USW SD-6 was 734.84 m, compared to the observed head of 731.2 m. This is a more direct use of borehole USW SD-6 water-level data than is the incorporation of this information into the potentiometric surface. The site-scale saturated zone flow model (BSC 2003) contains the same results for USW SD-6. Moreover, as indicated in Section C.4.3, this information would not materially change the potentiometric surface depicted

in *Water-Level Data Analysis for the Saturated Zone Site-Scale Flow and Transport Model* (USGS 2001, Figure 6-1).

The recorded water level in borehole USW SD-6 was 731.2 m, and including data from that borehole would not require a change in the shape and spacing of the potentiometric contours. USW SD-6 water level elevation could be plotted on the potentiometric map without any changes to the contours.

Information from borehole USW SD-6 was used by the NRC Center for Nuclear Waste Regulatory Analysis in *Revised Site-Scale Potentiometric Surface Map For Yucca Mountain, Nevada* (Hill et al. 2002), which states that the revised potentiometric surface map agrees favorably with the map provided in the water-level report (USGS 2001). The differences are:

- The contour intervals used
- The interpreted potentiometric surface in Hill et al. (2002) is limited to the Yucca Mountain area north of the Amargosa Farms area
- Recent Nye County water-level data, which includes preliminary data for Phase-3 boreholes and the most recent water-level measurements for Phase-2 boreholes, were used in the interpretation for the revised potentiometric surface map.

None of these differences would be affected by the addition of data from borehole USW SD-6. There are no noted differences between the water levels measured at borehole USW SD-6 and those measured at adjacent boreholes. Differences at other sites are not important because they principally apply to areas away from the potential flow paths, and updates from preliminary to final results for Nye County Phase-2 and Phase-3 boreholes are unlikely to result in changes beyond the current uncertainty range of the water-level interpretations.

Response to AIN-1 #2—The high potentiometric level in borehole USW H-5 has been attributed to the presence of a splay of the Solitario Canyon fault penetrated by the borehole (Ervin et al. 1994, pp. 9 to 10). This splay is believed to be an extension of the hydrologic barrier to west-to-east groundwater flow from Crater Flat (related to the Solitario Canyon fault). The high heads in USW H-5 (about 775 m) are related to heads in Crater Flat (ranging from about 780 to 775 m), and this borehole defines part of the moderate hydraulic gradient along the western edge of Yucca Mountain. Borehole USW UZ-14 is in a transition zone between the large and moderate hydraulic-gradient areas, and the high potentiometric level (about 779 m) is related to either of these areas. Rousseau et al. (1999, p. 172) hypothesized that perched water in borehole USW UZ-14 could be caused by a nearby projected growth fault that impedes percolation of water from the surface. This fault may also impede groundwater flow in the saturated zone. The high heads in borehole USW UZ-14 also could be caused by the low-permeability rocks in the upper part of the saturated zone at that borehole.

Response to AIN-1 #3—There are not enough data to unequivocally prove the presence of perched-water at boreholes USW G-2 and UE-25 WT#6. The evidence for the possibility of perched water is presented by Czarnecki et al. (1997), which was cited in the water-level report (USGS 2001). However, the USGS (2001, p. 7) presents an alternative concept for the large

hydraulic gradient. Both conceptual models of the large hydraulic gradient were tested with the flow model, and both yielded nearly identical flow fields and flow paths. The potentiometric surface map presented in the water-level report (USGS 2001) was not intended as a replacement for the previous maps (except in the south where there are new data from Nye County boreholes). The purpose of the report (USGS 2001) was to provide an alternate concept that could be tested with the site-scale saturated zone model and to update data with water levels from borehole USW WT-24 and the latest available Nye County data. The concept of semi-perched conditions (Flint et al. 2001) differs only in that the underlying rocks are fully saturated, rather than unsaturated as in the perched-water concept. An expert elicitation panel (CRWMS M&O 1998) concluded that the existence of the large hydraulic gradient or perched conditions does not impact the performance of Yucca Mountain. The panel suggested that to understand the cause, a borehole could be drilled and tested, which led to the drilling of borehole USW WT-24. Drilling, testing, and monitoring of borehole USW WT-24 indicated the existence of perched conditions and a regional water-table elevation of 840 m. After the water-bearing fracture was penetrated, the water level remained constant after the borehole was deepened by more than 100 m, indicating the probability that the water level represents the regional potentiometric surface rather than another perched zone. However, because borehole USW WT-24 is completed within the relatively low permeability Calico Hills Formation, as are boreholes USW G-2 and UE-25 WT#6, it cannot be ruled out that the 840-m water level in borehole USW WT-24 could represent a second perched zone. Because the water encountered was from a fracture below a long interval of dry rock, it may be more reasonable to conclude that the water level represents a regional potentiometric surface (connected by a network of water-bearing fractures within tight, dry rocks) rather than a second perched zone of saturated rocks. The alternative conceptual models were implemented and evaluated in the saturated zone flow model base case.

Response to AIN-1 #4—As the water-level report (USGS 2001) was being prepared, there were only two water levels for borehole NC-EWDP-7S, and no subsurface information was available. Contouring the 830-m potentiometric level would have produced an anomalously high bulls-eye pattern that was unjustified based on available data. With no additional evidence, it was assumed that the water level represented a perched condition. Since the water-level report (USGS 2001) was written, data from a new Nye County borehole, borehole NC-EWDP-7SC, provides evidence for alternative interpretations other than perched-water conditions. Large downward gradients are observed between the deep and shallow monitored intervals at borehole NC-EWDP-1DX (head difference of 38 m) and NC-EWDP-7SC (head differences ranging from about 9 m to as much as 78 m). The depth to water at both of these locations is anomalously shallow and probably represents locally perched conditions or the presence of a low permeability confining unit close to the surface that effectively impedes the downward migration of water to the more contiguous tuff and alluvium aquifers at greater depths.

Borehole NC-EWDP-7SC is completed at 4 depth intervals. The head in the uppermost interval is high, about 818 m, but heads decrease with depth to a level of about 740 m. However, the rocks appear to be at least partially saturated below the uppermost water-bearing zone. The high water levels in the uppermost zone may be partially perched by clay layers present below the uppermost zone. This is similar to conditions in Ash Meadows, although water levels there are above the land surface. Water-quality data from borehole NC-EWDP-7S indicate that the water may be more related to carbonate-aquifer water than volcanic-aquifer water. Another possible

explanation raised by Nye County consultants (Questa Engineering Corporation 2002) suggests that results for spinner surveys and a 48-hour pump test indicate that the well set (NC-EWDP-7S and NC-EWDP-7SC) were insufficiently developed and that lower screens monitored zones of lower permeability. The testing also suggested that there was a zone of severely damaged formation in the immediate vicinity of the well consistent with the history of large amounts of polymer and bentonite gel mud being lost to the hole during completion. Thus, data from this well is questionable. Because it is distant from the predicted flow paths from Yucca Mountain and outside of the compliance boundaries, the effect of the uncertainty in this data is minor relative to potential radionuclide transport to the accessible environment.

C.4 BASIS FOR THE RESPONSE

The basis for the response to the request for an updated potentiometric surface, an analysis of vertical gradients, and additional information regarding specific issues about the potentiometric surface are provided below. Additional related discussion can be found in Sections 2.2.2 and 2.3.3.

C.4.1 Updated Potentiometric Surface

The analysis of water level data was updated (USGS 2001) and provided as part of the original response. That analysis included water level data collected through December 2000, including water-level data obtained from the expanded Nye County Early Warning Drilling Program, and data from borehole USW WT-24. Using standard practices, in a manner similar to USGS (2000), a potentiometric surface map representative of the upper part of the saturated zone in the early 1990s was generated. Besides new water level data, the primary difference in the approach taken to generate the new potentiometric surface was the assumption that water levels in the northern portion of the model domain, acquired from boreholes USW G-2 and UE-25 WT#6, represent perched conditions rather than a continuous regional potentiometric surface. As a result, the revised potentiometric surface map represents an alternate concept from that presented by the USGS (2000) for the large hydraulic gradient area north of Yucca Mountain. Another difference in the preparation of the two maps is the use of hand contouring for the USGS (2001) map rather than using an automated (computerized) contouring approach.

The older (USGS 2000, Figure 1-2) and newer (USGS 2001, Figure 6-1) potentiometric surface maps are similar (potentiometric contours are similar). The most important difference is the portrayal of the large hydraulic gradient area north of Yucca Mountain. The concept that water levels in boreholes USW G-2 and UE-25 WT #6 represent perched conditions is used to create the newer potentiometric surface map (USGS 2001, Figure 6-1). Neglecting the data from those two boreholes, the large hydraulic gradient is reduced from about 0.11 m/m (Tucci and Burkhardt 1995, p. 9) to between 0.06 m/m to 0.07 m/m, and the potentiometric contours are more widely spaced. Another important difference is that potentiometric contours are no longer offset where they cross faults. Such offsets (USGS 2000) are not expected where the contours are perpendicular or nearly perpendicular to fault traces. Direct evidence of offset, which would be provided by boreholes that straddle the fault, does not exist at Yucca Mountain. Faults were used, however, to help in the placement of contours that are oriented parallel or approximately parallel to faults. The contour interval used in the newer map (USGS 2001, Figure 6-1) is somewhat different from that used in the older map (USGS 2000, Figure 1-2), which used a

uniform contour interval of 25 m. The contour interval used in the newer (USGS 2001) map has an interval of 50 m for contours greater than 800 m, and 25 m is used for contours less than 800 m. Two additional contours, 730 m and 720 m, are also included in the newer map (USGS 2001). The inclusion of these contours helps to visualize the effect of the fault along Highway 95 (south of Yucca Mountain) on the groundwater flow system. USGS (2000) maps were used as input for the base case model. *Water-Level Data Analysis for the Saturated Zone Site-Scale Flow and Transport Model* (USGS 2001) was used as, and evaluated as, an alternative conceptual model.

The current potentiometric surface analysis (USGS 2001) and analyses in previously published reports imply that a hydraulically well-connected flow system exists within the uppermost saturated zone (Tucci and Burkhardt 1995).

Water-level data from Nye County phase 3 and phase 4 boreholes, drilled since completion of the current report (USGS 2001) provide an update to the potentiometric surface south of Yucca Mountain. Nye County Phase 3 boreholes include boreholes NC-EWDP-10S, NC-EWDP-18P, NC-EWDP-22S, and NC-EWDP-23S at the south end of Jackass Flats. Water levels from these boreholes range from about 724 m to about 728 m. The 720-m and 725-m potentiometric contours based on these data would be placed south of those shown on the current potentiometric surface map (USGS 2001). The revised placement of these contours results in a hydraulic gradient in Jackass Flats of less than 0.0001 m/m, which is less than that in the previous report (USGS 2001; i.e., 0.0001 m/m to 0.0004 m/m). Nye County Phase 4 boreholes NC-EWDP-16P, NC-EWDP-27P, and NC-EWDP-28P were drilled directly south of Yucca Mountain, north of the Lathrop Wells cone, and west of the Stagecoach Road fault. Water levels from these boreholes ranged from 729 to 730 m, and were from 2 m to more than 10 m less than levels that can be interpolated from the contours shown for that area in the newer report (USGS 2001). Revised potentiometric contours in this area would have the 730-m contour placed about 1.5 to 2 km to the west of the position shown in the water-level report (USGS 2001), and would result in flow vectors in a more southerly direction for groundwater flow south of Yucca Mountain. This is being assessed in the TSPA-LA.

C.4.2 Analysis of Vertical Gradients

Within the saturated zone site-scale flow and transport model area (USGS 2001, Figure 1-1), 18 boreholes are currently used to monitor water levels in more than one vertical interval (Table C-1). These intervals were selected to monitor water levels between different geologic units or between different permeable intervals within the same geologic unit. Water-level data from these boreholes allow for the calculation of the difference in potentiometric heads at each monitored interval. Upward (head increases with depth) and downward (head decreases with depth) vertical gradients have been observed. Fewer downward gradients (6 cases) are observed than upward gradients (12 cases). Upward vertical head differences range from 0.1 m to almost 55 m, and downward vertical head differences range from 0.5 m to 78 m.

Table C-1. Vertical Head Differences

Borehole	Open Interval (m below land surface)	Potentiometric Level (m above sea level)	Head Difference deepest to shallowest intervals (m)
USW H-1 tube 4	573-673	730.94	54.7
USW H-1 tube 3	716-765	730.75	
USW H-1 tube 2	1097-1123	736.06	
USW H-1 tube 1	1783-1814	785.58	
USW H-3 upper	762-1114	731.19	28.9
USW H-3 lower	1114-1219	760.07	
USW H-4 upper	525-1188	730.49	0.1
USW H-4 lower	1188-1219	730.56	
USW H-5 upper	708-1091	775.43	0.2
USW H-5 lower	1091-1219	775.65	
USW H-6 upper	533-752	775.99	2.2
USW H-6 lower	752-1220	775.91	
USW H-6	1193-1220	778.18	
UE-25 b #1 upper	488-1199	730.71	-1.0
UE-25 b #1 lower	1199-1220	729.69	
UE-25 p #1 (volcanic)	384-500	729.90	21.4
UE-25 p #1 (carbonate)	1297-1805	751.26	
UE-25 c #3	692-753	730.22	0.4
UE-25 c #3	753-914	730.64	
USW G-4	615-747	730.3	-0.5
USW G-4	747-915	729.8	
UE-25 J -13 upper	282-451	728.8	-0.8
UE-25 J -13	471-502	728.9	
UE-25 J -13	585-646	728.9	
UE-25 J -13	820-1063	728.0	
NC-EWDP-1DX (shallow)	WT-419	786.8	-38.0
NC-EWDP-1DX (deep)	658-683	748.8	
NC-EWDP-2D (volcanic)	WT-493	706.1	7.6
NC-EWDP-2DB (carbonate)	820-937	713.7	

Table C-1. Vertical Head Differences (Continued)

Borehole	Open Interval (m below land surface)	Potentiometric Level (m above sea level)	Head Difference deepest to shallowest intervals (m)
NC-EWDP-3S probe 2	103-129	719.8	-1.5
NC-EWDP-3S probe 3	145-168	719.4	
NC-EWDP-3D	WT-762	718.3	
NC-EWDP-4PA	124-148	717.9	5.7
NC-EWDP-4PB	225-256	723.6	
NC-EWDP-7SC probe 1	24-27	818.1	
NC-EWDP-7SC probe 2	55-64	786.4	
NC-EWDP-7SC probe 3	82-113	756.6	-77.9
NC-EWDP-7SC probe 4	131-137	740.2	
NC-EWDP-9SX probe 1	27-37	766.7	0.1
NC-EWDP-9SX probe 2	43-49	767.3	
NC-EWDP-9SX probe 4	101-104	766.8	
NC-EWDP-12PA	99-117	722.9	2.2
NC-EWDP-12PB	99-117	723.0	
NC-EWDP-12PC	52-70	720.7	
NC-EWDP-19P	109-140	707.5	5.3
NC-EWDP-19D	106-433	712.8	

Source: Based on USGS 2001, Table 6-1.

NOTE: Negative values indicate downward gradient.

Only two sites, UE-25 p#1 and NC-EWDP-2D/2DB (Table C-1), provide information on vertical gradients between volcanic rocks and the underlying Paleozoic carbonate rocks. At borehole UE-25 p#1, water levels currently are monitored only in the carbonate aquifer; however, water-level data were obtained from within the volcanic rocks as the borehole was drilled and tested. At this site, water levels in the Paleozoic carbonate rocks are about 20 m higher than those in the overlying volcanic rocks. Borehole NC-EWDP-2DB penetrated Paleozoic carbonate rocks toward the bottom of the borehole (Spengler 2001). Water levels measured within the deep part of the borehole are about 6 m higher than levels measured in volcanic rocks penetrated by borehole NC-EWDP-2D (for NC-EWDP-2DB, DTN: MO0306NYE05111.151; for NC-EWDP-2D, DTN: MO0306NYE05354.152).

Water levels monitored in the lower part of the volcanic-rock sequence are higher than levels monitored in the upper part of the volcanics. Boreholes USW H-1 (tube 1) and USW H-3 (lower interval) monitor water levels in the lower part of the volcanic-rock sequence, and upward gradients are observed at these boreholes (head differences of 54.7 m, and 28.9 m, respectively). The gradient at USW H-3 is not completely known because the water levels in the lower interval had been rising continuously before the packer that separates the upper and lower intervals failed in 1996.

An upward gradient also is observed between the alluvial deposits monitored in borehole NC-EWDP-19P and the underlying volcanic rocks monitored in borehole NC-EWDP-19D. The vertical head difference at this site is 5.3 m; however, levels reported for NC-EWDP-19D represent a composite water level for alluvium and volcanics, so the true head difference between those units is not known.

Downward gradients also are observed within the saturated zone site-scale flow and transport model area. The largest downward gradient is between the deepest and shallowest monitored intervals at borehole NC-EWDP-7SC (i.e., head difference of nearly 80 m). The depth to water at this site is shallow (20 m) and within Tertiary spring deposits. Other downward gradients are smaller. In all, vertical gradient information is consistent with its implementation in the saturated zone flow model base case.

C.5 REFERENCES

C.5.1 Documents Cited

BSC (Bechtel SAIC Company) 2001. *Calibration of the Site-Scale Saturated Zone Flow Model*. MDL-NBS-HS-000011 REV 00 ICN 01. Las Vegas, Nevada: Bechtel SAIC Company. ACC: MOL.20010713.0049.

BSC 2003. *Site-Scale Saturated Zone Flow Model*. MDL-NBS-HS-000011 REV 01A. Las Vegas, Nevada: Bechtel SAIC Company. ACC: MOL.20030626.0296.

CRWMS M&O (Civilian Radioactive Waste Management System Management and Operating Contractor) 1998. *Saturated Zone Flow and Transport Expert Elicitation Project*. Deliverable SL5X4AM3. Las Vegas, Nevada: CRWMS M&O. ACC: MOL.19980825.0008.

Czarnecki, J.B.; Faunt, C.C.; Gable, C.W.; and Zyvoloski, G.A. 1997. *Hydrogeology and Preliminary Three-Dimensional Finite-Element Ground-Water Flow Model of the Site Saturated Zone, Yucca Mountain, Nevada*. Milestone SP23NM3. Denver, Colorado: U.S. Geological Survey. ACC: MOL.19990812.0180.

Ervin, E.M.; Luckey, R.R.; and Burkhardt, D.J. 1994. *Revised Potentiometric-Surface Map, Yucca Mountain and Vicinity, Nevada*. Water-Resources Investigations Report 93-4000. Denver, Colorado: U.S. Geological Survey. ACC: NNA.19930212.0018.

Flint, A.L.; Flint, L.E.; Kwicklis, E.M.; Bodvarsson, G.S.; and Fabryka-Martin, J.M. 2001. "Hydrology of Yucca Mountain, Nevada." *Reviews of Geophysics*, 39, (4), 447-470. Washington, D.C.: American Geophysical Union.

Hill, M.; Winterle, J.; and Green, R. 2002. *Revised Site-Scale Potentiometric Surface Map for Yucca Mountain, Nevada*. San Antonio, Texas: Center for Nuclear Waste Regulatory Analyses (CNWRA). TIC: 254765.

Questa Engineering Corporation. 2002. Preliminary Analysis of Pump-Spinner Tests and 48-Hour Pump Tests in Wells NC-EWDP-19IM1 and -19IM2, Near Yucca Mountain, Nevada. NWRPO-2002-05. Pahrump, Nevada: Nye County Nuclear Waste Repository Project Office. ACC: MOL.20030821.0001.

Reamer, C.W. and Williams, D.R. 2000. Summary Highlights of NRC/DOE Technical Exchange and Management Meeting on Unsaturated and Saturated Flow Under Isothermal Conditions. Meeting held August 16-17, 2000, Berkeley, California. Washington, D.C.: U.S. Nuclear Regulatory Commission. ACC: MOL.20001201.0072.

Rousseau, J.P.; Kwicklis, E.M.; and Gillies, D.C., eds. 1999. *Hydrogeology of the Unsaturated Zone, North Ramp Area of the Exploratory Studies Facility, Yucca Mountain, Nevada*. Water-Resources Investigations Report 98-4050. Denver, Colorado: U.S. Geological Survey. ACC: MOL.19990419.0335.

Spengler, R. 2001. "Pz in NC-EWDP-2DB." E-mail from R. Spengler to P. McKinley, August 30, 2001. ACC: MOL.20010907.0001.

Tucci, P. and Burkhardt, D.J. 1995. *Potentiometric-Surface Map, 1993, Yucca Mountain and Vicinity, Nevada*. Water-Resources Investigations Report 95-4149. Denver, Colorado: U.S. Geological Survey. ACC: MOL.19960924.0517.

USGS (U.S. Geological Survey) 2000. *Water-Level Data Analysis for the Saturated Zone Site-Scale Flow and Transport Model*. ANL-NBS-HS-000034 REV 00. Denver, Colorado: U.S. Geological Survey. ACC: MOL.20000830.0340.

USGS 2001. *Water-Level Data Analysis for the Saturated Zone Site-Scale Flow and Transport Model*. ANL-NBS-HS-000034 REV 01. Denver, Colorado: U.S. Geological Survey. ACC: MOL.20020209.0058.

Ziegler, J.D. 2002. "Transmittal of Reports Addressing Key Technical Issues (KTI)." Letter from J.D. Ziegler (DOE/YMSCO) to J.R. Schlueter (NRC), April 26, 2002, 0430022458, OL&RC:TCG-1032, with enclosures. ACC: MOL.20020730.0383.

C.5.2 Source Data, Listed by Data Tracking Number

MO0306NYE05111.151. Manual Water Level Data for EWDP Phase II Wells, 11/01 - 04/02. Submittal date: 06/17/2003.

MO0306NYE05354.152. Manual Water Level Data for EWDP Phase 1 Wells Revision 4. Submittal date: 06/17/2003.

APPENDIX D

REGIONAL MODEL AND CONFIDENCE BUILDING
(RESPONSE TO USFIC 5.02, USFIC 5.12, AND USFIC 5.11 AIN-1)

Note Regarding the Status of Supporting Technical Information

This document was prepared using the most current information available at the time of its development. This Technical Basis Document and its appendices providing Key Technical Issue Agreement responses that were prepared using preliminary or draft information reflect the status of the Yucca Mountain Project's scientific and design bases at the time of submittal. In some cases this involved the use of draft Analysis and Model Reports (AMRs) and other draft references whose contents may change with time. Information that evolves through subsequent revisions of the AMRs and other references will be reflected in the License Application (LA) as the approved analyses of record at the time of LA submittal. Consequently, the Project will not routinely update either this Technical Basis Document or its Key Technical Issue Agreement appendices to reflect changes in the supporting references prior to submittal of the LA.

APPENDIX D

REGIONAL MODEL AND CONFIDENCE BUILDING (RESPONSE TO USFIC 5.02, USFIC 5.12, AND USFIC 5.11 AIN-1)

This appendix provides a response for Key Technical Issue (KTI) agreements Unsaturated and Saturated Flow under Isothermal Conditions (USFIC) 5.02, USFIC 5.12, and an additional information needed (AIN) request on USFIC 5.11. These KTI agreements relate to providing more information about the use of the regional model in the site-scale model and the Solitario Canyon Alternative Conceptual Model.

D.1 KEY TECHNICAL ISSUE AGREEMENTS

D.1.1 USFIC 5.02, USFIC 5.12, and USFIC 5.11

KTI agreements USFIC 5.02, USFIC 5.12, and USFIC 5.11 were reached during the NRC/DOE technical exchange and management meeting on unsaturated and saturated flow under isothermal conditions held October 31 through November 2, 2000 in Albuquerque, New Mexico. The saturated zone portion of KTI subissues 5 and 6 were discussed at that meeting (Reamer and Williams 2000).

At the NRC/DOE technical exchange DOE explained that it had used mathematical groundwater models: (1) that incorporate site-specific climatic and subsurface information; (2) that are reasonably calibrated and reasonably represent the physical system; (3) whose fitted aquifer parameters compare reasonably well with observed site data; (4) whose implicitly or explicitly simulated fracturing and faulting are consistent with the data in the 3D geologic framework model (GFM) and hydrogeologic framework model (HFM); (5) whose abstractions are based on initial and boundary conditions consistent with site-scale modeling and the regional model of the Death Valley groundwater flow system. DOE has used mathematical groundwater models whose abstractions of the groundwater models for use in PA simulations use the appropriate spatial and temporal averaging techniques.

The NRC asked several questions regarding the analysis of alternative conceptual models and the propagation of such models through performance assessment. The NRC also asked the DOE if permeabilities along the Solitario Canyon Fault could be revised to permit additional flow from Crater Flat into the regional deep aquifer beneath Yucca Mountain. The NRC indicated that in this way, the model can be used to evaluate alternate conceptual flow models. The DOE indicated this alternative model could be evaluated.

Wording of these agreements is as follows:

USFIC 5.02

Provide the update to the saturated zone PMR, considering the updated regional flow model. A revision of the Saturated Zone Flow and Transport PMR is expected to be available and will reflect the updated United States Geological Survey (USGS) Regional Groundwater Flow Model in FY 2002, subject to receipt of the model report from the USGS (reference item 9).

USFIC 5.12

Provide additional supporting arguments for the Site-Scale Saturated Zone Flow model validation or use a calibrated model that has gone through confidence-building measures. The model has been calibrated and partially validated in accordance with AP 3.10Q, which is consistent with NUREG-1636. Additional confidence-building activities will be reported in a subsequent update to the Calibration of the Site-Scale Saturated Zone Flow Model AMR, expected to be available during FY 2002.

USFIC 5.11

In order to test an alternative conceptual flow model for Yucca Mountain, run the saturated zone flow and transport code assuming a north-south barrier along the Solitario Canyon fault whose effect diminishes with depth or provide justification not to. DOE will run the saturated zone flow and transport model assuming the specified barrier and will provide the results in an update to the Calibration of the Site-Scale Saturated Zone Flow Model AMR expected to be available during FY 2002.

A letter report responding to KTI agreement USFIC 5.11 (Ziegler 2002) was prepared. Specific additional information was requested by the U. S. Nuclear Regulatory Commission after the staff's review of this letter report was completed, resulting in USFIC 5.11 AIN-1 (Schlueter 2003).

Wording of the additional information need request is as follows:

USFIC 5.11 AIN-1

1. To examine flow and potential radionuclide transport in the deeper aquifer system, a vertical cross-sectional figure showing the flowpaths is needed. As an example, the left diagram of Figure 8 in the Calibration of the Site-Scale Saturated Zone Flow Model AMR (CRWMS M&O 2000) shows such a cross-sectional view. Two such particle tracking figures showing distance vs. depth are needed: one for the calibrated model and another for the shallow Solitario Canyon Fault alternative model.
2. To test the hypothesis that potential contaminant releases on the west side of a shallow Solitario Canyon Fault might enter the lower carbonate aquifer, DOE should provide an analysis of flow paths from the west side of a shallow Solitario Canyon Fault. Alternatively, DOE could provide an explanation of repository design and site characteristics that would preclude contaminant releases to the west side of the Solitario Canyon Fault.

DOE responded to the NRC on April 9, 2003 (Ziegler 2003), and agreed to provide information that would satisfy USFIC 5.11 AIN-1.

D.1.2 Related Key Technical Issue Agreements

None.

D.2 RELEVANCE TO REPOSITORY PERFORMANCE

The subject of these agreements is the construction and calibration of the saturated zone site-scale flow and transport model and the evaluation of the alternative conceptual model. These subjects directly affect the saturated zone model and, subsequently, the performance assessment.

The saturated zone flow and transport model domain lies within the Alkali Flat-Furnace Creek groundwater basin, which is part of the larger Death Valley regional groundwater flow system. The Death Valley regional groundwater flow model (D'Agnese et al. 2002) provides a representation of the groundwater flow patterns within the Alkali Flat-Furnace Creek groundwater basin, and thus can be used to define boundary conditions and calibration targets for the site-scale model. Accordingly, constant-potential boundary conditions and distributed vertical recharge for the site-scale saturated zone model can be derived from the regional model. Recharge from the unsaturated zone site-scale model area and from Fortymile Wash can also be included in the model. These boundary fluxes are used as calibration targets for validation of the revised site-scale saturated zone model

The understanding of the moderate hydraulic gradient is important because water-level data collected in Yucca Mountain boreholes indicate areas of moderate and high hydraulic gradients west and north of Yucca Mountain. East and southeast of Yucca Mountain, the hydraulic potential and the hydraulic gradient reflected in water levels are lower than those to the west and north. Water levels in boreholes east of the Solitario Canyon fault support the conceptual model of eastward groundwater flow directly beneath Yucca Mountain that gradually turns southward in the vicinity of Fortymile Wash. The moderate hydraulic gradient area west of Yucca Mountain is characterized by higher water table elevations in boreholes just west of the Solitario Canyon fault, indicating the moderate gradient likely is caused by a zone of reduced permeability in the volcanic tuffs along the Solitario Canyon fault.

Additional discussion associated with this topic can be found in *Technical Basis Document No. 11* "Saturated Zone and Transport" (Section 2.2) that describes the regional and site-scale models used to assess the flow of groundwater and transport of potential radionuclides in the saturated zone beneath and downgradient from Yucca Mountain. Regional and site-scale geochemical interpretations (Section 2.3) are used to develop confidence in the site-scale flow and transport representation.

D.3 RESPONSE

Response to USFIC 5.02—Revision of the saturated zone flow and transport model which reflects the USGS update of the regional groundwater flow model (USFIC 5.09 update of USGS Regional Groundwater Flow Model) is documented in the revised saturated zone flow model (BSC 2003a). The *Saturated Zone Process Model Report* (CRWMS M&O 2000a) will not be revised.

The 1997 Death Valley regional flow system (DVRFS) model (D'Agnese et al. 1997) was used in the development and calibration of the saturated zone site-scale flow model. The 2001 steady-state version of the DVRFS model (D'Agnese et al. 2002) is used in the development and calibration of the alternate model, which, in turn, is used as part of the validation and confidence building of the saturated zone site-scale flow model. Boundary fluxes play an important role in the saturated zone site-scale flow model. These fluxes provide the communication with the DVRFS model, which is based on a regional mass balance and calibrated to spring flow data. Averaged fluxes derived from the DVRFS model are used for calibration targets in the saturated zone site-scale flow model calibration process in much the same way water levels are used for targets. These targets are weighted differently based on the importance of a given average flux to the saturated zone site-scale flow model. Because of differences in the two models (differences in scale, resolution and layer definitions in HFM), only general agreement regarding fluxes is expected between the two models.

Response to USFIC 5.12—Confidence building through model validation is documented in the revised *Site-Scale Saturated Zone Flow Model* (BSC 2003a, Section 7) using (1) water level data, (2) hydrogeologic data, and (3) temperature data not used in development and calibration of the model.

A comparison of the predicted and recently obtained water levels from the newly drilled Nye County EWDP boreholes demonstrates that the base-case flow model can reliably predict the water levels and gradients along the flow path from the repository. An analysis of the impact of the differences between observed and predicted hydraulic gradients on the specific discharge along the flow path from the repository has identified only a minimal impact on the specific discharge. A comparison of permeability measurements from the Alluvial Testing Complex (ATC) with the calibrated permeability value for the alluvium has similarly indicated close agreement between calibrated and measured values. An analysis of the impact of differences between calibrated and measured permeability on the specific discharge along the flow path from the repository has also demonstrated only a minimal impact on the specific discharge. An analysis of the combined effect on specific discharge of the difference between observed and predicted hydraulic gradients and permeability values in the area of the ATC similarly indicates minimal impact. The comparison between the flow paths predicted by the base-case model and those indicated by hydrochemical analysis demonstrates close agreement between these flow paths, with the flow paths derived from hydrochemical analysis generally enveloping those predicted by the base-case model. Thermal modeling indicates that the thermal model developed from the base-case model is capable of modeling thermal transport in the saturated zone reasonably well (Section 2.3.7).

Response to USFIC 5.11—To investigate the importance of Solitario Canyon Fault depth, an alternative conceptualization was simulated in which the fault extends from the water table only to the top of the Carbonate Aquifer. This alternative is referred to as the Shallow Fault Alternative model and was identical to the saturated zone site-scale flow model in all other respects except for the Solitario Canyon Fault properties. The alternative resulted only in changes to the computation grid that were necessary to implement this alternate formulation of the fault. The alternative model was calibrated in a manner identical to that previously used to calibrate the base-case saturated zone flow model.

A comparison of the results of the simulations with the two conceptualizations of the Solitario Canyon fault indicates that both simulations produce essentially the same results. Both conceptualizations of the Solitario Canyon fault yield the same flow paths from the water table underneath the proposed repository to the accessible environment. The results of this investigation indicate that simulated water levels, hydraulic gradients, and transport pathways are not significantly affected by this alternative conceptualization of the Solitario Canyon fault. The small differences between the permeabilities and flow paths of the two models indicate that travel times will not be affected by Solitario Canyon fault depth. The influence of reducing the depth of the Solitario Canyon fault on total system performance is expected to be minor. An alternative conceptualization of the Solitario Canyon fault extending only from the water table to the top of the carbonate aquifer resulted in no significant changes to the flow system and thus will have no consequences for transport.

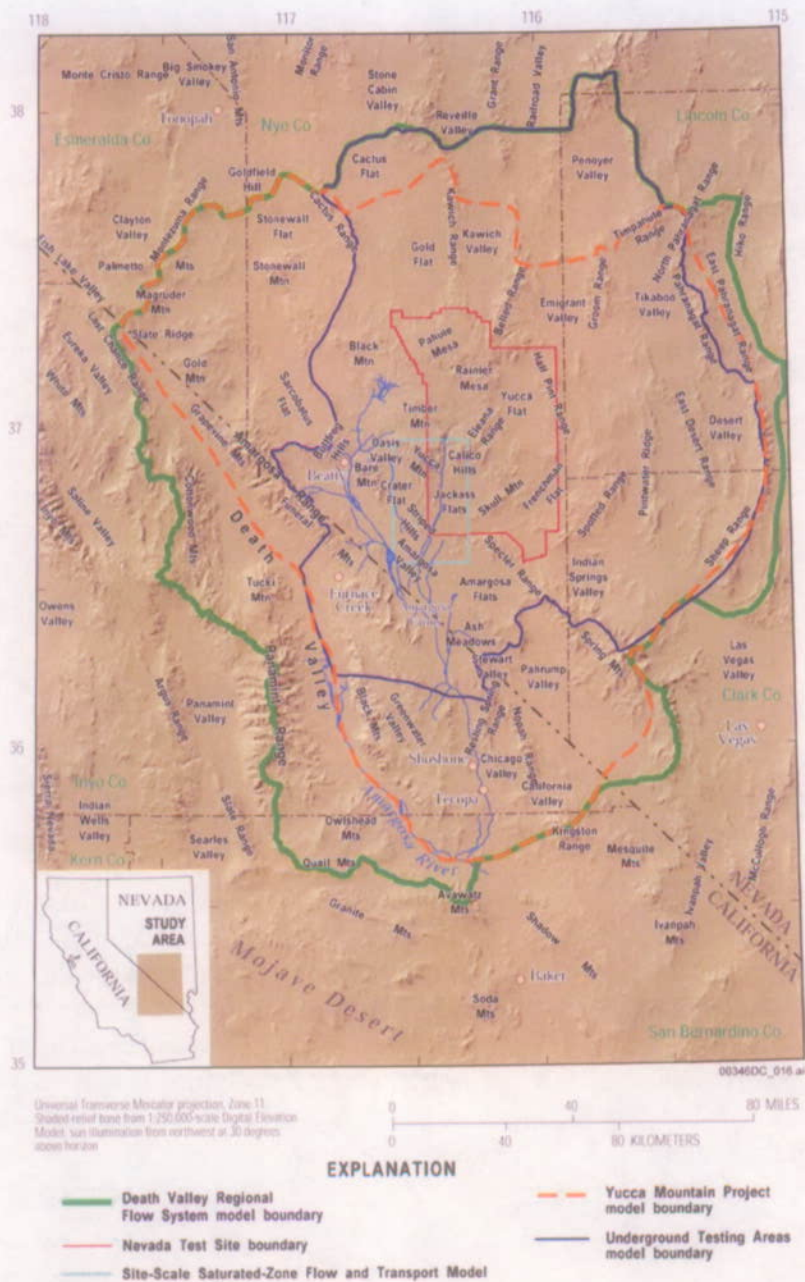
Based on current design, the repository is located east of the Solitario Canyon Fault. The study of the potential radionuclide flow paths in the unsaturated zone indicates a negligible number of particles arrive to the west of the Solitario Canyon at the water table within the 10,000 year regulatory period. Therefore, alternative conceptualizations of the Solitario Canyon Fault have little impact on transport in the saturated zone.

D.4 BASIS FOR THE RESPONSE

D.4.1 Use of the Regional Model and Update to the Site-Scale Model (USFIC 5.02)

D.4.1.1 Regional Model

The DVRFS is a large model developed by the USGS that covers about 70,000 km² and includes natural groundwater divides and discharge areas. The Yucca Mountain site-scale flow and transport model comprises a small portion (two percent) of the area of the larger model. The relationship of the two models is shown in Figure D-1. The DVRFS model was developed and documented by D'Agnese et al. (1997). The *Technical Basis Document No. 11: Saturated Zone Flow and Transport*, Section 2.2.3, describes the regional model and its use in conceptual understanding relevant to modeling and assessing the flow and transport of potential radionuclides in the saturated zone beneath and downgradient from Yucca Mountain.



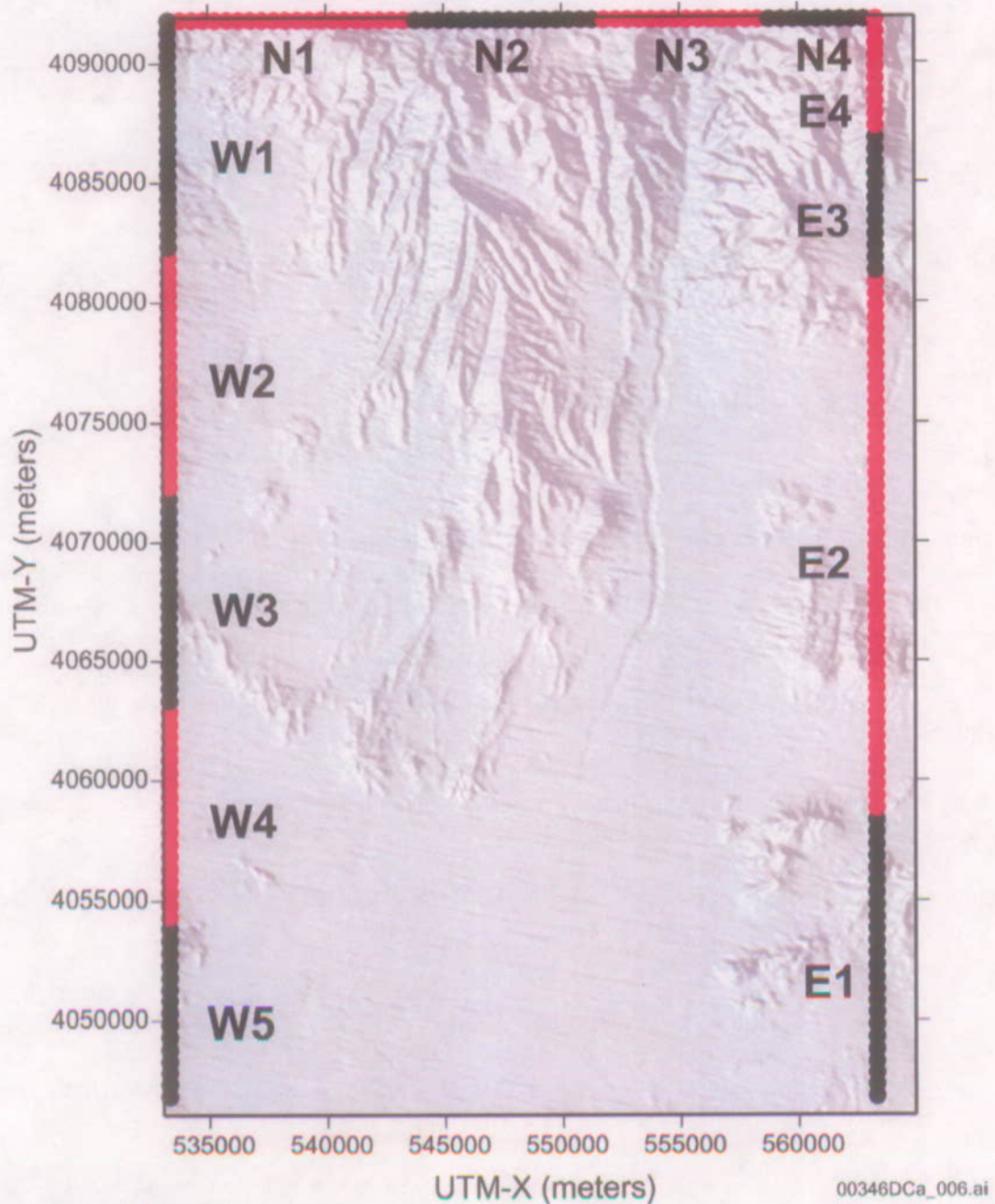
Source: Belcher et al. 2002, Figure 1.

NOTE: The different model boundaries reflect different regional model studies that are discussed and referenced in the source.

Figure D-1. Major Physiographic Features in the Death Valley Regional Flow System

Because the size of the system covers the entire basin and the model incorporates the discharge zones and groundwater divides, the fluxes in the regional model can be predicted with sufficient accuracy. Therefore, the fluxes from the regional model would be useful to constrain flow at the site-scale, as the site-scale model does not have discharge areas and uses fixed-head boundary conditions. Consequently, the 1997 regional model has been used to identify fluxes along the

boundaries of the site-scale flow model. These boundary fluxes have been used as targets during calibration of the site-scale flow model. Fluxes derived from the regional model were subdivided along each boundary of the site-scale model (Figure D-2). The flux targets and site-scale flow and transport model results are shown in Table D-1. Table D-1 also identifies which flux segments were used as a calibration target for the site-scale model. Figure D-2 identifies the segments of the north, east, and west lateral boundaries listed in Table D-1.



Source: BSC 2001, Figure 16.

Figure D-2. Flux Zones Used for Comparing Regional and Site-Scale Fluxes

Table D-1. Comparison of Regional and Site-Scale Fluxes

Boundary Zone	Regional Flux (kg/s)	Site-Scale Flux (kg/s)	Calibration Target
N1	-101	-60.0	Yes
N2	-16.5	-33.4	Yes
N3	-53.0	-30.6	Yes
N4	-18.4	-44.8	Yes
W1	3.45	4.17	No
W2	-71	-0.00719	No
W3	-6.9	-0.000078	No
W4	2.73	-0.000223	No
W5	-47.0	-6.85	No
E1	-555	-554	Yes
E2	-5.46	3.53	Yes
E3	2.65	16.5	Yes
E4	-3.07	16.8	Yes
S	918	724	No

Source: BSC 2003a, Table 15.

NOTES: A negative value indicates flow into the model.
 Information in the last column indicates whether the regional-mix flux for a zone was used as a calibration target for the site-scale model.
 Some numbers in this table were rounded to three significant figures compared to those reported in the source document.

A comparison of the fluxes on the northern and eastern boundaries indicates a reasonable match between the fluxes from the regional and site-scale models (Table D-1) within the uncertainty range of the specific discharge (10 times and divide by 10 the value predicted by the model). The northern boundary, for example, has a total flux of 189 kg/s in the regional model and 169 kg/s in the saturated zone calibrated model. However, the distribution is somewhat different. The match was good on the east side of the model within the lower thrust area (E1). The other zones showed small flows in both models. Because the western boundary fluxes were not used as a calibration target, the match between the two models was not as good on the western boundary. The southern boundary flux, which is simply a sum of the other boundary fluxes plus the recharge, is also a good match.

A number of factors affect the applicability of the 1997 DVRFS model results to the site-scale flow model analyses, including:

- The 1997 DVRFS model uses an older hydrologic model than the one used during the development of the site-scale flow model.
- The horizontal resolution of the site-scale model is three times finer than the 1997 DVRFS model (500-m versus 1500-m gridblock size).
- The 1997 DVRFS has three vertical layers, while the site-scale model has 38 vertical layers.

- The 1997 DVRFS model used the concept of hydraulic conductivity classes and did not explicitly relate these classes to permeabilities in boundary fluxes predicted by the regional and site-scale models.
- Prediction residuals and unquantified uncertainties in the regional model. That model does not exactly reproduce observed heads (especially in the site-model area), as well as errors in reproducing discharges at springs and evapotranspiration areas.
- Prediction residuals in the site model.
- The updated regional model is calibrated to predevelopment conditions (no pumping in the Amargosa), while the previous model and the site model are for more recent (1990s/present) conditions.

These differences help to explain differences in boundary fluxes predicted by the regional and site-scale models.

Since 1997, the DVRFS model has been updated and improved, including an increased resolution in the vertical dimension, with the number of vertical layers increasing from 3 in the 1997 model to 15 in the 2002 updated DVRFS model. In addition, the 1997 DVRFS model used a concept of permeability classes, while nodal values of permeability are assigned in the updated DVRFS model. The 2002 updated DVRFS is also based on an updated and improved hydrogeologic framework model. These and other enhancements to the updated DVRFS model (D'Agnese et al. 2002) will make it easier to compare estimates of fluxes along the boundary of the site-scale flow model. A comparison of fluxes along the boundaries of the site-scale model predicted by the 1997 and updated DVRFS model is presented in Table D-2.

Table D-2. Comparison of the Site-Scale Flow Model Boundary Fluxes Predicted by 1997 and Updated DVRFS Models.

Base-Case Model (extracted from the 1997 DVRFS model ^a)			Alternate Model (extracted from the 2002 DVRFS ^b model)		
West Boundary					
From (m)	To (m)	Flux (kg/s)	From (m)	To (m)	Flux (kg/s)
4,046,780	4,054,280	3.45	4,046,500	4,052,500	210.45
4,054,280	4,063,280	-71.00	4,052,500	4,057,000	-0.08
4,063,280	4,072,280	-6.90	4,057,000	4,067,500	-56.12
4,072,280	4,082,780	2.73	4,067,500	4,085,500	-1.31
4,082,780	4,091,780	-46.99	4,085,500	4,091,500	-28.43
Sum		-118.71	Sum		124.51
East Boundary					
From (m)	To (m)	Flux (kg/s)	From (m)	To (m)	Flux (kg/s)
4,046,780	4,058,780	-555.45	4,046,500	4,054,000	-69.71
4,058,780	4,081,280	-5.46	4,054,000	4,058,500	0.01
4,081,280	4,087,280	2.65	4,058,500	4,078,000	-138.06
4,087,280	4,091,780	-3.07	4,078,000	4,084,000	0.09
			4,084,000	4,091,500	-1.53
Sum		-561.33	Sum		-209.21

Table D-2. Comparison of the Site-Scale Flow Model Boundary Fluxes Predicted by 1997 and Updated DVRFS Models (Continued)

Base-Case Model (extracted from the 1997 DVRFS model ^a)			Alternate Model (extracted from the 2002 DVRFS ^b model)		
North Boundary					
From (m)	To (m)	Flux (kg/s)	From (m)	To (m)	Flux (kg/s)
533,340	543,840	-101.24	533,000	545,000	-219.47
543,840	551,840	-16.48	545,000	552,500	-57.07
551,840	558,840	-63.39	552,500	558,500	6.90
558,840	563,340	-18.41	558,500	563,000	-1.39
Sum		-199.52	Sum		-271.03
South Boundary					
From (m)	To (m)	Flux (kg/s)	From (m)	To (m)	Flux (kg/s)
533,340	563,340	918.00	533,000	563,000	430.02
Total Fluxes (kg/s)					
Sum		38.44	Sum		74.30

Source: BSC 2003a, Table 7.5-5.

NOTE: ^aDVRFS base-case model (D'Agnese et al. 1997).

^bDVRFS alternate model is (D'Agnese et al. 2002).

The boundary flux targets have changed from the base-case to the alternate model (Table D-2). The biggest differences occur on the east and west sides of the site-scale flow model. In particular, the thrust zone in the southeastern corner of the model was removed from the most recent DVRFS model (D'Agnese et al. 2002). As a result, the flux target decreased from -555.45 kg/s to -69.71 kg/s in the southern-most zone on the eastern boundary. Overall, flow out of the southern boundary in the alternate model is approximately one-half of that (430/918) used in the base-case model. The large differences in the flux targets can be traced to the evolution of the DVRFS model.

Despite improvements in the DVRFS model, challenges to the applicability to the site-scale flow model remain:

- The updated DVRFS model (D'Agnese et al. 2002) has more vertical layers than the 1997 model (15 versus 3), but it still has fewer than the site-scale model, which uses 38 layers.
- The updated DVRFS model is based on a different HFM than the current site-scale model.
- The updated DVRFS model uses the hydraulic unit flow package in MODFLOW 2000 (Harbaugh et al. 2000) to calculate cell permeabilities in the coordinate directions. The hydraulic unit flow package limits the use of permeability information and, hence, fluxes on a unit by unit basis.

Current modeling efforts, including the analysis of a number of alternate conceptual models, reveal a pervasive upward gradient from the carbonate aquifer to the overlying volcanic aquifer. Graphical analysis of simulations of fluid particles leaving the repository region confirms that no

particle enters the carbonate aquifer. Recent Nye County borehole data also support this finding (USGS 2001a). This evidence, in turn, supports the theory that the local volcanic aquifers near Yucca Mountain (which as depicted in the site-scale model, are the ones expected to transport potential released radionuclides), are independent of the regional aquifer and, thus, little influenced by flux uncertainties in the regional model. Farther south along the predicted transport path lines, according to the site-scale model, fluid close to the water table transitions from volcanic aquifers to alluvium. In this area, model results indicate stronger influence of lateral boundary fluxes. The influence of boundary fluxes (and therefore the regional model) on site-scale flow and transport depends on the position of the path lines and how much alluvial material they encounter.

In addition to providing estimates of boundary fluxes for the site-scale model, the updated DVFRS model (D'Agnese et al. 2002) allows for the comparison of calibrated permeabilities between the two models and the analysis of the sensitivity to permeability of fluxes in both the regional and site-scale models. The ability of the updated DVFRS model to provide information on fluxes on a unit-by-unit basis should provide further insight on the role of regional fluxes in determining the flow pathways from the repository.

D.4.1.2 Development of an Alternate Model

The understanding of the site-scale flow system continues to evolve as new information becomes available. These additional data and analyses include additional water-level data, a reinterpreted HFM, revised recharge distribution, updated boundary fluxes, additional permeability data, and further evaluation of alternative conceptual models. To evaluate the effects of additional knowledge on modeling the site-scale flow system, a model update has been formulated and is being calibrated for the purpose of validating the site-scale base case flow model (BSC 2003a). Until the model is completely calibrated, the comparison of the model update to the site-scale base case model is limited to comparison of the hydrogeology, boundary flux targets, and model construction and formulation. Flow-field and flow-path predictions will be completed when calibration of the model update is completed.

The mathematical formulation used in the model update is identical to that used in the base-case site-scale model. The FEHM code (Zyvoloski et al. 1997) used in the site-scale model to obtain a numerical solution to the mathematical equation describing groundwater flow is also used in the model update. However, inputs for the model update have been revised to reflect the most recent data and analyses currently available for formulating the site-scale model.

The computational grid used in the model update has been modified from that used in the site-scale model. The 500-m grid in the site-scale model was retained in the model update. However, the grid was offset slightly in the north-south direction and expanded by 500 m in the east-west direction, resulting in a slightly larger model domain. The grid for the model update was expanded from the water table to the ground surface, although nodes above the water table are not computationally active. A confined aquifer solution using the water-table elevation to define the top of the flow system continues to be implemented as it was in the site-scale model. The depth of the model update has been extended to match the depth of the HFM, which was increased primarily to include more of the regional carbonate aquifer. The vertical grid spacing of the model update is equivalent to that of the base-case site-scale model.

Since the development of the HFM used in the base-case site-scale model, the Yucca Mountain HFM has been reinterpreted with data recently obtained from the Nye County EWDP and through the reinterpretation of existing data from other areas, including geophysical data in the northern area of the site (USGS 2001b). The major changes in the southern part of the model are the depths and extent of the alluvial layers. The HFM for the northern part of the model domain was changed substantially. This is largely the result of reinterpretation of geophysical data regarding the depth of the carbonate aquifer. As a result, the shape and extent of the carbonate aquifer has changed substantially. In particular, the carbonate aquifer no longer is believed to intersect the northern boundary of the site-scale model. As a result of the re-interpretation of the HFM, the number and distribution of hydrogeologic units was modified in the HFM that is used in the model update. While there were 19 hydrogeologic units in the original HFM, there are 27 hydrogeologic units in the revised HFM.

The changes in the revised HFM resulted in notable differences between the original and revised HFM in the hydrogeology at the water table in the area of Nye County and along the anticipated flow path from the repository. The important changes occurred in the hydrogeologic units at the water table in the southern part of the model where the Volcanic and Sedimentary units replace the Valley-fill Aquifer as the most pervasive unit in the alternate HFM. The revised HFM has new zones inserted into lower Fortymile Wash to correct for known deficiencies in the earlier HFM. The northern-most zone, the alluvial uncertainty zone, represents a transition from the volcanic to the alluvial aquifer system. It replaces the older HFM because, based on logs from borehole NC-EWDP-19-D, the alluvial aquifer extended farther north than what is presented in the earlier HFM. The permeability associated with this zone is a calibration parameter and, thus, can represent either aquifer system. A second zone, the Lower Fortymile Wash zone, was inserted to achieve a good calibration in the site-scale model. It represents a distinct subset of the alluvial aquifer that is characterized by the higher proportion of gravels in the lower-most portion of Fortymile Wash. The Calico Hills Volcanic unit has replaced the Upper Volcanic Confining Unit in the HFM revision. In the model update, however, there is no longer any of this Calico Hills material separating the upper and lower portions of the Fortymile Wash. Further north, the Paintbrush Volcanic Aquifer replaces the Upper Volcanic Aquifer as the dominant unit, at least near the water table. The Yucca Mountain block remains composed of the Crater Flat Group: Prow Pass, Bullfrog, and Tram units. The Crater Flat units are more continuous to the north and west of Yucca Mountain in the HFM revision than in the earlier HFM. Because the Crater Flat Group has relatively high permeability, the new representation provides a high permeability path at the water table to Yucca Mountain that was not present in the earlier model.

Development of the HFM revision was influenced primarily by data from the new Nye County boreholes. The most pronounced difference in the two models based on these new data is the relative abundance of the Crater Flat Group to the west of Yucca Mountain in the HFM revision. The Crater Flat Group represents relatively high permeability rock. However, the flow paths of fluid particles leaving the repository area are likely to be to the east of Yucca Mountain. Thus, this change in the HFM may not greatly influence the ability of the updated model to replicate flow paths predicted by the site-scale model. The Crater Flat Group is more continuous on the east side of Yucca Mountain, possibly influencing the calibration and specific discharge predictions of the model update.

Based on the flow paths previously predicted by the site-scale model, the differences in the two HFMs along the expected flow paths from the repository can be identified. Flow near the repository area in the model update is expected to be similar to that in the base-case site-scale model because the HFM changes were small in this region. However, the recharge in the model update is considerably larger than the recharge in the base-case site-scale model; and therefore the specific discharge is expected to increase in the model update. Flow in the Upper Fortymile Wash, in the area also known as the low-gradient area, might change because the character of the Bullfrog unit is different in the two HFMs. The model update is thinner and more continuous. Flow in the Lower Fortymile Wash is expected to be different. The correction in the extent of the alluvial aquifer is the major difference. The alluvial uncertainty zone included in the site-scale model, however, has mitigated this difference.

Seventeen hydrogeologic features were incorporated into the site-scale flow model (BSC 2003a, Section 6.5.3.4). These features were modified in the model update, largely due to changes necessary to incorporate an alternate conceptual model for the large hydraulic gradient area north of Yucca Mountain. The alternative conceptualization, referred to as the Altered Width Fault/Ghost Dance Fault conceptualization of the large hydraulic gradient area, was used in the model update. This conceptualization does not make use of the extensive feature set north of Yucca Mountain. This was removed from the model grid, thereby simplifying the grid in the model update. Instead, the hydrogeologic units have been divided into northern and southern zones at the Claim Canyon Caldera boundary to represent a zone of hydrothermal alteration in the area of the caldera. Differing permeabilities can be assigned in each zone to each hydrogeologic unit. In addition, a zone has been added to represent the northwest-southeast trending fault zone just north of Yucca Mountain, and features have been added to account for the Ghost Dance fault and the Dune Wash fault. Although there are fewer discrete features in the model update than in the site-scale model, there are more calibration parameters because the hydrogeologic units are divided into independent northern and southern zones. Also, the alluvial uncertainty zone was removed from the model update.

Boundary conditions were established in the model update in the same manner as in the base-case site-scale model. However, the constant head boundaries around the periphery of the model at each boundary node are based on the updated 2001 potentiometric surface (USGS 2001a).

Recharge is applied to the top surface of the computational grid as a flux boundary condition in the model update in an identical manner to the site-scale model. However, an updated recharge distribution was used in the model update. The update recharge distributions result in 40 percent more recharge to the model update (BSC 2003a).

The model update is calibrated in a manner similar to the site-scale model. The same automated procedure is used during calibration to adjust calibration parameters, and manual adjustments were used when necessary to calibrate the model update. Water levels and boundary fluxes were used as calibration targets during the calibration of the model update. However, the water levels used as calibration targets during the base-case site-scale model calibration were augmented by new water-level data from boreholes recently installed as part of the Nye County EWDP. Twenty-six water-level measurements are now available from the Nye County EWDP.

boreholes, bringing the number of water-level measurements used as targets during the calibration of the model update to 130.

Boundary fluxes used during calibration of the base-case site-scale model were derived from the 1997 DVRFS model (D'Agnese et al. 1997). However, since 1997, the DVRFS model has been updated and improved, including increasing the resolution in the vertical dimension from 3 to 15 layers. In addition, the 1997 DVFRS model used a concept of permeability classes, while nodal values of permeability are assigned in the updated DVRFS model. Due to these and other enhancements, the updated DVRFS model (D'Agnese et al. 2002) offers improved discretization to obtain estimates of fluxes along the boundary of the site-scale flow model and has been used to establish boundary flux targets for the model update. Although the resulting boundary flux targets have changed, with the biggest change along the southern boundary (about 490 kg/s vs. about 240 kg/s on west and about 350 kg/s on east). Part of the reason for the reduction in flux across the southern boundary is probably due to the lack of pumping in the predevelopment conditions simulated in the revised regional model. The impact on flow and transport is expected to be small because of the small transmissivities of the shallow volcanic aquifers that control flow and transport in the saturated zone beneath Yucca Mountain as compared to that of the underlying regional aquifers.

In an approach similar to that employed in the base-case site-scale model, permeability was optimized during calibration of the model update. Permeability zones were created for hydrogeologic units identified in the HFM and for specific hydrogeologic features established in the model. In the base-case site-scale model, a permeability zone was established for each hydrogeologic unit, with the exception of the basal unit that served as a lower boundary for the model. In the model update, a second permeability zone was created for each hydrogeologic unit in the Claim Canyon Caldera to allow for modifying unit permeabilities in this area. This modification was necessary to implement the alternative conceptual model used to simulate the large hydraulic gradient area in the north of the model domain. As in the base-case site-scale model, upper and lower bounds were placed on each permeability variable during parameter optimization, but these bounds were updated based on permeability data available since calibration of the base-case site-scale model. In a manner similar to the base-case site-scale model, vertical anisotropy was assigned a value of 10:1 (horizontal to vertical) in the volcanic and valley-fill units in the model update.

Based on the updated and improved HFM, more consistent flux targets from the DVRFS model, and additional calibration targets from the Nye County EWDP, the alternate model more accurately represents the saturated flow system near Yucca Mountain. The results indicate that the important parameters in the site-scale model are the most sensitive parameters in the model update. Target values and spatial variability for fluxes are important in the model update. Probable flow paths, considering the HFM, are similar in both models. Based on these studies the alternate model validates the base-case site-scale flow model.

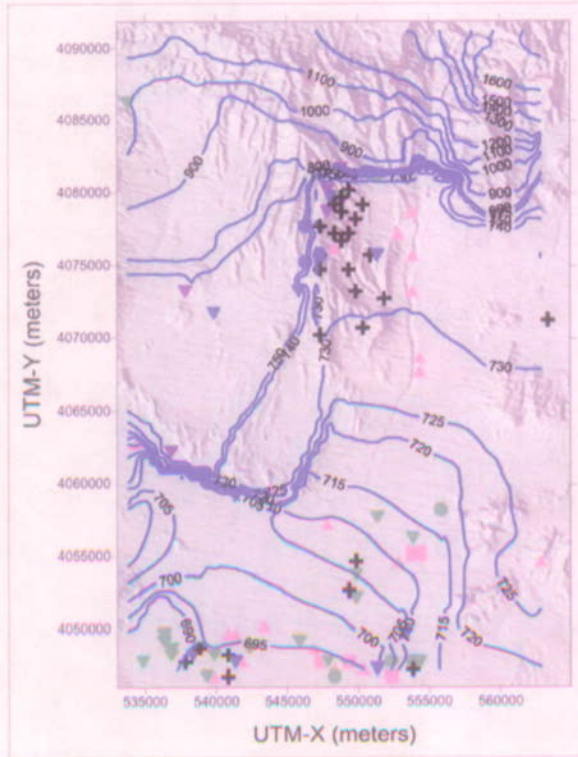
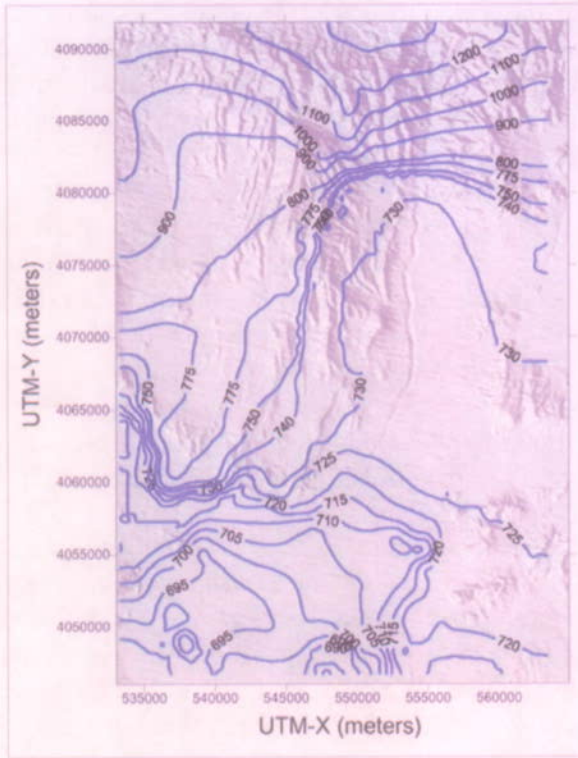
D.4.2 Site-Scale Model Confidence Building Activities (USFIC 5.12)

The saturated zone site-scale flow and transport model is designed to provide an analysis tool that facilitates understanding of solute transport in the aquifer beneath and down gradient from the repository. It is also a computational tool for performing potential radionuclide migration

predictions in the saturated zone. For these predictions to be credible, it must be demonstrated that the saturated zone flow and transport model has been validated for its intended use. This statement means that there is established "confidence that a mathematical model and its underlying conceptual model adequately represents with sufficient accuracy the phenomenon, process, or system in question" (AP-SIII.10Q, *Models*, Section 3.14). Confidence building activities for the saturated zone flow and transport model included pre-development and post-development activities. Pre-development activities consisted of using field and laboratory testing: to identify pertinent processes and to derive model parameters, using established mathematical formulations to describe pertinent processes, and using calibration processes to estimate hydraulic parameters for best fit of field data. Post-development confidence building activities involved comparison of observed and predicted water levels, comparison of permeability data to calibrated permeability values, comparison of hydrochemical data trends with calculated particle pathways, thermal modeling, and comparison of the predicted groundwater velocity to velocity estimates from ATC single-borehole tracer test.

Water Levels—The adequacy of the model can be assessed by its ability to accurately predict observed water levels and its ability to reproduce the observed potentiometric surface. The model is calibrated through an optimization process that seeks to minimize differences between observed and predicted water levels at each target location by adjusting model permeability parameters. Observed and predicted water levels at each target water-level location are presented in *Site-Scale Saturated Zone Flow Model* (BSC 2003a, Table 6.6-1).

A comparison of the predicted and observed potentiometric surface as well as the residual water levels (i.e., the difference between the predicted and observed) at each of the target water-level locations are presented in Figure D-3. The average, unweighted residual over the entire model domain is 30 m. However, as shown on Figure D-3, larger residuals are distributed unevenly throughout the domain. The largest residuals (about 100 m) are in the northern part of the model domain in the high-gradient area. These head values are largely the result of the low weighting factor applied during calibration and the uncertainty in these measurements, possibly due to perched conditions. The next highest group of heads borders the East-West barrier and Solitario Canyon fault. These residuals (about 50 m) likely result from the inability of the 500-m grid blocks to resolve the 780-m to 730-m drop in head in the short distance just east of these features. Figure D-3 also shows that residuals east and south east of the repository in Fortymile Wash area generally are small. This is the expected flow path from the repository, and the generally good agreement between predicted and observed water levels in this area provides confidence that the calibrated flow model reliability simulates flow from the repository.



Source: BSC 2003a, Figure 6.6-2.

Figure D-3. Contour Plot of Water-Level Data (left panel) and Simulated Water-Level Data with Residual Heads (right panel)

Comparison of the predicted and observed potentiometric surface also indicates that the two potentiometric surfaces are similar. When comparing the two, it should be noted that both surfaces are contoured and that the data distribution for both surfaces is not uniform. Evident in the comparison is the low-gradient region in the Fortymile Wash region, the high-gradient region north of Yucca Mountain, and the flow disruption caused by the Solitario Canyon fault. These results indicate that the model, at least qualitatively, represents the current water table in the vicinity of Yucca Mountain.

Since the calibration of the site-scale flow model, a number of boreholes have been installed as part of the Nye County EWDP. These include boreholes installed at new locations and boreholes completed at depths different from those previously available at existing locations. Comparison of the water levels in the new Nye County EWDP boreholes with water levels predicted by the calibrated site-scale flow model at these new locations and depths offers an opportunity to validate the site-scale flow model using new data not available during calibration.

The site-scale flow model was calibrated using 115 water-level and head measurements from boreholes within the model domain. Eight of these measurements were from boreholes drilled and completed as part of the Nye County EWDP. With the addition of the new Nye County boreholes, the number of water-level observations available in the Nye County area has increased to 26. These boreholes are identified in Table D-3, and their locations are shown in Figure D-4. The calibrated flow model has been used to predict the water level at the location and depth of each of these additional measurements (Table D-1). It should be noted that water-level data from new completion intervals at previously existing borehole locations are now available and, for the purpose of this comparison, are replacing water levels previously available at this location in Table D-3. Although NC-EWDP-2D, NC-EWDP-3D, and NC-Washburn-1X were previously used as calibration targets, water levels from these boreholes also are included in Table D-3.

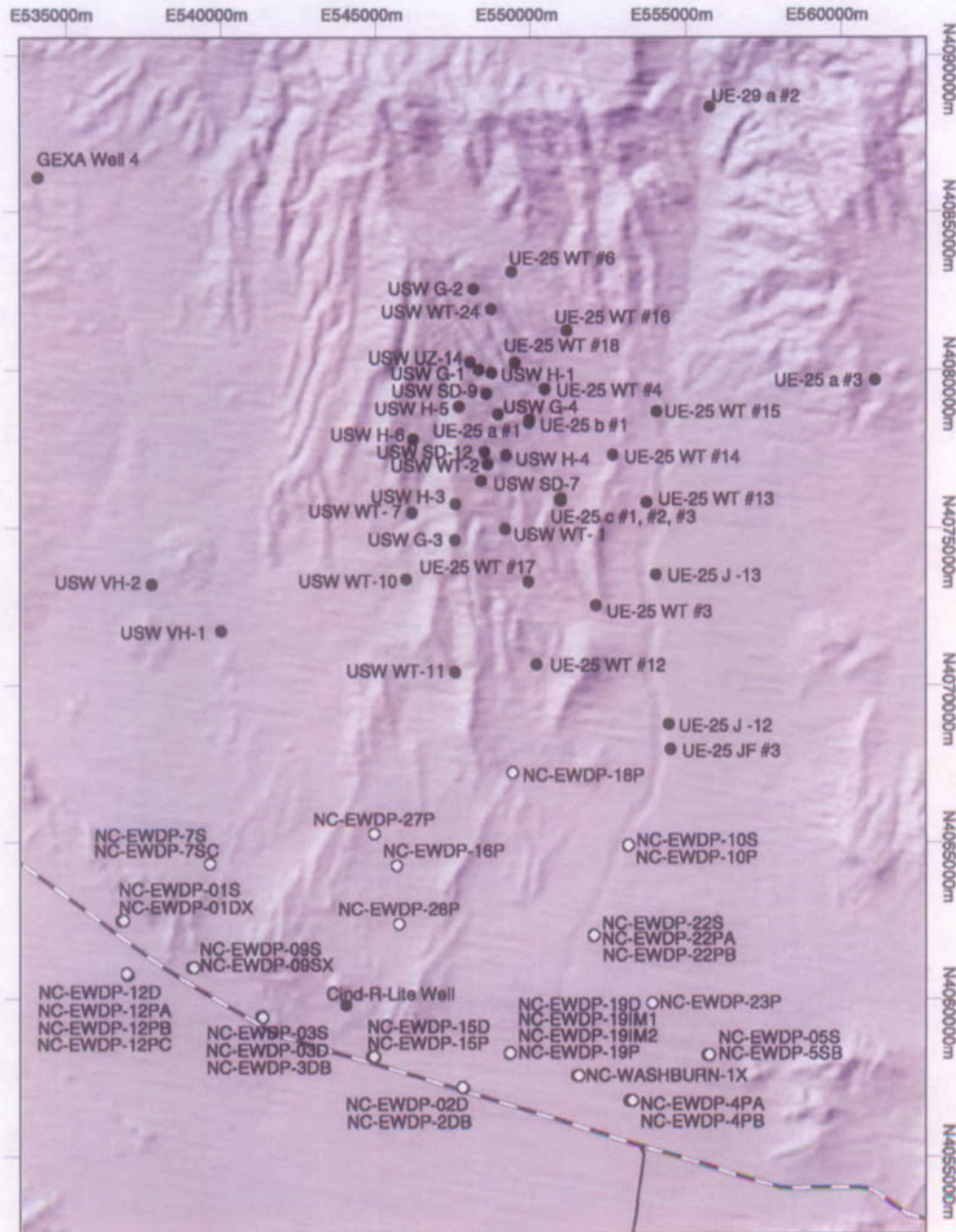
A comparison of the predicted and observed water levels (Table D-3) can be used to evaluate the calibrated flow model. Examination of the residuals (Table D-3) indicates that the errors in predicted water levels depend on the location within the site-scale model domain. The residuals generally are higher in the more western portion of the EWDP area. The gradients are steep in this area and the calibrated model is generally less capable of predicting these rapid water level changes. A more detailed discussion of the residuals observed in this area is available in *Site-Scale Saturated Zone Flow Model* (BSC 2003a, Section 7.1).

Table D-3. Comparison of Water Levels Observed and Predicted at Nye County EWDP Boreholes

Site Name	x (UTM) (m)	y (UTM) (m)	z (elevation) (m)	Observed Head (m)	Modeled Head (m)	Residual Difference (m)
NC-EWDP-1DX, deep	536768	4062502	585.7	748.8	762.7	13.9
NC-EWDP-1DX, shallow	536768	4062502	133.1	786.8	756.7	-30.1
NC-EWDP-1S, P1	536771	4062498	751.8	787.1	767.3	-19.8
NC-EWDP-1S, P2	536771	4062498	730.8	786.8	767.3	-19.5
NC-EWDP-2DB	547800	4057195	-77	713.7	717.0	4.3
NC-EWDP-2D	547744	4057164	-77	706.1	709.2	3.3
NC-EWDP-3D	541273	4059444	377.9	718.3	703.7	-14.6
NC-EWDP-3S, P2	541269	4059445	682.8	719.8	702.5	-17.3
NC-EWDP-3S, P3	541269	4059445	642.3	719.4	702.6	-16.8
NC-EWDP-5SB	555676	4058229	707.8	723.6	718.0	-6.6
NC-EWDP-9SX, P1	539039	4061004	765.3	766.7	731.7	-35.0
NC-EWDP-9SX, P2	539039	4061004	751.3	767.3	731.7	-35.6
NC-EWDP-9SX, P4	539039	4061004	694.8	766.8	731.7	-35.1
NC-Washburn-1X	551465	4057563	687.0	714.6	714.5	-0.1
NC-EWDP-4PA	553167	4056766	687.0	717.9	715.5	-2.4
NC-EWDP-4PB	553167	4056766	582.5	723.6	715.5	-8.1
NC-EWDP-7S	539638	4064323	826.6	818.1	769.6	-48.5
NC-EWDP-12PA	536951	4060814	666.7	722.9	705.3	-17.6
NC-EWDP-12PB	536951	4060814	666.7	723.0	705.3	-17.7
NC-EWDP-12PC	536951	4060814	713.7	720.7	704.3	-16.4
NC-EWDP-15P	544848	4058158	716.9	722.5	711.0	-11.5
NC-EWDP-19P	549329	4058292	694.7	707.5	713.2	5.7
NC-EWDP-19D	549317	4058270	549.7	712.8	713.2	0.4
NC-EWDP-16P	545648	4064247	723.8	730.9	711.0	-19.9
NC-EWDP-27P	544936	4065266	724.9	730.3	713.2	-17.1
NC-EWDP-28P	545723	4062372	719.2	729.7	713.2	-16.5

Source: Based on BSC 2003a, Table 7.1-2.

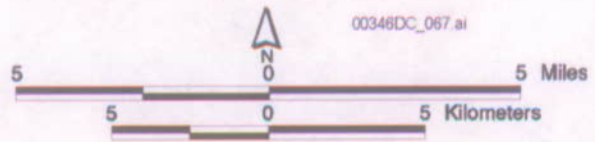
NOTE: z-elevation refers to the mid point of the open interval of an uncased well.



Legend

- Saturated Zone Borehole
- Nye County Early Warning Drilling Program Borehole

Map Projection: Universal Transverse Mercator, Zone 11



YMP-03-042_0

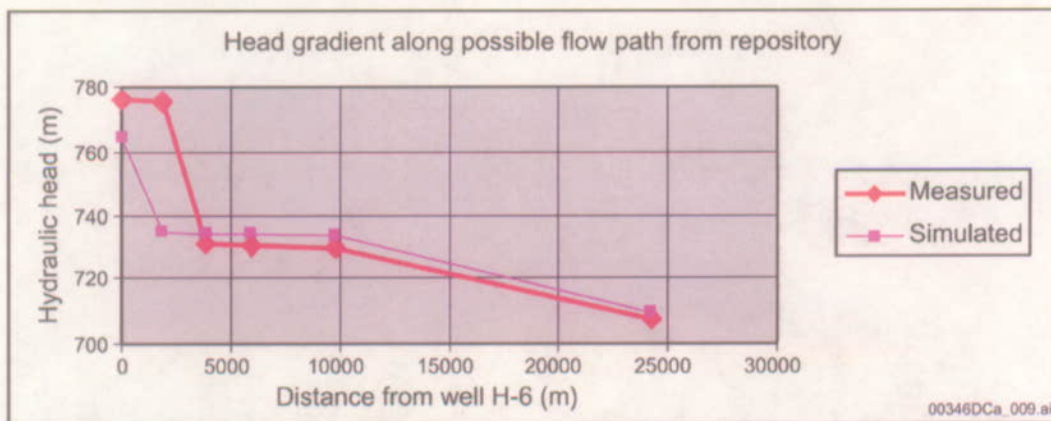
Source: CRWMS M&O 2000a, Figure 3-7.

Figure D-4. Location of Boreholes used to Characterize the Site-Scale Groundwater Flow System in the Vicinity of Yucca Mountain

The residuals tend to be smaller in boreholes located further to the east. Residuals at the NC-EWDP-3 borehole cluster range from -14.6 to -17.3 m. With an observed residual of -11.5 m at NC-EWDP-15P, the residuals decrease in borehole locations further east. At the NC-EWDP-19 cluster location (the Alluvial Testing Complex), the residuals improve further, with observed values of only +0.4 and +5.7 m. Residuals in this general area (NC-Washburn-1X, NC-EWDP-4, and NC-EWDP-5) are similarly low. These boreholes are in the predicted flow path from the repository. Thus, the additional water-level data confirm the capability of the site-scale flow model to predict water levels accurately in this portion of the flow path.

For validation and confidence building, a comparison of hydraulic gradients along the flow path from the repository observed through field data and predicted by the site-scale flow model has been performed. These gradients have a direct effect on the prediction of specific discharge along the flow path from the repository and can be used to determine the potential effect of model error on the calculation of specific discharge.

Water-level data from a series of six boreholes extending from near the repository to Nye County borehole NC-EWDP-19P are presented in Figure D-5. The predicted and observed hydraulic gradients between these boreholes are presented in Table D-4.



Source: BSC 2003a, Figure 7.1-2.

NOTE: Data results computed from Table 6.6-1.

Figure D-5. Measured and Simulated Head

Table D-4. Predicted and Observed Hydraulic Gradient for Identified Wells

Flow Segment	$\Delta H/\Delta L$ (Measured)	$\Delta H/\Delta L$ (Simulated)
H-6 to W-2	0.012	0.0078
WT-2 to WT-1	0.000095	0.00015
WT-1 to WT-3	0.00021	0.00021
WT-3 to 19P/2D	0.0015	0.0016

Source: BSC 2003a, Table 7.1-3.

NOTE: Data results computed from Table 6.6-1.

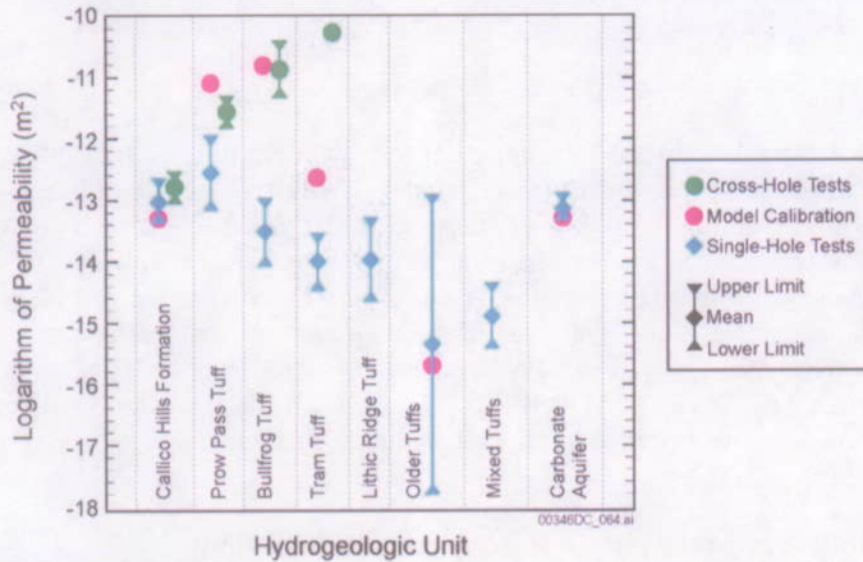
The observed and predicted gradients along the flow path are in good agreement, except in the very northernmost part of the flow path (Figure D-5, Table D-4). The discrepancies between boreholes USW H-6 and USW WT-2 are the result of the manner in which the model accounts for the effect of the splay of the Solitario Canyon Fault, which lies in the general area of these boreholes. However, while the model does not accurately predict the precise location for the drop in head across the fault, the overall drop in head predicted between USW H-6 and USW WT-2 agrees reasonably well with the observed water levels. With the exception of the segment between USW WT-2 and USW WT-1, in which the predicted gradient is 55 percent greater than the observed gradient, all the predicted gradients are within 50 percent of the observed gradient.

Comparison of Permeability Data to Calibrated Permeability Values—The site-scale flow model was calibrated by adjusting permeability values for individual hydrogeologic units in the model until the sum of the weighted-residuals squared (the objective function) was minimized. The residuals include the differences between the measured and simulated hydraulic heads and the differences between the groundwater fluxes simulated with the regional- and site-scale models. Permeabilities estimated from hydraulic tests were neither formally included in the calibration as prior information nor considered in the calculation of the objective function. Instead, field-derived permeabilities were used to guide the selection of bounds on the permissible range of permeabilities to be considered during calibration and to check on the reasonableness of the final permeability estimates produced by the calibration. Consequently, a comparison of the permeability data to calibrated permeability values can be used to provide confidence in the ability of calibrated model to adequately represent the Yucca Mountain saturated zone flow system. In addition, new permeability data are now available from the Alluvial Testing Complex that were not used in calibrating the site-scale flow model. Comparisons of these new measurements with calibrated permeability values provide a further opportunity to validate the model using new data.

Site-Scale Saturated Zone Flow Model (BSC 2003a, Section 7.2) provides a discussion of the data available to determine the permeability of individual hydrogeologic units in the saturated zone at Yucca Mountain. These data include permeability data from Yucca Mountain and the nearby Nevada Test Site. In addition general inferences about permeability can be drawn from regional observations.

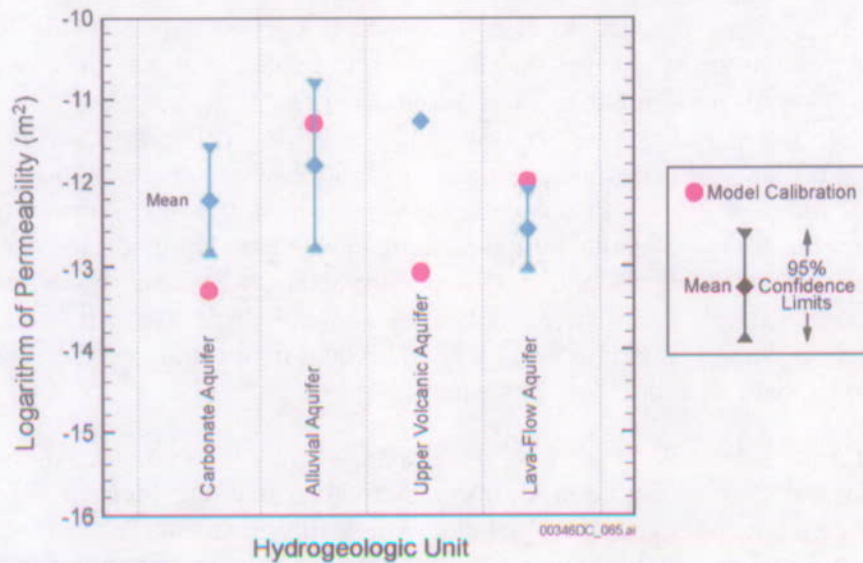
To check if the permeabilities estimated during the calibration of the site-scale model are representative of measured permeabilities, the logarithms of the calibrated permeabilities are compared to the mean logarithms of permeabilities estimated from pump-test data from Yucca

Mountain in Figure D-6 and to data from elsewhere at the Nevada Test Site in Figure D-7. Where they could be estimated, the 95-percent confidence limits for the mean logarithm of the permeability data also are shown in Figures D-6 and D-7. For the Calico Hills Formation, the Prow Pass Tuff, the Bullfrog Tuff, the Tram Tuff, and the MVA, permeabilities are shown for both the single-hole and for the cross-hole tests at the C-wells complex.



Source: BSC 2003a, Figure 7.2-1.

Figure D-6. Logarithms of Permeabilities Estimated during Model Calibration Compared to Mean Logarithms of Permeability Determined from Pump-Test Data from Yucca Mountain



Source: BSC 2003a, Figure 7.2-2.

Figure D-7. Logarithms of Permeabilities Estimated during Model Calibration Compared to Mean Logarithms of Permeability Determined from Pump-Test Data from the Nevada Test Site

As shown in Figure D-6, the calibrated permeability for the Calico Hills Formation, the Pre-Lithic Ridge Tuffs, and the Carbonate Aquifer are within the 95 percent confidence limits of the mean permeabilities estimated from single-hole pump test analyses at Yucca Mountain. The calibrated permeability for the Bullfrog Tuff is within the 95 percent confidence limits of the mean-measured permeability determined from the cross-hole tests. The calibrated permeability of the Prow Pass Tuff is slightly higher than the mean permeability estimated from the cross-hole tests, whereas the calibrated permeability of the Tram Tuff is between the mean permeabilities estimated for the unit from the single-hole and cross-hole tests (Figure D-6).

Overall, the calibrated permeabilities are consistent with most of the permeability data from Yucca Mountain and elsewhere at the Nevada Test Site, except for the Upper Volcanic Aquifer. The calibrated permeability of the Tram Tuff is lower than the mean permeability derived from the cross-hole tests but higher than the permeability estimated from the single-hole tests. The relatively high permeability estimated for the Tram Tuff from the cross-hole tests may be at least partially attributable to local conditions at the site of these tests. A breccia zone is present in the Tram Tuff at boreholes UE-25 c#2 and UE-25 c#3 (Geldon et al. 1997, Figure 3), which is a factor that may have caused a local enhancement in the permeability of the Tram Tuff.

The permeability data recently obtained from single-hole and cross-hole testing in the alluvial testing complex have not been included in Figure D-6. Single-borehole hydraulic testing of the saturated alluvium in borehole NC-EWDP-19D1 of the ATC was conducted between July 2000 and November 2000. During this testing, a single-borehole test of the alluvial aquifer to a depth of 247.5 m below land surface was initiated to determine the transmissivity and hydraulic conductivity of the entire alluvium system at the NC-EWDP-19D1 location. Analyses of these data resulted in a permeability measurement of $2.7 \times 10^{-13} \text{ m}^2$ for alluvial aquifer (BSC 2003a; Section 7.2.1.2). A cross-hole hydraulic test was also conducted at the ATC in January 2002. During this test, borehole NC-EWDP-19D1 was pumped in the open-alluvium section, while water level measurements were made in two adjacent boreholes. The intrinsic permeability measured in this test for the tested interval of alluvium is $2.7 \times 10^{-12} \text{ m}^2$. The calibrated permeability for the Alluvial Uncertainty Zone was $3.20 \times 10^{-12} \text{ m}^2$. Thus, the calibrated permeability for the Alluvial Uncertainty Zone was only 19 percent greater than the permeability value measured in the cross-hole test at the ATC. While the permeabilities reported from the single-hole tests for the alluvial materials are about an order of magnitude less than the calibrated value, the cross-hole tests yield a permeability measurement similar to the calibrated permeability values for the alluvial aquifer (BSC 2003b, Section 6.4).

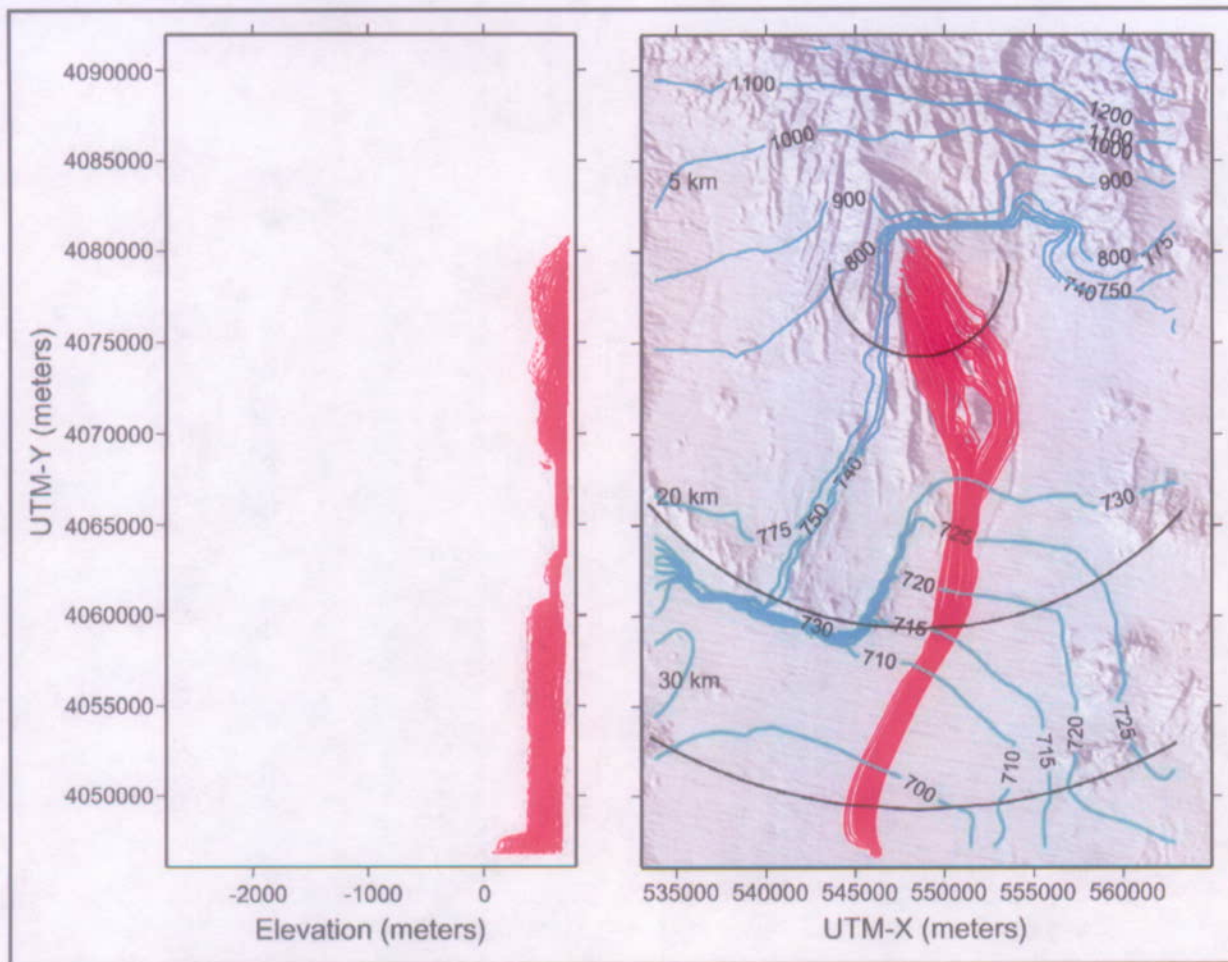
While the calibrated permeability of the many geologic units and features represented in the site-scale flow model may indirectly influence to a limited extent the specific discharge predicted by the site-scale model, the calibrated permeabilities of those geologic units along the flow path from the repository to the compliance boundary most directly determine the specific discharge predicted by the site-scale model. Particle tracking using the site scale flow model (BSC 2003a, Section 7.3) has indicated that fluid particles migrating from the repository generally travel downward until they reach the Crater Flat Bullfrog unit. Because of the high permeability of the Bullfrog unit, the particles remain in that unit until it ends. At this point, fluids particles generally enter the alluvial portion of the flow system after briefly transitioning the Upper Volcanic Confining Unit. The flow path through the alluvial deposits is represented in the site-scale flow model by the Alluvial Uncertainty Zone and the Lower Fortymile Wash Zone.

Thus, those calibrated permeabilities that most directly control the prediction of specific discharge by the site-scale flow model are those for the Bullfrog Unit and the Alluvial Uncertainty and Lower Fortymile Wash zones.

The calibrated value for the Bullfrog unit was $1.54 \times 10^{-11} \text{ m}^2$ (BSC 2003a, Table 6.6-2). The mean permeability for the cross-hole measurements of the Bullfrog unit at Yucca Mountain was $1.37 \times 10^{-11} \text{ m}^2$ (BSC 2003a, Table 6.8.1). Thus, the calibrated permeability for the Bullfrog unit was only 12 percent greater than the mean of the measured value for this unit. As previously discussed, the calibrated permeability for the Alluvial Uncertainty Zone was only 19 percent greater than the permeability value measured in the cross-hole test at the ATC.

Since both new water level data and permeability measurements are available at the ATC, predicted and observed values of both hydraulic gradient and permeability at this location can be used to calculate specific discharge. These calculated specific discharge values can then be compared to evaluate their combined impact on specific discharge for purposes of post-model development validation. As previously discussed in (the water level section above), the predicted hydraulic gradient between UE-25 WT#3 and NC-EWDP-19P/NC-EWDP-2D is only 7 percent greater than the observed gradient between these two locations (Table D-2). The calibrated permeability for the Alluvial Uncertainty Zone was 19 percent greater than the measured value at the ATC. Because the combined effect of the differences between predicted and observed values of these parameters on specific discharge is the product of their individual impacts, the calculated specific discharge based on predicted value of hydraulic gradient and the calibrated value of permeability is only 27 percent greater than is the value calculated using the respective observed values of these parameters. This independent validation of the site-scale flow model further enhances the confidence in the model's ability to predict the specific discharge along the flow path from the repository to the accessible environment.

Comparison of Hydrochemical Data Trends with Calculated Particle Pathways—A comparison of the flow paths identified using analysis of hydrochemical data with the flow paths predicted by the calibrated site-scale flow model provides a further opportunity to build confidence in and validate the site-scale flow model. Using its particle-tracking capabilities, the calibrated site-scale model has been used to identify predicted flow paths throughout the model domain. Figure D-8 shows the flow paths predicted by the model from the repository. Groundwater flow paths and mixing zones were also identified in the analyses of the areal distributions of measured and calculated geochemical and isotopic parameters, scatterplots, and inverse mixing and reaction models with PHREEQC (Parkhurst and Appelo 1999). The flow paths and mixing zones identified using this analysis of hydrochemical data are shown on Figure D-9. Additional discussion of the underlying analysis used to determine these flow paths and mixing zones is available in *Site-Scale Saturated Zone Flow Model* (BSC 2003a, Section 7.3).

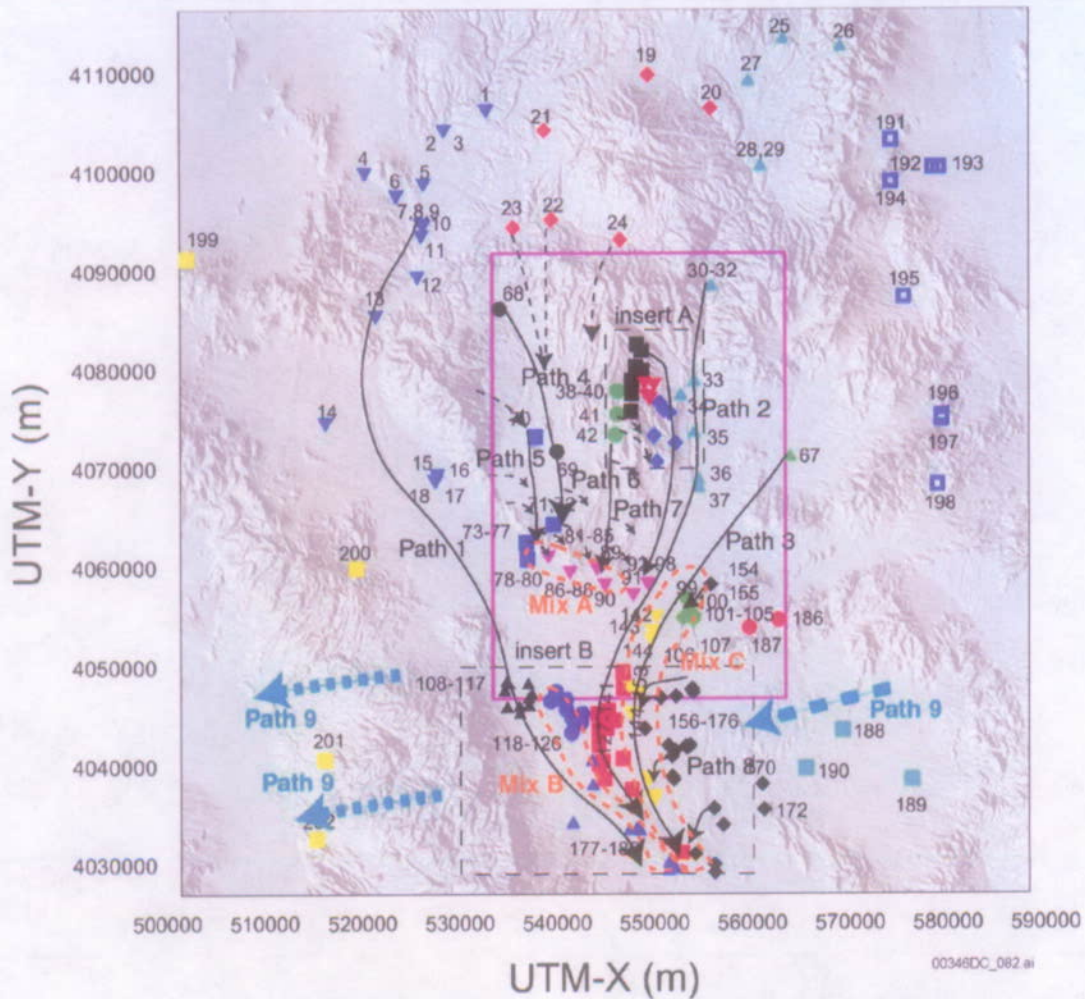


00346DCa_012.ai

Source: BSC 2003a, Figure 6.6-3.

NOTE: Blue lines refer to head contours; red lines refer to particles. Circles correspond to the 5-km boundary and the 18-km and 30-km compliance boundaries. The left panel is the north-south vertical plane; the right panel is the plan view.

Figure D-8. Flow Paths from the Proposed Repository with Simulated Hydraulic Head Contours



Source: BSC 2003c, Figure 62.

NOTE: The termination of flow paths implies that the flow paths could not be traced from geochemical information downgradient from these areas because of mixing or dilution by more actively flowing groundwater; flow path terminations do not imply that groundwater flow has stopped.

Figure D-9. Location of Geochemical Groundwater Types and Regional Flow Paths Inferred from Hydrochemical and Isotopic Data

A comparison of these flow paths indicates that the flow paths from the repository predicted by the site-scale flow model generally correspond well with those identified through geochemical analysis. The generally good agreement between the two sets of flow paths qualitatively supports the validation of the site-scale model, particularly in demonstrating the capability of the site-scale model to simulate flow paths accurately from the proposed repository to the compliance boundaries.

Thermal Modeling—Measurements of temperature in the saturated zone constitute an independent data set that was not used in the calibration of the saturated zone site-scale flow model and may, thus, be used in the validation of the flow model. The transport of heat in the geosphere occurs generally upward toward the Earth's surface, leading to higher temperatures with depth. However, heat is also redistributed by groundwater flow and can potentially serve as a tracer for the movement of groundwater in the saturated zone. To evaluate heat transport in the saturated zone, modeling of heat transport through conduction only and through conduction with convective transport was undertaken. A comparison of the heat distribution predicted by the conduction only model and the coupled conduction with convective transport model was then used to evaluate the site-scale saturated zone flow model.

The temperature data used in the thermal modeling are taken from temperature profiles measured in boreholes within the model domain. The temperature data were extracted at 200-m intervals from these temperature profiles and a total of 94 observations from 35 boreholes were obtained (BSC 2003a, Section 7.4.2).

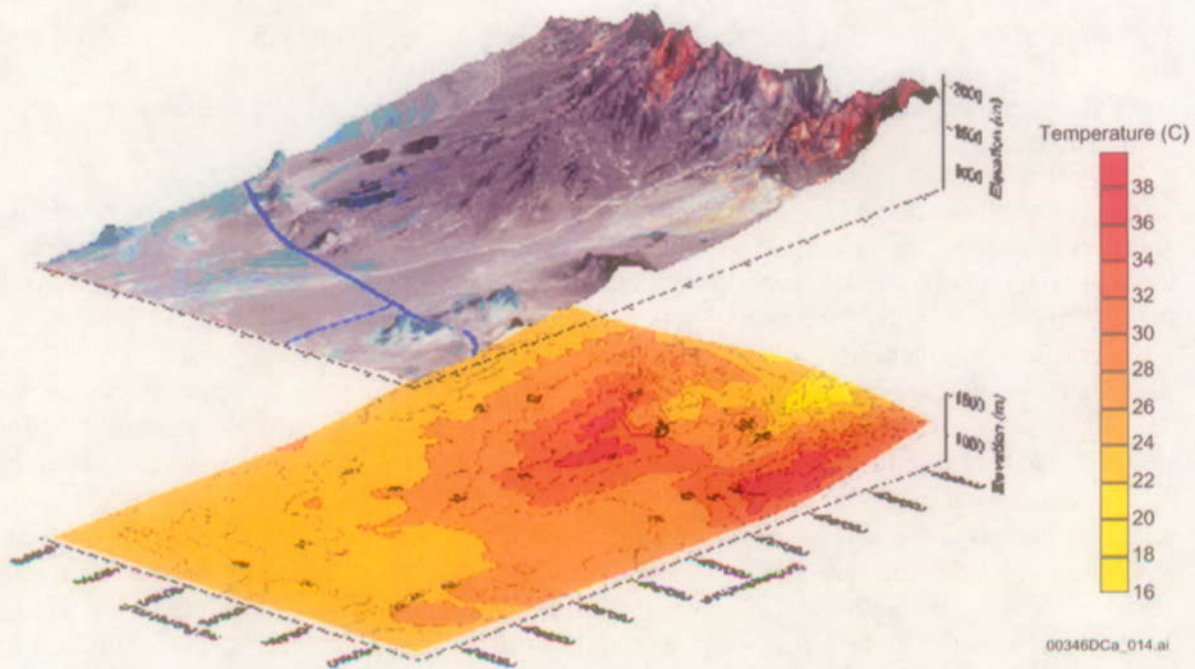
The site-scale flow model is used as the basis for the conduction only model. The model domain and definitions of the hydrogeologic units are retained from the site-scale model. Values of thermal conductivity are designated on a unit-by-unit basis. Values of thermal conductivity for the hydrogeologic units in the conduction-only model are taken from a variety of sources available from the literature. The lateral boundaries of the conduction-only model are set as no thermal flow. These boundary conditions represent the essentially vertical transport of heat in the subsurface. The upper boundary condition is specified as a temperature-dependent heat flux, in which the heat flux to the land surface is calculated as a function of the simulated temperature at the water table and the specified temperature at the land surface. The average annual temperature was computed based on the land surface elevation and varies by as much as 22°C over the model domain. A variable thermal conductance was established for the unsaturated zone to account for the variable thickness of the unsaturated zone. The bottom boundary is specified as heat flux to reflect upward heat transport from the deeper crust. A uniform heat flux was assumed, since insufficient information on variations in deep heat flow are available to justify establishing a spatially variable heat flux at the bottom of the model.

The conduction model was calibrated by adjusting the upper and lower thermal boundary conditions in a trial-and-error method. The model was run to steady-state thermal conditions and the simulated temperatures were compared to the observed temperatures in a cross plot. The calibration process sought to minimize the coefficient of determination (R^2) for this cross plot.

The best calibration of the conduction only model is obtained with a uniform heat flux of 35 mW/m² at the lower boundary and an equivalent thermal conductivity of 0.3 W/mK for the unsaturated zone at the upper boundary. The calibrated value of the heat flux at the lower

boundary of 35 mW/m^2 is somewhat lower than previously estimated by Sass et al. (1988), but is within the estimated range of error ($40 \pm 9 \text{ mW/m}^2$) from that study. The calibrated value of the equivalent thermal conductivity for the unsaturated zone is quite low relative to the units in the saturated zone. However, this equivalent value may also account for the effects of unsaturated conditions, variations in rock type, and percolation of groundwater.

The simulated temperatures at the water table in the calibrated conduction-only model are shown in Figure D-10. The values of simulated temperature are projected onto the water-table surface, and the topographic surface is shown in this figure. There is considerable variation in the simulated temperature at the water table, primarily as a function of the unsaturated zone. The higher simulated temperatures correspond to the relatively thick unsaturated zone under Yucca Mountain in the north-central portion of the area and under the Calico Hills in the northeastern part of the model. The lower simulated temperatures occur in areas where the water table is closer to the land surface, in the southern part of the model, and under Fortymile Canyon in the north. The pattern of simulated temperatures at the water table is influenced to a lesser extent by refraction of heat flow in the Lower Carbonate Aquifer with its higher thermal conductivity.

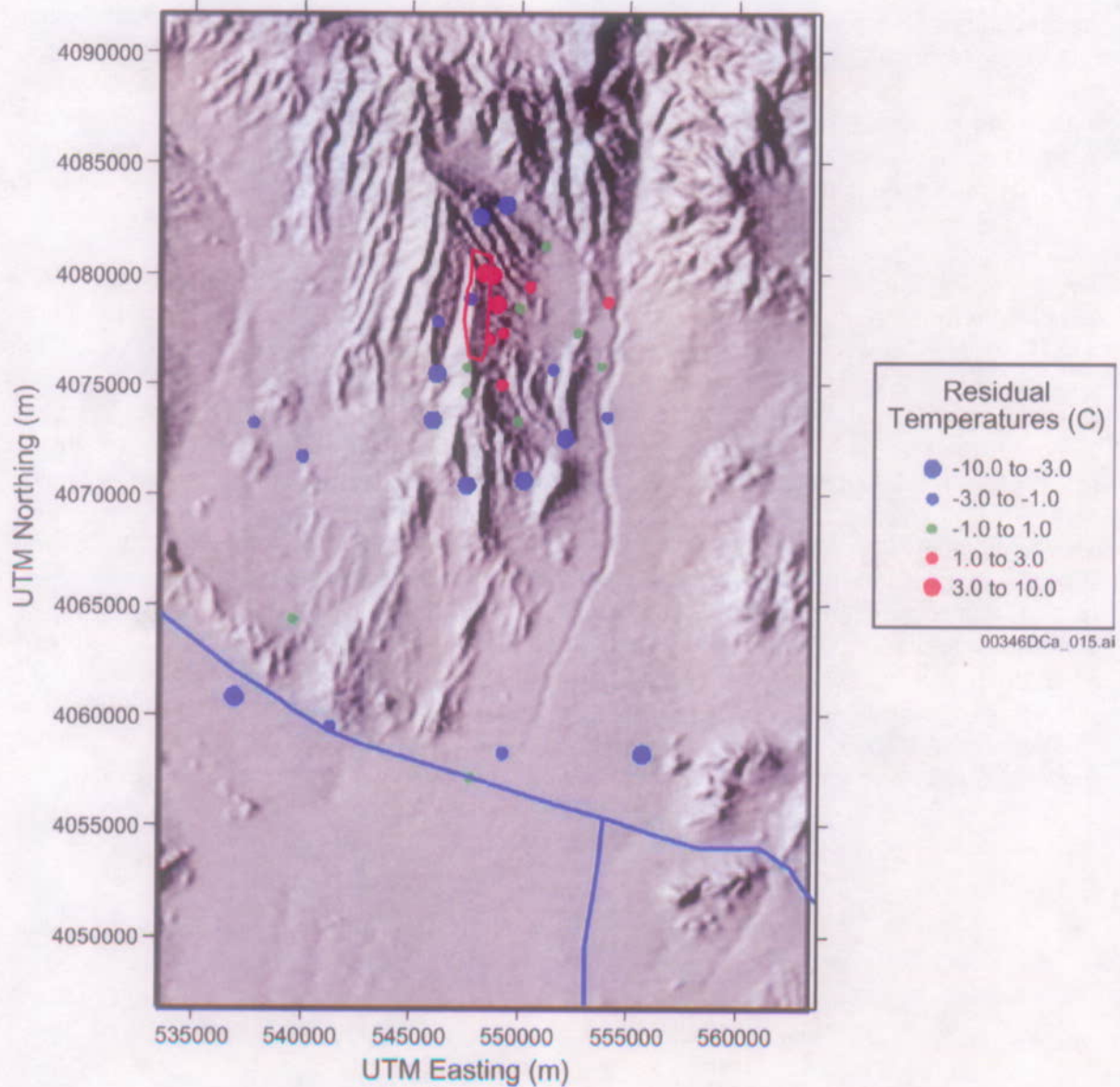


Source: BSC 2003a, Figure 7.4-3.

Figure D-10. Simulated Temperatures at the Water Table for the Thermal Conduction Model

The cross plot of the 94 observations of temperatures in boreholes versus simulated temperatures for the calibrated thermal conduction-only model indicates that there is generally good agreement between observed and simulated temperatures in the model. The R^2 value for these results is 0.80. There is, however, an apparent tendency for the calibrated conduction model to underestimate temperatures between 20°C and 35°C , to overestimate temperatures between 35°C and 50°C , and to underestimate temperatures over 50°C .

The spatial distribution of residuals in simulated temperature at the water table is examined in the map shown in Figure D-11. This figure indicates that there is some systematic pattern to the spatial distribution of residuals in simulated temperature. The positive residuals tend to cluster near and to the east of Yucca Mountain; whereas, the residuals farther to the south and immediately to the north of Yucca Mountain tend to be negative. The positive residuals indicate that the simulated temperature at the water table is too high.



Source: BSC 2003a, Figure 7.4-6.

NOTE: For illustration purposes only.

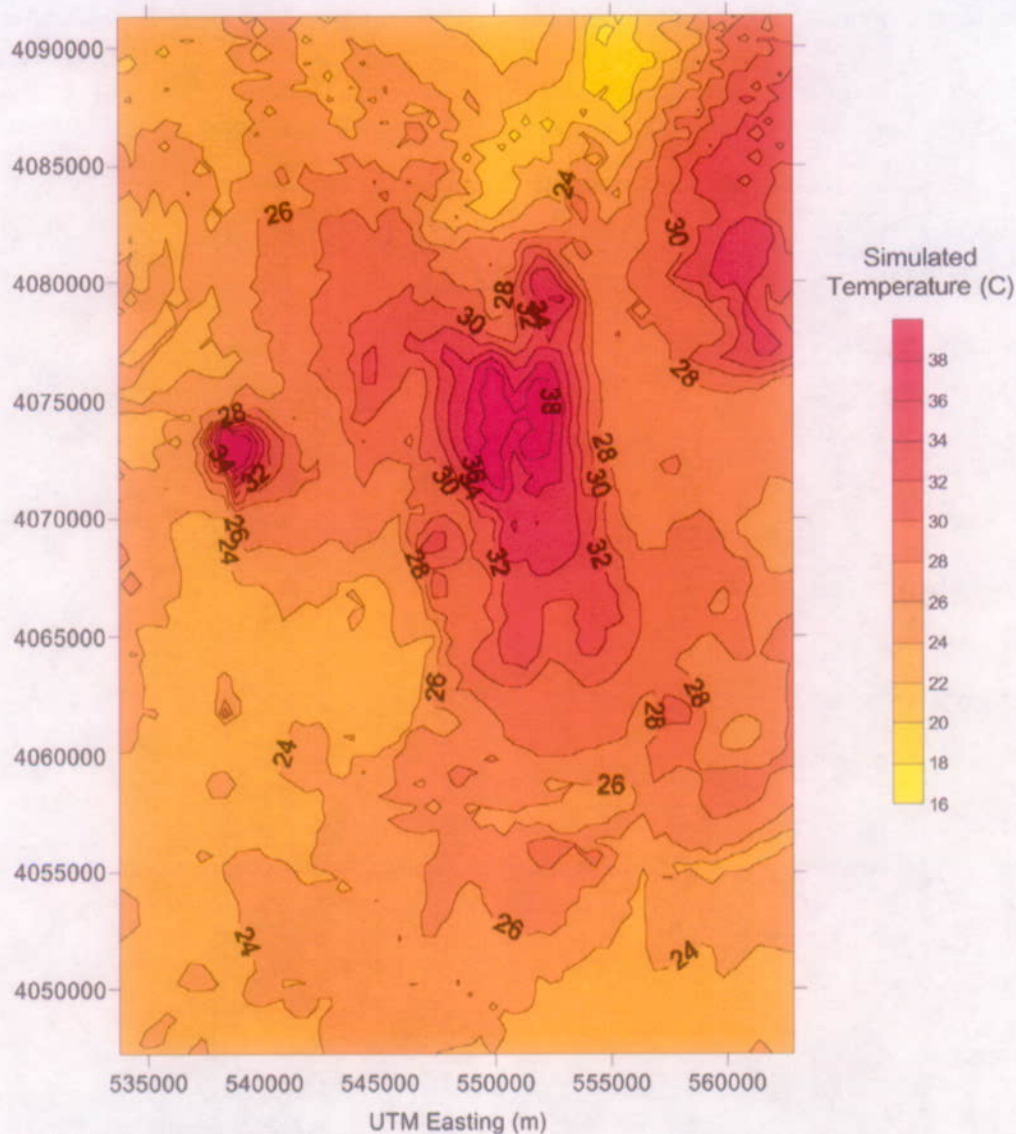
Figure D-11. Residuals in Simulated Temperature at the Water Table for the Thermal Conduction Model

Coupled thermal modeling of groundwater flow and heat transport provides a more complete representation of thermal transport processes in the saturated zone than the conduction-only modeling. Groundwater flow redistributes heat in both the lateral and vertical directions. In addition, variations in the density and viscosity of groundwater as a function of temperature influence the groundwater flow field.

Both the site-scale flow model and the site-scale conduction only model are used as the basis for the modeling of coupled thermal transport. The calibrated upper and lower thermal boundary conditions from the conduction-only model are used in the coupled thermal model. The temperature of groundwater flowing into the coupled thermal model at the lateral boundaries is specified to be equal to the simulated temperatures at those nodes in the saturated zone site-scale thermal conduction model. Similarly, the specified groundwater flux from recharge on the upper boundary of the coupled thermal model is specified to be at the simulated temperatures from the conduction-only model.

The site-scale coupled thermal model is run to steady-state thermal and flow conditions for comparison to the observed temperatures in boreholes. Joint calibration of the coupled thermal model to water-level and temperature measurements was not possible given the long computer run-times necessary to achieve a steady-state solution. Ideally, joint calibration of the saturated zone site-scale model would provide explicit constraints on the groundwater flow field. Nonetheless, the uncalibrated coupled heat and groundwater flow model can provide independent validation of the flow model and subjective indications to improve the flow model.

The resulting steady-state, simulated temperatures at the water table for coupled groundwater flow and thermal transport are shown in Figure D-12. Simulated temperatures at the water table for the coupled model differ significantly from the conduction-only model in the area directly to the east of Yucca Mountain and in a small area in Crater Flat. The simulated temperatures are generally higher in the area between Yucca Mountain and Fortymile Wash in the coupled model, indicating significant upward vertical advective heat transfer in this area of the model. The smaller area of higher simulated temperatures in Crater Flat indicates another area of simulated upward groundwater flow.

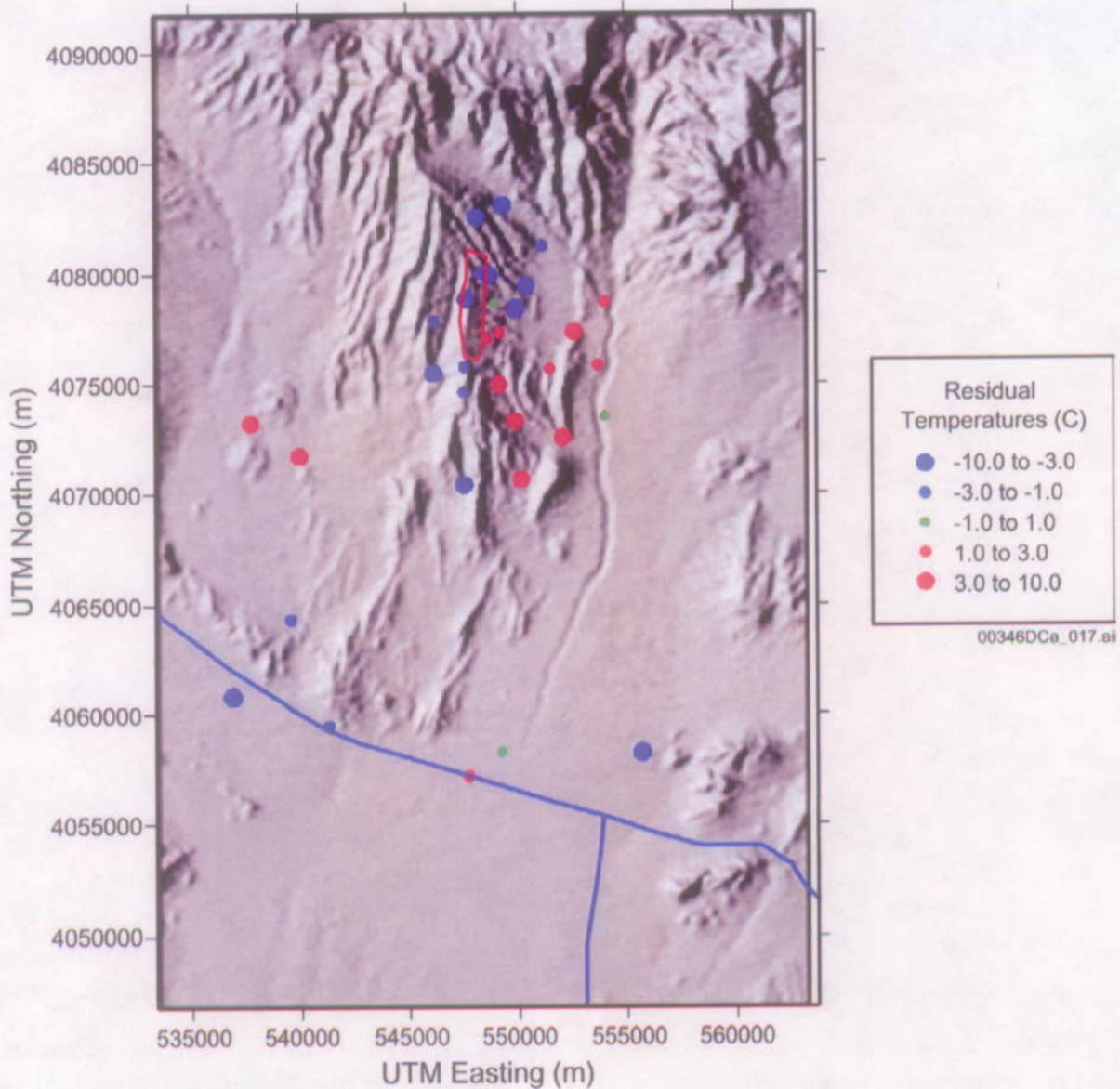


Source: BSC 2003a, Figure 7.4-7.

Figure D-12. Simulated Temperatures at the Water Table for the Coupled Thermal Model

Results of combining the calibrated site-scale flow model and the calibrated thermal conduction model indicate a significant reduction in the R^2 of observed and simulated temperatures from the conduction-only model (0.62 versus 0.80). However, the cross plot of simulated temperatures versus observed temperatures for the coupled thermal model indicates that the simulated temperatures for the deeper, higher-temperature measurement locations have both positive and negative residuals from the coupled model, whereas, the conduction-only model consistently underestimated the temperatures at these locations. The statistical distribution of residuals in simulated temperature for the coupled model has a broader range than for the conduction-only model with an average of -0.13°C .

The spatial distribution of residuals in simulated temperature at the water table for the coupled thermal model is shown in the map shown in Figure D-13. The largest positive residuals generally occur in the area to the east and southeast of Yucca Mountain and in a relatively small area in Crater Flat. The largest negative residuals occur to the north of Yucca Mountain.



Source: BSC 2003a, Figure 7.4-9.

Figure D-13. Residuals in Simulated Temperature at the Water Table for the Coupled Thermal Model

The results of the coupled thermal transport model show that this jointly uncalibrated model is unbiased, but less accurate than the heat conduction-only model.

Although some discernable spatial pattern in residuals has been noted, the results of the coupled thermal model indicate that more than 90 percent of the simulated temperatures are within

10°C of the measured temperatures. Thus, the results of the coupled thermal modeling provide an independent validation of the saturated zone site-scale flow model.

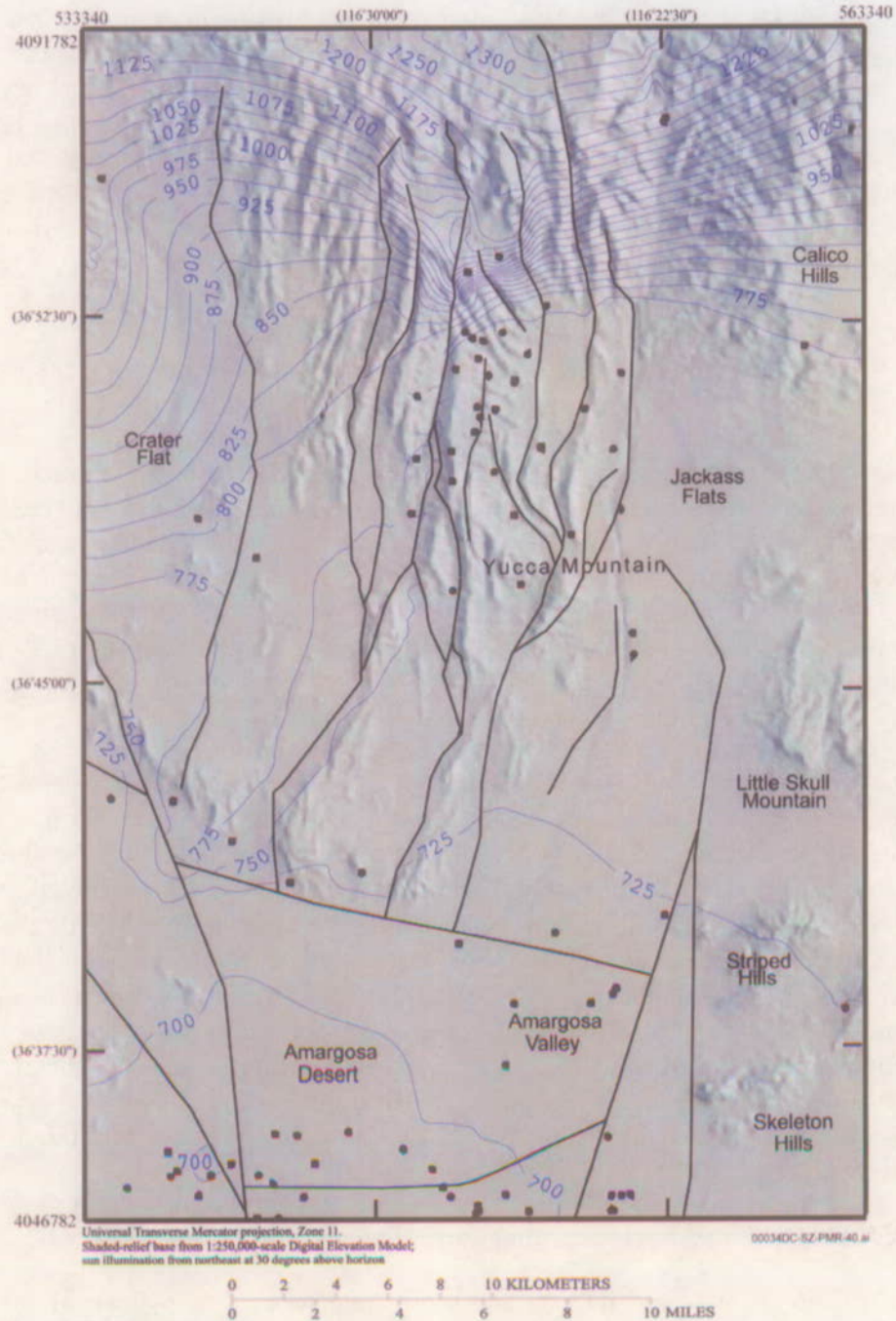
Comparison of Predicted Ground-Water Velocity to Velocity Estimates from ATC Single-Borehole Tracer Test—The ambient ground-water velocity in the saturated alluvium south of Yucca Mountain, Nye County, Nevada has been estimated by comparing the responses of nonsorbing solute tracers in three single-borehole injection-withdrawal tracer tests conducted in borehole NC-EWDP-19D1, located just outside the southwest corner of the Nevada Test Site (BSC 2003b, Sections 6.3 and 6.5). The primary difference between the three tests was that the tracers were allowed to “drift” with the ambient ground-water flow for different periods of time in each test (0, 2 and 30 days) before being pumped back out of the borehole. Four methods were used to estimate ground-water velocities from the single-borehole tracer tests. The first three methods involved between-test comparisons of the peak, mean, and late tracer arrival times, respectively, with the underlying assumption that the differences in the arrival times were due to the different times allowed for movement of the tracer “plume” with the ambient flow field. The three methods assumed a confined aquifer, with the tracer mass corresponding to the arrival times assumed to be injected either directly upgradient or downgradient from the borehole. The resulting ground-water velocity estimates were dependent on the assumed flow porosity. The fourth estimation method assumed a homogeneous, isotropic, and confined aquifer. Although these assumptions are difficult to verify, they allow estimates of longitudinal dispersion and flow porosity to be obtained from the single-borehole tracer tests in addition to ground-water velocity. Assuming that the true flow porosity in the alluvium is between 0.05 and 0.30, the groundwater velocity estimates from the first three methods ranged from 10 to 77 m/yr, with the lower value being associated with the peak arrival analysis and an assumed flow porosity of 0.30, and the higher value being associated with the late arrival analysis and a flow porosity of 0.05. The fourth method yielded a groundwater velocity estimate of 15 m/yr, with a flow porosity of 0.10 and a longitudinal tracer dispersivity of 5 m. The range of specific discharge estimates from all four methods was 1.3 to 9.4 m/yr.

Using the calibrated flow model, specific discharge has been estimated for a nominal fluid path leaving the proposed repository area and traveling 0 to 5-km, 5-km to 20-km, and 20-km to 30-km (BSC 2003a, Section 6.6.2.3). The specific discharge simulated by the flow model for each segment of the flow path from the repository was determined using the median travel time for a group of particles released beneath the repository. Values for specific discharge of 0.67, 2.3, and 2.5 m/yr were obtained, respectively, for the three segments of the flow path. The expert elicitation panel (CRWMS M&O 1998, Figure 3-2e) estimated a median specific discharge of 0.71 m/yr for the 5-km distance. The expert elicitation panel did not consider other travel distances. The range of specific discharge estimates used in Yucca Mountain performance assessments is between 0.25 to 25 m/yr, with a most probable value being 2.5 m/yr. Thus, the range of specific discharge estimates from all four single borehole test methods is well within those established for the TSPA.

D.4.3 Solitario Canyon Alternate Conceptual Model (USFIC 5.11 AIN)

The Solitario Canyon fault and its east and west branches make up three of the 17 discrete geologic features and regions represented with distinct hydrological properties in the site-scale saturated-zone flow and transport model. The location of the Solitario Canyon fault in the

saturated zone model domain is shown in Figure D-14. The Solitario Canyon fault consists of generally north-south trending features just to the west of Yucca Mountain. Both east and west branches consist of generally north-northeast trending linear features, also just to the west of Yucca Mountain. The hydrological characteristics of these features in the model provide both zones of permeability enhancement in the vertical and fault-parallel directions and permeability reduction normal to the fault.



Source: USGS 2001b, Figure 1-2.

Figure D-14. Location of Faults in the Yucca Mountain Region.

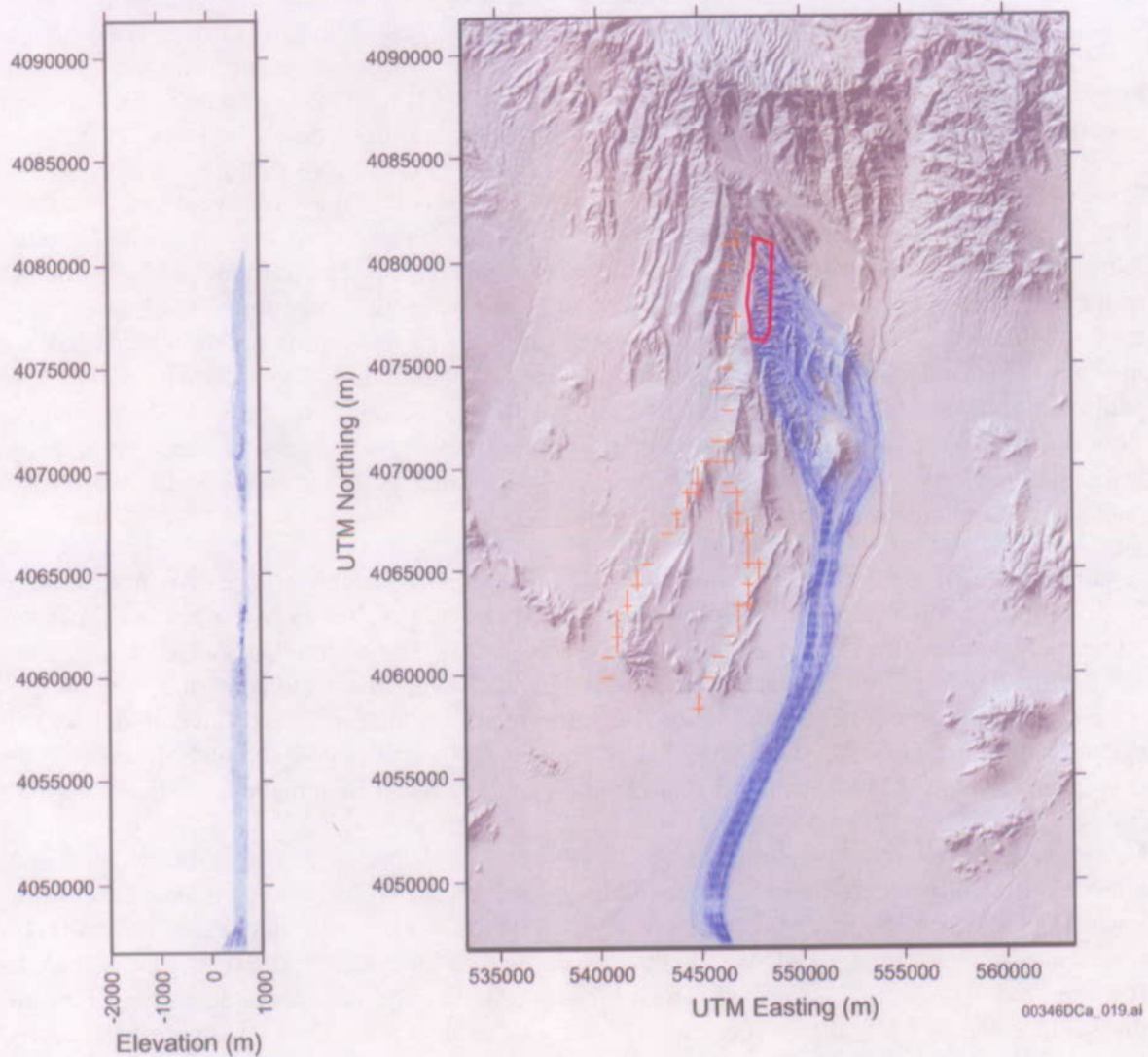
The parameterization of the Solitario Canyon fault is an important part of the saturated zone flow and transport model because it can potentially control flow from Crater Flat to Fortymile Wash. The impact on the model of these features is to generate a higher head gradient to the west of Yucca Mountain and to impede flow from Crater Flat to Yucca Mountain. This effect on flow is important in determining the amount of alluvial material that groundwater flowing from beneath the potential repository region passes through en route to the accessible environment. This fault is included as a discrete feature in the site-scale saturated zone flow and transport model. Simulations performed for the Total System Performance Assessment–Site Recommendation (TSPA-SR) (CRWMS M&O 2000b) included this fault as a feature that extended from the bottom of the model to the top of the water table. While the Solitario Canyon fault has been identified as a major fault in the site-scale model region, conceptual uncertainty remains in the hydrogeologic framework model as to the depth of this fault. This uncertainty translates into uncertainty regarding the likely hydraulic behavior of this feature at depth.

To investigate the importance of Solitario Canyon Fault depth, an alternative conceptualization was simulated in which the fault extends from the water table only to the top of the Carbonate Aquifer. This alternative is referred to as the Shallow Fault Alternative model and was identical to the saturated zone site-scale flow model in all other respects except for the Solitario Canyon Fault properties. The alternative resulted only in changes to the computation grid that were necessary to implement this alternate formulation of the fault. The alternative model was calibrated in a manner identical to that previously used to calibrate the base-case saturated zone flow model. Water-level contour maps and particle tracks were generated based on the water levels predicted by the alternative model in a manner similar to that previously described for the base-case saturated zone flow model.

A comparison of the modeled head values from the Shallow Fault Alternative model for the 32 boreholes in the low-gradient region to the south and east of Yucca Mountain with measured values and values from the base-case flow model has been presented in *Site-Scale Saturated Zone Flow Model* (BSC 2003a, Table 6.7-3). As this comparison indicates the Shallow Fault Alternative model produced essentially the same result as the base-case flow model with the deeper fault zone. For the shallow fault case, however, the calibrated permeability for the fault was approximately 25 percent lower than the permeability for the original deeper fault.

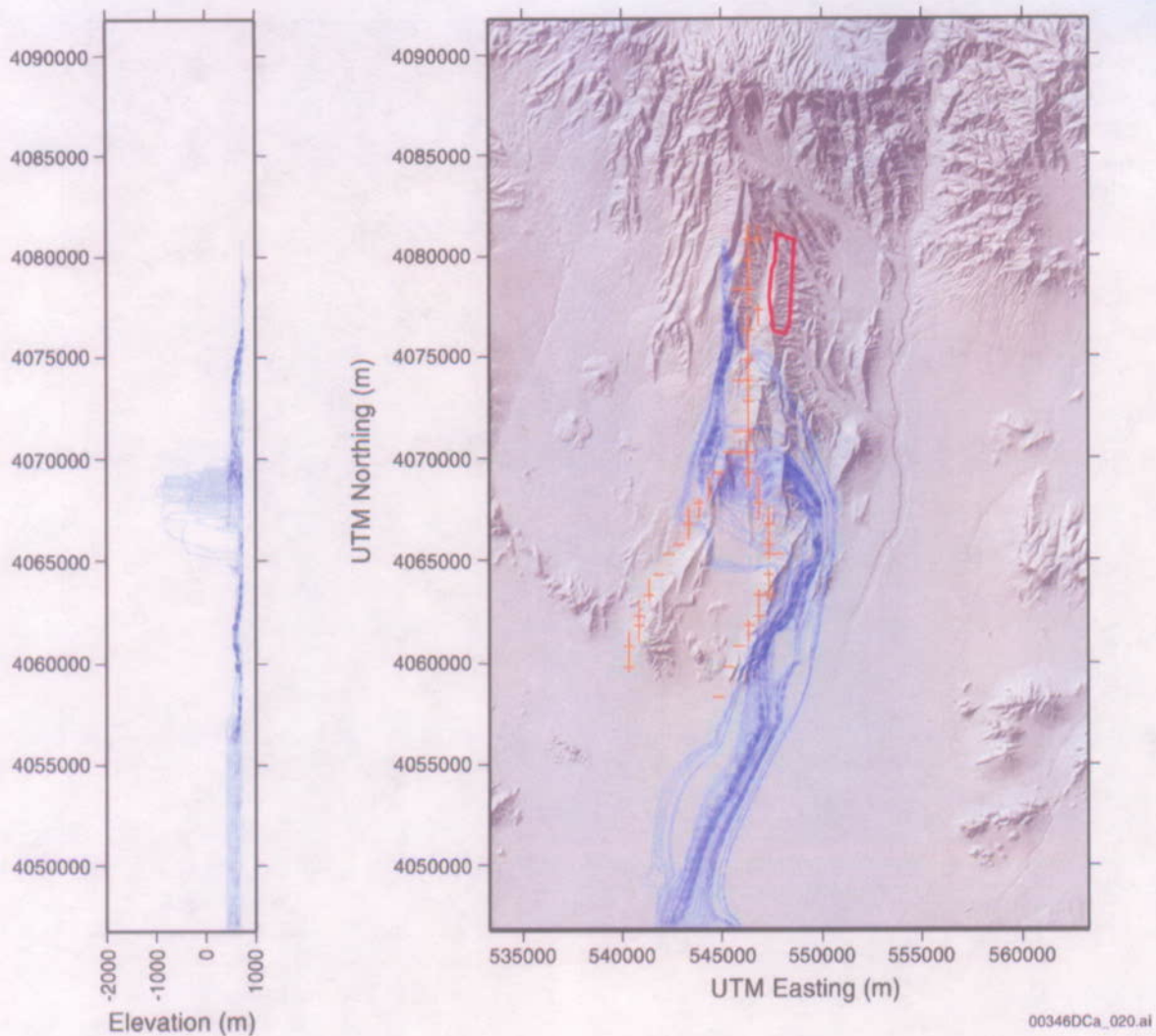
Groundwater flow paths in the base case saturated zone site-scale flow model and in the alternative shallower Solitario Canyon fault model were evaluated using particle tracking. Particle paths from beneath the repository with the base case saturated zone site-scale flow model are shown in Figure D-15. Note that the particle paths are generally restricted to the upper few hundred meters of the saturated zone, with some spreading to deeper paths in the alluvium to the south of Yucca Mountain. Figure D-16 shows the flow paths from a source area near the water table to the west of the Solitario Canyon fault, near the repository for the base case saturated zone site-scale flow model. Flow paths are generally to the south and parallel to the Solitario Canyon fault to distances of five to ten kilometers south of the repository, where flow paths cross the southern branches of the Solitario Canyon fault from west to east. Some flow pathways cross the Solitario Canyon fault branches at depths of up to 1500 m below the water table in the area between five and ten kilometers south of the repository.

Particle paths from beneath the repository with the alternative Solitario Canyon fault model are shown in Figure D-17. Simulated flow paths for the alternative model are very similar to the base case model in both the map view and in the cross-section view. Figure D-18 shows the flow paths from a source area to the west of Solitario Canyon fault for the alternative (shallow) Solitario Canyon model. The flow paths shown in the map view are generally very similar in the alternative model to those in the base case model; however, the flow paths in the cross section indicate that the paths crossing the southern branches of the Solitario Canyon fault do not extend to depths as great as in the base case saturated zone site-scale flow model.



Source: BSC 2003a, Figure 6.7-5.

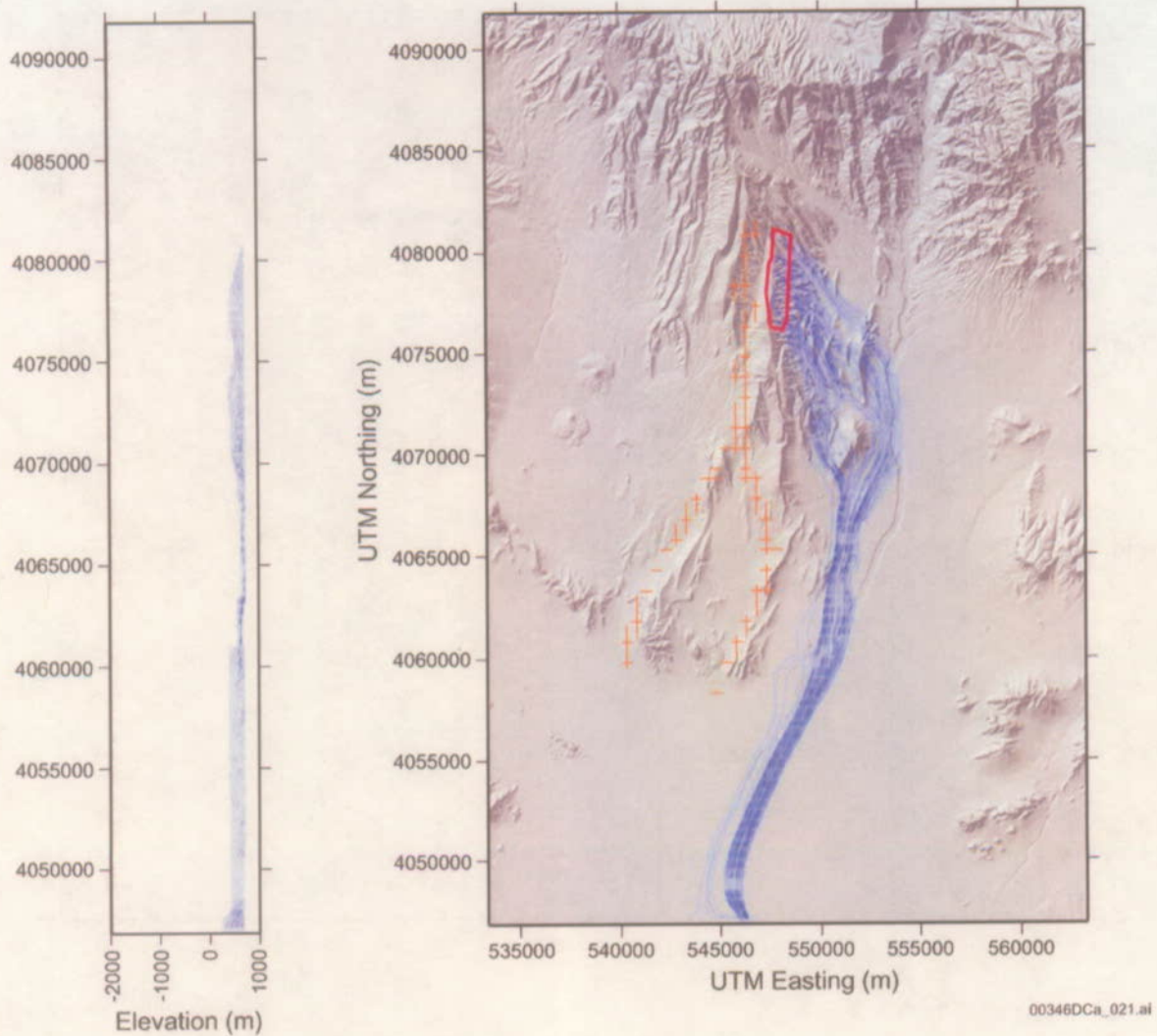
Figure D-15. Simulated Groundwater Flow Paths from Beneath the Repository (Blue Lines) for the Base-Case (Deep Solitario Canyon Fault) Saturated Zone Site-Scale Flow Model



Source: BSC 2003a, Figure 6.7-6.

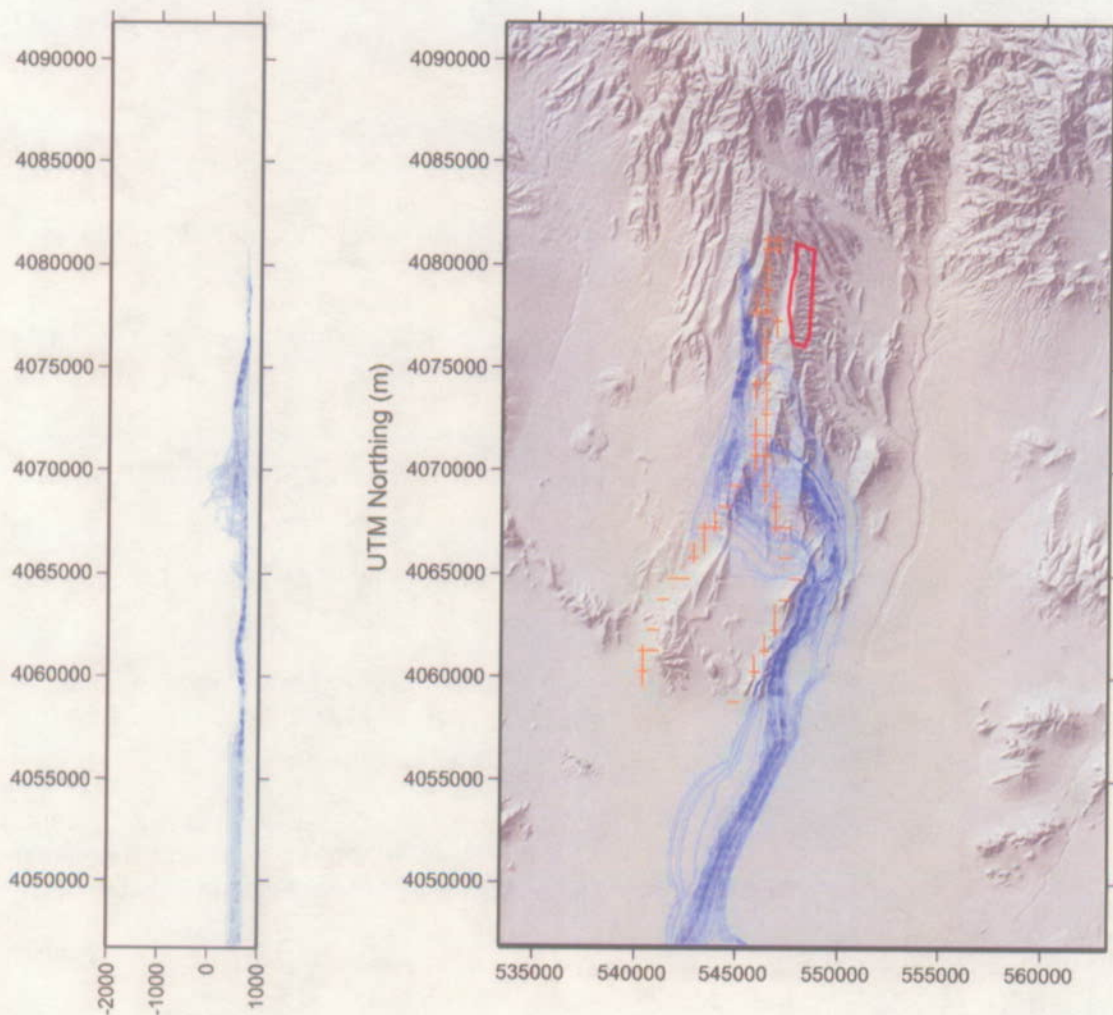
NOTE: Particle paths start west of Solitario Canyon Fault, outside of the repository footprint and do not represent the paths of potential radionuclides that may be released from the repository.

Figure D-16. Simulated Groundwater Flow Paths from the West Side of Solitario Canyon Fault (Blue Lines) for the Base-Case (Deep Solitario Canyon Fault) Saturated Zone Site-Scale Flow Model



Source: BSC 2003a, Figure 6.7-7.

Figure D-17. Simulated Groundwater Flow Paths from Beneath the Repository (Blue Lines) for the Alternative Case (Shallow Solitario Canyon Fault) Saturated Zone Site-Scale Flow Model



Source: BSC 2003a, Figure 6.7-8.

00346DCa_022.ai

Figure D-18. Simulated Groundwater Flow Paths from the West Side of Solitario Canyon Fault (Blue Lines) for the Alternative Case (Shallow Solitario Canyon Fault) Saturated Zone Site-Scale Flow Model

A comparison of the results of the simulations with the two conceptualizations of the Solitario Canyon fault indicates that both simulations produce essentially the same results. Both conceptualizations of the Solitario Canyon fault yield the same flow paths from the water table underneath the proposed repository to the accessible environment. Thus, travel times for the shallow fault case would not be shorter. The results of this investigation indicate that simulated water levels, hydraulic gradients, and transport pathways are not significantly affected by this alternative conceptualization of the Solitario Canyon fault. The small differences between the permeabilities and flow paths of the two models indicates that travel times will not be affected by Solitario Canyon fault depth. The influence of reducing the depth of the Solitario Canyon fault on Total System Performance is expected to be minor. An alternative conceptualization of the Solitario Canyon fault extending only from the water table to the top of the carbonate aquifer resulted in no significant changes to the flow system and thus will have no consequences for transport.

D.5 REFERENCES

D.5.1 Documents Cited

Belcher, W.R.; Faunt, C.C.; and D'Agnese, F.A. 2002. *Three-Dimensional Hydrogeologic Framework Model for Use with a Steady-State Numerical Ground-Water Flow Model of the Death Valley Regional Flow System, Nevada and California*. Water-Resources Investigations Report 01-4254. Denver, Colorado: U.S. Geological Survey. TIC: 252875.

BSC (Bechtel SAIC Company) 2001. *Calibration of the Site-Scale Saturated Zone Flow Model*. MDL-NBS-HS-000011 REV 00 ICN 01. Las Vegas, Nevada: Bechtel SAIC Company. ACC: MOL.20010713.0049.

BSC 2003a. *Site-Scale Saturated Zone Flow Model*. MDL-NBS-HS-000011 REV 01A. Las Vegas, Nevada: Bechtel SAIC Company. ACC: MOL.20030626.0296

BSC 2003b. *Saturated Zone In-Situ Testing*. ANL-NBS-HS-000039 REV 00A. Las Vegas, Nevada: Bechtel SAIC Company. ACC: MOL.20030602.0291.

BSC 2003c. *Geochemical and Isotopic Constraints on Groundwater Flow Directions and Magnitudes, Mixing, and Recharge at Yucca Mountain*. ANL-NBS-HS-000021 REV 01A. Las Vegas, Nevada: Bechtel SAIC Company. ACC: MOL.20030604.0164.

CRWMS M&O (Civilian Radioactive Waste Management System Management and Operating Contractor) 1998. *Saturated Zone Flow and Transport Expert Elicitation Project*. Deliverable SL5X4AM3. Las Vegas, Nevada: CRWMS M&O. ACC: MOL.19980825.0008.

CRWMS M&O 2000a. *Saturated Zone Flow and Transport Process Model Report*. TDR-NBS-HS-000001 REV 00 ICN 02. Las Vegas, Nevada: CRWMS M&O. ACC: MOL.20001102.0067.

CRWMS M&O 2000b. *Total System Performance Assessment for the Site Recommendation*. TDR-WIS-PA-000001 REV 00 ICN 01. Las Vegas, Nevada: CRWMS M&O. ACC: MOL.20001220.0045.

D'Agnese, F.A.; Faunt, C.C.; Turner, A.K.; and Hill, M.C. 1997. *Hydrogeologic Evaluation and Numerical Simulation of the Death Valley Regional Ground-Water Flow System, Nevada and California*. Water-Resources Investigations Report 96-4300. Denver, Colorado: U.S. Geological Survey. ACC: MOL.19980306.0253.

D'Agnese, F.A.; O'Brien, G.M.; Faunt, C.C.; Belcher, W.R.; and San Juan, C. 2002. *A Three-Dimensional Numerical Model of Predevelopment Conditions in the Death Valley Regional Ground-Water Flow System, Nevada and California*. Water-Resources Investigations Report 02-4102. Denver, Colorado: U.S. Geological Survey. TIC: 253754.

Geldon, A.L.; Umari, A.M.A.; Fahy, M.F.; Earle, J.D.; Gemmell, J.M.; and Darnell, J. 1997. *Results of Hydraulic and Conservative Tracer Tests in Miocene Tuffaceous Rocks at the C-Hole Complex, 1995 to 1997, Yucca Mountain, Nye County, Nevada*. Milestone SP23PM3. [Las Vegas, Nevada]: U.S. Geological Survey. ACC: MOL.19980122.0412.

Harbaugh, A.W.; Banta, E.R.; Hill, M.C.; and McDonald, M.G. 2000. *MODFLOW-2000, The U.S. Geological Survey Modular Ground-Water Model—User Guide to Modularization Concepts and the Ground-Water Flow Process*. Open-File Report 00-92. Reston, Virginia: U.S. Geological Survey. TIC: 250197.

Parkhurst, D.L. and Appelo, C.A.J. 1999. *User's Guide to PHREEQC (Version 2)—A Computer Program for Speciation, Batch-Reaction, One-Dimensional Transport, and Inverse Geochemical Calculations*. Water-Resources Investigations Report 99-4259. Denver, Colorado: U.S. Geological Survey. TIC: 253046.

Reamer, C.W. and Williams, D.R. 2000. Summary Highlights of NRC/DOE Technical Exchange and Management Meeting on Unsaturated and Saturated Flow Under Isothermal Conditions. Washington, D.C.: U.S. Nuclear Regulatory Commission. ACC: MOL.20001128.0206.

Sass, J.H.; Lachenbruch, A.H.; Dudley, W.W., Jr.; Priest, S.S.; and Munroe, R.J. 1988. *Temperature, Thermal Conductivity, and Heat Flow Near Yucca Mountain, Nevada: Some Tectonic and Hydrologic Implications*. Open-File Report 87-649. [Denver, Colorado]: U.S. Geological Survey. TIC: 203195.

Schlueter, J.R. 2003. "Additional Information needed for Unsaturated and Saturated Flow Under Isothermal Conditions (USFIC).5.11 Agreement and Completion of General (GEN).1.01, Comment 103." Letter from J.R. Schlueter (NRC) to J.D. Ziegler (DOE/ORD), February 5, 2003, 0210036017, with enclosure. ACC: MOL.20030805.0395.

USGS (U.S. Geological Survey) 2001a. *Water-Level Data Analysis for the Saturated Zone Site-Scale Flow and Transport Model*. ANL-NBS-HS-000034 REV 01. Denver, Colorado: U.S. Geological Survey. ACC: MOL.20020209.0058.

USGS 2001b. *Hydrogeologic Framework Model for the Saturated-Zone Site-Scale Flow and Transport Model*. ANL-NBS-HS-000033 REV 00 ICN 02. Denver, Colorado: U.S. Geological Survey. ACC: MOL.20011112.0070.

Ziegler, J.D. 2002. "Transmittal of Report Addressing Key Technical Issue (KTI) Agreement Item Unsaturated and Saturated Zone Flow Under Isothermal Conditions (USFIC) 5.11." Letter from J.D. Ziegler (DOE/YMSCO) to J.R. Schlueter (NRC), July 5, 2002, 0709023235, OL&RC:TCG-1357, with enclosure. ACC: MOL.20020911.0130.

Ziegler, J.D. 2003. "Response to Additional Information Needed on Key Technical Issue (KTI) Agreement Item Unsaturated and Saturated Flow Under Isothermal Conditions (USFIC) 5.11." Letter from J.D. Ziegler (DOE/ORD) to J.R. Schlueter (NRC), April 9, 2003, 0410036845, OLA&S:TCG-0976. ACC: MOL.20030529.0290.

Zyvoloski, G.A.; Robinson, B.A.; Dash, Z.V.; and Trease, L.L. 1997. *User's Manual for the FEHM Application—A Finite-Element Heat- and Mass-Transfer Code*. LA-13306-M. Los Alamos, New Mexico: Los Alamos National Laboratory. TIC: 235999.

D.5.2 Codes, Standards, Regulations, and Procedures

AP-SIII.10Q, Rev. 1, ICN 0. *Models*. Washington, D.C.: U.S. Department of Energy, Office of Civilian Radioactive Waste Management. ACC: DOC.20030312.0039

APPENDIX E
HORIZONTAL ANISOTROPY
(RESPONSE TO USFIC 5.01)

Note Regarding the Status of Supporting Technical Information

This document was prepared using the most current information available at the time of its development. This Technical Basis Document and its appendices providing Key Technical Issue Agreement responses that were prepared using preliminary or draft information reflect the status of the Yucca Mountain Project's scientific and design bases at the time of submittal. In some cases this involved the use of draft Analysis and Model Reports (AMRs) and other draft references whose contents may change with time. Information that evolves through subsequent revisions of the AMRs and other references will be reflected in the License Application (LA) as the approved analyses of record at the time of LA submittal. Consequently, the Project will not routinely update either this Technical Basis Document or its Key Technical Issue Agreement appendices to reflect changes in the supporting references prior to submittal of the LA.

APPENDIX E

HORIZONTAL ANISOTROPY (RESPONSE TO USFIC 5.01)

This appendix provides a response for key technical issue (KTI) agreement Unsaturated and Saturated Flow under Isothermal Conditions (USFIC) 5.01. This KTI agreement relates to providing more information about horizontal anisotropy in the tuff.

E.1 KEY TECHNICAL ISSUE AGREEMENT

E.1.1 USFIC 5.01

KTI agreement USFIC 5.01 was reached during the NRC/DOE technical exchange and management meeting on unsaturated and saturated flow under isothermal conditions held October 31 through November 2, 2000 in Albuquerque, New Mexico. The saturated zone portion of KTI subissues 5 and 6 were discussed at that meeting (Reamer and Williams 2000).

During the technical exchange, NRC and DOE discussed the appropriate degree of anisotropy for the site-scale saturated zone flow and transport model, the calibration of the model, and the use of alternative conceptual models. DOE asserted that the isotropic case is really anisotropic given the discrete features, such as faults, included in the site-scale model. NRC asked if the calibration was based on the isotropic or anisotropic case. DOE replied that calibration was performed with the isotropic case. Following the discussion, agreement USFIC 5.01 was reached to perform additional evaluation of anisotropy.

Wording of the agreement is as follows:

USFIC 5.01

Anisotropy in the site scale model should be reevaluated to ensure that a reasonable range for uncertainty is captured. The data from the C-Wells testing should provide a technical basis for an improved range. As part of the C-Wells report, DOE should include an analysis of horizontal anisotropy for wells that responded to the long-term tests. Results should be included for the tuffs in the calibrated site scale model. DOE will provide the results of the requested analyses in C-Wells report(s) in October 2001, and will carry the results forward to the site-scale model, as appropriate.

E.1.2 Related Key Technical Issues

None.

E.2 RELEVANCE TO REPOSITORY PERFORMANCE

The subject of USFIC 5.01 is the further evaluation of the affects of anisotropy on model performance. This is directly relevant to the sensitivity of parameter uncertainty on model output and, subsequently performance assessment.

Because potential radionuclides released from the proposed repository at Yucca Mountain must travel through the saturated fractured tuff and the saturated alluvium before reaching the compliance boundary, it is important to characterize the hydrogeologic properties of the downgradient media. In these volcanic tuffs, fractures and faults often have common orientations and it is likely that preferential flowpaths exist along these features. Anisotropy in hydraulic properties of the volcanic tuffs affects uncertainty in flow paths. Large-scale anisotropy and heterogeneity were implemented in the SZ site-scale flow model through direct incorporation of known hydraulic features, faults, and fractures. Small-scale anisotropy was derived from the analysis of hydraulic testing at the C-Wells (BSC 2003a, Section 6.2.6).

Additional analysis of anisotropy was needed for the site-scale saturated zone model for proper calibration of the model and for use of alternative conceptual models. If the uncertainty is very large, with a range that could span an isotropic model to a highly anisotropic model, model prediction results could be different.

Section 2.3.5.3 describes horizontal anisotropy in the tuffs and its use in assessing the flow of groundwater and potential transport of radionuclides in the saturated zone beneath and downgradient from Yucca Mountain.

E.3 RESPONSE

Since completion of the C-Wells complex in 1983, several single and cross-hole tracer and hydraulic tests have been conducted to gain a better understanding of the hydrogeology of the region. The purpose of the testing was to characterize the hydrologic properties of the saturated zone at and around Yucca Mountain. Data from the testing were used for a more detailed analysis of anisotropy than the analyses originally performed. Although data from the C-Wells tests were not intended to be used for an analysis of anisotropy, because drawdown was measurable at several distant wells, an estimate of anisotropy ratio could be completed. The analyses were presented in BSC (2003a, Section 6.2.6). Based on this analysis, a wider range of horizontal anisotropy than was used in SR was considered for the license application. Sensitivity analyses using the site-scale model indicated that variation in anisotropy impacted flow paths length in the volcanic tuffs and alluvium.

E.4 BASIS FOR THE RESPONSE

Understanding saturated flow and transport near the proposed high-level nuclear waste repository at Yucca Mountain is critical to a thorough understanding of the saturated zone flow and potential radionuclide transport. Because potential radionuclides released from the proposed repository at Yucca Mountain must travel through the saturated fractured tuff and the saturated alluvium before reaching the compliance boundary, it is important to characterize the hydrogeologic properties of downgradient media. In these volcanic tuffs, fractures and faults often have common orientations and it is likely that preferential flowpaths exist along these features. A number of published studies have assigned transmissivities, storativities, and anisotropy ratios to the saturated zone in this area. In this analysis, reviews of several studies are used in conjunction with an independent re-analysis of the data to suggest a distribution of anisotropy ratios between 0.05 and 20 used in the saturated zone flow code (i.e., FEHM; LANL 2003).

E.4.1 Background of the Site-Scale Flow Models

It should be noted that, in general, large-scale hydraulic features (e.g., major faults, fault zones, and zones of chemical alteration) have been incorporated directly into TSPA-LA (BSC 2003b) models as zones of enhanced or reduced permeability. However, the fractured volcanic tuffs found in the area bounded by the coordinates listed in Table E-1 is assigned a stochastically selected horizontal anisotropy, which is the focus of this appendix. Originally, an isotropic representation of this area was used as the base-case conceptual model with horizontal anisotropy in permeability considered an alternative conceptual model. For the TSPA-SR, two alternative models were examined to evaluate the effect of uncertainty in anisotropy: an isotropic case and an anisotropic case with a 5:1 north-south anisotropy ratio. When calibrating the TSPA-SR model (CRWMS M&O 2000a), a slightly better match to water level data was achieved when a 5:1 north-south anisotropy ratio was used. In addition, the differences in predicted heads and the impacts on the specific discharge, the flow-path direction, and flow-path lengths in volcanic tuffs and alluvium were within the uncertainty ranges allowed in the TSPA-SR (CRWMS M&O 2000a). Although only minor differences in model performance were recorded between the isotropic and 5:1 north-south anisotropic cases, it was felt that these discrete values were not representative of the system. Since then, a more detailed analysis of anisotropy has been performed with results presented in *Saturated Zone In-Situ Testing* (BSC 2003a, Section 6.2.6) and used in *SZ Flow and Transport Model Abstraction* (BSC 2003b, Section 6.5.2.10).

Table E-1. Boundaries of the Horizontally Anisotropic Uncertainty Zone

Vertex	UTM Northing (m)	UTM Easting (m)
1	548712	4065570
2	554390	4067050
3	553647	4080900
4	547317	4081090

Source: BSC 2003b.

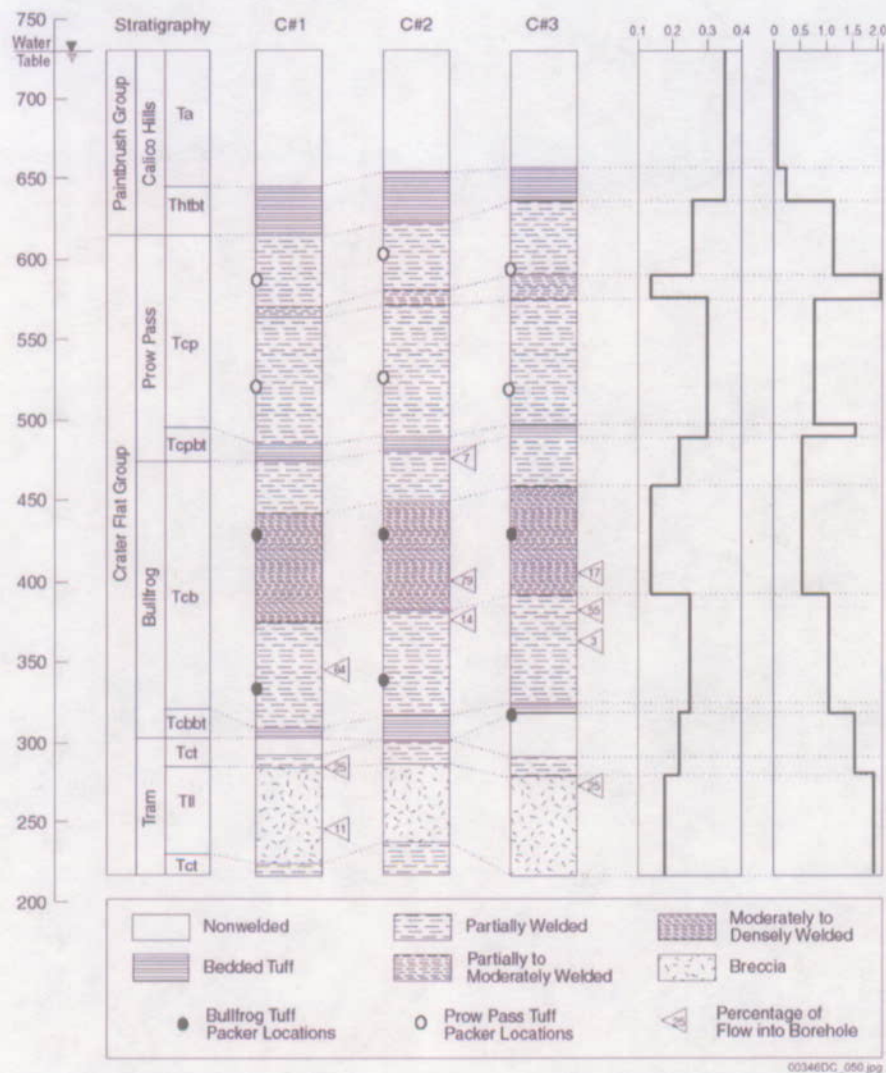
E.4.2 Analyses of Data from the C-Wells

A geologic description of the C-Wells complex and the surrounding area is presented elsewhere (e.g., Geldon et al. 1998; Farrell et al. 1999; Ferrill et al. 1999; Winterle and La Femina 1999; CRWMS M&O 2000b; BSC 2003a). Furthermore, a detailed description of the analysis and derivation of the distribution of anisotropy ratio in the saturated zone near the C-Wells complex is presented in *Saturated Zone In-Situ Testing* (BSC 2003a, Section 6.2.6). Well logs for the C-Wells are shown in Figure E-1. Interpretation of well-test data with analytical solutions consists of inferring the hydraulic properties of a system based on measured responses to an assumed flow geometry (i.e., radial). The system geometry cannot be specified with reasonable certainty. In a layered sedimentary system lacking extreme heterogeneity, flow might reasonably be expected to be radial during a hydraulic test. However, when hydraulic tests are conducted at an arbitrary point within a three-dimensional fractured rock mass, the flow geometry is complex (Hsieh et al. 1985). Radial flow would occur only if the test were performed in a single uniform fracture of effectively infinite extent or within a network of fractures confined to a planar body in which the fractures were so densely interconnected that the network behaves like an equivalent

porous medium. Flow in fractured tuff is nonradial and variable, as fracture terminations and fracture intersections are reached by the cone of depression. Therefore, assumptions required in the analytical treatment of anisotropy may not be strictly consistent with site geology.

There is considerable heterogeneity in hydraulic properties throughout the fractured tuff and alluvium near Yucca Mountain, which differ spatially and differ depending on the direction in which they are measured (horizontally and vertically). In this analysis, transmissivity and storativity are required to calculate and define large-scale anisotropy, and their measured values reflect heterogeneity in the media. The concept of anisotropy typically is associated with homogeneous medium, a criterion not met here. Nevertheless, there are spatial and directional variations in transmissivity, and the notion remains that, over a large enough representative elementary volume, there exists a preferential flow direction that can be termed "anisotropy." Structural features (e.g., fractures and faults) are indirectly incorporated into the anisotropy ratio applied to this area through the anisotropy analysis that considered the media as a homogeneous representative elementary volume.

Data from a long-term pumping test (May 8, 1996 to November 12, 1997) were used to evaluate anisotropy near the C-Wells complex. For this test, the most productive portion of the Bullfrog-Tram lithologic interval in well UE-25 c#3 was isolated with downhole packers and water levels were monitored at several distant wells (USW-H4, UE-25 ONC#1, UE-25 WT#3, and UE-25 WT#14). Data from the other C-Wells (UE-25 c#1 and UE-25 c#2) were not used in the anisotropy analysis because over the small scale of observation at the C-Wells, pump test results are likely dominated by discrete fractures (i.e., inhomogeneities), three-dimensional flow effects are likely, and recirculation from simultaneous tracer tests obscured results. Furthermore, because anisotropy is conceptually difficult to define for heterogeneous media, it is more easily described as an average preferential flow over as large a representative elementary volume as possible. Thus, it makes little sense to attempt to define anisotropy over a heterogeneous area as small as that of the C-Wells complex. The non-radial nature of the cone of depression near the C-Wells is illustrated in Figure E-2. After filtering (USGS 2002) the drawdown data in response to pumping at UE-25 c#3, transmissivity and storativity were calculated at four distant wells (USW H-4, UE-25 ONC#1, UE-25 WT#3, and UE-25 WT#14). Figure E-3 is a plot of the filtered drawdowns fit with the Cooper-Jacob straight-line method (CRWMS M&O 2000c). The inconsistent slope of the fit to drawdown in well USW H-4 resulted in a lower transmissivity at this well, which could be due to the Antler Wash fault that runs north-north-east between wells UE-25 c#3 and USW H-4. Transmissivity and storativity values are presented in Table E-2. The variations in transmissivity and storativity support the alternative conceptual model in which there is large-scale horizontal anisotropy in permeability in the saturated zone volcanic units to the southeast of the repository.



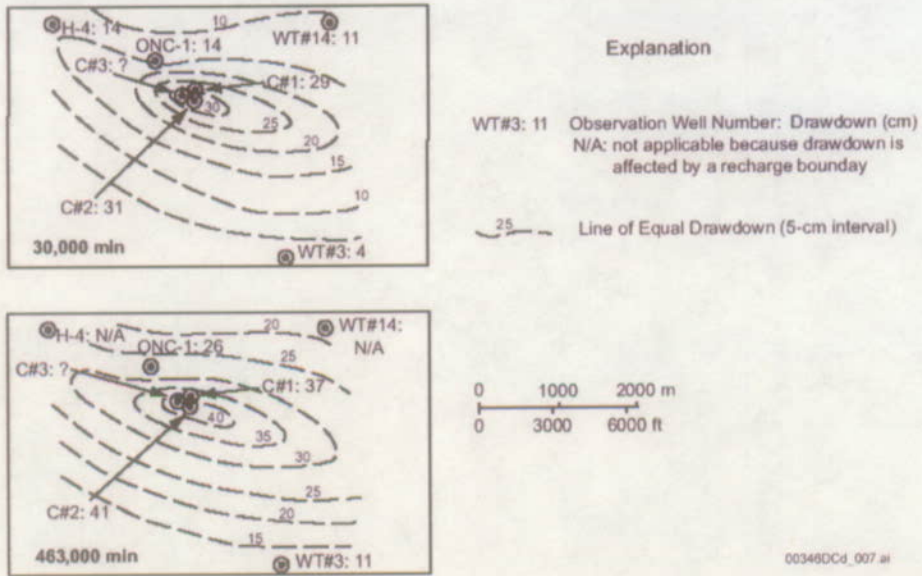
Source: Information derived from Geldon (1993 [101045, WRIR 92-4016 (pp. 35-37, 68-70). Packer locations from Scientific Notebook SN-USGS-SCI-036 [162854], [162856], [162857], [162858].

NOTE: Packer locations indicate intervals in which tracer tests described in this report were conducted. (note that the tracer tests were conducted between UE-25 c#2 and c#3).

Source: Information derived from Geldon 1993, pp. 35-37, 68-70. Packer locations from Umari 2002.

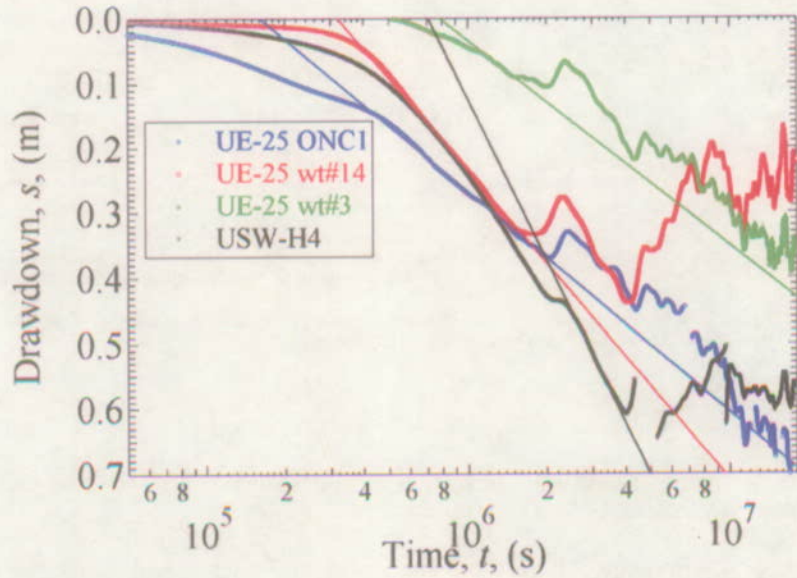
NOTE: Packer locations indicate intervals in which tracer tests described in this report were conducted. (Note that the tracer tests were conducted between UE-25 c#2 and c#3.)

Figure E-1. Stratigraphy, Lithology, Matrix Porosity, Fracture Density, and Inflow from Open-Hole Flow Surveys at the C-Well



Source: BSC 2003a, Figure 6.2-36.

Figure E-2. Distribution of Drawdown in Observation Wells at Two Times after Pumping Started in UE-25 c#3 on May 8, 1996



Source: BSC 2003a, Figure 6.2-39.

Figure E-3. Linear Fits to Filtered Data from Four Monitoring Wells

Table E-2. Transmissivities and Storativities Calculated Using the Cooper-Jacob Method with Filtered Data

Well	T (m ² /day)	S (-)
UE-25 ONC-1	446	0.003
UE-25 wt#3	477	0.0005
UE-25 wt#14	318	0.0008
USW H-4	182	0.0007

Source: BSC 2003a.

E.4.3 Previously Reported Results

Winterle and La Femina (1999) processed the long-term pumping data with AQTESOLV and their transmissivity and storativity results (obtained with the Theis method) are shown in Table E-3. *Saturated Zone In-Situ Testing* (BSC 2003a) also analyzed the drawdown data from the long-term pumping test using the analytical methods of Theis (1935), Neuman (1975), and Streltsova-Adams (1978), and these results also are presented in Table E-3. There are obvious discrepancies between the results presented in Tables E-2 and E-3. Such variability is not surprising considering the differences in data reduction methods and solution techniques.

Table E-3. Transmissivities and Storativities of Distant Wells for the Long Term Pumping Tests

Well	Winterle and La Femina ^a		Geldon et al. ^b	
	T (m ² /day)	S (-)	T (m ² /day)	S (-)
UE-25 ONC1	1,340	0.008	1,000	0.001
UE-25 wt#3	1,230	0.005	2,600	0.002
UE-25 wt#14	1,330	0.002	1,300	0.002
USW-H4	670	0.002	700	0.002

Source: Entire table from BSC 2003a, Table 6.2-11.

NOTES: ^a Winterle and La Femina (1999)

^b Geldon et al. (2002).

E.4.4 Anisotropy Ratios

Anisotropy ratio analyses (BSC 2003a) use the analytical solutions of Papadopulos (1967) combined with PEST (Watermark Computing 2002), hereafter referred to as the Papadopulos-PEST method, and Hantush (1966), both implemented with standard formulas of ellipses and coordinate transformations. Both techniques are applicable to homogeneous confined aquifers with radial flow to the pumping well, although small deviations from these assumptions may still yield reasonable estimates of anisotropy. These methods require transmissivity, storativity, and the locations of a minimum of three monitoring wells as input. With this information, anisotropy ratios and principle directions are calculated. Results from three analyses are presented in Table E-4.

Table E-4. Calculated and Reported Anisotropies and Principle Directions

Data Set Used	T_{max} (m ² /day)	T_{min} (m ² /day)	Anisotropy	Azimuth
BSC (2003a); Hantush (1966)	748	229	3.3	15°E
BSC (2003a) $T=1,000$ m ² /day (Papadopulos-PEST))	1,863	537	3.5	79°W
BSC (2003a $T=700-2,600$ m ² /day (Papadopulos-PEST))	3,272	599	5.5	1°E
BSC (2003a $T=700-1,230$ m ² /day (Papadopulos-PEST))	3,047	271	11.3	35°W
Ferrill et al. (1999)	5,400	315	17	30°E
Winterle and La Femina (1999)	2,900	580	5	33°E

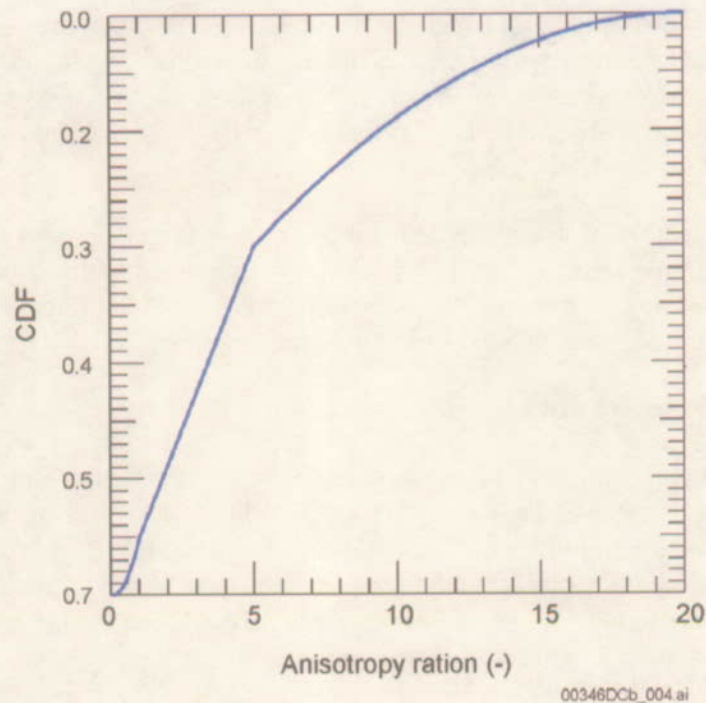
Source: BSC 2003a, Table 6.2-12.

E.4.5 Interpretation and Assignment of the Anisotropy Distribution

A distribution of anisotropies is specified so that an anisotropy ratio can be selected for each stochastic realization of the *SZ Flow and Transport Abstraction* (BSC 2003b). Because the current version of FEHM (LANL 2003) can only implement anisotropy aligned with the grid direction, the north-northeasterly principal direction is not directly applicable in the model, which further increases uncertainty. For example, the analytical result for anisotropy using the Cooper-Jacob (1946) method is a ratio of 3.3 in a direction 15° east of north. A projection that orients the principal direction north south (0°) results in an anisotropy ratio of 2.5, and depending on the principle direction, it is possible for the projected north-south anisotropy ratio to be less than one.

To reflect uncertainty in the anisotropy data near the C-wells, a relatively large range of anisotropies (large uncertainty) was used in the flow and transport abstraction models. All authors who have previously investigated anisotropy ratios in this area (Farrell et al. 1999; Ferrill et al. 1999; Winterle and La Femina 1999), agree that the assumptions made in the anisotropy analysis are difficult to support and that the analysis is sensitive to the input parameters. Reported anisotropies range from 3.3 (BSC 2003a, Table 6.2-12) to 17 (Ferrill et al. 1999), but “because of the considerable degree of uncertainty in the anisotropy ratio and direction obtained from [these analyses], the degree of confidence in [the] horizontal anisotropy analysis should be regarded as low” (Winterle and La Femina 1999, p 4-25). Based on the ratio of a maximum of 3,800 m²/day (Winterle and La Femina 1999, p 4-12) to a minimum calculated transmissivity of 182 m²/day (BSC 2003a, Table 6.2-10), and on the highest reported anisotropy ratio of 17 (Ferrill et al. 1999), the upper limit of the distribution of the projected north-south anisotropy ratio was conservatively set at 20. Although most anisotropy calculations and geologic interpretations report the direction of maximum principal hydraulic conductivity as approximately north-north-east, it cannot be ruled out that the direction of anisotropy could lie in the east-west direction (BSC 2003a, Table 6.2-12), causing the projected north-south to east-west anisotropy ratio to be less than 1. Therefore, the lower limit was set as the inverse of the upper limit, 1/20 or 0.05. This lower limit on anisotropy ratio is consistent with the Antler Wash fault found near the C-Wells complex. Thus, a small (10 percent) probability of the projected north south to east-west anisotropy being less than 1 is assigned. Because 3 of 6 anisotropy analyses yielded ratios of anisotropy between 1 and 5 (BSC 2003a, Table 6.2-12), a 50 percent probability for the projected north south to east-west anisotropy ratio falling between 1 and 5 is assigned.

This leaves a 40 percent probability of projected anisotropy ratios between 5 and 20. The resulting cumulative distribution function is shown in Figure E-4. For the flow model, it is only possible to specify “projected” anisotropies in the north-south or east-west directions (independent of calculated principle direction) further justifying the large range of anisotropies.



Source: Based on BSC 2003b, Figure 6-19.

Figure E-4. Cumulative Distribution of Anisotropy Ratio

There are several noteworthy points based on three distinct regions of the anisotropy ratio distribution:

Anisotropy Ratio Between 5 and 20—The maximum anisotropy ratio of 20:1 is based on the highest reported anisotropy ratio 17:1 (Ferrill et al. 1999). To be conservative, the maximum reported value of 17:1 was rounded to 20:1 and set as the upper limit for horizontal anisotropy. Furthermore, although features such as high transmissivity zones and fractures may yield large local anisotropy ratios, their effects are globally attenuated and 20 is a reasonable maximum. The 5.5 anisotropy ratio calculated by the second approach of the modified Papadopulos-PEST method (BSC 2003a, Table 6.2-12) lies in this range. Therefore, between 5 and 20, a triangularly distributed anisotropy ratio was constructed that decreases to zero probability at 20. A 40 percent probability was assigned to this portion of the probability density function.

Anisotropy Ratio Between 0.05 and 1—Based on the existence of the Antler Wash fault and the uncertainty associated with the projected anisotropy discussed above, it is possible the media

could be isotropic, and there is a small probability that the principal direction could be east-west. Correspondingly, a north-south anisotropy ratio of less than one is possible, and the minimum anisotropy ratio was set equal to the inverse of the maximum, 1:20, with a triangularly distributed 10 percent probability decreasing to zero at a ratio of 0.05. One Papadopoulos solution yielding an anisotropy ratio of 3.5 at 79° west of north falls in this range (BSC 2003a).

Anisotropy Ratio Between 1 and 5—A uniformly distributed 50 percent probability is assigned to the range of anisotropy ratio between 1 and 5. This interval comprises the more likely values of anisotropy ratios with no specific value likelier than another. In addition, in the TSPA-SR model (CRWMS M&O 2000a) of the saturated zone near Yucca Mountain, anisotropy was binomially distributed with a 50 percent probability of isotropy (1:1) and a 50 percent probability of a 5:1 ratio (CRWMS M&O 2000a).

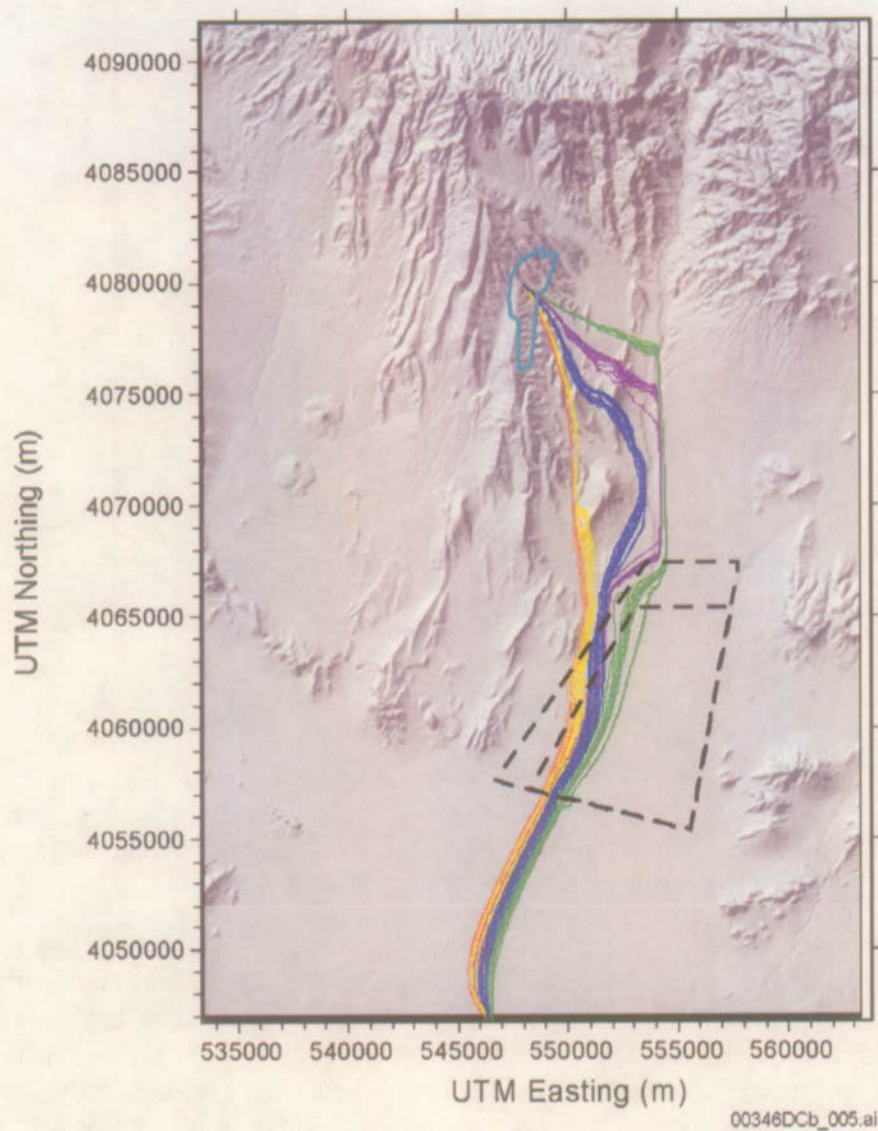
Based on a reevaluation of horizontal anisotropy in the site-scale model using a reinterpretation of the C-Wells testing data, Figure E-4 is the best estimate for the cumulative distribution of north-south anisotropy ratios in the saturated zone used as stochastic input to FEHM (LANL 2003) in the *SZ Flow and Transport Abstraction* (BSC 2003b).

E.4.6 Effects on Flow Path Length

There is considerable variation in the simulated flow paths (BSC 2003b) over the range of uncertainty in the horizontal anisotropy in permeability considered in the model (Figure E-5). The uncertainty distribution for horizontal anisotropy assigns 90 percent probability to a value of greater than 1 for the ratio of north-south to east-west permeability, and consequently, the most likely flow paths are to the west of the blue particle paths shown in Figure E-5.

E.4.7 FEHM Model Sensitivity Study

The sensitivity analysis of anisotropy ratio using the site-scale flow model (FEHM code) revealed that the modeled heads are only slightly sensitive to anisotropy ratio. Figure E-6 illustrates how varying the anisotropy ratio affects the weighted root-mean-square error between measured and FEHM modeled heads. The root-mean-square error ranges only between 6.9 and 7.6. Although this short range demonstrates relative insensitivity of the modeled heads to the anisotropy ratio, it is encouraging that the root-mean-square error decreases for anisotropy ratios between 0.05 to 20 and then subsequently increases.



Source: Repository outline: BSC 2003c; alluvial uncertainty zone: BSC 2003b.

NOTE: Green lines, purple lines, blue lines, yellow lines, and red lines show simulated particle paths for horizontal anisotropy values of 0.05, 0.20, 1.0, 5.0, and 20.0, respectively. The dashed lines show the minimum and maximum boundaries of the alluvial uncertainty zone.

Figure E-5. Simulated Particle Paths for Different Values of Horizontal Anisotropy in Permeability

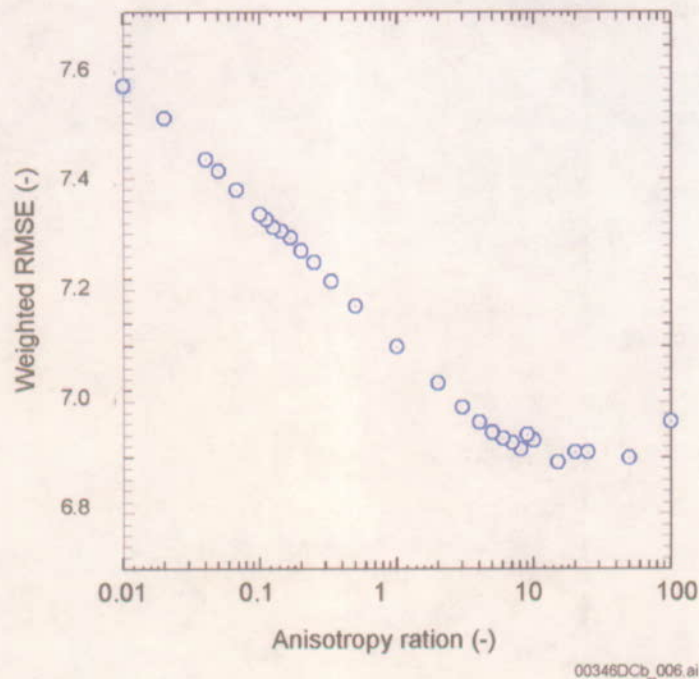


Figure E-6. Weighted Root-Mean-Square Error between Measured Heads and FEHM Modeled Heads Subject to a Range of Anisotropy Ratios between 0.01 and 100

Although analytical and graphical techniques yield a single, specific anisotropy ratio, this value is sensitive to the solution technique and interpretations of the data by the analyst (e.g., assumptions, filtering parameters, and how the slopes of drawdown were calculated). A wide distribution of anisotropy ratios is suggested to account for the uncertainty in this hydrogeologic property. Each run of FEHM must have a single value of anisotropy assigned to the appropriate zone, and although this is unrealistic (no single value of anisotropy truly applies to such a large heterogeneous area), drawing an anisotropy ratio from the specified distribution and running FEHM stochastically effectively accounts for the uncertainty in this model parameter.

Field data were analyzed to identify anisotropy in flow direction. The data was used to derive anisotropy distribution used in TSPA-LA.

E.5 REFERENCES

BSC (Bechtel SAIC Company) 2003a. *Saturated Zone In-Situ Testing*. ANL-NBS-HS-000039 REV 00A. Las Vegas, Nevada: Bechtel SAIC Company. ACC: MOL.20030602.0291.

BSC 2003b. *SZ Flow and Transport Model Abstraction*. MDL-NBS-HS-000021 REV 00A. Las Vegas, Nevada: Bechtel SAIC Company. ACC: MOL.20030612.0138.

BSC 2003c. *Repository Design, Repository/PA IED Subsurface Facilities*. 800-IED-EBS0-00401-000-00C. Las Vegas, Nevada: Bechtel SAIC Company. ACC: ENG.20030303.0002.

Cooper, H.H., Jr. and Jacob, C.E. 1946. "A Generalized Graphical Method for Evaluating Formation Constants and Summarizing Well-Field History." *Transactions, American Geophysical Union*, 27, (IV), 526-534. Washington, D.C.: American Geophysical Union. TIC: 225279.

CRWMS M&O (Civilian Radioactive Waste Management System Management and Operating Contractor) 2000a. *Total System Performance Assessment for the Site Recommendation*. TDR-WIS-PA-000001 REV 00 ICN 01. Las Vegas, Nevada: CRWMS M&O. ACC: MOL.20001220.0045.

CRWMS M&O 2000b. *Saturated Zone Flow and Transport Process Model Report*. TDR-NBS-HS-000001 REV 00 ICN 02. Las Vegas, Nevada: CRWMS M&O. ACC: MOL.20001102.0067.

CRWMS M&O 2000c. *Development Plan for Engineered Barrier System Features, Events and Processes, and Degradation Modes Analysis*. Development Plan TDP-EBS-MD-000010 REV 02. Las Vegas, Nevada: CRWMS M&O. ACC: MOL.20000421.0225.

Farrell, D.A.; Armstrong, A.; Winterle, J.R.; Turner, D.R.; Ferrill, D.A.; Stamatakos, J.A.; Coleman, N.M.; Gray, M.B.; and Sandberg, S.K. 1999. *Structural Controls on Groundwater Flow in the Yucca Mountain Region*. San Antonio, Texas: Center for Nuclear Waste Regulatory Analyses. TIC: 254265.

Ferrill, D.A.; Winterle, J.; Wittmeyer, G.; Sims, D.; Colton, S.; Armstrong, A.; and Morris, A.P. 1999. "Stressed Rock Strains Groundwater at Yucca Mountain, Nevada." *GSA Today*, 9, (5), 1-8. Boulder, Colorado: Geological Society of America. TIC: 246229.

Geldon, A.L. 1993. *Preliminary Hydrogeologic Assessment of Boreholes UE-25c #1, UE-25c #2, and UE-25c #3, Yucca Mountain, Nye County, Nevada*. Water-Resources Investigations Report 92-4016. Denver, Colorado: U.S. Geological Survey. ACC: MOL.19960808.0136.

Geldon, A.L.; Umari, A.M.A.; Earle, J.D.; Fahy, M.F.; Gemmell, J.M.; and Darnell, J. 1998. *Analysis of a Multiple-Well Interference Test in Miocene Tuffaceous Rocks at the C-Hole Complex, May-June 1995, Yucca Mountain, Nye County, Nevada*. Water-Resources Investigations Report 97-4166. Denver, Colorado: U.S. Geological Survey. TIC: 236724.

Geldon, A.L.; Umari, A.M.A.; Fahy, M.F.; Earle, J.D.; Gemmell, J.M.; and Darnell, J. 2002. *Results of Hydraulic Tests in Miocene Tuffaceous Rocks at the C-Hole Complex, 1995 to 1997, Yucca Mountain, Nye County, Nevada*. Water-Resources Investigations Report 02-4141. Denver, Colorado: U.S. Geological Survey. TIC: 253755.

Hantush, M.S. 1966. "Analysis of Data from Pumping Tests in Anisotropic Aquifers." *Journal of Geophysical Research*, 71, (2), 421-426. [Washington, D.C.: American Geophysical Union]. TIC: 225281.

Hsieh, P.A.; Neuman, S.P.; Stiles, G.K.; and Simpson, E.S. 1985. "Field Determination of the Three-Dimensional Hydraulic Conductivity Tensor of Anisotropic Media. 2. Methodology and Application to Fractured Rocks." *Water Resources Research*, 21, (11), 1667-1676. Washington, D.C.: American Geophysical Union. TIC: 254511.

LANL (Los Alamos National Laboratory) 2003. *Software Code: FEHM*. V2.20. SUN, PC. 10086-2.20-00.

Neuman, S.P. 1975. "Analysis of Pumping Test Data from Anisotropic Unconfined Aquifers Considering Delayed Gravity Response." *Water Resources Research*, 11, (2), 329-342. Washington, D.C.: American Geophysical Union. TIC: 222414.

Papadopoulos, I.S. 1967. "Nonsteady Flow to a Well in an Infinite Anisotropic Aquifer." *Hydrology of Fractured Rocks, Proceedings of the Dubrovnik Symposium, October 1965*. 1, 21-31. Gentbrugge, [Belgium]: Association Internationale d'Hydrologie Scientifique. TIC: 223152.

Reamer, C.W. and Williams, D.R. 2000. Summary Highlights of NRC/DOE Technical Exchange and Management Meeting on Unsaturated and Saturated Flow Under Isothermal Conditions. Meeting held August 16-17, 2000, Berkeley, California. Washington, D.C.: U.S. Nuclear Regulatory Commission. ACC: MOL.20001201.0072.

Streltsova-Adams, T.D. 1978. "Well Hydraulics in Heterogeneous Aquifer Formations." Volume 11 of *Advances in Hydroscience*. [Chow, V.T., ed.]. Pages 357-423. [New York, New York: Academic Press]. TIC: 225957.

Theis, C.V. 1935. "The Relation Between the Lowering of the Piezometric Surface and the Rate and Duration of Discharge of a Well Using Ground-Water Storage." *Transactions of the American Geophysical Union Sixteenth Annual Meeting, April 25 and 26, 1935, Washington, D.C.* Pages 519-524. Washington, D.C.: National Academy of Science, National Research Council. TIC: 223158.

Umari, M.J. 2002. Performing Various Hydraulic and Tracer Tests Using Prototype Pressure Transducer and Packer Assemblies. Scientific Notebook SN-USGS-SCI-036-V1. ACC: MOL.20020520.0364; MOL.20020520.0368; through; MOL.20020520.0382.

USGS (U.S. Geological Survey) 2002. *Software Code: Filter.vi*. V 1.0. PC, Windows 2000/NT 4.0/98. 10970-1.0-00.

Watermark Computing 2002. *Software Code: PEST*. V5.5. SUN, PC, Linux. 10289-5.5-00.

Winterle, J.R. and La Femina, P.C. 1999. *Review and Analysis of Hydraulic and Tracer Testing at the C-Holes Complex Near Yucca Mountain, Nevada*. San Antonio, Texas: Center for Nuclear Waste Regulatory Analyses. TIC: 246623.

APPENDIX F
FLOW-C14 RESIDENCE TIME
(RESPONSE TO USFIC 5.06)

Note Regarding the Status of Supporting Technical Information

This document was prepared using the most current information available at the time of its development. This Technical Basis Document and its appendices providing Key Technical Issue Agreement responses that were prepared using preliminary or draft information reflect the status of the Yucca Mountain Project's scientific and design bases at the time of submittal. In some cases this involved the use of draft Analysis and Model Reports (AMRs) and other draft references whose contents may change with time. Information that evolves through subsequent revisions of the AMRs and other references will be reflected in the License Application (LA) as the approved analyses of record at the time of LA submittal. Consequently, the Project will not routinely update either this Technical Basis Document or its Key Technical Issue Agreement appendices to reflect changes in the supporting references prior to submittal of the LA.

APPENDIX F

FLOW-C14 RESIDENCE TIME (RESPONSE TO USFIC 5.06)

This appendix provides a response for Key Technical Issue (KTI) agreement Unsaturated and Saturated Flow under Isothermal Conditions (USFIC) 5.06. This KTI agreement relates to providing more information about groundwater flow directions based on residence time of naturally occurring carbon-14 isotopes.

F.1 KEY TECHNICAL ISSUE AGREEMENT

F.1.1 USFIC 5.06

KTI agreement USFIC 5.06 was reached during the NRC/DOE technical exchange and management meeting on unsaturated and saturated flow under isothermal conditions held October 31 through November 2, 2000 in Albuquerque, New Mexico. The saturated zone portion of KTI subissues 5 and 6 were discussed at that meeting (Reamer and Williams 2000).

Wording of the agreement is as follows:

USFIC 5.06

Provide a technical basis for residence time (for example, using C-14 dating on organic carbon in groundwater from both tuffs and alluvium). DOE will provide the technical basis for residence time in an update to the Geochemical and Isotopic Constraints on Groundwater Flow Directions, Mixing, and Recharge at Yucca Mountain, Nevada AMR during FY 2002.

F.1.2 Related Key Technical Issue Agreements

None.

F.2 RELEVANCE TO REPOSITORY PERFORMANCE

Understanding and confirming groundwater flow paths and mixing zones using independent datasets is beneficial for ensuring that the results of predictive model can be relied on for the license application. Although advective transport properties are reasonably constrained by in situ observations from boreholes, these observations are limited by the time and space over which the testing was conducted. For example, the scale of the C-wells complex and the Alluvial Testing Complex are representative of spatial scales of 10s of meters and temporal scales of days to months. The transport processes of relevance to repository performance occur over spatial scales of kilometers and temporal scales of thousands of years.

One of the few methods to investigate relevant transport processes over the spatial and temporal scale of interest to repository performance is the use of naturally-occurring radioisotopes such as carbon-14. Section 3.2.3 describes the use of naturally-occurring radioisotopes for assessing the

flow of groundwater and radionuclide transport in the saturated zone beneath and downgradient from Yucca Mountain.

F.3 RESPONSE

The activity of carbon-14 has been measured (in percent modern carbon, pmc) in several boreholes in and adjacent to the site-scale model area (Figure F-1). Most boreholes had less than 30 pmc, but there were a few notable exceptions in northern Fortymile wash. The general trend of the data did not support decreasing carbon-14 along potential flow pathways from the proposed repository. The carbon reservoir (principally as bicarbonate) in groundwater is readily modified through reactions with aquifer rock along a flow pathway. Therefore, it is necessary to evaluate potential sources of carbon in the groundwater before using carbon-14 data to evaluate flow pathways or residence times.

Due to the non-conservative nature of carbon in groundwater, carbon isotopes are not used to evaluate flow pathways. Rather, the approach used was to evaluate potential flow pathways based on conservative species, principally chlorine and sulfate, in conjunction with the potentiometric surface map. After identifying potential flow paths, additional hydrochemical species were considered to evaluate whether they behave conservatively and are consistent with the flow paths, or if non-conservative behavior can be explained through reasonable chemical reactions. This iterative process resulted in determining the final potential flow paths. Carbon-14 data from groundwater along the potential flow pathways were then evaluated to determine transport time. Measured carbon-14 activities were corrected to account for decreases in carbon-14 activity that resulted from water-rock interactions and the mixing of groundwaters, as identified by the PHREEQC mixing and chemical reaction models. This process resulted in estimates of decreases in carbon-14 activity due to radioactive decay during transit between boreholes, which can be converted into transit time using the radioactive decay equation (Equation F-1). After determining the transit time between boreholes, linear groundwater velocities were determined by dividing the distance between the boreholes by the transit time. In a similar fashion, carbon-14 activity was used to evaluate the range of ages of water and the components of young water present in areas thought to be dominated by local recharge.

Given the distribution of ages calculated for perched waters, an average residence time was in the range of 10,000 to 13,000 yrs. This result is comparable with the range in ages (8,000 to 16,000 yr) calculated for saturated zone waters from carbon-14 measurements on dissolved organic carbon-14.

Carbon-13 results suggest that groundwater under Yucca Mountain is not simply groundwater that flowed southward from recharge areas to the north (e.g., Timber Mountain), but represents local recharge at Yucca Mountain and in areas immediately to the north (e.g., Yucca Wash and Pinnacles Ridge).

F.4 BASIS FOR THE RESPONSE

F.4.1 Identification of Flow Paths

Groundwater flow paths and mixing zones were identified based on measured and calculated geochemical and isotopic parameters. The hydraulic gradient, shown on the potentiometric

surface map (BSC 2003, Figure 4), was used to constrain flow directions. Chemical and isotopic composition of groundwater was then used to locate flow pathways in the context of the hydraulic gradient, considering the possibility that flow paths can be oblique to the potentiometric gradient because of anisotropy in permeability.

The analysis of flow paths assumes that chloride (Cl⁻) and sulfate (SO₄⁻²) values are conservative, and that changes to these species are due to mixing along flow paths. Flow paths can be traced using conservative constituents where compositional differences exist that allow some directions to be eliminated as possible flow directions. However, no single chemical or isotopic species varies sufficiently in the study area to determine flow paths everywhere. Therefore, multiple lines of evidence were used to construct flow paths, including the areal distribution of multiple chemical and isotopic species, potential sources of recharge, groundwater ages, and the evaluation of mixing and groundwater evolution through scatterplots and inverse mixing and reaction models.

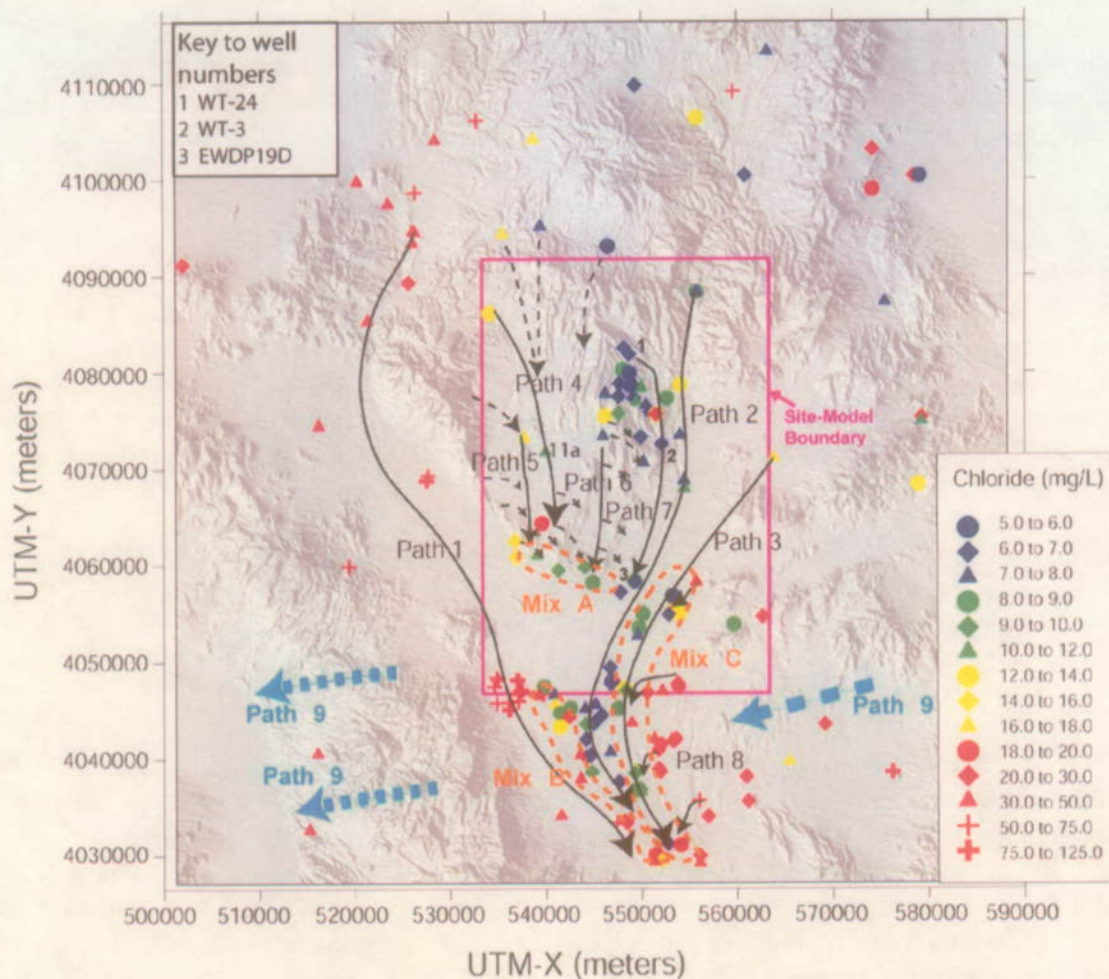
Figure F-1 presents flow pathways inferred from hydrochemical data (Cl⁻ illustrated). Groundwater transport time, based on carbon-14 activities, was evaluated for specific samples along flow paths near the repository, as discussed below.

F.4.2 Carbon Isotopes in the Environment

Carbon has two stable isotopes (carbon-12 and carbon-13) and a third isotope, carbon-14, which is radioactive. Carbon-14 is produced in the atmosphere by a variety of nuclear reactions, the most important of which is the interaction of cosmic ray neutrons with nitrogen-14. Carbon-14 is rapidly mixed in the atmosphere and incorporated into carbon dioxide (CO₂) where it is then available for incorporation into terrestrial carbonaceous materials. The radioactive decay of carbon-14, with a half-life of 5,730 years, forms the basis for radiocarbon dating. The carbon-14 age of a groundwater sample is calculated as

$$t = (-1/\lambda) \ln (^{14}A/^{14}A_0) \quad (\text{Eq. F-1})$$

where t is the mean groundwater age (yr), λ is the radioactive decay constant $1.21 \times 10^{-4} \text{ yr}^{-1}$; (Clark and Fritz 1997, p. 201), ^{14}A is the measured carbon-14 activity, and $^{14}A_0$ is the assumed initial activity. Carbon-14 activities (ages) typically are expressed in percent modern carbon (pmc). A carbon-14 activity of 100 pmc is taken as the carbon-14 activity of the atmosphere in the year 1890, before the natural ^{14}A of the atmosphere was diluted by large amounts of carbon-14-free carbon dioxide gas from burning fossil fuels (Clark and Fritz 1997, p. 18).



00346DCb_007.ai

Source: Based on BSC 2003, Figure 62.

Figure F-1. Regional Flow Paths Inferred from Hydrochemical and Isotopic Data

Theoretically, the activity of carbon-14 in a groundwater sample reflects the time at which the water was recharged. Unfortunately, precipitation generally is dilute and has a high affinity for dissolution of solid phases in the soil zone, unsaturated zone, and saturated zone. In particular, in the transition from precipitation compositions to groundwater compositions, the concentration of combined bicarbonate and carbonate in the water commonly increases by orders of magnitude (Langmuir 1997, Table 8.7; Meijer 2002). Because bicarbonate is the principal carbon-14-containing species in most groundwaters, the source of the additional bicarbonate can have a major impact on the “age” calculated from the carbon-14 activity of a given sample. If the source primarily is decaying plant material in an active soil zone, the calculated “age” for the water sample should be close to the real age. In contrast, if the source of the bicarbonate is the dissolution of old (i.e., older than 10^4 yr) calcite with low carbon-14 activity, or oxidation of old organic material, then the calculated age for the sample will be over estimated.

A useful measure of the source of the carbon in a water sample is the delta carbon-13 ($\delta^{13}\text{C}$) value of the sample because this value is different for organic materials and calcites. The $\delta^{13}\text{C}$ value, in units of per mil, is defined as

$$\delta^{13}\text{C} = \left[\frac{(^{13}\text{C}/^{12}\text{C})_{\text{sample}}}{(^{13}\text{C}/^{12}\text{C})_{\text{standard}}} - 1 \right] \times 1000 \quad (\text{Eq. F-2})$$

The standard used for reporting stable carbon isotope measurements is carbon from a belemnite fossil from the Cretaceous Peedee formation in South Carolina (Clark and Fritz 1997, p. 9).

The $\delta^{13}\text{C}$ values of plant matter in arid soils generally range from -25 to -13 per mil (Forester et al. 1999, p. 36). Soil waters can also dissolve atmospheric CO_2 , which has a $\delta^{13}\text{C}$ value of about -8 percent at Yucca Mountain. Pedogenic carbonate minerals at Yucca Mountain have $\delta^{13}\text{C}$ values that generally are between -8 and -4 per mil, although early-formed calcites from deep within Yucca Mountain (from the Exploratory Studies Facility) have $\delta^{13}\text{C}$ values greater than 0 per mil (Forester et al. 1999, Figure 16; Whelan et al. 1998, Figure 5). Paleozoic carbonate rocks typically have $\delta^{13}\text{C}$ values close to 0 per mil (Clark and Fritz 1997, Figure 5-12).

F.4.3 Delta Carbon-13 Data and Discussion

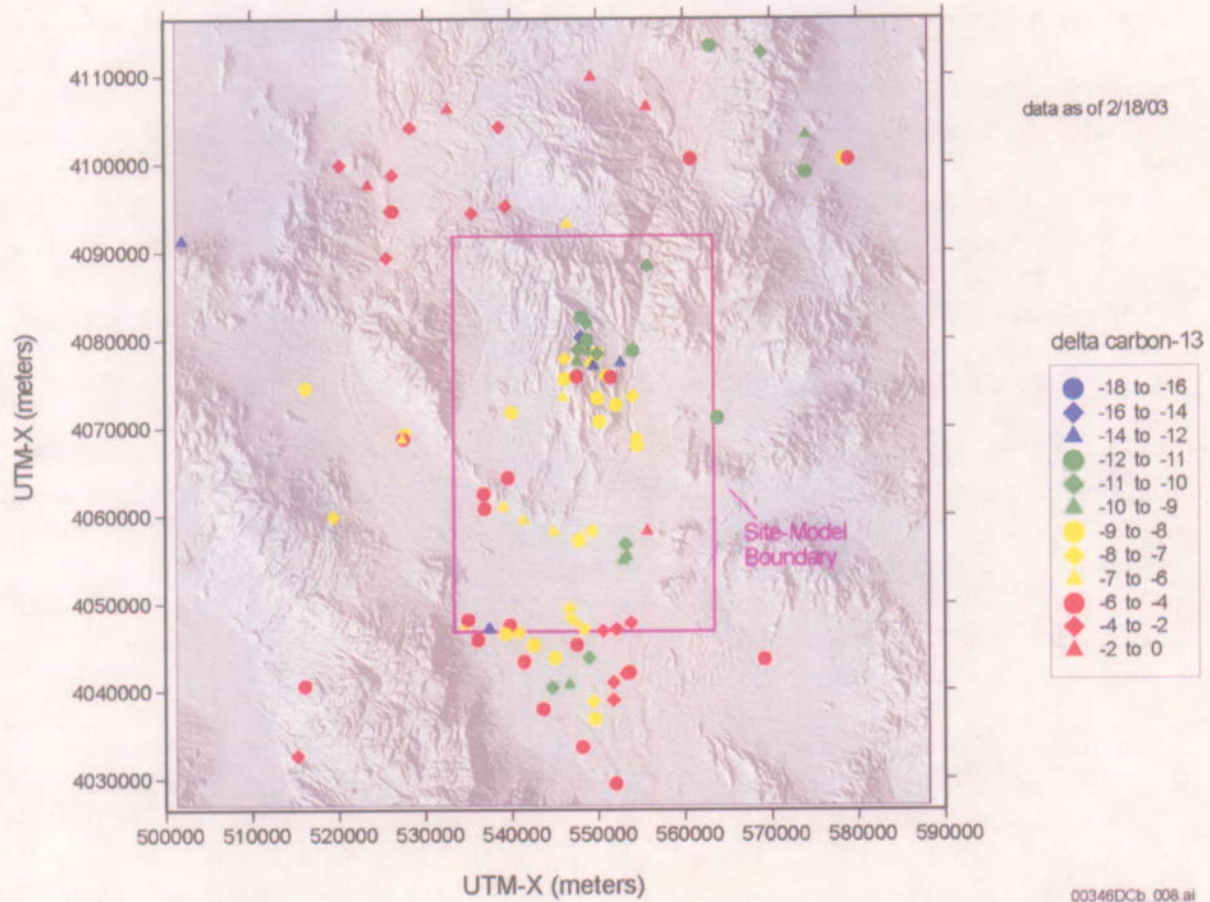
The areal distribution of delta carbon-13 ($\delta^{13}\text{C}$) values are shown in Figure F-2. Excluding data from borehole UE-25 p#1, where groundwater has $\delta^{13}\text{C}$ values of -2.3 per mil in the carbonate aquifer and -4.2 per mil in the volcanic aquifer, the $\delta^{13}\text{C}$ values of groundwater in the volcanic aquifer at Yucca Mountain vary between -14.4 per mil at borehole USW UZ-14 to -4.9 per mil at borehole USW H-3. Although patterns are complex on a borehole-by-borehole basis, groundwater in the northernmost part of Yucca Mountain is generally lighter in $\delta^{13}\text{C}$ than groundwaters toward the central and southern parts of the mountain.

North of Yucca Mountain, groundwater $\delta^{13}\text{C}$ values are generally considerably heavier than the groundwater $\delta^{13}\text{C}$ values found at Yucca Mountain. This suggests that groundwater at Yucca Mountain is not simply groundwater that flowed southward from recharge areas to the north (e.g., Timber Mountain). Only groundwater from borehole ER-EC-07 in Beatty Wash has a $\delta^{13}\text{C}$ within the range of values found at Yucca Mountain, Solitario Canyon Wash, and Crater Flat (borehole USW VH-1). The most likely explanation for these data is that there is substantial local recharge at Yucca Mountain and areas immediately to the north (e.g., Yucca Wash and Pinnacles Ridge).

The $\delta^{13}\text{C}$ values of groundwater in Nye County Early Warning Drilling Program (NC-EWDP) boreholes at the southern edge of Crater Flat are similar in value to those in groundwaters from boreholes in the southern portion of Yucca Mountain. Thus, these data provide little evidence of water-rock interaction (e.g., calcite dissolution) between groundwaters from these two areas. The westernmost NC-EWDP boreholes appear to sample groundwater from carbonate rocks with relatively large $\delta^{13}\text{C}$ values.

The $\delta^{13}\text{C}$ values of groundwater near Fortymile Wash generally increase from north to south within the site-model area, although local reversals in this trend are evident. The north-south variations in groundwater $\delta^{13}\text{C}$ values near Fortymile Wash are similar to those observed in

groundwaters from boreholes on Yucca Mountain (Figure F-2). This may reflect a major Yucca Mountain component in groundwaters in Fortymile Wash. Alternatively, it reflects similar processes operating on groundwater from north to south. Groundwater in Jackass Flats, and some groundwater at Lathrop Wells, has relatively light $\delta^{13}\text{C}$ values, despite the proximity of the Lathrop Wells group samples to groundwater near the Gravity fault with considerably higher $\delta^{13}\text{C}$ values.



Source: BSC 2003, Figure 27.

Figure F-2. Areal Distribution of Delta Carbon-13 in Groundwater

F.4.4 Carbon-14 Activity Data and Discussion

The areal distribution of carbon-14 activity is shown in Figure F-3. Excluding data from borehole UE-25 p#1, which has a carbon-14 activity of 2.3 pmc in the carbonate aquifer and 3.5 pmc in the volcanic aquifer, the carbon-14 activity of groundwater at Yucca Mountain ranges from 10.5 pmc at borehole USW H-3 to 27 pmc at borehole USW WT-24 in northern Yucca Mountain. Groundwater at the eastern edge of Crater Flat near Solitario Canyon has some of the lowest carbon-14 activities of groundwater in the map area, with values as low as 7.3 pmc at borehole USW WT-10 and 10 pmc in a sample from borehole USW H-6. Groundwater carbon-14 activities are slightly higher farther to the west in Crater Flat at borehole USW VH-1 (12 pmc). Groundwater samples collected from several NC-EWDP boreholes in the Yucca

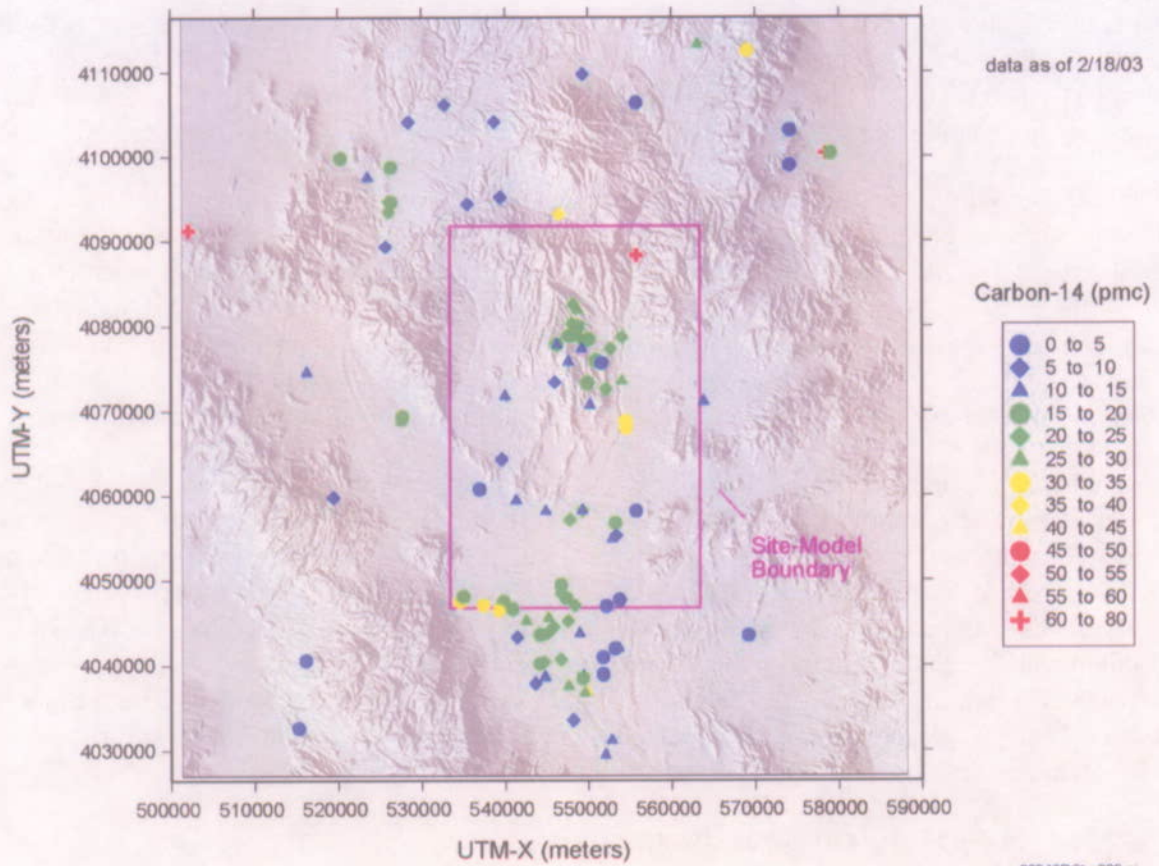
Mountain-South group to the south of borehole USW VH-1 had similar carbon-14 activities. Groundwater samples collected from boreholes NC-EWDP-2D, NC-EWDP-19P, and some zones in NC-EWDP-19D had carbon-14 activities of 20 pmc or more, similar to the carbon-14 activities of groundwater in Dune Wash and Fortymile Wash.

These data do not indicate a clear decrease in carbon-14 activity from north to south along likely flow paths. There is a relatively rapid decrease in carbon-14 activity in groundwater in boreholes between northern and central Yucca Mountain. Conversely, there is little variation in carbon-14 activities between central Yucca Mountain and the Nye County boreholes. As with the $\delta^{13}\text{C}$ data, the carbon-14 activity in groundwater samples from boreholes north of Beatty Wash is low. This is additional evidence that groundwater at Yucca Mountain has a large component of local recharge and is not simply groundwater that flowed southward from recharge areas to the north.

Groundwater samples collected near Fortymile Wash had carbon-14 activities that ranged from about 76 pmc at borehole UE-29 a#1 near the northern boundary of the model area, to values under 20 pmc near the southern boundary of the model area. The decrease in carbon-14 activities from north to south was irregular (Figure F-3) with the highest value in the northern-most borehole (UE-29 a#1) and the lowest value in borehole NC-EWDP-19D, which is a composite borehole sample. The decreasing trend in carbon-14 values would appear more consistent if data from boreholes between UE-29 a#1 and J-13 were removed. These boreholes have carbon-14 values lower than expected, which may reflect enhanced flow from the Yucca Mountain area into the Fortymile Wash flow path.

F.4.5 Carbon-14 Ages of Groundwater

Carbon-14 Ages of Dissolved Organic Carbon—Groundwater ages can be calculated directly from the carbon-14 activities of dissolved organic carbon if the carbon-14 activity of the recharge water is known. These ages, however, are maximum ages because organic material in the aquifer would contain no carbon-14 (except for newly drilled boreholes that can be contaminated by modern dissolved organic carbon). The carbon-13 activity of dissolved organic carbon is a good indicator of contamination problems if dissolved organic carbon from drilling fluids is present in the sample, or if old (potentially isotopically light) organic carbon is being leached from aquifer materials. Thirteen dissolved organic carbon measurements have been made on samples of ground water in the Yucca Mountain area. Most of the dissolved inorganic carbon ages for these waters are greater than 12,000 yrs, but range from 8,000 to 16,000 yrs. The youngest dissolved organic carbon and dissolved inorganic carbon radiocarbon ages are for water from upper Fortymile Canyon. These ages show a slight reverse discordance, such that the dissolved inorganic carbon ages are slightly younger than the dissolved organic carbon ages (Figure F-4).



00346DCb_009.ai

Source: BSC 2003, Figure 28.

Figure F-3. Areal Distribution of Carbon-14 in Groundwater

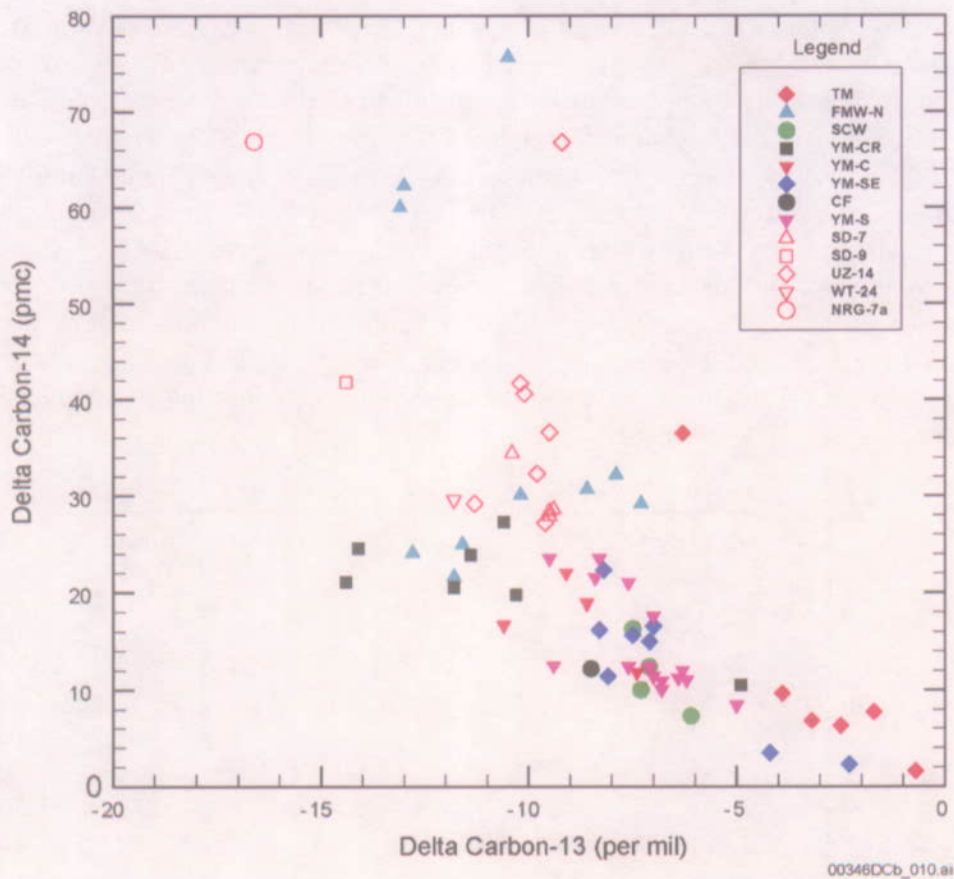
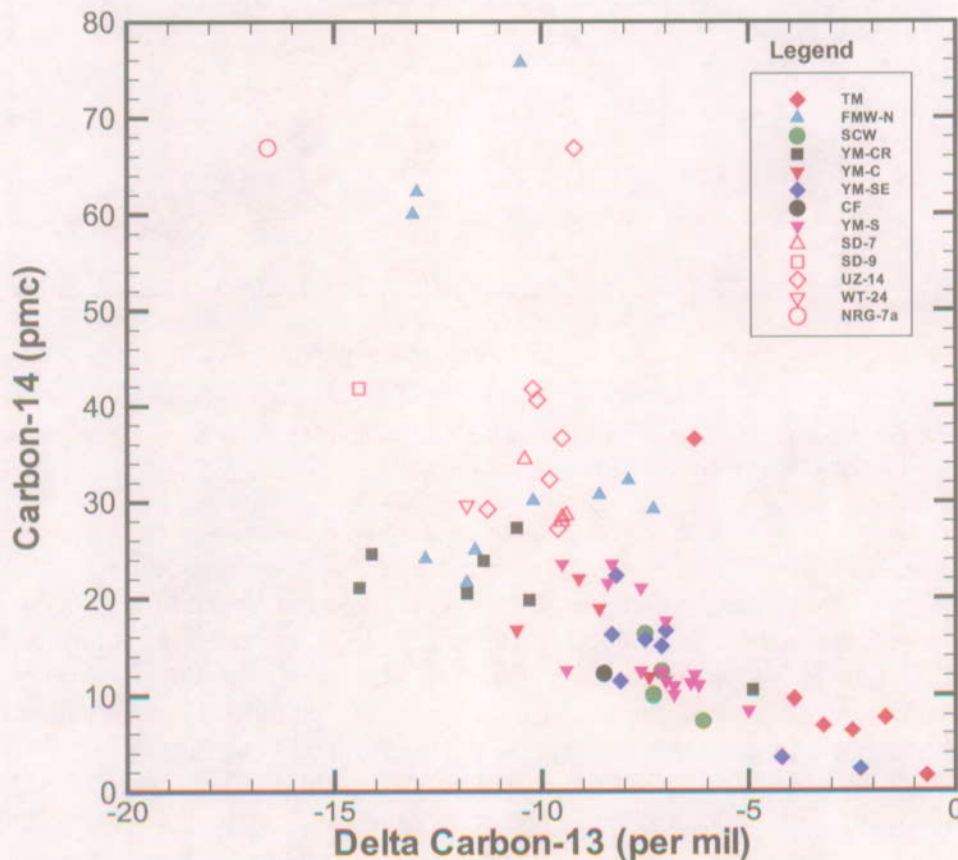


Figure F-4. Comparison of Observed Dissolved Organic and Inorganic Carbon-14 Ages in Groundwaters in the Vicinity of Yucca Mountain

Carbon-14 Ages of Perched Water—Although groundwater ages based on inorganic carbon are susceptible to modification through water-rock reactions, various observations indicate that the carbon-14 ages of the perched-water samples from boreholes on Yucca Mountain do not require substantial correction for the dissolution of carbonate. First, the ratios of chlorine-36 to stable chlorine ($^{36}\text{Cl}/\text{Cl}$) of the perched-water samples are similar to those expected for their uncorrected carbon-14 age, based on reconstructions of $^{36}\text{Cl}/\text{Cl}$ ratios in precipitation throughout the late Pleistocene and Holocene from pack-rat midden data (Plummer et al. 1997, Figure 3; DTN: LAJF831222AQ97.002; DTN: GS950708315131.003; DTN: GS960308315131.001). Second, Winograd et al. (1992, Figure 2) presented data from calcite deposits that indicated the $\delta^{18}\text{O}$ values in precipitation during the Pleistocene were, on average, 1.9 per mil more depleted during pluvial periods compared to interpluvial periods. The $\delta^{18}\text{O}$ values of the perched-water samples generally are more depleted than pore-water samples from the shallow unsaturated zone at Yucca Mountain by more than 1.0 per mil (BSC 2003, Figure 48). This consistent difference suggests that, at some boreholes, the perched water may contain a substantial component of Pleistocene-age water.

Carbon-14 Ages of Groundwater Based on Dissolved Inorganic Carbon—Values for $\delta^{13}\text{C}$ and carbon-14 in perched waters and groundwaters from the Yucca Mountain area are plotted in Figure F-5. Excluding perched-water samples and the Fortymile Wash area (FMW-N; a group

of boreholes east and northeast of Yucca Mountain), the $\delta^{13}\text{C}$ and carbon-14 values reported for the groundwater samples are negatively correlated. In the absence of chemical reactions or mixing, waters moving from source areas to Yucca Mountain should experience no change in $\delta^{13}\text{C}$, but the carbon-14 activity should decrease with time. If waters infiltrating into the source area have approximately constant $\delta^{13}\text{C}$ values, data points for waters infiltrated at different times would form a vertical trend in Figure F-5. The fact that the data points do not form a vertical trend suggests that the $\delta^{13}\text{C}$ of waters infiltrated at the source areas are not constant or that chemical reactions or mixing have affected the carbon isotope values. If waters that infiltrate into the source areas have randomly variable $\delta^{13}\text{C}$ ratios, then a random relation between $\delta^{13}\text{C}$ and carbon-14 values would be expected. Rather, the $\delta^{13}\text{C}$ and carbon-14 values for Yucca Mountain and Crater Flat groundwaters are well correlated, suggesting a relationship between these parameters.



Source: BSC 2003, Figure 45.

NOTE: Solid symbols are groundwater; open symbols are perched water.

Figure F-5. Carbon-14 Activity Versus Delta Carbon-13 of Perched Water and Groundwater Near Yucca Mountain

The $\delta^{13}\text{C}$ values of infiltrating waters reflect the types of vegetation present at the infiltration point. The $\delta^{13}\text{C}$ values of modern water that infiltrate in cooler climates (or at higher elevations) are more negative than the values for water that infiltrates in warmer climates (or at lower elevations; Quade and Cerling (1990, p. 1,550). This relation should produce in a positive correlation in Figure F-5 because the older samples (i.e., lowest pmc) would tend to have the most negative $\delta^{13}\text{C}$ (i.e., they infiltrated when the climate was cooler than it is now). Because the observed correlation in the groundwater values is negative, the primary cause of the correlation involves other processes.

Possible explanations for the observed trend are calcite dissolution and mixing with groundwater from the carbonate aquifer. Both of these processes tend to introduce dissolved inorganic carbon with heavy $\delta^{13}\text{C}$ and little carbon-14. This explanation assumes that points on the regression line are of the same age, but that the water dissolved different amounts of calcite. However, the scatter of points about the regression line could be due to inclusion of samples of different ages.

Carbon-14 ages, based on inorganic carbon, were calculated for locations at Yucca Mountain where groundwater had been identified (from anomalously high $^{234}\text{U}/^{238}\text{U}$ ratios) as originating mostly from local recharge (Paces et al. 1998). Corrections were also made to the carbon-14 ages of groundwater from several locations for which $^{234}\text{U}/^{238}\text{U}$ activity ratios were not measured, but which may contain substantial fractions of local Yucca Mountain recharge (based on proximity to groundwater with high $^{234}\text{U}/^{238}\text{U}$ activity ratios). As the local recharge would most likely have compositions close to that of perched water, perched water was used as a starting composition.

To calculate the correction factor, q , for the dissolution of calcite (i.e., dead inorganic carbon), the bicarbonate concentrations of the groundwaters were compared with the bicarbonate concentration of perched water. The difference was attributed to dissolution of calcite. The corrections assume that dissolved inorganic carbon of local recharge (as $\text{mDIC}_{\text{rech}}$) varies between 128.3 and 144 mg/L bicarbonate (HCO_3^-), based on values measured in perched water at Yucca Mountain (Yang et al. 1996). The correction factor ranges from 0.74 at borehole UE-25 WT #12, to 1.0 at several other boreholes (Table F-1). Corrected carbon-14 ages for groundwater range from 11,430 years at borehole UE-25 WT #3, to 16,390 years at borehole UE-25 WT #12 (Table F-1). These calculations show that only minor corrections to the groundwater carbon-14 ages are necessary for samples located along the estimated flow path from the repository.

Table F-1. Chemistry and Ages (Eq. F-1) of Groundwaters from Seven Boreholes at Yucca Mountain

Borehole	²³⁴ U/ ²³⁸ U Activity Ratio	carbon-14 Activity (pmc)	DIC, as HCO ₃ , (mg/L)	Log P _{CO2} (atm)	Log (IAP/K _{cal}) ^a	Factor q	Corrected carbon-14 age (years)	Uncorrected carbon-14 age (years)
USW G-2	7 to 8	20.5	127.6	-2.352	-0.791	1	13,100	13,100
UE-25 WT #17	7 to 8	16.2	150.0	-1.958	-1.175	0.86 to 0.96	13,750 to 14,710	15,040
UE-25 WT #3	7 to 8	22.3	144.3	-2.413	-0.515	0.89 to 1.0	11,430 to 12,380	12,400
UE-25 WT #12	7 to 8	11.4	173.9	-2.327	-0.313	0.74 to 0.83	15,430 to 16,390	17,950
UE-25 C #3	7 to 9	15.7	140.2	-2.458	-0.319	0.92 to 1.0	14,570 to 15,300	15,300
UE-25 B #1 (Tcb) ^b	---	18.9	152.3	-1.892	-0.757	0.84 to 0.95	12,350 to 13,300	13,770
USW G-4	---	22.0	142.8	-2.490	-0.305	0.90 to 1.0	11,630 to 12,510	12,500

NOTES: DIC = dissolved inorganic carbon.

^a Log (IAP/K_{cal}) is the calcite saturation index. Negative values indicate undersaturation with calcite.

^b The sample from borehole UE-25 B#1 came from the Bullfrog Tuff (Tcb).

F.4.6 Evaluation of Groundwater Velocities in the Yucca Mountain Region

Groundwater velocities were estimated along various flow path segments using the groundwater carbon-14 activities along the flow path. Measured carbon-14 activities at the upgradient borehole were adjusted to account for decrease in carbon-14 activity that results from water-rock interactions between boreholes, as identified by PHREEQC mixing and chemical reaction models (described in BSC 2003). The adjustment is necessary to distinguish between the decrease in carbon-14 activity caused by water-rock interaction and the decrease in activity due to transit time between the boreholes. After determining the transit time between boreholes, linear groundwater velocities were determined by dividing the distance between the boreholes by the transit time.

The transit time between boreholes was calculated from the radioactive decay equation for carbon-14 (Equation F-1). A variety of methods have been used to estimate the value of ¹⁴A₀ for use with the radioactive decay law (Clark and Fritz 1997, Chapter 8). One simple method, which can be used to correct for the effects of calcite (or dolomite) dissolution when the downgradient groundwater evolves from a single upgradient source, is to compare the total dissolved inorganic carbon in the upgradient borehole (*m*_{DIC-U}) with the dissolved inorganic carbon of the downgradient groundwater (*m*_{DIC-D}) (Clark and Fritz 1997, p. 209):

$$q_{\text{DIC}} = \frac{m_{\text{DIC-U}}}{m_{\text{DIC-D}}} \quad (\text{Eq. F-3})$$

The value of q_{DIC} represents the fraction of dissolved inorganic carbon in the downgradient water that originated from the upgradient borehole, with the remainder acquired from water-rock-gas interactions. Therefore, the initial value of $^{14}\text{A}_0$ is the product of q_{DIC} and the measured carbon-14 activity at the upgradient borehole ($^{14}\text{A}_\text{U}$):

$$^{14}\text{A}_0 = ^{14}\text{A}_\text{U} \times q_{\text{DIC}} \quad (\text{Eq. F-4})$$

This method assumes that after infiltration reaches the saturated zone, the water is effectively isolated from further interaction with carbon dioxide gas in the unsaturated zone, and that any downgradient increases in the dissolved inorganic carbon of the groundwater are a result of interactions with carbon-bearing minerals. The carbon-14 content of these minerals is assumed to be depleted, which is probably the case because most saturated zone calcite was formed during a 10-million-year-old hydrothermal event or during deposition under unsaturated conditions when the water table was lower than today (Whelan et al. 1998). Thus, although the proportions of dissolved carbon dioxide gas, bicarbonate, and carbonate may change with pH as the groundwater interacts with the rock, the total dissolved inorganic carbon is fixed unless the groundwater reacts with calcite. This method would not account for interactions between groundwater and calcite after the groundwater became saturated with calcite, nor would it account for the effects of groundwater mixing. This method was applied to obtain preliminary estimates where the upgradient groundwater was undersaturated with calcite and mixing was not considered an important process (based on the PHREEQC inverse models).

For flow path segments where PHREEQC inverse models indicate that downgradient groundwater evolves from a single upgradient borehole, the value of $^{14}\text{A}_\text{U}$ is simply groundwater ^{14}A at the upgradient borehole, and q_{DIC} is computed as

$$q_{\text{DIC}} = (\text{DIC}_\text{u}) / (\text{DIC}_\text{U} + \text{DIC}_{\text{carbonate}}) \quad (\text{Eq. F-5})$$

where DIC_U is the dissolved inorganic carbon at the upgradient borehole, and $\text{DIC}_{\text{carbonate}}$ is the amount of carbon contributed by water-rock interactions involving carbonate rocks.

For flow path segments where the PHREEQC inverse models identified mixing as having an important affect on the downgradient groundwater chemistry, the values of $^{14}\text{A}_\text{U}$ and q_{DIC} are calculated as

$$^{14}\text{A}_\text{U} = (f_1 ^{14}\text{A}_1 \text{DIC}_1 + f_2 ^{14}\text{A}_2 \text{DIC}_2 + \dots + f_i ^{14}\text{A}_i \text{DIC}_i) / (f_1 \text{DIC}_1 + f_2 \text{DIC}_2 + \dots + f_i \text{DIC}_i) \quad (\text{Eq. F-6})$$

and

$$q_{\text{DIC}} = (f_1 \text{DIC}_1 + f_2 \text{DIC}_2 + \dots + f_i \text{DIC}_i) / (f_1 \text{DIC}_1 + f_2 \text{DIC}_2 + \dots + f_i \text{DIC}_i + \text{DIC}_{\text{carbonate}}) \quad (\text{Eq. F-7})$$

where, f_1 to f_i are the fractions of various upgradient components in the mixture and the subscripts 1, 2, ... i indicate the component in the mixture. The equations do not consider the effects of CO_2 degassing, dissolution, or calcite precipitation. This simplification is acceptable because the fractionation factor for carbon-14 is small (Clark and Fritz 1997) and the carbon-14 in the CO_2 or calcite exiting the groundwater should leave the carbon-14 in the groundwater

relatively unchanged. Gas dissolution by the groundwater should not occur in most instances because the log P_{CO_2} of the groundwater is higher than that of the overlying unsaturated zone (BSC 2003, Section 6.5.5).

Flow path segment USW WT-3 to NC-EWDP-19D—Results from the PHREEQC inverse models (BSC 2003, Section 6.5.8) indicate that groundwater sampled from various zones in borehole NC-EWDP-19D could have evolved from groundwater in the vicinity of borehole USW WT-3. Transit times were calculated using the dissolved inorganic carbon of groundwater at borehole USW WT-3 and PHREEQC estimates of the carbon dissolved by this groundwater as it moves toward various zones at borehole NC-EWDP-19D (Table F-2). Groundwater in the composite borehole and alluvial groundwaters require approximately 1,000 to 2,000 years to travel between boreholes USW WT-3 and NC-EWDP-19D, a distance of approximately 15-km. This equates to linear groundwater velocities of approximately 7.5 to 15 m/yr. The groundwater in the deeper alluvial zones (Zones 3 and 4) of borehole NC-EWDP-19D requires approximately 1,500 to 3,000 years, and therefore travels at a linear groundwater velocity of 5 to 10 m/yr. In contrast, the transit times calculated for groundwater from shallow Zones 1 and 2 have transit times that range from 0 to about 350 years. Most of the calculated groundwater transit times were negative, indicating that the differences between carbon-14 activities in the groundwater at borehole USW WT-3 and these zones in borehole NC-EWDP-19D was too small, and that the uncertainty in dissolved inorganic carbon reactions estimated by PHREEQC too large, to adequately resolve the transit times. Using the upper age of 350 years, groundwater flow from borehole USW WT-3 to Zones 1 and 2 in borehole NC-EWDP-19D is about 40 m/yr. This relatively high velocity may indicate that some of the shallow groundwater at borehole USW WT-3 moves along major faults (e.g., the Paintbrush Canyon fault).

Flow path segment USW WT-24 to USW WT-3—Transit times were calculated using the dissolved inorganic carbon of groundwater at borehole USW WT-24 and PHREEQC estimates of the carbon dissolved by the groundwater as it moves toward borehole USW WT-3 (Table F-3). Transit times based on the PHREEQC models range from 0 to slightly over 1,000 years. The transit time estimate based on the differences in dissolved inorganic carbon of groundwater at boreholes USW WT-24 and USW WT-3 is 216 years. Using this estimate of transit time and a linear distance between boreholes USW WT-24 and USW WT-3 of 10 km, the linear groundwater velocity is 46 m/yr. The longest transit time (1,023 years) results in a groundwater velocity of about 10 m/yr.

Table F-2. Calculated Groundwater Transport Times between Borehole USW WT-3 and Various Depth Zones in Borehole NC-EWDP-19D

Model Number ^a	Open Borehole	Alluvium Composite	Zone 1 ^b	Zone 2	Zone 3	Zone 4
1	2332	2048	0	0	2151	2802
2	2275	2535	0	0	2521	2802
3	2325	2334	0	0	2894	2800
4	2325	2535	359	70	2968	2800
5	2332	2048	0	0	2941	2798
6	2273	2049	0	295	2149	2798
7	2328	2049	0	0	2149	---
8	2275	2501	359	0	2521	---
9	2328	2050	0	0	2521	---
10	2324	2050	186	0	2521	---
11	2273	---	305	---	3027	---
12	2325	---	0	---	---	---
13	2325	---	0	---	---	---
DIC estimate ^c	866	1063	0	188	1601	1681

NOTES: DIC = dissolved inorganic carbon. "—" means that no model was produced beyond those indicated by the numerical values.

^a Model number refers to various PHREEQC models produced for that zone using groundwater from USW WT-3 as the source groundwater.

^b Zones 1 to 4 are all isolated zones in alluvium. When negative transit times were calculated, the value was set to 0 years.

^c DIC estimate refers to the transit time estimate made from the measured dissolved inorganic carbon at borehole USW WT-3 and that particular zone in borehole NC-EWDP-19D.

Table F-3. Calculated Groundwater Transport Times between Boreholes USW WT-24 and USW WT-3

PHREEQC model	Transit time (yr)
1	0
2	555
3	725
4	0
5	0
6	749
7	430
8	717
9	567
10	0
11	1,023
12	883
13	0
DIC estimate	216

NOTE: When negative transit times were calculated, the value was set to 0 years. DIC = dissolved inorganic carbon.

Under ideal circumstances, the decrease in groundwater carbon-14 activities along a flow path can be used to calculate groundwater velocities. The calculation is straightforward when groundwater recharge occurs in a single location and groundwater downgradient from this location does not receive additional recharge or mix with other groundwater. In the Yucca Mountain area, calculating groundwater velocity based on carbon-14 activity is complicated by the possible presence of multiple, distributed recharge areas. If relatively young recharge were added along a flow path, the carbon-14 activity of the mixed groundwater would be higher and the calculated transport times shorter than for the premixed groundwater without the downgradient recharge. Unfortunately, the chemical and isotopic characteristics of the recharge from various areas at Yucca Mountain may not be sufficiently distinct to identify separate sources of local recharge in the groundwater. Conversely, if groundwater from the carbonate aquifer were to mix downgradient with Yucca Mountain recharge, the mixture would have a lower carbon-14 activity than the Yucca Mountain recharge component because of the high carbon alkalinity and low carbon-14 activity of the carbonate aquifer groundwater. However, the presence of groundwater from the carbonate aquifer in the mixture would be recognized because of the distinct chemical and isotopic composition of that groundwater compared with the recharge water, and the effect on the carbon-14 activity of the groundwater mixture could be calculated.

F.4.7 Residence Times

The residence time for water that originates at the repository level and subsequently moves to the accessible environment is calculated as the sum of the average age of perched water corrected for travel time from the surface to the perched water horizon and the transit times calculated for water moving from USW WT-24 to the accessible environment. The ages calculated for perched water range from 7,000 to 11,000 yr based on the carbon-14 activities of perched water samples assuming $^{14}\text{A}_0$ equals 100 pmc (BSC 2003). The travel times calculated for water infiltrated at the surface and percolated to the perched water zones range from 1,000 to 4,000 yr (Letter Report from Ed Kwicklis to Al Eddebbahr, December 2001). Most of this travel time is taken up in the bedded tuffs of the PTn. Thus, the residence time for water in the perched zones ranges from 3,000 to 10,000 yr. A single sample from borehole NRG-7a, and one of several samples from UZ-14, had much younger carbon-14 ages of about 3,300 yr. These samples were obtained with bailers instead of pumps. They are waters that stagnated in the borehole for some period of time. Therefore, it is more likely for them to have been compromised by mixing with atmospheric gases than waters pumped from the formation. If these samples are included, the water residence time in the perched zones would range from 0 to 10,000 yr.

When the residence time of water in the perched zones is combined with the estimates of travel time between WT-24 and the accessible environment, a range of total residence times of 0 to 10,000 yr is obtained. The low end of this range is very model dependent (PHREEQC) and likely an underestimate. When compared to the range in ages (8,000 to 16,000 yr) calculated for saturated zone waters from carbon-14 measurements on dissolved organics, the 0 to 10,000 yr range also appears to underestimate the true range in residence times unless saturated zone waters are on the order of 8,000 yr old when they reach Yucca Mountain from upgradient locations. The strong evidence for local recharge (i.e., uranium-234/uranium-238, carbon-13, and carbon-14 data) suggests this scenario is not correct. Thus, the carbon-14 analysis of

residence times appears to underestimate the residence times for water between the repository and the accessible environment.

F.5 REFERENCES

F.5.1 Documents Cited

BSC (Bechtel SAIC Company) 2003. *Geochemical and Isotopic Constraints on Groundwater Flow Directions and Magnitudes, Mixing, and Recharge at Yucca Mountain*. ANL-NBS-HS-000021 REV 01A. Las Vegas, Nevada: Bechtel SAIC Company. ACC: MOL.20030604.0164.

Clark, I.D. and Fritz, P. 1997. *Environmental Isotopes in Hydrogeology*. Boca Raton, Florida: Lewis Publishers. TIC: 233503.

Forester, R.M.; Bradbury, J.P.; Carter, C.; Elvidge-Tuma, A.B.; Hemphill, M.L.; Lundstrom, S.C.; Mahan, S.A.; Marshall, B.D.; Neymark, L.A.; Paces, J.B.; Sharpe, S.E.; Whelan, J.F.; and Wigand, P.E. 1999. *The Climatic and Hydrologic History of Southern Nevada During the Late Quaternary*. Open-File Report 98-635. Denver, Colorado: U.S. Geological Survey. TIC: 245717.

Langmuir, D. 1997. *Aqueous Environmental Geochemistry*. Upper Saddle River, New Jersey: Prentice Hall. TIC: 237107.

Meijer, A. 2002. "Conceptual Model of the Controls on Natural Water Chemistry at Yucca Mountain, Nevada." *Applied Geochemistry*, 17, ([6]), 793-805. [New York, New York]: Elsevier. TIC: 252808.

Paces, J.B.; Ludwig, K.R.; Peterman, Z.E.; Neymark, L.A.; and Kenneally, J.M. 1998. "Anomalous Ground-Water ²³⁴U/²³⁸U Beneath Yucca Mountain: Evidence of Local Recharge?" *High-Level Radioactive Waste Management, Proceedings of the Eighth International Conference, Las Vegas, Nevada, May 11-14, 1998*. Pages 185-188. La Grange Park, Illinois: American Nuclear Society. TIC: 237082.

Plummer, M.A.; Phillips, F.M.; Fabryka-Martin, J.; Turin, H.J.; Wigand, P.E.; and Sharma, P. 1997. "Chlorine-36 in Fossil Rat Urine: An Archive of Cosmogenic Nuclide Deposition During the Past 40,000 Years." *Science*, 277, 538-541. Washington, D.C.: American Association for the Advancement of Science. TIC: 237425.

Quade, J. and Cerling, T.E. 1990. "Stable Isotopic Evidence for a Pedogenic Origin of Carbonates in Trench 14 Near Yucca Mountain, Nevada." *Science*, 250, 1549-1552. Washington, D.C.: American Association for the Advancement of Science. TIC: 222617.

Reamer, C.W. and Williams, D.R. 2000. Summary Highlights of NRC/DOE Technical Exchange and Management Meeting on Unsaturated and Saturated Flow Under Isothermal Conditions. Washington, D.C.: U.S. Nuclear Regulatory Commission. ACC: MOL.20001128.0206.

Whelan, J.F.; Moscati, R.J.; Roedder, E.; and Marshall, B.D. 1998. "Secondary Mineral Evidence of Past Water Table Changes at Yucca Mountain, Nevada." *High-Level Radioactive Waste Management, Proceedings of the Eighth International Conference, Las Vegas, Nevada, May 11-14, 1998*. Pages 178-181. La Grange Park, Illinois: American Nuclear Society. TIC: 237082.

Winograd, I.J.; Coplen, T.B.; Landwehr, J.M.; Riggs, A.C.; Ludwig, K.R.; Szabo, B.J.; Kolesar, P.T.; and Revesz, K.M. 1992. "Continuous 500,000-Year Climate Record from Vein Calcite in Devils Hole, Nevada." *Science*, 258, 255-260. Washington, D.C.: American Association for the Advancement of Science. TIC: 237563.

Yang, I.C.; Rattray, G.W.; and Yu, P. 1996. Interpretation of Chemical and Isotopic Data from Boreholes in the Unsaturated Zone at Yucca Mountain, Nevada. Water-Resources Investigations Report 96-4058. Denver, Colorado: U.S. Geological Survey. ACC: MOL.19980528.0216.

F.5.2 Source Data, Listed by Data Tracking Number

GS950708315131.003. Woodrat Midden Age Data in Radiocarbon Years Before Present. Submittal date: 07/21/1995.

GS960308315131.001. Woodrat Midden Radiocarbon (C14). Submittal date: 03/07/1996.

LAFJ831222AQ97.002. Chlorine-36 Analyses of Packrat Urine. Submittal date: 09/26/1997.

APPENDIX G

**UNCERTAINTY IN FLOW PATH LENGTHS IN TUFF AND ALLUVIUM
(RESPONSE TO RT 2.08, RT 3.03, AND USFIC 5.04)**

Note Regarding the Status of Supporting Technical Information

This document was prepared using the most current information available at the time of its development. This Technical Basis Document and its appendices providing Key Technical Issue Agreement responses that were prepared using preliminary or draft information reflect the status of the Yucca Mountain Project's scientific and design bases at the time of submittal. In some cases this involved the use of draft Analysis and Model Reports (AMRs) and other draft references whose contents may change with time. Information that evolves through subsequent revisions of the AMRs and other references will be reflected in the License Application (LA) as the approved analyses of record at the time of LA submittal. Consequently, the Project will not routinely update either this Technical Basis Document or its Key Technical Issue Agreement appendices to reflect changes in the supporting references prior to submittal of the LA.

APPENDIX G

UNCERTAINTY IN FLOW PATH LENGTHS IN TUFF AND ALLUVIUM (RESPONSE TO RT 2.08, RT 3.03, AND USFIC 5.04)

This appendix provides a response for Key Technical Issue (KTI) agreements Radionuclide Transport (RT) 2.08, RT 3.03, and Unsaturated and Saturated Flow under Isothermal Conditions (USFIC) 5.04. These KTI agreements relate to providing additional information about flow path uncertainties in the alluvium and tuff.

G.1 KEY TECHNICAL ISSUE AGREEMENTS

G.1.1 RT 2.08, RT 3.03, and USFIC 5.04 Agreements

KTI agreements RT 2.08 and RT 3.03 were reached during the NRC/DOE technical exchange and management meeting on radionuclide transport held December 5 through 7, 2000, in Berkeley, California. Radionuclide transport KTI subissues 1, 2 and 3 were discussed at that meeting (Reamer and Williams 2000a).

KTI agreement USFIC 5.04 was reached during the NRC/DOE technical exchange and management meeting on unsaturated and saturated flow under isothermal conditions held October 31 through November 2, 2000 in Albuquerque, New Mexico. The saturated zone portion of KTI subissues 5 and 6 were discussed at that meeting (Reamer and Williams 2000b).

Wording of these agreements is as follows:

RT 2.08

Provide additional information to further justify the uncertainty distribution of flow path lengths in the alluvium. This information currently resides in the Uncertainty Distribution for Stochastic Parameters AMR. DOE will provide additional information, to include Nye County data as available, to further justify the uncertainty distribution of flowpath lengths in alluvium in updates to the Uncertainty Distribution for Stochastic Parameters AMR and to the Saturated Zone Flow and Transport PMR, both expected to be available in FY 2002.

RT 3.03

Provide additional information to further justify the uncertainty distribution of flow path lengths in the tuff. This information currently resides in the Uncertainty Distribution for Stochastic Parameters AMR. DOE will provide additional information, to include Nye County data as available, to further justify the uncertainty distribution of flowpath lengths from the tuff at the water table through the alluvium at the compliance boundary in updates to the Uncertainty Distribution for Stochastic Parameters AMR and to the Saturated Zone Flow and Transport Process Model Report, both expected to be available in FY 2002.

USFIC 5.04

Provide additional information to further justify the uncertainty distribution of flow path lengths in the alluvium. This information currently resides in the Uncertainty Distribution for Stochastic Parameters AMR. DOE will provide additional information, to include Nye County data as available, to further justify the uncertainty distribution of flowpath lengths in alluvium in updates to the Uncertainty Distribution for Stochastic Parameters AMR and to the Saturated Zone Flow and Transport PMR, both expected to be available in FY 2002.”

G.1.2 Related Key Technical Issue Agreements

RT 2.08, RT 3.03 and USFIC 5.04 all pertain to questions regarding flow paths. RT 3.03 only differs in that it discusses flow paths in tuff rather than alluvium. All three agreements are addressed in this appendix.

G.2 RELEVANCE TO REPOSITORY PERFORMANCE

The subject of these agreements is the further definition of flow path length uncertainty in the tuffs and alluvium. This is directly relevant to the uncertainty of saturated zone flow and transport model output and, subsequently, to performance assessment. Characterization of the flow paths, including uncertainty, comprises part of the characterization work and a description of the hydrology. Flow paths are part of the output of the saturated zone flow and transport model, therefore, directly affect performance assessment.

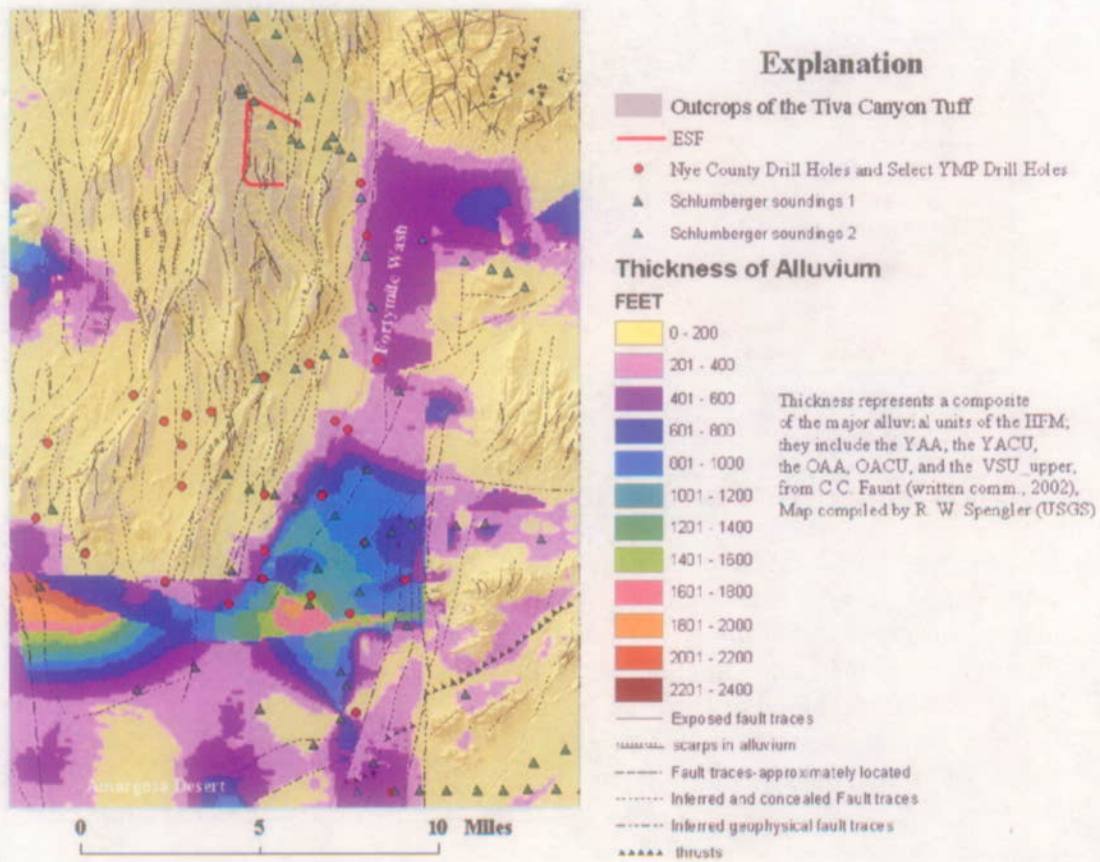
Groundwater flow path lengths in the saturated zone to the accessible environment affect the potential transport of radionuclides. Because the flow paths are close to the water table and transition from the volcanic tuffs to the alluvium, flow-path uncertainty directly affects the length of flow in the volcanic tuffs and in the alluvium. In particular, the relative lengths of the flow path in the tuff and the alluvium may have a large effect on the transport times of potential radionuclides through the saturated zone system because of different transport characteristics in the two media. The tuff aquifer is a fractured medium in which groundwater flow is limited to the fracture network and access to the rock matrix porosity depend on the relatively slow process of matrix diffusion. The alluvium aquifer is a porous medium in which the groundwater flow is more widely distributed and groundwater velocities are slower relative to the tuff aquifer. In addition, the sorption coefficient for some radionuclides (e.g., ²³⁷Np) may be higher in alluvium than in the tuff matrix, leading to longer transport times in the alluvium relative to the tuff aquifer.

Additional discussion related to this subject is provided in Section 3.

G.3 RESPONSE

Uncertainty in the length of the saturated zone flow paths in tuff and alluvium is related to uncertainties in two underlying characteristics of the saturated zone system. First, there is uncertainty in the contact location between the tuff and the alluvium. Second, there is uncertainty in the specific groundwater flow directions and the resulting flow pathways from beneath the repository to the accessible environment. Interaction between these two sources of

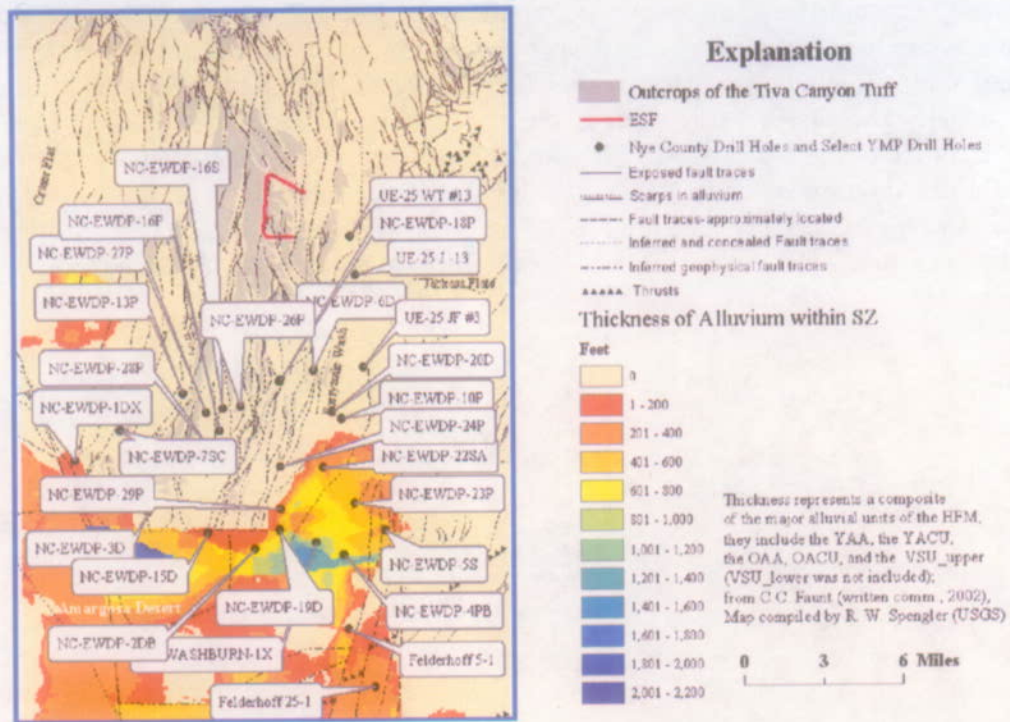
uncertainty accounts for the overall uncertainty in the flow path lengths in the tuff and alluvium. Uncertainty in the subsurface geology has been reduced in the area near the contact between the tuff and alluvium at the water table by wells in the Nye County Early Warning Drilling Program (Figure G-1a and G-1b). Figure G-1 shows saturated alluvium thickness. Lithologic and water-level data from wells have been used to constrain the uncertainty in the location at which groundwater flow moves from the tuff to the alluvium. Uncertainty in flow paths through the tuff aquifer has been evaluated through analyses and quantification of uncertainty in the horizontal anisotropy of permeability (Appendix E). These analyses are based on reevaluation of pumping test data from the C-wells Complex (BSC 2003a).



00346DCb_011.ai

Source: DTN: GS021008312332.002

Figure G-1a. Thickness of Alluvial Deposits in the Vicinity of Yucca Mountain



003460Cb_012.ai

Source: DTN: GS021008312332.002

Figure G-1b. Saturated Thickness of Alluvial Deposits in the Vicinity of Yucca Mountain

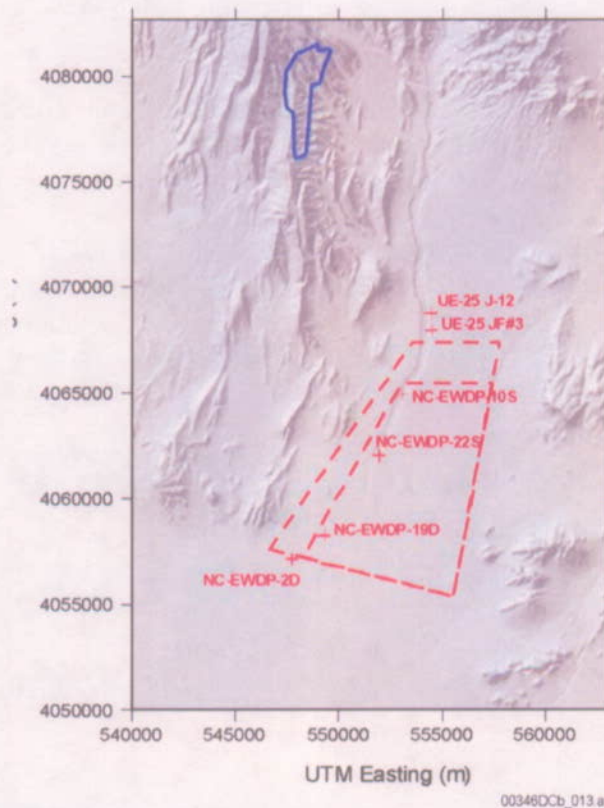
The total flow path length from beneath the repository to the compliance boundary varies from about 14.5 km to 22 km, depending on the source location beneath the repository and the horizontal anisotropy in permeability in the volcanic units (BSC 2003b, Table 6-7). Uncertainty in the flow path length in the alluvium varies from about 1 to 10 km, also depending on the source location beneath the repository, the horizontal anisotropy in permeability in the volcanic units, and the location of the western boundary of the alluvium uncertainty zone (BSC 2003b, Table 6-7). The technical bases for the uncertainty in flow path lengths in tuff and alluvium is currently provided in *SZ Flow and Transport Model Abstraction* (BSC 2003b). Technical discussions on this subject, originally presented in *Uncertainty Distribution for Stochastic Parameters* (CRWMS M&O 2000), have been incorporated into *SZ Flow and Transport Model Abstraction* (BSC 2003b).

G.4 BASIS FOR THE RESPONSE

G.4.1 Hydrogeologic Uncertainty

Uncertainty in the geology below the water table exists along the inferred flowpath from the repository at distances of approximately 10 to 20 km downgradient of the repository. The uncertainty in the northerly and westerly extent of the alluvium in the saturated zone of the site-scale flow and transport system is abstracted as a polygonal region that is assigned radionuclide transport properties representative of the valley-fill aquifer hydrogeologic unit (alluvium). The dimensions of the polygonal region are randomly varied in BSC (2003b) for the

multiple realizations used in probabilistic assessment of uncertainty. The northern boundary of the uncertainty zone is varied between the dashed lines at the northern end of the polygonal area shown in Figure G-2. The western boundary of the uncertainty zone is varied between the dashed lines along the western side of the polygonal area shown in the Figure G-2.



Sources: Repository outline: BSC 2003c; alluvial uncertainty zone: BSC 2003b; and well locations: DTN: GS010908312332.002

NOTE: Repository outline is shown by the solid line and the minimum and maximum boundaries of the alluvium uncertainty zone are shown by the dashed lines. Key well locations and well numbers are shown with the cross symbols.

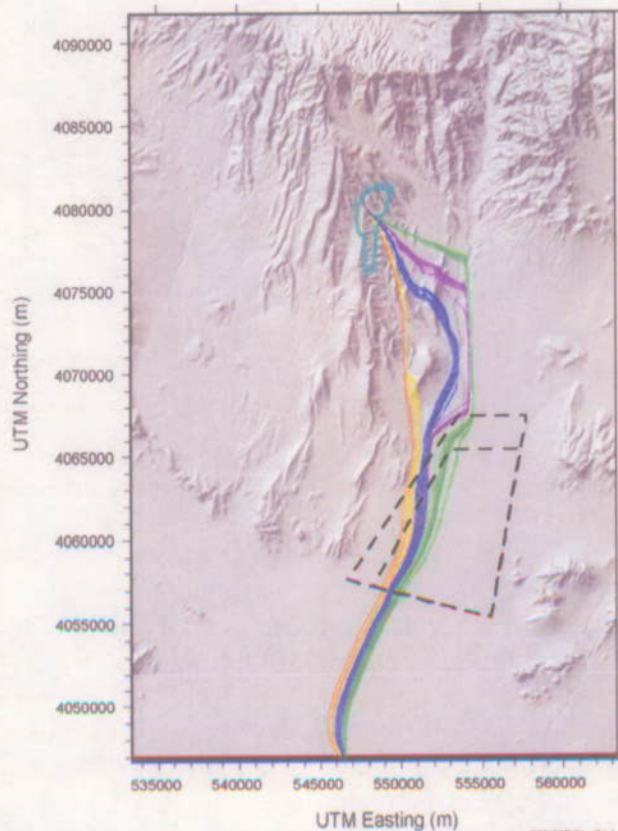
Figure G-2. Minimum and Maximum Extent of the Alluvium Uncertainty Zone

Uncertainty in the contact between volcanic rocks and alluvium at the water table along the northern part of the uncertainty zone is approximately bounded by the location of well UE-25 JF#3, in which the water table is below the contact between the volcanic rocks and the overlying alluvium, and by the location of well NC-EWDP-10S, in which the water table is above the contact between the volcanic rocks and the alluvium (Figure G-2). Uncertainty in the contact along the western part of the uncertainty zone is defined by the locations of wells NC-EWDP-10S, NC-EWDP-22S, and NC-EWDP-19D, in which the water table is above the contact between volcanic rocks and the overlying alluvium, and outcrops of volcanic bedrock to the west.

G.4.2 Flow Path Uncertainty

Uncertainty in flow paths is affected by anisotropy in hydraulic properties of the volcanic tuffs. Large-scale anisotropy and heterogeneity were implemented in the saturated zone site-scale flow model through incorporation of known hydraulic features, faults, and fractures. Small-scale anisotropy was derived from analysis of hydraulic testing at the C-wells complex (BSC 2003a, Section 6.2.6; see also Appendix E).

There is notable variation in the simulated saturated zone flow paths (BSC 2003b) over the range of uncertainty in the horizontal anisotropy in permeability considered in that model. The uncertainty distribution for horizontal anisotropy assigns 90 percent probability to a value of greater than 1 for the ratio of north-south to east-west permeability. Consequently, the most likely flow paths are to the west of the blue particle paths (Figure G-3). Figures G-4 and G-5, for comparison, show flow trajectories from the approximate footprint of the repository in the north to the 18-km compliance boundary in the south. The trajectories are predicted for two calibration cases using the Center for Nuclear Waste Regulatory Analyses three-dimensional site-scale model as described by Winterle et al. (2003).



Source: Repository outline: BSC 2003c; alluvial uncertainty zone: BSC 2003b

NOTE: Green lines, purple lines, blue lines, yellow lines, and red lines show simulated particle paths for horizontal anisotropy values of 0.05, 0.20, 1.0, 5.0, and 20.0, respectively. The dashed lines show the minimum and maximum boundaries of the alluvial uncertainty zone.

Figure G-3. Simulated Particle Paths for Different Values of Horizontal Anisotropy in Permeability



00346DCb_015.ai

Source: Winterle et al 2003, Figure 4

Figure G-4 Case 1 predicted flow trajectories from the approximate footprint of the proposed repository in the north to the 18-km compliance boundary in the south.



00346DCb_016.ai

Source: Winterle et al. 2003, Figure 8

Figure G-5. Case 2 predicted flow trajectories from the approximate footprint of the proposed repository in the north to the 18-km compliance boundary in the south.

G.4.3 Aggregate Uncertainty in Flow Path Lengths in the Tuff and Alluvium

The effects of uncertainty in flow path lengths are evaluated in the saturated zone flow and transport abstraction model (BSC 2003b) in an aggregate sense. In addition, the flow path lengths are estimated for implementation in the saturated zone 1-D transport model (BSC 2003b). Factors influencing the flow path lengths in the tuff and alluvium are the source location at the water table beneath the repository, the horizontal anisotropy, and the location of the contact between tuff and alluvium at the water table. Except for some values of the horizontal anisotropy ratio of less than 1, the uncertainty in the simulated flow path length in the alluvium is only a function of the location of the western boundary of the alluvial uncertainty zone (Figure G-3). Uncertainty in the northern location of the contact between the tuff and alluvium at the water table has been reduced by lithologic information from wells NC-EWDP-10S and NC-EWDP-22S. However, sufficient uncertainty remains regarding the western location of the contact between the tuff and alluvium to affect uncertainty in the flow path lengths in the alluvium.

The total flow path lengths from beneath the repository to the compliance boundary varies from about 14.5 km to 22 km, depending on the source location beneath the repository and the

horizontal anisotropy in permeability in the volcanic units (BSC 2003b, Table 6-7). Uncertainty in the flow path length in the alluvium varies from about 1 to 10 km, also depending on the source location beneath the repository, the horizontal anisotropy in permeability in the volcanic units, and the location of the western boundary of the alluvium uncertainty zone (BSC 2003b, Table 6-7).

The evaluation of uncertainty of flow path lengths in tuff and alluvium has been incorporated into the saturated zone transport model for license application by identifying an alluvium uncertainty zone and then abstracted as a polygonal region that is assigned radionuclide transport properties representative of the valley-fill aquifer hydrogeologic unit (alluvium). The dimensions of the polygonal region (shown in Figure G-2) are randomly varied in the *SZ Flow and Transport Model Abstraction* (BSC 2003b) for the multiple realizations used in probabilistic assessment of uncertainty which allows for the range of uncertainty to be reflected in the results. The flow path lengths in the alluvium and fracture tuffs are justified using field data and analyses. Uncertainty associated with the flow path lengths is propagated to the TSPA-LA assessments.

G.5 REFERENCES

G.5.1 Documents Cited

BSC (Bechtel SAIC Company) 2003a. *Saturated Zone In-Situ Testing*. ANL-NBS-HS-000039 REV 00A. Las Vegas, Nevada: Bechtel SAIC Company. ACC: MOL.20030602.0291.

BSC 2003b. *SZ Flow and Transport Model Abstraction*. MDL-NBS-HS-000021 REV 00A. Las Vegas, Nevada: Bechtel SAIC Company. ACC: MOL.20030612.0138.

BSC 2003c. *Repository Design, Repository/PA IED Subsurface Facilities*. 800-IED-EBS0-00401-000-00C. Las Vegas, Nevada: Bechtel SAIC Company. ACC: ENG.20030303.0002.

CRWMS M&O (Civilian Radioactive Waste Management System Management and Operating Contractor) 2000. *Uncertainty Distribution for Stochastic Parameters*. ANL-NBS-MD-000011 REV 00. Las Vegas, Nevada: CRWMS M&O. ACC: MOL.20000526.0328.

Reamer, C.W. and Williams, D.R. 2000a. Summary Highlights of NRC/DOE Technical Exchange and Management Meeting on Radionuclide Transport. Meeting held December 5-7, 2000, Berkeley, California. Washington, D.C.: U.S. Nuclear Regulatory Commission. ACC: MOL.20010117.0063.

Reamer, C.W. and Williams, D.R. 2000b. Summary Highlights of NRC/DOE Technical Exchange and Management Meeting on Unsaturated and Saturated Flow Under Isothermal Conditions. Meeting held August 16-17, 2000, Berkeley, California. Washington, D.C.: U.S. Nuclear Regulatory Commission. ACC: MOL.20001201.0072.

Winterle, J.R.; Claisse, A.; and Arlt, H.D. 2003. "An Independent Site-Scale Groundwater Flow Model for Yucca Mountain." *Proceedings of the 10th International High-Level Radioactive Waste Management Conference (IHLRWM), March 30-April 2, 2003, Las Vegas, Nevada*. Pages 151-158. La Grange Park, Illinois: American Nuclear Society. TIC: 254559.

G.5.2 Source Data, Listed by Data Tracking Number

GS010908312332.002. Borehole Data from Water-Level Data Analysis for the Saturated Zone Site-Scale Flow and Transport Model. Submittal date: 10/02/2001.

GS021008312332.002. Hydrogeologic Framework Model for the Saturated-Zone Site-Scale Flow and Transport Model, Version YMP_9_02. Submittal date: 12/09/2002.

APPENDIX H
TRANSPORT PROPERTIES
(RESPONSE TO RT 1.05, RT 2.01, RT 2.10, GEN 1.01 (#28 AND #34),
AND RT 2.03 AIN-1)

Note Regarding the Status of Supporting Technical Information

This document was prepared using the most current information available at the time of its development. This Technical Basis Document and its appendices providing Key Technical Issue Agreement responses that were prepared using preliminary or draft information reflect the status of the Yucca Mountain Project's scientific and design bases at the time of submittal. In some cases this involved the use of draft Analysis and Model Reports (AMRs) and other draft references whose contents may change with time. Information that evolves through subsequent revisions of the AMRs and other references will be reflected in the License Application (LA) as the approved analyses of record at the time of LA submittal. Consequently, the Project will not routinely update either this Technical Basis Document or its Key Technical Issue Agreement appendices to reflect changes in the supporting references prior to submittal of the LA.

APPENDIX H

TRANSPORT PROPERTIES (RESPONSE TO RT 1.05, RT 2.01, RT 2.10, GEN 1.01 (COMMENTS 28 AND 34), AND RT 2.03 AIN-1)

This appendix provides a response for Key Technical Issue (KTI) agreements Radionuclide Transport (RT) 1.05, RT 2.01, RT 2.10, General Agreement (GEN) 1.01, Comments 28 and 34, and a U.S. Nuclear Regulatory Commission (NRC) additional information needed (AIN) request for KTI agreement RT 2.03. These KTI agreements relate to providing more information justifying transport properties for the parameters derived.

H.1 KEY TECHNICAL ISSUE AGREEMENTS

H.1.1 RT 1.05, RT 2.01, RT 2.10, GEN 1.01 (Comments 28 and 34), and RT 2.03 AIN-1

KTI agreements RT 1.05, RT 2.01, RT 2.03 and RT 2.10 were reached during the NRC/DOE technical exchange and management meeting on radionuclide transport held December 5 through 7, 2000, in Berkeley, California. Radionuclide transport KTI subissues 1, 2 and 3 were discussed at that meeting (Reamer and Williams 2000).

A letter report responding to this agreement (Ziegler 2002) was prepared. Specific additional information was requested by the U. S. Nuclear Regulatory Commission after the staff's review of this letter report was completed, resulting in RT 2.03 AIN-1 (Schlueter 2002).

During the NRC/DOE technical exchange and management meeting on thermal operating temperatures, held September 18 through 19, 2001, the NRC provided additional comments relating to these RT KTI agreements (Reamer and Gil 2001). These comments (GEN 1.01, comments 28 and 34) relate specifically to transport properties. DOE provided initial responses to these comments (Reamer and Gil 2001).

At the September technical exchange, the NRC stated that additional documentation is needed to enable a thorough evaluation of the use of expert judgement to obtain ranges and probabilities for transport parameters used in the total system performance assessment (TSPA) code. The NRC staff expressed the concern that retardation (K_{ds}) distributions were obtained from inadequately documented expert judgments. For transport parameters derived from expert judgements, the judgements should be conducted and documented in accordance with the guidance in NUREG-1563 (Kotra et al. 1996), as applicable. For those species for which K_{ds} were measured or referenced, the selected ranges of K_{ds} used to model transport of chemical species either through porous rock or fractures should be technically supported.

At the time of the meeting, DOE planned to provide additional documentation to explain how transport parameters obtained from expert judgments and used for performance assessment were derived. Specifically, for alluvium properties, the DOE suggested that testing at the Alluvial Testing Complex would help confirm the applicability of laboratory-determined transport parameters. If performed, testing at the Alluvial Testing Complex would also help verify whether the alluvial aquifer could be considered a single continuum porous medium.

As indicated by their associated comments and responses, GEN 1.01 comments 28 and 34 are addressed implicitly through the response to KTI agreements RT 1.05 and RT 2.10, which are addressed in this appendix.

The wording of these agreements and of DOE's initial response to the general agreement comments is as follows:

RT 1.05

Provide additional documentation to explain how transport parameters used for performance assessment were derived in a manner consistent with NUREG-1563, as applicable. Consistent with the less structured approach for expert judgment acknowledged in NUREG-1563 guidance and consistent with DOE procedure AP-3.10Q, DOE will document how it derived the transport parameter distributions for performance assessment, in a report expected to be available in FY 2002.

RT 2.01

Provide further justification for the range of effective porosity in alluvium, considering possible effects of contrasts in hydrologic properties of layers observed in wells along potential flow paths. DOE will use data obtained from the Nye County Drilling Program, available geophysical data, aeromagnetic data, and results from the Alluvial Testing Complex testing to justify the range of effective porosity in alluvium, considering possible effects of contrasts in hydrologic properties of layers observed in wells along potential flow paths. The justification will be provided in the Alluvial Testing Complex report due in FY 2003.

RT 2.03

Provide a detailed testing plan for alluvial testing (the ATC and Nye County Drilling Program) to reduce uncertainty (for example, the plan should give details about hydraulic and tracer tests at the well 19 complex and it should also identify locations for alluvium complex testing wells and tests and logging to be performed). NRC will review the plan and provide comments, if any, for DOE's consideration. In support and preparation for the October/November 2000 Saturated Zone meeting, DOE provided work plans for the Alluvial Testing Complex and the Nye County Drilling Program (FWP-SBD-99-002, Alluvial Tracer Testing Field Work Package, and FWP-SBD-99-001, Nye County Early Warning Drilling Program, Phase II and Alluvial Testing Complex Drilling). DOE will provide test plans of the style of the Alcove 8 plan as they become available. The plan will be amended to include laboratory testing. In addition, the NRC On Site Representative attends DOE/Nye County planning meetings and is made aware of all plans and updates to plans as they are made.

RT 2.03 AIN-1

The purpose of the testing is to support the development of a conceptual model of groundwater flow and radionuclide transport in saturated alluvium south of Yucca Mountain, and to quantify flow and transport parameters. The distance between wells is less than 30 meters. The parameters used in performance assessment are applied to cells 500 meters on a side. Provide the justification for the use of parameter values, determined at one scale (30 meters between drill holes of the ATC test), in the total system performance assessment model that uses a different scale.

RT 2.10

Provide additional documentation to explain how transport parameters used for PA were derived in a manner consistent with NUREG-1563, as applicable. Consistent with the less structured approach for expert judgment acknowledged in NUREG-1563 guidance and consistent with AP-3.10Q, DOE will document how it derived the transport distributions for performance assessment, in a report expected to be available in FY 2002.

GEN 1.01 (Comment 28)

The different analyses in the SSPA use different values and distributions for Np sorption. This type of inconsistency makes it difficult to compare the results of the different types of analyses and their effects on repository performance. Also, the effects of coupled thermal-hydrological-chemical effects on transport parameters are not considered.

Basis: Sections 11.3.1.5.3 and 11.3.4.5 use different values and distributions for Np sorption in the analyses presented in the SSPA. This type of inconsistency makes it difficult to compare the results of the different types of analyses and their effects on repository performance. Also, although the effects of coupled thermal-hydrological-chemical effects on permeability are considered (Section 11.3.5.4.2), the effects of the temperature on sorption parameters are not addressed directly.

These comments fall under Agreement RT 1.05.

DOE Response to GEN 1.01 (Comment 28)

Section 11.3.1.5.3 of SSPA Volume 1 used a single, conservative value of Kd (0.3 mL/g) for Np in illustrating the effects of drift shadow zone. Section 11.3.4.5 used a range of Kds (1-3 mL/g) for Np-237 that was selected based on AMR UZ and SZ Transport Properties (ANL-NBS-HS-000019) Rev 00. The difference will be reconciled should any one of these analyses be carried forward into a potential LA.

With regard to sorption in the EBS, partition coefficients are anticipated to vary from those in the UZ because of the large mass of iron-based corrosion products and other materials in the waste package and in the invert. The rationale for the ranges of partition coefficients in the EBS is discussed in Section 10.3.4 with final values defined in Table 10.4.4-1 of Section 10.4.4. If sorption in the EBS is carried forward to a potential LA, rationale for selected ranges for sorption coefficients will be provided per KTI agreements RT 1.05 and RT 2.10.

GEN 1.01 (Comment 34)

If radionuclide retardation is to be modeled in the EBS, sorption coefficient distributions will need to be justified in a manner consistent with existing agreements RT 1.05 and RT 2.10. For example, non-zero K_d values for technetium and iodide have not been used previously in TSPA; any future adoption of such values, as were used in the SSPA, will require stronger technical basis.

DOE Initial Response to GEN 1.01 (Comment 34)

DOE understands that a strong basis must be provided for sorption coefficient distributions for all radionuclides that are important to performance. If retardation in the EBS is carried forward to the potential LA, implementation of KTI agreements RT 1.05 and 2.10 will provide justification for the use of radionuclide transport parameters in the performance assessment.

H.1.2 Related Key Technical Issue Agreements

RT 1.05 and RT 2.10 are identical agreements and will both be addressed by this appendix. RT 1.05, RT 2.01, RT 2.06, RT 2.07 and RT 2.10 all relate to the alluvial testing program, although they address different aspects of the testing program. RT 2.06 and RT 2.07 are related to K_d experiments in alluvium and are addressed separately in Appendix K.

H.2 RELEVANCE TO REPOSITORY PERFORMANCE

The subject of these agreements is transport properties and justification for parameters and their use in performance assessment. Appendix K focuses on agreements that relate to recent work to document K_{ds} (Sorption Coefficient, also known as distribution coefficient) in alluvium. The discussion of K_{ds} for alluvium is presented there. This appendix is focused principally on the K_{ds} in tuff since those were the transport properties that we derived using a modified expert judgement methodology. Other parameters also are addressed in this appendix, but because they are a key part of the technical basis for saturated zone performance, they are discussed in the main text.

Radionuclide delay through the saturated zone at Yucca Mountain is considered in the repository performance assessment. The degree of radionuclide sorption on mineral surfaces within the rock matrix of the tuff aquifer system and in the alluvial aquifer system is the most important process affecting the ability of the saturated zone to attenuate and delay potentially released radionuclides. Matrix diffusion, a process whereby aqueous radionuclides diffuse from actively flowing pore spaces into the relatively stagnant pore space within the rock matrix, is another important process to be considered because the majority of saturated pore volume in the saturated tuff aquifer system comprises relatively stagnant water within the rock matrix.

The importance of the saturated zone in total system performance is reflected in its status as a principal factor, chiefly as a component of defense in depth. Furthermore, a NRC performance assessment sensitivity analysis concluded that retardation in the saturated zone is important based on much higher modeled doses that result from its removal from the analysis (NRC 1999). In particular, neptunium retardation has been shown to have a significant dose effect (NRC 1999; Codell et al. 2001).

Additional discussion associated with this subject is presented in Sections 3.2 and 3.3.

H.3 RESPONSE

This appendix focuses on the transport parameters that are most important to overall saturated zone performance. These are sorption coefficients, effective porosity, and dispersivity. Other transport parameters that are mentioned in this appendix, but for which detailed discussion of their treatment is referred to other documents, include flowing interval spacing (volcanics), flowing interval porosity (volcanics), effective diffusion coefficient (for matrix diffusion in volcanics), matrix porosity (volcanics), and bulk density of volcanic matrix and alluvium. The models are less sensitive to these parameters. The issue of parameter scaling is also addressed in this appendix. Colloid transport parameters, such as filtration rate constants, retardation factors, and the mass fraction transporting unretarded are addressed in *Saturated Zone Colloid Transport* (BSC 2003a). Radionuclide transport in the SZ is also very sensitive to specific discharge, but specific discharge is considered a flow parameter, not a transport parameter, so it is not discussed in this appendix.

Expert judgment is used in the interpretation and synthesis of data for the purposes of defining uncertainty distributions in a manner consistent with the guidance of NUREG-1563 (Kotra et al. 1996). Expert judgment is used in the consideration of factors that may influence the direct application of data to the development of uncertainty distributions in transport parameters. One consideration is the potential impact of the scale of measurement relative to the scale at which the parameter is applied in the radionuclide transport models. For many parameters, variability in its value at the small scale of measurement is greater than at the scale of a single numerical grid cell in the transport model. This result comes about because populating a large volume element (i.e., a grid cell) with spatially-distributed parameter values that are randomly sampled from statistical distributions will result in an "effective" parameter value for the entire volume element that is a "weighted average" of the individual small-scale parameters populating the element. The effective parameter values from a large number of such volume elements will tend to have less variability than the variability of the original distribution of smaller-scale parameter values. However, parameters that have values that inherently increase with scale, such as

dispersivity (longitudinal or transverse), will not necessarily follow this behavior because variability in an absolute sense will increase as absolute parameter values increase. Another consideration is general lack-of-knowledge uncertainty, which is generally incorporated into the uncertainty distribution by extending the "tails" of the distribution. This qualitative assessment of uncertainty may extend the distribution to parameter values that are plausible, but are not necessarily directly linked to data. Another consideration is the potential impacts of features, events, and processes (FEPs) on the uncertainty in parameter values. There may be FEPs that are not explicitly associated with the available data, but are given consideration in defining the uncertainty distributions for transport parameters.

A detailed technical basis for sorption coefficient probability distributions for the license application is provided in *Site-Scale Saturated Zone Transport* (BSC 2003b, Attachment I) and in a revision to *Radionuclide Transport Models Under Ambient Conditions* (BSC 2003c; see DTN: LA0302AM831341.002). The attachments include discussion of the parameters that affect sorption behavior of radionuclides of interest, laboratory measurements, and the results of sorption modeling using the PHREEQC v.2.3 computer code.

Laboratory measurements were performed with samples of rock and water from the Yucca Mountain site. For some radionuclides (i.e., Pa and Th), these laboratory measurements were augmented with laboratory measurements reported in the literature for sorption on pure silica in simple electrolytes or waters similar in composition to those from well UE-25 J-13. Pure silica is a useful surrogate for tuff in sorption coefficient determinations because Yucca Mountain tuffs contain 70 to 80 wt. percent SiO₂. The PHREEQC v.2.3 modeling was used primarily to evaluate the impact of variations in water chemistry on sorption coefficients for Am, Np, Pu, and U.

For alluvium, sorption coefficient distributions for Np and U were derived on the basis of laboratory measurements using alluvium and water samples from boreholes drilled during Phase 2 of the Nye County Early Warning Drilling Program (NC-EWDP-10S, NC-EWDP-19D, and NC-EWDP-22S). Laboratory measurements obtained with water samples from borehole NC-EWDP-3S were not used in the derivation of the sorption coefficient distributions for Np. For the radionuclides Am, Pu, and Cs, sorption coefficient distributions derived for devitrified tuff were used to represent sorption coefficient distributions in alluvium. The mineralogic composition of alluvium clearly reflects its volcanic provenance. Because alluvium tends to contain more clay and zeolite than devitrified tuff, this approach should yield conservative estimates of transport through lower measured sorption coefficients.

H.4 BASIS FOR THE RESPONSE

The evaluation of uncertainty in saturated zone transport parameters used for the performance assessment includes consideration of data from the Yucca Mountain site, nonsite-specific data, expert judgment, and, in the case of dispersivity, formal expert elicitation results. Appropriate site-specific data are used as the primary basis for the development of uncertainty distributions in transport parameters. These data are augmented with process model studies, where appropriate. In some cases, data from the surrounding region are included in the evaluation. Regional data are directly utilized in some cases and are used as corroborative to site data in other cases.

The results of formal expert elicitation are used to define the uncertainty distributions for longitudinal and transverse dispersivity in the saturated zone transport simulations (CRWMS M&O 1998). This saturated zone expert elicitation was conducted in accordance with the guidance provided by Kotra et al. (1996).

H.4.1 Sorption Coefficient Probability Distributions

The technical basis for K_d distributions in the three major volcanic rock types (devitrified, zeolitic, and vitric) to be used in TSPA is provided in *Site-Scale Saturated Zone Transport* (BSC 2003b, Attachment I) and in a revision to *Radionuclide Transport Models Under Ambient Conditions* (BSC 2003c; see DTN: LA0302AM831341.002). The technical basis includes an evaluation of the parameters that could influence the sorption behavior of the radionuclides of interest, an evaluation of the potential ranges for these parameters in the Yucca Mountain flow system, laboratory measurements of sorption coefficients, and the results of sorption modeling using the PHREEQC v.2.3 computer code.

Laboratory experiments were performed with samples of rock and water from the Yucca Mountain site. Two water compositions were used in the experiments (from wells UE-25 J-13 and UE-25 p#1). These water compositions bracket the water compositions expected in the Yucca Mountain flow system over time. The potential effects of variations in water chemistry on sorption coefficients were further evaluated for some radionuclides (i.e., Am, Np, Pu, and U) with modeling studies using the PHREEQCv2.3 computer code. For sorption coefficients on volcanic rock, samples were obtained from various boreholes drilled on Yucca Mountain. The samples used reflect a range of rock compositions (i.e., mineral abundances and mineral compositions). For some radionuclides (i.e., Pa and Th), these laboratory measurements were augmented with those reported in the literature for sorption on pure silica in simple electrolytes or waters similar to UE-25 J-13 in composition. Pure silica is a useful substrate for sorption measurements because Yucca Mountain tuffs contain 70-80 wt. percent SiO_2 .

Sorption coefficient probability distributions were derived for the three major volcanic rock types (devitrified, zeolitic, and vitric) using the results of laboratory measurements, computer modeling, and expert judgment. Separate distributions were derived for the unsaturated zone and the saturated zone. The differences in these distributions include differences in water compositions, mineral compositions, and radionuclide concentrations. On average, pore waters in the unsaturated zone have higher ionic strengths than waters in the saturated zone. Thus, the sorption coefficient probability distributions for the unsaturated zone were more heavily weighted toward the laboratory results and modeling studies involving UE-25 p#1 water compared to sorption coefficient probability distributions for the saturated zone. Secondary mineral compositions in the unsaturated zone are generally more enriched in alkaline earth elements compared to secondary minerals in the saturated zone. Therefore, the sorption coefficient probability distributions for the unsaturated zone were weighted towards the results of laboratory measurements with rock samples enriched in alkaline earth elements compared to sorption coefficient probability distributions in the saturated zone. Finally, radionuclide concentrations in the unsaturated zone are expected to be higher on average than the concentrations in the saturated zone. Therefore, the sorption coefficient probability distributions for the unsaturated zone are weighted towards experiments carried out at the higher radionuclide concentrations compared to sorption coefficient probability distributions in the saturated zone.

In the saturated zone, each TSPA realization (i.e., calculation) uses a single value for the sorption coefficient of each radionuclide of interest. To incorporate the impact of the variability in major mineral content in saturated zone hydrologic units, distributions of effective sorption coefficients were derived. The approach used to derive these distributions involved modeling the sorption behavior of selected radionuclides in a 500-m grid block with mineral distributions reflecting the range of mineral distributions encountered along potential flow paths to the accessible environment. These mineral distributions were combined with sorption coefficient distributions for the major rock types to obtain effective sorption coefficient distributions for the 500-m grid blocks. Breakthrough curves were obtained for the grid blocks using discrete values for sorption coefficients relative to the mineralogy of the block and using the effective sorption coefficient. The resulting breakthrough curves were nearly identical.

For alluvium, sorption coefficient distributions for Np and U were derived on the basis of laboratory measurements using alluvium and water samples from boreholes drilled during Phase 2 of the Nye County Early Warning Drilling Program (NC-EWDP-10S, NC-EWDP-19D, and NC-EWDP-22S). Laboratory measurements obtained with water samples from borehole NC-EWDP-3S were not used in the derivation of the sorption coefficient distributions for Np. For the radionuclides Am, Pu and Cs, sorption coefficient distributions derived for devitrified tuff were used to represent sorption coefficient distributions in alluvium. The mineralogic composition of alluvium clearly reflects its volcanic provenance. Because alluvium tends to contain more clay and zeolite than devitrified tuff, this approach should yield conservative estimates of transport.

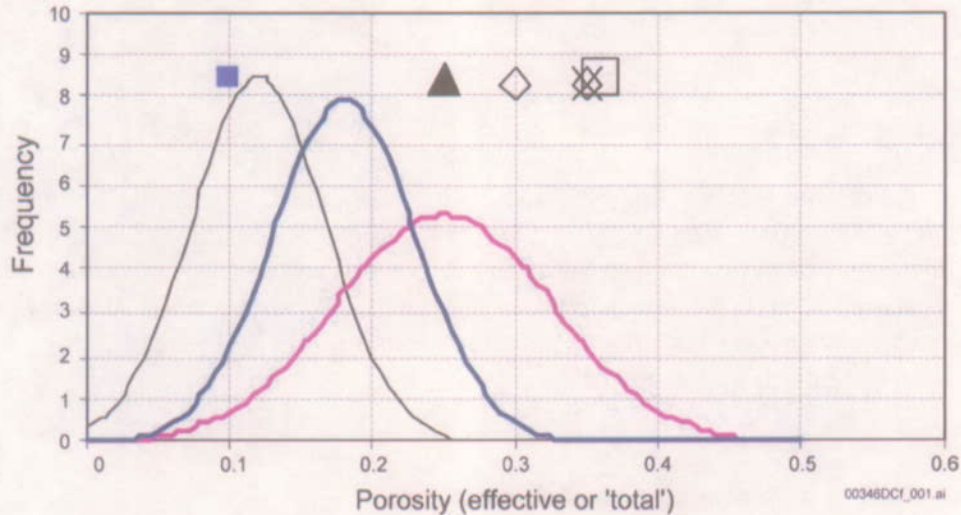
H.4.2 Effective Porosity of the Alluvium

A site-specific value was determined for effective porosity from well NC-EWDP-19D1 at the ATC based on a single-well pumping test (BSC 2003d). There are also total porosity values from the same well based on borehole gravimeter surveys, which are used in developing the upper bound of the effective porosity in the alluvium uncertainty distribution.

Effective porosity is important in determining the average linear ground water velocities used in the simulation of radionuclide transport, which is customarily calculated by dividing the specific discharge of groundwater through a model grid cell by the effective porosity, ϕ_e . Groundwater velocities are more accurate when dead-end pores and low permeability zones that flow bypasses are eliminated from consideration because they do not transmit water. As a result ϕ_e will always be less than or equal to total porosity, ϕ_T . The retardation coefficient, R_f , is also a function of porosity. However, it should be a function of the total porosity *within* flowing pathways, which is better approximated by ϕ_T than by ϕ_e .

Effective porosity is treated as an uncertain parameter for the two alluvium units of the nineteen saturated zone model hydrogeologic units. Uncertain, in this sense, means that ϕ_e will be constant spatially for each unit for any particular model realization, but that value will vary from one realization to the next. In comparison, constant parameters are constant spatially and also do not change from realization to realization.

The effective porosity uncertainty distribution used for TSPA for the site recommendation is shown in Figure H-1. Figure H-1 compares the distribution of Bedinger et al. (1989) to distributions, ranges, and values from the other sources that were considered when developing the uncertainty distribution. The site-specific effective porosity data point from well NC-EWDP-19D1 of 0.1 (BSC 2003d, Section 6.5) is shown on Figure H-1. This is considered a corroborative data point and falls within the uncertainty distribution.



Source: BSC 2003e, Figure 6-8

NOTES: The single value data points do not have a Y-scale value, but do correspond to the X-axis. These points are shown for comparison only.

Solid black line is Neuman (MO0003SZFWTEEP.000)

Solid blue line is Bedinger et al. (1989)

Solid pink line is Gelhar (MO0003SZFWTEEP.000)

Solid blue block is effective porosity value from NC-EWDP-19D1 (BSC 2003d, Section 6.5)

Solid black triangle is mean matrix porosity (DOE 1997, Table 8-1)

Diamond outlined shapes are total porosity (Burbey and Wheatcraft 1986)

X is total porosity (DOE 1997, Table 8-2)

Square outlined shape is mean bulk porosity (DOE 1997, Table 8-1).

Figure H-1. Effective Porosity Distributions and Point Estimates of Effective and Total Porosity in Alluvium

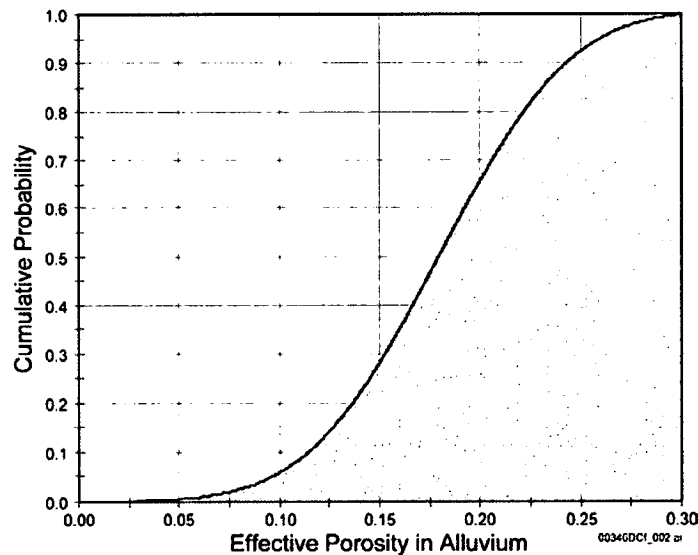
The upper bound of the uncertainty distribution for effective porosity is re-evaluated because of new site-specific data obtained since the TSPA for the site recommendation. The new upper bound is based on the total porosity values from well NC-EWDP-19D1 and corroborative data. The total porosity values from corroborative sources are shown in Table H-1, which have an average value of 0.35. A borehole gravimetry log of NC-EWDP-19D1 (BSC 2003d) resulted in an average porosity estimate of 0.24 for the saturated alluvium at this location, with a minimum value of 0.18 (local value from one measurement "station") and a maximum value of 0.29 (DTN: MO0105GPLOG19D.000).

Table H-1. Summary of Corroborative Values of Total Porosity (ϕ_T)

Reference	Total Porosity	Comments
DOE (1997, Table 8-1)	0.36	Mean bulk porosity
DOE (1997, Table 8-2)	0.35	Total porosity
Burbey and Wheatcraft (1986, pp. 23-24)	0.34	Average of porosity values from Table 3 of that study
Average of above	0.35	N/A

Source: BSC 2003e, Table 6-10

The average of the corroborative values in Table H-1 and the average of the site-specific data from well NC-EWDP-19D1 were used to develop the upper bound of the effective porosity uncertainty distribution. The average value of 0.35 from Table H-1 and the average value from NC-EWDP-19D1 of 0.24 yield a mean of 0.30. Figure H-2 shows the truncated normal distribution developed in this analysis for effective porosity in the alluvium with a mean of 0.18, standard deviation of 0.051, a lower bound of 0, and an upper bound of 0.30. Note that the effective porosities for the two different alluvium units in the SZ flow and transport model are sampled independently from this distribution.



Source: BSC 2003e, Figure 6-10

Figure H-2. Cumulative Distribution Function for Uncertainty in Effective Porosity in the Alluvium

H.4.3 Flowing Intervals for Tuffs

H.4.3.1 Flow Interval Spacing

The flowing interval spacing is a key parameter in the dual porosity model that is included in the saturated zone transport abstraction model (BSC 2003e). A flowing interval is defined as a fractured zone that transmits fluid in the saturated zone, as identified through borehole flow meter surveys (see Figure 3-2 and associated discussion). A detailed description of how uncertainty in the flowing interval spacing is accounted for in *SZ Flow and Transport Model Abstraction* (BSC 2003e, Section 6.5.2.4).

H.4.3.2 Flowing Interval Porosity

The flowing interval porosity, as described in Section 3.2.1 of the Technical Basis Document, is defined as the volume of the pore space through which significant groundwater flow occurs, relative to the total volume. At Yucca Mountain, rather than attempt to define the porosity within all fractures, a flowing interval is defined as the region in which significant groundwater flow occurs at a well. The flowing interval porosity then characterizes these flowing intervals rather than all fractures. The advantage to this definition of flowing interval porosity is that in-situ well data may be used to characterize the parameter. The flowing interval porosity may also include the matrix porosity of small matrix blocks within fracture zones that potentially experience rapid matrix diffusion. A detailed description of how uncertainty in the flowing interval porosity is accounted for is found in *SZ Flow and Transport Model Abstraction* (BSC 2003e, Section 6.5.2.5).

H.4.4 Effective Diffusion Coefficient

Matrix diffusion, as described in Section 3.3.1.3 of the Technical Basis Document, is a process in which diffusing particles move, via Brownian motion, through both mobile and immobile fluids. A detailed description of how uncertainty in the effective diffusion coefficient is accounted for in *SZ Flow and Transport Model Abstraction* (BSC 2003e, Section 6.5.2.6).

H.4.5 Longitudinal and Transverse Dispersion

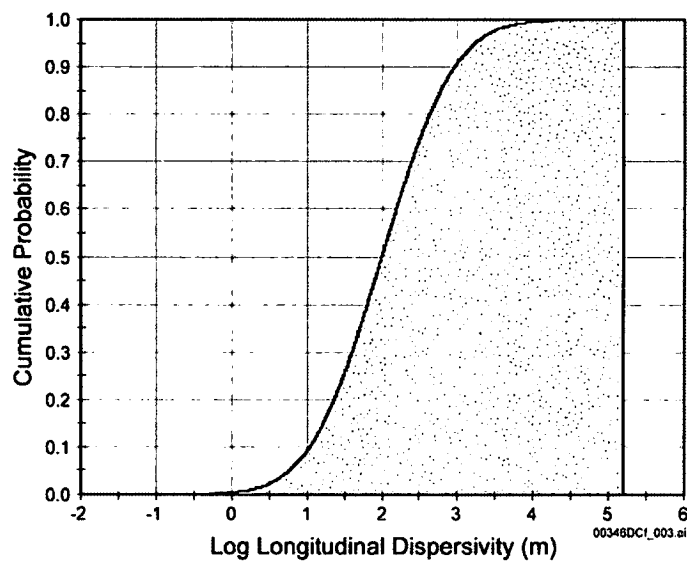
Longitudinal dispersion is the mixing of a solute in groundwater that occurs along the direction of flow (BSC 2003e, Section 6.5.2.9). This mixing is a function of many factors including the relative concentrations of the solute, the velocity pattern within the flow field, and the host rock properties. An important component of this dispersion is the dispersivity, a coarse measure of the solute (mechanical) spreading properties of the rock. The dispersion process causes spreading of the solute in directions transverse to the flow path as well as in the longitudinal flow direction (Freeze and Cherry 1979, p. 394). Longitudinal dispersivity will be important only at the leading edge of the advancing plume, while transverse dispersivity (horizontal transverse and vertical transverse) is the strongest control on plume spreading and dilution for the Yucca Mountain repository (CRWMS M&O 1998, p. LG-12). Because the entire mass of radionuclides potentially released is mixed into the regulatory volume the plume spreading effect of transverse dispersion are irrelevant for TSPA calculations.

Temporal changes in the groundwater flow field may significantly increase the apparent dispersivity displayed by a contaminant plume, particularly with regard to transverse dispersion. However, the thick unsaturated zone in the area of Yucca Mountain likely dampens the response of the saturated zone flow system to seasonal or decadal variations in infiltration.

These dispersivities (longitudinal, vertical transverse, and horizontal transverse) are used in the advection-dispersion equation governing solute transport and are implemented into the saturated zone transport abstraction model report (BSC 2003e) as stochastic parameters. Recommendations from the expert elicitation were used as the basis for specifying the distribution for longitudinal and transverse dispersivity. As part of the expert elicitation, Dr. Lynn Gelhar provided statistical distributions for longitudinal dispersivity at 5 and 30 km (CRWMS M&O 1998, p. 3-21). These distributions for longitudinal dispersivity are consistent with his previous work (Gelhar 1986, pp. 135s to 145s). *Modeling Sub Gridblock Scale Dispersion in Three-Dimensional Heterogeneous Fractured Media (S0015)* (CRWMS M&O 2000, p. 53) provided estimates of the transverse and longitudinal dispersion that may occur at the sub gridblock scale within the saturated zone site-scale model. The estimation of dispersivity using sub-gridblock scale modeling is also described by McKenna et al. (2003). The results from this report are in general agreement with the estimates by the expert elicitation panel (CRWMS M&O 2000, p. 55). However, it should be noted that there is a significant difference in the spatial scale at which the analyses in *Modeling Sub Gridblock Scale Dispersion in Three-Dimensional Heterogeneous Fractured Media (S0015)* (CRWMS M&O 2000) (500 m) were conducted and the scales at which the expert elicitation (CRWMS M&O 1998) estimates were made (5 and 30 km). Nonetheless, both sources of information on dispersivity are mutually supportive.

In the saturated zone transport abstraction model report (BSC 2003e), the longitudinal dispersivity parameter is sampled as a log-transformed parameter and the transverse dispersivities are then calculated as indicated by *Saturated Zone and Transport Expert Elicitation Project* (CRWMS M&O 1998, p. 3-21).

The log-normal distribution for longitudinal dispersivity over the approximately 18 km transport distance in the saturated zone is specified as $E[\log_{10}(\alpha_L)] = 2.0$ and $S.D.[\log_{10}(\alpha_L)] = 0.75$. The CDF of uncertainty in longitudinal dispersivity is shown in Figure H-3.



Source: BSC 2003e, Figure 6-10

Figure H-3. Cumulative Distribution Function for Uncertainty in Longitudinal Dispersivity over the Approximately 18-km Travel Distance in the Saturated Zone

H.4.6 Other Transport Parameters

The remaining solute transport parameters show less variability and have less of an impact on transport predictions. These parameters include matrix porosity (BSC 2003e, Section 6.5.2.18) and bulk density of the volcanic matrix (BSC 2003e, Section 6.5.2.19), plus bulk density of the alluvium (BSC 2003e, Section 6.5.2.7).

H.4.7 Scaling of Field Parameters to Models

The request for additional information addresses the practice of using saturated zone flow and transport parameter estimates derived from field-scale (30 to 100 m) tests in flow and transport simulations over much larger scales.

The issue of extrapolation is complex and is being addressed in various ways by the project. However, it is first important to note that the long-term pump test in the Bullfrog Tuff at the C-Wells yielded flow parameter estimates over an approximately 21 km² area. It is conceivable that an area much larger than the local spacing between wells could also be affected by long-term pumping at the Alluvium Testing Complex. Thus, for flow parameters, field tests can yield parameter estimates at scales relevant to PA.

Some of the ways that the project addresses upscaling include:

1. For most flow and transport parameters, estimates derived from field-scale tests are not used directly in performance assessment models. Rather, PA models randomly sample probability distributions in Monte-Carlo fashion to obtain parameter values for individual simulations. The probability distributions are constructed from a variety of different information sources, including the literature, expert elicitation, and laboratory- and field-scale test results. The parameter estimates obtained from field-scale tests are used to refine these distributions and to ensure that the distributions are consistent with field observations (a parameter estimate from a YMP field test should probably not be an outlier of a distribution). Furthermore, most of the probability distributions tend to be conservative in that the field-derived parameters fall into the less conservative end of the distribution. This is practiced, in part, to allow for uncertainty associated with a lack of understanding of the scaling of flow and transport processes. The probability distributions also tend to be quite broad (often using log-normal or log-uniform distributions) for the same reason.
2. For some parameters, valuable insights into scaling are obtained by comparing field-scale parameter estimates with laboratory-scale parameter estimates. Although a straight-line extrapolation to larger scales is not necessarily advisable, some extrapolation can be employed to help in the construction of the probability distributions mentioned. For instance, extrapolation of parameter estimates for matrix diffusion and colloid transport from laboratory to field to larger scales tends to lead the analyst to construct more conservative probability distributions than might be constructed if only field data were considered.
3. The use of geostatistical methods in two-dimensional and three-dimensional models help address scaling issues associated with parameters that may be expected to have more spatial variability at repository scales than at field-test scales. These methods will help refine the probability distributions mentioned as well as yield additional insights into scaling phenomena.

KTI RT 2.01 can no longer be addressed prior to license application. Conducting the Alluvial Testing Complex cross-hole tracer testing had been planned beginning in the second quarter of FY 2002. The DOE maintained a policy of submitting permit requests to the State of Nevada Underground Injection Control (UIC) and the State Water Engineer. The State of Nevada denied the Underground Injection Control permit request and rescinded the existing water withdrawal waiver. The testing described in the subject ATC Scientific Investigation Test Plan has been delayed pending resolution of permitting issues or a decision to proceed in another direction. Information that could be collected in the future can not be used to support saturated zone process models or the total systems performance assessment for the license application. Therefore, the request:

DOE should address the potential for scale dependency of the total system performance assessment parameters developed from Alluvial Testing Complex tests.

can no longer be met prior to initial license application submittal because the majority of the testing described in the ATC SITP is no longer able to feed the TSPA. Parameters developed from the ATC tests have been obtained from single well tracer tests and cross-hole hydraulic tests. No additional testing can be conducted that could feed the license application. Those parameters that have been obtained are single data points and will not be used directly in TSPA, but only as confirmation that the ranges in TSPA are reasonable from site-specific results.

H.5 REFERENCES

H.5.1 Documents Cited

Bedinger, M.S.; Sargent, K.A.; Langer, W.H.; Sherman, F.B.; Reed, J.E.; and Brady, B.T. 1989. *Studies of Geology and Hydrology in the Basin and Range Province, Southwestern United States, for Isolation of High-Level Radioactive Waste—Basis of Characterization and Evaluation*. U.S. Geological Survey Professional Paper 1370-A. Washington, D.C.: U.S. Government Printing Office. ACC: NNA.19910524.0125.

BSC (Bechtel SAIC Company) 2003a. *Saturated Zone Colloid Transport*. ANL-NBS-HS-000031 REV 01A. Las Vegas, Nevada: Bechtel SAIC Company. ACC: MOL.20030602.0288.

BSC 2003b. *Site-Scale Saturated Zone Transport*. MDL-NBS-HS-000010 REV 01A. Las Vegas, Nevada: Bechtel SAIC Company. ACC: MOL.20030626.0180.

BSC 2003c. *Radionuclide Transport Models Under Ambient Conditions*. MDL-NBS-HS-000008 REV 01. Las Vegas, Nevada: Bechtel SAIC Company. ACC: TBD.

BSC 2003d. *Saturated Zone In-Situ Testing*. ANL-NBS-HS-000039 REV 00A. Las Vegas, Nevada: Bechtel SAIC Company. ACC: MOL.20030602.0291.

BSC 2003e. *SZ Flow and Transport Model Abstraction*. MDL-NBS-HS-000021 REV 00A. Las Vegas, Nevada: Bechtel SAIC Company. ACC: MOL.20030612.0138.

Burbey, T.J. and Wheatcraft, S.W. 1986. *Tritium and Chlorine-36 Migration from a Nuclear Explosion Cavity*. DOE/NV/10384-09. Reno, Nevada: University of Nevada, Desert Research Institute, Water Resources Center. TIC: 201927.

Codell, R.B.; Byrne, M.R.; McCartin, T.J.; Mohanty, S.; Weldy, J.; Jarzempa, M.; Wittmeyer, G.W.; Lu, Y.; and Rice, R.W. 2001. *System-Level Repository Sensitivity Analyses, Using TPA Version 3.2 Code*. NUREG-1746. Washington, D.C.: U.S. Nuclear Regulatory Commission (NRC). TIC: 254763.

CRWMS M&O (Civilian Radioactive Waste Management System Management and Operating Contractor) 1998. *Saturated Zone Flow and Transport Expert Elicitation Project*. Deliverable SL5X4AM3. Las Vegas, Nevada: CRWMS M&O. ACC: MOL.19980825.0008.

CRWMS M&O 2000. *Modeling Sub Gridblock Scale Dispersion in Three-Dimensional Heterogeneous Fractured Media (S0015)*. ANL-NBS-HS-000022 REV 00 ICN 01. Las Vegas, Nevada: CRWMS M&O. ACC: MOL.20001107.0376.

DOE (U.S. Department of Energy) 1997. *Regional Groundwater Flow and Tritium Transport Modeling and Risk Assessment of the Underground Test Area, Nevada Test Site, Nevada*. DOE/NV-477. Las Vegas, Nevada: U.S. Department of Energy. ACC: MOL.20010731.0303.

Freeze, R.A. and Cherry, J.A. 1979. *Groundwater*. Englewood Cliffs, New Jersey: Prentice-Hall. TIC: 217571.

Gelhar, L.W. 1986. "Stochastic Subsurface Hydrology from Theory to Applications." *Water Resources Research*, 22, (9), 135S-145S. Washington, D.C.: American Geophysical Union. TIC: 240749.

Kotra, J.P.; Lee, M.P.; Eisenberg, N.A.; and DeWispelare, A.R. 1996. *Branch Technical Position on the Use of Expert Elicitation in the High-Level Radioactive Waste Program*. NUREG-1563. Washington, D.C.: U.S. Nuclear Regulatory Commission. TIC: 226832.

McKenna, S.A.; Walker, D.D.; and Arnold, B. 2003. "Modeling Dispersion in Three-Dimensional Heterogeneous Fractured Media at Yucca Mountain." *Journal of Contaminant Hydrology*, 62-63, 577-594. New York, New York: Elsevier. TIC: 254205.

NRC (U.S. Nuclear Regulatory Commission) 1999. *NRC Sensitivity and Uncertainty Analyses for a Proposed HLW Repository at Yucca Mountain, Nevada, Using TPA 3.1, Results and Conclusions*. NUREG-1668. Volume 2. Washington, D.C.: U.S. Nuclear Regulatory Commission. TIC: 248805.

Reamer, C.W. and Gil, A.V. 2001. Summary Highlights of NRC/DOE Technical Exchange and Management Meeting of Range of Thermal Operating Temperatures, September 18-19, 2001. Washington, D.C.: U.S. Nuclear Regulatory Commission. ACC: MOL.20020107.0162.

Reamer, C.W. and Williams, D.R. 2000. Summary Highlights of NRC/DOE Technical Exchange and Management Meeting on Radionuclide Transport. Meeting held December 5-7, 2000, Berkeley, California. Washington, D.C.: U.S. Nuclear Regulatory Commission. ACC: MOL.20010117.0063.

Schlueter, J. 2002. "Radionuclide Transport Agreement 2.03 and 2.04." Letter from J. Schlueter (NRC) to J.D. Ziegler (DOE/YMSCO), August 30, 2002, 0909024110, with enclosure. ACC: MOL.20020916.0098.

Ziegler, J.D. 2002. "Transmittal of Reports Addressing Key Technical Issues (KTI)." Letter from J.D. Ziegler (DOE/YMSCO) to J.R. Schlueter (NRC), April 30, 2002, 0501022470, OL&RC:TCG-1045, with enclosures. ACC: MOL.20020730.0636.

H.5.2 Source Data, Listed by Data Tracking Number

LA0302AM831341.002. Unsaturated Zone Distribution Coefficients (KDS) for U, NP, PU, AM, PA, CS, SR, RA, and TH. Submittal date: 02/04/2003.

MO0003SZFWTEEP.000. Data Resulting from the Saturated Zone Flow and Transport Expert Elicitation Project. Submittal date: 03/06/2000.

MO0105GPLOG19D.000. Geophysical Log Data from Borehole NC EWDP 19D. Submittal date: 05/31/2001.

INTENTIONALLY LEFT BLANK

APPENDIX I
TRANSPORT—SPATIAL VARIABILITY OF PARAMETERS
(RESPONSE TO RT 2.02, TSPA I 3.32, AND TSPA I 4.02)

Note Regarding the Status of Supporting Technical Information

This document was prepared using the most current information available at the time of its development. This Technical Basis Document and its appendices providing Key Technical Issue Agreement responses that were prepared using preliminary or draft information reflect the status of the Yucca Mountain Project's scientific and design bases at the time of submittal. In some cases this involved the use of draft Analysis and Model Reports (AMRs) and other draft references whose contents may change with time. Information that evolves through subsequent revisions of the AMRs and other references will be reflected in the License Application (LA) as the approved analyses of record at the time of LA submittal. Consequently, the Project will not routinely update either this Technical Basis Document or its Key Technical Issue Agreement appendices to reflect changes in the supporting references prior to submittal of the LA.

APPENDIX I

TRANSPORT—SPATIAL VARIABILITY OF PARAMETERS (RESPONSE TO RT 2.02, TSPAI 3.32, AND TSPAI 4.02)

This appendix provides a response for key technical issue (KTI) agreements Radionuclide Transport (RT) 2.02, Total System Performance Assessment Integration (TSPAI) 3.32 and TSPAI 4.02. These agreements relate to providing more information about the treatment of spatial variability and uncertainty in transport parameters.

I.1 KEY TECHNICAL ISSUE AGREEMENTS

I.1.1 RT 2.02, TSPAI 3.32, and TSPAI 4.02

KTI agreement RT 2.02 was reached during the NRC/DOE technical exchange and management meeting on radionuclide transport held December 5 through 7, 2000, in Berkeley, California. Radionuclide transport KTI subissues 1, 2 and 3 were discussed at that meeting (Reamer and Williams 2000).

KTI agreements TSPAI 3.32 and TSPAI 4.02 were reached during the NRC/DOE technical exchange and management meeting on total system performance assessment and integration held August 6 through 10, 2001, in Las Vegas, Nevada. TSPAI KTI subissues 1, 2, 3, and 4 were discussed at that meeting (Reamer 2001).

Wording of the agreements is as follows:

RT 2.02

The DOE should demonstrate that TSPA captures the spatial variability of parameters affecting radionuclide transport in alluvium. DOE will demonstrate that TSPA captures the variability of parameters affecting radionuclide transport in alluvium. This information will be provided in the TSPA-LA document due in FY 2003.

TSPAI 3.32

Provide the technical basis that the representation of uncertainty in the saturated zone as essentially all lack-of-knowledge uncertainty (as opposed to real sample variability) does not result in an underestimation of risk when propagated to the performance assessment (SZ2.4.1).

DOE will provide the technical basis that the representation of uncertainty (i.e., lack-of-knowledge uncertainty) in the saturated zone does not result in an underestimation of risk when propagated to the performance assessment. A deterministic case from Saturated Zone Flow Patterns and Analyses AMR (ANL-NBS-HS-000038) will be compared to TSPA analyses. The comparison will be documented in the TSPA for any potential license application expected to be available to NRC in FY 2003.

TSPAI 4.02

DOE will provide the documentation that supports the representation of distribution coefficients (K_d 's) in the performance assessment as uncorrelated is consistent with the physical processes and does not result in an underestimation of risk. This will be documented in the TSPA for any potential license application in FY2003.

I.1.2 Historical Basis of Agreement

At the RT technical exchange (Reamer and Williams 2000), DOE noted that future TSPA analyses would be revised to better incorporate the effects of heterogeneity in the alluvium. Furthermore, it was indicated that heterogeneity in the alluvial aquifer would be incorporated into TSPA analyses by the use of effective porosity distributions. The DOE indicated that gravimeter logs would be run to supplement the Nye County well grain-size distribution data (BSC 2003a) to obtain further estimates of average formation porosity.

At the TSPAI technical exchange (Reamer 2001), NRC and DOE discussed the NRC comments pertaining to the radionuclide transport in the saturated zone model abstraction. NRC asked if changes in radionuclide concentration in the saturated zone model in the TSPA changes as a result of the inclusion of FEP 2.2.08.01.00. DOE responded that the code did not simulate changes in radionuclide concentration in the saturated zone. Individual realizations included spatially variable K_d s only through the distinction between volcanic and alluvium units, but temporally constant K_d values. The NRC expressed concern that the TSPA code would not show potential increases in dose if the K_d decreased in the future.

I.1.3 Related Key Technical Issue Agreements

None.

I.2 RELEVANCE TO REPOSITORY PERFORMANCE

The purpose of the site-scale saturated zone flow and transport model is to describe the spatial and temporal distribution of groundwater as it moves from the water table below the potential repository, through the saturated zone, and to the point of uptake by the receptor of interest. The saturated zone processes that control the movement of groundwater and the movement of dissolved radionuclides and colloidal particles that might be present, and the processes that reduce radionuclide concentrations in the saturated zone, are affected by spatial variability of the saturated zone materials.

The geologic media encountered at Yucca Mountain are inherently heterogeneous, reflected in spatial variabilities in their physical and chemical properties. It would be ideal if all of such variabilities could be incorporated in numerical modeling of subsurface flow and transport, but that is neither possible nor practical for a number of reasons. Yucca Mountain Project model development allows for consideration of variability in a number of ways, mainly in its understanding and propagation of uncertainties from experimental data into the abstraction process. The abstraction of radionuclide transport in the saturated zone for total system performance assessment analyses is developed using a site-scale, three-dimensional,

single-continuum, particle-tracking transport model. Particle transport pathways are calculated based on spatially variable groundwater flux vectors (flow fields) derived from the site-scale saturated zone flow model. It is necessary to provide experimental and field information to constrain data uncertainty for transport parameters relevant to the saturated zone system performance.

The Technical Basis Document Saturated Zone Flow and Transport summary main text that describes spatial variability in the context of the saturated zone conceptual understanding relevant to assessing the flow of groundwater and transport of radionuclides in the saturated zone beneath and downgradient from Yucca Mountain is found in Section 3.2.

I.3 RESPONSE

RT 2.02—Geologic systems are inherently heterogeneous, reflected in considerable spatial variability in physical and chemical properties. It would be ideal if all of such variability were incorporated in numerical modeling of subsurface flow and transport. However, such an approach quickly becomes impractical for most real-world problems due to data and computational limitations. In order to best account for the effects of spatial variability in a model that already accounts for numerous complex processes, the Performance Assessment model uses the Monte Carlo approach in conjunction with parameter distributions of effective parameters to predict flow and transport at Yucca Mountain. Parameter uncertainties are quantified using uncertainty distributions, which numerically represent the state of knowledge about a particular parameter on the scale of the model domain. The uncertainty distribution of a parameter (either cumulative distribution function [CDF] or probability density function), represents what is known about the parameter, and it reflects the current understanding of the range and likelihood of the appropriate parameter values when used in these models (BSC 2002a, p. 45). The uncertainty distributions incorporate uncertainties associated with field or laboratory data, knowledge of how the parameter will be used in the model, and theoretical considerations. The subgrid-scale spatial variability is implicitly considered in these parameter value distributions. The key assumption is that correlation lengths for a particular parameter be smaller than the model domain in order to use these effective parameters. Small correlation lengths result in a simulation sampling the entire distribution making it possible to represent the small-scale heterogeneity with an effective parameter. In other words, there is no “connected pathway” of high effective porosity, low effective sorption coefficient, etc., in the alluvium that could invalidate the use of effective parameters in the TSPA model. Finally, it is assumed that correlations between various parameters in the model do not need to be considered. Painter et al. (2000) examined the correlation between hydraulic conductivity and distribution coefficient and did not find the correlation to be important. In general, due to the large transport distances of interest and the small correlation lengths, the effects would be mitigated due to averaging that invariably occurs at the large scales of interest. Section 4 provides the technical justification for these positions for the cases of flow, transport, and sorption.

TSPAI 3.32—By definition, lack-of-knowledge uncertainty is difficult to quantify. The modeling approach attempts to ensure that lack-of-knowledge uncertainty does not underestimate risk by avoiding the phenomena of risk dilution. As commonly used, risk dilution refers to the apparent paradoxical result of higher mean doses if the parameter distributions are narrowed (indicating less uncertainty) versus lower mean doses if the parameter distributions are widened (indicating

greater uncertainty) in the nominal scenario. This paradox is a result of narrowly defining risk as the expected value (i.e., probability-weighted consequence), and risk dilution as the lowering of the expected value. A broader view of risk would consider the spread of all possible outcomes (i.e., the variance of dose) and the likelihood of adverse outcomes (i.e., the probability of dose greater than 15 mrem/yr with such metrics, widening the parameter distributions would lead to a higher risk (greater variance, higher likelihood of adverse outcomes), even though the expected value might decrease. Thus, a conclusion regarding risk dilution based on the central tendency of system performance ignores other risk insights. In order to prevent risk dilution, parameter distributions are chosen to be as narrow as possible while ensuring that the distribution is based on field or laboratory data, knowledge of how the parameter will be used in the model, and theoretical considerations.

TSPA I 4.02—Correlation factors have been derived for the sampling of sorption coefficient probability distribution functions for cesium, neptunium, plutonium, and uranium transported in the saturated zone (BSC 2003b, Attachment I). These are the radionuclides that are most likely to contribute to dose at the compliance boundary.

I.4 BASIS FOR THE RESPONSE

I.4.1 Spatial Variability (Response to RT 2.02)

I.4.1.1 Background on Spatial Variability

Geologic formations are inherently heterogeneous, reflecting considerable spatial variability in their physical and chemical properties. It would be ideal if all such variabilities were incorporated in numerical modeling of subsurface flow and transport. However, such an approach quickly becomes impractical for most real-world problems, including the Yucca Mountain Project. A large, and sometimes overwhelmingly large, number of nodes are needed for a numerical model to precisely represent spatial variability. For example, when the scale of variability is on the order of meters, 10^{13} nodes are required for a problem on the scale of $100 \times 100 \times 1 \text{ km}^3$. Clearly, the computational burden exceeds the capacity of available computers. In addition, it is impossible to take all measurements at the meter scale, without greatly altering the physical and chemical properties of the formation. Recently, much research has been devoted to effectively and efficiently incorporate the impacts of geologic variability in subsurface flow and transport (reviewed by Zhang 2002).

Formation material properties, including fundamental parameters such as permeability and porosity, are ordinarily observed at only a few locations despite the fact that they exhibit a high degree of spatial variability at all length scales. This combination of considerable spatial heterogeneity with a relatively small number of observations leads to uncertainty about the values of the formation properties, and thus, to uncertainty in estimating or predicting flow in such formations. The theory of stochastic processes provides a natural method for evaluating uncertainties. In stochastic formalism, uncertainty is represented by probability (or by related quantities such as statistical moments). Because material parameters such as permeability and porosity are not purely random, they are treated as random space functions with variabilities exhibiting some spatial correlation structures. The spatial correlations may be quantified by joint (multi-variable, multi-point, or both) probability distributions or joint statistical moments such as

cross- and auto-covariances. In turn, equations governing subsurface flow and transport become stochastic differential equations, the solutions of which are no longer deterministic, but probability distributions of flow and transport quantities. Generally, stochastic differential equations cannot be solved exactly, but estimates of the first few moments of the corresponding probability distribution can be made (namely the mean, variance, and covariances). These moments are sufficient to approximate the confidence intervals.

Moment equation and Monte Carlo simulation are two commonly used methods for solving (approximating) stochastic differential equations. In moment equation methods, equations governing the statistical moments of flow quantities are first derived from the (original) stochastic differential equations, which are then solved numerically or analytically. This method directly yields the statistical moments. Monte Carlo simulation is an alternative, and perhaps the most straightforward method, for solving stochastic equations. This widely used approach is conceptually simple and is based on the idea of approximating stochastic processes using a large number of equally probable realizations.

The moment equation and Monte Carlo simulation methods have been used to derive effective parameters of flow and transport, including hydraulic conductivity, porosity, dispersivity, and retardation coefficients (reviewed by Zhang 2002). The effective parameters are commonly used for describing the mean behaviors of the systems or subsystems under study. However, not only the mean behaviors, but also uncertainties about them, are needed for better describing flow and transport in the subsurface.

The TSPA model uses the Monte Carlo approach in conjunction with parameter distributions of effective parameters to predict flow and transport at Yucca Mountain. Parameter uncertainties are quantified using uncertainty distributions, which numerically represent the state of knowledge about a particular parameter on the scale of the model domain. The uncertainty distribution of a parameter (either cumulative distribution function [CDF] or probability density function), represents what is known about the parameter, and it reflects the current understanding of the range and likelihood of the appropriate parameter values when used in these models (BSC 2002a, p. 45). The uncertainty distributions incorporate uncertainties associated with field or laboratory data, knowledge of how the parameter will be used in the model, and theoretical considerations. The subgrid-scale spatial variability is implicitly considered in the parameter value distributions. The Monte Carlo approach, which samples from these parameter distributions, includes the effects of spatially variable parameters on overall system uncertainty. The following sections provide the technical justification for this position for the cases of flow, transport, and sorption.

I.4.1.2 Spatial Variability in Flow and Transport Parameters

The principal parameters for which subgrid-block spatial variability are of concern for performance predictions are permeability, effective porosity, and sorption coefficients. Analysis of the impact of spatial variability of flow and transport parameters (e.g., permeability and effective porosity) is treated in this section, whereas the spatial variability of sorption coefficients is treated in detail for the fractured volcanic tuffs in the next section.

It is important to recognize the role of permeability and porosity in flow and transport model predictions. Travel times through the alluvium are governed by the water flux, the effective porosity through which radionuclides travel, and sorption coefficients. Average permeabilities are estimated by calibrating the saturated zone flow model to potentiometric and water flux data. Because the model assumes homogeneity within a hydrostratigraphic unit, this approach inherently provides an estimate of the mean permeability of the unit (i.e., the effective permeability at the scale of a hydrogeologic unit). There is considerable uncertainty in the estimation of the effective permeability, as evidenced by the fact that the groundwater flux in the TSPA model of saturated zone flow ranges from 1/30 to 10 times the base case value (BSC 2003c). Therefore, any compound uncertainty due to small-scale permeability variations is considered to be negligible with respect to estimating groundwater flux through the alluvium.

In addition to groundwater flux, the effective porosity used in large-scale flow and transport simulations could also be influenced by heterogeneity in the medium. The approach to considering these effects is through the use of an "effective porosity" approach that considers the possibility of nonuniform transport through the alluvium. Consider a system in which the groundwater flux through a portion of the medium is obtained from flow model calibration assuming homogenous, intra-unit properties. If the medium is highly heterogeneous at smaller scales, water and radionuclides will likely travel through only a portion of the available pore space. A method for capturing this effect in large-scale simulations is by applying a lower porosity for the medium than would be obtained from examination of cores. Under steady state flow conditions, a lower porosity would have no impact on groundwater flow simulations, but would decrease travel times, all else being equal. Estimates of the total porosity of the alluvial material fall in the range of 0.12 to 0.36 (Bedinger et al. 1989, p. A18, Table 1; Burbey and Wheatcraft 1986, pp. 23 and 24; DOE 1997). However, the effective porosity used in TSPA modeling has a mean of 0.18, and a range from 0.02 to 0.3 (BSC 2003c). For the sake of example, assume 0.3 for total porosity as a means for discussing the issue, the mean value implies transport through $0.18/0.3 = 0.6$ or 60 percent of the entire medium. In contrast, the lower limit of 0.02 yields transport through $0.02/0.3 = 0.067$ or 6.7 percent of the medium, and the upper limit on effective porosity is essentially homogeneous transport ($0.3/0.3 = 1$). In essence, the model accounts for preferential flow and transport caused by heterogeneous properties through a reduction of the effective porosity. By using values as low as 6.7 percent of the total available porosity, even though the unit is porous and fairly permeable, the influence of heterogeneities in alluvium porosity has been conservatively bounded.

I.4.1.3 Spatial Variability of the Distribution Coefficient

In this section, the impact of small-scale variability in the distribution coefficient on travel times is studied. The basic conclusions from this sorption analysis would be transferable to transport in the alluvium if a key assumption is valid: that the correlation length of the distribution coefficient is much smaller than the model domain. Specifically, that there are no large connected pathways of permeability or distribution coefficient in the alluvium. If this is the case, a transporting radionuclide will sample the entire range of distribution coefficients distribution. A transported particle that spans the entire distribution can be represented by an effective distribution coefficient.

Radionuclide transport is affected by natural spatial variability in hydrologic and chemical properties. Proper assessment of the impact of these variabilities on radionuclide transport is important when determining the long-term fate of radionuclides and associated exposure risks. Effects of small-scale variability on groundwater flow and transport have been studied using stochastic techniques (Gelhar 1993; Zhang 2002). This appendix outlines the derivations of distributions of effective sorption coefficients for multiple radionuclides. These distributions are used to simulate transport of radionuclides in the saturated zone site-scale model during TSPA calculations. In TSPA calculations, radionuclide transport is modeled using a single value of K_d for grid blocks with dimensions $500 \times 500 \text{ m}^2$ in the x and y directions. It is assumed that the uniform single value captures the processes that affect transport through the grid block. In the field, values of K_d are variable at scales smaller than 500 m. Thus, if a uniform single value of K_d is used to model sorption, it is important to use a value that effectively captures variability at smaller scale and results in the same sorption behavior as if the small-scale processes were represented explicitly. The factors that affect the sorption behavior of the rock matrix include mineral composition, ground water chemistry, and the type of radionuclide. Mineral composition and groundwater chemistry are spatially variable at a scale smaller than 500 m. This spatial variability should be taken into account when modeling sorption behavior. In addition, if laboratory measurements are used to model sorption at scales much larger than the scale of laboratory measurements, it is important to consider the effect of scale. It should be noted that the stochastic nature of the flow model will effectively account for small-scale heterogeneities through use of a wide range of K_d s for the single model grid blocks.

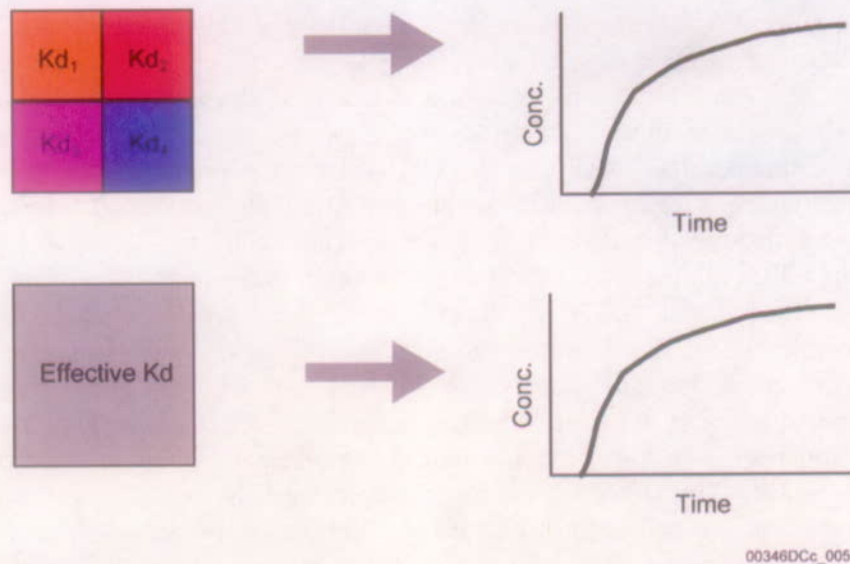
This section summarizes the approach used to calculate effective values of K_d for a $500\text{-m} \times 500\text{-m} \times 100\text{-m}$ grid block while incorporating the effect of small-scale spatial heterogeneity in K_d values, the effect of upscaling, and the effect of mineralogy. The approach includes generating spatially heterogeneous distributions of K_d at a scale much smaller than 500 m using the heterogeneous distributions to calculate effective K_d values. The heterogeneous distributions were generated by incorporating the effect of spatial variability in rock mineralogy. A stochastic approach was used to generate distributions of effective K_d values, and multiple K_d realizations were used to calculate effective K_d values. The input data used to generate the heterogeneous K_d distributions were derived from experimental data described in BSC (2003b, Attachment I).

I.4.1.3.1 Approach

Definition of Effective K_d —Effective K_d is defined as the value of K_d that would result in a radionuclide sorption behavior that is similar to the sorption behavior resulting from a heterogeneous distribution of small-scale K_d values as illustrated in Figure I-1, in which a two-dimensional grid block with a uniform effective K_d produces radionuclide breakthrough behavior that is similar to that shown by the same grid block with four subgrid blocks with different K_d properties.

With the above definition, the following approach was used to compute an effective K_d . The retardation coefficient and K_d are related to each other as

$$K_d = (\text{retardation coefficient} - 1) \frac{\text{Porosity}}{\text{Bulk Density}} \quad (\text{Eq. I-1})$$



Source: BSC 2003b, Figure III-1

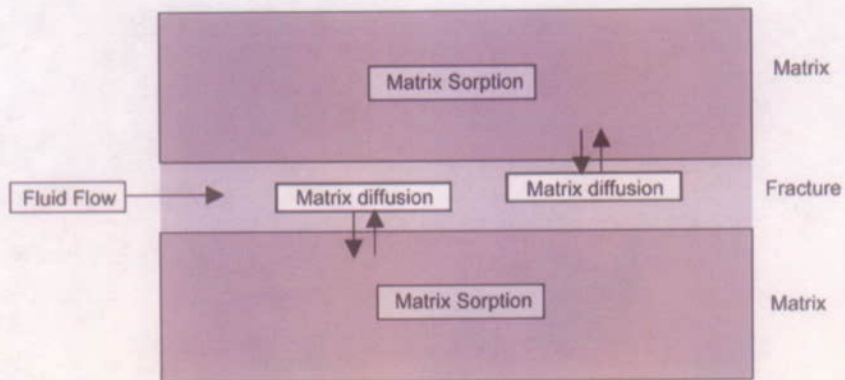
Figure I-1. A Schematic Representation of the Definition of Effective K_d

Thus, if the retardation behavior of a system is well characterized, it can be used to calculate the effective K_d . Effective retardation behavior of a grid block for a particular radionuclide was determined by comparing two breakthrough curves for the same grid block under identical flow conditions. A breakthrough curve was calculated assuming dual-porosity transport in which the radionuclide can diffuse from fracture to matrix subject to retardation (Figure I-2a). A second curve was calculated with identical diffusion behavior but assuming no retardation in matrix (Figure I-2b). In both calculations, retardation on fracture surfaces was neglected. Using these two curves, effective matrix retardation was calculated by comparing the breakthrough times for 50 percent relative concentration. These breakthrough curves are illustrated, with and without matrix sorption, in Figure I-3.

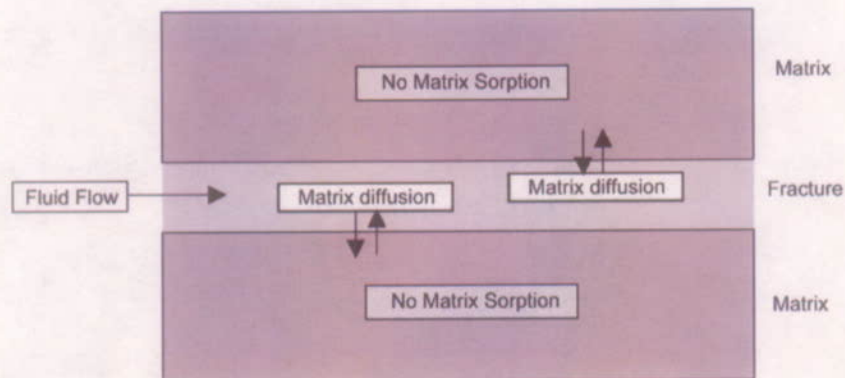
The breakthrough curve for the case with no matrix sorption is much steeper than that for the case with matrix sorption. The times at which 50 percent breakthrough takes place are marked as T_1 and T_2 for the cases without matrix sorption and with matrix sorption, respectively. The effective retardation coefficient was calculated as the ratio of these two times:

$$\text{Effective Retardation } (R_{\text{eff}}) = \frac{T_2}{T_1} \quad (\text{Eq. I-2})$$

a)



b)

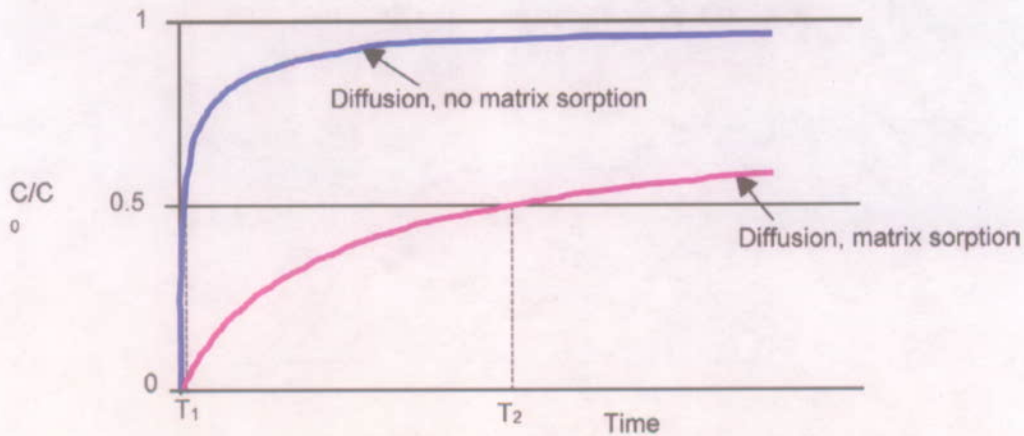


00346DCc_008

Source: BSC 2003b, Figure III-2

NOTE: (a) Transport with diffusion followed by matrix sorption.
(b) Transport with diffusion followed by no matrix sorption.

Figure I-2. The Processes During Transport of a Radionuclide in Fractured Media



00346DCc_007

Source: BSC 2003b, Figure III-3

Figure I-3. Representation of the Breakthrough Curves Used to Calculate Effective Matrix Retardation Behavior

This definition of effective retardation was used to calculate effective K_d values using Equation I-1. Multiple values of effective K_d were calculated using multiple spatially heterogeneous realizations of K_d and subsequently were used to generate statistical distribution of effective K_d . The heterogeneous K_d distributions were generated geostatistically. Before describing the approach, a brief discussion on the method used to perform transport calculations follows.

Transport Calculations—A dual-porosity transport model was used to calculate the breakthrough curves. The calculations were performed using the streamline particle-tracking macro ‘*sptr*’ in the Finite Element Heat and Mass Transport (FEHM) Code (LANL 2003). The dual-porosity transport model in the *sptr* macro is based on the analytical solution developed by Sudicky and Frind (1982) for radionuclide transport in a system of parallel fractures. This solution takes into account advective transport in the fractures, molecular diffusion from the fracture into the porous matrix, and adsorption on the fracture surface as well as within the matrix. In this model all of the above mentioned processes except adsorption on the fracture surface are represented. It is conservatively assumed that there is no sorption on the fracture surfaces.

Stochastic Realizations of K_d —The value of K_d depends on several factors, including rock mineralogy and water chemistry, as well as spatial location. This dependence was taken into account when developing K_d realizations. Groundwater chemistry was treated as a spatially random variable, and its effect on K_d values was incorporated in the K_d distribution used as input for generating stochastic realizations (BSC 2003b). Dependence on rock mineralogy was captured with spatial realizations of rock mineralogy. Data on mineral abundance in rock were available from x-ray diffraction analysis of samples from multiple wells. These mineral abundance data were used to determine prevalent mineralogic rock types. Spatial correlation functions were calculated from these data and were subsequently used to generate multiple realizations of spatial distribution of rock types using sequential indicator simulations.

Sequential indicator simulation is a powerful tool that can be used to generate stochastic realizations of parameters. It uses cumulative distribution functions (CDFs) of observed data as input and estimates a discrete, nonparametric true CDF of a simulated parameter. An indicator is a variable used to indicate the presence or absence of any parameter qualitatively or quantitatively. For example, an indicator can be used to define the presence of a particular rock type at any spatial location. It can also be used to define whether the value of a parameter falls within a certain range of parameter values defined as cutoffs.

After the spatial distributions of rock types were generated, experimental data on K_d values were used to generate spatial distributions of K_d values. The experimental data were analyzed to derive rock-type specific statistical distributions for K_d . The statistical distributions were used to derive the CDF for each radionuclide. Next, indicators were defined at four CDF cutoffs of 0.2, 0.4, 0.6, and 0.8. These cutoffs, along with the spatial correlation information, were used to generate spatial distributions. Unlike mineral abundance data, spatial information on K_d observations was not available. As a result, no spatial correlation functions were available for K_d data. Four different values were used for correlation length in the horizontal direction to investigate its effects on spatial K_d distributions:

- Correlation length equal to a single grid block dimension (4 m) that represents spatially random realizations;
- Correlation length equal to the correlation length used to generate permeability realizations (60 m);
- Correlation length equal to the large grid block length (500 m); and,
- Correlation length equal to the correlation length used to generate rock-type data.

The above values represent the expected range of correlation lengths for K_d . The K_d correlation length in the vertical direction, as well as the correlation lengths for rock types and permeability, were not varied. The spatial distributions of K_d realizations were also generated using the sequential indicator simulation approach. These spatial distributions of K_d values were generated for individual rock types. Distributions for each rock type were generated independent of other rock-type distributions. Finally, the rock-type specific K_d distributions and rock-type distributions were used to generate integrated K_d distributions. The approach used is explained schematically below:

$$\begin{aligned}
 &K_d \text{ distribution for rock-type '1': } K_{d1}^1, K_{d2}^1, K_{d3}^1, K_{d4}^1, K_{d5}^1, K_{d6}^1, K_{d7}^1, \dots, K_{dn}^1 \\
 &K_d \text{ distribution for rock-type '0': } K_{d1}^0, K_{d2}^0, K_{d3}^0, K_{d4}^0, K_{d5}^0, K_{d6}^0, K_{d7}^0, \dots, K_{dn}^0 \\
 &\text{Rock-type distribution: } 1, 0, 1, 1, 1, 0, 0, \dots, 1 \\
 &\text{Combined } K_d \text{ distribution: } K_{d1}^1, K_{d2}^0, K_{d3}^1, K_{d4}^1, K_{d5}^1, K_{d6}^0, K_{d7}^0, \dots, K_{dn}^1
 \end{aligned}$$

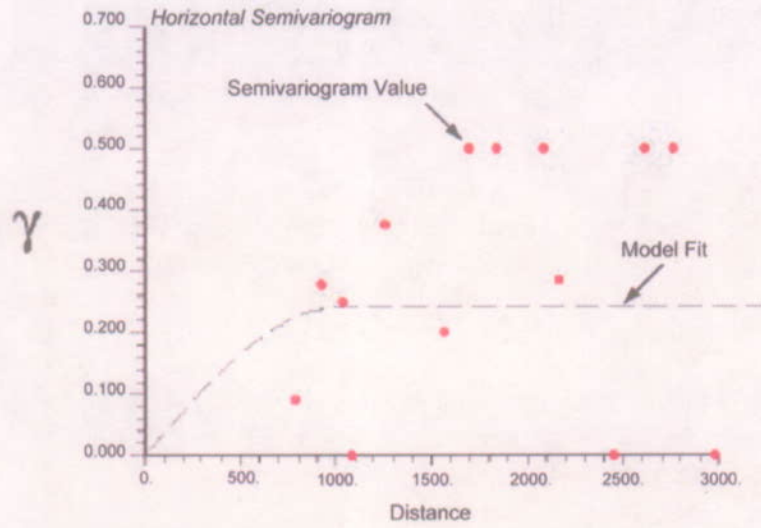
The approach explained above incorporates the effect of spatial heterogeneity and rock mineralogy on the spatial distribution of K_d . Multiple realizations for the spatial distribution of K_d values were generated with this approach.

Stochastic Realizations of Permeability—Similar to the K_d distributions, spatial distributions of permeability were generated using the stochastic approach. The approach and data used were similar to that found in CRWMS M&O (2000). These permeability realizations represent and encompass continuum distributions of permeability for fractured rocks. In this analysis, permeability and K_d were treated as independent, uncorrelated parameters.

I.4.1.3.2 Results

Stochastic Realizations of K_d —As mentioned in BSC (2003b, Section III.2.3), the first step in generating realizations for the spatial distribution of K_d values was to generate a mineralogic rock-type realization. Mineral abundance data for rock samples from multiple wells were used. The mineral abundance data include the following minerals: smectites, zeolites, tridymite, cristobalite, quartz, feldspar, volcanic glass, analcime, mica, and calcite. These data were used to identify rock types using the following definition: the rock type was labeled as zeolitic if the zeolitic abundance was greater than 20 percent, as vitric if glass abundance was greater than 80 percent, and as devitrified otherwise.

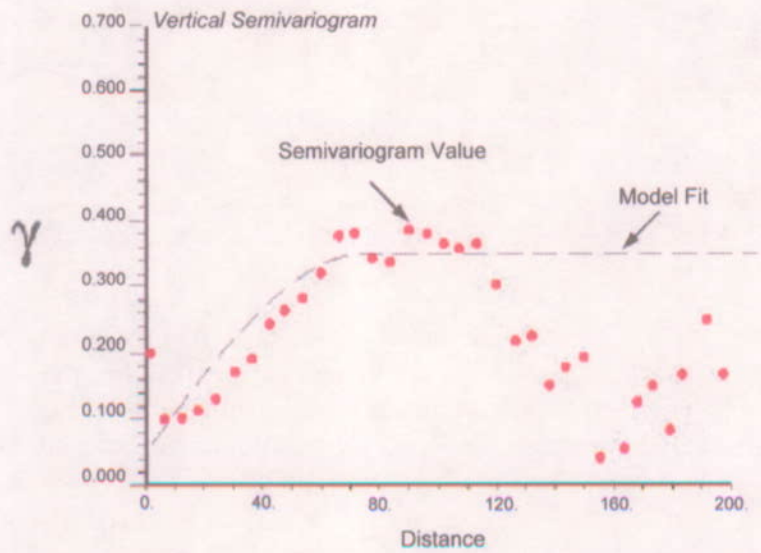
Only the data that were part of the saturated zone extending 200 m below the water table were used in this analysis. When mineralogic abundance data were converted to rock-type data with the above definition, it was observed that only zeolitic and devitrified rocks were present for the top 200 m of the saturated zone. The observed proportions of the rocks were 60 percent zeolitic and 40 percent devitrified. The data set also included information on the spatial location of rock samples. These data were used to calculate spatial correlation information through indicator semivariograms. Two directional semivariograms were calculated: one in the horizontal direction and another in the vertical direction. The semivariograms were used to calculate the correlation information. The semivariograms and the correlation functions fit to them are shown in Figures I-4 and I-5. For the horizontal semivariogram the sill is assumed to be the variance of the input data due to lack of sufficient pairs at higher separations. The parameters for the model fit are shown in Table I-1.



00346DCc_008

Source: BSC 2003b, Figure III-4

Figure I-4. Calculated Semivariogram and Model Fit in the Horizontal Direction



00346DCc_009

Source: BSC 2003b, Figure III-5

Figure I-5. Calculated Semivariogram and Model Fit in the Vertical Direction

Table I-1. Spatial Correlation Parameters for Mineralogic Rock Type Data

Direction	Range (m)	Sill
Horizontal	1000	0.25
Vertical	75	0.35

Source: BSC 2003b, Table III-2

These correlation parameters were used to generate spatial distributions of rock types. The sequential indicator simulation algorithm SISIM, which is part of GSLIB, was used to generate these distributions. Five different rock-type realizations were generated using this approach. The proportions of zeolitic and devitrified rocks in the five output realizations were in good agreement with the input proportions.

Spatial realizations for K_d were generated for four different radionuclides: uranium, neptunium, cesium, and plutonium. The statistical distributions of the experimentally available data for these radionuclides are given in Table I-2.

Table I-2. Statistical Distributions of Experimentally Observed K_d Values

Radionuclide	Rock-type	Distribution	Mean	Standard Deviation	Minimum	Maximum
Uranium	zeolitic	Normal	12.0	3.6	5.0	20.0
	devitrified	Normal	2.0	0.6	0.0	4.0
Cesium	zeolitic	Exponential	16942.0	14930.0	2000.0	42000.0
	devitrified	Normal	728.0	464.0	100.0	1000.0
Neptunium	zeolitic	Normal	2.88	1.47	0.0	6.0
	devitrified	Exponential	0.69	0.707	0.0	2.0
Plutonium	zeolitic	Beta	100.0	15.0	50.0	300.0
	devitrified	Beta	100.0	15.0	50.0	300.0

Source: BSC 2003b, Table III-4

These distributions were used to derive the CDFs for each radionuclide for each rock type. For each CDF, indicators were defined at four CDF cutoffs: 0.2, 0.4, 0.6, and 0.8. In the absence of spatial data, correlation lengths were parameterized, and four different correlation lengths were used to generate stochastic realizations. This effect of correlation length was studied only for uranium. For other radionuclides, a correlation length of 500 m was used. Fifty different realizations were generated for each radionuclide and each rock type. Statistics of the output realizations were calculated and found to be in very good agreement with the input data statistics. These rock-type specific K_d distributions were combined to generate distributions that were conditioned to the realizations of rock types.

Results of Breakthrough Curve Calculations Using the Particle-Tracking Algorithm—These multiple K_d realizations were used to compute breakthrough curves and model the sorption behavior of each radionuclide. A two-step approach was used. In the first step, steady-state flow fields were computed for fifty different permeability realizations. The properties used for these calculations are shown in Table I-3. Note that the parameters such as matrix porosity, fracture porosity, and fracture density were not treated as stochastic variables in this analysis.

Table I-3. Values of Properties Used in Flow and Transport Calculations

Property	Value
Matrix Porosity	0.22
Rock Bulk Density (Kg/m ³)	1997.5
Fracture Porosity	0.001
Fracture Spacing (m)	19.49
Hydraulic Gradient (m/m)	2.9×10^{-4}

Source: BSC 2003b, Table III-9

The above values were obtained from experimental measurements taken at the Yucca Mountain site. Values for fracture spacing and aperture are the mean of available measurements. Values for matrix porosity and rock bulk density are averages for the following units: Topopah, Calico Hills, Prow Pass, Bullfrog, and Tram. These are the main units observed in the saturated zone 200 m below the water table.

Steady-state flow fields were used in the particle-tracking calculations. The flow fields were calculated using constant head at two ends and no flux boundary conditions on the sides, top, and bottom. As mentioned earlier, the particle-tracking macro *sptr* of the Finite Element Heat and Mass Transport Code (LANL 2003) was used to model transport. In these calculations, 4,000 particles were released along one face of a 500-m model element and were allowed to move under the influence of the steady-state flow field. The locations of the particle releases were determined by a flux-weighted placement scheme. Two sets of particle-tracking calculations were performed for each steady-state flow field. In the first set of calculations, the baseline breakthrough curve was calculated assuming transport with diffusion from fracture to matrix without matrix sorption. In the second set of calculations, the breakthrough curve was calculated assuming transport with diffusion followed by sorption on the matrix. For these calculations, the stochastically generated K_d distributions were used. The values of the diffusion coefficient used for these calculations are shown in Table I-4. The diffusion coefficient was not treated as a stochastic variable and the values fall in the range of the effective diffusion coefficient used for TSPA calculations.

Table I-4. Values of Diffusion Coefficients Used for the Particle-Tracking Calculations

Radionuclide	Diffusion Coefficient (m ² /s)
Uranium	3.2×10^{-11}
Plutonium, Cesium, Neptunium	1.6×10^{-10}

Source: BSC 2003b, Table III-10

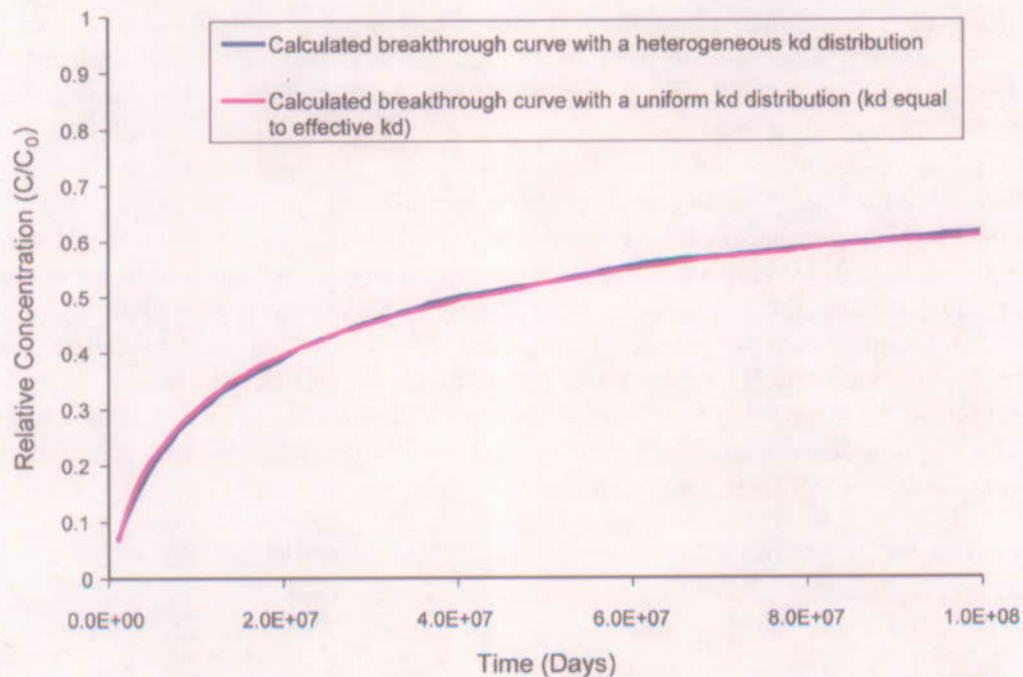
Breakthrough curves subject to effective K_d values were generated for 50 realizations of K_d . The statistics of the calculated effective K_d values are provided in Table I-5. These calculations of stochastic realizations of K_d were performed using a correlation length of 500 m. As indicated in Table I-5, the effective K_d distributions are very narrow compared to the distributions of experimentally observed K_d values (see Table I-2).

Table I-5. Statistics of Calculated Effective K_d Values

Radionuclide	Mean	Standard Deviation	Minimum	Maximum
Uranium	6.61	0.61	5.39	8.16
Cesium	5188.72	941.55	3000.59	6782.92
Plutonium	110.17	7.45	89.90	129.87
Neptunium	1.48	0.23	0.99	1.83

Source: BSC 2003b, Table III-11

A comparison was made as to how well the calculated effective K_d values predicted the particle breakthrough behavior with respect to the breakthrough behavior predicted by the heterogeneous K_d field (from which the effective value was calculated). In these calculations, a uniform value of K_d equal to the effective K_d value was used. Figure I-6 shows the two breakthrough curves for one of the K_d realizations. The effective value of K_d calculated for this realization was 7.32. As can be seen from the figure, the calculated effective K_d value captures the breakthrough behavior of the heterogeneous K_d field well.



00348DCc_010

Source: BSC 2003b, Figure III-16

Figure I-6. Comparison of Breakthrough Behavior Predicted by the Calculated Effective K_d

Effect of Horizontal Correlation Length on Effective K_d Distributions of Uranium—The effect of correlation length in the horizontal direction on effective K_d values was investigated. In these calculations the correlation length in the vertical direction was not varied. The correlation length for permeability is provided by *Modeling Sub Gridblock Scale Dispersion in Three-Dimensional Heterogeneous Fractured Media* (CRWMS M&O 2000). In these calculations permeability and K_d are assumed to be uncorrelated. Table I-6 details the statistics

of the calculated effective K_d values along with the correlation length used to generate the heterogeneous K_d distributions. As can be seen from the results, variation in the correlation length does not greatly affect the calculated statistics of effective K_d values.

Table I-6. Effect of Changes in Correlation Length on Effective K_d Distributions

Correlation Length (m)	Mean	Standard Deviation	Minimum	Maximum
4	6.71	0.49	5.70	8.13
60	6.79	0.47	5.42	8.14
500	6.61	0.61	5.39	8.16
1000	6.58	0.62	4.46	7.85

Source: BSC 2003b, Table III-16

Effect of Variability in the Hydraulic Gradient—The effect of variability in the hydraulic gradient on calculated effective K_d values was studied. These calculations were performed only for uranium and used K_d realizations generated with a correlation length of 500 m. Two different values of hydraulic gradient were used: 8.7×10^{-4} m/m (3 times mean hydraulic gradient) and 0.967×10^{-4} m/m (one-third of mean hydraulic gradient). Steady-state flow fields were calculated with these hydraulic gradients and were subsequently used to calculate particle breakthrough curves. The statistics of the resulting effective K_d values are compared to those calculated using a mean hydraulic gradient of 0.14 m/m in Table I-7. Variability of an order of magnitude in hydraulic gradient has little affect on the effective K_d distributions.

Table I-7. Statistics of Calculated Effective K_d Values for Different Hydraulic Gradients

Hydraulic Gradient	Mean	Standard Deviation	Minimum	Maximum
0.967×10^{-4}	6.55	0.59	5.13	7.53
2.9×10^{-4}	6.61	0.61	5.39	8.16
8.7×10^{-4}	6.27	0.56	4.97	7.65

Source: BSC 2003b, Table III-20

I.4.1.3.3 Summary

Studies were performed to calculate distributions of effective K_d for uranium, neptunium, cesium, and plutonium. These effective K_d distributions are used in the TSPA calculations. The effective K_d distributions were calculated through a stochastic approach in which multiple values of effective K_d were calculated. The value of effective K_d was determined by calculating effective retardation resulting from a spatially heterogeneous K_d field. The spatially heterogeneous K_d fields were calculated using geostatistics. The factors affecting the spatial distribution of K_d , such as rock mineralogy and spatial heterogeneity, were taken into account while generating the heterogeneous K_d fields. The correlation lengths used to generate the fields were parameterized. The conclusions of the study are that:

- The calculated effective K_d values closely reproduced the sorption behavior of the heterogeneous K_d field, validating the approach used to determine the effective K_d values;

- The distributions of calculated effective K_d fields were much narrower than the distributions used as the input. This is to be expected because, in any upscaling study, as the scale gets larger the variability in parameter values gets smaller;
- Variability in correlation length had little effect on the effective K_d distributions for uranium; and,
- Variability in hydraulic gradient did not greatly change the effective K_d distributions.

Once again, it must be reiterated that these small scale studies of heterogeneity should be viewed in the context of the entire site-scale model. Even though results of the present analysis indicate that variability at a correlation length of 1,000 m is not significantly different than that at 500 m, it should be noted that there may be an upper limit to the correlation length that will yield a single effective K_d value. However, so long as the correlation lengths are smaller than the scale of transport, effective K_d values appear to be tightly clustered around a weighted average of the mean K_d s for the different rock types present in the control volume and it is appropriate to use a single effective parameter for the control volume. The implication is that over 18 km of transport distance, the effective K_d value for a given radionuclide should approximate the weighted average of the mean K_d value for the various rock types encountered along the flow pathway. Furthermore, uncertainty is inherently taken into account in the model through Monte Carlo selections from the distributions of parameters (which inherently include the effects of small scale heterogeneity) for each model realization. Thus the practice of choosing single K_d values from distributions for each rock type throughout the entire saturated zone domain for a given TSPA realization should result in greater variability in dose predictions over multiple realizations than if spatial variability in K_d values were represented in each realization.

I.4.2 Risk Dilution (Response to TSPAI 3.32)

The uncertainty in the saturated zone parameters is characterized and documented as described in *Guidelines for Developing and Documenting Alternative Conceptual Models, Model Abstractions, and Parameter Uncertainty in the Total System Performance Assessment for the License Application* (BSC 2002a) and the *Total System Performance Assessment-License Application Methods and Approach* (BSC 2002b). The approach has been to ensure a realistic characterization of the uncertainty in the saturated zone parameters based on analogues, experimental data and sensitivity studies; therefore no risk dilution should be expected from the saturated zone modeling.

As commonly used, risk dilution refers to the apparent paradoxical result of possibly higher mean doses if the parameter distributions are narrowed (indicating less uncertainty) versus lower mean doses if the parameter distributions are widened (indicating greater uncertainty) in the nominal scenario. This paradox is a result of narrowly defining risk as the expected value (i.e., probability-weighted consequence), and risk dilution as the lowering of the expected value. A broader view of risk would consider the spread of all possible outcomes (i.e., the variance of dose) and/or the likelihood of adverse outcomes (i.e., the probability of dose greater than 15 mrem/yr) with such metrics, widening the parameter distributions could lead to a higher risk (greater variance, higher likelihood of adverse outcomes), even though the expected value might

decrease. In other words, a conclusion regarding risk dilution based on the central tendency of system performance for ignores the other risk insights that are available.

The proposed comparison of stochastic and a single deterministic realization does not yield useful risk insight. The choice of single values for parameters for the deterministic simulations is at least as problematic as choices of parameter distributions. Further, interpretation of the results with respect to a comparison with the full stochastic TSPA would not readily lead to any conclusions regarding risk dilution by way of saturated zone parameters without also interrogating the selection of all deterministic values in the model and understanding the nature of the non-linear model response to the inputs. Any meaningful comparison would first require statistical sensitivity analyses (e.g., regression analyses) to determine which parameters are most driving the total system.

I.4.3 Correlations of K_d Distributions (Response to TSPAI 4.02)

Correlation factors for the sampling of sorption coefficient probability distribution functions for cesium, neptunium, plutonium, and uranium transported in the saturated zone (Saturated Zone Transport AMR, Attachment 1) have been derived. These are the radionuclides that are most likely to contribute to dose at the compliance boundary.

I.5 REFERENCES

Bedinger, M.S.; Sargent, K.A.; Langer, W.H.; Sherman, F.B.; Reed, J.E.; and Brady, B.T. 1989. *Studies of Geology and Hydrology in the Basin and Range Province, Southwestern United States, for Isolation of High-Level Radioactive Waste—Basis of Characterization and Evaluation*. U.S. Geological Survey Professional Paper 1370-A. Washington, D.C.: U.S. Government Printing Office. ACC: NNA.19910524.0125.

BSC (Bechtel SAIC Company) 2002a. *Guidelines for Developing and Documenting Alternative Conceptual Models, Model Abstractions, and Parameter Uncertainty in the Total System Performance Assessment for the License Application*. TDR-WIS-PA-000008 REV 00, ICN 01. Las Vegas, Nevada: Bechtel SAIC Company. ACC: MOL.20020904.0002.

BSC 2002b. *Total System Performance Assessment-License Application Methods and Approach*. TDR-WIS-PA-000006 REV 00. Las Vegas, Nevada: Bechtel SAIC Company. ACC: MOL.20020923.0175.

BSC 2003a. *Saturated Zone In-Situ Testing*. ANL-NBS-HS-000039 REV 00A. Las Vegas, Nevada: Bechtel SAIC Company. ACC: MOL.20030602.0291.

BSC 2003b. *Site-Scale Saturated Zone Transport*. MDL-NBS-HS-000010 REV 01A. Las Vegas, Nevada: Bechtel SAIC Company. ACC: MOL.20030626.0180.

BSC 2003c. *SZ Flow and Transport Model Abstraction*. MDL-NBS-HS-000021 REV 00A. Las Vegas, Nevada: Bechtel SAIC Company. ACC: MOL.20030612.0138.

Burbey, T.J. and Wheatcraft, S.W. 1986. *Tritium and Chlorine-36 Migration from a Nuclear Explosion Cavity*. DOE/NV/10384-09. Reno, Nevada: University of Nevada, Desert Research Institute, Water Resources Center. TIC: 201927.

CRWMS M&O (Civilian Radioactive Waste Management System Management and Operating Contractor) 2000. *Modeling Sub Gridblock Scale Dispersion in Three-Dimensional Heterogeneous Fractured Media (S0015)*. ANL-NBS-HS-000022 REV 00 ICN 01. Las Vegas, Nevada: CRWMS M&O. ACC: MOL.20001107.0376.

DOE (U.S. Department of Energy) 1997. *Regional Groundwater Flow and Tritium Transport Modeling and Risk Assessment of the Underground Test Area, Nevada Test Site, Nevada*. DOE/NV-477. Las Vegas, Nevada: U.S. Department of Energy. ACC: MOL.20010731.0303.

Gelhar, L.W. 1993. *Stochastic Subsurface Hydrology*. Englewood Cliffs, New Jersey: Prentice-Hall. TIC: 240652.

LANL (Los Alamos National Laboratory) 2003. *Software Code: FEHM*. V2.20. SUN, PC. 10086-2.20-00.

Painter, S., Cvetkovic, and Turner, D. R. 2001. "Effect of Heterogeneity on Radionuclide Retardation in the Alluvial Aquifer Near Yucca Mountain, Nevada" *Journal of Ground Water*, 39, no. 3. Westerville, Ohio National Ground Water Association. ACC: Ordered-TBD

Reamer, C.W. 2001. "U.S. Nuclear Regulatory Commission/U.S. Department of Energy Technical Exchange and Management Meeting on Total System Performance Assessment and Integration (August 6 through 10, 2001)." Letter from C.W. Reamer (NRC) to S. Brocoum (DOE/YMSCO), August 23, 2001, with enclosure. ACC: MOL.20011029.0281.

Reamer, C.W. and Williams, D.R. 2000. Summary Highlights of NRC/DOE Technical Exchange and Management Meeting on Radionuclide Transport. Meeting held December 5-7, 2000, Berkeley, California. Washington, D.C.: U.S. Nuclear Regulatory Commission. ACC: MOL.20010117.0063.

Sudicky, E.A. and Frind, E.O. 1982. "Contaminant Transport in Fractured Porous Media: Analytical Solutions for a System of Parallel Fractures." *Water Resources Research*, 18, (6), 1634-1642. Washington, D.C.: American Geophysical Union. TIC: 217475.

Zhang, D. 2002. *Stochastic Methods for Flow in Porous Media: Coping with Uncertainties*. San Diego, California: Academic Press. TIC: 254707.

APPENDIX J

**DETERMINATION OF WHETHER KINETIC EFFECTS SHOULD
BE INCLUDED IN THE TRANSPORT MODEL
(RESPONSE TO RT 1.04)**

Note Regarding the Status of Supporting Technical Information

This document was prepared using the most current information available at the time of its development. This Technical Basis Document and its appendices providing Key Technical Issue Agreement responses that were prepared using preliminary or draft information reflect the status of the Yucca Mountain Project's scientific and design bases at the time of submittal. In some cases this involved the use of draft Analysis and Model Reports (AMRs) and other draft references whose contents may change with time. Information that evolves through subsequent revisions of the AMRs and other references will be reflected in the License Application (LA) as the approved analyses of record at the time of LA submittal. Consequently, the Project will not routinely update either this Technical Basis Document or its Key Technical Issue Agreement appendices to reflect changes in the supporting references prior to submittal of the LA.

APPENDIX J

DETERMINATION OF WHETHER KINETIC EFFECTS SHOULD BE INCLUDED IN THE TRANSPORT MODEL (DOE'S RESPONSE TO RT 1.04)

This appendix provides a response for key technical issue (KTI) RT 1.04, which relates to providing more information about sensitivity studies on K_d s for plutonium, uranium, and protactinium, and to evaluate the adequacy of the K_d data.

J.1 KEY TECHNICAL ISSUE AGREEMENT

J.1.1 RT 1.04

KTI agreement RT 1.04 was reached during the NRC/DOE technical exchange and management meeting on radionuclide transport held December 5 through 7, 2000, in Berkeley, California. Radionuclide transport KTI subissues 1, 2 and 3 were discussed at that meeting (Reamer and Williams 2000).

During the meeting, experiments for plutonium were discussed that showed kinetic effects that make the high flow rates used for the column tests non-representative. Additional sensitivity studies and a review of available data were suggested to evaluate the adequacy of the data. To evaluate the adequacy of the data, the DOE indicated that the effect of plutonium sorption on performance could be investigated in sensitivity studies. As a result of these discussions, KTI agreement RT 1.04 was reached.

The wording of the agreement is as follows:

RT 1.04

Provide sensitivity studies on K_d for plutonium, uranium, and protactinium to evaluate the adequacy of the data. DOE will analyze column test data to determine whether, under the flow rates pertinent to the Yucca Mountain flow system, plutonium sorption kinetics are important to performance. If they are found to be important, DOE will also perform sensitivity analyses for uranium, protactinium, and plutonium to evaluate the adequacy of K_d data. The results of this work will be documented in an update to the AMR Unsaturated Zone and Saturated Zone Transport Properties available to the NRC in FY 2002.

J.1.2 Related Key Technical Issue Agreements

The response to KTI agreement RT 2.05, which was delivered to NRC in FY02, provided a work plan describing the laboratory radionuclide column testing for colloidal facilitated transport to be performed for YMP.

The response to KTI agreement RT 1.04 will also satisfy the RT 3.10 agreement, which addresses the unsaturated zone aspect of the same question. KTI agreement RT 3.10 will be

addressed in the context of the unsaturated zone processes in Group Code X, Unsaturated Zone Transport.

J.1.3 Related Key Technical Issue Agreements

RT 2.05, which was delivered to NRC in FY02 provided a work plan describing the laboratory radionuclide column testing for colloidal facilitated transport to be performed for YMP.

The response to RT 1.04 will also satisfy the RT 3.10 agreement that addresses the unsaturated zone aspect of the same question. RT 3.10 will be addressed in the context of the unsaturated zone process in Group Code X, Unsaturated Zone Transport.

J.2 RELEVANCE TO REPOSITORY PERFORMANCE

Radionuclide retardation in the alluvium might delay the movement of most radionuclides for long time periods, varying from thousands to tens of thousands of years for nuclides that tend to sorb onto porous materials. Key sorbing radionuclides include neptunium-237, americium-241, and plutonium-240. Particularly, neptunium-237 which is the most important radionuclide affected by retardation in the alluvium because it has a long half-life, a large inventory and energetic.

Experiments on plutonium show kinetic effects that make the high flow rates used in the column tests non-representative. Additional sensitivity studies and a data review will be used to evaluate the adequacy of the data. The criterion to confirm the K_d for plutonium determined in the static tests (that are appropriate for calculating retardation in dynamic systems) was evaluated for the adequacy of the data. The effect of plutonium sorption on performance has been investigated in sensitivity studies, and external information on plutonium sorption has been reviewed.

A general discussion of the influence of sorption coefficients on radionuclide transport in the saturated zone is found in Section 3.3.2 of this Technical Basis Document.

J.3 RESPONSE

Sorption kinetics of plutonium have been evaluated to determine if kinetic effects can be neglected in the transport models. If kinetic effects can be neglected, retardation factors, that are based on the validity of the local equilibrium assumption, can be used in the transport equations that simulate the transport of plutonium. The study presented in this response demonstrates that sorption kinetics are relatively unimportant for plutonium and that the assumption of local equilibrium can be used when evaluating transport of plutonium in the saturated zone. Under the conditions in which the Yucca Mountain sorption experiments were performed, the kinetics of plutonium sorption were slower than those of other sorbing radionuclides. Therefore for typical Yucca Mountain geochemical conditions, kinetic limitations of the sorption reaction do not need to be considered when predicting the transport of radionuclides through the saturated zone.

J.4 BASIS FOR THE RESPONSE

To assess whether sorption kinetic processes need to be included in the transport model, column test data collected under flow rates pertinent to the Yucca Mountain flow system were used to

calculate Damköhler (Da) numbers (Triay et al. 1997). Da is a dimensionless number used for comparing transport and reaction time-scales to determine if kinetic limitations apply to a particular reactive transport system. Therefore, Da can be used to determine if local equilibrium assumptions are valid, and if so, kinetic effects can be neglected and computationally efficient equilibrium models with retardation factors as input can be used.

Plutonium kinetics were examined (BSC 2003, Attachment IV) because plutonium sorption kinetics are slower than the sorption kinetics of other radionuclides in the Yucca Mountain inventory examined in *Site-Scale Saturated Zone Transport* (BSC 2003, Attachment I). Plutonium kinetics may not always be slower than that of other radionuclides. However, for the representative Yucca Mountain geochemical conditions examined in *Site-Scale Saturated Zone Transport* (BSC 2003, Attachment IV), plutonium sorption kinetics were slower than that of the other sorbing radionuclides and plutonium was therefore chosen for study in this analysis. Thus, if the assumption of local equilibrium is valid for plutonium in these relatively short time-scale experiments (on the order of days), it should be valid for other radionuclides in the Yucca Mountain inventory at relatively long saturated zone travel time scales (on the order of years). By using plutonium in short time-scale experiments, this analysis provides a stringent test for assessing the validity of the local equilibrium assumption.

Da is defined as the rate constant, k , multiplied by a representative residence time, T

$$Da = k \times T \quad (\text{Eq. J-1})$$

where k is a first order reaction rate constant (1/time). The rate constant, k , quantifies the reaction time scale of the system, and the residence time, T , quantifies the transport time scale. Da provides a basis for evaluating which time scale dominates the system. If the reaction time is much faster than the transport time, Da is large, and the assumption of local equilibrium is valid.

For evaluating sorption behavior, separate Da numbers, Da_{att} and Da_{det} , can be computed for attachment and detachment of the sorbing contaminant using k_{att} and k_{det} , which, respectively, are the attachment and detachment rate constants for plutonium sorbing onto mineral surfaces. Bahr and Rubin (1987, p. 450) found that equilibrium is well approximated when the sum of the two Da numbers is greater than 100, and it is reasonably well estimated when the sum is greater than 10. Thus, the larger the sum of the two Da numbers, the more appropriate is the assumption of equilibrium.

Valocchi (1985, Figure 2) found similar results, although only the reverse rate k_{det} was used to compute the Da number. The Valocchi approach is used here because a single first order rate best fit the column experiments. Because the Valocchi approach uses only one Da number and gives a lower Da number than the Bahr and Rubin method, the Bahr and Rubin (1987, p. 450) criteria of 10 and 100 can also be used with the Valocchi approach.

To estimate the Da number for the saturated zone transport model (Equation J-1), the reaction rate constants for plutonium sorption must be determined. This is done with laboratory data from column experiments (BSC 2003, Attachment IV). The general idea behind the calculation is to fit a first order reaction rate constant to plutonium-239 column data. This rate constant, along with a conservative travel time through the fractured volcanics, can be used to estimate a

Da number. In *Site-Scale Saturated Zone Transport* (BSC 2003, Attachment IV), the *Da* number was determined to be greater than 100, indicating that kinetic limitations are not important for plutonium in the saturated zone at Yucca Mountain. Under the conditions in which the Yucca Mountain sorption experiments were performed, the kinetics of plutonium sorption were slower than those of other sorbing radionuclides (BSC 2003, Attachment IV). Therefore for typical Yucca Mountain geochemical conditions, kinetic limitations of the sorption reaction do not need to be considered when predicting the transport of radionuclides through the saturated zone.

It should be noted that colloid facilitated transport cannot be ruled out in the Triay et al. (1997) column experiments used in this analysis. The kinetic interpretation of these column studies is also consistent with a colloid transport interpretation where the sorption and desorption rate constants are equivalent to colloid filtration and detachment rate constants. However, if the early plutonium breakthroughs in the column experiments were a result of colloid-facilitated transport of a portion of the plutonium, then the sorption of rate constants for the soluble plutonium fraction would have to be greater than those deduced assuming that all the plutonium was soluble. This scenario would only strengthen the conclusion that the equilibrium approximation is valid for soluble plutonium over large time scales.

J.5 REFERENCES

- Bahr, J.M. and Rubin, J. 1987. "Direct Comparison of Kinetic and Local Equilibrium Formulations for Solute Transport Affected by Surface Reactions." *Water Resources Research*, 23, (3), 438-452. Washington, D.C.: American Geophysical Union. TIC: 246894.
- BSC (Bechtel SAIC Company) 2003. *Site-Scale Saturated Zone Transport*. MDL-NBS-HS-000010 REV 01A. Las Vegas, Nevada: Bechtel SAIC Company. ACC: MOL.20030626.0180.
- Reamer, C.W. and Williams, D.R. 2000. Summary Highlights of NRC/DOE Technical Exchange and Management Meeting on Radionuclide Transport. Meeting held December 5-7, 2000, Berkeley, California. Washington, D.C.: U.S. Nuclear Regulatory Commission. ACC: MOL.20010117.0063.
- Triay, I.R.; Meijer, A.; Conca, J.L.; Kung, K.S.; Rundberg, R.S.; Strietelmeier, B.A.; and Tait, C.D. 1997. *Summary and Synthesis Report on Radionuclide Retardation for the Yucca Mountain Site Characterization Project*. Eckhardt, R.C., ed. LA-13262-MS. Los Alamos, New Mexico: Los Alamos National Laboratory. ACC: MOL.19971210.0177.
- Valocchi, A.J. 1985. "Validity of the Local Equilibrium Assumption for Modeling Sorbing Solute Transport Through Homogeneous Soils." *Water Resources Research*, 21, (6), 808-820. Washington, D.C.: American Geophysical Union. TIC: 223203.

APPENDIX K
TRANSPORT- K_{ds} IN ALLUVIUM
(RESPONSE TO RT 2.06, RT 2.07, AND GEN 1.01 (#41 AND #102))

Note Regarding the Status of Supporting Technical Information

This document was prepared using the most current information available at the time of its development. This Technical Basis Document and its appendices providing Key Technical Issue Agreement responses that were prepared using preliminary or draft information reflect the status of the Yucca Mountain Project's scientific and design bases at the time of submittal. In some cases this involved the use of draft Analysis and Model Reports (AMRs) and other draft references whose contents may change with time. Information that evolves through subsequent revisions of the AMRs and other references will be reflected in the License Application (LA) as the approved analyses of record at the time of LA submittal. Consequently, the Project will not routinely update either this Technical Basis Document or its Key Technical Issue Agreement appendices to reflect changes in the supporting references prior to submittal of the LA.

APPENDIX K

TRANSPORT- K_d s IN ALLUVIUM (RESPONSE TO RT 2.06, RT 2.07, AND GEN 1.01 (COMMENTS 41 AND 102))

This appendix provides a response for key technical issues (KTI) agreements Radionuclide Transport (RT) 2.06, RT 2.07 and General Agreement (GEN) 1.01 Comments 41 and 102. These KTI agreements relate to providing more information about how DOE used testing in the alluvium to develop K_d s for use in the model.

K.1 KEY TECHNICAL ISSUE AGREEMENTS

K.1.1 RT 2.06, RT 2.07, and GEN 1.01 (Comments 41 and 102)

KTI agreements RT 2.06 and RT 2.07 were reached during the NRC/DOE technical exchange and management meeting on radionuclide transport held December 5 through 7, 2000, in Berkeley, California. Radionuclide transport KTI subissues 1, 2 and 3 were discussed at that meeting (Reamer and Williams 2000).

At this technical exchange, NRC suggested that, for the valid application of the constant K_d s approach, DOE should demonstrate that the flow path acts as a single continuum porous medium. DOE stated that evidence that the alluvium can be modeled as a single continuum porous medium would be obtained by testing at the Alluvium Testing Complex.

NRC further suggested that, for the valid application of the constant K_d s approach, the DOE should demonstrate that appropriate sorption values have been adequately considered (e.g., experimentally determined or measured). DOE responded that preliminary transport parameter values derived from lab measurements in performance assessment analyses would be used. The DOE would refine and confirm these parameter values after multiple borehole tracer testing of radionuclide surrogates at the Alluvium Testing Complex and after laboratory batch and column radionuclide transport studies.

During the NRC/DOE technical exchange and management meeting on thermal operating temperatures, held September 18 through 19, 2001, the NRC provided additional comments relating to these RT KTI agreements (Reamer and Gil 2001). Those comments relating to transport K_d s in alluvium resulted in KTI agreement GEN 1.01, Comments 41 and 102. DOE provided initial responses to these comments (Reamer and Gil 2001).

Wording of the agreements is as follows:

RT 2.06

If credit is taken for retardation in alluvium, the DOE should conduct K_d testing for radionuclides important to performance using alluvium samples and water compositions that are representative of the full range of lithologies and water chemistries present within the expected flow paths (or consider alternatives such as testing with less disturbed samples, use of samples from more accessible analog sites (e.g., 40-mile Wash), detailed process level modeling, or other

means). DOE will conduct K_d experiments on alluvium using samples from the suite of samples obtained from the existing drilling program; or, DOE will consider supplementing the samples available for testing from the alternatives presented by the NRC. This information will be documented in an update to the SZ In Situ Testing AMR, available in FY 2003. K_d parameter distributions for TSPA will consider the uncertainties that arise from the experimental methods and measurements.

RT 2.07

Provide the testing results for the alluvial and laboratory testing. DOE will provide testing results for the alluvial field and laboratory testing in an update to the SZ In Situ Testing AMR available in FY 2003.

GEN 1.01 (Comment 41)

The new N_p sorption coefficient distribution for the saturated zone used in the uncertainty analysis needs further analysis. Any future adoption of this distribution in TSPA will require a technical basis consistent with agreements RT 1.05 and RT 2.10.

DOE Initial Response to GEN 1.01 (Comment 41)

Alluvium K_d distributions are based on data obtained using EWDP-3S water and alluvium from saturated zone 3S, 9Sx, and 2D. However, DOE acknowledges that 3S water was contaminated with a polymer / surfactant used during well development. The effect of this polymer / surfactant on K_d values is being investigated by conducting additional experiments using alluvium samples and water from Nye County EWDP well locations along Fortymile wash, which were drilled without using polymer or surfactant additives. These locations are essentially along the projected SZ flow pathway from the proposed repository. The technical basis for sorption coefficients will be provided consistent with the cited agreements for data used in any potential license application.

GEN 1.01 (Comment 102)

The DOE states in Section 12 (p. 12-4) that 'new data from column and batch experiments have been used to define the K_{ds} estimate for neptunium-237.' Previous work used uranium K_d values to characterize the K_d values for neptunium-237. Has this been improved by using neptunium studies?

DOE Initial Response to GEN 1.01 (Comment 102)

K_d values obtained directly from neptunium sorption measurements are superior to assuming that uranium K_d values also apply to neptunium. A description of column and batch Neptunium 237 experiments and results will be provided in the next revision of the transport properties report, per KTI agreements RT 1.05 and RT 2.10.

K.1.2 Related Key Technical Issue Agreements

None.

K.2 RELEVANCE TO REPOSITORY PERFORMANCE

The subject of these agreements is the assessment of K_d testing to evaluate the retention capacities of Yucca Mountain alluvium for iodine-129, technecium-99, neptunium-237, and uranium-233 as part of the characterization of saturated zone flow and transport. The adequate characterization of saturated zone flow and transport is important to performance assessment. Characterization of K_{ds} comprises part of the site characterization activities and a description of radionuclide transport. As direct input to the SZ flow and transport model, K_{ds} potentially effect the model output and performance assessment. The assessment of K_{ds} supports the characterization of the saturated zone processes and their effectiveness; subsequently, it supports the performance assessment.

A discussion of the influence of sorption coefficients on radionuclide transport in the saturated zone is found in Section 3.3.2.

K.3 RESPONSE

K.3.1 Response Summary

The alluvium south of Yucca Mountain is expected to retard the migration of radionuclides from the repository to the accessible environment. The alluvium consists primarily of materials of volcanic origin, with some enrichment of clays and zeolites relative to the volcanic tuffs at Yucca Mountain. Analyses of selected samples by X-ray diffraction indicate the dominant phases in the alluvium are quartz, feldspar, and cristobalite, followed by smectite and clinoptilolite. These results are consistent with a volcanic provenance for the alluvium south of Yucca Mountain.

A series of experiments were conducted to better characterize the retardation potential of saturated alluvium. The objectives of the experiments were:

- To evaluate the retardation potential of alluvium for iodine-129, technecium-99, neptunium-237, and uranium-233 by determining distribution coefficients (K_d ; ml/g) using alluvium samples and water collected from boreholes in saturated alluvium along potential flowpaths to the accessible environment.
- To study chemical reaction mechanisms between these four radionuclides and alluvium
- To estimate sorption and transport parameters for use in predictive models.

To achieve these objectives, batch sorption, batch desorption, and flow-through column experiments were conducted under ambient conditions (room temperature, contact with atmosphere) to determine K_d values for the four radionuclides in alluvium samples from different boreholes. The first set of sorption experiments was carried out with alluvium samples from the boreholes drilled in Phase 1 of the Nye County drilling program (NC-EWDP-1X, 2D, 3S, 9SX,

19D). Groundwater from borehole 3S was used in experiments with samples from boreholes 1D, 2D, 3S, and 9SX while groundwater from borehole 19D was used in experiments with alluvium samples from 19D. Because groundwater from borehole 3S may not be representative of in situ conditions in this borehole (i.e., the water obtained from 3S may have contained materials used in well construction), the results obtained in experiments with samples from boreholes 2D, 3S, and 9S, were not used in the derivation of sorption coefficient probability distributions used in TSPA-LA. The second set of experiments was carried out with alluvium samples from boreholes NC-EWDP-10SA, 19M1A, and 22SA and groundwater from different zones in NC-EWDP-19D (Zones 1 and 4) and NC-EWDP-10SA.

As a group, the samples selected for sorption experiments are taken to be representative of alluvium in the flowpath to the accessible environment. Boreholes NC-EWDP-10SA, 19D, 19M1A, and 22SA are located within or close to the active channel in Forty Mile Wash. The groundwater in these boreholes is, on average, more oxidizing than groundwater measurements from boreholes west (NC-EWDP-1D, 3S, 7S, 9S, 12PA, 12PB, 12PC, 15D, and 15P) or east (NC-EWDP-4P, 5S) of the Forty Mile Wash channel (DTN: LA0206AM831234.002). Oxidizing groundwater should result in smaller K_d values for neptunium and uranium when compared to reducing groundwater. For neptunium, the change in sorption behavior occurs at approximately 230 ± 30 mv at near-neutral pH (Langmuir 1997, p. 538). For uranium, the change in sorption behavior occurs at lower Eh values in the range 0.0-100 mv at near-neutral pH (Langmuir 1997, p. 506). Thus, the derivation of sorption coefficient probability distributions using sorption data obtained on samples from boreholes NC-EWDP-10SA, 19D, and 19M1A, leads to conservatism in the prediction of transport rates in alluvium.

Results of the batch tests suggest that the interaction of iodine-129 and technecium-99 with the alluvium is negligible. Therefore, no additional credit is taken in TSPA for retardation of these radionuclides in alluvium.

Measured K_d values for neptunium-237 in alluvium ranged from about 3 to 13 ml/g excluding experiments with 3S water and experiments with particle sizes less than $75 \mu\text{m}$. The less than $75 \mu\text{m}$ size fraction is enriched in clays and represents a small weight fraction of in situ alluvium. Column experiments with 19D alluvium and water indicate that the extent of neptunium retardation is dependent on the flow rate through the columns. A column with a flow rate (43 m/yr) in the range of flow rates predicted in the alluvial aquifer (10-80 m/yr) (BSC 2003) did not show effective neptunium breakthrough even after the elution of about 12.5 pore volumes. This result implies the neptunium sorption coefficient in this column was greater than 2.7 ml/g. The batch K_d measured for this material was 6.9 ml/g. In column experiments with an effective flow rate of 210 m/yr, a fraction of the Np broke through with an effective K_d value of 1.5 ml/g, and when the flow rate was ~ 700 m/yr, a fraction broke through with an effective K_d value of only 0.1 ml/g. However, most of the neptunium was retained on the columns in these experiments. The difference between the batch result and the minimum K_d values from the column tests can not be explained entirely by a single first-order kinetic reaction mechanism. The results are more consistent with multiple sorption sites with different sorption rates and K_d values in the alluvium. Mass transfer processes may also be contributing to the observed column behavior. However, the result of an effective K_d value greater than 2.7 ml/g in the column experiment with a linear flow velocity approximating estimated flow velocities in

the alluvium is consistent with the concept that, as flow rates approach in situ conditions, the use of batch neptunium K_d values is justified in TSPA calculations.

For uranium-233, K_d values measured in batch experiments ranged from about 1 to 9 ml/g in alluvium. The experimental results indicate that water chemistry has a strong influence on the sorption behavior of uranium in contact with alluvium. When groundwater from Zone #1 in borehole 19D was used in sorption experiments with alluvium samples from boreholes 19IM1A and 22SA, sorption coefficient values of 3 to 9 ml/g are obtained. When groundwater from Zone #4 in borehole 19D was used in the sorption experiments with separate aliquots of the same alluvium samples, sorption coefficient values of 1 to 3 ml/g are obtained. The main differences in the chemistry of groundwater from Zones #1 and #4 in 19D include lower Ca^{2+} in #4 (0.92 versus 3.7 mg/L), higher pH in #4 (7.7 versus 9.0), and lower dissolved oxygen content in #1 (0.7 mg/L versus 3.3 mg/L). The low dissolved oxygen content of Zone #1 groundwater implies more reducing conditions and may cause the differences in uranium sorption behavior in experiments with these two waters. In addition, higher pH in #4 cause its greater carbonate content resulting in uranium carbonate complex formation, thus decreasing its sorption capacity.

A limited number of uranium column experiments were carried out with alluvium. The experiments were all run at an elution rate of 10 ml/hr, which corresponds to a linear flow velocity at least an order of magnitude greater than estimated in situ alluvium flow velocities. At this elution rate, a small fraction of the uranium loaded onto the column breaks through with tritium. That is, this fraction of uranium is transported through the column with no retardation. However, the bulk of the uranium loaded onto the columns was not eluted over the duration of the experiments. Long tails on the uranium breakthrough curves, as well as the incomplete recovery of uranium from the column experiments, suggest that the bulk of the uranium-233 loaded onto the columns is slow to desorb even at an elution rate of 10 ml/hr.

When compared to the results obtained for neptunium columns, the retardation of uranium in the columns at flow rates similar to those anticipated in the natural system, is expected to be close to that predicted by the results of batch experiments. However, more column tests at lower flow velocities are required to verify this expectation and ultimately to validate the use of batch uranium K_d values in alluvium in TSPA calculations. In effect, the results of the uranium column experiments are not appropriate for use in the derivation of the uranium sorption coefficient probability distribution in alluvium because flow rates exceeded in situ rates expected in the alluvium.

There is a range of redox conditions in alluvial groundwaters, as measured in groundwaters pumped from Nye County boreholes. Groundwater along the eastern-most (i.e., NC-EWDP-5S) and western-most (i.e., NC-EWDP-1DX, 3D) potential flow paths to the accessible environment show reducing characteristics. Groundwater measurements from boreholes along the central portion (e.g., NC-EWDP-19D, 22S) of the flow system generally show more oxidizing conditions although not exclusively, as indicated by the 19D Zone #1 water. The sorption coefficient probability distribution for uranium in alluvium was formulated to take this variability into account.

K.4 BASIS FOR THE RESPONSE

K.4.1 Materials Used in Recent Alluvium Batch Sorption and Column Transport Experiments (Used for Developing K_d Distributions)

Alluvium samples were obtained at various depths from three boreholes located south of Yucca Mountain (NC-EWDP-19IM1A, NC-EWDP-10SA, and NC-EWDP-22SA). For the batch experiments, the alluvium samples were dry sieved. For the column experiments, alluvium samples with particle sizes ranging from 75 to 2000 μm were wet sieved to remove fine particles that would clog the columns. Groundwater was used in the experiments, which was obtained from boreholes NC-EWDP-19D (Zones 1 and 4) and NC-EWDP-10SA. The chemical composition of NC-EWDP-19D waters is summarized in Table K-1. Field measurements of the redox conditions in groundwater samples in alluvium are shown in Table K-2.

Table K-1. Chemical Composition of NC-EWDP-19D Waters

Species	Concentration (mg/L) in Zone 1	Concentration (mg/L) in Zone 4
Temperature ($^{\circ}\text{C}$)	32	31
pH	7.66	9.02
Eh (mV-SHE)	342.1	493.9
Na^+	91.50	107.30
K^+	3.70	3.40
Ca^{2+}	3.70	0.92
Mg^{2+}	0.31	0.03
SiO_2	22.0	18.7
F^-	2.0	2.7
Cl^-	6.10	5.60
SO_4^{2-}	22.0	18.7
HCO_3^-	189	212

NOTES: pH and Eh were measured in the laboratory under the conditions of the batch sorption and column transport experiments (DTN: LA0302MD831341.004). Major ion concentrations are from USGS measurements reported in DTN: GS011180312322.006.

Table K-2. Redox Measurements in Groundwater in Nye County Boreholes

NC-EWDP Well No.	Sand-Pack Depth (feet bgs)	Sampling Date	pH	Dissolved Oxygen (mg/L)	Eh mv-SHE	T (degrees C)
01SX	152-189	5/17/99	7.1	4.3	327	27.5
		11/8/99	7.0	0.9-3.8	128-272	25.9-26.7
		5/18/00	7.1	3.5-3.9	347-407	27.5-27.9
01SX	204-340	5/17/99	7.2	2.7	249	28.4
		11/8/99	7.0	1.4	172	26.9
		5/18/00	7.1-7.2	1.6-1.9	133-146	28.2-28.8
01D	2180.0-2294.7	5/24/00	6.6	0.02	(-51 to -131)	25.9-26.14
03S	245-275	5/20/99	8.6	1.2	370	32.9
		11/15/99	8.3-8.5	1.7-2.2	366-386	30.3-31.9
03S	295-524.3	5/20/99	8.7	0	154	32.5
	Open Hole	11/15/99	8.5-8.9	0.1-0.4	204-299	27.8-32.0
		5/17/00	8.8-9.1	0.08-0.12	(-29 to 41)	32.4-33.9
04PA	394.7-496	5/16/00	8.5-9.8	3.0-6.3	340-456	23.8-26.3
		10/26/00	7.8-7.9	3.8-4.7	309-339	23.5-24.0
04PB	718-849.5	5/26/00	6.4-8.1	6.4-8.1	244-249	26.6-26.9
		10/26/00	9.7-9.9	2.8-3.6	217-242	21.6-23.2
05SB	366.0-499.4	5/17/00	7.5-7.7	0.04-1.5	(-10 to 37)	24.2-27.0
		10/23/00	7.6	0.01-0.09	(-26 to 49)	22.8-24.0
07S	26-53.2	10/23/00	7.0-7.1	0.7-2.4	144-211	19.7-20.6
		3/28/01	6.9-7.0	2.3-2.4	283-301	21.1-21.2
09SX	85.0-126.1	5/19/99	8.3	1.6	388	28.6
		11/10/99	7.6-8.6	2.1-6.4	317-369	25.8-26.6

Table K-2. Redox Measurements in Groundwater in Nye County Boreholes (Continued)

NC-EWDP Well No.	Sand-Pack Depth (feet bgs)	Sampling Date	pH	Dissolved Oxygen (mg/L)	Eh mv-SHE	T (degrees C)
09SX	134.8-167.1	5/19/99	7.7	5.2	432	28.1
		11/10/99	7.5-7.7	3.6-6.0	354-452	26.1-27.4
09SX	245.4-295.6	5/18/99	7.7	2.9	430	28.5
		11/9/99	7.7-8.1	1.3-3.3	196-251	27.1-27.4
09SX	325-397	5/18/99	7.7	4.8	232	29.0
		11/9/99	7.6-7.7	3.2-4.9	223-303	27.0-27.9
12PA	317.5-389.5	10/25/00	6.4-6.5	0.3-0.5	122-153	27.2-28.9
12PB	316.2-399.75	5/25/00	6.6-6.9	0.6-3.9	33-167	30.5-30.8
		10/25/00	6.5	0.5-0.8	147-160	27.2-27.6
12PC	160.4-249.6	5/25/00	7.1	4.3-5.2	282-302	27.8-27.9
		10/26/00	7.1	5.2-5.5	209-230	24.2-24.4
15P	192.6-274.5	5/23/00	7.7	4.0-4.7	413-424	32.1-32.7
		10/26/00	7.8	4.2-4.4	374-400	26.6-27.5
19D	Zone # 1	10/17/00	8.5-8.7	0.8	358-423	31.0-31.3
	408.5-437.0					
19D	Zone # 3	9/13/00	8.4	4.8-5.0	388-463	30.3-30.6
	568.0-691.0					
19D	Zone # 4	8/27/00	8.8-8.9	3.2-3.4	291-376	31.5-31.6
	717.0-795.0					
19D	Zone # 5	1/5/02	9.0	2.7-3.1	N/A	31.0-32.6
19P	351.5-474.5	5/23/00	8.6-8.7	6.7-7.0	324-396	28.9-29.5
Airport Well		6/10/99	8.3	9.5	370	28.4
YMP WELLS						
WT-17	1312-1359	7/1/98	6.1-6.7	0.0	(-23 to -65)	27.3-29.7
WT-3	1053-1093	6/22/98	7.1-7.6	3.7-6.5	273-422	31.6-33.0

DTN: LA0206AM831234.002.

NOTE: All measurements in this table were conducted in the field using water freshly pumped from the wells.

Four radionuclides (^{129}I , ^{99}Tc , ^{233}U , and ^{237}Np) were used in the experiments.

Mineral characterization of the alluvium used in the experiments was determined by quantitative X-ray diffraction (Table K-3). The major phases in the Yucca Mountain alluvium samples are silica (i.e., quartz, tridymite, cristobalite), K-feldspar, and plagioclase. The amount of smectite and clinoptilolite, which are two major absorptive mineral phases in alluvium, differs among samples. Among these samples, the sum of the smectite and clinoptilolite in NC-EWDP-22SA is larger than in NC-EWDP-19IM1A or NC-EWDP-10SA.

Table K-3. Quantitative X-ray Diffraction Results of Representative Alluvium used in the Experiments

Minerals	Samples (75-500 μm fraction, dry sieve)					
	NC-EWDP-19IM1A		NC-EWDP-10SA		NC-EWDP-22SA	
	725-730 ^{a, b}	785-790	665-670 ^b	695-700	522-525 ^b	660-665
Smectite	6.9 ^b	6.2	5.7 ^b	2.6	8.3 ^b	4.7
Kaolinite	1.2	1.3	0.8	0.5	2.0	1.1
Clinoptilolite	7.7 ^b	8.5	7.0 ^b	4.1	14.3 ^b	7.9
Tridymite	7.6	7.9	3.5	2.3	8.5	10.2
Cristobalite	5.8	6.4	7.0	5.9	5.6	7.2
Quartz	19.2	16.1	14.0	6.0	12.8	17.3
K-Feldspar	23.7	25.8	29.7	32.5	22.7	25.0
Plagioclase	25.0	26.5	30.5	40.7	19.1	21.2
Biotite	1.0	3.0	3.1	2.5	2.4	2.1
Hematite	0.7	0.7	0.8	2.4	1.0	2.5
Total	98.8	102.3	102.3	99.6	96.7	99.2

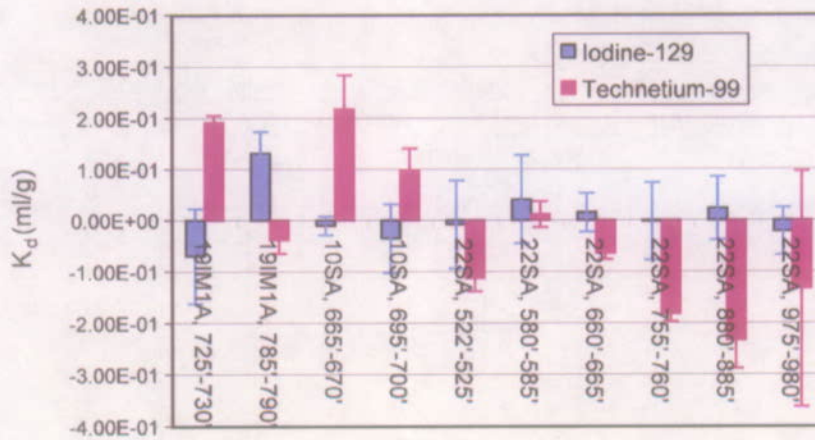
Source: Ding 2003, Attachment B.

NOTES: ^a Interval below land surface (feet)

^b Samples selected to conduct kinetic adsorption of uranium-233.

K.4.2 Summary of Batch K_d Values for ^{129}I , ^{99}Tc , ^{233}U , and ^{237}Np in Alluvium

Under ambient conditions, measured K_d values were not statistically distinguishable from zero for iodine-129 and technecium-99 sorption onto alluvium (Figure K-1).



NOTE: Experiments terminated after two weeks. Liquid to solid ratio (L/S) of the experiments is 20 ml/g. NC-EWDP-19D Zone 1 water was used for the experiments with alluvium from NC-EWDP-19IM1A and NC -EWDP-22SA, and NC -EWDP-10 S water was used for the experiments with alluvium from NC-EWDP-10SA.

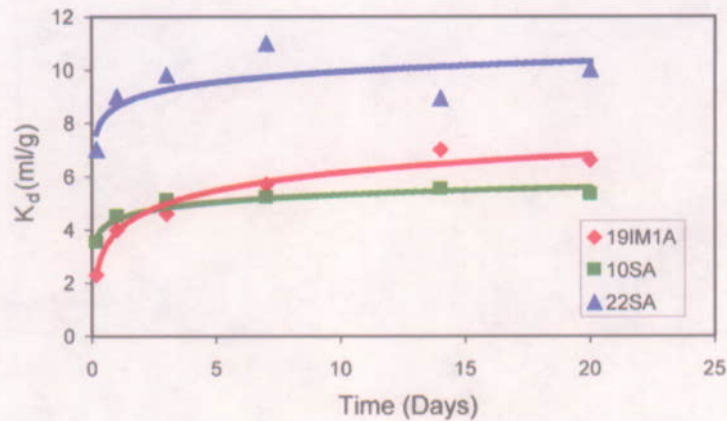
00346DCc_011

DTNs: LA0302MD831341.001, LA0302MD831341.002

NOTE: Experiments terminated after two weeks. Liquid to solid ratio (L/S) of the experiments is 20 ml/g. NC-EWDP-19D Zone 1 water was used for the experiments with alluvium from NC-EWDP-19IM1A and NC-EWDP-22SA, and NC-EWDP-10 S water was used for the experiments with alluvium from NC-EWDP-10SA.

Figure K-1. Batch K_d Values for iodine-129 and technetium-99 in Alluvium

Neptunium-237 and uranium-233 K_d values were determined experimentally in alluvium samples (Figure K-2). The K_d of neptunium-237 and uranium-233 in the alluvium differs from sample to sample depending on the depths and types of the tested alluvium. The K_d values range between 3 and 13 ml/g for neptunium-237 and about 3 to 9 ml/g for uranium-233. The sorption capacity of alluvium for neptunium-237 is larger than that for uranium-233.



NOTE: L/S = 20 ml/g. NC-EWDP-19D Zone 1 water was used for the experiments with alluvium from NC-EWDP-19IM1A and NC-EWDP-22SA, and NC-EWDP-10S water was used for the experiments with alluvium from NC-EWDP-10SA.

00346DCc_012

DTNs: LA0302MD831341.003, LA0302MD831341.004

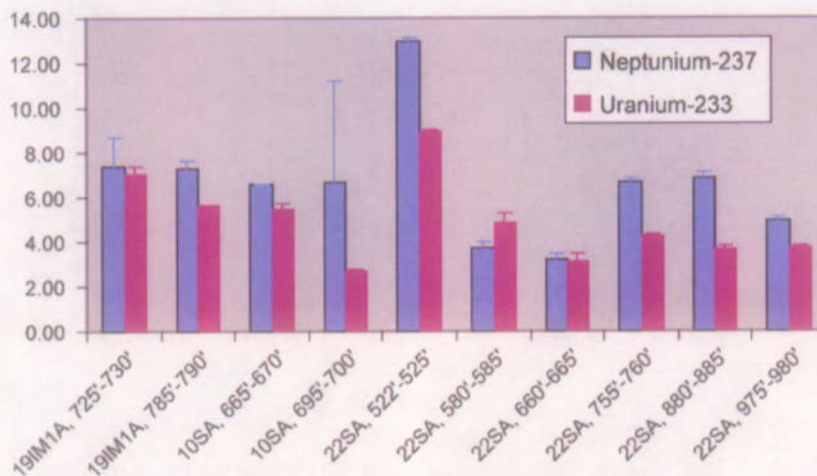
NOTE: Experiments terminated after two weeks. Liquid to solid ratio (L/S) of the experiments is 20 ml/g. NC-EWDP-19D Zone 1 water was used for the experiments with alluvium from NC-EWDP-19IM1A and NC-EWDP-22SA, and NC-EWDP-10S water was used for the experiments with alluvium from NC-EWDP-10SA.

Figure K-2. K_d Values for Neptunium-237 and Uranium-233 in Alluvium

K.4.3 Uranium Sorption Behavior in Alluvium

K.4.3.1 Uranium Sorption Experiments

Sorption kinetics of uranium-233 was measured in three alluvium samples (Table K-3). After 1 day of exposure, the amount of uranium-233 adsorbed onto alluvium changed little during the remainder of the tests. Thus, the equilibration rate for the uranium sorption reaction is relatively fast (Figure K-3). Higher K_d values from the NC-EWDP-22SA sample may be the result of higher smectite and clinoptilolite content (Table K-3).



NOTE: Experiments terminated after two weeks. Liquid to solid ratio (L/S) of the experiments is 20 ml/g. NC-EWDP-19D Zone 1 water was used for the experiments with alluvium from NC-EWDP-19IM1A and NC-EWDP-22SA, and NC-EWDP-10S water was used for the experiments with alluvium from NC-EWDP-10SA.

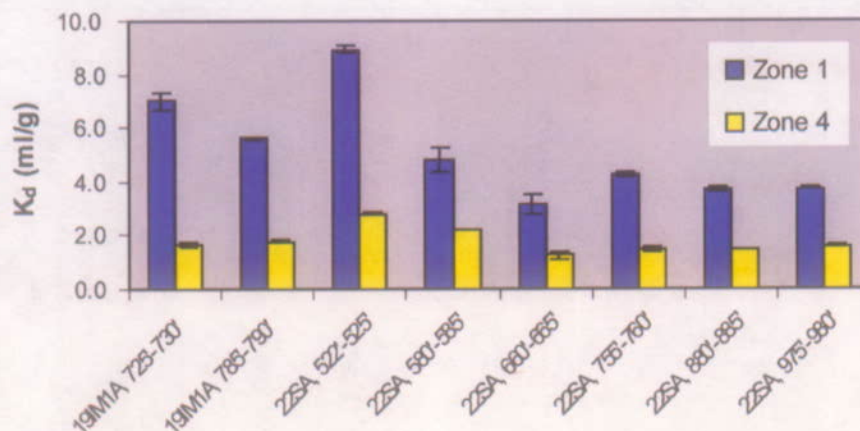
00346DCc_013

Source: Ding 2003, Attachment B.

NOTE: L/S = 20 ml/g. NC-EWDP-19D Zone 1 water was used for the experiments with alluvium from NC-EWDP-19IM1A and NC-EWDP-22SA, and NC-EWDP-10S water was used for the experiments with alluvium from NC-EWDP-10SA.

Figure K-3. Batch K_d Values for uranium-233 onto Alluvium as a Function of Time

To test if uranium-233 sorption is a function of water composition, adsorption experiments were performed with uranium-233 using water from NC-EWDP-19D Zones 1 and 4. The K_d values of uranium-233 measured in Zone 4 water were lower than those for Zone 1 (Figure K-4). Major differences in these two waters under the conditions of the laboratory experiments are the pH of Zone #4 water is considerably higher than that of Zone #1 water (Table K-1), and the dissolved oxygen content of Zone #4 water is higher than water from Zone #1. Note that the pH of the waters in the laboratory experiments were significantly different than those measured in the field; the two waters had similar pH in the field, but the Zone #1 water decreased to pH = 7.7 in the lab and the Zone #1 water increased to pH = 9. The reasons for these differences in the change in pH are not fully understood. The lower pH of the water from Zone #1 is likely a major cause for the higher sorption coefficients obtained in experiments using this water. The high pH of the zone #4 water would have resulted in a significant amount of carbonate ion (CO_3^{2-}) present in this water, whereas the Zone #1 water would have had very little carbonate ion present at a pH of 7.7. Uranium is known to form stable complexes with carbonate ion in solution (Langmuir 1997), so it would have been more likely to remain in solution at the higher pH of the Zone #4 water.



NOTE: Experiments terminated after two weeks. Liquid to solid ratio (L/S) of the experiments was 20ml/g.

00346DCc_014

DTN: LA0302MD831341.004

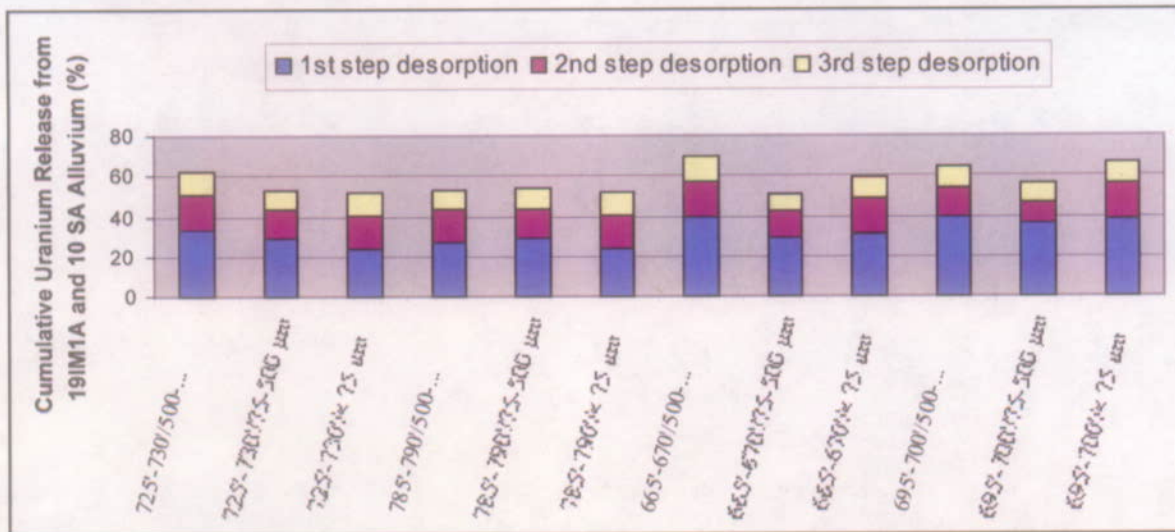
NOTE: Experiments terminated after two weeks. Liquid to solid ratio (L/S) of the experiments was 20 ml/g.

Figure K-4. Batch K_d Values for ranium-233 in NC-EWDP-19D Zone 1 and Zone 4 Waters

K.4.3.2 Uranium Desorption Experiments

Multi-step batch desorption experiments of sorbed ^{233}U were conducted (Figure K-5). Most of the uranium desorbed from the alluvium samples was desorbed during the first step. Less uranium was desorbed in subsequent desorption steps. A large fraction (30-50 percent) of the sorbed ^{233}U remained sorbed on the solid phase even after three desorption steps. These results suggest that the ^{233}U desorption kinetics were relatively slow and that they may have been slowing down as the experiments progressed.

Continuous-flow ^{233}U desorption experiments were conducted after the end of some of the sorption experiments. The alluvium material containing sorbed ^{233}U was removed from the test tubes used in the batch experiments and placed in a small "column", where it was then subjected to a continuous flow of fresh water. The effluent from the column was analyzed for ^{233}U . The results showed that the release of sorbed ^{233}U slowed down after first 100 ml of ground water had contacted the alluvium (Figure K-6), but release continued at a finite rate for the remainder of the experiment. The total duration of the experiment was about 5.5 days, including a ~2.5-day flow interruption just after 100 ml eluted. The concentrations of eluted ^{233}U near the end of the experiment were very close to the detection limit. These results suggest that the desorption of the sorbed ^{233}U was quite slow.. Simple linear extrapolation of the trends at the end of the experiments suggests that the total desorption after 3 weeks would be similar to the total desorption measured after 3 weeks in the multi-step batch desorption experiments shown in Figure K-5.



NOTE: The time period for each step of desorption was one week. L/S ratio for the desorption is about 20 ml/g.

00346DCc_015

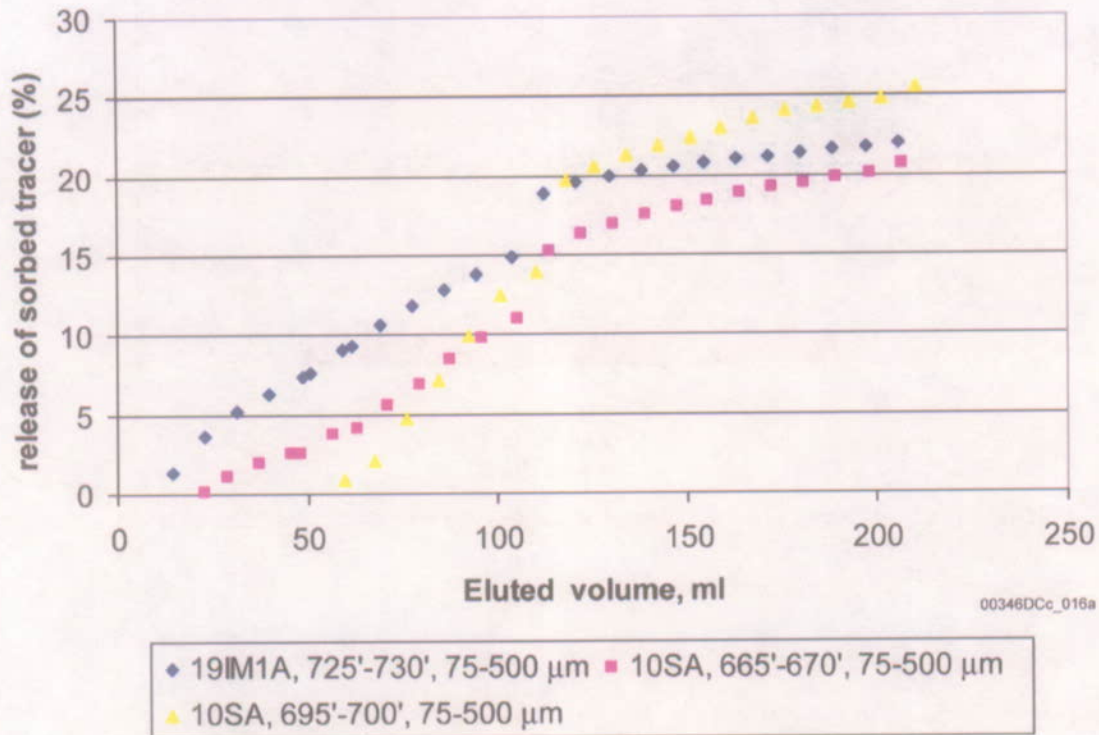
Source: Ding 2003, Attachment B.

NOTE: The time period for each step of desorption was one week. L/S ratio for the desorption is about 20 ml/g.

Figure K-5. Cumulative Release of Sorbed uranium-233 from NC-EWDP-19IM1A and NC-EWDP-10SA Alluvium

K.4.3.3 Uranium Column Experiments

Continuous-flow column experiments were conducted at room temperature and under ambient conditions at an elution rate of 10 ml/hr. The elution rate was decreased first to 5 ml/hr and then very quickly to 3 ml/hr as the experiments progressed. Experimental conditions are presented in Table K-4. The ^{233}U breakthrough curves relative to $^3\text{H}_2\text{O}$ are shown in Figure K-7. In all cases, a small fraction of the uranium broke through at almost the same time as the $^3\text{H}_2\text{O}$, but the vast majority of the uranium mass was significantly retarded. Total uranium recoveries ranged from 25 to 62 percent of the uranium injected. The long tails and incomplete recoveries observed in the column experiments indicate that some of the ^{233}U was slow to desorb from the columns within the time frame of the experiments. These experiments have not yet been interpreted to obtain estimates of uranium sorption parameters.



Source: Ding 2003, Attachment B.

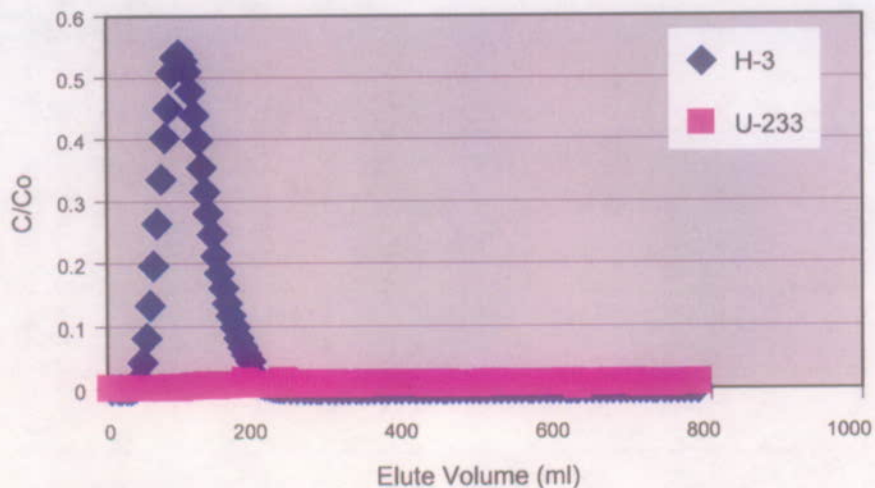
NOTE: The flow rate is 3 ml/h. NC-EWDP-19D Zone 1 water was used for NC-EWDP-19IM1A sample, 10 S water was used for NC-EWDP-10SA samples.

Figure K-6. Release of Sorbed uranium-233 as a Function of Elute Volume of Groundwater

Table K-4. Uranium Column Experiments

	Column #1	Column #2	Column #3
Geological Medium	19IM1A	10SA	22SA
Interval (ft. BLS)	725-730	665-670	522-525
Particle Size (μm)	75-2000	75-2000	75-2000
Water Used	19D Zone 1	10S	19D Zone 1
pH range	8.4-8.7	8.2-8.5	8.4-8.7
Diameter, cm	2.5	2.5	2.5
Dry alluvium packed in column (g)	374.61	356.59	390.72
Water weight after the saturation (g)	89.82	102.4	85.98
Porosity in column	0.41	0.44	0.39

Source: Ding 2003, Attachment B.

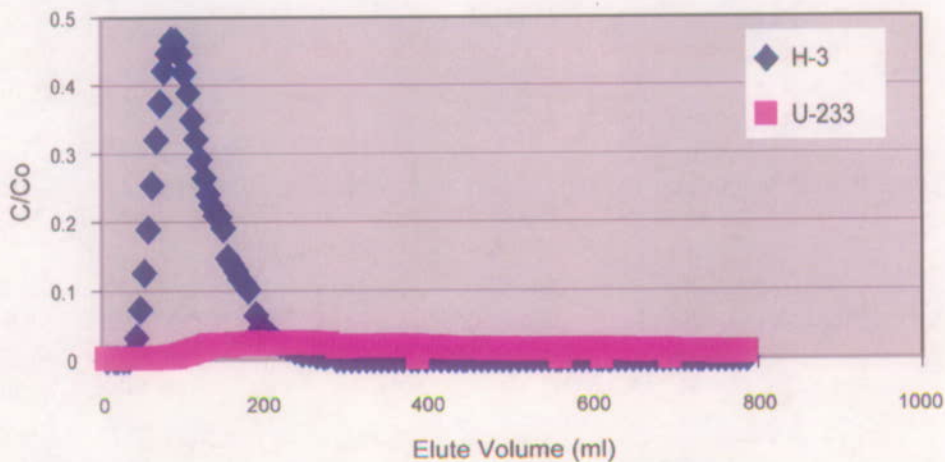


NOTE: The total recovery of ^3HHO was about 94%, while that of uranium-233 was about 10%. The flow rate was 10 ml/h.

00346DCc_017

NOTE: The total recovery of ^3HHO was about 94 percent, while that of uranium-233 was about 10 percent. The flow rate was 10 ml/h.

Figure K-7a. Column #1, ^3HHO and Uranium-233 Breakthrough Curve

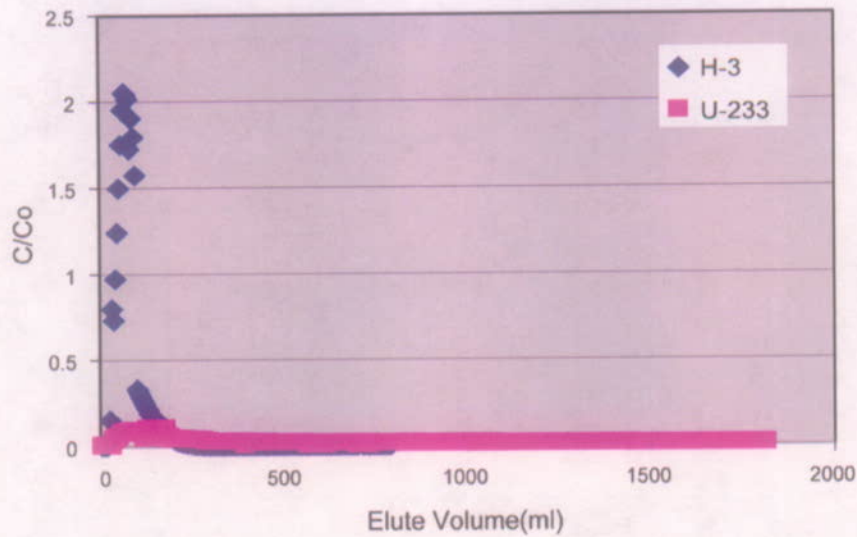


NOTE: The total recovery of ^3HHO was about 87%, and that of uranium-233 was about 23%. The flowrate was 10 ml/h.

00346DCc_018

NOTE: The total recovery of ^3HHO was about 87 percent, and that of uranium-233 was about 23 percent. The flow rate was 10 ml/h.

Figure K-7b. Column #2, ^3HHO and Uranium-233 Breakthrough Curves



NOTE: The total recovery of ^3HHO was about 92%, and that of uranium-233 was about 65%. The flowrate was 10 ml/h.

00346DCc_019

NOTE: The total recovery of ^3HHO was about 92 percent, and that of uranium-233 was about 65 percent. The flow rate was 10 ml/h.

Figure K-7c. Column #3, ^3HHO and Uranium-233 Breakthrough Curves

K.4.4 Neptunium Sorption Behavior in Alluvium

K.4.4.1 Materials used in Early Neptunium Experiments

The alluvium materials used in the early Np experiments were obtained from different intervals within five boreholes located south of Yucca Mountain (i.e., boreholes NC-EWDP-2D, NC-EWDP-9S, NC-EWDP-3S, NC-EWDP-1X, NC-EWDP-19D). The alluvium samples used and preparation methods are presented in Table K-5.

Table K-5. Boreholes and Sample Preparation Methods

Borehole Location	Depth (ft BLS)	Sample Preparation Method ^a	Particle Size Fraction (wt %)		
			75-2000 μm	75-500 μm	< 75 μm
2D	395-400	A	ND	59	41
2D	400-405	A	ND	60	40
2D	405-410	A	ND	56	44
2D	410-415	A	ND	56	44
9S	145-150	A	ND	66	34
9S	150-155	A	ND	62	38
9S	155-160	A	ND	61	39
9S	160-165	A	ND	61	39
3S	60-65	A	ND	54	46
3S	65-70	A	ND	64	36
3S	70-75	A	ND	59	41
3S	75-80	A	ND	66	44
1X	390-395	B+A	40	39	21
1X	395-400	B+A	71	19	10
1X	400-405	B+A	33	45	22
1X	405-410	B+A	51	33	16
19D	405-425	A	ND	ND	ND
19D	405-425	C	100	0	0
19D	405-425	C	0	0	100

Source: Ding et al. 2003.

NOTES: BLS = below land surface; ND = not determined.

^a Sample Preparation Method: A) Grind, crush, and dry sieve; B) collect 75-2000 μm size particle materials by dry sieving without grinding or crushing, followed by process A; C) collect 75-2000 μm size particle materials by dry sieving without grinding or crushing processes, follow with washing out the fine particles and collecting particle size range 75-2000 μm materials by wet sieving.

The water used in the experiments came from boreholes NC-EWDP-03S and two zones in NC-EWDP-19D. The water compositions are shown in Table K-6. The compositions of NC-EWDP-03S and NC-EWDP-19D (1 and 2) water were similar. Groundwater from NC-EWDP-03S had a lower dissolved oxygen concentration, lower Eh, and a higher organic carbon concentration than the 19D groundwater measurements. Thus, groundwater from 3S is more reducing than groundwater from different zones in 19D.

Table K-6. Borehole NC-EWDP-03S and NC-EWDP-19D Waters Composition

Species	Concentration (mg/L)		
	3S (449 ft BLS)	19D1 (412-439 ft + 490-519 ft BLS)	19D2 (412-437 ft BLS)
Na ⁺	141	69.4	73.2
K ⁺	2.99	3.61	3.92
Li ⁺	0.26	0.087	0.081
Ca ²⁺	0.94 ± 0.01	7.59	7.70
Mg ²⁺	0.14	0.65	0.69
Mn ²⁺	< 0.002	0.0088	< 0.0001
Fe ^{2+/3+}	0.02	0.09	< 0.01
Al ³⁺	0.34	0.05	0.002
SiO ₂	48.4	58.0	58.4
F ⁻	3.24	1.78	1.96
Cl ⁻	8.68	5.61	6.52
NO ₃ ⁻	0.28	4.18	4.84
SO ₄ ²⁻	50.0	23.0	23.8
HCO ₃ ⁻	261	168	146
CO ₃ ²⁻	ND	0	17.9
Alkalinity (CaCO ₃)	193	ND	ND
PH	8.67	8.11	9.02
Eh (mv/SHE) ^a	190	ND	ND
DO	0.02	ND	ND
TOC	1.5	<0.6	0.67
Ionic strength (mol/kg)	0.007	0.004	0.005

Source: Ding 2003.

NOTES: ND = not determined; DO = dissolved oxygen; TOC = total organic carbon; SHE = standard hydrogen electrode.

^a SHE is the reference electrode for reporting Eh data. $Eh(SHE)_{\text{sample}} = Eh(SHE)_{\text{measured for sample}} + \frac{RT}{F} \ln \left(\frac{a_{\text{H}^+}}{a_{\text{H}_2}} \right)$

Alluvium samples were characterized primarily using quantitative X-ray diffraction and N₂-BET surface area measurements (Table K-7). Samples were selected from different borehole locations, intervals, sieving methods, and particle sizes.

The mineralogy of the alluvium used in the experiments is summarized in Table K-7. The amount of organic carbon in the samples was negligible. Trace amounts of calcite and hematite were detected in some samples. Alluvium from borehole NC-EWDP-03S contained a considerable amount of calcite. Dry sieved samples were used for all the experiments except for a column experiment with material from NC-EWDP-19D. Note that the sieving technique (wet vs. dry) had only a minor effect on the mineral composition of the 75-500 μm fraction of the 19D sample.

Table K-7. Mineral Abundance and Surface Areas for Selected Alluvium Samples used in Early Np Sorption Tests

Alluvium		Quantitative mineral abundance for alluvium samples (wt %)													Surface area (m ² /g)	Organic Carbon (wt %)
Sieve Method	Bore-hole	Depth (ft BLS)	PS (µm)	Smectite	Clinoptilolite	Kaolinite	Mica	Tridymite	Cristobalite	Quartz	Feldspar	Calcite	Hematite	Total		
Dry	2D	410-415	75-500	2±1	4±1	1±1	trace	3±1	16±1	18±1	54±8	---	1±1	99±8	1.97	---
	9Sx	160-165	75-500	6±2	3±1	---	trace	1±1	18±1	14±1	58±8	---	trace	100±8	2.80	---
	3S	75-80	75-500	1±1	13±1	1±1	1±1	---	10±1	17±1	53±8	4±1	---	100±8	3.67	---
	19D	405-425	75-500	5±2	7±1	1±1	trace	3±1	13±1	20±2	52±8	trace	trace	101±9	7.60	0.22
	2D	410-415	<75	4±1	7±1	1±1	1±1	5±1	14±1	17±1	53±8	---	1±1	103±8	4.27	---
	2D	395-400	<75	10±3	13±1	1±1	trace	4±1	13±1	11±1	47±7	1±1	trace	100±8	5.55	---
	9S	155-160	<75	19±6	3±1	trace	1±1	4±1	14±1	12±1	50±7	---	trace	103±9	5.69	---
	3S	60-65	<75	7±2	13±1	2±1	1±1	1±1	11±1	12±1	44±7	9±1	trace	100±8	11.94	---
	19D	405-425	75-2000	4±1	5±1	1±1	1±1	3±1	16±1	16±1	49±7	---	1±1	96±8	5.42	0.15
	19D	405-425	<75	48±14	6±1	1±1	1±1	2±1	5±1	8±1	29±4	1±1	---	101±15	73.65	0.76
3S	65-70	<75	30±9	21±2	1±1	2±1	trace	2±1	2±1	25±4	12±1	---	98±10	37.49	---	

Source: Ding 2003, Attachment C.

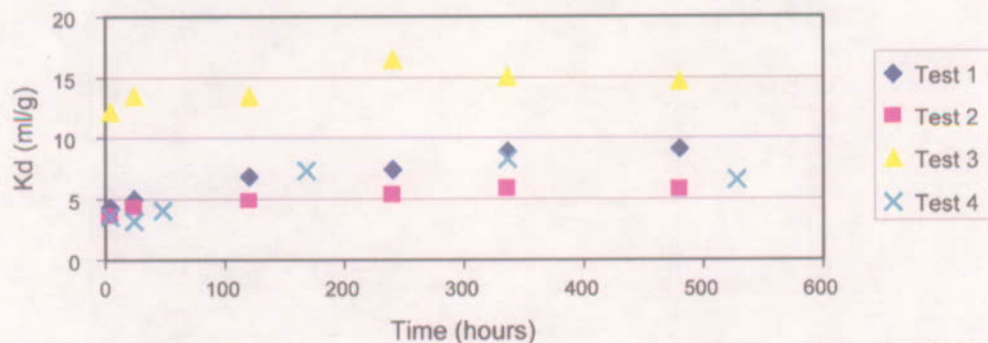
NOTES: PS = particle size; "----" = not detected; trace = amount at less than 0.5 wt%. Surface area measurements were conducted using MONOSORB N₂-BET Single Point Surface Area Analyzer.

K.4.4.2 Neptunium Batch Sorption Results from Early Experiments

Kinetics of Neptunium(V) Interaction with Alluvium—Kinetic experiments, using the experimental conditions described in Table K-8, were conducted to examine the interaction of neptunium(V) and alluvium. The initial sorption kinetics were fast (Figure K-8). After 1 day of exposure, the amount of neptunium(V) adsorbed onto alluvium changed little with time in all four tests. The effects of different waters and concentrations of neptunium(V) on the kinetic processes of reaction between neptunium(V) and alluvium were not systematically evaluated but they appeared to be of less importance than the alluvium characteristics.

Table K-8. Experimental Conditions for Kinetics of neptunium(V) Interaction with Alluvium

Test	Alluvium			Neptunium(V) Initial Concentration	Water used
	Borehole	Depth (ft BLS)	Particle Size (μm)		
Test 1	2D	410-415	75-500	1×10^{-7} mol/L	NC-EWDP-3S
Test 2	9S	160-165	75-500	1×10^{-7} mol/L	NC-EWDP-3S
Test 3	3S	75-80	75-500	1×10^{-7} mol/L	NC-EWDP-3S
Test 4	19D	405-425	75-2000	1×10^{-6} mol/L	NC-EWDP-19D1



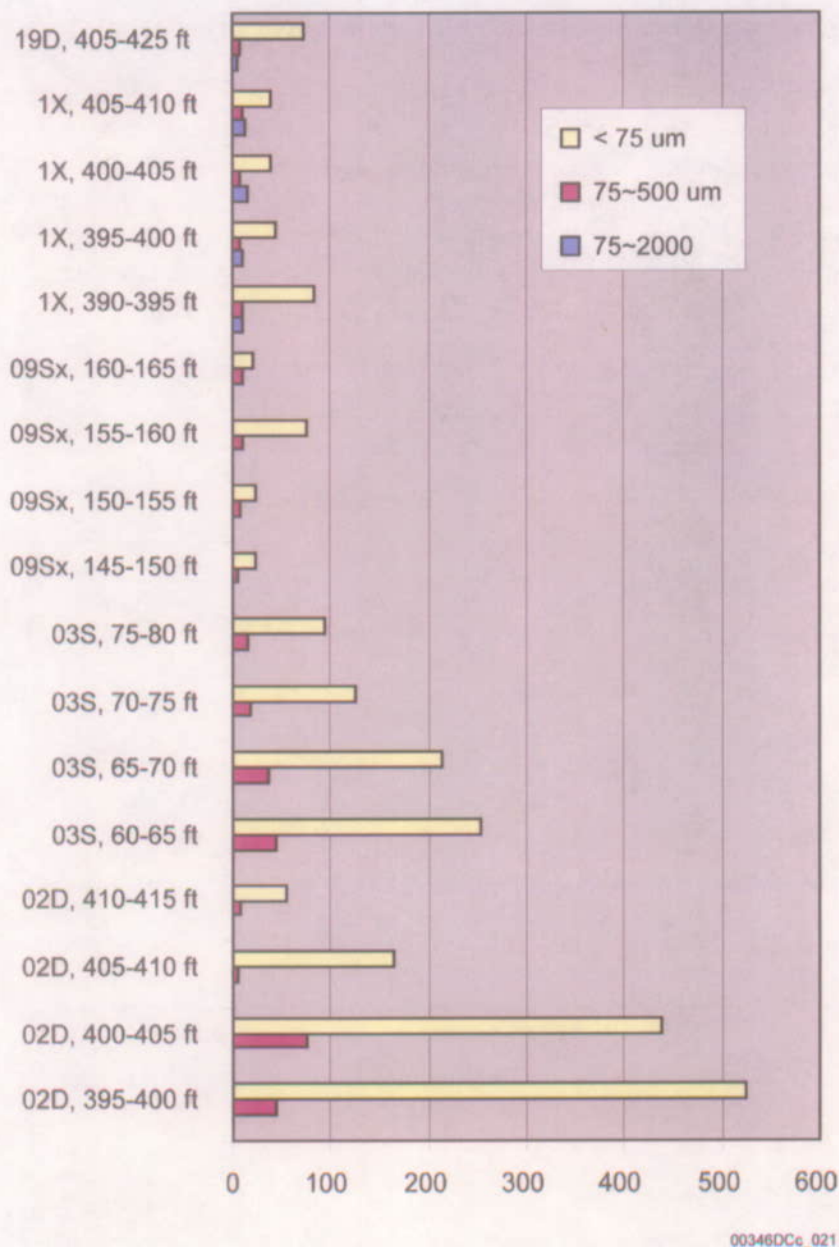
003460Cc_020

DTN: LA0106MD831341.001

Source: Ding 2003, Attachment A, C.

Figure K-8. Sorption Kinetic of neptunium-237 in Yucca Mountain Alluvium

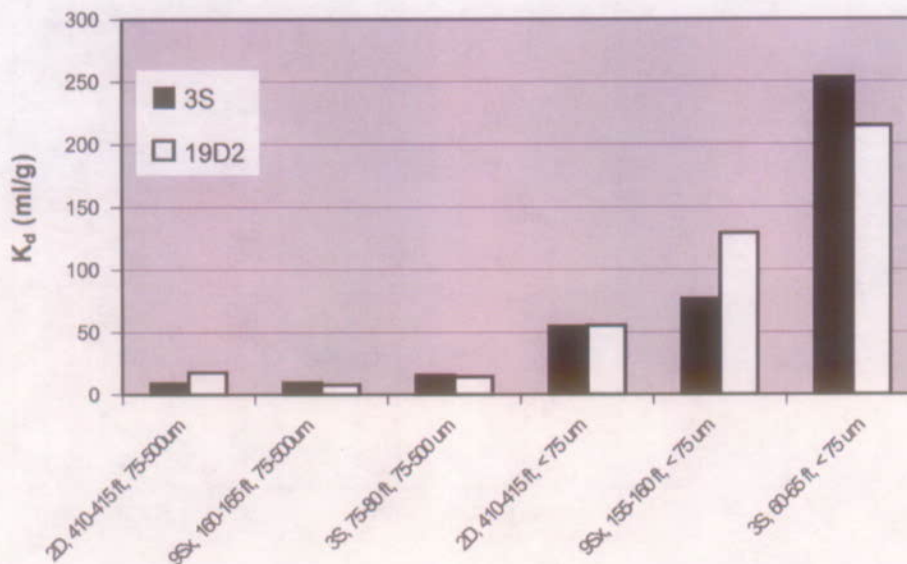
Range of K_d Values for Neptunium(V)—The experimentally determined K_d values for all the alluvium samples listed in Table K-5 are presented in Figure K-9. The experimental period for these tests was 2 weeks. The water used for NC-EWDP-19D alluvium test was NC-EWDP-19D1 groundwater. The water used for all other experiments was NC-EWDP-3S groundwater. The results suggest that the K_d of neptunium(V) in alluvium differs from sample to sample and range from about 4 to 500 ml/g. The particle size of the sample appears to play an important role with respect to K_d value. In general, the smaller the particle size, the larger the K_d value. Alluvium samples from near the surface of boreholes NC-EWDP-2D and NC-EWDP-3S boreholes have a large adsorption capability for neptunium(V).



Source: Ding 2003, Attachment A, C.

Figure K-9. Batch K_d Values for Neptunium(V) in Different Intervals and Size Fractions

Effect of Groundwater Chemistry on Neptunium(V) K_d Values—Adsorption experiments were conducted using neptunium-237 and alluvium and groundwater from the same boreholes (NC-EWDP-03S and NC-EWDP-19D). The K_d values obtained for a given sample with the two different waters were similar (Figure K-10). This result suggests that the different redox states of the two waters did not have a significant impact on neptunium sorption behavior or that the waters used in the experiments had equilibrated with the atmosphere before they were used.



NOTE: The initial concentration of neptunium(V) was 1×10^{-6} M. The liquid to solid ratio for all experiments was 20 ml/g. The testing period was 2 weeks.

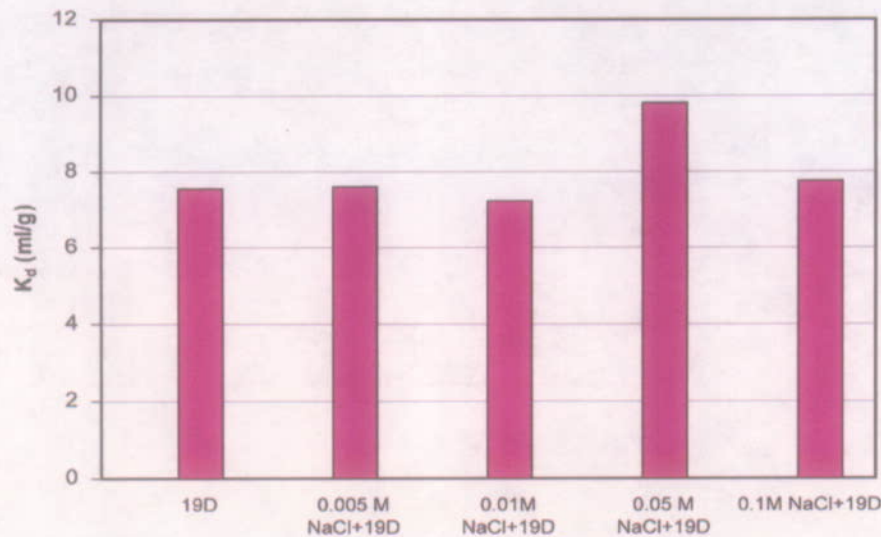
00346DCc_022

Source: Ding 2003, Attachment A, C.

NOTE: The initial concentration of neptunium(V) was 1×10^{-6} M. The liquid to solid ratio for all experiments was 20 ml/g. The testing period was 2 weeks.

Figure K-10. Batch K_d Values for Neptunium(V) in Waters from Boreholes NC-EWDP-3S and NC-EWDP-19D

Effects of Ionic Strength on Neptunium-237 K_d Values—The adsorption of ^{237}Np adsorption in alluvium from borehole NC-EWDP-19D was examined under various ionic strengths. The original ionic strength of NC-EWDP-19D water was 0.004, but this was modified by adding NaCl. The K_d of ^{237}Np did not change significantly with increasing ionic strength (Figure K-11). These results suggest that the reaction mechanism is probably dominated by surface complexation rather than ion exchange. An additional experiment (not shown) indicated a much larger K_d value in deionized water than in the 19D water, suggesting a possible role of carbonate in suppressing Np sorption in the 19D water (carbonate was not present in the deionized water).



NOTE: Equilibration period is two weeks

00346DCc_023

Source: Ding 2003, Attachment A, C.

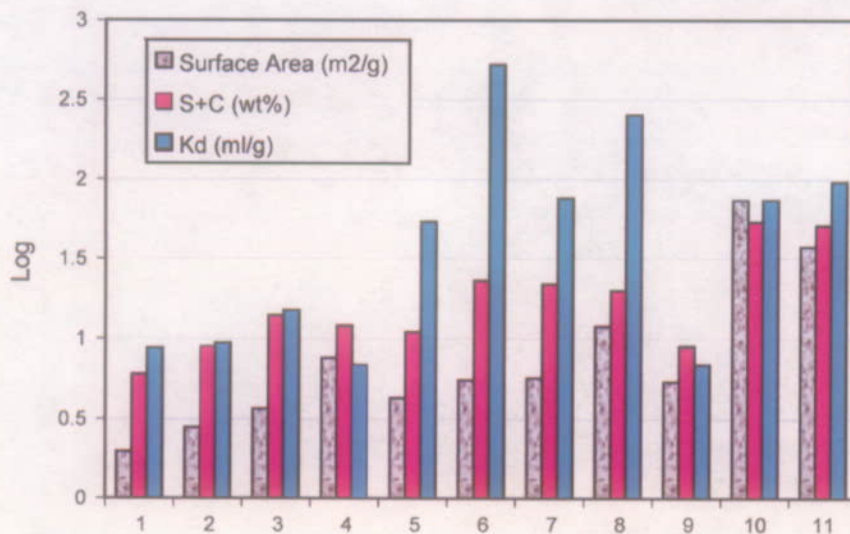
NOTE: Equilibration period is two weeks.

Figure K-11. Batch K_d Values for neptunium-237 in Solutions with Different Ionic Strengths

Alluvium K_d values in Relation to Surface Area and Secondary Mineral Content—Surface reactions (e.g., sorption) depend on the surface properties of the geosorbents (e.g., surface area). The larger the surface area of the sample, the larger will be the K_d value obtained under the same experimental conditions. Clays and zeolites have larger surface areas than do primary minerals. Thus, alluvium containing more clay and zeolites would be expected to have larger K_d values.

Experiments were conducted to examine the relationships among surface area, the amount of secondary minerals (combined amounts of smectite and clinoptilolite), and the K_d values of neptunium-237 in alluvium. The results of these experiments are presented in Figure K-12.

The surface area of the alluvium samples was related to the amount of smectite and clinoptilolite in the sample, such that the larger the amount of smectite and clinoptilolite, the larger the surface area. However, two samples with high K_d values did not have high contents of smectite and clinoptilolite, and they did not have the highest surface areas. Thus, while Np sorption is positively correlated with surface area and mineralogy, trace amounts of minerals such as amorphous Fe and Mn oxides, which were not identified by quantitative X-ray diffraction, may ultimately exert more influence on Np K_d values in the alluvium. Studies of sorption by neptunium, plutonium, and americium in the vitric tuffs of Busted Butte indicated that sorption increases with increasing levels of smectite, Fe, and Mn oxides in the rock (Turin et al. 2002).



NOTE: Surface area units = m²/g, S = smectite (wt %); C = clinoptilolite (wt %), K_d units = ml/g.

00346DCc_024

Source: Ding 2003, Attachment A, C.

NOTE: Surface area units = m²/g, S = smectite (wt %); C = clinoptilolite (wt %), K_d units = ml/g.

Figure K-12. Surface Area, Combined Smectite and Clinoptilolite, and K_d Values for neptunium(V)

K.4.4.3 Neptunium Column Transport Experiments

Two sets of column studies were performed to investigate neptunium(V) transport behavior in saturated alluvium under flowing conditions. Tables K-9 and K-10 list individually the columns used and parameters for the two studies. In all the column experiments, tritium (³HHO) was used as conservative tracer. Water from NC-EWDP-03S was used in the experiment in column #1 and water from NC-EWDP-19D was used in the experiments in columns #2 through #4. The latter experiments were reported by Ding et al. (2003).

Table K-9. Column Study (I)

	Column #1
Geological Medium	-03S
Interval (ft. BLS)	65-70
Particle Size (μm)	75-500
Water Used	-03S
pH range	8.5-9.0
Diameter, cm	1.0
Length of column (cm)	60
Porosity in column	0.45
Flow rate (ml/h)	2 (reduced to 0.5 ml/h late in the test)

Source: Ding 2003, Attachment A.

Table K-10. Column Study (II)

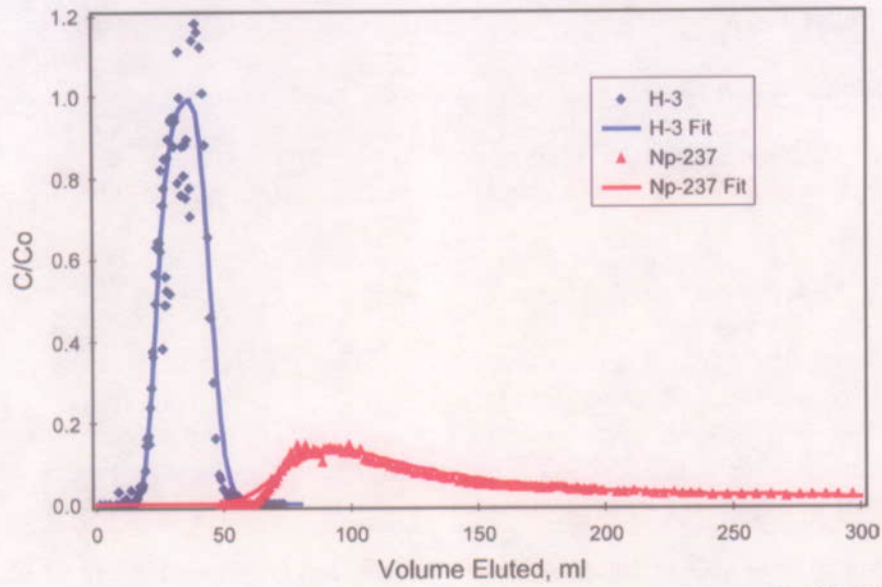
	Column #2	Column #3	Column #4
Geological Medium	-19D	-19D	-19D
Interval (ft. BLS)	405-425	405-425	405-425
Particle Size (μm)	75-2000	75-2000	75-2000
Water Used	19D	19D	19D
pH range	8.4-8.7	8.4-8.7	8.4-8.7
Diameter, cm	2.5	2.5	2.5
Length of alluvium in the column (cm)	45	45	45
Porosity in column	0.38	0.37	0.34
Flow rate (ml/h)	0.6	3	10
Np recovery (%)	NA	32	9

Source: Ding 2003, Attachment C.

Results—Figure K-13 shows the breakthrough curve of neptunium from column #1, and Figure K-14 shows the breakthrough curves of neptunium from columns # 2, #3 and #4. As Figure K-14 shows, there was no breakthrough of neptunium after ~12.5 pore volumes had been eluted in the 0.6 ml/hr test. The K_d value corresponding to a breakthrough at 12.5 pore volumes is approximately 2.7 ml/g for the column in which this test was conducted. Thus, all of the neptunium in the 0.6 ml/hr test had an effective K_d value of greater than 2.7 ml/g. This test is significant because the linear flow velocity in the column was 43 m/yr, which is consistent with estimates of linear flow velocities in the alluvial aquifer (10-80 m/yr) (BSC 2003).

Figure K-14 indicates that higher flow rates result in a lower effective K_d value for at least a portion of the neptunium traveling through the columns. However, despite the early breakthroughs in the experiments at the two higher flow rates, the recoveries of neptunium were still quite low (32 percent or less), suggesting very slow desorption rates for most of the neptunium in the columns. Furthermore, the long tails in these experiments suggest a wide range of desorption rates for neptunium. The minimum possible K_d value in the lowest flow rate column test (2.7 ml/g) agrees better with the batch studies ($K_d = 6.9$ ml/g) than the K_d values for the earliest arriving neptunium in the higher flow rate tests.

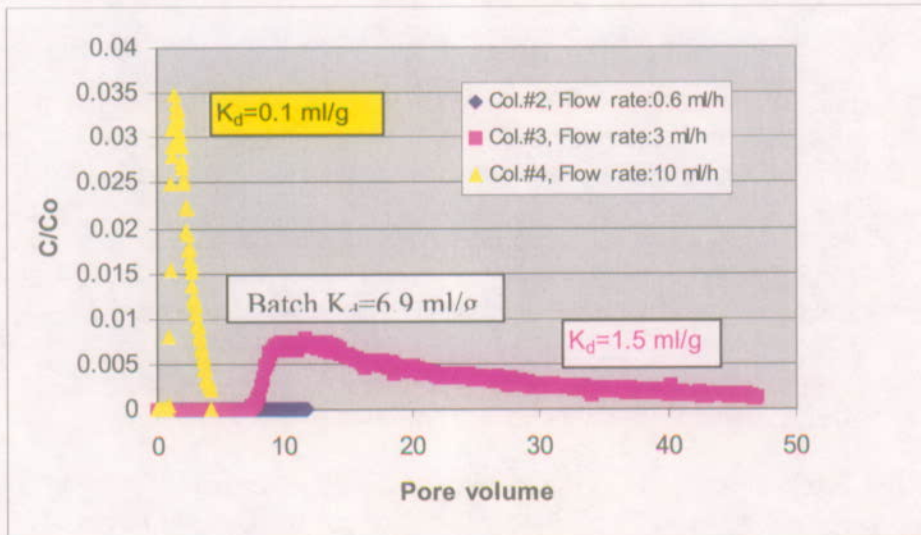
The observed differences in neptunium transport as a function of flow rate cannot be explained by a single rate-limited sorption reaction. A dual-porosity model was used to model the data of Figure K-13 after a single-porosity kinetic sorption model could not provide a reasonable fit. A good fit by the dual-porosity model in this case is not taken to imply that there is a significant amount of stagnant water in the columns that the flowing water is in diffusive communication with. Rather, this result is taken to indicate that there may be a mass transport step occurring in series with a sorption reaction in the column. However, the column results could also be explained by multiple sorption reactions occurring at different rates and with different effective K_d values (because of different sorption sites). Preliminary modeling of the column experiments shown in Figure K-14 suggests that this latter explanation is more consistent with the results of these experiments. The column experiments reveal that reactive transport processes in heterogeneous alluvium, even at a relatively small scale, are quite complicated and not amenable to simple transport models, at least when flow velocities are high.



00346DCc_025

Source: Ding 2003, Attachment A.

Figure K-13. Tritiated water and Neptunium Breakthrough Curves in Column #1



Source: Ding 2003, Attachment C.

Figure K-14. Neptunium Breakthrough Curves in Columns #2 and #3

K.5 REFERENCES

K.5.1 Documents Cited

BSC (Bechtel SAIC Company) 2003. *Saturated Zone In-Situ Testing*. MDL-NBS-HS-000039 REV 00A. Las Vegas, Nevada: Bechtel SAIC Company. ACC: MOL.20030602.0291.

Ding, M. 2003. YMP Alluvium Sorption II Notebook: SN-LANL-SCI-273-V1. Los Alamos, New Mexico: Los Alamos National Laboratory. ACC: TBD.

Ding, M.; Reimus, P.W.; Ware, S.D.; and Meijer, A. 2003. "Experimental Studies of Radionuclide Migration in Yucca Mountain Alluvium." *Proceedings of the 10th International High-Level Radioactive Waste Management Conference (IHLRWM), March 30-April 2, 2003, Las Vegas, Nevada*. Pages 126-135. La Grange Park, Illinois: American Nuclear Society. TIC: 254559.

Langmuir, D. 1997. *Aqueous Environmental Geochemistry*. Upper Saddle River, New Jersey: Prentice Hall. TIC: 237107.

Reamer, C.W. and Gil, A.V. 2001. Summary Highlights of NRC/DOE Technical Exchange and Management Meeting on Range of Thermal Operating Temperatures held September 18-19, 2001, Las Vegas, Nevada; Rockville, Maryland; and San Antonio, Texas. [Washington, D.C.]: U.S. Nuclear Regulatory Commission. ACC: MOL.20020107.0162.

Reamer, C.W. and Williams, D.R. 2000. Summary Highlights of NRC/DOE Technical Exchange and Management Meeting on Radionuclide Transport. Meeting held December 5-7, 2000, Berkeley, California. Washington, D.C.: U.S. Nuclear Regulatory Commission. ACC: MOL.20010117.0063.

Turin, H.J.; Groffman, A.R.; Wolfsberg, L.E.; Roach, J.L.; and Strietelmeier, B.A. 2002. "Tracer and Radionuclide Sorption to Vitric Tuffs of Busted Butte, Nevada." *Applied Geochemistry*, 17, (6), 825-836. New York, New York: Elsevier. TIC: TBD.

K.5.2 Source Data, Listed by Data Tracking Number

GS011108312322.006. Field and Chemical Data Collected between 1/20/00 and 4/24/01 and Isotopic Data Collected between 12/11/98 and 11/6/00 from Wells in the Yucca Mountain Area, Nye County Nevada. Submittal date: 11/20/2001.

LA0106MD831341.001. Adsorption of Np-237 in Three Types of Alluvium as a Function of Time and Stratigraphic Position. Submittal date: 06/21/2001.

LA0302MD831341.001. Iodine-129 Sorption in Alluvium from NC-EWDP Wells 19IM1A, 10SA, and 22SA under Ambient Conditions. Submittal date: 02/13/2003.

LA0302MD831341.002. Technetium-99 Sorption in Alluvium from NC-EWDP Wells 19IM1A, 10SA, and 22SA under Ambient Conditions. Submittal date: 02/11/2003.

LA0302MD831341.003. Neptunium-237 Sorption in Alluvium from NC-EWDP Wells 19IM1A, 10SA, and 22SA under Ambient Conditions. Submittal date: 02/11/2003.

LA0206AM831234.002. Geochemical Field Measurements on Nye County EWDP Wells. Submittal date: 06/21/2002.

LA0302MD831341.004. Uranium Sorption in Alluvium from NC-EWDP Wells 19IM1A, 10SA, and 22SA Under Ambient Conditions. Submittal date: 02/11/2003.

INTENTIONALLY LEFT BLANK

APPENDIX L
TRANSPORT-TEMPORAL CHANGES IN HYDROCHEMISTRY
(RESPONSE TO TSPA I 3.31)

Note Regarding the Status of Supporting Technical Information

This document was prepared using the most current information available at the time of its development. This Technical Basis Document and its appendices providing Key Technical Issue Agreement responses that were prepared using preliminary or draft information reflect the status of the Yucca Mountain Project's scientific and design bases at the time of submittal. In some cases this involved the use of draft Analysis and Model Reports (AMRs) and other draft references whose contents may change with time. Information that evolves through subsequent revisions of the AMRs and other references will be reflected in the License Application (LA) as the approved analyses of record at the time of LA submittal. Consequently, the Project will not routinely update either this Technical Basis Document or its Key Technical Issue Agreement appendices to reflect changes in the supporting references prior to submittal of the LA.

APPENDIX L

TRANSPORT-TEMPORAL CHANGES IN HYDROCHEMISTRY (RESPONSE TO TSPA I 3.31)

This appendix provides a response for Key Technical Issue (KTI) agreement Total System Performance Assessment Integration (TSPA I) 3.31. This KTI agreement relates to providing more information about effects in temporal changes in water chemistry on transport parameters.

L.1 KEY TECHNICAL ISSUE AGREEMENT

L.1.1 TSPA I 3.31

KTI agreement TSPA I 3.31 was reached during the NRC/DOE TSPA I technical exchange and management meeting on total system performance assessment and integration held August 6 through 10, 2001, in Las Vegas, Nevada. TSPA I KTI subissues 1, 2, 3, and 4 were discussed at that meeting (Reamer 2001).

During the technical exchange (Reamer 2001), the U.S. Nuclear Regulatory Commission (NRC) and the DOE discussed NRC comments pertaining to radionuclide transport in the saturated zone model abstraction. The NRC asked if changes in radionuclide concentration in the saturated zone model used in the Total System Performance Assessment (TSPA) changes as a result of the inclusion of FEP 2.2.08.01.00, Groundwater Chemistry/Composition in Unsaturated Zone and Saturated Zone. The DOE responded that the code did not simulate changes in radionuclide concentration in the saturated zone. Individual realizations included spatially variable K_{ds} only through the distinction between volcanic and alluvium units, but temporally constant K_d values. The NRC expressed concern that the TSPA code would not show potential increases in dose if the K_d decreased in the future.

Wording of the agreement is as follows:

TSPA I 3.31

Evaluate the effects of temporal changes in saturated zone chemistry on radionuclide concentrations (SZ2.3.2).

DOE will reexamine the FEPs, currently included in the performance assessment, that may lead to temporal changes in saturated zone hydrochemistry. If the DOE determines that these FEPs can be excluded, the results will be documented in the FEP Saturated Zone Flow and Transport AMR (ANL-NBS-MD-000002) in FY 2003. If the DOE determines that these FEPs cannot be excluded from the performance assessment, the DOE will evaluate the effects of temporal changes in the saturated zone chemistry on radionuclide concentrations and will document this evaluation in above-mentioned AMR.

L.1.2 Related Key Technical Issue Agreements

None.

L.2 RELEVANCE TO REPOSITORY PERFORMANCE

The subject of the agreement is the further evaluation of the affects of temporal changes in water chemistry on radionuclide concentrations. This is directly relevant to the output of the saturated zone transport model and, subsequently to the performance assessment. Adequate characterization of saturated zone transport is required by following sections of 10 CFR Part 63 (66 FR 55732).

Retardation of radionuclides by sorption is an important component of the saturated zone performance, and the geochemical processes potentially affecting radionuclide sorption must be fully evaluated. Temporal changes in saturated zone chemistry that might alter sorption and, consequently, the transport of radionuclides require evaluation. Analysis of the potential effects of temporal changes in saturated zone chemistry on the determination of sorption coefficients is provided in this appendix, and the treatment of these potential effects in the TSPA is identified and discussed.

L.3 RESPONSE

The effects of temporal changes in saturated zone chemistry on radionuclide concentrations have been evaluated. Temporal changes in saturated zone chemistry could include changes in rock chemistry, changes in water chemistry, or changes in both. The evaluation indicated that the effects relating to potential changes in rock chemistry have been included in the TSPA through the sorption coefficient probability density functions (PDFs) used in the TSPA. The effects of changes in water chemistry through changes in major ion concentrations and in pH have similarly been accounted for in the sorption coefficient PDFs. Potential changes in Eh and dissolved oxygen have not been incorporated into the PDFs. PDFs were derived under the assumption that conditions in the flow system are oxidizing, which leads to more rapid radionuclide transport than reducing conditions.

However, concern has been expressed regarding the potential impact of transient reducing conditions. The potential for transient reducing conditions to occur has been examined and found to be unlikely. Consequently, this scenario has been discounted. A scenario in which existing reducing conditions are altered during the regulatory timeframe is considered more likely and has also been evaluated. Locations have been examined where water quality data indicate that reducing conditions currently exist. Some of these locations are not in the main flow paths from the repository, and one is suspected of being affected by drilling operations. Reducing conditions in areas affected by drilling are expected to dissipate. However, at least one of the locations is in the main flow path and not likely influenced by drilling operations. This location requires further investigation before firm conclusions are drawn from the available data. Thus, the most likely temporal changes in saturated-zone chemistry are included in the TSPA, while changes thought to be unlikely have been discounted and excluded from the TSPA. For this reason, the main text of this report does not specifically include a discussion of temporal changes in hydrochemistry.

L.4 BASIS FOR THE RESPONSE

Temporal changes in saturated zone chemistry could include changes in rock chemistry, changes in water chemistry, or both. The potential effect of such changes would primarily be on the sorption behavior of the radionuclides of interest. Potential changes in rock chemistry that could impact the transport behavior of radionuclides primarily are changes in ion exchanger (e.g., clays and zeolites) compositions and changes in mineral surface compositions. Variation in ion exchanger compositions and mineral surface compositions were built into the sorption coefficient PDFs used in TSPA (BSC 2003a, Attachment 1). More specifically, the PDFs are based on sorption coefficient data obtained on rock samples taken from different locations on Yucca Mountain. For example, zeolitic samples used in laboratory experiments to obtain sorption coefficients reflect a range of zeolite compositions (Broxton et al. 1986). Similarly, laboratory experiments on devitrified or vitric tuffs used samples from different locations within Yucca Mountain in an attempt to sample the variation in surface chemical heterogeneities. To be conservative, the derived PDFs are biased toward data on rock samples that primarily contain (greater than 95 percent) the major mineral phases or glass (e.g., feldspar, silica phases, zeolite, and glass; BSC 2003a, Attachment 1).

Temporal changes in water chemistry could include changes in the major ion concentrations as well as changes in pH, Eh, dissolved oxygen, and organic carbon content. Potential changes in major ion concentrations are included in the sorption coefficient PDFs (BSC 2003a, Attachment 1). Two end-member water compositions were used in laboratory experiments to obtain sorption coefficients. These two water compositions (from boreholes UE-25 J-13 and UE-25 p#1) are considered to bracket the range in water compositions expected along potential radionuclide flowpaths in the saturated zone over the next 10,000 years. Basically, water from borehole UE-25 J-13 is used to represent the average composition of saturated zone waters. Although water that infiltrated during glacial times may be somewhat more dilute than water from borehole UE-25 J-13, the differences in the major ion compositions of these waters are small (e.g., the concentration of Cl⁻ in glacial-aged groundwater ranges from 5 to 6.5 mg/L, while young groundwater in borehole UE-29 a#2 has a Cl⁻ concentration of 8.3 mg/L; BSC 2003b).

The water composition in the volcanic portion of borehole UE-25 p#1 (BSC 2003b) is used to represent unsaturated zone pore waters that may percolate into the saturated zone beneath Yucca Mountain and possible upward flow from the Paleozoic aquifer into the shallow saturated zone. Because these waters are unlikely to comprise a major percentage of the flow along potential radionuclide pathways, the results of sorption experiments with these waters are given less emphasis in the derivation of the PDFs.

Potential changes in pH are included in the PDFs. Laboratory sorption coefficient experiments were carried out over a range of pH values, 6.8 to 8.6 (BSC 2003a, Attachment 1). Thus, by using the results of these experiments in the derivation of the PDFs, the potential impacts of pH variations were addressed. The impacts of variations in organic content of saturated zone waters were addressed in experiments by using waters from the site. These waters contain small amounts of dissolved organic matter (DTN: GS980908312322.008). Thus, using these waters in laboratory experiments allows the impact of dissolved organic matter to be included in the PDFs.

Potential temporal changes in Eh and dissolved oxygen were not incorporated in the PDFs. The PDFs were derived under the assumption that conditions in the flow system will be oxidizing. The laboratory experiments on which the PDFs are based were carried out in contact with atmospheric oxygen (BSC 2003a, Attachment 1). Thus, the results of these experiments reflect oxidizing conditions. In general, oxidizing conditions lead to more rapid radionuclide transport in the saturated zone than reducing conditions (Langmuir 1997, p.485). However, the NRC has pointed out that the assumption that conditions are oxidizing might lead to dose dilution. In particular, it was pointed out that transient-reducing conditions in some part of the flow field could lead to the accumulation of some radioelements (e.g., Np, Pu, Tc, and U). A subsequent return to oxidizing conditions within the regulatory timeframe could result in enhanced groundwater concentrations of these radioelements. In the following discussion, it is concluded that transient reducing conditions are unlikely to develop during the regulatory time frame.

Possible scenarios in which transient reducing conditions might occur in the flow field include anthropogenic inputs (e.g., from sewage treatment plants, landfills, dairy farms, and leaks from tanks containing petroleum products). Because the land above the potential flowpaths will be under deed restrictions, these potential sources of transient reducing conditions need not be considered further. Even in the absence of deed restrictions, the potential impact of anthropogenic inputs would be limited by the areal extent of the inputs relative to the width of the radionuclide flowfield. Transient reducing conditions also could be imposed from below the potential flowpaths by the upward migration of hydrocarbons (e.g., methane) from the deep saturated zone. However, the hydrocarbon potential for the Yucca Mountain region is classified as low (French 2000), and therefore this scenario is also discounted.

A more likely scenario involving reducing conditions is one in which the reducing conditions are not transient. Some groundwaters in deep boreholes at Yucca Mountain (e.g., USW H-1, USW H-3, USW H-4, UE-25 b#1) and shallow boreholes directly east of Yucca Mountain (UE-25 WT-17) currently show reducing conditions (BSC 2003a). In addition, some of the boreholes drilled by Nye County (NC-EWDP-1DX, 3D, 5S) also contain groundwaters that show reducing conditions.

The reducing conditions observed in deep boreholes such as USW H-3 (Ogard and Kerrisk 1984) are most likely due to the presence of reducing agents in the aquifer matrix. The main reducing agent appears to be pyrite, although biotite and other ferrous-iron-bearing minerals may contribute to the reduction capacity of the aquifer matrix. In borehole USW H-3, pyrite is found deep in the Tram member of the Crater Flat tuff (Thordarson et al. 1984). Pyrite is present in the Tram member as a primary (i.e., volcanic) constituent. The fact that pyrite is still present in the Tram Member after millions of years indicates the existence of substantial reducing capacity in this member. Thus, these reducing conditions are not likely to be transient in a 10,000-year timeframe.

Flow modeling (BSC 2003c) has shown that potential radionuclide flowpaths are primarily through the Prow Pass and Bullfrog members of the Crater Flat Tuff. The Tram member is located directly beneath the Bullfrog member. Thus, radionuclides potentially released from the repository will not come into contact with the reducing conditions present in the Tram member according to the flow model. Mineralogical analyses of samples from the Prow Pass and Bullfrog Members of the Crater Flat Tuff from boreholes in the Yucca Mountain area do not

indicate the presence of pyrite in these units (CRWMS M&O 2000). Thus, it is unlikely that reducing conditions of the type found at borehole USW H-3 will be encountered by radionuclides transported through the volcanic units in the vicinity of Yucca Mountain.

Groundwater pumped from borehole UE-25 WT-17 showed reducing characteristics (Eh < 0.0 mV, little or no dissolved oxygen and nitrate, high organic carbon), which were maintained over a pumping interval during which more than 4,000 gallons were pumped (DTN: LA0206AM831234.001). Analyses of the waters showed that organic carbon concentrations were unusually high (up to 20 mg/L; DTN: GS980908312322.008) for a well completed in volcanic rocks. One explanation for these observations is that drilling fluids containing organic materials were left in the borehole after it was drilled (i.e., the borehole was not properly developed). These fluids may have migrated in a downgradient direction from the borehole but were eventually drawn back into the borehole by the pumping event. This scenario would explain the low Eh, the low dissolved oxygen and nitrate concentrations, and particularly explain the high organic carbon concentrations. If this explanation is correct, the reducing conditions at this location should dissipate, as the groundwater containing drilling fluid is advected downgradient. An alternative explanation for the reducing conditions in borehole UE-25 WT-17 is that the site is located above a source of hydrocarbons in the deeper saturated zone (i.e., the Paleozoic aquifer). However, Yucca Mountain is considered to be an area with low hydrocarbon potential (French 2000), and this possibility is excluded or at least minimized.

Groundwater pumped from the Bullfrog Member in borehole UE-25b#1 also showed reducing conditions (Ogard and Kerrisk 1984). Water pumped during the 4th day of pumping was more reducing than the water pumped during the 28th day of pumping (Eh = -18 vs. 160 mv/SHE; dissolved oxygen = 0.6 vs. 2.2 mg/L; nitrate = 2.2 vs. 4.5 mg/L). After 28 days of pumping, the well was thought to be cleared of any drilling fluids that may have been used in its construction. In fact, the organic carbon concentration was reported to be only 0.55 mg/L (Ogard and Kerrisk 1984). This is a higher concentration than observed in well J-13 water (0.15 mg/L), but it is consistent with the reducing conditions observed in UE-25b#1 and lower than the value of 20 mg/L observed in WT-17. Thus, in this case, the reducing conditions appear to reflect in-situ conditions in the Bullfrog Member. The cause for these reducing conditions is not known. Therefore, the longevity of reducing conditions in this well cannot be evaluated at present.

Reducing conditions have been observed in the alluvial aquifer in boreholes located east and west of Forty Mile Wash (e.g., EWDP-NC-5SB, EWDP-NC-1DX, EWDP-NC-3S; (DTN: LA0206AM831234.002). The cause of reducing conditions in groundwater from borehole NC-EWDP-5SB is not clear. For boreholes EWDP-NC-1DX and EWDP-NC-3S, the reducing conditions likely reflect the presence of pyrite. It may be that pyrite was present in borehole 5SB but was not noted in the cuttings. To the extent that the reducing conditions in these boreholes are maintained over the regulatory time-frame, redox-sensitive radionuclides will be strongly retarded over the regulatory time-frame along flowpaths along the eastern and western edges of the potential flow field. Assuming the presence of pyrite is the main cause of reducing conditions in alluvium, these conditions are expected to be present over the regulatory time-frame.

L.5 REFERENCES

L.5.1 Documents Cited

Broxton, D.E.; Warren, R.G.; Hagan, R.C.; and Luedemann, G. 1986. *Chemistry of Diagenetically Altered Tuffs at a Potential Nuclear Waste Repository, Yucca Mountain, Nye County, Nevada*. LA-10802-MS. Los Alamos, New Mexico: Los Alamos National Laboratory. ACC: MOL.19980527.0202.

BSC (Bechtel SAIC Company) 2003a. *Site-Scale Saturated Zone Transport*. MDL-NBS-HS-000010 REV 01A. Las Vegas, Nevada: Bechtel SAIC Company. ACC: MOL.20030626.0180.

BSC 2003b. *Geochemical and Isotopic Constraints on Groundwater Flow Directions and Magnitudes, Mixing, and Recharge at Yucca Mountain*. ANL-NBS-HS-000021 REV 01A. Las Vegas, Nevada: Bechtel SAIC Company. ACC: MOL.20030604.0164.

BSC 2003c. *Site-Scale Saturated Zone Flow Model*. MDL-NBS-HS-000011 REV 01A. Las Vegas, Nevada: Bechtel SAIC Company. ACC: MOL.20030626.0296. TBV-5203

CRWMS M&O (Civilian Radioactive Waste Management System Management and Operating Contractor) 2000. *Mineralogical Model (MM3.0)*. MDL-NBS-GS-000003 REV 00 ICN 01. Las Vegas, Nevada: CRWMS M&O. ACC: MOL.20000120.0477.

French, D.E. 2000. *Hydrocarbon Assessment of the Yucca Mountain Vicinity, Nye County, Nevada*. Open-File Report 2000-2. Reno, Nevada: Nevada Bureau of Mines and Geology. ACC: MOL.20000609.0298.

Langmuir, D. 1997. *Aqueous Environmental Geochemistry*. Upper Saddle River, New Jersey: Prentice Hall. TIC: 237107.]

Ogard, A.E. and Kerrisk, J.F. 1984. *Groundwater Chemistry Along Flow Paths Between a Proposed Repository Site and the Accessible Environment*. LA-10188-MS. Los Alamos, New Mexico: Los Alamos National Laboratory. ACC: HQS.19880517.2031.

Reamer, C.W. 2001. "U.S. Nuclear Regulatory Commission/U.S. Department of Energy Technical Exchange and Management Meeting on Total System Performance Assessment and Integration (August 6 through 10, 2001)." Letter from C.W. Reamer (NRC) to S. Brocoum (DOE/YMSCO), August 23, 2001, with enclosure. ACC: MOL.20011029.0281.

Thordarson, W.; Rush, F.E.; Spengler, R.W.; and Waddell, S.J. 1984. *Geohydrologic and Drill-Hole Data for Test Well USW H-3, Yucca Mountain, Nye County, Nevada*. Open-File Report 84-149. Denver, Colorado: U.S. Geological Survey. ACC: NNA.19870406.0056.

L.5.2 Codes, Standards, Regulations, and Procedures

66 FR 55732. *Disposal of High-Level Radioactive Wastes in a Proposed Geologic Repository at Yucca Mountain, NV*. Final Rule 10 CFR Part 63. Readily available.

L.5.3 Source Data, Listed by Data Tracking Number

GS980908312322.008. Field, Chemical, and Isotopic Data from Precipitation Sample Collected Behind Service Station in Area 25 and Ground Water Samples Collected at Boreholes UE-25 C #2, UE-25 C #3, USW UZ-14, UE-25 WT #3, UE-25 WT #17, and USW WT-24, 10/06/97 to 07/01/98. Submittal date: 09/15/1998.

LA0206AM831234.001. Eh-pH Field Measurements on Nye County EWDP Wells. Submittal date: 06/21/2002.

LA0206AM831234.002. Geochemical Field Measurements on Nye County EWDP Wells. Submittal date: 06/21/2002.

INTENTIONALLY LEFT BLANK

APPENDIX M
MICROSPHERES AS ANALOGS
(RESPONSE TO RT 3.08 AIN-1 AND GEN 1.01 (#43 AND #45))

Note Regarding the Status of Supporting Technical Information

This document was prepared using the most current information available at the time of its development. This Technical Basis Document and its appendices providing Key Technical Issue Agreement responses that were prepared using preliminary or draft information reflect the status of the Yucca Mountain Project's scientific and design bases at the time of submittal. In some cases this involved the use of draft Analysis and Model Reports (AMRs) and other draft references whose contents may change with time. Information that evolves through subsequent revisions of the AMRs and other references will be reflected in the License Application (LA) as the approved analyses of record at the time of LA submittal. Consequently, the Project will not routinely update either this Technical Basis Document or its Key Technical Issue Agreement appendices to reflect changes in the supporting references prior to submittal of the LA.

APPENDIX M

MICROSPHERES AS ANALOGS (RESPONSE TO RT 3.08 AIN-1 AND GEN 1.01 (COMMENTS 43 AND 45))

This appendix provides a response for additional information needed (AIN) request for Key Technical Issue (KTI) agreements Radionuclide Transport (RT) 3.08 and General Agreement (GEN) (1.01) Comments 43 and 45. These KTI agreements relate to providing more information about the justification for the use of carboxylate-modified latex (CML) polystyrene microspheres as analogs for natural colloids.

M.1 KEY TECHNICAL ISSUE

M.1.1 RT 3.08 AIN-1 and GEN 1.01 (Comments 43 and 45)

KTI agreement RT 3.08 was reached during the NRC/DOE technical exchange and management meeting on radionuclide transport held December 5 through 7, 2000, in Berkeley, California. Radionuclide transport KTI subissues 1, 2 and 3 were discussed at that meeting (Reamer and Williams 2000). At the meeting, DOE indicated that they had completed tests at the C-well complex using microspheres, which will be used as part of the basis for justifying the use of microspheres as analogs for natural colloids. DOE considered these tests to be representative of transport for colloids. This discussion resulted in KTI agreement RT 3.08.

During the NRC/DOE technical exchange and management meeting on thermal operating temperatures, held September 18 through 19, 2001, the NRC provided additional comments relating to this RT KTI agreement (Reamer and Gil 2001). Those comments relating to microspheres as analogs resulted in KTI agreement GEN 1.01, Comments 43 and 45. DOE provided initial responses to these comments (Reamer and Gil 2001).

A letter report responding to agreement RT 3.08 (Ziegler 2002) was prepared. Specific additional information was requested by the U. S. Nuclear Regulatory Commission after the staff's review of this letter report was completed, resulting in RT 3.08 AIN-1 (Schlueter 2002). The NRC response to the letter report states that DOE needs to provide a stronger technical basis and adequate experimental evidence to indicate that carboxylate-modified latex microspheres can be used as analogues for colloids in alluvium. In addition, NRC stated that the DOE response to the agreement did not address General Agreement 1.01 (Comment 45), as discussed during the September 18-19 technical exchange.

As indicated by their associated comments and responses, GEN 1.01 Comments 43 and 45 are addressed implicitly through the response to KTI agreement RT 3.08 AIN-1.

Wording of the agreements is as follows:

RT 3.08

Provide justification that microspheres can be used as analogs for colloids (for example, equivalent ranges in size, charge, etc.). DOE will provide documentation in the C-Wells AMR to provide additional justification that

microspheres can be used as analogs for colloids. The C-Wells AMR will be available to the NRC in October 2001.

RT 3.08 AIN-1

1. Provide a stronger technical basis and adequate experimental evidence to indicate that CML microspheres can be used as analogs for colloids in alluvium.
2. Provide a response to General Agreement 1.01 (#45) to address the potential for remobilization of microspheres and/or colloids.

GEN 1.01 (Comment 43)

The SSPA presents a new distribution for retardation of colloids with irreversibly-attached radionuclides. The distribution takes into account new site-specific alluvium data. However, any future use of this distribution in TSPA will require comparison with results of field and laboratory tests. This concern is indirectly related to agreement TSPA I.3.30.

DOE Initial Response to GEN 1.01 (Comment 43)

DOE acknowledges that any future use of this distribution in TSPA will require comparison with results of field and laboratory tests. This concern is indirectly related to KTI agreements RT 3.07 and RT 3.08. Laboratory testing of microsphere and silica colloid retardation in alluvium-packed columns is in progress. Microspheres will be used as colloid tracers in ATC cross-hole tracer testing.

GEN 1.01 (Comment 45)

In discussing preliminary microsphere transport tests at the Alluvial Testing Complex, it is mentioned that flow transients can remobilize microspheres. Is such a process possible in the repository system? If so, how can it be accommodated in models? These questions may be addressed under agreement RT 3.08, although that agreement specifically discusses fractured rock rather than alluvium.

DOE Initial Response to GEN 1.01 (Comment 45)

Flow transients are likely to occur, but it is unlikely that they will be as rapid or extreme as the transients associated with stopping and starting the pump at ATC during single-well testing. However, it may be important to incorporate sudden transients associated with seismicity into models (it is well known that earthquakes can turn well water turbid for a while). Transients in water chemistry could also result in some remobilization of colloids. This issue is related to KTI agreement RT 3.08 and will address both fractured rock and alluvium.

M.1.2 Related Key Technical Issues

None.

M.2 RELEVANCE TO REPOSITORY PERFORMANCE

The transport of colloids can influence the transport of radionuclides through the natural system. Therefore, this process is included in the transport model and is important in evaluating the saturated zone for the time scales of interest. Because natural colloids are omnipresent in the saturated zone and make it difficult to distinguish between natural and introduced colloids during field testing, YMP scientists and many other researchers have relied on the use of polystyrene microspheres as surrogates for natural colloids in field tracer tests (McKay et al. 2000, Auckenthaler et al. 2002, Harvey et al. 1989, Goldscheider et al. 2003, Becker et al. 1999, and Reimus and Haga 1999). Numerous laboratory studies involving microspheres as colloid analogs have also been conducted (Abdel-Fattah and El-Genk 1998, Anghel 2001, Reimus 2003, Vilks and Bachinski. 1996, Toran and Palumbo 1992, McCaulou et al. 1995, and Wan and Wilson 1994).

Even though they have different physical and chemical properties, the benefit of using microspheres as colloid tracers in these field tests overshadows the limitations because they can be obtained with a narrow range of diameters and with various fluorescent dyes incorporated into the polymer matrix, which allows them to be detected at low concentrations and to be discriminated from natural, nonfluorescing colloids. CML microspheres have been used in testing by the YMP because these microspheres have more hydrophilic surfaces than other types of polystyrene microspheres. The hydrophilic surface is more representative of inorganic colloids, which also have hydrophilic surfaces.

Sections 3.2.1 and 3.3.2 contain summaries of how microsphere test results have been used to support Yucca Mountain performance assessments. Section 6.8 of *Saturated Zone Colloid Transport* (BSC 2003) provides details of laboratory tests conducted to compare the transport behavior of microspheres and inorganic colloids in both saturated fractured tuffs and saturated alluvium. These test results and their interpretation provide the basis for the DOE response to KTI RT 3.08.

M.3 RESPONSE

CML microspheres were used as surrogates for colloid tracers in the multiple-tracer tests in the Bullfrog Tuff and the Prow Pass Tuff at the C-Wells complex. CML microspheres were also used in one of the three single-well tracer tests in the saturated alluvium at borehole NC-EWDP-19D1, and they will be used in at least one cross-hole tracer test at the ATC (when permitting conditions allow further aquifer testing).

CML microspheres were selected as colloid tracers in these field tests because they are nearly monodisperse (i.e., they have a narrow range of diameters) and they can be obtained with various fluorescent dyes incorporated into the polymer matrix, which allows them to be detected at low concentrations and to be discriminated from natural, nonfluorescing colloids using methods such as epifluorescent microscopy and flow cytometry. Flow cytometry was used as the microsphere detection and quantification method for all field tracer tests in which microspheres were used as

tracers. This technique allows quantification at microsphere concentrations as low as 100/mL in the presence of natural background colloid concentrations that are 2 to 4 orders of magnitude higher. These levels of detection and discrimination are not attainable using other types of colloid tracers, except perhaps viruses or bacteriophages (Bales et al. 1989, pp. 2063 to 2064).

Recent laboratory experiments (BSC 2003) conducted to evaluate the applicability of CML microspheres as field-test surrogates for inorganic colloids in saturated fractured media and saturated alluvium have demonstrated that CML microspheres can be used as conservative analogs in fractured tuffs and that small microspheres (<200 nm diameter) transport with nearly the same attenuation as natural colloids in alluvium. In laboratory fracture experiments, 330-nm-diameter CML microspheres consistently experienced less filtration and attenuation than 100-nm silica colloids. Additional tests showed that silica colloids transported with less attenuation than montmorillonite clay colloids. Furthermore, 640-nm-diameter microspheres transported with less attenuation in the C-wells Prow Pass Tuff field tracer test than 280-nm-diameter microspheres. The combination of the laboratory and field test results suggest that microspheres in the 280- to 640-nm size range should transport conservatively relative to inorganic colloids. In alluvium-packed column experiments, natural colloids (wide range of diameters, most less than 100 nm) transported with slightly less filtration than 190-nm-diameter CML microspheres and with considerably less filtration than 500-nm microspheres. These results suggest that:

1. Small (less than 200-nm-diameter) CML microspheres should be reasonable surrogates for inorganic colloids in saturated alluvium
2. CML microspheres in the 280- to 640-nm diameter size range should be conservative colloid tracers in saturated fractured media (yielding transport parameter estimates that result in overprediction of inorganic colloid transport).

M.4 BASIS FOR THE RESPONSE

M.4.1 Introduction to Microspheres as Analogs for Colloids

Substantial additional laboratory analyses and interpretations have been completed since the original DOE submittal for RT 3.08 (Ziegler 2002; BSC 2003).

M.4.2 Summary of Recent Laboratory Experiments Conducted for the U.S. Department of Energy

Colloid filtration rate constants and retardation factors for the fractured volcanics have been estimated in a number of laboratory and field experiments conducted for the YMP and the Underground Test Area Project. The field measurements in fractured tuffs involved fluorescent CML microspheres ranging in diameter from 280- to 640-nm. Microsphere analogs were used because testing with natural colloids is not practical in the saturated zone at Yucca Mountain where natural colloids are abundant, and it would not be possible to determine when exogenous colloids showed breakthrough in tracer testing. CML polystyrene microspheres can be tagged with fluorescent dyes that allow them to be detected and quantified using specific wavelengths of light in recovered samples.

To evaluate potential differences in transport characteristics between the CML microspheres and natural colloids, additional laboratory analyses were conducted and re-evaluated previous interpretations at Yucca Mountain and elsewhere in the DOE complex.

The process for determining colloid filtration and detachment rate constants, k_{filt} and k_{det} , respectively, from laboratory or field transport experiments is:

1. Nonsorbing solute tracers were always injected simultaneously with the colloid tracer(s). The mean residence time (L/V , where L is travel distance and V is velocity) and dispersivity (D/V , where D is the dispersion coefficient) in the flow system were determined using RELAP (LANL 2002) to fit the nonsorbing solute breakthrough curves. In dual-porosity systems, diffusive mass-transfer parameters were estimated for the solutes so that the effects of diffusion and dispersion could be distinguished in the flow system. Diffusive mass-transfer parameters were determined by simultaneously fitting the responses of two nonsorbing tracers with different diffusion coefficients or fitting the responses of the same nonsorbing tracer at different flow rates through the systems. In field tests, because of the low tracer recovery in many cases, the fraction of tracer mass observed in the test was allowed to be an additional adjustable parameter for fitting the solute breakthrough curves. The best-fitting fraction for solutes was then applied to the colloids (although the colloids were assumed to not diffuse into the matrix) with the rationale that the flow pathways resulting in incomplete recovery of solutes would affect the simultaneously injected colloids similarly. This practice has been consistently followed in interpretations of microsphere and colloid transport tests, as colloid transport is generally reported relative to solute transport. The issue is *not* that colloids travel faster than solutes (in fact, this is not consistently observed unless travel times are extremely short, as in laboratory experiments) but that (1) they can carry strongly-sorbing radionuclides along with them and (2) they do not readily diffuse into the matrix, which makes their effective travel time shorter than solutes in systems with significant solute matrix diffusion. The latter difference between colloids and solutes is accounted for in the interpretive procedure. The velocity of colloids and solutes in fractures should be the same over long enough distances and times.
2. The mean residence time, dispersivity, and mass fraction (for field tests) obtained from fitting the solute breakthrough curves were assumed to apply to the colloids in each experiment.
3. RELAP was used to fit colloid breakthrough curves by adjusting k_{filt} and k_{det} (and fixing the mean residence time, dispersivity, and mass fraction to be equal to that of the solutes). The colloids are also assumed to not diffuse into the matrix. The procedure involved adjusting the colloid retardation factor, R_{col} , and k_{filt} . The relationship between R_{col} , k_{filt} and k_{det} is $R_{col} = 1 + k_{filt}/k_{det}$, so if R_{col} and k_{filt} are adjusted, k_{det} is adjusted by default.
4. R_{col} (and therefore, k_{det}) was constrained primarily by fitting the tails of the colloid breakthrough curves. k_{filt} was constrained primarily by fitting the early (unretarded) colloid response (i.e., the peak arriving at about the same time as nonsorbing solutes).

Essentially, k_{filt} was adjusted until it was small enough that the fraction of colloids not filtered in the system matched the early arriving peak. Therefore, the early colloid response was implicitly interpreted as being a fraction of colloids that moved through the system without filtering. Similarly, R_{col} was adjusted until an appropriate fraction of filtered colloids was predicted to detach, thereby yielding a modeled response that approximated the tails of the colloid breakthrough curves. [For any given test, a single best-fitting k_{filt} is obtained. In most cases, this estimate is neither a lower or an upper bound. A lower bound is obtained if there is no colloid breakthrough (which happened at least once) because there is some lower limit of k_{filt} that will result in no predicted breakthrough (all higher values will also result in no breakthrough). An upper bound is obtained if 100 percent of the colloids transport conservatively. In this case, there is some maximum value of k_{filt} that will result in 100 percent conservative transport (all smaller values will also result in 100% conservative transport)].

In some tests, an inadvertent flow transient occurred that resulted in a "spike" in colloid concentrations in the tail of the breakthrough curve. This is presumably because of enhanced detachment caused by the flow transient. In these instances, the value obtained for R_{col} (and k_{det}) was not considered to be representative of steady-flow conditions. However, the value obtained for k_{filt} , which was constrained primarily by the colloid response occurring before the flow transient, was assumed to be representative of steady-flow conditions. Thus, k_{filt} values obtained from such tests were used in the development of cumulative distribution functions for filtration rate constants, but R_{col} values from these tests were not used in the development of cumulative distribution functions for retardation factors.

M.4.3 The Use of Polystyrene Microspheres as Tracer Surrogates for Inorganic Groundwater Colloids

Many of the laboratory and field experiments used to develop the R_{col} distributions in this analysis used CML polystyrene microspheres to study colloid transport. This section describes the effectiveness of CML microspheres as analogs to inorganic groundwater colloids. CML microspheres were used as colloid tracers in the multiple-tracer tests in the Bullfrog Tuff and the Prow Pass Tuff at the C-Wells complex. CML microspheres were also used in a single-well tracer tests in the saturated alluvium at borehole NC-EWDP-19D1, and they will be used in at least one cross-hole tracer test at the ATC. CML microspheres were selected as colloid tracers in these field tests because they are nearly monodisperse and coated with various fluorescent dyes, that allows them to be detected at very low concentrations and to be discriminated from natural, nonfluorescing colloids using methods such as epifluorescent microscopy and flow cytometry. Flow cytometry has been used as the microsphere detection and quantification method for all field tracer tests in which microspheres have been used as tracers. This technique allows quantification at microsphere concentrations as low as 100/mL in the presence of natural background colloid concentrations that are 2 to 4 orders of magnitude higher. These levels of detection and discrimination are not attainable using other types of colloid tracers, except perhaps viruses or bacteriophages (Bales et al. 1989, pp. 2063 and 2064).

CML microspheres were chosen over other types of polystyrene latex microspheres as field colloid tracers for two reasons:

1. They have surface carboxyl groups that give them a negative surface charge at pH greater than about 5.
2. They have relatively hydrophilic surfaces compared to other types of polystyrene microspheres (Wan and Wilson 1994, Table 1).

These properties are consistent with those of natural inorganic groundwater colloids. In addition to providing better consistency with surface characteristics of inorganic colloids, these properties result in greater resistance to flocculation and less attachment to negatively charged hydrophilic rock surfaces. Fluorescent dyes are generally incorporated into the microspheres by swelling the spheres in an organic solvent containing the dye, and then washing the spheres in an aqueous solution to expel the solvent and shrink them back to the original size. Dye molecules tend to remain in the spheres because of their affinity for the organic matrix. As discussed above, the dyes in the matrix provide the means for discriminating tracer colloids from natural colloids and for quantifying tracer colloid concentrations at low levels.

The CML microspheres used in Yucca Mountain field tracer tests were purchased from Interfacial Dynamics Corporation because they use a surfactant-free synthesis process that does not require microspheres to be cleaned (by dialysis or centrifugation) to remove trace levels of surfactant before they are used in tests. Small levels of surfactants can affect microsphere surface characteristics, resulting in inconsistency and irreproducibility of the transport behavior.

CML microspheres have properties that make them a suitable choice among synthetic polystyrene microspheres as reasonable surrogates for inorganic colloids. A comparison of properties of CML microspheres and naturally-occurring inorganic groundwater colloids is presented in Table M-1. Although the two types of colloids differ in density, shape, and specific surface chemistry, both have negative surface charges (at groundwater pHs) and hydrophilic surfaces.

Table M-1. Comparison of Properties of CML Microspheres and Inorganic Groundwater Colloids

Property	CML Microspheres	Inorganic Groundwater Colloids
Size	Monodisperse but greater than 200nm-diameter to ensure good fluorescence detection	Polydisperse, ranging from less than 50 nm to greater than 1000 nm (1 μ m)
Density	1.055 g/cm ³	2.0 to 2.6 g/cm ³
Shape	Spherical	Variable, including polygons, rods, and platelets
Surface Chemistry	Carboxyl groups with many polymer chains extending into solution	Variable, with silicate, iron oxide, aluminum oxide, manganese oxide, and other surface groups possible
Zeta potential	-30 mV or less in low ionic strength water at neutral pH	-30 mV or less in low ionic strength water at neutral pH
Hydrophobicity	Hydrophilic	Hydrophilic
pH at point of zero charge	about 5.0	Variable, but generally less 6

To address the suitability of using CML microspheres as surrogates for natural inorganic colloids, a limited number of laboratory experiments were conducted in which the transport behavior of CML microspheres was compared with that of silica microspheres in saturated volcanic-tuff fractures and saturated alluvium-packed columns. Tests were conducted using the

same CML microspheres (330-nm-diameter spheres from Interfacial Dynamics Corporation dyed with a fluorescent yellow-green dye) and silica spheres (100-nm-diameter spheres from Nissan Chemical). Further information on the two colloid tracers is presented in Table M-2. Most of the tests involving the CML microspheres and silica colloids were conducted in vertically-oriented systems, but in one test in a horizontally-oriented fracture demonstrated that silica colloid transport was significantly more attenuated in this orientation than in the vertical orientation, presumably because of settling. The CML microspheres, on the other hand, were affected only slightly by the change from vertical to horizontal orientation. Silica microspheres were used in the comparison studies because previous testing indicated that silica microspheres transport with less attenuation through vertically oriented fractures than clay (montmorillonite) colloids (Kersting and Reimus 2003). Therefore, because CML microspheres transport with less attenuation than silica microspheres, they would also be expected to be transported with less attenuation than clay colloids.

The 330-nm CML microspheres were selected to be representative of microspheres with diameters ranging from about 250 to 500 nm, which represents a practical size range that can be used in field tests (detection-limited at the small end and cost-limited at the large end). Microspheres at the upper end of this size range will settle about twice as fast and diffuse about one-third slower than 330-nm-diameter spheres, and microspheres at the lower end of this range will settle about half as fast and diffuse about one-fourth faster than 330-nm-diameter spheres.

However, when comparing CML to silica, the CML microspheres ranging in size from 250 to 500 nm (diameter) will settle slower and diffuse slower than 100-nm silica microspheres. Both of these characteristics (slower settling and diffusion) are desirable for reducing the number of colloid collisions with aquifer surfaces. Thus, if electrostatic or double-layer interactions between colloids and aquifer surfaces are similar for both types of microspheres (as suggested by the similar zeta potentials; Table M-2), the CML microspheres would be expected to transport with less attenuation relative to the silica microspheres.

Testing in fractured volcanic rock was conducted in two different fractured cores from Pahute Mesa at the Nevada Test Site, with the majority of the testing being done in fractured lava. At the time of the testing, fractured cores from the saturated zone near Yucca Mountain were not readily available. Testing in the lava core was conducted at several flow rates and residence times.

Table M-2. Properties of CML and Silica Microspheres Used in Experiments

Property	CML Microspheres	Silica Microspheres
Particle Diameter (nm)	330 ± 11	100
% Solids (g/100g) ^a	2 ± 0.1	40.7
Stock Conc. (number/mL) ^a	1 x 10 ¹²	3.8 x 10 ¹⁴
Density (g/cm ³)	1.055	2.65
Dye Excitation/Emission Wavelengths (nm)	505/515	No Dye
Diffusion Coefficient (cm ² /s) ^b	1.34 x 10 ⁻⁸	4.43 x 10 ⁻⁸
Specific Surface Area (cm ² /g)	1.7 x 10 ⁵	2.3 x 10 ⁵
Surface Charge (meq/g) ^c	0.08	not measured
Zeta Potential in U-20WW Water (mV) ^d	-42.7 ± 9.1	-41.2 ± 4.1
Zeta Potential in NC-EWDP-19D1 Water (mV)	NM	-45.15 ± 2.9

Source: Information from manufacturers' certificates of analyses or calculated as described in Note b, below, except for zeta potentials. Zeta potentials are reported by Anghel (2001, Chapter 2).

- NOTES: ^a Manufacturer's stock solution in deionized water; solutions used in experiments were diluted in groundwater to several orders of magnitude below these concentrations.
- ^b Calculated using the Stokes-Einstein equation, $D = kT/(6\pi\mu R)$, where k = Boltzmann's constant (1.38×10^{-16} ergs/K), T = temperature (°K), μ = fluid viscosity (g/cm-s), and R = colloid radius (cm). Calculations assume water at 25°C (298°K).
- ^c Value reported by the manufacturer (Interfacial Dynamics Corporation).
- ^d The zeta potential is the potential measured at the "surface of shear" near the colloid surface in solution (Hiemenz 1986, p. 745). The surface of shear occurs where ions transition from being immobile to being mobile relative to the colloid surface when the colloid moves relative to the surrounding solution. The zeta potential is generally considered to be the best experimental measure of the strength of electrostatic interactions between colloids or between colloids and surfaces in solution.

Conclusions from the testing suggests that CML microspheres in the size range of 280 to 640 nm in diameter should transport similarly to, or with less attenuation relative to, natural inorganic groundwater colloids in saturated fractured systems. However, in saturated alluvium systems, CML microspheres should be smaller than about 200-nm diameter to serve as reasonable analogs for inorganic colloids.

Two sets of experiments were conducted in which the transport of CML microspheres was compared to that of inorganic colloids in saturated alluvium. In the first set of experiments, 330-nm-diameter CML microspheres and 100-nm-diameter silica spheres were simultaneously injected into columns packed with alluvium from the uppermost-screened interval of borehole NC-EWDP-19D1. Water from the same interval was used in these experiments. In the second set of experiments, 190-nm- and 500-nm-diameter CML microspheres were injected simultaneously with natural colloids collected from borehole NC-EWDP-19D1. The alluvium and water in these experiments were taken from the lowest screened interval completed in the alluvium at the ATC (the water came from borehole NC-EWDP-19D1, and the alluvium came from borehole NC-EWDP-19IM1A). In this set of experiments, Pu(V) was sorbed onto the natural colloids prior to injecting the colloids into the columns. Thus, these experiments also provided a test of colloid-facilitated Pu transport in saturated alluvium, but the Pu transport results are beyond the scope of this summary. Although the amount of colloid filtration was considerably different in the two sets of alluvium colloid-transport experiments, the results were consistent in that the inorganic colloids transported with similar or less filtration than the CML

microspheres in both sets of tests. However, it was also apparent in the second set of experiments that smaller CML microspheres tend to more closely approximate the transport behavior of natural inorganic colloids than larger microspheres in saturated alluvium. This result supports the hypothesis that interception may be a dominant mechanism of colloid filtration in alluvium because of the small pore throat sizes that are present. It also suggests that the smallest detectable CML microspheres should be used in field tracer tests in saturated alluvium to obtain field-scale colloid-transport parameters that are most representative of natural colloids.

M.4.4 Remobilization of Colloids by Flow Transients

The need for incorporating sudden transients into the transport models using the Features, Events and Processes process was evaluated. A response to the transient issue in the previous RT 3.08 submittal was not included because the DOE was still in the process of developing its conceptualization of the appropriate models and had not yet decided on what transient processes (if any) would be important to incorporate into the models. Remobilization of colloids as a result of flow transients is not explicitly included in the process models carried forward to total system performance assessment for the license application. However, parameter distributions developed for colloid retardation factors in the saturated zone will be partially based on detachment rate constants derived from field tests in which such flow transients occurred. These flow transients were the result of pumping interruptions and subsequent resumptions, so the transients were probably much more severe than any that are likely to be encountered under ambient conditions. Thus, the effect of these transients on the retardation factor distributions is expected to be a reduction in the retardation factors such that the remobilization of colloids due to naturally-occurring flow transients is effectively overestimated. Therefore the explicit inclusion of minor transient colloid mobilization processes as they apply to the overall total system performance assessment for license application modeling effort is screened out.

M.4.5 Ionic Strength

Colloidal suspensions are sensitive to the ionic strength of the solution, and the results of previous investigations at the C-wells complex and at Busted Butte suggest that the effects of ionic strength may have played important roles in those studies. The original letter report (Ziegler 2002) did not discuss ionic strength of experimental fluids. Ionic strength effects should be explicitly considered in any studies involving transport of colloids or an explanation of why the exclusion of this effect would not have an adverse impact on performance should be documented.

It was an oversight to not include the ionic strengths of the ground waters used in the fractured core and alluvium column experiments involving CML microspheres and silica colloids. The ionic strengths were about 0.0035 M for the water used in the fractured core experiments (borehole U-20WW water) and about 0.004 M for the water used in the alluvium experiments (borehole EWDP-19D water from zones 1 and 2). Furthermore, the divalent cation concentrations (mostly Ca^{2+}) in the two waters were low and almost identical (divalent cations have a greater destabilizing effect on colloids than monovalent cations). The solute tracers used in conjunction with the colloid tracers increased the ionic strength of the injection solutions by 0.001 to 0.0014 M in the experiments (up to a maximum of about 0.005 M).

These differences in solution ionic strength should not, by themselves, have been large enough to cause large differences in the transport behavior of the microspheres and silica colloids. It is expected that the silica colloids would be more sensitive to ionic strength than the CML microspheres because the microspheres have polymer strands extending from their surfaces that contribute to stability in aqueous solutions, whereas silica colloids are stabilized primarily by their negative surface charge. Thus, silica colloids would be expected to be more attenuated, instead of less attenuated, relative to CML microspheres in a higher ionic strength alluvium groundwater if all other things were equal. Therefore, CML microspheres are expected to be on the conservative side of realistic, but not by a large degree.

Ionic strength was not varied in the experiments because the experimental objective was to compare the transport behavior of the colloid tracers in groundwaters considered to be representative of different saturated zone hydrogeologic settings. This study was limited in scope to saturated zone transport. Varying ionic strength would be more important in studies addressing transport in the unsaturated zone or in the engineered barrier system where greater potential variability in ionic strength could be expected.

M.5 REFERENCES

Abdel-Fattah, A.I. and El-Genk, M.S. 1998. "On Colloid Particle Sorption onto a Stagnant Air/Water Interface." *Advances in Colloid and Interface Science*, 78, 237-266. Amsterdam, The Netherlands: Elsevier. TIC: 253147.

Anghel, I. 2001. *Comparison of Polystyrene and Silica Colloids Transport in Saturated Rock Fractures*. Master's. Thesis. Albuquerque, New Mexico: University of New Mexico. TIC: 253148.

Auckenthaler, A., Raso, G., and Huggenberger, P. 2002. "Particle Transport in a Karst Aquifer: Natural and Artificial Tracer Experiments with Bacteria, Bacteriophages and Microspheres," *Water Science and Technology*, 46 (3), 131-138. New York, New York: Pergamon Press. TIC: TBD.

Bales, R.C.; Gerba, C.P.; Grondin, G.H.; and Jensen, S.L. 1989. "Bacteriophage Transport in Sandy Soil and Fractured Tuff." *Applied and Environmental Microbiology*, 55, (8), 2061-2067. Washington, D.C.: American Society for Microbiology. TIC: 224864.

Becker, M.W.; Reimus, P.W.; and Vilks, P. 1999. "Transport and Attenuation of Carboxylate-Modified Latex Microspheres in Fractured Rock Laboratory and Field Tracer Tests." *Ground Water*, 37, (3), 387-395. Westerville, Ohio: National Ground Water Association. TIC: 254522.

BSC (Bechtel SAIC Company) 2003. *Saturated Zone Colloid Transport*. ANL-NBS-HS-000031 REV 01A. Las Vegas, Nevada: Bechtel SAIC Company. ACC: MOL.20030602.0288.

Goldscheider, N.; Hotzl, H.; Kass, W.; and Ufrecht, W. 2003. "Combined Tracer Tests in the Karst Aquifer of the Artesian Mineral Springs of Stuttgart, Germany." *Environmental Geology*, 43, (8), 922-929. New York, New York: Springer-Verlag. TIC: 254772.

Harvey, R.W.; George, L.H.; Smith, R.L.; and LeBlanc, D.R. 1989. "Transport of Microspheres and Indigenous Bacteria Through a Sandy Aquifer: Results of Natural- and Forced-Gradient Tracer Experiments." *Environmental Science & Technology*, 23, (1), 51-56. Washington, D.C.: American Chemical Society. TIC: 224869.

Hiemenz, P.C. 1986. *Principles of Colloid and Surface Chemistry*. 2nd Edition, Revised and Expanded. Undergraduate Chemistry Volume 9. Lagowski, J.J., ed. New York, New York: Marcel Dekker. TIC: 246392.

Kersting, A.P. and Reimus, P.W., eds. 2003. *Colloid-Facilitated Transport of Low-Solubility Radionuclides: A Field, Experimental, and Modeling Investigation*. UCRL-ID-149688. Livermore, California: Lawrence Livermore National Laboratory. TIC: 254176.

LANL (Los Alamos National Laboratory) 2002. *RELAP*. V2.0. PC, Windows 2000/NT. 10551-2.0-00.

McCaulou, D.R.; Bales, R.C.; and Arnold, R.G. 1995. "Effect of Temperature-Controlled Motility on Transport of Bacteria and Microspheres through Saturated Sediment." *Water Resources Research*, 31, (2), 271-280. Washington, D.C.: American Geophysical Union. TIC: 252318.

McKay, L.D.; Sanford, W.E.; and Strong, J.M. 2000. "Field-Scale Migration of Colloidal Tracers in a Fractured Shale Saprolite." *Ground Water*, 38, (1), 139-147. Westerville, Ohio: National Ground Water Association. TIC: 254705.

Reamer, C.W. and Gil, A.V. 2001. Summary Highlights of NRC/DOE Technical Exchange and Management Meeting on Range of Thermal Operating Temperatures held September 18-19, 2001, Las Vegas, Nevada; Rockville, Maryland; and San Antonio, Texas. Washington, D.C.: U.S. Nuclear Regulatory Commission. ACC: MOL.20020107.0162.

Reamer, C.W. and Williams, D.R. 2000. Summary Highlights of NRC/DOE Technical Exchange and Management Meeting on Radionuclide Transport. Meeting held December 5-7, 2000, Berkeley, California. Washington, D.C.: U.S. Nuclear Regulatory Commission. ACC: MOL.20010117.0063.

Reimus, P.W. 2003. Laboratory Testing in Support of Saturated Zone Investigations. Scientific Notebook: SN-LANL-SCI-280-V1. ACC: MOL.20030313.0036.

Reimus, P.W. and Haga, M.J. 1999. *Analysis of Tracer Responses in the BULLION Forced-Gradient Experiment at Pahute Mesa, Nevada*. LA-13615-MS. Los Alamos, New Mexico: Los Alamos National Laboratory. TIC: 249826.

Schlueter, J. 2002. "Radionuclide Transport Agreement 3.08." Letter from J. Schlueter (NRC) to J.D. Ziegler (DOE/YMSCO), August 16, 2002, 0822023934, with enclosure. ACC: MOL.20021014.0097.

Toran, L. and Palumbo A.V. 1992. "Colloid transport through Fractured and Unfractured Laboratory Sand Columns." *Journal of Contaminant Hydrology*, 9, 289-303. Amsterdam, The Netherlands: Elsevier. TIC: 224871.

Vilks, P. and Bachinski, D.B. 1996. "Colloid and Suspended Particle Migration Experiments in a Granite Fracture." *Journal of Contaminant Hydrology*, 21, 269-279. Amsterdam, The Netherlands: Elsevier. TIC: 245730.

Wan, J. and Wilson, J.L. 1994. "Colloid Transport in Unsaturated Porous Media." *Water Resources Research*, 30, (4), 857-864. Washington, D.C.: American Geophysical Union. TIC: 222359.

Ziegler, J.D. 2002. "Transmittal of Reports Addressing Key Technical Issues (KTI)." Letter from J.D. Ziegler (DOE/YMSCO) to J.R. Schlueter (NRC), April 26, 2002, 0430022458, OL&RC:TCG-1032, with enclosures. ACC: MOL.20020730.0383.

INTENTIONALLY LEFT BLANK